

701cy4
PLEASE RETURN TO
KAMAN AVIDYNE
LIBRARY

L-1477-79

WT-31
Copy 4 A

UNCLASSIFIED

TEMPO
KTL 0205
Copy No.

HANDLED AS RESTRICTED IN
FOREIGN DISSEMINATION
SECTION 144b ATOMIC ENERGY ACT 1954

OPERATION

GREENHOUSE

SCIENTIFIC DIRECTOR'S REPORT

ANNEX 8.1

BLAST EFFECTS ON AIRCRAFT IN FLIGHT

NUCLEAR
EXPLOSIONS

1951

DISTRIBUTION STATEMENT A

Approved for public release
Distribution Unlimited

PHOTIC QUALITY INSPECTED 4

DECLASSIFIED BY DNA ISTS, DDE, + AF
DISTRIBUTION STATEMENT "A" APPLIES

DATE 7/24/95

19960212 136

UNCLASSIFIED



Defense Nuclear Agency
6801 Telegraph Road
Alexandria, Virginia 22310-3398

31 August 1995

MEMORANDUM FOR DEFENSE TECHNICAL INFORMATION CENTER
ATTENTION: OCD/MR. BILL BUSH

SUBJECT: WITHDRAWAL OF AD-A995424 FROM DTIC SYSTEM

The Defense Nuclear Agency Security Office (ISTS) requests the withdrawal of the subject report (AD-A995424, WT-31-EX) from the DTIC system.

This action is being requested, because the original report (WT-31) is now **declassified** and **approved for public release**.

Since this office shows no record of DTIC ever receiving a copy of the original report, a reproduced copy is enclosed. Please notify us of your assigned accession number.

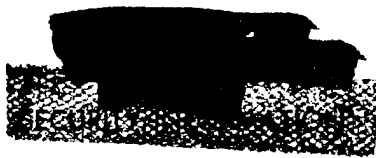
FOR THE DIRECTOR:

A handwritten signature in cursive script, reading "Josephine B. Wood", is positioned above the typed name and title.

JOSEPHINE B. WOOD
Chief, Technical Support

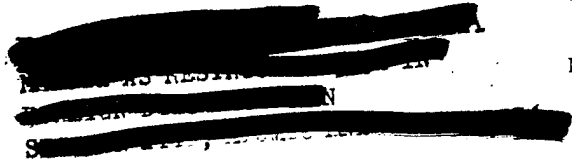
Enclosure:
A/S

UNCLASSIFIED



This document consists of 314 plus 4 pages
(counting preliminary pages)

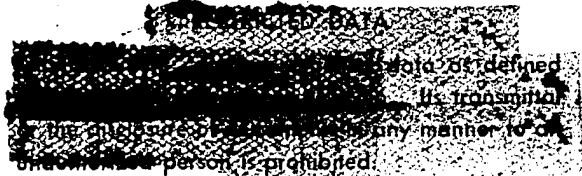
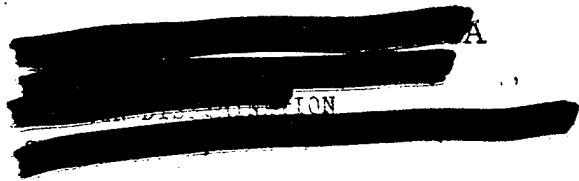
No. 4 of 150 copies, Series A



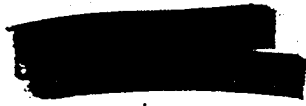
Scientific Director's Report of Atomic Weapon Tests at Eniwetok, 1951

Annex 8.1

Blast Effects on Aircraft in Flight



UNCLASSIFIED



UNCLASSIFIED

Distribution

	Copy		Copy
DEPARTMENT OF DEFENSE		AIR FORCE	
Armed Forces Special Weapons Project (Sandia)	1-3	Deputy Chief of Staff for Development (AFDRD)	53
Armed Forces Special Weapons Project (Washington)	4-15	Director of Operations (Operations Analysis Division)	54
		Director of Plans (AFOPD-P1)	55
		Director of Requirements	56-57
		Director of Research and Development	58-59
ARMY		Eglin Air Force Base, Air Proving Ground	60-61
Army Field Forces	16	Ent Air Force Base, Air Defense Command	62-63
Assistant Chief of Staff, G-3	17	Kirtland Air Force Base, Special Weapons Center	64-66
Assistant Chief of Staff, G-4	18-19	Langley Air Force Base, Tactical Air Command	67-68
Chief of Ordnance	20-24	Maxwell Air Force Base, Air University	69-70
Operations Research Office (Johns Hopkins University)	25-26	Offutt Air Force Base, Strategic Air Command	71-73
Quartermaster General	27-31	1009th Special Weapons Squadron	74
		Rand Corporation	75-76
		Scott Air Force Base, Air Training Command	77-78
		Wright Air Development Center	79-81
		Wright Air Development Center	82-83
NAVY		ATOMIC ENERGY COMMISSION	
Bureau of Aeronautics	32-35	Atomic Energy Commission, Washington	84-86
Bureau of Ordnance	36-37	Los Alamos Scientific Laboratory, Report Library	87-91
Chief of Naval Operations	38-39	Sandia Corporation	92-93
Chief of Naval Research	40	Technical Information Service, Oak Ridge (surplus)	94-149
Commandant, Marine Corps	41	Weapon Test Reports Group, TIS	150
AIR FORCE			
Air Force Cambridge Research Center	42		
Air Research and Development Command	43-46		
Air Targets Division, Directorate of Intelligence (Phys. Vul. Branch)	47-48		
Assistant for Atomic Energy	49-50		
Assistant for Development Planning	51		
Assistant for Materiel Program Control	52		

UNCLASSIFIED

UNCLASSIFIED



BLAST EFFECTS ON AIRCRAFT IN FLIGHT

by

JAY C. WAYNE

and

JOEL C. LEHMKUHL

Approved by: ROBERT E. JARMON
Colonel, USAF
Director, Program 8

Approved by: ALVIN C. GRAVES
Scientific Director

Aircraft Laboratory
Aeronautical Division
Wright Air Development Center
Wright-Patterson Air Force Base
Dayton, Ohio

October 1951

UNCLASSIFIED



[REDACTED]

Because of its limited interest to the readers of Operation Greenhouse Program 8 reports, "Calibration Curves," Annex 8.1, Appendixes A to H (WT-32 Ref.) has been reproduced in 26 copies and given the following limited distribution:

	Copy
Los Alamos Scientific Laboratory, Report Library	1-4
Atomic Energy Commission, Washington	5-7
Armed Forces Special Weapons Project, Washington	8-12
Armed Forces Special Weapons Project, Albuquerque	13
Kirtland Air Force Base, SWC	14
Air Force Cambridge Research Center	15
Wright Air Materiel Command (WCNSS)	16-18
Wright Air Development Center	19-20
Air Research and Development Command	21-22
Director of Research and Development (USAF)	23
Bureau of Aeronautics	24
Chief of Naval Research	25
Weapon Test Reports Group, TIS	26



Preface

The primary mission of Project 8.1 was the collection of data concerning the effects of an atomic explosion on aircraft. This report is essentially designed around the function of presenting those data in such a manner that they are readily available for further analysis or exploitation.

The presentation of the data is precluded by descriptions of the instruments used, their installation, and their calibration in order that those who make further use of the data may do so with discretion. Furthermore, this report attempts to describe the techniques and equipment in order that persons concerned can reproduce the conditions as they existed in order to verify the measurements or repeat the tests.

The quantity of data collected and the limits of time precluded a complete analysis. Also, such analyses and reductions to airplane design criteria are the function of another project, Project 8.0. In this report the data are merely presented as functions versus time and catalogued; in some instances, obvious regroupings of related data are performed. For the most part, the analysis and application of the data to theory are left to Project 8.0. It is hoped that these efforts are successful.

~~SECRET~~

Acknowledgments

When one considers the scope of the tests performed under Project 8.1, it is readily apparent that credit for much earnest effort is due many people. Because of the scope of the project, the amount of detail work to be done, and the number of persons involved, it is impossible to acknowledge the contributions of each individual. The authors are, however, grateful to all who participated in this project and indebted to those who provided the assiduous effort which is so necessary to the success of any operation of such magnitude. Special acknowledgment should be given to the following contributing authors:

T. S. Lewis, Maj, USAF (TG 3.1)	Electronics, Project 8.1
D. L. Diehi, Capt, USAF (AMC)	Radar-data Recorders
C. W. Orr, 1st Lt, USAF (TG 3.1)	Sections on B-50D's and XB-47
J. A. Petersen, 1st Lt, USAF (TG 3.4)	Operation of Instruments
C. W. Luchsinger (TG 3.1)	Sections on QB-17 Drones
C. K. Fredricks (TG 3.1)	Heat Measurements
F. C. Karabaich (TG 3.4)	Telemetry Equipment

The direct collaboration of the contributing authors was invaluable in the preparation of this report.

JAY C. WAYNE
JOEL C. LEHMKUHL

CONTENTS

	Page
PREFACE	v
ACKNOWLEDGMENTS	vii
ABSTRACT	1
CHAPTER 1 INTRODUCTION	3
1.1 Description of Report	3
1.1.1 Organization	3
1.1.2 Definitions and Sign Conventions	3
1.1.3 Data Presentation	4
1.2 Problem	4
1.3 Background	5
1.4 General Plan	5
1.4.1 Selection of Airplanes	5
1.4.2 Selection of Instrumentation	6
1.4.3 Airplane Collocation	6
CHAPTER 2 INSTRUMENTS	8
2.1 General Instrument Requirements	8
2.2 Recorders	8
2.2.1 Selection	8
2.2.2 Principles of Operation	9
2.2.3 Air-borne Amplifier	13
2.2.4 Air-borne Recorder	13
2.2.5 12-channel Playback	13
2.2.6 2-channel Playback	13
2.3 Telemetry	23
2.3.1 System	23
2.3.2 Principles of Operation	23
2.3.3 Accessories	28
2.4 Timing and Synchronization	30
2.4.1 System	30
2.4.2 Description of Equipment	31
2.4.3 Theory of Operation	31
2.4.4 Blue-box Fiducial Marker	33
2.5 High-frequency Pressure Recorder	33
2.5.1 System	35
2.5.2 Calibration	35

CONTENTS (Continued)

	Page
2.6 Sensing Instruments	37
2.6.1 Airspeed and Altitude Gauges	37
2.6.2 Accelerometers	37
2.6.3 Elevator-position Indicator	39
2.6.4 Strain Gauges	39
2.6.5 Pressure Transducers	39
2.7 Radar-data Recorders	40
2.7.1 System	40
2.7.2 Description of Equipment	40
2.7.3 Theory of Operation	43
2.7.4 Reading Radar Data	44
2.8 Temperature Survey Instruments (Temp-Tape)	44
2.9 Instrument Performance	46
2.9.1 Recorders	46
2.9.2 Telemetry	46
2.9.3 Timing and Synchronization	48
2.9.4 High-frequency Pressure Recorder	48
2.9.5 Sensing Instruments	49
2.9.6 Radar-data Recorders	49
2.9.7 Aircraft Installation	49
CHAPTER 3 AIRPLANE PREPARATIONS	53
3.1 Instrumentation	53
3.2 Calibrations	54
3.2.1 Direct Method	56
3.2.2 Indirect Method	56
3.2.3 Analytical Method	61
3.2.4 Presentation	61
3.3 QB-17 Drones	65
3.3.1 Instrumentation	65
3.3.2 Calibration	69
3.4 QT-33 Drones	70
3.4.1 Instrumentation	71
3.4.2 Calibration	77
3.5 B-50D Airplanes	79
3.5.1 Instrumentation	79
3.5.2 Calibration	84
3.6 XB-47 Airplane	87
3.6.1 Instrumentation	87
3.6.2 Calibration	92
3.7 Temp-Tapes	93
3.7.1 Installation	93
3.7.2 Calibration	100
CHAPTER 4 OPERATION PLANS	101
4.1 General Operation Objectives	101

~~SECRET~~

CONTENTS (Continued)

	Page
4.2 Plan for Dog Shot	101
4.3 Plan for Easy Shot	101
4.4 Plan for George Shot	104
4.5 Standard Operating Procedure	110
CHAPTER 5 DOG SHOT	111
5.1 General Information	111
5.2 Alice Position, QT-33 Drone 2	111
5.2.1 Flight Log	111
5.2.2 Airplane Condition	112
5.2.3 Radar Position Data	112
5.2.4 Load Data	115
5.2.5 Heat Data	115
5.2.6 Analysis	115
5.3 Betty Position, QT-33 Drone 1	125
5.4 Carol Position, QB-17 Drone M	125
5.4.1 Flight Log	125
5.4.2 Airplane Condition	125
5.4.3 Radar Position Data	126
5.4.4 Load Data	126
5.4.5 Heat Data	137
5.4.6 Analysis	137
5.5 Doris Position, QB-17 Drone N	137
5.6 Elaine Position, XB-47 Airplane, No. 46-066	139
5.6.1 Flight Log	139
5.6.2 Airplane Condition	139
5.6.3 Load Data	139
5.6.4 Analysis	150
5.7 Frances Position, B-50D Airplane, No. 49-340	150
5.7.1 Flight Log	150
5.7.2 Airplane Condition	150
5.7.3 Load Data	152
5.7.4 Analysis	152
5.8 Grace Position, B-50D Airplane, No. 49-290	152
5.8.1 Flight Log	152
5.8.2 Airplane Condition	162
5.8.3 Load Data	162
5.8.4 Analysis	162
5.9 General Conclusions from Dog Shot	162
CHAPTER 6 EASY SHOT	168
6.1 General Information	168
6.2 Alice Position, QT-33 Drone 3	169
6.2.1 Flight Log	169
6.2.2 Radar Position Data	169
6.3 Betty Position, QT-33 Drone 2	169
6.3.1 Flight Log	171

CONTENTS (Continued)

	Page
6.3.2 Airplane Condition	171
6.3.3 Radar Position Data	172
6.3.4 Load Data	172
6.3.5 Heat Data	172
6.3.6 Analysis	172
6.4 Carol Position, QB-17 Drone M	172
6.4.1 Flight Log	172
6.4.2 Airplane Condition	180
6.4.3 Radar Position Data	180
6.4.4 Load Data	186
6.4.5 Heat Data	186
6.4.6 Radiological Data	186
6.4.7 Analysis	186
6.5 Doris Position, QB-17 Drone N	186
6.5.1 Flight Log	186
6.5.2 Airplane Condition	196
6.5.3 Radar Position Data	196
6.5.4 Load Data (Shock)	199
6.5.5 Load Data (Cloud)	199
6.5.6 Heat Data	199
6.5.7 Radiological Data	199
6.5.8 Analysis	199
6.6 Elaine Position, XB-47 Airplane, No. 46-066	211
6.6.1 Flight Log	211
6.6.2 Airplane Condition	211
6.6.3 Load Data	211
6.6.4 Analysis	211
6.7 Frances Position, B-50D Airplane, No. 49-290	220
6.7.1 Flight Log	220
6.7.2 Airplane Condition	220
6.7.3 Load Data	220
6.7.4 Analysis	220
6.8 Grace Position, B-50D Airplane, No. 49-340	229
6.8.1 Flight Log	229
6.8.2 Airplane Condition	229
6.8.3 Load Data	229
6.8.4 Analysis	229
6.9 General Conclusions from Easy Shot	248
 CHAPTER 7 GEORGE SHOT	
7.1 General Information	249
7.2 Alice Position, QT-33 Airplane 5	249
7.3 Betty Position, QT-33 Airplane 4	249
7.4 Carol Position, QB-17 Airplane O	250
7.4.1 Flight Log	250
7.4.2 Airplane Condition	250
7.4.3 Radar Position Data	250
7.4.4 Load Data	250

CONTENTS (Continued)

	Page
7.5 Doris Position, QB-17 Airplane N	255
7.5.1 Flight Log	255
7.5.2 Airplane Condition	255
7.5.3 Load Data	256
7.6 Elaine Position, XB-47 Airplane, No. 46-066	256
7.7 Frances Position, B-50D Airplane, No. 49-290	256
7.7.1 Flight Log	256
7.7.2 Airplane Condition	256
7.7.3 Load Data	256
7.8 Grace Position, B-50D Airplane, No. 49-340	265
7.8.1 Flight Log	265
7.8.2 Airplane Condition	265
7.8.3 Load Data	265
7.9 Sally Position, QB-17 Airplane P	265
7.9.1 Flight Log	279
7.9.2 Airplane Condition	279
7.9.3 Load Data	279
7.10 General Conclusions from George Shot	279
CHAPTER 8 SUMMARY	284
8.1 Instrumentation	284
8.2 Operation	284
8.2.1 Organization	285
8.2.2 Facilities	285
8.2.3 Personnel	285
8.3 Data	286
8.4 Future Plans	287

ILLUSTRATIONS

CHAPTER 2 INSTRUMENTS

2.1 Deriving Phase Shift from Strain-gauge Output	10
2.2 Functional Block Diagram, One Channel of 24-channel Recorder	11
2.3 Functional Block Diagram, One Channel of Playback System	12
2.4 24-channel Recording System	14
2.5 Air-borne Amplifier Unit	15
2.6 Plug-in Amplifier (Standard Accuracy)	16
2.7 Plug-in Amplifier (High Accuracy)	17
2.8 Air-borne Recorder Unit	18
2.9 12-channel Playback	19

ILLUSTRATIONS (Continued)

	Page
2.10 Control Rack, 12-channel Playback	20
2.11 Channel Rack, 12-channel Playback	21
2.12 2-channel Playback	22
2.13 Coder-Multiplexer Unit, Telemetry Set AN/AKT-6	24
2.14 Transmitter Unit, Telemetry Set AN/AKT-6	25
2.15 Receiver Unit, Telemetry Set AN/UKR-1	26
2.16 Block Diagram of Telemetry Set AN/AKT-6	27
2.17 Block Diagram of Telemetry Set AN/UKR-1	29
2.18 Block Diagram of Coder and Decoder Systems	32
2.19 Blue-box Fiducial, Type A-2	34
2.20 Block Diagram of High-frequency Pressure Recorder	36
2.21 Transfer Function for Shock Tube Used to Calibrate High-frequency Pressure Recorders	38
2.22 Radar-data Recorder	41
2.23 Radar-data Recorder with Camera in Place	42
2.24 Presentation of Data from Radar-data Recorder	45
2.25 Assembly and Application of Temp-Tapes	47
2.26 High-frequency-pressure-recorder Installation and Sample Records	50
2.27 Typical Instrument-engineer's Control Station	51
2.28 Installation of Equipment below Table at Instrument-engineer's Station	52
CHAPTER 3 AIRPLANE PREPARATIONS	
3.1 Schematic Wiring Diagram for Test Airplane	55
3.2 Schematic Wiring Diagram for Connection of Calibration Box in Intelligence Channel	57
3.3 Example Calibration of Sensing Element	58
3.4 Example Calibration of Recorder-Amplifier	59
3.5 Example Calibration of Recorder-Playback Combination	63
3.6 Example Calibration of Complete Channel	64
3.7 Instrumentation of QB-17 Drones	67
3.8 Instrumentation of QT-33 Drones	73
3.9 Installation of Instrumentation in Aft Cockpit of QT-33 Drones	74
3.10 Mounting of Pressure Transducers, QT-33	76
3.11 Calibration of Bending and Shear Gauges, QT-33	78
3.12 Instrumentation of B-50D Airplanes	80
3.13 Permissible and Maximum Applied Shear for Calibration of B-50D Wing Shear Gauges	85
3.14 Permissible and Maximum Applied Moments for Calibration of B-50D Wing-bending Gauges	86
3.15 Instrumentation of XB-47 Airplane	88
3.16 Painted Areas on QB-17 Flaps	94
3.17 Space Diagram for Computation of Angles of Incidence	99
CHAPTER 4 OPERATION PLANS	
4.1 Array of Test Airplanes for Dog Shot	103
4.2 Estimates of Heat Effects on Test Airplanes	105

ILLUSTRATIONS (Continued)

	Page
4.3 Array of Test Airplanes for Easy Shot	106
4.4 Array of Test Airplanes for George Shot	109

CHAPTER 5 DOG SHOT

5.1 Heat Damage to QT-33 No. 2, Dog Shot	113
5.2 Track of QT-33 Drone 2, Dog Shot	114
5.3 Normal Acceleration, c.g., Channel 3, QT-33 No. 2, Dog Shot	116
5.4 Normal Acceleration, Nose, Channel 5, QT-33 No. 2, Dog Shot	116
5.5 Wing Bending, Right Root, Channel 7, QT-33 No. 2, Dog Shot	117
5.6 Stabilizer Bending, Right Root, Channel 9, Before Shock Wave, QT-33 No. 2, Dog Shot	117
5.7 Stabilizer Bending, Right Root, Channel 9, Shock Wave, QT-33 No. 2, Dog Shot	118
5.8 Wing Bending, Outer Panel, Right Wing Station 129, Channel 10, QT-33 No. 2, Dog Shot	118
5.9 Wing Shear, Right Root, Channel 12, QT-33 No. 2, Dog Shot	119
5.10 Differential Pressure, 10% Chord, Right Wing Station 128, Channel 17, QT-33 No. 2, Dog Shot	119
5.11 Differential Pressure, 26% Chord, Right Wing Station 128, Channel 18, QT-33 No. 2, Dog Shot	120
5.12 Differential Pressure, 42% Chord, Right Wing Station 128, Channel 19, QT-33 No. 2, Dog Shot	120
5.13 Differential Pressure, 58% Chord, Right Wing Station 128, Channel 20, QT-33 No. 2, Dog Shot	121
5.14 Differential Pressure, 80% Chord, Right Wing Station 124, Channel 21, QT-33 No. 2, Dog Shot	121
5.15 Aerodynamic Pressure, Nose, Channel 22, QT-33 No. 2, Dog Shot	122
5.16 Summary of Differential Pressures at Wing Station 128, QT-33 No. 2, Dog Shot	123
5.17 Pitching Acceleration, QT-33 No. 2, Dog Shot	123
5.18 Apparent Temperature Variation in Horizontal Stabilizer, QT-33 No. 2, Dog Shot	124
5.19 Heat Damage to Elevators, QB-17 M, Dog Shot	127
5.20 Heat Damage to Ailerons, QB-17 M, Dog Shot	128
5.21 Ground Track, Radar-data Recorder, Drone Carol, Dog Shot	129
5.22 Altitude, Channel 1, QB-17 M, Dog Shot	129
5.23 Airspeed, Channel 2, QB-17 M, Dog Shot	130
5.24 Wing Bending, Right Wing Root, Channel 7, QB-17 M, Dog Shot	130
5.25 Wing Bending, Left Wing Root, Channel 8, QB-17 M, Dog Shot	131
5.26 Stabilizer Bending, Right Horizontal Stabilizer, Channel 9, QB-17 M, Dog Shot	131
5.27 Wing Bending, Outer Panel, Right Wing Station 19, Channel 10, QB-17 M, Dog Shot	132
5.28 Wing Bending, Mid-span, Right Wing Station 8.8, Channel 14, QB-17 M, Dog Shot	132
5.29 Elevator Position, Channel 15, QB-17 M, Dog Shot	133

~~SECRET~~

ILLUSTRATIONS (Continued)

	Page
5.30 Differential Pressure, 5% Chord, Right Wing Station 25.5, Channel 16, QB-17 M, Dog Shot	133
5.31 Differential Pressure, 10% Chord, Right Wing Station 25.5, Channel 17, QB-17 M, Dog Shot	134
5.32 Differential Pressure, 20% Chord, Right Wing Station 25.5, Channel 18, QB-17 M, Dog Shot	134
5.33 Differential Pressure, 40% Chord, Right Wing Station 25.5, Channel 19, QB-17 M, Dog Shot	135
5.34 Differential Pressure, 40% Chord, Right Wing Station 8.8, Channel 22, QB-17 M, Dog Shot	135
5.35 Differential Pressure, 40% Chord, Right Horizontal Stabilizer, Channel 24, QB-17 M, Dog Shot	136
5.36 Normal Acceleration, No. 3 Engine, Channel A3, XB-47, Dog Shot	140
5.37 Normal Acceleration, No. 1 Engine, Channel A4, XB-47, Dog Shot	140
5.38 Normal Acceleration, Bomb Bay, Forward, Channel A6, XB-47, Dog Shot	141
5.39 Normal Acceleration, c.g., Channel A7, XB-47, Dog Shot	141
5.40 Normal Acceleration, Aft Fuselage at Horizontal Stabilizer, Channel A8, XB-47, Dog Shot	142
5.41 Wing Shear, Right Wing Root, Wing Station 307, Channel A12, XB-47, Dog Shot	142
5.42 Wing Bending, Right Wing Root, Wing Station 307, Channel A13, XB-47, Dog Shot	143
5.43 Wing Shear, Left Wing Root, Wing Station 307, Channel A16, XB-47, Dog Shot	143
5.44 Wing Bending, Left Wing Root, Wing Station 307, Channel A17, XB-47, Dog Shot	144
5.45 Wing Shear, Left Wing Outboard, Wing Station 660, Channel A21, XB-47, Dog Shot	144
5.46 Fuselage Bending, Aft End of Bomb Bay, Fuselage Station 718, Channel A24, XB-47, Dog Shot	145
5.47 Airspeed, Channel B2, XB-47, Dog Shot	145
5.48 Gauge Aerodynamic Pressure, Left-hand Side of Vertical Fin, Channel B6, XB-47, Dog Shot	146
5.49 Gauge Aerodynamic Pressure, 5% Chord, Bottom Left Wing Station 515, Channel B7, XB-47, Dog Shot	146
5.50 Gauge Aerodynamic Pressure, 11.7% Chord, Bottom Left Wing Station 515, Channel B9, XB-47, Dog Shot	147
5.51 Gauge Aerodynamic Pressure, 20% Chord, Bottom Left Wing Station 515, Channel B11, XB-47, Dog Shot	147
5.52 Gauge Aerodynamic Pressure, 40% Chord, Bottom Left Wing Station 515, Channel B15, XB-47, Dog Shot	148
5.53 Gauge Aerodynamic Pressure, 61.3% Chord, Top Left Wing Station 515, Channel B16, XB-47, Dog Shot	148
5.54 Gauge Aerodynamic Pressure, Left-hand Side of Fuselage, Aft of Bomb Bay, Channel B19, XB-47, Dog Shot	149

~~SECRET~~

ILLUSTRATIONS (Continued)

	Page
5.55 Gauge Aerodynamic Pressure, 5% Chord, Top Left Wing Station 523, Channel B24, XB-47, Dog Shot	149
5.56 Summary of Gauge Pressures at Left Wing Station 515, XB-47, Dog Shot	151
5.57 Pitching Acceleration, XB-47, Dog Shot	151
5.58 Elevator Position, Elevator Torque Tube, Channel A1, B-50D (340), Dog Shot	153
5.59 Wing Bending, Left Wing Outboard, Wing Station 505, Channel A2, B-50D (340), Dog Shot	153
5.60 Normal Acceleration, Forward Bomb Bay, Aft, Channel A5, B-50D (340), Dog Shot	154
5.61 Normal Acceleration, Nose-wheel Well, Aft, Channel A6, B-50D (340), Dog Shot	154
5.62 Normal Acceleration, Aft Fuselage, in Tail-gunner's Compartment, Channel A7, B-50D (340), Dog Shot	155
5.63 Wing Bending, Right Wing Mid-span, Wing Station 266, Channel A10, B-50D (340), Dog Shot	155
5.64 Wing Bending, Right Wing Root, Wing Station 79, Channel A11, B-50D (340), Dog Shot	156
5.65 Wing Bending, Left Wing Root, Wing Station 79, Channel A12, B-50D (340), Dog Shot	156
5.66 Wing Bending, Left Wing Inboard, Wing Station 120, Channel A13, B-50D (340), Dog Shot	157
5.67 Wing Shear, Right Wing Mid-span, Wing Station 269, Channel A16, B-50D (340), Dog Shot	157
5.68 Wing Shear, Right Wing Root, Wing Station 78, Channel A17, B-50D (340), Dog Shot	158
5.69 Wing Shear, Left Wing Root, Wing Station 78, Channel A18, B-50D (340), Dog Shot	158
5.70 Wing Shear, Left Wing Inboard, Wing Station 122, Channel A19, B-50D (340), Dog Shot	159
5.71 Wing Shear, Left Wing Mid-span, Wing Station 269, Channel A20, B-50D (340), Dog Shot	159
5.72 Wing Torsion, Right Wing Root, Wing Station 78, Channel A22, B-50D (340), Dog Shot	160
5.73 Wing Torsion, Left Wing Root, Wing Station 78, Channel A23, B-50D (340), Dog Shot	160
5.74 Overpressure, High-frequency Recorder, B-50D (340), Dog Shot	161
5.75 Normal Acceleration, c.g., Channel A5, B-50D (290), Dog Shot	163
5.76 Normal Acceleration, Aft Fuselage, in Tail-gunner's Compartment, Channel A7, B-50D (290), Dog Shot	163
5.77 Wing Shear, Right Wing Root, Wing Station 78, Channel A17, B-50D (290), Dog Shot	164
5.78 Wing Shear, Left Wing Outboard, Wing Station 506, Channel A21, B-50D (290), Dog Shot	164
5.79 Wing Torsion, Right Wing Root, Wing Station 78, Channel A22, B-50D (290), Dog Shot	165

ILLUSTRATIONS (Continued)

	Page
5.80 Wing Torsion, Left Wing Inboard, Wing Station 122, Channel A24, B-50D (290), Dog Shot	165
5.81 Airspeed, Channel B2, B-50D (290), Dog Shot	166
5.82 Normal Acceleration, Rear Bomb Bay, Aft, Channel B3, B-50D (290), Dog Shot	166
CHAPTER 6 EASY SHOT	
6.1 Track, Radar-data Recorder, QT-33 Drone No. 3, Easy Shot	170
6.2 Track, Radar-data Recorder, QT-33 Drone No. 2, Easy Shot	173
6.3 Normal Acceleration, Nose, Channel 5, QT-33 No. 2, Easy Shot	174
6.4 Wing Bending, Right Root, Channel 7, QT-33 No. 2, Easy Shot	174
6.5 Stabilizer Bending, Right Root, Channel 9, QT-33 No. 2, Easy Shot	175
6.6 Wing Bending, Outer Panel, Right Wing Station 129, Channel 10, QT-33 No. 2, Easy Shot	175
6.7 Wing Shear, Right Root, Channel 12, QT-33 No. 2, Easy Shot	176
6.8 Wing Torsion, Right Root, Channel 13, QT-33 No. 2, Easy Shot	176
6.9 Differential Pressure, 10% Chord, Right Wing Station 128, Channel 17, QT-33 No. 2, Easy Shot	177
6.10 Differential Pressure, 26% Chord, Right Wing Station 128, Channel 18, QT-33 No. 2, Easy Shot	177
6.11 Differential Pressure, 42% Chord, Right Wing Station 128, Channel 19, QT-33 No. 2, Easy Shot	178
6.12 Differential Pressure, 58% Chord, Right Wing Station 128, Channel 20, QT-33 No. 2, Easy Shot	178
6.13 Differential Pressure, 80% Chord, Right Wing Station 124, Channel 21, QT-33 No. 2, Easy Shot	179
6.14 Summary of Differential Pressures at Wing Station 128, QT-33 No. 2, Easy Shot	179
6.15 Damage to QB-17 Drone M, Easy Shot	181
6.16 Heat Damage to Tire, QB-17 Drone M, Easy Shot	182
6.17 Blast Damage to QB-17 Drone M, Easy Shot	183
6.18 Blast Damage to QB-17 Drone M, Easy Shot	184
6.19 Blast Damage to QB-17 Drone M, Easy Shot; Flexible Coupling of Exhaust Duct, No. 2 Engine	185
6.20 Track, Radar-data Recorder, QB-17 Drone Carol, Easy Shot	188
6.21 Altitude, Channel 1, QB-17 M, Easy Shot	189
6.22 Wing Bending, Right Wing Root, Channel 7, QB-17 M, Easy Shot	189
6.23 Wing Bending, Left Wing Root, Channel 8, QB-17 M, Easy Shot	190
6.24 Stabilizer Bending, Right Horizontal Stabilizer, Channel 9, QB-17 M, Easy Shot	190
6.25 Wing Bending, Outer Panel, Right Wing Station 19, Channel 10, QB-17 M, Easy Shot	191
6.26 Wing Shear, Right Wing Root, Channel 12, QB-17 M, Easy Shot	191
6.27 Wing Bending, Mid-span, Right Wing Station 8.8, Channel 14, QB-17 M, Easy Shot	192
6.28 Differential Pressure, 5% Chord, Right Wing Station 25.5, Channel 16, QB-17 M, Easy Shot	192

ILLUSTRATIONS (Continued)

	Page
6.29 Differential Pressure, 10% Chord, Right Wing Station 25.5, Channel 17, QB-17 M, Easy Shot	193
6.30 Differential Pressure, 40% Chord, Right Wing Station 25.5, Channel 19, QB-17 M, Easy Shot	193
6.31 Differential Pressure, 60% Chord, Right Wing Station 25.5, Channel 20, QB-17 M, Easy Shot	194
6.32 Differential Pressure, 40% Chord, Right Horizontal Stabilizer, Channel 24, QB-17 M, Easy Shot	194
6.33 Overpressure, High-frequency Pressure Recorder, QB-17 Drone M, Easy Shot	195
6.34 Damage to QB-17 Drone N, Easy Shot	197
6.35 Damage to QB-17 Drone N, Easy Shot	198
6.36 Track, Radar-data Recorder, QB-17 Drone Doris, Easy Shot	201
6.37 Wing Bending, Left Wing Root, Channel 8, QB-17 N, Easy Shot	202
6.38 Stabilizer Bending, Right Horizontal Stabilizer, Channel 9, QB-17 N, Easy Shot	202
6.39 Wing Bending, Outer Panel, Right Wing Station 19, Channel 10, QB-17 N, Easy Shot	203
6.40 Wing Shear, Right Wing Root, Channel 12, QB-17 N, Easy Shot	203
6.41 Wing Bending, Mid-span, Right Wing Station 8.8, Channel 14, QB-17 N, Easy Shot	204
6.42 Elevator Position, Channel 15, QB-17 N, Easy Shot	204
6.43 Differential Pressure, 5% Chord, Right Wing Station 25.5, Channel 16, QB-17 N, Easy Shot	205
6.44 Differential Pressure, 20% Chord, Right Wing Station 25.5, Channel 18, QB-17 N, Easy Shot	205
6.45 Differential Pressure, 40% Chord, Right Wing Station 25.5, Channel 19, QB-17 N, Easy Shot	206
6.46 Differential Pressure, 85% Chord, Right Wing Station 25.5, Channel 21, QB-17 N, Easy Shot	206
6.47 Differential Pressure, 40% Chord, Right Wing Station 25.5, Channel 22, QB-17 N, Easy Shot	207
6.48 Differential Pressure, 40% Chord, Right Horizontal Stabilizer, Channel 24, QB-17 N, Easy Shot	207
6.49 Wing Bending, Left Wing Root, Channel 8, QB-17 N, Cloud Pass, Easy Shot	208
6.50 Stabilizer Bending, Right Horizontal Stabilizer, Channel 9, QB-17 N, Cloud Pass, Easy Shot	208
6.51 Wing Bending, Outer Panel, Right Wing Station 19, Channel 10, QB-17 N, Cloud Pass, Easy Shot	209
6.52 Wing Shear, Right Wing Root, Channel 12, QB-17 N, Cloud Pass, Easy Shot	209
6.53 Wing Bending, Mid-span, Right Wing Station 8.8, Channel 14, QB-17 N, Cloud Pass, Easy Shot	210
6.54 Elevator Position, Channel 15, QB-17 N, Cloud Pass, Easy Shot	210
6.55 Normal Acceleration, Bomb Bay, Forward, Channel A6, XB-47, Easy Shot	212
6.56 Fuselage Bending, Forward of Vertical Fin, Fuselage Station 985, Channel A9, XB-47, Easy Shot	212

ILLUSTRATIONS (Continued)

	Page
6.57 Wing Shear, Right Wing Root, Wing Station 307, Channel A12, XB-47, Easy Shot	213
6.58 Wing Bending, Right Wing Root, Wing Station 307, Channel A13, XB-47, Easy Shot	213
6.59 Wing Shear, Left Wing Root, Wing Station 307, Channel A16, XB-47, Easy Shot	214
6.60 Wing Bending, Left Wing Root, Wing Station 307, Channel A17, XB-47, Easy Shot	214
6.61 Wing Shear, Left Wing Outboard, Wing Station 660, Channel A21, XB-47, Easy Shot	215
6.62 Horizontal-stabilizer Bending, Left-horizontal-stabilizer Station 64, Channel A23, XB-47, Easy Shot	215
6.63 Fuselage Bending, Aft End of Bomb Bay, Fuselage Station 718, Channel A24, XB-47, Easy Shot	216
6.64 Altitude, Channel B1, XB-47, Easy Shot	216
6.65 Differential Aerodynamic Pressure, 61.3% Chord, Right Wing Station 515, Channel B4, XB-47, Easy Shot	217
6.66 Gauge Aerodynamic Pressure, 11.7% Chord, Top Left Wing Station 515, Channel B8, XB-47, Easy Shot	217
6.67 Gauge Aerodynamic Pressure, 11.7% Chord, Bottom Left Wing Station 515, Channel B9, XB-47, Easy Shot	218
6.68 Gauge Aerodynamic Pressure, 61.3% Chord, Bottom Left Wing Station 515, Channel B17, XB-47, Easy Shot	218
6.69 Gauge Aerodynamic Pressure, Forward of 50% Chord, Bottom Left-horizontal-stabilizer Station 110, Channel B22, XB-47, Easy Shot	219
6.70 Gauge Aerodynamic Pressure, 5% Chord, Top Left Wing Station 523, Channel B24, XB-47, Easy Shot	219
6.71 Airspeed, Channel B2, B-50D (290), Easy Shot	221
6.72 Normal Acceleration, Aft Rear Bomb Bay, Fuselage Station 628, Channel B3, B-50D (290), Easy Shot	221
6.73 Differential Aerodynamic Pressure, 23% Chord, Right Wing Station 525, Channel B4, B-50D (290), Easy Shot	222
6.74 Gauge Aerodynamic Pressure, Bottom Forward Fuselage, Fuselage Station 26, Channel B6, B-50D (290), Easy Shot	222
6.75 Gauge Aerodynamic Pressure, Right Side of Fuselage, Fuselage Station 783, Channel B7, B-50D (290), Easy Shot	223
6.76 Gauge Aerodynamic Pressure, Right Side of Vertical Fin, Fuselage Station 974, Channel B9, B-50D (290), Easy Shot	223
6.77 Gauge Aerodynamic Pressure, Left Side of Vertical Fin, Fuselage Station 974, Channel B10, B-50D (290), Easy Shot	224
6.78 Gauge Aerodynamic Pressure, 23% Chord, Top Left Wing Station 524, Channel B13, B-50D (290), Easy Shot	224
6.79 Gauge Aerodynamic Pressure, 60% Chord, Top Left Wing Station 524, Channel B15, B-50D (290), Easy Shot	225
6.80 Gauge Aerodynamic Pressure, 85% Chord, Top Left Wing Station 524, Channel B16, B-50D (290), Easy Shot	225
6.81 Gauge Aerodynamic Pressure, 5% Chord, Bottom Left Wing Station 524, Channel B17, B-50D (290), Easy Shot	226

ILLUSTRATIONS (Continued)

	Page
6.82 Gauge Aerodynamic Pressure, 23% Chord, Bottom Left Wing Station 524, Channel B19, B-50D (290), Easy Shot	226
6.83 Gauge Aerodynamic Pressure, 43% Chord, Bottom Left Wing Station 524, Channel B20, B-50D (290), Easy Shot	227
6.84 Gauge Aerodynamic Pressure, 60% Chord, Bottom Left Wing Station 524, Channel B21, B-50D (290), Easy Shot	227
6.85 Gauge Aerodynamic Pressure, Bottom Right-horizontal-stabilizer Station 170, Channel B23, B-50D (290), Easy Shot	228
6.86 Gauge Aerodynamic Pressure, Bottom Left-horizontal-stabilizer Station 170, Channel B24, B-50D (290), Easy Shot	228
6.87 Elevator Position, Elevator Torque Tube, Channel A1, B-50D (340), Easy Shot	230
6.88 Normal Acceleration, Forward Bomb Bay, Channel A5, B-50D (340), Easy Shot	230
6.89 Normal Acceleration, Nose-wheel Well, Channel A6, B-50D (340), Easy Shot	231
6.90 Normal Acceleration, Aft Fuselage, in Tail-gunner's Compartment, Channel A7, B-50D (340), Easy Shot	231
6.91 Horizontal-stabilizer Bending, Right-horizontal-stabilizer Station 34, Channel A8, B-50D (340), Easy Shot	232
6.92 Horizontal-stabilizer Bending, Left-horizontal-stabilizer Station 34, Channel A9, B-50D (340), Easy Shot	232
6.93 Wing Bending, Right Wing Mid-span, Wing Station 266, Channel A10, B-50D (340), Easy Shot	233
6.94 Wing Bending, Right Wing Root, Wing Station 79, Channel A11, B-50D (340), Easy Shot	233
6.95 Wing Bending, Left Wing Root, Wing Station 79, Channel A12, B-50D (340), Easy Shot	234
6.96 Wing Shear, Right Wing Mid-span, Wing Station 269, Channel A16, B-50D (340), Easy Shot	234
6.97 Wing Shear, Right Wing Root, Wing Station 78, Channel A17, B-50D (340), Easy Shot	235
6.98 Wing Shear, Left Wing Root, Wing Station 78, Channel A18, B-50D (340), Easy Shot	235
6.99 Wing Shear, Left Wing Inboard, Wing Station 122, Channel A19, B-50D (340), Easy Shot	236
6.100 Wing Shear, Left Wing Mid-span, Wing Station 269, Channel A20, B-50D (340), Easy Shot	236
6.101 Wing Torsion, Right Wing Root, Wing Station 78, Channel A22, B-50D (340), Easy Shot	237
6.102 Wing Torsion, Left Wing Root, Wing Station 78, Channel A23, B-50D (340), Easy Shot	237
6.103 Wing Torsion, Left Wing Inboard, Wing Station 122, Channel A24, B-50D (340), Easy Shot	238
6.104 Altitude, Channel B1, B-50D (340), Easy Shot	238
6.105 Airspeed, Channel B2, B-50D (340), Easy Shot	239
6.106 Normal Acceleration, Aft Rear Bomb Bay, Fuselage Station 628, Channel B3, B-50D (340), Easy Shot	239

ILLUSTRATIONS (Continued)

	Page
6.107 Differential Aerodynamic Pressure, 23% Chord, Right Wing Station 525, Channel B4, B-50D (340), Easy Shot	240
6.108 Differential Aerodynamic Pressure, 60% Chord, Right Wing Station 525, Channel B5, B-50D (340), Easy Shot	240
6.109 Gauge Aerodynamic Pressure, Bottom Forward Fuselage, Fuselage Station 26, Channel B6, B-50D (340), Easy Shot	241
6.110 Gauge Aerodynamic Pressure, Right Side of Fuselage, Fuselage Station 783, Channel B7, B-50D (340), Easy Shot	241
6.111 Gauge Aerodynamic Pressure, Right Side of Vertical Fin, Fuselage Station 974, Channel B9, B-50D (340), Easy Shot	242
6.112 Gauge Aerodynamic Pressure, Left Side of Vertical Fin, Fuselage Station 974, Channel B10, B-50D (340), Easy Shot	242
6.113 Gauge Aerodynamic Pressure, 5% Chord, Top Left Wing Station 524, Channel B11, B-50D (340), Easy Shot	243
6.114 Gauge Aerodynamic Pressure, 15% Chord, Top Left Wing Station 524, Channel B12, B-50D (340), Easy Shot	243
6.115 Gauge Aerodynamic Pressure, 43% Chord, Top Left Wing Station 524, Channel B14, B-50D (340), Easy Shot	244
6.116 Gauge Aerodynamic Pressure, 60% Chord, Top Left Wing Station 524, Channel B15, B-50D (340), Easy Shot	244
6.117 Gauge Aerodynamic Pressure, 5% Chord, Bottom Left Wing Station 524, Channel B17, B-50D (340), Easy Shot	245
6.118 Gauge Aerodynamic Pressure, 23% Chord, Bottom Left Wing Station 524, Channel B19, B-50D (340), Easy Shot	245
6.119 Gauge Aerodynamic Pressure, 43% Chord, Bottom Left Wing Station 524, Channel B20, B-50D (340), Easy Shot	246
6.120 Gauge Aerodynamic Pressure, 85% Chord, Bottom Left Wing Station 524, Channel B22, B-50D (340), Easy Shot	246
6.121 Gauge Aerodynamic Pressure, Bottom Right-horizontal-stabilizer Station 170, Channel B23, B-50D (340), Easy Shot	247
6.122 Gauge Aerodynamic Pressure, Bottom Left-horizontal-stabilizer Station 170, Channel B24, B-50D (340), Easy Shot	247
CHAPTER 7 GEORGE SHOT	
7.1 Track, Radar-data Recorder, QB-17 Airplane O, Carol Position, George Shot	251
7.2 Airspeed, Channel 2, QB-17 O, George Shot	251
7.3 Normal Acceleration, c.g., Channel 3, QB-17 O, George Shot	252
7.4 Normal Acceleration, Aft Fuselage, Channel 4, QB-17 O, George Shot	252
7.5 Wing Bending, Right Wing Root, Channel 7, QB-17 O, George Shot	253
7.6 Wing Bending, Outer Panel, Right Wing Station 19, Channel 10, QB-17 O, George Shot	253
7.7 Wing Bending, Mid-span, Right Wing Station 8.8, Channel 14, QB-17 O, George Shot	254
7.8 Elevator Position, Channel 15, QB-17 O, George Shot	254
7.9 Wing Bending, Left Wing Root, Channel 8, QB-17 N, George Shot	257
7.10 Stabilizer Bending, Right Horizontal Stabilizer, Channel 9, QB-17 N, George Shot	257

ILLUSTRATIONS (Continued)

	Page
7.36 Wing Torsion, Left Wing Root, Wing Station 78, Channel A23, B-50D (340), George Shot	272
7.37 Airspeed, Channel B2, B-50D (340), George Shot	272
7.38 Normal Acceleration, Aft Rear Bomb Bay, Fuselage Station 628, Channel B3, B-50D (340), George Shot	273
7.39 Differential Aerodynamic Pressure, 60% Chord, Right Wing Station 525, Channel B5, B-50D (340), George Shot	273
7.40 Gauge Aerodynamic Pressure, Left Side of Vertical Fin, Fuselage Station 974, Channel B10, B-50D (340), George Shot	274
7.41 Gauge Aerodynamic Pressure, 5% Chord, Top Left Wing Station 524, Channel B11, B-50D (340), George Shot	274
7.42 Gauge Aerodynamic Pressure, 15% Chord, Top Left Wing Station 524, Channel B12, B-50D (340), George Shot	275
7.43 Gauge Aerodynamic Pressure, 60% Chord, Top Left Wing Station 524, Channel B15, B-50D (340), George Shot	275
7.44 Gauge Aerodynamic Pressure, 5% Chord, Bottom Left Wing Station 524, Channel B17, B-50D (340), George Shot	276
7.45 Gauge Aerodynamic Pressure, 23% Chord, Bottom Left Wing Station 524, Channel B19, B-50D (340), George Shot	276
7.46 Gauge Aerodynamic Pressure, 85% Chord, Bottom Left Wing Station 524, Channel B22, B-50D (340), George Shot	277
7.47 Gauge Aerodynamic Pressure, Bottom Right-horizontal-stabilizer Station 170, Channel B23, B-50D (340), George Shot	277
7.48 Gauge Aerodynamic Pressure, Bottom Left-horizontal-stabilizer Station 170, Channel B24, B-50D (340), George Shot	278
7.49 High-frequency Pressure Record, Grace Position, George Shot	278
7.50 Normal Acceleration, c.g., Channel 3, QB-17 P, George Shot	280
7.51 Normal Acceleration, Aft Fuselage, Channel 4, QB-17 P, George Shot	280
7.52 Wing Bending, Left Wing Root, Channel 8, QB-17 P, George Shot	281
7.53 Stabilizer Bending, Right Horizontal Stabilizer, Channel 9, QB-17 P, George Shot	281
7.54 Wing Bending, Outer Panel, Right Wing Station 19, Channel 10, QB-17 P, George Shot	282
7.55 Elevator Position, Channel 15, QB-17 P, George Shot	282
7.56 High-frequency Pressure Record, Sally Position, George Shot	283

ILLUSTRATIONS (Continued)

	Page
7.11 Wing Bending, Outer Panel, Right Wing Station 19, Channel 10, QB-17 N, George Shot	258
7.12 Wing Bending, Mid-span, Right Wing Station 8.8, Channel 14, QB-17 N, George Shot	258
7.13 Elevator Position, Channel 15, QB-17 N, George Shot	259
7.14 Airspeed, Channel B2, B-50D (290), George Shot	259
7.15 Normal Acceleration, Rear Bomb Bay, Fuselage Station 628, Channel B3, B-50D (290), George Shot	260
7.16 Differential Aerodynamic Pressure, 23% Chord, Right Wing Station 525, Channel B4, B-50D (290), George Shot	260
7.17 Gauge Aerodynamic Pressure, Right Side of Vertical Fin, Fuselage Station 974, Channel B9, B-50D (290), George Shot	261
7.18 Gauge Aerodynamic Pressure, Left Side of Vertical Fin, Fuselage Station 974, Channel B10, B-50D (290), George Shot	261
7.19 Gauge Aerodynamic Pressure, 60% Chord, Top Left Wing Station 524, Channel B15, B-50D (290), George Shot	262
7.20 Gauge Aerodynamic Pressure, 5% Chord, Bottom Left Wing Station 524, Channel B17, B-50D (290), George Shot	262
7.21 Gauge Aerodynamic Pressure, 43% Chord, Bottom Left Wing Station 524, Channel B20, B-50D (290), George Shot	263
7.22 Gauge Aerodynamic Pressure, 60% Chord, Bottom Left Wing Station 524, Channel B21, B-50D (290), George Shot	263
7.23 Gauge Aerodynamic Pressure, Bottom Left-horizontal-stabilizer Station 170, Channel B24, B-50D (290), George Shot	264
7.24 Wing Bending, Left Wing Outboard, Wing Station 505, Channel A2, B-50D (340), George Shot	266
7.25 Normal Acceleration, Nose-wheel Well, Channel A6, B-50D (340), George Shot	266
7.26 Normal Acceleration, Aft Fuselage in Tail-gunner's Compartment, Channel A7, B-50D (340), George Shot	267
7.27 Horizontal-stabilizer Bending, Right-horizontal-stabilizer Station 34, Channel A8, B-50D (340), George Shot	267
7.28 Horizontal-stabilizer Bending, Left-horizontal-stabilizer Station 34, Channel A9, B-50D (340), George Shot	268
7.29 Wing Bending, Right Wing Mid-span, Wing Station 266, Channel A10, B-50D (340), George Shot	268
7.30 Wing Bending, Right Wing Root, Wing Station 79, Channel A11, B-50D (340), George Shot	269
7.31 Wing Shear, Right Wing Mid-span, Wing Station 269, Channel A16, B-50D (340), George Shot	269
7.32 Wing Shear, Left Wing Root, Wing Station 78, Channel A18, B-50D (340), George Shot	270
7.33 Wing Shear, Left Wing Inboard, Wing Station 122, Channel A19, B-50D (340), George Shot	270
7.34 Wing Shear, Left Wing Mid-span, Wing Station 269, Channel A20, B-50D (340), George Shot	271
7.35 Wing Torsion, Right Wing Root, Wing Station 78, Channel A22, B-50D (340), George Shot	271

TABLES

	Page
CHAPTER 3 AIRPLANE PREPARATIONS	
3.1 Example Data for Calibration of Sensing Element	60
3.2 Example Data for Calibration of Recorder-Amplifier	60
3.3 Example Data for Calibration of Recorder-Playback Combination	62
3.4 Example of Correlated Data for Channel Calibration	62
3.5 Recorder-channel Assignments for QB-17 Drones	66
3.6 Recorder-channel Assignments for QT-33 Drones	72
3.7 Recorder-channel Assignments for B-50D Airplanes	81
3.8 Recorder-channel Assignments for XB-47 Airplane	90
3.9 Temp-tape Locations, QB-17 Drones	95
3.10 Temp-tape Locations, QT-33 Drones	96
3.11 Temp-tape Color Code	96
3.12 Temp-tape Locations, Incidence Angles	97
CHAPTER 4 OPERATION PLANS	
4.1 Assigned Airplane Positions, Dog Shot	102
4.2 Assigned Airplane Positions, Easy Shot	107
4.3 Assigned Airplane Positions, George Shot	108
CHAPTER 5 DOG SHOT	
5.1 Heat Measurements at Alice Position, Dog Shot	122
5.2 Heat Measurements at Carol Position, Dog Shot	138
5.3 Comparison of Loads on QB-17 Drone M, Dog Shot	138
CHAPTER 6 EASY SHOT	
6.1 Heat Measurements at Betty Position, Easy Shot	173
6.2 Heat Measurements at Carol Position, Easy Shot	187
6.3 Radiological Data at Carol Position, Easy Shot	188
6.4 Heat Measurements from QB-17 Drone N, Easy Shot	200
6.5 Radiological Data from QB-17 Drone N, Easy Shot	201



Abstract

The primary objective of this report is to present data concerning the structural and aerodynamic loads as measured on various types of aircraft, in flight, in the vicinity of an atomic explosion. A secondary objective is to describe the instrumentation (installation, calibration, and operation) in order to provide for the future planning and conduct of similar tests.

The data presented herein were obtained on Dog, Easy, and George shots of Operation Greenhouse. The airplanes used to collect these data were B-17's, T-33's, B-50D's and one XB-47. These instrumented airplanes were arrayed at preassigned locations in the air-space above the explosions. A total of approximately 250 channels of information were obtained which essentially consisted in wing bending, torsion, and shear at the root, mid-span, and outer panel; horizontal-stabilizer bending at the root; normal accelerations at the nose, c.g., and tail; aerodynamic pressures at various locations on the airplanes; and temperatures experienced by various critical components of the airplane.

The positions of the airplanes at the time of shock arrival were accurately determined by means of radar tracking. The measured data were correlated by means of time signals, every second, from a land-based radio-transmitter station, and with reference to time zero, by means of a photoelectric cell. The majority

of the data are presented relative to level-flight conditions and time zero (T_0).

The recorded data show that the loads produced by the shock wave were in general accord with theory. The loading experienced by an airplane while passing through the "puff" of the atomic cloud is shown to be considerably higher than that caused by the shock wave. For this reason the penetration of the puff should be avoided even by "sampling" drones. The effects and magnitude of radiant heating were originally underestimated. This was proved by the charring of fabric control surfaces, the scorching of metal surfaces, the apparent thermal loading of structures, and the high temperatures indicated by the temperature survey.

In view of the primary purpose of this report, no complete analysis was attempted. However, the data are believed to be accurate to within 10 per cent, suitable for further analysis, and satisfactory for the development or correction of a technique for calculating the effects of atomic explosions on aircraft structures.

The organization responsible for collecting these data proved to be workable but deficient in operation and authority. As a result of these deficiencies and of the unproved instruments, many of the potentially available data were not obtained. Chapter 8, therefore, contains recommendations concerning personnel requirements, facilities, and organizational level for guidance in planning future tests of this nature.

Chapter 1

Introduction

Project 8.1 is the "in-flight" phase of a larger program designed to identify the nature and magnitude of the various loads imposed on aircraft structures by an atomic explosion.

1.1 DESCRIPTION OF REPORT

1.1.1 Organization

The fundamental purpose of this report is the presentation of the data collected; therefore the majority of the sections are allotted to that function. The remaining sections are devoted to the description, preparation, discussion, or justification of these data. The supporting chapters and appendixes (reproduced elsewhere; see page iv) concern the instruments, installations, techniques, and missions employed in the collection of the data with which the principal chapters are concerned. There are three such principal chapters, each containing the data from one specific shot or test. These chapters are subdivided into sections, each presenting the data collected from a specific mission. An attempt has been made to make each of these sections a separate entity, complete in itself. Each section includes the predicted conditions, the actual conditions as reported by the Air Task Unit, and the measured conditions as determined from the various equipments employed.

It may be noted that the reported conditions vary somewhat from the data as reported in the Final Report, Task Group 3.4. However, the data presented here are taken from the data sheets prepared by the flight crews or by the Unit Navigator for Task Unit 3.4.2, Maj. H. S. Leffel, and as included in the Navigator's Report as forwarded from that Task Unit to Project 8.1.

1.1.2 Definitions and Sign Conventions

The following terms are defined in the sense as used in this report:

m.a.c. — The mean aerodynamic chord of a wing is the chord of an imaginary airfoil which will have force vectors approximating those of the wing. The m.a.c. is considered to lie in the plane of symmetry, parallel to the longitudinal reference axis of the aircraft. The m.a.c. is a convenient reference for use in pitching-moment calculations and for locating the center of gravity.

Engine numbers — In a multiengine aircraft it is customary to refer to the individual engines by number, counting from the pilot's left to right from his position in the cockpit.

Normal direction — The direction parallel to a line lying in the plane of symmetry and perpendicular to the longitudinal reference axis of the airplane.

Class A and Class B parts — In an installation the Class A parts include brackets, fittings, wiring, plugs, and other accessories; the Class B parts are the actual operating components such as the recorders, amplifiers, and sensing instruments.

Gauge pressure — The pressure difference between that measured and the ambient pressure (rather than 1 atm as normally used).

T_0 — Used to denote blast time; sometimes called "H-hour."

Point zero — Referred to in locations, the point or location of the explosion.

For purposes of this report an arbitrary sign convention has been adopted. Positive sense has been assigned as follows:

- Bending (wings and stabilizers) — Tip deflection upward; compression on the upper surface.
- Bending (fuselage) — Nose and tail deflection upward with respect to the center section; compression on the upper surface.
- Torsion (wing) — Leading-edge deflection upward.
- Shear (wing) — Associated with positive bending; outboard-surface deflection upward with respect to the inboard surface.
- Normal acceleration (c.g.) — Increase in upward velocity or decrease in downward velocity of the airplane; same direction as that produced by increased lift on the wings.
- Normal acceleration (other than c.g.) — Parallel to and in the same direction as positive c.g. normal acceleration.
- Lateral acceleration (XB-47 engine) — That produced by increasing the velocity of the engine from left to right.
- Pressure, differential aerodynamic (wing or stabilizer) — Increased pressure on the bottom surface or decreased pressure on the top surface.
- Pressure, gauge aerodynamic (wing, stabilizer, or fuselage) — Increased pressure.

1.1.3 Data Presentation

The data collected for Project 8.1 are intended for further analysis and incorporation into tactical or design criteria. It is important, therefore, that the data be presented in the simplest and most convenient form. Such form is considered to be a graph of the variation in value with respect to time, and all the measured data are so presented. For clarity and in order to expand the graphs as much as possible within the limits of the permissible page dimensions, the data from each channel are presented as a separate figure. A single page containing all the data from one test mission (one airplane on a single test) referred to a common time axis would have been more convenient for correlation, but either the page would have been

larger than permissible or the data would have been so small as to have been obscured.

The time interval selected for abscissas of the graphs is, in each instance, sufficient to include the initial peaks as well as the majority of the ensuing disturbances. The interval is, at the same time, as small as practicable in order to permit maximum scale expansion. This expansion of the time scale is necessary to identify the various frequencies excited in the structure and is well within the limits imposed by the capabilities of the tape recorder. Where necessary, the extraneous frequencies (sensing-element ringing, engine-induced vibrations, etc.) have been removed from the traces.

Incremental values of data, rather than absolute values, are selected for the ordinates of the graphs. Incremental values (Δ load) are obtained by the algebraic subtraction of the steady-state level-flight value of the load from the instantaneous value of the load at a particular time. Thus the increment is the variation in load from the level-flight condition. The absolute or total value of the load is, in reality, referred to a rather nebulous datum, particularly in the strain-gauge channels. The ground-balance condition for these channels is not the no-load condition used as a reference in the stress analyses. This no-load condition is practically unobtainable. However, the incremental loads may be added to the level-flight loads from the stress analyses for reference to theory. The practice of plotting incremental values has been followed for all data except airspeed and altitude, wherein the absolute value is the important datum.

1.2 PROBLEM

In general, the problem presented to Project 8.1 concerned the collection and reduction of sufficient data from aircraft in flight on Operation Greenhouse to substantiate or correct a technique for calculating the effects of the explosion on aircraft structures. The complete problem of blast loads and thermal effects on aircraft is divided into two parts. The first is the development of a theoretical analysis and the evaluation of generalized equations and computation techniques. This part is discussed in Greenhouse Report, Annex 8.0. The second part is the actual measurement of the loads

[REDACTED]

under defined conditions to prove the validity of, or indicate corrections to, the theoretical analysis. These measurements were made in the air by Project 8.1 and on the ground by Project 8.2.

The problem of the measurements in the air was essentially threefold. First, the collection of data from a variety of aircraft was important in order to ensure the application of the theory to all types of aircraft structures. Second, measurements on each structure had to be judiciously chosen to permit correlation between types and to provide sufficient data to prove the theoretical loading. Third, the data had to be collected at a suitable variety of locations to justify the application of the theory to the entire airspace above the explosion.

1.3 BACKGROUND

Although the problem of the effect of the explosion on the carrier aircraft was undoubtedly considered on the early atomic explosions, at least by the crew of the B-29 Enola Gay, there is no record of any attempt to measure, or even to compute, the effects on the airplane. Strictly speaking, there was no definite theory or technique for even approximating the loads to any reasonable degree of accuracy. The first attempt to obtain even an approximate value of the airplane loads was the recording of vertical (center of gravity) accelerations on the various airplanes engaged in Operation Crossroads. These measurements were made by means of the Air Force type C-1 flight analyzer. This instrument is a recording accelerometer of very low-frequency response (approximately 8 cps) which includes simultaneous records of airspeed and altitude. No missions were specifically assigned for the measurement of airplane response; rather, the records were made at whatever locations the airplanes happened to occupy at the time of the explosion. Since the various airplanes carried similar instruments having the same accuracies and limitations, it was possible to draw a few conclusions regarding the distribution of the effects in the general vicinity of the explosion and the general nature of the "bump" experienced by the airplane.

On Operation Sandstone four of the twelve "drones" were instrumented with more-sensitive equipment having a faster response. How-

ever, the primary mission of these drones was still not the collection of structural data. On Yoke and Zebra shots of Operation Sandstone, permission was obtained to assign one of the drones to a primary mission of collecting load data, and the first records of structural loads were obtained. Detailed analysis of these data indicated several faults due to the lack of information on which to base the selection of gauge locations, ranges of sensing instruments, and the particular functions to be measured. These results also indicated the need for a quantity of data in order to satisfy all the variables inherent in such an investigation. However, these data formed the initial effort and indicated the general nature of the loads involved. This information was essential to the planning for Operation Greenhouse.

1.4 GENERAL PLAN

The possibility of active participation by the Air Force in the 1951 atomic weapons test was presented in a conference at Headquarters, Air Materiel Command, in February 1949. Very soon thereafter, detailed proposals and plans were required for submittal to Headquarters, Air Force, for approval.

Obviously, it would be impossible to satisfy completely all the requirements of all the problems. The first task, therefore, was to define the feasible limits or extent of the participation and next to determine what distribution of effort would best satisfy the problems.

1.4.1 Selection of Airplanes

The selection of the test airplanes for this project was influenced by the variations in types of structures, by a necessity for obtaining sufficiently severe loads at least to indicate failure, and by the limitations imposed by the scope of the operation. Thus it was decided that only four drones would be permitted for the primary mission of measuring blast loads. The radio-control equipment and techniques for B-17, B-29, and F-80 type aircraft had been or were being developed. In view of experience, operational characteristics (take-off and landing distances), and spread of structural design, the B-17 and F-80 (two-place version is the T-33) were selected as the drones. In addition, plans were made for including three manned

[REDACTED]

test airplanes in the array. Two B-50 airplanes were selected as representing the types presently in use and available. A B-47 was included as representing an elastic structure, indicative of probable trends for future aircraft design, as well as permitting a study of other features such as swept wings and jet engines. Inasmuch as a quantity of data at a variety of points in space was important, it was decided to instrument at least some of those drones whose primary mission was the collection of "samples" for Project 1.7. Although these airplanes would undoubtedly be at greater distances when struck by the blast wave, the data would be of value in the extrapolation of the data from the other test airplanes. It was decided that six of the twelve drones in this category would be instrumented for the collection of blast load data.

In summary, it was decided that the test array for Project 8.1 on each shot would consist of the two B-17G drones, two T-33 drones, two B-50D manned airplanes, and one XB-47 airplane, together with whatever additional B-17G drones of Project 1.7 that happened to be instrumented.

1.4.2 Selection of Instrumentation

A detailed description of the instrumentation of each airplane is presented in Chap. 3. The general instrumentation layout for the test airplanes was the same regardless of airplane type. A few minor modifications were required to allow for variations by the airplane types, and the manned aircraft were more completely instrumented. However, the installations were essentially as follows:

1. Flight parameters. Altitude and airspeed were measured on each airplane. The location of the drone airplanes was established by means of ground-based radar, and the location of the manned airplanes was determined by the navigators and radar operators in the airplanes.

2. Airplane response. The response of the airplane and the elements was determined by measuring accelerations at the center of gravity, at the tail, and in the engines on the right wing. The pitching of the airplane was measured by an elevator-position indicator. Inasmuch as the elevators of the drones are controlled through a gyroscope which tends to hold each airplane in a level-flight attitude, a "pitching-up" tendency

was indicated by a down deflection of the elevator. The amount of elevator deflection, in holding the airplane level, was measured by the elevator-position indicator.

3. Structural loads. Bending moments were measured at the root section of each wing, at mid-span of the right wing, and at the root section of the right horizontal stabilizer. Shear and torsion measurements were also made at the root section of the wing and at other stations as the number of channels permitted.

4. Aerodynamic loads. The aerodynamic loads and their distribution were determined by pressure measurements. One chord, in an area free from disturbance, was instrumented to get the distributions of differential pressures over the upper and lower surfaces of the wing. Additional pressure transmitters were placed at other selected points to obtain comparison pressures from which the change in aerodynamic loads on the complete airplane could be determined.

5. Transcription of data. In order to assure the collection of the data despite the possible loss of the critical drones, telemetering was necessary in addition to local recording. The six AEC B-17 drones were to have been instrumented in the afore-mentioned manner without telemetering, and the manned aircraft were equipped with two recorders each to permit the recording of additional data.

1.4.3 Airplane Collocation

The pattern of arrangement of the test airplanes was primarily concerned with two factors: obtaining the highest practicable loads on each airplane and attaining the greatest variety of loading conditions possible. In general, the allowable peak overpressure for each airplane was computed on the basis of the theoretical loading and approximate permissible slant ranges for each airplane determined for each shot strength. The slant range for one of each pair of drones was increased somewhat to ensure the safety of at least one of the drones of each type. The slant ranges for the manned airplanes were so selected as to ensure the safety of each airplane and its crew. The actual locations for the airplanes were originally selected arbitrarily on two 45° slant rays. The airplanes were located along two lines to limit,

[REDACTED]

as much as possible, the differences in applied loading to the variable of distance only. A 45° angle to the shock was selected as the best division of the vector of blast load into its two components: the velocity vector in the direction of flights and the gust vector perpendicular to the line of flight. Subsequent considera-

tions of a necessity for increasing the altitude of one of the B-17 drones without changing the slant range and of an investigation of the effect of the gust component alone prescribed the changes to the plans as finally used. The detailed plans for each test shot are presented in Chap. 4.

Chapter 2

Instruments

2.1 GENERAL INSTRUMENT REQUIREMENTS

In the basic planning for the instrumentation for this project, several fundamental requisites were evident from previous experience. Certain of these conditions were common to each of the various equipments employed.

The first condition to be considered for all the air-borne equipment was that of vibration and shock acceleration. Besides the usual vibration and acceleration effects to which air-borne equipment is normally subjected, the response of the airplane to the very blast that was being studied imposed more severe shock on the equipment. This effect was considered very carefully because of the nature of the shock (very sharp) and the fact that shock effects on the equipments were likely to obscure the data at precisely the critical time.

Environmental conditions were also given careful consideration. The corrosive effects of the high humidity and the salt spray and the detrimental effects of the fungi were proved to be important by previous experience. Along with the conditions natural to the geographical location of the tests, the climatic conditions inherent in aircraft flight were present. The latter conditions include the reduced pressures and low temperatures encountered at altitudes. It was necessary, therefore, that the equipment be designed to operate both at high and low temperatures, under conditions of high humidity, in the presence of severe corrosive stimuli, and under low ambient pressure.

The operational details of the project also imposed requirements on the instrumentation. The equipment was, for the most part, installed in drone aircraft. Thus the equipment was required to operate automatically at some time

(usually more than 1 hr) after it was checked by an operator prior to take-off. The operations required to initiate the recording cycle had to be reduced to a minimum so that they could be performed remotely, and a means of terminating the cycle at the conclusion of the record was necessary. The requirement for unattended operation also emphasized reliability and thus simplicity of design and construction. The fact that it would be necessary to maintain and operate the equipment under very severe field conditions further emphasized simplicity not only of each piece of equipment but also of the overall instrumentation plan as far as possible. One more specification arising from the operational situation was the logistical benefit to be derived from the use of standard parts and as few different components as possible.

2.2 RECORDERS

2.2.1 Selection

In view of the severe conditions described in Sec. 2.1, the selection of the appropriate technique of recording for this project required considerable research. In the first place, standard methods of recording by means of bifilar-type galvanometers were impossible because of the severe shock conditions. It was necessary, therefore, to select a recorder which was primarily impervious to shock. The natural selection in this regard was a magnetic-tape type of recorder. A prototype of this type of recorder had been recently completed by the Webster-Chicago Corporation, and preliminary tests indicated several desirable features of benefit to this test. Some of these features included a suitable fast response, satisfactory

operation with resistance-type sensing instruments, satisfactory operation at altitude, and good performance under adverse climatic conditions. A contract was awarded to Webster-Chicago during the fiscal year 1949 for the development of four prototype 24-channel magnetic-tape recorders and one 12-channel playback. A production order for an additional 21 recorders and a 2-channel playback was awarded to Webster-Chicago early in the fiscal year 1950.

2.2.2 Principles of Operation

The recording system operated on a phase-shift principle. A 3,750-cps signal was impressed upon the sensing element, and the return signal was added to a voltage at quadrature in order to produce a signal which was shifted in phase as a function of strain with respect to a 7,500-cps reference signal. Both of these signals were recorded simultaneously on a single trace of the tape in order to record one channel of data. There were 24 such channels across the tape.

The fundamental principle of operation of the system was the comparison of the phase of two recorded signals. The technique of deriving phase shift from the output of a strain gauge is illustrated in Fig. 2.1. Vector A is the quadrature vector which is constant in amplitude and phase position. Vector B is the sense vector representing the strain-gauge output, the amplitude of which is a function of strain and the phase of which is always $\pm 90^\circ$ from vector A, depending on the algebraic sign of the strain-gauge output. Vector C is the resultant of the vector addition of vectors A and B and varies in phase with respect to vector A as a function of strain-gauge output. It is obvious that the phase angle Φ of vector C is not directly proportional to the value of the strain; rather, the strain is proportional to the tangent of the phase angle. For large amplitudes of vector B (with respect to vector A) this fact becomes important. It was necessary, therefore, to develop and include a circuit within the system to correct or compensate for this nonlinearity. This correcting circuit was originally incorporated into the data transcription or playback forward area.

The gauge drive voltage derived from the gauge source generator was applied to various

bridge-type sensing elements (strain gauges, etc.). (See Fig. 2.2 for functional block diagram.) The voltage (vector B, Fig. 2.1) due to response of the sensing element was returned to the gauge amplifier, where it was combined with the quadrature voltage (vector A, Fig. 2.1), thus producing a combined voltage shifted in phase (vector C, Fig. 2.1). This voltage was, in turn, combined with the 7,500-cps reference voltage to produce a composite wave form, which was amplified and recorded on a magnetic tape. It will be noted that the 3,750-cps gauge drive voltage, the 3,750-cps quadrature voltage, and the 7,500-cps reference voltage were all derived from the same source so that they were proportional in magnitude and fixed in phase angle relative to each other. This factor eliminated the source of error arising from the possibility of fluctuation of one or more of these voltages. All voltages, unless otherwise specified, were sine-wave voltages containing negligible harmonics.

The magnetic tape was played back at one-half the recording speed through a magnetic-pickup head similar to the recording head, so that the recorded composite voltage wave form was reproduced at half the recorded frequency. (See Fig. 2.3 for functional block diagram.) This wave form was amplified and was impressed upon two sets of filters, one tuned to pass 1,875 cps and the other tuned to pass 3,750 cps. The composite wave form is thus broken down into its two components. A voltage which is proportional to vector C, Fig. 2.1, is obtained from one set of filters, and a voltage proportional to the reference frequency (now 3,750 cps) is obtained from the other set of filters. Pulses are derived from each of these voltages and are applied to a stable multivibrator (Eccles-Jordan circuit).

The reference frequency is fixed in time relation to vector A, Fig. 2.1, since both are derived from the same source. Therefore any time variation of vector C, Fig. 2.1, with respect to vector A also will be a time variation with respect to the reference voltage. Thus the pulses derived from vector C vary in time relation with those derived from the reference voltage. This variation is proportional to the original variation of phase angle Φ , Fig. 2.1. The time relation of these derived pulses is continuously interpreted by the Eccles-Jordan multivibrator and was to have been corrected

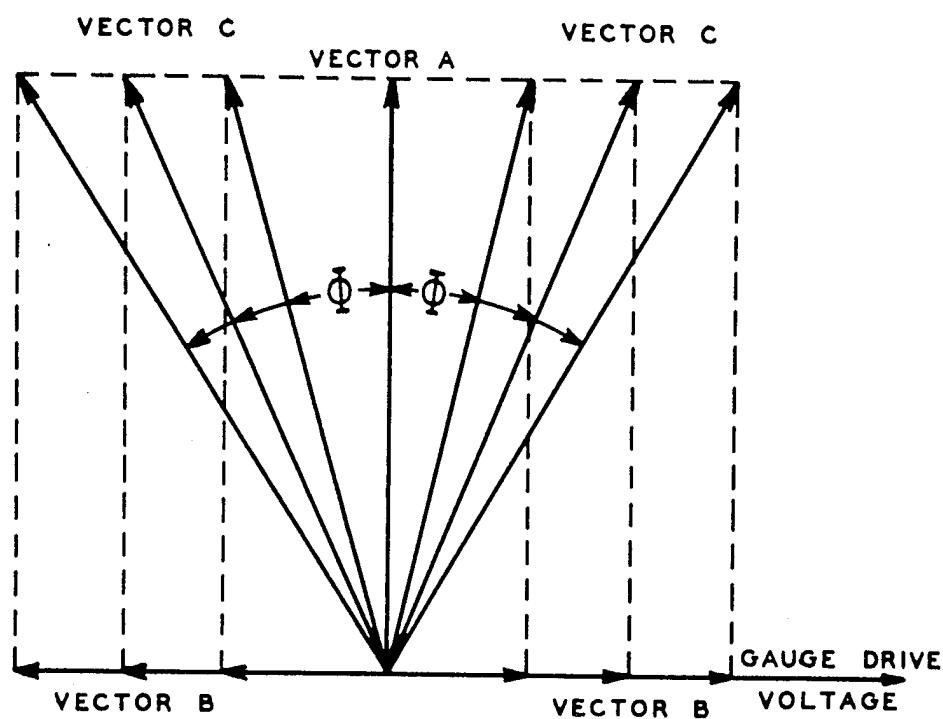


Fig. 2.1 Deriving Phase Shift from Strain-gauge Output. Vector A, quadrature voltage (fixed in phase-relation amplitude with respect to gauge drive voltage). Vector B, gauge output voltage (proportional to the gauge drive voltage and degree of gauge unbalance and in phase with or 180° out of phase with gauge drive voltage). Vector C, vector sum or resultant of vectors A and B.

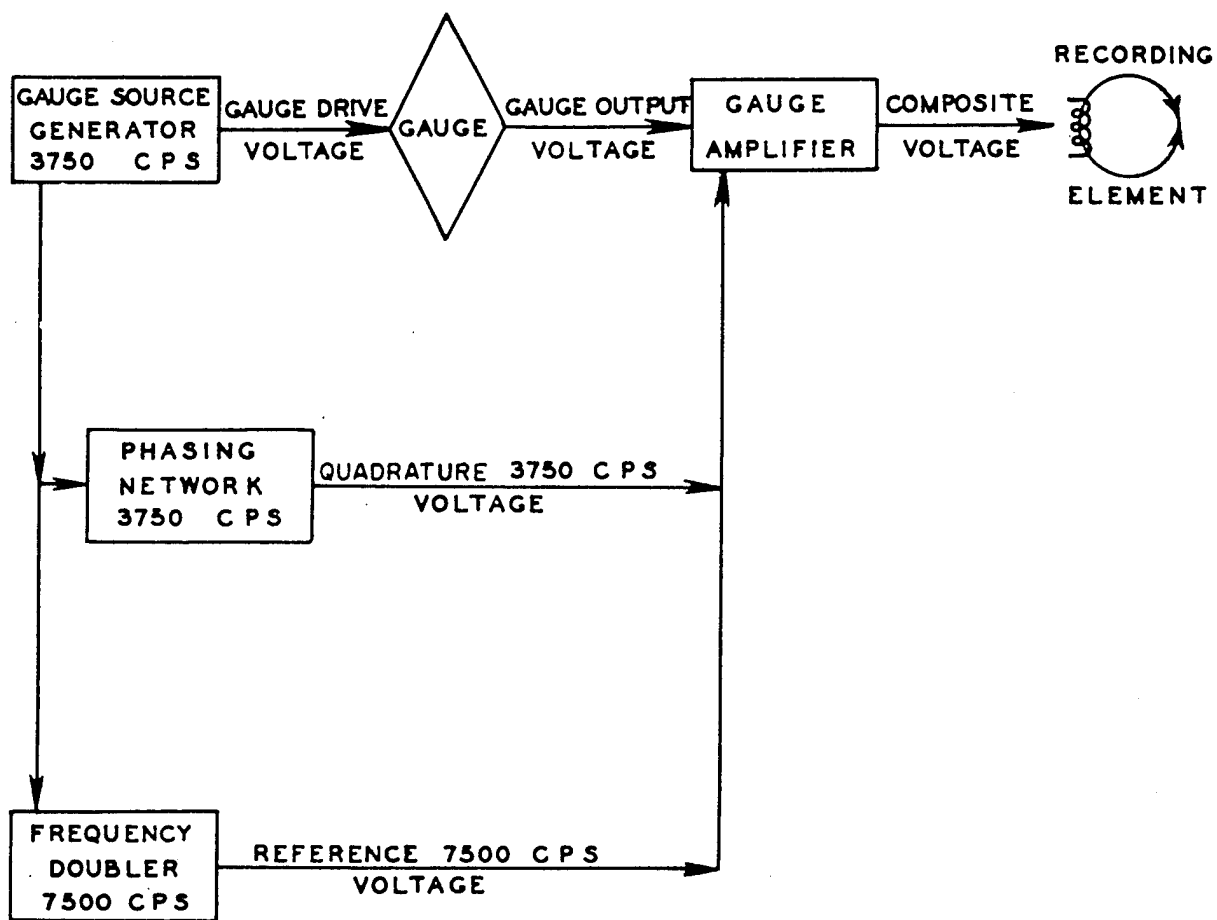


Fig. 2.2 Functional Block Diagram, One Channel of 24-channel Recorder

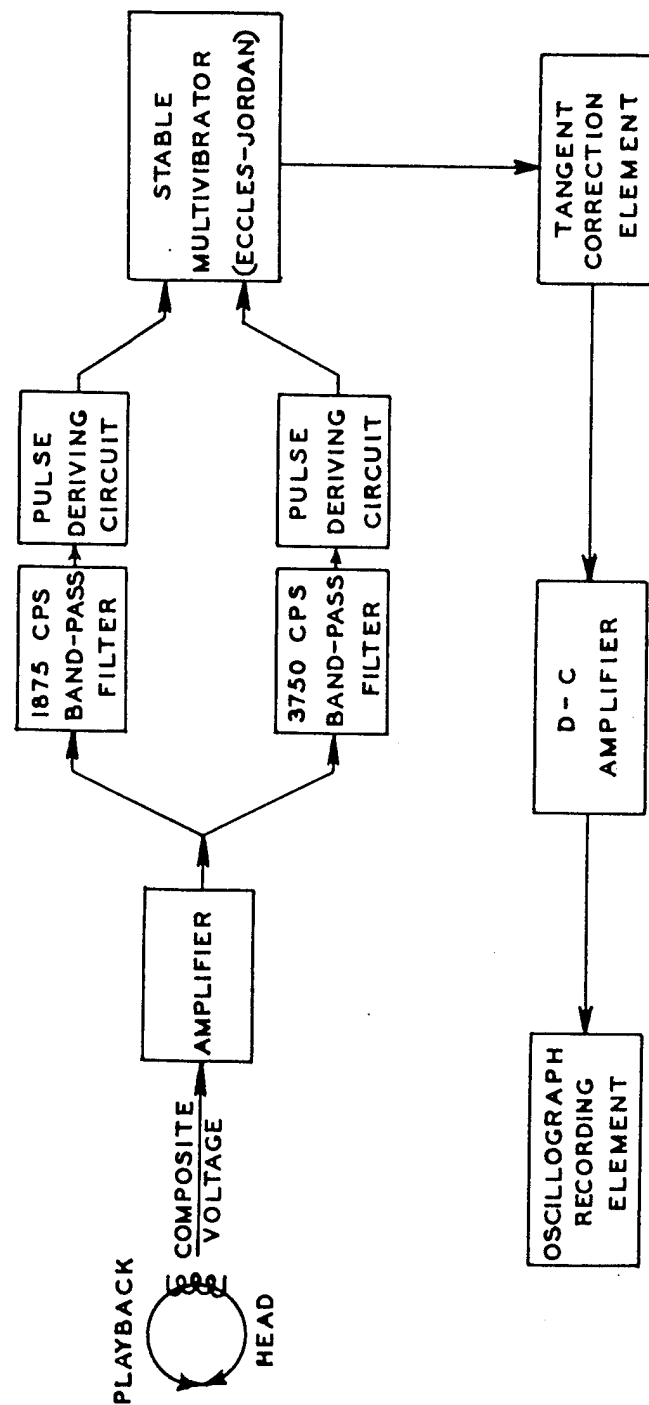


Fig. 2.3 Functional Block Diagram, One Channel of Playback System

by the tangent correcting circuit so that the output from the correcting circuit was proportional to the tangent of the phase angle Φ and therefore was proportional to the original vector B. This was the information that was ultimately desired; it was recorded either by an oscillograph or by a Brush Penmotor recorder. Physically the recorder consisted of the two units shown in Fig. 2.4. The first of these was the air-borne amplifier, which contained the individual gauge circuits and the necessary controls for balancing and adjusting each circuit. The second unit was the air-borne recorder, which consisted of a tape transport mechanism and the power supply and control circuits.

2.2.3 Air-borne Amplifier

The air-borne amplifier consisted of the gauge source generators and power components common to all channels, together with 24 separate plug-in amplifiers (Fig. 2.5). The plug-in amplifiers were of two types. The first of these was the standard amplifier, which provided a frequency response of 500 cps and an accuracy of approximately ± 2 per cent of full scale. This type of amplifier is shown in Fig. 2.6. The second type of amplifier was termed the "high-accuracy amplifier" and is illustrated in Fig. 2.7. This amplifier was capable of accuracies of approximately ± 0.25 per cent, with a frequency response of approximately 100 cps. Controls were provided on the front surface of each amplifier unit for resistance and capacitance balance. This permitted adjustment for variations in gauges and connecting circuits. The high-accuracy amplifiers were to have been used in those channels in which the data were likely to be slowly changing but of greater importance in accuracy of recording, for example, airspeed and altitude. However, because of repeated malfunction and complexity of maintenance, the high-accuracy amplifiers were discarded, and only standard amplifiers were used throughout.

2.2.4 Air-borne Recorder

The air-borne recorder contained the power and starting circuits along with the tape transport mechanism and is shown in Fig. 2.8. The tape was $3\frac{1}{2}$ in. wide and was made of a plastic coated on one surface with magnetic particles.

The tape was contained on an aluminum reel and was driven past the recording heads at a speed of approximately 24 in./sec. An automatic switch was provided to shut off the recorder automatically at the end of a preset period of time. Another switch was provided which turned off the recorder when the tape was completely exhausted on the supply spool. Two means of starting the recorder were provided. Through one plug, initiation of the recording cycle was made by shorting two pins; through the other, the cycle was initiated by 24 volts dc applied from an external source. A third plug provided an indication that (1) power was provided to the recorder so that it was ready to run and (2) the tape was being run past the recording heads.

2.2.5 12-channel Playback

The 12-channel playback consisted of four relay racks as illustrated in Fig. 2.9. One of the relay racks contained the tape transport mechanism, the recording oscillograph, and the necessary distribution and control circuits. This rack is illustrated in Fig. 2.10. The remaining racks housed the individual playback amplifiers. One of these racks is illustrated in Fig. 2.11.

The tape was carried past a recording head assembly similar to those in the air-borne recorder, and the signals were distributed to the various playback amplifiers. The resulting output signals were returned to an oscillographic recorder employing bifilar-type galvanometers. Eleven of the playback signals were of the standard-accuracy type, and one playback amplifier was of the high-accuracy type. The 12-channel playback was housed in a mobile laboratory which provided the necessary facilities for power and for processing the records from the oscillographic recorder.

2.2.6 2-channel Playback

The 2-channel playback was used as portable transcription equipment to facilitate the adjustment and maintenance of the recorders at the airplanes. It was similar in operation to the 12-channel playback, containing similar tape transport mechanisms and two of the standard-accuracy playback amplifiers. The transcribed data were presented in a visible record by a Penmotor. This equipment is illustrated in Fig. 2.12.

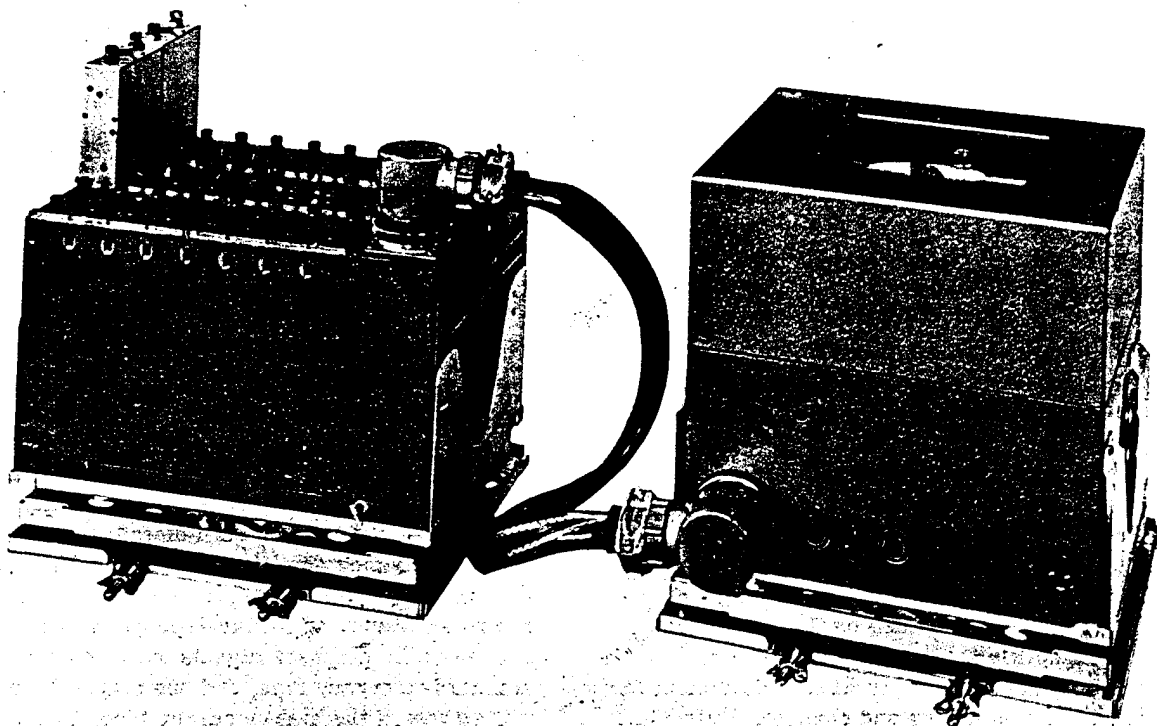


Fig. 2.4 24-channel Recording System

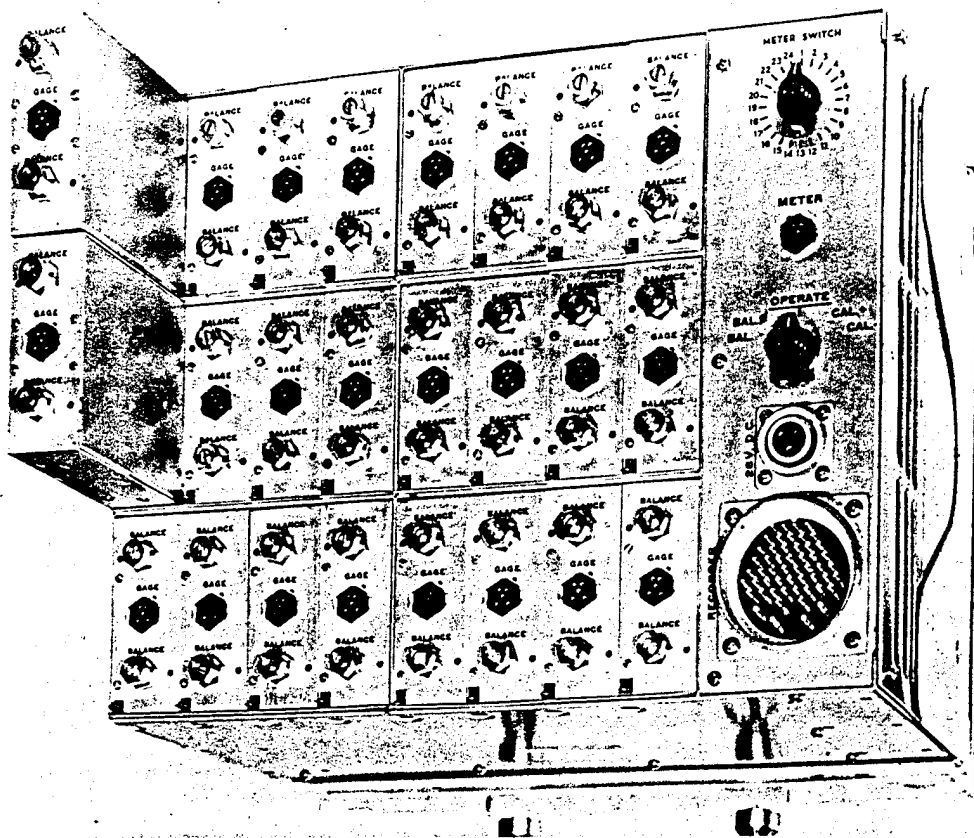


Fig. 2.5 Air-borne Amplifier Unit

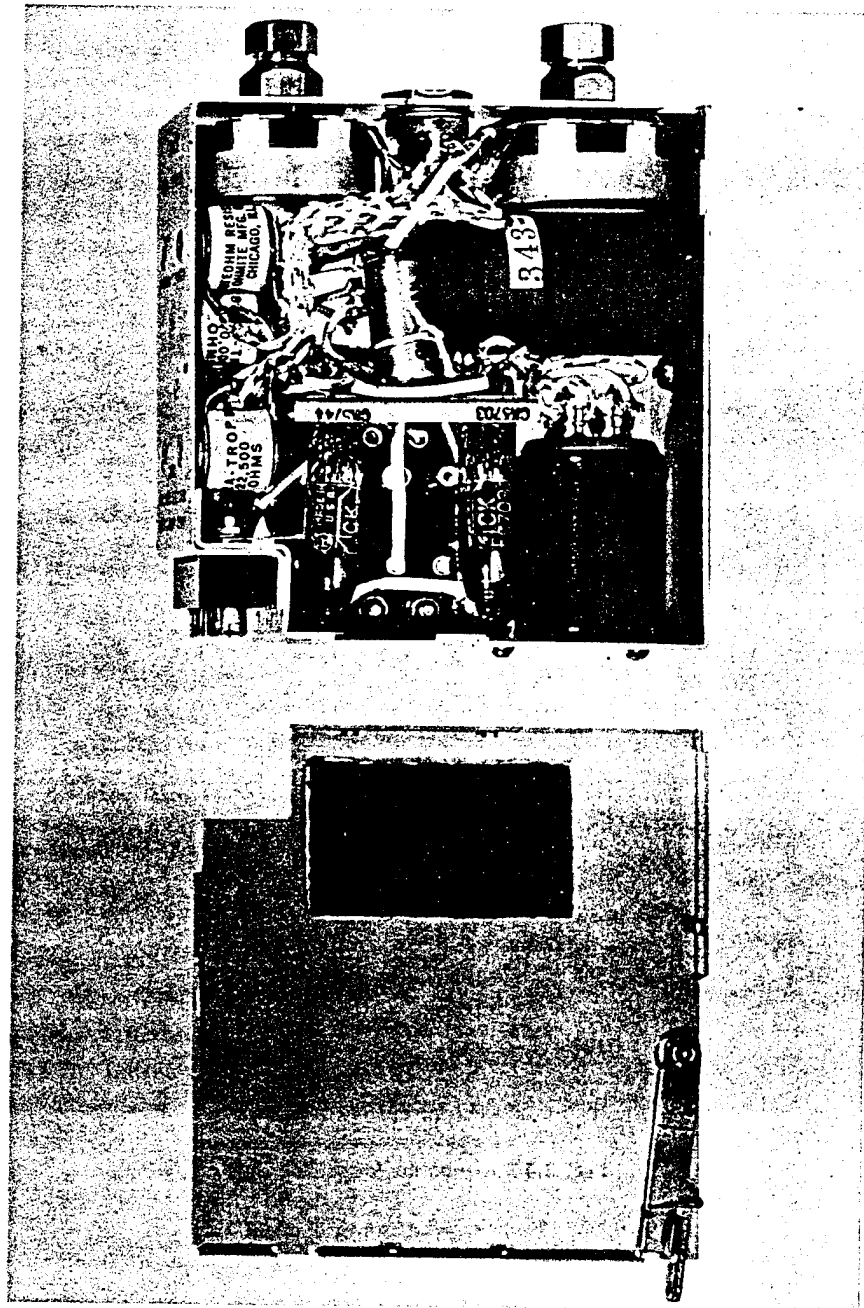


Fig. 2.6 Plug-in Amplifier (Standard Accuracy)

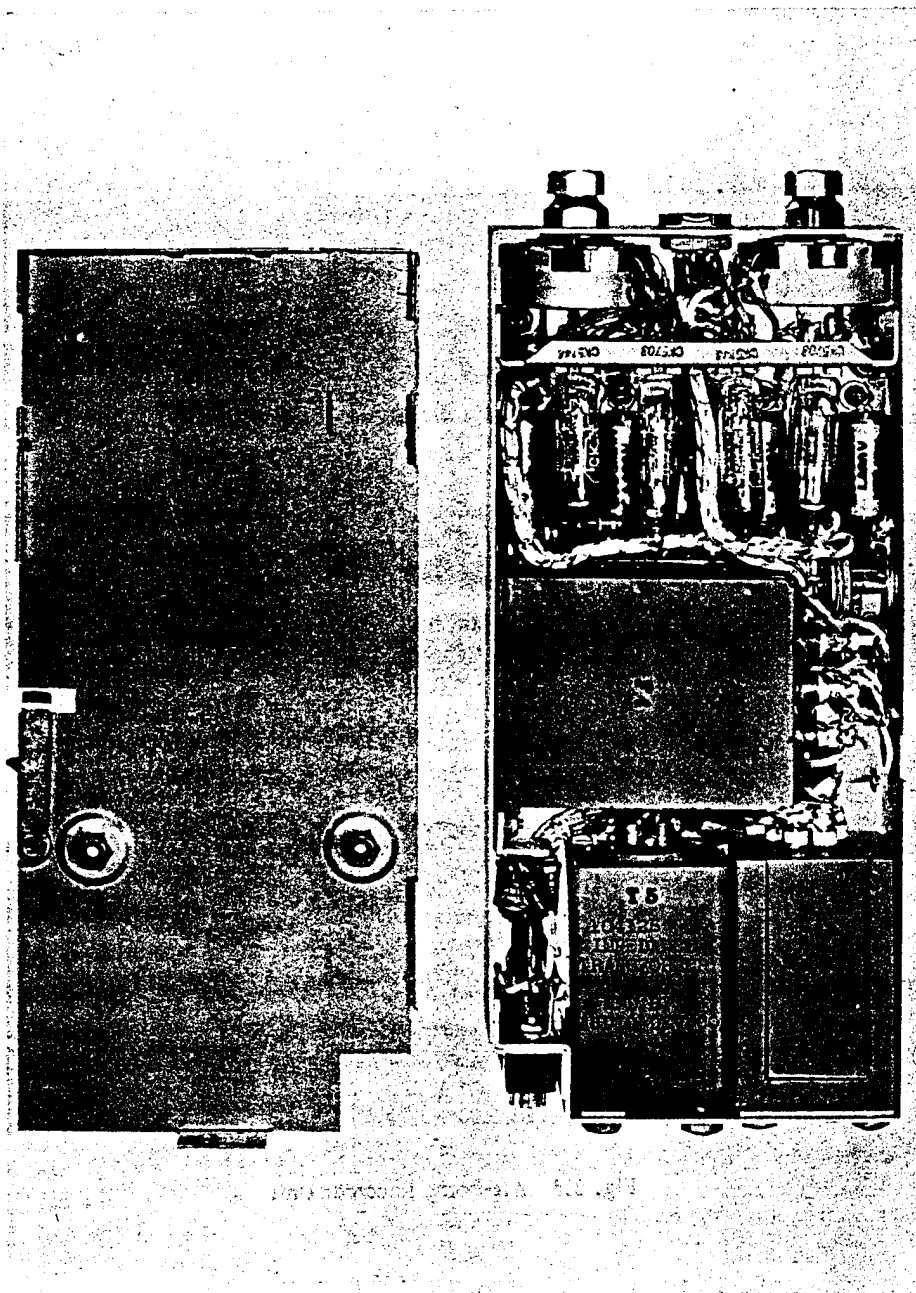


Fig. 2.7 Plug-in Amplifier (High Accuracy)

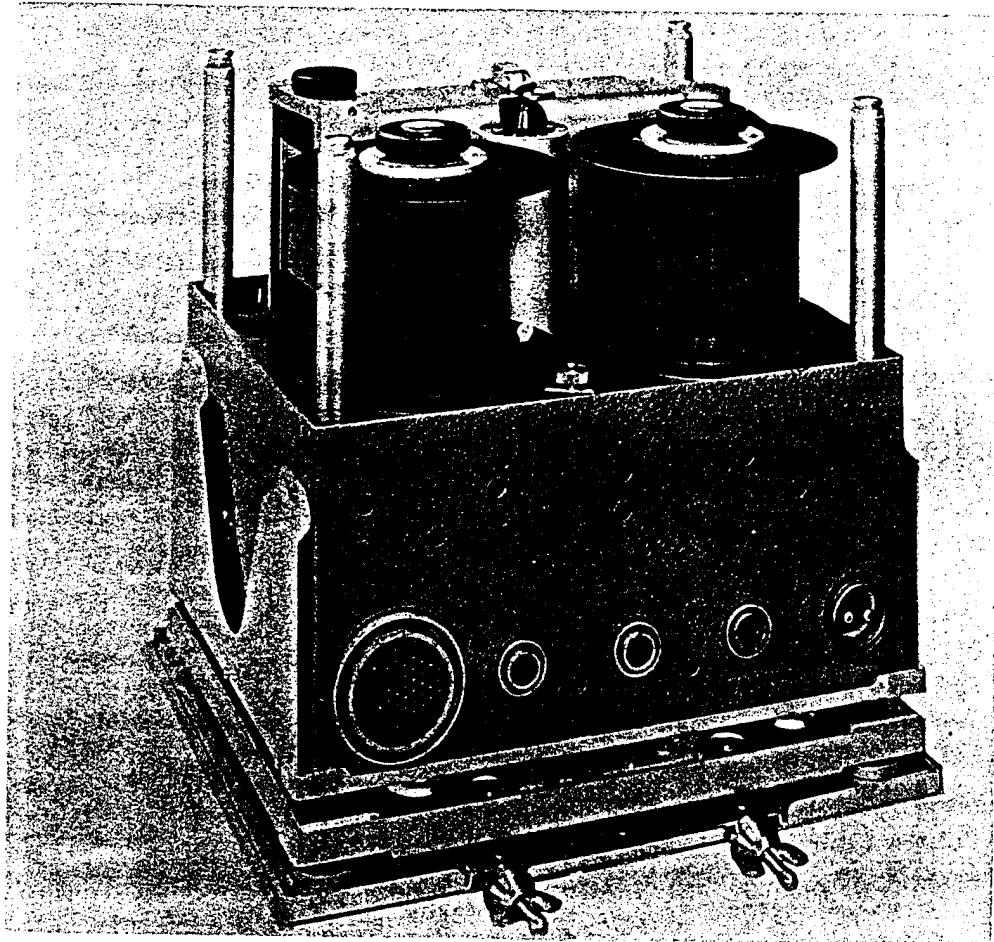


Fig. 2.8 Air-borne Recorder Unit

~~SECRET~~

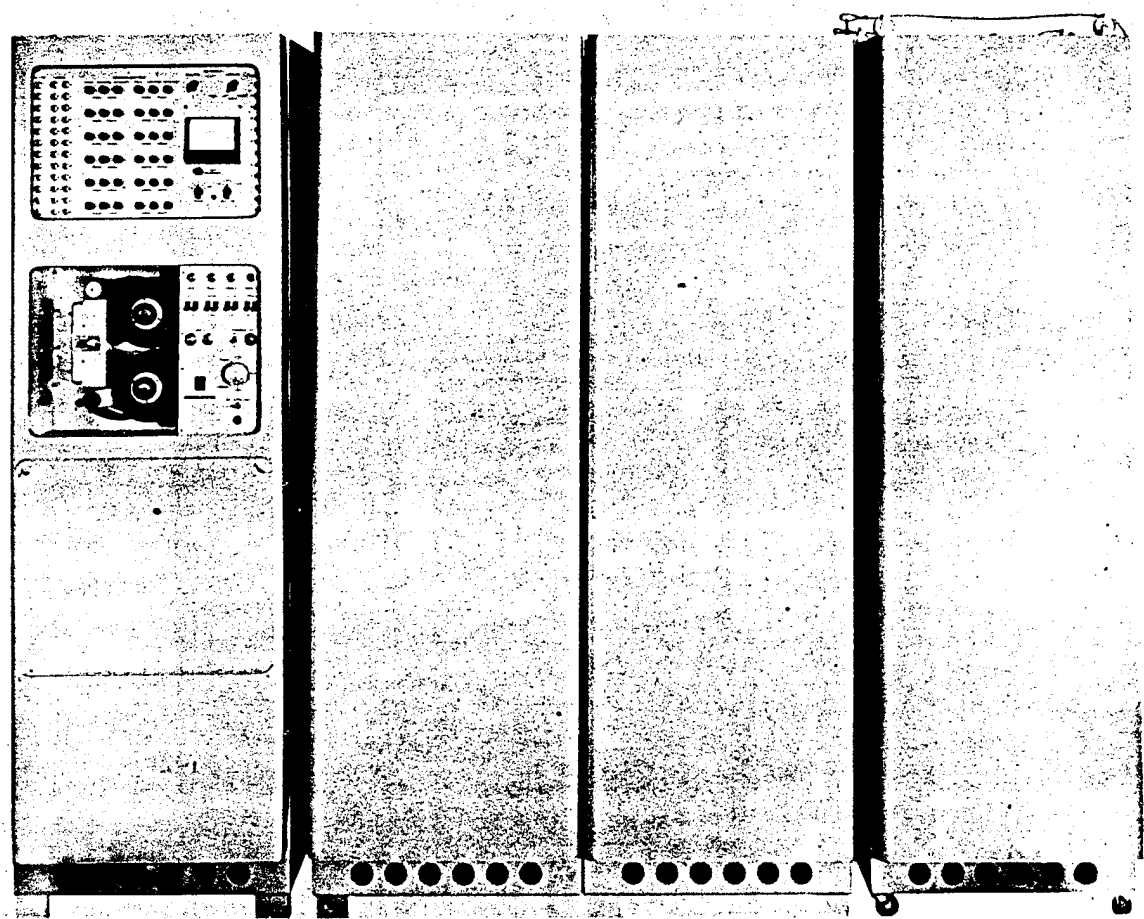


Fig. 2.9 12-channel Playback

~~SECRET~~

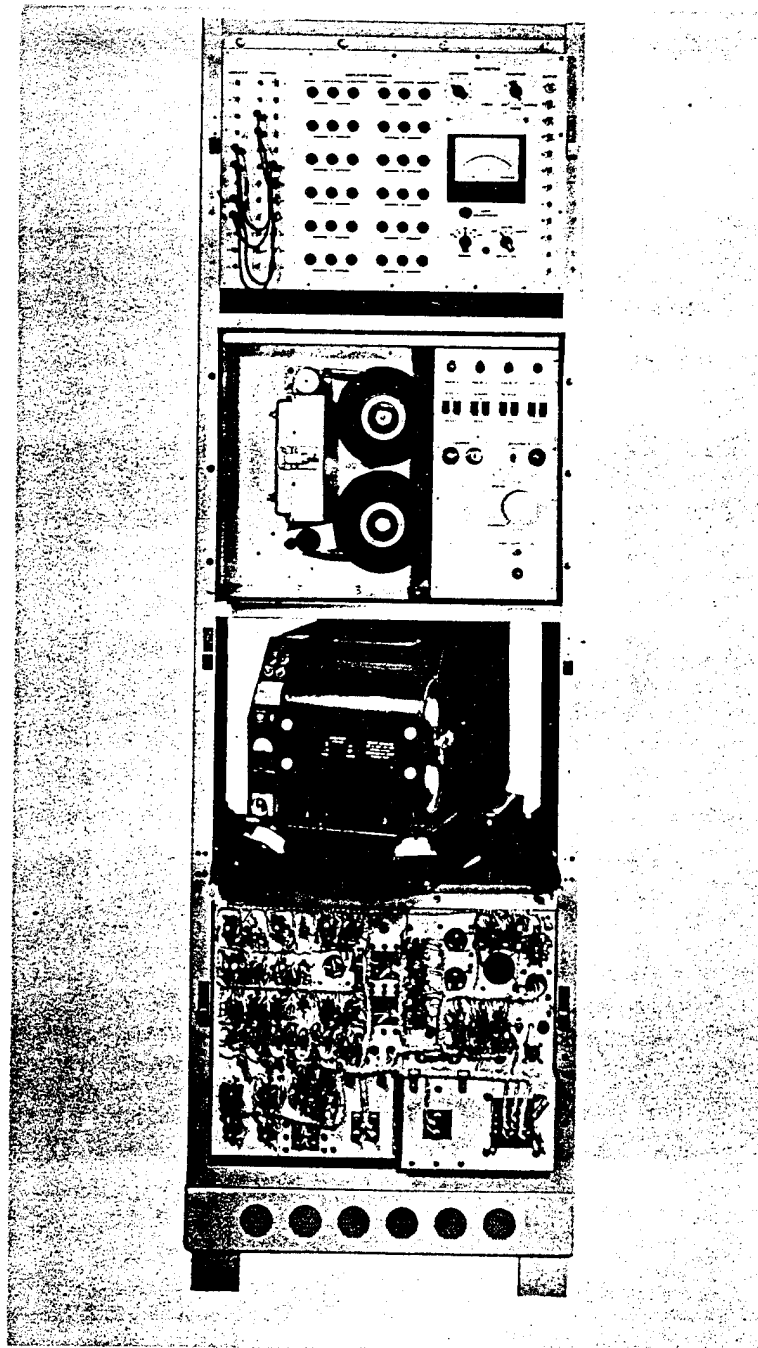


Fig. 2.10 Control Rack, 12-channel Playback

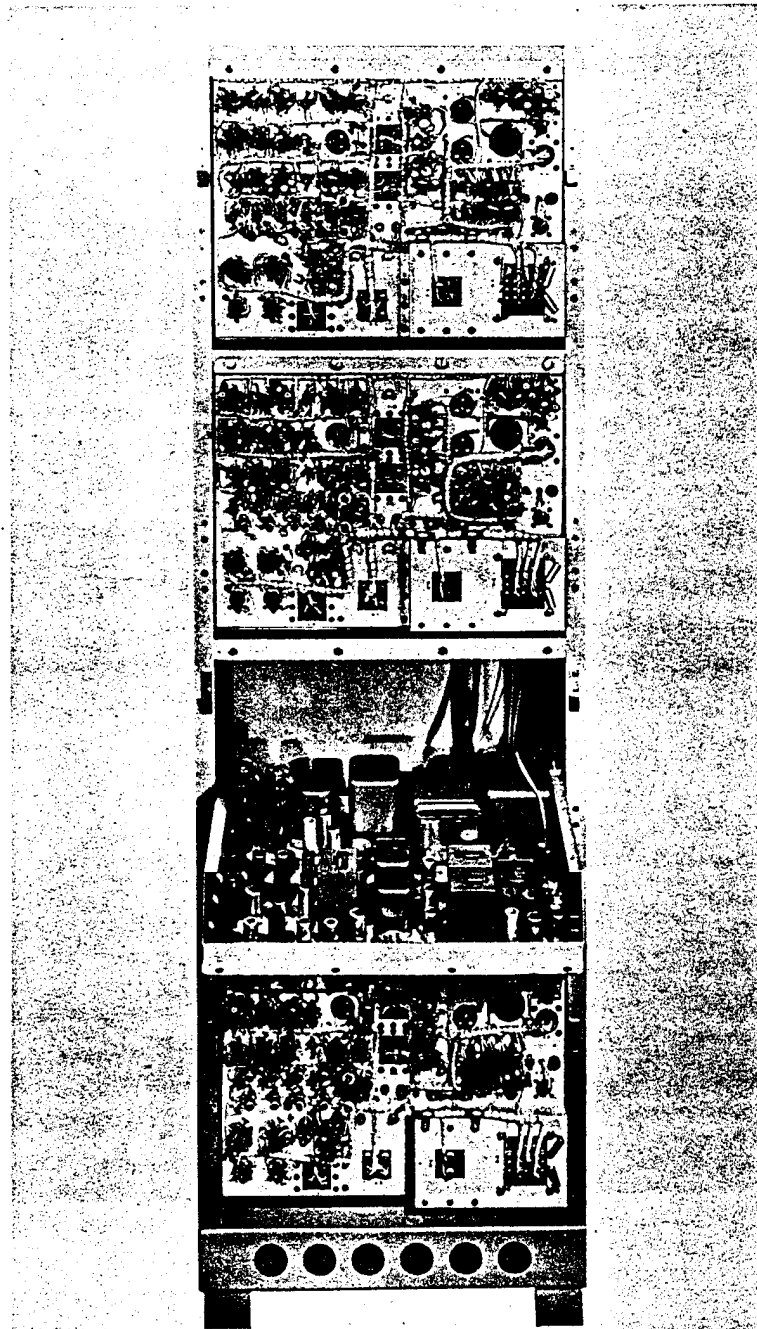


Fig. 2.11 Channel Rack, 12-channel Playback

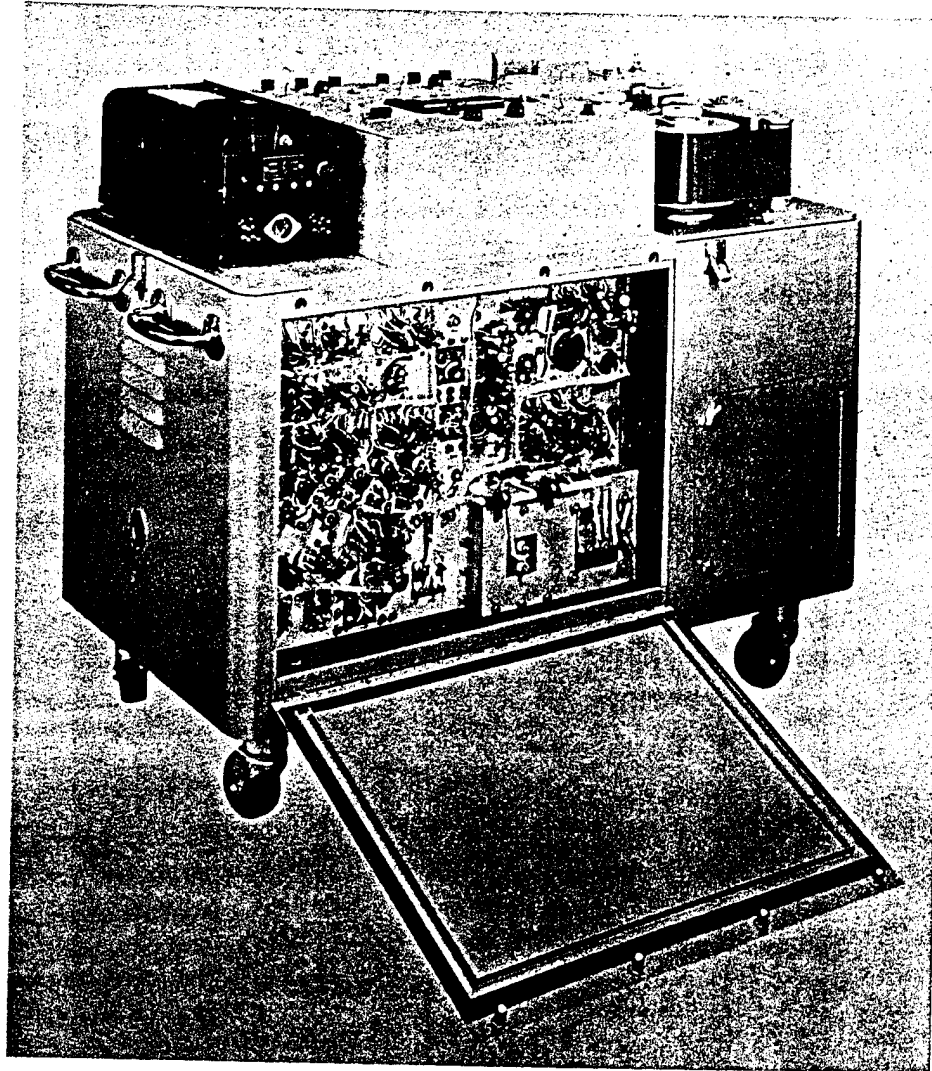


Fig. 2.12 2-channel Playback

2.3 TELEMETERING

Telemetry may be defined as the transmission of flight data such as strain, pressure, and acceleration from an air-borne vehicle and the reception, recording, and interpretation of these data at some point other than the test vehicle.

The data to be telemetered for this test included some flight information which was of interest to the pilots controlling the drone airplanes. Because of the possibility that one of the drone aircraft might be lost and because of the limitations of television as a means of transmitting flight information, it was necessary that a telemetering system be used. An important feature of telemetering is that a permanent record of the data is available despite loss of the test vehicle.

The air-borne telemetering components used in this project were required to be capable of operating continuously over the time of the test flight without the attention of technical personnel aboard. They were required to be capable of withstanding the severe shock and vibration produced during the actual test, as well as the high-temperature, high-humidity, and low-pressure conditions. Since the expected maximum line-of-sight distance at test time between the air-borne and ground equipment was approximately 35 miles, it was necessary that usable information be obtained at that distance.

2.3.1 System

The telemetering system used on this project was composed of the air-borne component, transmitting set AN/AKT-6, and the ground component, receiving set AN/UKR-1. The transmitting set AN/AKT-6 consists of two units: the coder-multiplexer, Fig. 2.13, and the transmitter unit, Fig. 2.14. The receiver unit AN/UKR-1 is illustrated in Fig. 2.15. This system was designed to provide, at a ground-based receiving station, a means of recording flight data from an air-borne vehicle. The system was capable of continuous transmission, reception, and recording of such data on 28 individual channels during any desired portions of the flight. Actually 29 separate channels were provided in the equipment; one of these, being used as a reference channel which transmitted a steady signal of one-half modulation,

served as a continuous check on the operation of the system.

The air-borne transmitting set operated on a transmitter frequency of 2,200 to 2,300 Mc and employed modified pulse-time modulation for transmission of data. The quantity measured by a channel of the equipment appeared as a graph plotted against time on the corresponding channel of a recording oscillograph into which the receiving equipment fed its output.

Since local recording was also to be used in the drones, a filter box was designed and installed for the purpose of supplying the data to both the local recording set and the telemetric transmitting set. The filter box was necessary in view of the voltage and frequency differences inherent in the two types of equipment.

2.3.2 Principles of Operation

A block diagram of the components of the air-borne telemetering set is presented as Fig. 2.16. Information was provided to the transmitting set from strain gauges, accelerometers, etc. These bridge drive voltages were obtained from the secondaries of a 750-cps 30-phase transformer. An unbalance on the data bridge caused by strain, acceleration, etc., appeared in the form of a 750-cps voltage sine wave and was fed into a preamplifier stage. This stage amplified the 750-cps wave, which was then fed into a modulation generator where it modulated a 1,500-cps timing sine wave coming in from the delay line. Where the 1,500-cps timing wave crossed the zero reference level going in a positive direction (above the zero level), a pulse was generated. The amplitude of the 750-cps wave being fed into the modulation generator from the preamplifier determined the time along the zero reference level at which the 1,500-cps wave went positive and hence time-modulated the resulting pulse. The pulse was amplified in either the video A or B stage and was sent into the mixer.

It should be noted that there were actually 28 sets of those stages up to and not including the video A stage, comprising 28 data channels. Channel 29, the reference channel, consisted of a modulation generator which gave a constant output of 50 per cent modulation as a running check on the equipment. The outputs of the 29 modulation generators were fed into the video A and B stages.

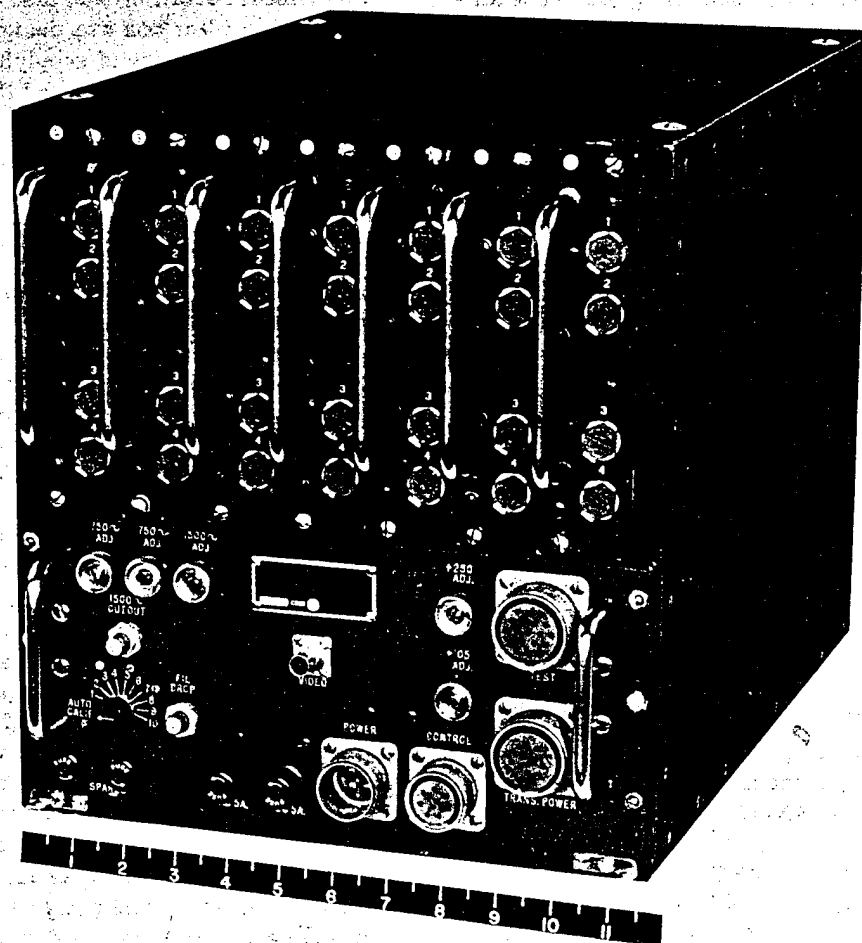


Fig. 2.13 Coder-Multiplexer Unit, Telemetering Set AN/AKT-6

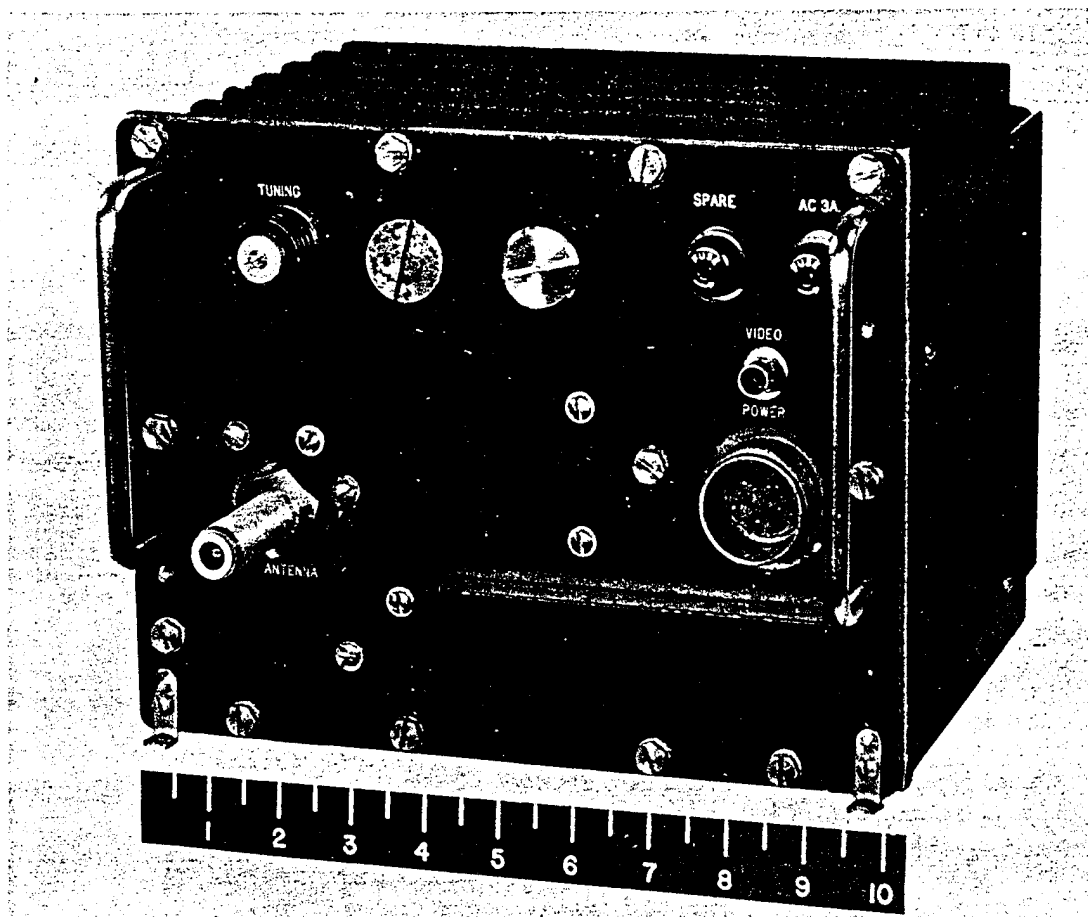


Fig. 2.14 Transmitter Unit, Telemetering Set AN/AKT-6

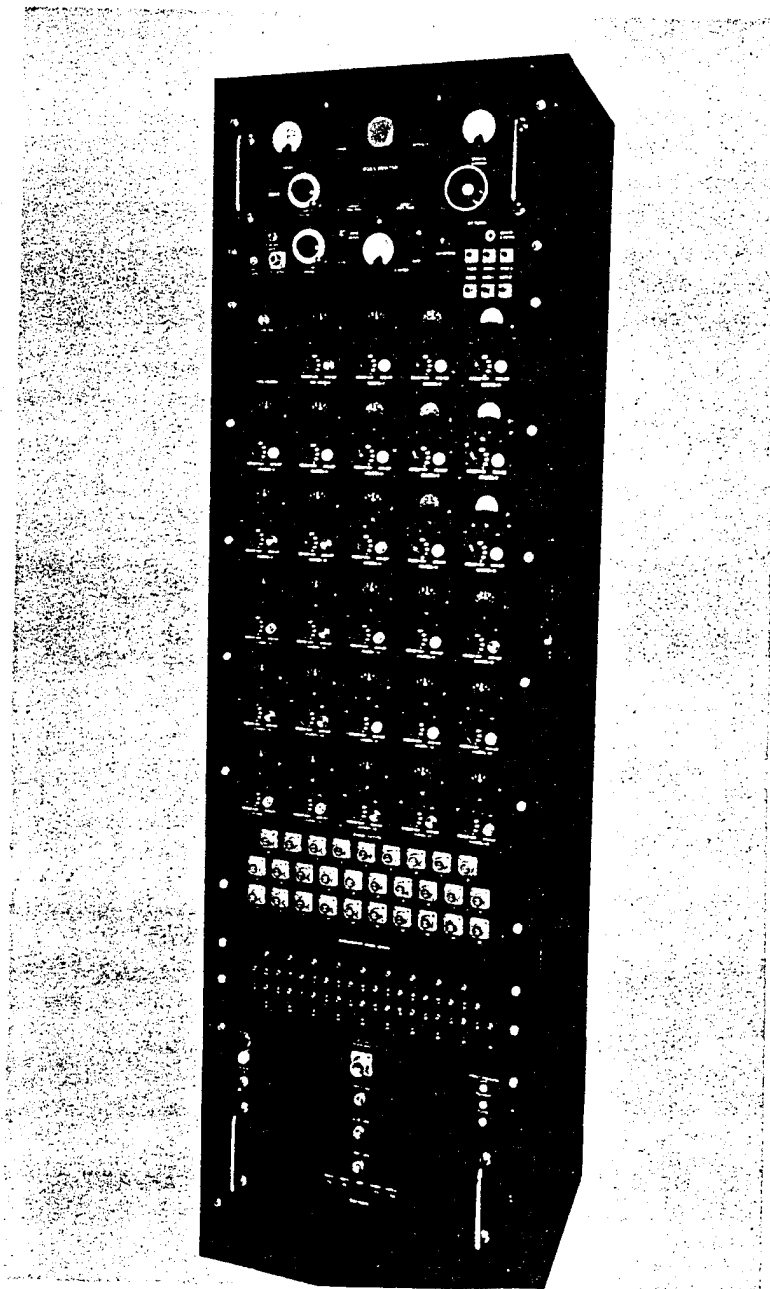
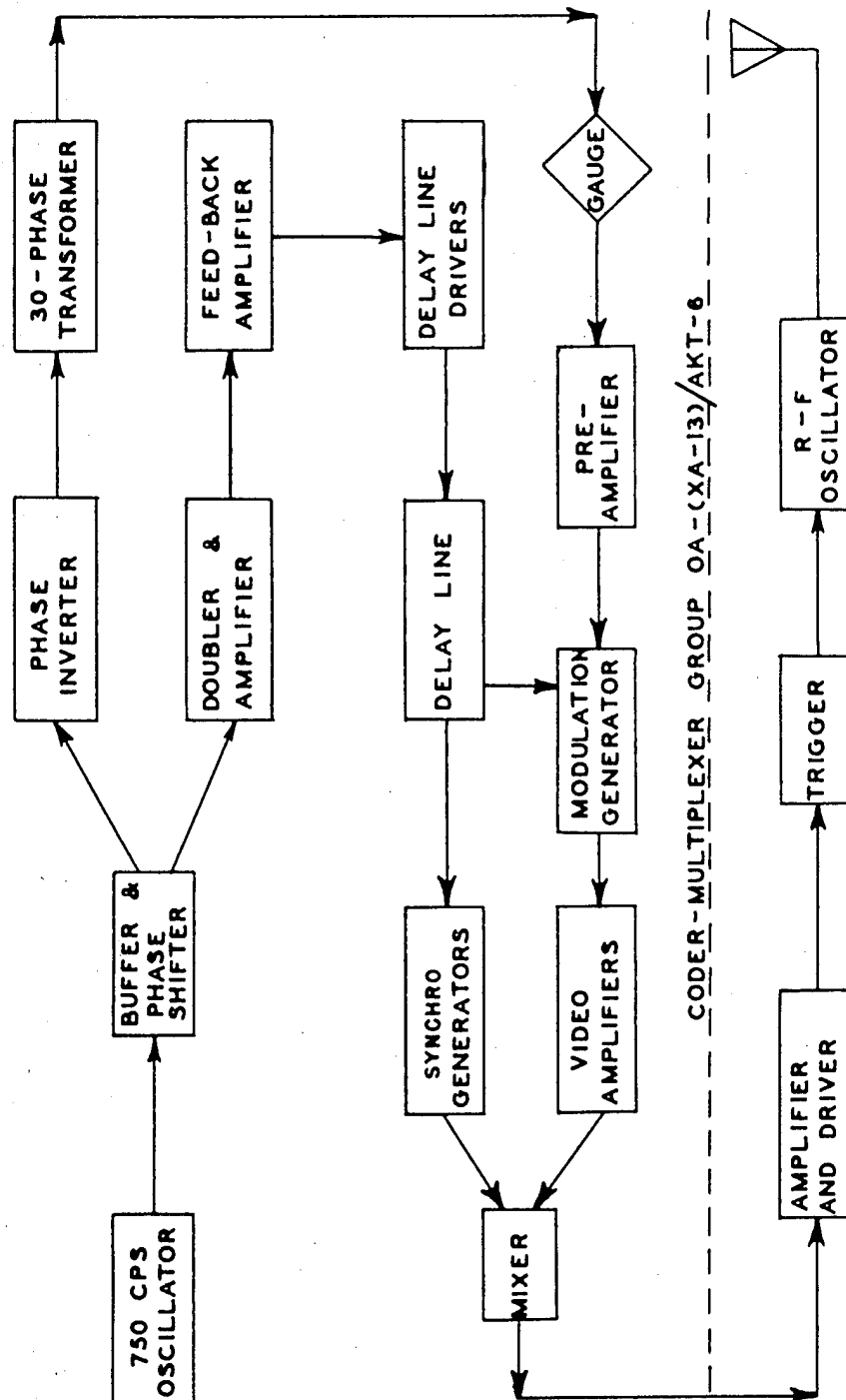


Fig. 2.15 Receiver Unit, Telemetering Set AN/UKR-1



CODER-MULTIPLEXER GROUP OA-(XA-13)/AKT-6

TRANSMITTER T-(XA-77)/AKT-6(XA-2)

Fig. 2.16 Block Diagram of Telemetry Set AN/AKT-6

In the mixer, two pulses, which were used at the receiving station for synchronization purposes, were added to the 29 channel pulses. Two pulses were used to reduce the possibility of losing synchronization as a result of outside interference. After leaving the mixer, the pulses were amplified and fed into a driver stage and thence to a trigger circuit for triggering an r-f oscillator.

The 750-cps oscillator was the network basis for the data bridge 750-cps drive voltages and for the 1,500-cps timing wave. The output of the oscillator was sent to a buffer and phase-shifting network which had two outputs. The output from the phase shifter went to a phase inverter which provided the 750-cps drive voltages for the four primaries of the 30-phase transformer. The other output from the buffer stage was doubled in frequency to 1,500 cps and was fed into a delay-line network which was tapped at intervals to provide a 1,500-cps timing signal for the 29 modulation generators and for the generation of the two synchronization pulses.

A block diagram of the ground telemetering receiving set is presented as Fig. 2.17. The pulse transmission of the air-borne transmitting set was picked up by the receiving antenna and fed to an r-f cavity tuned to the frequency (2,200 to 2,300 Mc) of the transmitter. The 29 channel pulses and two synchronizing pulses were fed to a mixer stage, where a local oscillator frequency 30 Mc below the transmitter frequency was also fed. The difference frequency of 30 Mc was present in the mixer output and was sent to the i-f detector strip. The i-f strip discriminated against multiples, sums, and differences of the local oscillator frequency at the received signal frequency and allowed only a 30-Mc signal to be amplified and passed. The automatic frequency-control stage obtained a signal from the last i-f stage with which to stabilize the local oscillator frequency and ensure an accurate 30-Mc difference frequency. The output of the i-f strip was also detected, filtered, and fed to a video-synchronizing-separator strip. In the video portion the pulses were cleaned and amplified, while in the synchronizing-separator portion the two synchronizing pulses were coincided into one master pulse which, in turn, was divided into two other synchronizing pulses, one coinciding with the master pulse and the other spaced much later in time. The output from the video-

synchronizing-separator stage, consisting of the cleaned data pulses and two new synchronizing pulses, was fed to all channel units in parallel.

The multivibrator in the reference-channel unit and in each data-channel unit was blocked off by a disabling voltage from the previous channel and could not be triggered until this disabling voltage was removed. The synchronizing-channel multivibrator was triggered until this disabling voltage was removed. The synchronizing-channel multivibrator was triggered by the synchronizing pulse No. 1 coinciding with the master pulse, and its sole purpose was to remove the disabling voltage from the reference channel. When the reference channel was triggered, it removed the disabling voltage from channel 1, and so on. In this manner all the channel units were triggered in sequence. By using the synchronizing channel any error that occurred in the triggering of a channel was corrected at the time of the next synchronizing signal and would not recur. Synchronizing pulse No. 1 was fed to the reference channel of channels 1 through 7 and 22 through 28 to retrigger the multivibrators.

The square-wave output from the channel multivibrator was fed through a cathode-follower stage which compensated for wiring and tube capacities. The cathode-follower square-wave output was fed through a sharp 450- to 1,050-cps band-pass filter, and its output consisted of a 750-cps sine wave varying in amplitude with the degree of modulation of the channel. This signal was amplified and rectified, appearing as a negative d-c signal of a magnitude directly proportional to the magnitude of the 750-cps signal input. This d-c signal was passed through a low-pass filter to eliminate 750- or 1,500-cps ripple; the output of this filter was the recorder signal.

2.3.3 Accessories

The filter unit was designed to permit the use of both the telemeter and the local recorder with one set of sensing elements. The use of such a unit eliminated (1) one source of difference between the data recorded on the recorder and that recorded on the telemeter, (2) the need for extra calibrations, and (3) the time, expense, and maintenance problems involved in dual sensing-element installations. The filter unit consisted of a pair of filters on the input and

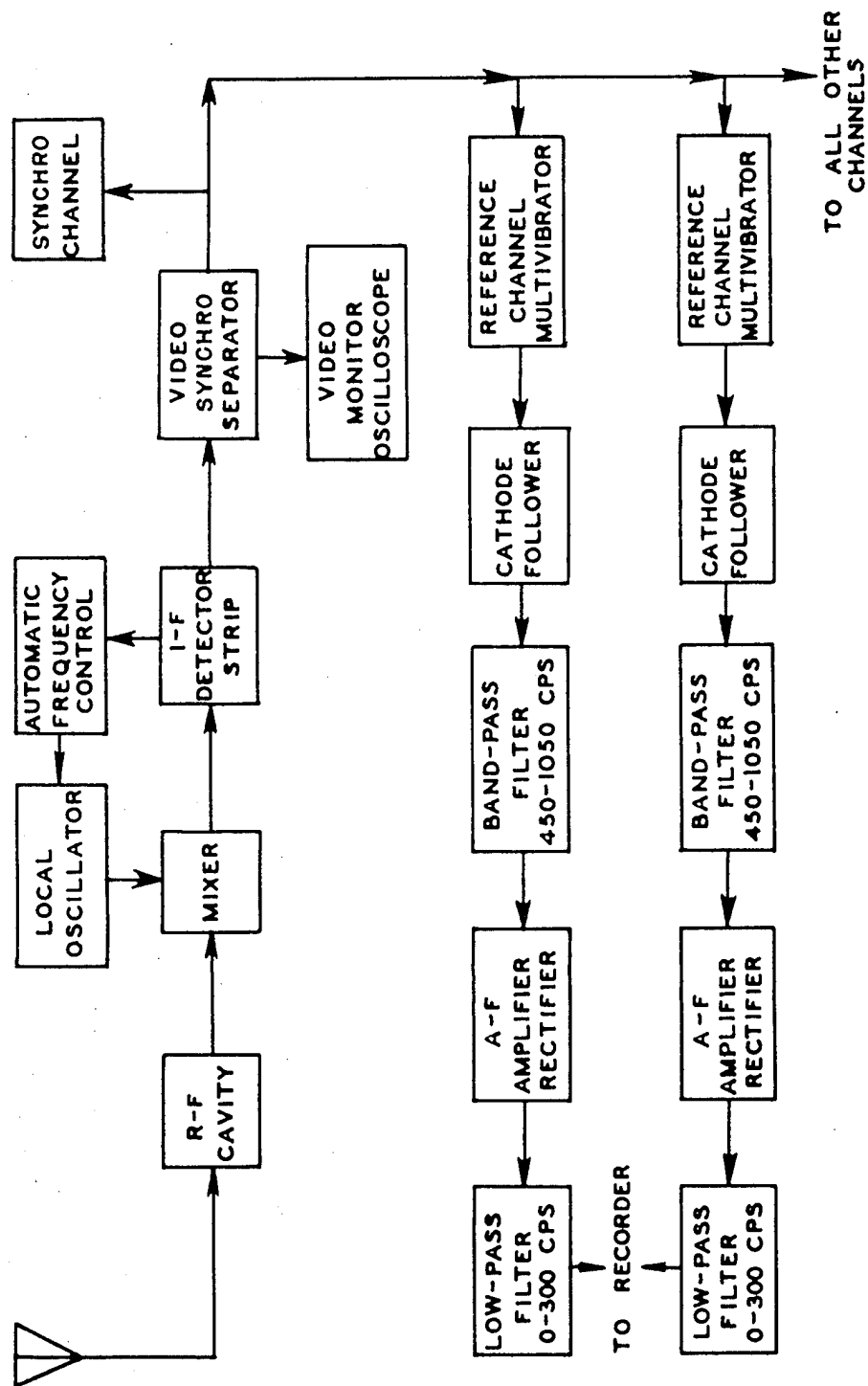


Fig. 2.17 Block Diagram of Telemetering Set AN/UKR-1

another pair on the output of each of 24 channels. One filter of each pair passed 3,750 cps, and the other passed 750 cps. The input filters were intended to prevent feedback from the telemeter into the recorder and vice versa. The output filters separated the signals intended for each equipment. Preliminary service tests showed high insertion losses in gain (66 per cent for the telemeter and 30 per cent for the recorder) and considerable feedback from the recorder to the telemeter. The units were returned to the manufacturer to be improved at the time of departure from the Z.I.

Inasmuch as telemetered data were transmitted from four drones simultaneously, it was necessary to provide a multiple-receiver station. Four operational receivers and one spare receiver were mounted in a van along with the necessary oscillographic recorders. The antennas for the receivers were mounted atop the van. In view of the directional characteristics of the receiving antennas, the necessary information for pointing the antennas toward the airplanes was to have been obtained continuously from the radar stations. The various elements of flight data as received at the ground station were to have been sent to the controlling pilots by means of remote repeater instruments.

2.4 TIMING AND SYNCHRONIZATION

In the collection of the data from these tests, a requirement was established that all recorded data obtained would be referenced to a common time. In order to meet this requirement, a timing system was developed which would provide starting signals for remote recording equipment at $T_0 - 5$ sec and timing signals every second beginning with $T_0 - 4$ sec.

The timing system consists of a time reference generator, a vhf radio link, and a number of time decoder units. The time reference generator was located in the telemetering trailer, and the time decoder units were located in the drone aircraft and other aircraft requiring time signals and/or starting signals.

2.4.1 System

The function of the time reference generator was to generate a coded time signal which indi-

cated seconds on the data records and also provided a starting signal to start remotely located equipment. The coded time signal was a 100-cps sine wave which was "blanked out" for 0.03 sec every 1 sec, 0.06 sec every 10 sec, and 0.09 sec every 100 sec. The starting of remote equipment at a specified time was accomplished by means of a control frequency of 2,000 cps which was mixed with the 100-cps signal already present. Both the 100- and 2,000-cps signals had to be received in order to effect starting of the remote equipment. This provided a measure of certainty that the equipment would not be started by noise signals, as would more likely be the case if only one frequency had been used.

Although not all the following aircraft were used on any one mission, timing and starting information was available in five Air Force B-17 drones, six combination B-17 drones, five Air Force T-33 drones, two B-50D aircraft, and one B-47 aircraft. Only starting information was available in the remaining six AEC B-17 drones and the two B-50A aircraft. Timing information was also supplied to 10 Consolidated Engineering recorders which were part of the telemetering receiver system. Four Veeder-Root counters which were part of the radar-data boxes used with the MSQ-1 tracking system were driven once each second by means of timing information from the time reference generator.

Two complete time reference generators were fabricated. The second generator was also located in the telemetering trailer and was used as a stand-by spare.

The function of the time decoder units was to convert the coded time signal into a form suitable for recording on a magnetic-tape recorder located in the aircraft. Another function of the decoder was to start the recording equipment in the aircraft. Starting was accomplished by means of a latching relay which closed two contacts to start the recording equipment. This latching relay did not close unless the 100-cps signal was also present. The Webster-Chicago magnetic-tape recorder located in the drone aircraft actually started recording upon receipt of the first time signal after closing of the latching relay, i.e., at $T_0 - 4$ sec. Other recording equipment in the aircraft started at $T_0 - 5$ sec.

2.4.2 Description of Equipment

A block diagram of the coder and decoder system is presented in Fig. 2.18. The time reference generator was composed of a crystal oscillator and frequency-divider circuits to produce a control frequency of 2,000 cps and a timing frequency of 100 cps. A start relay was included so that the control frequency could be turned on at time $T_0 - 5$ sec and then off at time T_0 from a remote point by means of landlines. A decade counter unit was included to provide outputs to the driving relay of the Veeder-Root counter and to the gating generator. The reference generator also contained a gating circuit which interrupted the 100-cps signal according to the pattern which has already been mentioned. Cathode-follower stages were included to provide output signals to the Consolidated recorders. A mixer stage combined the control frequency and time-signal output of the gating generator into a single signal, which was then sent to the vhf transmitter.

The vhf link was composed of a radio transmitter BC-640-D and either an ARC-3 or SCR-522 communication receiver.

The decoder units consisted of band-pass filters which separated the control and timing frequencies. Also included were relays; one was a latching type, and the other was the timing relay that operated once each second. The latching relay was operated by a combination of the control and timing signals, whereas the timing relay was operated by just the timing signal.

2.4.3 Theory of Operation

At some time prior to T_0 the time reference generator was turned on by means of a local power switch. This caused a 100-cycle sine wave to be sent out by the vhf transmitter to the remote time recorder units. No remote operation occurred at this time since both the 100- and 2,000-cps signals were required before operation began.

Two landlines from Parry Island provided input to the timer-starter relay as a result of shorting the lines at that island. One of the lines was shorted at time $T_0 - 5$ sec. This caused the control frequency, f_c , to be sent over the vhf link and also caused the decade counter unit in the reference generator to start

operation. The effect of the control frequency on the decoder unit is discussed in a later paragraph. The second line was shorted at time T_0 . This caused the control frequency to be shut off.

The two frequencies used in the timing system were generated by means of a 100-kc crystal oscillator and frequency-divider circuits. The output from the 100-kc oscillator was first fed into a pulse-shaping network which converted the sine wave into a square wave. The square wave form was necessary in order to operate the decade counter units and the frequency-divider circuits.

The first frequency division of the 100-kc signal was five, and the second division was ten. The signal frequency was then 2,000 cps. A portion of this signal was sent to further frequency-dividing circuits; the other portion was filtered to remove all but the fundamental frequency, which was a 2,000-cps sine wave. This sine wave was used as the control frequency for the timing system.

The third division of the 100-kc signal was ten, and the fourth and final division was two. The frequency of the square wave was then 100 cps. A portion of this 100-cps square wave was fed to the decimal counter units (DCU). The other portion was filtered so that only the fundamental sine wave of 100 cps remained. This sine wave was then applied to the control grids of a push-pull amplifier.

The counter unit consisted of four DCU's in cascaded counting series. The output of the first DCU had a repetition rate of 10 cps; the second, 1 cps; the third, 1 cycle every 10 sec; and the fourth, 1 cycle every 100 sec. The second DCU was connected to a gate-generating univibrator with a time constant such as to give a natural triggering time of 0.03 sec. The output of the third DCU was connected to a similar gate generator with a time constant of 0.06 sec, and the output of the fourth DCU was connected to a gate generator with a time constant of 0.09 sec.

The pulse outputs of these three gate generators were combined in a resistance network and applied to the suppressor grids of the push-pull amplifier. These pulses cut off the plate current in these tubes, reducing the gain of the push-pull amplifier to zero. This resulted in a 100-cps timing signal which was blanked once every second. Every 1 sec the blanking period was

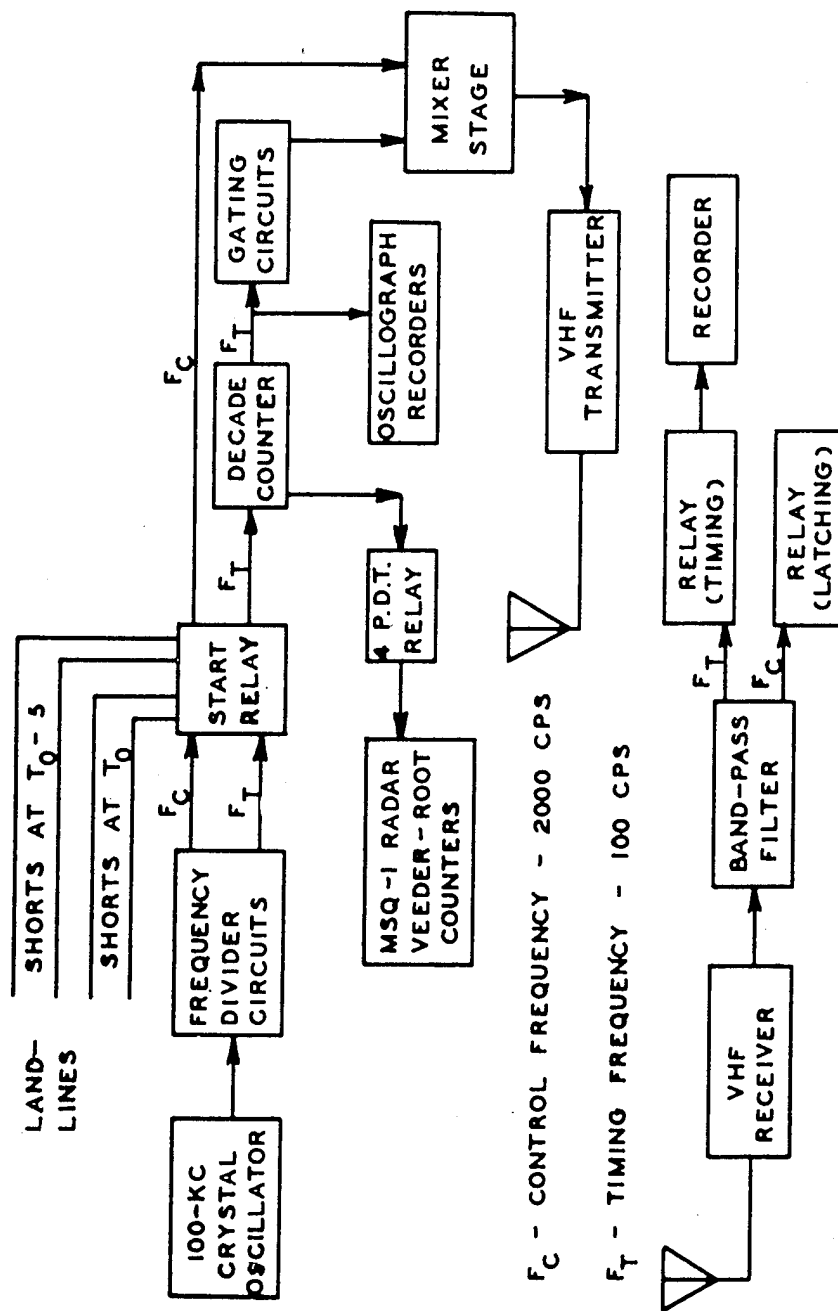


Fig. 2.18 Block Diagram of Code and Decoder Systems

0.03 sec, every 10 sec it was 0.06 sec, and every 100 sec it was 0.09 sec.

The 100-cps output of the push-pull amplifier, which had been modified by the gating generators as previously explained, was mixed with the control frequency f_c and put through an amplifier stage. The output of this amplifier was then sent to the vhf transmitter, where it was transmitted to the remote decoder units.

One output of the push-pull gating circuit was combined with the 2,000-cps signal and then sent to the transmitter. The other output was coupled to 10 parallel-connected cathode-follower stages. The output of the cathode-follower stages operated the Consolidated Engineering recorder units. Actually only eight of these telemetering recorders were used at one time. The remaining two were stand-by spares. The signal received at the recorder units was a 100-cps signal which was interrupted once every second in accordance with the established pattern.

The electrically operated Veeder-Root registers located in the radar-data boxes were driven by means of a counterdriving relay which was operated from the output of the second DCU. Remembering that the second DCU repetition rate was 1 cps, the counterdriving relay was operated once every second. The counterdriving relay is a four-pole relay whose contacts were closed for the period of time sufficient to drive the Veeder-Root registers. The power to drive the registers was supplied externally.

The time decoder units, upon receiving the transmitted signal, separated the control signal f_c and the timing signal f_t by means of band-pass filters.

The filtered 100-cps timing signal was applied to the grid of a vacuum tube. This signal caused the tube to conduct and to close a relay. Interruption of the 100-cps signal at the 1-, 10-, and 100-sec intervals caused the relay, which is normally closed, to open momentarily. Since the relay was of a fast-acting type, it was necessary to add a capacitance, the charge of which was sufficient to keep the relay closed between adjacent cycles and yet allow it to drop out during the blanking periods of the 100-cps timing signal. The output of the 100-cps filter was also applied to a cathode-follower stage so that it was possible to operate additional equipment without interfering with the primary system.

The output of the 2,000-cps filter was also

applied to the grid of a vacuum tube. This signal was sufficient to drive the tube into conduction and thus close the 2,000-cps relay. However, the 2,000-cps relay was not connected to the plate of this tube unless the 100-cps relay was energized. This means that the remote equipment would not start operation until both signals were present. A condenser was again added to keep the relay closed between adjacent cycles of the 2,000-cps wave. A cathode-follower stage was used so that additional equipment could be operated by the 2,000-cps signal.

2.4.4 Blue-box Fiducial Marker

In order to synchronize the various recording systems with the exact time of the blast, a photosensitive fiducial marker was developed and built by Edgerton, Germeshausen & Grier, Inc., and was designated as Type A-2. This instrument was identified as a "blue box" in order to avoid the complications and malfunctions inherent in the usual "black box."

The instrument consisted of a protected photocell which triggered a thyatron, which in turn closed a relay. The photocell was protected by a suitable optical filter and by electrical circuits to avoid untimely operation due to sunlight, reflected light, or other extraneous sources other than the actual atomic explosion. This equipment operated from a 400-cps 110-volt source and was so mounted as to be directed toward the expected location of the blast. The blue box is illustrated* in Fig. 2.19.

2.5 HIGH-FREQUENCY PRESSURE RECORDER

It was necessary to relate the loads on the aircraft structure to some function that is at least theoretically predictable from atomic explosions. This function was selected as "peak overpressure." Formulas are available by which to calculate (or at least approximate) the peak overpressure at a given distance from an explosion of a given strength. The measurement of peak overpressure is then a convenient link between the calculations concerning the

*Operating Instructions, Blue Box, Aircraft - Type A-2; Edgerton, Germeshausen & Grier, Inc., Boston, Mass.

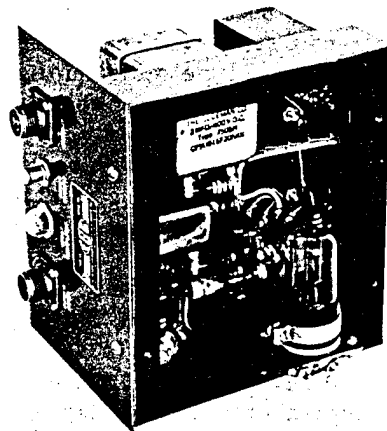
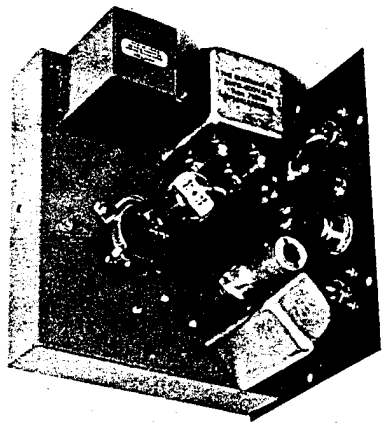
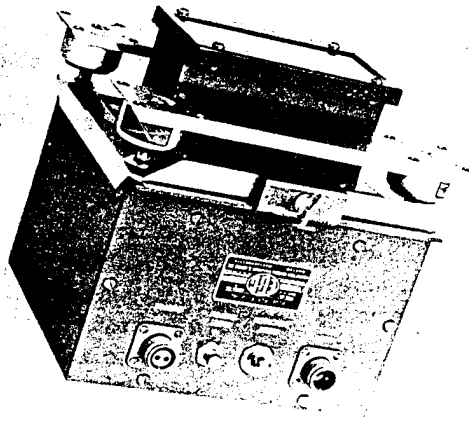


Fig. 2.19 Blue-box Fiducial, Type A-2

bomb on the one hand and the airplane limitations on the other.

Since the overpressure at a point rises almost instantaneously from zero to maximum, it was necessary that the measuring and recording equipment have extremely fast response. Other factors of paramount importance in the design of this recorder were the elimination of reflection effects of the wave itself, the reduction of noise from the airplane forward velocity and from the propellers, and the width of scale necessary to detect and evaluate the pressure accurately.

2.5.1 System

In view of the complexity of the problem it was decided that the peak-overpressure measurements would only be made on a few airplanes and that restrictions on size and weight would be kept to a minimum. A response frequency of 100 kc was selected as a reasonable response, with a desired response of 250 kc if possible. By this selection of top frequencies the possibility of zero frequency response (or static pressures) was practically eliminated. A low frequency of 20 cps was accepted.

In order to reduce interference from reflections from the airplane and to reduce the pickup of propeller noise, it was decided to mount the sensing element of the system on a cylindrical boom ahead of the airplane. The sensing crystal was located approximately 10 diameters of the crystal behind the tip of the boom in order to reduce pressure fluctuations due to turbulent flow around the boom. It was so located that the surface of the crystal was parallel to the expected line from the blast in order to reduce the reflection effects from the boom itself. The crystal was located approximately 6 ft ahead of the nearest projection of the airplane.

A preamplifier for the crystal was mounted within the boom immediately behind the crystal in order to reduce the length of the high-impedance cable required to connect the crystal to the recording equipment. This preamplifier was used as an impedance-matching device so that low-impedance connecting line could be used from the preamplifier to the recorder in order to reduce the signal attenuation and the noise pickup of the wiring. The output of the preamplifier was applied to a dual-beam oscilloscope which had been modified to have the required

sensitivity and frequency response. A dual-beam oscilloscope was used in order to provide sufficient scale width to ensure adequate, yet accurate, measurement of peak pressures. The two amplifiers for the oscilloscope were arranged so that full-scale deflection could be selected and preset on either beam to correspond to pressures ranging from 2.5 to 40 psi. This arrangement allowed one beam to be set up as a safety scale to ensure obtaining pressure readings from any phenomena that might cause off-scale deflections of the sensitive beam. The record of the beam deflections was made on a continuous (no shutter) 35-mm camera. The recording camera was started at T_0 from the air-borne blue box (see Sec. 2.4). Sufficient film was provided for approximately 5 min of recording. Timing marks were provided on the film from a time-pulse generator built into each piece of equipment. Time marks could be selected from the 10-cps generator in the equipment or from the 100-cps output of the time decoder in the aircraft (see Sec. 2.4). For the latter instance, the time-pulse generator was triggered by the 100-cps sine-wave output of the time decoder. This sine wave was interrupted once every second and thereby provided a master time indicator each second along with the 0.01-sec marks. A block diagram of the high-frequency pressure-recording system is shown in Fig. 2.20.

2.5.2 Calibration

Each system had a calibrating circuit built into it. A square wave of voltage of constant amplitude was impressed across the crystal element. This voltage furnished a signal through the preamplifier into the oscilloscope equivalent to that generated by a rapid pressure change of approximately 6 psi. Each system was calibrated by use of a shock tube. The crystal sensing element of each unit was installed in the test section of the shock tube and was subjected to a series of shock waves of known overpressure. The records of these shock waves were compared to that of the fixed calibrating signal to obtain a calibration curve for each system in terms of overpressure versus the ratio between trace deflection due to pressure and trace deflection due to the calibrate signal in per cent. The calibration curves are presented in the appendixes (not reproduced

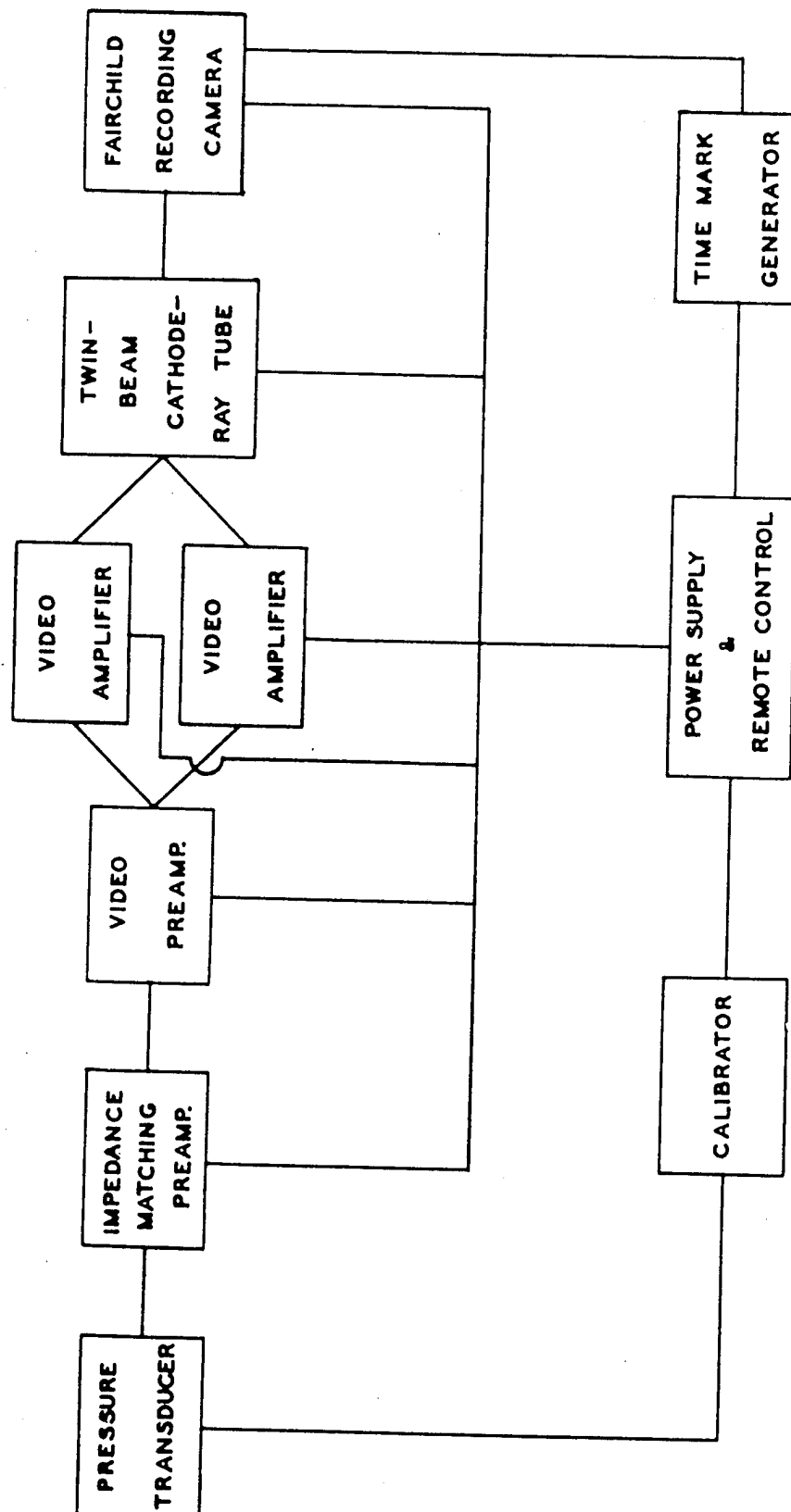


Fig. 2.20 Block Diagram of High-frequency Pressure Recorder

here; see page iv), along with the other calibration curves for each airplane concerned.

The shock tube used was one built by the Commonwealth Engineering Co. from plans of a similar shock tube developed and utilized by the Ballistic Research Laboratories, Aberdeen Proving Ground, Md. Basically, it is composed of a compression chamber separated from a long, open expansion chamber by a thin replaceable diaphragm. Shock waves were initiated by charging the compression chamber with compressed air to a predetermined pressure and then rupturing the diaphragm. The rate of travel of the shock wave was determined by measuring the time of its travel between two fixed points in the expansion chamber with a high-speed electronic counter. The overpressure of the shock wave was computed by relating its velocity to that of the speed of sound in free air at the same temperature.

$$\frac{u}{a_0} = \left(\frac{7 + 6z}{7} \right)^{\frac{1}{2}} \quad z = \frac{P - P_0}{P_0} \quad (2.1)$$

where u = velocity of shock wave

a_0 = speed of sound

P = pressure in shock wave (psi abs)

P_0 = atmospheric pressure (psi abs)

The overpressure in the shock wave can also be related to the compression-chamber pressure. If it is assumed that the air in the compression chamber is allowed to reach ambient temperature so that the temperatures on both sides of the shock front will be essentially equal, the following relation will hold:

$$\frac{P_c}{P_0} = \frac{Y}{\left(1 - \frac{Y-1}{\sqrt{7(1+6Y)}} \right)^7} \quad (2.2)$$

where P_c = compression-chamber pressure (absolute)

P_0 = expansion-chamber pressure (absolute)

Y = ratio of pressure in shock wave to expansion-chamber pressure, or
 $Y = P/P_0$

The transfer-function curve (Fig. 2.21) for calibration of the high-frequency pressure recorder was evolved from Eq. 2.2.

Accuracy of the equipment was determined by repeatability to be well within 5 per cent of full

scale. The noise level of the equipment was equivalent to approximately 0.05 psi. This noise was due to actual pressure variations plus the electrical noise inherent in this type of electronic equipment.

2.6 SENSING INSTRUMENTS

2.6.1 Airspeed and Altitude Gauges

The gauges used for determining the airspeed and the altitude of each test aircraft were the Statham Laboratories Model P-69 pressure transducers with a nominal resistance of 350 ohms. These transducers were connected to a pitot-static system installed on the right-hand side of the fuselage so as to correspond with the standard pitot-static system on the left-hand side of the fuselage. The altitude gauges were absolute-pressure transducers in the range 0 to 15 psi, while the airspeed gauges were of the differential type, in the ranges of ± 1.0 and ± 3.0 psi, depending upon the cruising speed of the test aircraft. One altitude transducer and one airspeed transducer were used with each set of recording equipment, local recorder and telemetering, in the QB-17 drones. Individual transducers were used with each recording medium in order to obtain greater sensitivity in the measurement of these functions. In the QT-33 drones space did not permit the dual installation, and in the manned airplanes it was not required since only local recording was used.

The P-69 pressure transducers offered a simple means for the conversion of pressure into electrical units for recording and telemetering purposes. Pressures applied to the transducers were translated into an electrical equivalent by means of a complete strain-gauge bridge of the unbonded resistance-wire principle. This method is linear, accurate, simple, and rugged. The acceleration response is less than 0.1 per cent of full scale per gravity (g) unit up to 10 g in any axis. Each transducer was individually temperature-compensated over the range -65 to $+250^\circ\text{F}$, and zero shift with temperature was specified to be not more than 0.01 per cent of full scale per degree Fahrenheit.

2.6.2 Accelerometers

The gauges used for determining the accelerations (normal and transverse) at various po-

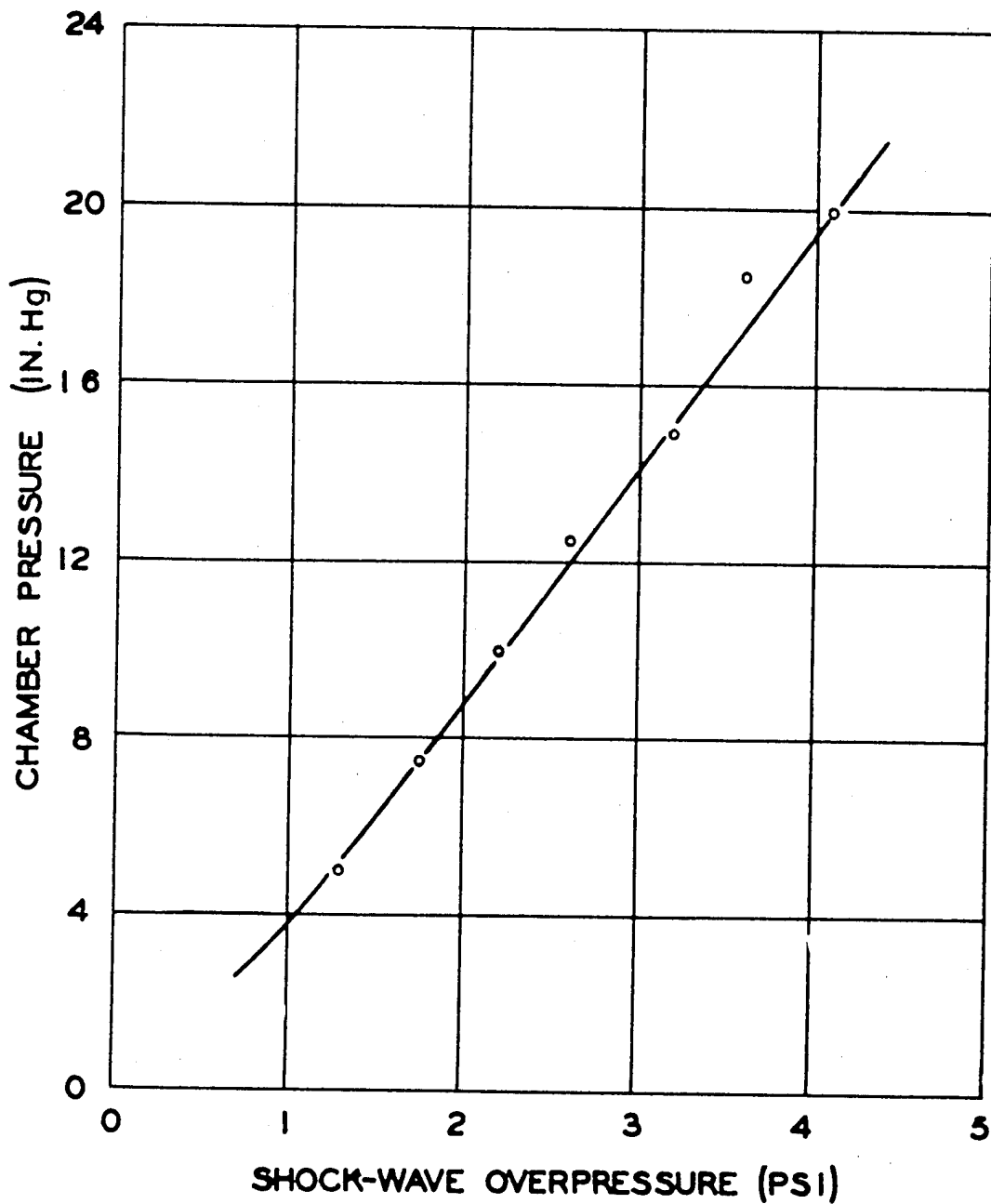


Fig. 2.21 Transfer Function for Shock Tube Used to Calibrate High-frequency Pressure Recorders

sitions in the test aircraft were the Statham Laboratories Models C and A-18 accelerometers with a nominal bridge resistance of 350 ohms. These accelerometers were used in ranges of ± 6 and ± 12 g and were mounted on specially designed brackets located in the required positions (locations of the various accelerometers in each type airplane are contained in Chap. 3). The range in which the accelerometers were used was dependent on the accelerations expected at the particular locations on the test airplanes. One accelerometer was used at each location, and the intelligence was furnished to both the local recorder and the telemetering.

The Statham accelerometers consisted of a mass-and-spring combination housed in a small, lightweight, rugged case. When the case was shaken, relative movement between the mass and case was produced. This relative displacement was translated into an electrical equivalent by means of a complete strain-gauge bridge of the unbonded resistance-wire principle. The accuracy and linearity of these gauges were approximately 1.0 per cent of full scale, and the response to transverse acceleration was less than 1.0 per cent. Each accelerometer was individually temperature-compensated over the range -65 to $+250^{\circ}\text{F}$, and the change in zero output was not greater than 0.01 per cent per degree Fahrenheit.

2.6.3 Elevator-position Indicator

Elevator-position indicators were used for determining the pitching tendency of the test airplanes. The indicators were designed as a cantilever beam and cam arrangement, the design being dependent upon the physical arrangement and size of the elevator mechanisms of the various types of aircraft. The cantilever beam was fitted with Baldwin-Southwark SR-4 Type A-13 strain gauges at the root and interconnected to produce a complete bridge sensitive only to bending. The beam was rigidly mounted to the structure of the aircraft, and the cam was mounted to the elevator torque tube. Upon rotation of the torque tube to produce a certain deflection of the elevator, the cam imparted a certain deflection to the cantilever beam, unbalancing the strain-gauge bridge and providing the recording equipment with an electrical signal proportional to the angular deflection of the elevator.

2.6.4 Strain Gauges

The Webster-Chicago tape recorder and the Melpar telemetering system were designed to be used in conjunction with sensing instruments having an effective resistance between 300 and 500 ohms. All strain gauges used on test aircraft were Baldwin-Southwark SR-4 Type A-13 gauges with a nominal resistance of 350 ohms. These gauges were selected because they are small and thermally stable and were known to be very reliable from previous experience in their use.

From Operation Sandstone it was known that the climatic conditions at the test site would have an adverse effect on strain gauges which were not given a protective coating. A contract was awarded to Purdue University to investigate commercial strain-gauge adhesives and protective coatings when subjected to high temperatures, high humidity, and salt spray. From the tests conducted by Purdue University it was determined that gauges cemented with General Radio cement and protected with a coating of Petrosene wax would endure the conditions of high temperature, high humidity, and salt spray better than other combinations of adhesives and protective coatings tested. All strain gauges installed in test aircraft were installed with these materials.

The function and location of the various strain-gauge bridge circuits for each type of aircraft are shown in Chap. 3.

2.6.5 Pressure Transducers

A long and extensive search was made for adequate pressure transducers to measure the overpressures encountered by the aircraft. Both AMC and Webster-Chicago attempted to determine the best available pressure transducer to be utilized in conjunction with the local recorder and the telemetering system. It was originally intended to use purely resistive-type sensing elements with an output directly proportional to the imposed pressures so that no electrical phase-shift problems would exist when the element was employed with a phase-sensitive recording system. These requisites were made known to several leading instrument manufacturers. Several prototypes were constructed and tested, but a gauge satisfying all the requirements could not be constructed at the deadline for awarding a contract. The gauge

best fulfilling the instrumentation requirements employed a variable-reluctance-type element and necessitated the use of an electrical coupling unit to avoid any objectionable phase variation. These gauges, Types 3PAD10W and 3PAD10S, were manufactured by the Wiancko Engineering Co., Alhambra, Calif. Owing to the characteristics of the reluctance-type gauges, it was impossible to supply intelligence to the local recorders and the telemetering system simultaneously. This fact made individual transmitters necessary for each system. These transducers were of the differential type capable of measuring pressures to ± 10 psi. The response was flat to within ± 3 per cent up to 500 cps, with a maximum rise time of 0.7 msec to 90 per cent of the full-scale output.

2.7 RADAR-DATA RECORDERS

In order to relate induced load to airplane location, it was required that an accurate time-correlated record be made of the position of the test aircraft at the instant the load was applied. To accomplish this, a radar-data recorder was developed for use with the MSQ-1 tracking system to make once every $\frac{1}{10}$ sec a film record of the data available at the MSQ-1 radar set.

2.7.1 System

The radar-data recorders were located at each of the four MSQ-1 radar sites. One additional set was available as a spare.

The function of the data recorder was to provide a time-correlated record of the radar slant range and antenna azimuth and elevation angles. The end product, or output, of this recorder was a length of 35-mm film with its latent image of the recorded data. The trajectory data may therefore be used at any later time to determine the exact position of the tracked aircraft. The location of each MSQ-1 radar was determined by means of a very accurate geographical survey.

The radar tracking system tracked the two B-17 drones and two T-33 drones from the time they were released by the mother aircraft until the data had been collected. It was extremely important that the exact position of these aircraft be known at any time during this interval. It was expected that these aircraft

would be located within 300 ft of the desired location at time T_0 as a result of using the MSQ-1 tracking system.

After control of the drones was returned to the mother aircraft, the MSQ-1 tracking system was able to track other aircraft whose positions in space needed to be accurately determined. Two such aircraft were the B-50A's of Project 4.6. Since there were four MSQ-1's being used, two of these radar sets were available for tracking any other aircraft which were equipped with beacons.

2.7.2 Description of Equipment

The radar-data recorder was divided into two functional units which were panel-mounted in cabinets. These two functional units were the range console and the servo console, as shown in Fig. 2.22. The range scope and included circuitry were mounted in the left cabinet (range console), and the data mask with its servo-driven dials and associated circuitry was mounted in the right cabinet (servo console). The recording camera was mounted at the edge of the servo console, as shown in Fig. 2.23, so that approximately half its field of view included the range scope, and the remainder included the mirrored image of the data mask, which was recessed 5 in. inside the servo console.

The range console consisted of a range-indicator unit which contained the cathode-ray tube that presented the fine range data. A range unit was included to provide pulse intensification, sweep generation, range-marker generation, and video amplification. A time-synchronizer unit was included which consisted of a free-running multivibrator producing 10 pulses per second capable of being synchronized with 1 pulse per second from an external source. Power and voltage-regulator units were included to provide power and voltage regulation to the above units.

The servo console consisted of a data-indicator unit which contained the coarse range and antenna azimuth and elevation dials. A servo-amplifier unit included the necessary selection and amplification of error signals such that the output of the servo amplifier was of the proper magnitude and phase for driving the servomotor in the data-indicator unit. A power unit was included to supply power to the above units.

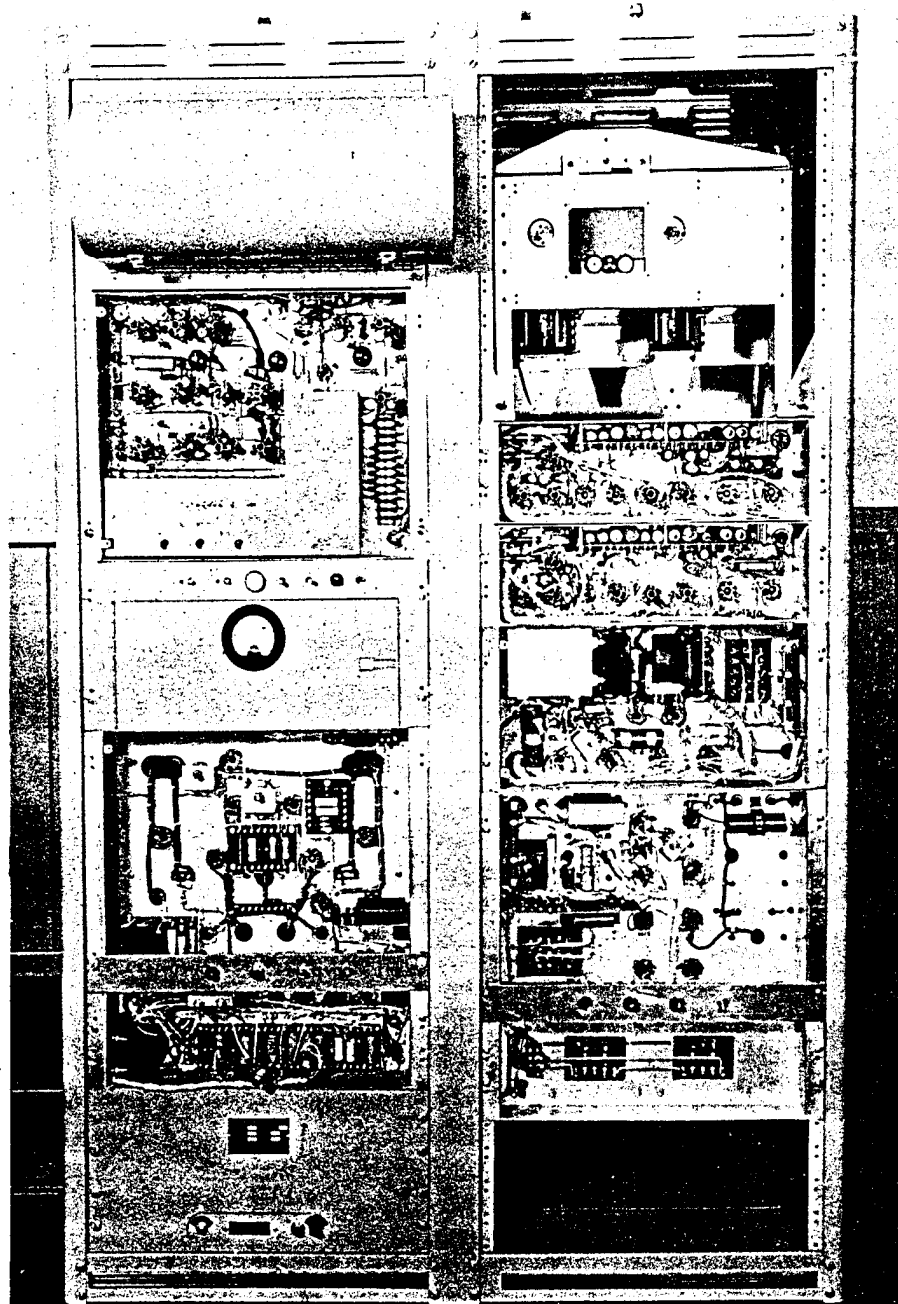


Fig. 2.22 Radar-data Recorder

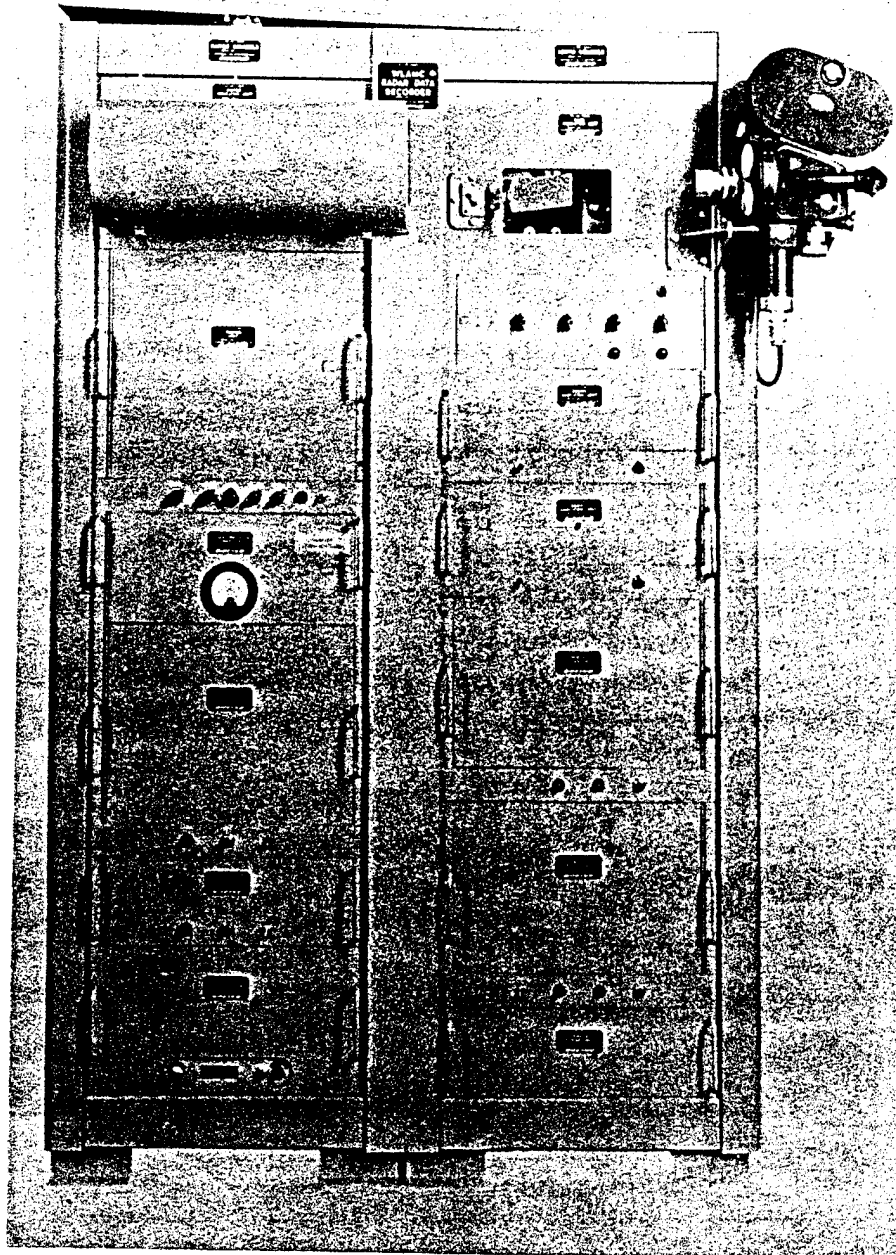


Fig. 2.23 Radar-data Recorder with Camera in Place

2.7.3 Theory of Operation

The radar-data recorder was used in conjunction with the MSQ-1 radar to determine airplane trajectory data by providing a time-correlated record of the radar slant range and antenna azimuth and elevation angles at a sampling rate of 10 per second. The sampling rate was controlled from a self-contained timing system which was synchronized with an external source of timing signals at a rate of 1 per sec. For accurate timing of the recorded data, an external source of accurate time signals was required. Such a source was available from the timing system used in the operation (see Sec. 2.4).

Recording of data was accomplished by means of a continuous-strip 35-mm movie camera. The camera was a USAF Type A-5 (Cineflex) camera which had been modified for continuous-strip close-up operation. This camera photographed a cathode-ray tube displaying the range information and indirectly photographed, through a mirror, a data mask that framed the coarse range and angle dials, operational indicators, and second counter. The translucent dials were pulse-illuminated from behind by a flash lamp triggered by timing signals at a rate of 10 per second. The light pulses were 0.1 to 0.2 msec in duration, which was short enough to eliminate blurring on the continuous-strip film. The range scope (cathode-ray tube) was pulse-intensified in coincidence with the flash lamp.

Recording of the slant range of the radar was accomplished by means of a coarse and a fine presentation. The coarse range was presented by two synchro-driven dials, a small one overlaying the larger, both mounted on concentric shafts with the unit being located behind the data mask. The smaller dial displayed twelve 100,000-ft increments; the larger dial displayed a hundred 1,000-ft increments. Fine range was presented by a cathode-ray tube displaying a selected 5,000-ft portion of the slant range of the radar, including the video signals, and with the addition of sawtooth-shaped markers accurately spaced at 1,000-ft intervals. The 1,000-ft range markers provided reference and calibration marks and facilitated film-reading ease and accuracy. These 1,000-ft range markers moved in synchronism with the 1,000-ft divisions on the range dial. When a target was being tracked quite closely,

the video signal of the target remained stationary with respect to the 5,000-ft sweep, and the 1,000-ft range markers moved past the video signal of the target at a rate dependent upon the radar range-tracking rate. At any instant the range of the target was determined by measuring the range of the video signal from the nearest range-marker value.

The azimuth and elevation-angle information from the radar antenna was presented by two high-performance servo systems, each driving two translucent concentric dials mounted behind the data mask. The smaller one-speed dial was graduated in 10° increments; the larger 36-speed dial was graduated in 0.05° increments, easily readable to 0.01° . The performance of the servo system was such that the angle dials followed the movement of the radar antenna to an accuracy of better than $\pm 0.02^\circ$.

Timing of the recorded data was accomplished by means of a magnetic counter operated by the external time signals received from the time reference generator of the timing system. This counter, which was mounted behind the data mask, had three translucent dials, each reading from 0 to 9 and permitting an elapsed time count of 999 sec. Timing of the individual frames on the film was inherent with the illumination system of this recorder, in which the cathode-ray tube was pulse-intensified and the dials were pulse-illuminated at exactly 0.1-sec intervals.

Provision for the timing of the various operations was made through the use of shutter- and lamp-type operational indicators. Closure of a remotely actuated switch operated these indicators and displayed the time of their operation on the film. Two shutter-type indicators were available which, when operated, opened a shutter on the data mask and permitted light from the flash lamp to shine through the data mask. Since the flash lamp operated only every 0.1 sec, the timing accuracy of these shutter-type indicators was limited to a maximum error of ± 0.10 sec. Three lamp-type operational indicators were located on the front of the data mask. They could be operated at any time, irrespective of the 10-per-second flash lamp, and thus permitted the timing of an operation of the moving film to a higher accuracy than that for the shutter-type indicator. It was anticipated that these lamp-type indicators would be used to indicate when the magnetic

counter had gone through 999 counts (16.7 min).

The timing system incorporated in the radar-data recorder was based on the use of an external time-signal system which supplied pulses once each second. The pulses arrived on an open two-wire line, and during the 30-msec duration of the pulse the wire line was shorted. These timing pulses were used to operate the seconds counter and to synchronize the self-contained 10-per-second time pulses generated in the time-synchronizer unit. The seconds counter was a modified Veeder-Root magnetic counter, and the time-synchronizer unit consisted of a free-running multivibrator with a repetition rate of 10 per second. The synchronized 10-per-second pulses were used to operate the flash lamps which illuminated the translucent dials of the data-indicator unit.

2.7.4 Reading Radar Data

An illustration of the data presentation as recorded by the camera is shown in Fig. 2.24. The upper half of the frame presents the range scope as photographed directly by the camera, and the lower half presents the data mask as photographed from the mirror. The dial lettering and range-scope sweep appear normal when viewed directly by the operator. Reversion of the mirrored image of the data mask, as recorded by the camera, is compensated for when analyzing the film by placing the film upside down in the Recordak or projector and reading the range-scope trace in the reverse of its normal direction. The sketch in Fig. 2.24 of the presentation of the camera is shown with the film in this manner. The azimuth and elevation dials each consisted of two concentric dials and were marked accordingly. Identification of the 1,000-ft range markers on the range scope was provided by two concentric translucent dials, the larger dials being marked in 1,000-ft intervals to 100,000 ft and the smaller dial being marked in 100,000-ft intervals to 1,200,000 ft. These dials with their triangular indices were located directly under the range-scope trace. The five divisions in view through the window in the data mask (see Fig. 2.24) correspond to the five range markers shown in the scope trace. In the sketch shown, the radar echo is at a distance of 226,330 ft (the sweep travels from right to left on the projected image of the film because of the afore-mentioned image rever-

sion). Time identification was provided by the counter dials which appear in the three windows at the bottom of the frame. The counter dials indicated time from the start of recording in seconds and thus advanced one digit every 10 frames. The two shutter-type operational indicators were located near the center of the data mask and permitted light to shine through the cut-out letters (A and B) when the individual shutters for each of the windows were actuated by solenoids. Three lamp-type operational indicators were located near the edge of the data mask: No. 1 at the upper left was identified by a large circle, No. 2 at the upper right was also identified by a large circle, and No. 3 at the lower left was identified by a small circle.

2.8 TEMPERATURE SURVEY INSTRUMENTS (TEMP-TAPE)

At a late stage in the development of the instrumentation for the drones it was decided that a survey of the skin temperatures would be necessary. An instrument was needed which would allow installation at any convenient time prior to the temperature rise and examination for results at some time after cooling. It was necessary that the temperature sensing instrument operate with no observer or attendant during the test and that it need a minimum of auxiliary instrumentation, power, weight, and space.

An instrument was developed which fulfilled these requirements. Essentially, the device (named "temp-tape") consists of a series of low-melting-point alloys held in place on the adhesive side of a heat-resistant tape strip, the assembly somewhat resembling the familiar Band Aid adhesive bandage. A temperature range of 117 to 511°F was covered in distinct steps of melting points, with a differential of about 20°F.

The final design of the instrument uses two small strips of alloy foil, about 0.0025 in. in thickness, superimposed one on the other. The two strips are sandwiched between two sheets of aluminum foil, or between a sheet of aluminum foil and one of thin paper, and the entire assembly is attached to the adhesive side of a strip of temperature-resistant adhesive tape. The tape serves the dual purpose of holding the foil sand-

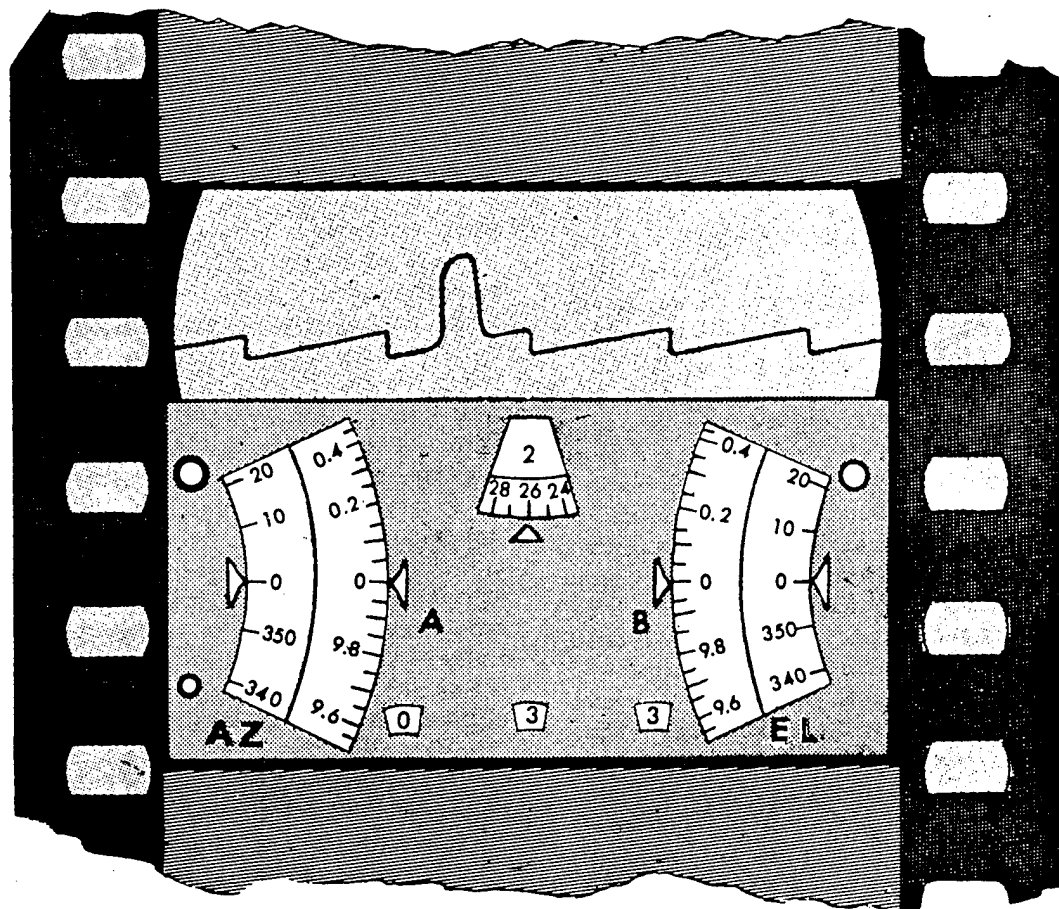


Fig. 2.24 Presentation of Data from Radar-data Recorder

wich together and of allowing a simple method of attaching the foil sandwich to the surface whose temperature is to be measured (see Fig. 2.25).

It was a simple matter to measure the peak temperature of the back side (the side away from the radiation source) of a sheet-metal structure using the temp-tapes. The tape was attached to the surface in a manner similar to that in which a Band Aid would be applied. After the test it was removed, and the protective covering was cut away from the alloy foils. The foils were then examined for melting and fusion, and comparison was made with the calibration curves to determine the peak temperature reached.

2.9 INSTRUMENT PERFORMANCE

The operation of the instruments was acceptable in that data were collected in quantities which are generally consistent with similar flight tests under severe field conditions. It was necessary, however, to modify the details of the planning to alleviate the work load of the operating organization and to account for the malfunction of equipment. Details of the problems connected with the maintenance and operation of the equipment may be found in the report prepared by the Electronics Section of TU 3.4.2. The majority of the problems could be related, either directly or indirectly, to the late delivery of the equipment. Had deliveries been such that the faults in the equipment could have been discovered and corrected through use and that the operating personnel could have gained experience with the equipment, many of the difficulties could have been avoided, or provision could have been made to provide corrective equipment or facilities.

The major problems and difficulties arising from the use of the various items of equipment are here identified for the benefit of those who may attempt another project of this type and magnitude. The most important lesson to be learned from the instrument performance on this project was that service or operational testing of equipment should not be combined with the collection of such important data from tests as strictly controlled as atomic weapons tests must necessarily be.

2.9.1 Recorders

The operation of the recorders was seriously hampered by late delivery. One component, the high-frequency bias generator, was delivered directly to the forward area with no opportunity to check its operation. This component was intended to straighten the calibration curves as produced by the recorder. When the units failed to operate properly, they were discarded, because neither the facilities nor the time were available to investigate or correct the fault. Since it was then necessary to calibrate each channel of each recorder, the arc-tangent function of the playback was also eliminated in order to reduce noise, with a resultant increased complexity of data reduction. This complexity is discussed in Chap. 3. The high-accuracy channels were also discarded because of malfunctions. On the recorders in the manned airplanes it was necessary to modify the channel amplifiers to increase the sensitivity. The problem of expansion and contraction of the recording tape with variations in atmospheric humidity was never satisfactorily solved. This problem was discovered in the brief low-temperature test at the aircraft laboratory, but time did not permit a thorough investigation. As a stopgap solution the width of the spools was increased to permit room for expansion and to prevent wrinkling of the tape under conditions of high humidity. However, under low humidity the tape did not fit the spools and the resultant lateral motion of the tape seriously complicated the problem of playback. Other minor problems with the recording equipment are discussed in the report prepared by TU 3.4.2; however, the equipment did operate, was calibrated, and did collect data.

2.9.2 Telemetry

Generally, the operation of the telemetry was unsatisfactory. Many factors contributed to the failure of this equipment, and these factors are discussed in detail in the report prepared by TU 3.4.2. Of these factors two predominate: tracking or coordination with the radars and loss of signal at the critical time.

The problem with tracking arose from the lack of proper landlines. The requirement for the landlines was submitted to TG 3.4 on Aug. 8, 1950, and again on Nov. 10, 1950. When

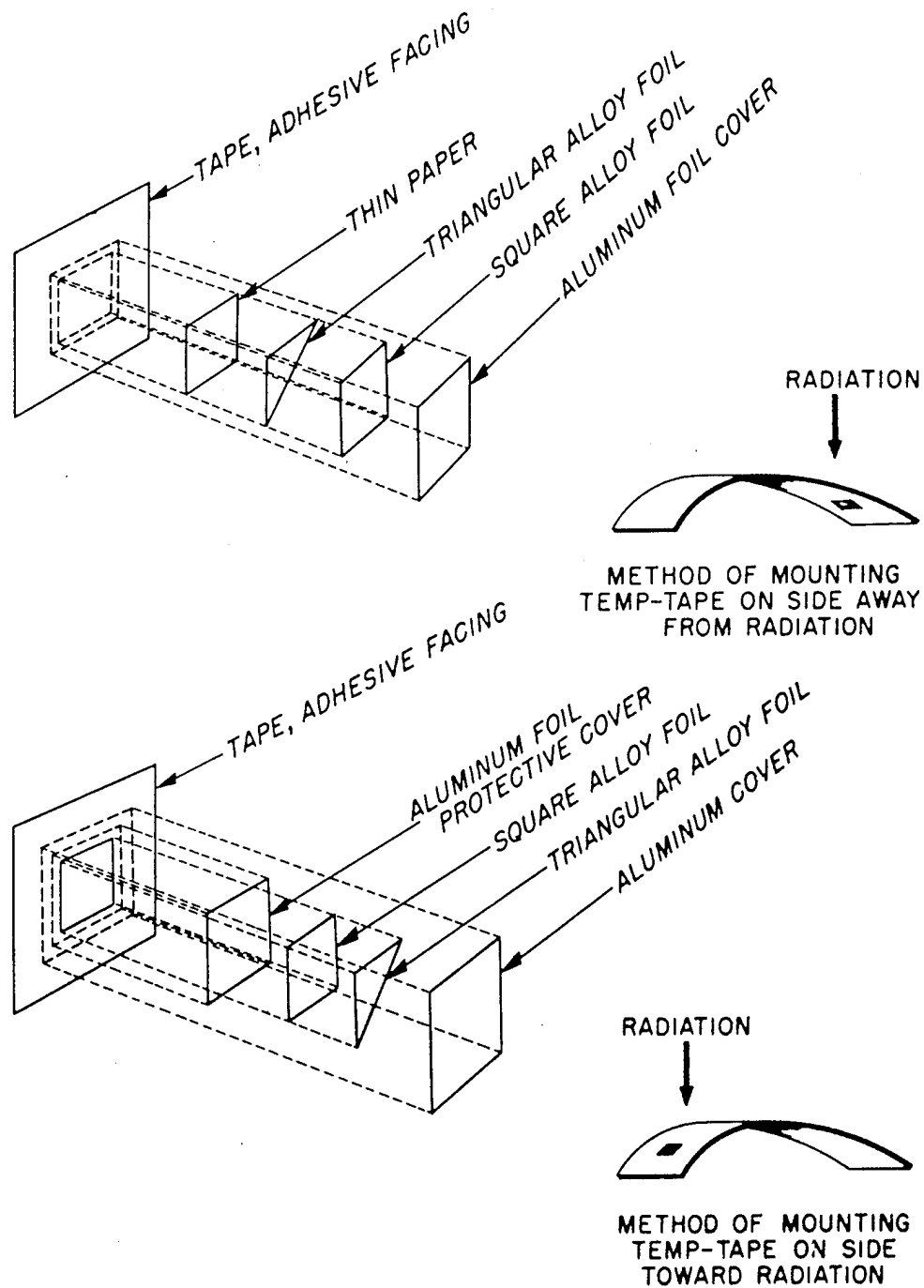


Fig. 2.25 Assembly and Application of Temp-Tapes

the organization moved into the forward area, about Feb. 15, 1951, the only indications of planning for landlines were the messenger cables on which the conductors were to be strung. This situation existed to some degree up to the time of Dog shot, when, through a determined effort, conductors were strung by Lieutenant Lusk of the AACS contingent. These conductors were made of odds and ends of wire collected at the last minute from all over the South Pacific area. They were wholly unsatisfactory because of open circuits from hasty splicing and low-resistance shorts from scraped or broken insulation or from moisture. The tracking system was proved to be workable by an improvised hookup with the radar set which was adjacent to the telemeter-receiver station but which was not usable because of the absence of adequate landlines.

The loss of signal at the critical time has been attributed to one or more of several possible causes. The first suggestion was microphonics or shock response of the transmitter-multiplexer. However, this explanation appears to be improbable because the equipment was tested to 15 g during vibration tests, and the loss of signal occurred on fighters and bombers alike with no apparent relation to the magnitude of shock encountered. Another explanation involves the change in density of the air at the shock wave and the reflection or diffusion of enough of the transmitted signal to weaken the received pulses below usable level. This theory may have merit since the shock wave is of such a nature as to reflect radar waves, which are only 500 Mc above the telemeter frequencies, and to present a picture on a radar screen. It is expected that considerable effort will be spent on the telemeter to improve the operation.

2.9.3 Timing and Synchronization

The timing signals operated essentially according to plan. It was necessary that the radio receiver used for the timing signal in the B-17 drones be changed from SCR-522 to the AN/ARC-3 standard vhf communication receiver because of the level of the noise in the older equipment. The operation of the coder was complicated in some of the airplanes by the necessity for providing starting signals for other equipment. Had these requirements been

foreseen, sufficient contacts and/or relays could have been provided.

The operation of the blue-box fiducial marker was generally satisfactory. This equipment was checked prior to each test by using a photoflash bulb. On several occasions this equipment operated prematurely owing to electrical impulses from the aircraft power supply. This premature operation was remedied by preflight checkout procedure.

2.9.4 High-frequency Pressure Recorder

The operation of the high-frequency pressure-recording systems was adversely affected by late delivery. The recording systems were delivered directly to the forward area where they were installed and calibrated. There was insufficient time to perform adequate operational checks on the equipment in order to find and correct all defects incidental to assembly (cold-soldered joints, loose connections, microphonic tubes, etc.) before it was installed or to make full-scale operational checks of the systems in flight with all other associated equipment in operation. As a result, there were some control-circuit malfunctions when all the air-borne equipment was operated simultaneously that were not indicated upon operation of individual systems. This factor prevented the operation of some of the high-frequency recording systems until the difficulties could be overcome.

Two other factors contributing to malfunctioning of the equipment were the collection of moisture, as a result of incessant rain, and the manual operation of the recorders in manned aircraft by untrained personnel. Manual operation of the systems was not contemplated; therefore personnel had not been assigned and trained for that function.

In one instance (B-17 drone Doris, Easy shot) recorded data were obscured by exposure of the recording film to radiation when the airplane flew through the radioactive cloud. The high-frequency recording systems did record some data, and, although the techniques of recording the overpressures encountered in an airplane passing through a shock-wave disturbance are very difficult, these data agreed very closely with theoretical values which were predetermined for the particular aircraft locations in space.

13 ~~SECRET~~

An example of a section of the record from the high-frequency pressure recorder is presented in Fig. 2.26, along with a calibration record and pictures of a typical installation.

2.9.5 Sensing Instruments

In general, the operation of the resistive-type gauges was satisfactory. The Statham accelerometers and pressure gauges operated, with few exceptions, without malfunction. The strain-gauge operation was very reliable; however, installation techniques should be improved to simplify installation, maintenance, and operation. The operation of the reactance-type pressure gauges was not reliable because of numerous shorts which occurred at the connecting terminals. These shorted currents, which were caused by poor design and moisture, affected the balance of the gauge. Calibration of the pressure gauges was difficult because of the complexity of the electronics equipment necessary to make the reactance gauge appear resistive to the recording systems.

2.9.6 Radar-data Recorders

In general, the operation of the radar-data recorders was satisfactory, and excellent correlations with the reports by the controlling pilots were obtained. Some difficulties arose in the early missions because of inexperience with the equipment and the photographic techniques. Only one record was lost by physical failure of the equipment: loss of the range indicator on Alice position on Dog shot. The "jitter" in the scales made analysis of the records somewhat difficult. Analysis of the elevation record was particularly difficult because the changes in elevation, which were small, were obscured by the jitter of the scale. The changes in azimuth were relatively large and continuous so that the jitter could be averaged out during the analysis.

One desirable improvement in the radar-data recorder would be the addition of a marker which would indicate the passage of the shock wave past the airplane. Conceivably this could be done by means of an indication from the

radar beacon in the test airplane and could be marked on the radar record.

2.9.7 Aircraft Installation

Making a complete aircraft instrumentation installation of this nature presented many problems. The modifications of aircraft were leading the development of equipment; therefore many revisions of the installations were necessary as the physical configuration of the equipment changed. Many of these revisions and modifications had to be performed in the forward area, and this fact created additional problems. The telemetering wire used was hygroscopic, and the wire-to-wire resistance changed with the humidity, which made it rather difficult to keep a balanced line for use with bridge-type networks. The wire was also rather fragile, and, where considerable handling was necessary (such as at the plug into the recorders), many shorted and opened circuits were created. Accessible test points on the aircraft telemetering wire at the equipment positions would have greatly assisted the maintenance and trouble-shooting of the telemetering wire and sensing elements.

Figure 2.27 illustrates the installation of the recording and control instruments at a single point where possible. The installation shown was made in a B-50D airplane, and a seat for the instrument engineer is shown in the foreground. The amplifier units for the local recorder are mounted on the table, and the control switches can be seen against the wall behind the amplifiers. The plug-in panel for the connection of the particular strain-gauge bridges was mounted directly above the amplifiers. The valve which controlled the venting of the reference pressure (see Sec. 3.4.1) is shown just behind the right-hand edge of the seat, below the oxygen control. Figure 2.28 is a view of the equipment mounted under the table shown in Fig. 2.27. The Wiancko coupling units (see Sec. 2.6) were mounted in a row against the rear bulkhead, and the timing decoder (see Sec. 2.4.2) is shown on the left-hand side of Fig. 2.28.

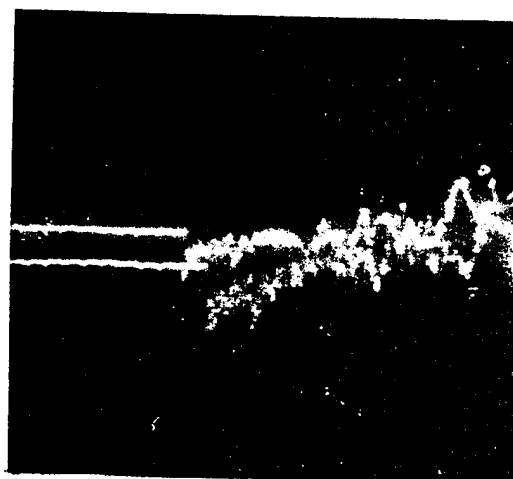
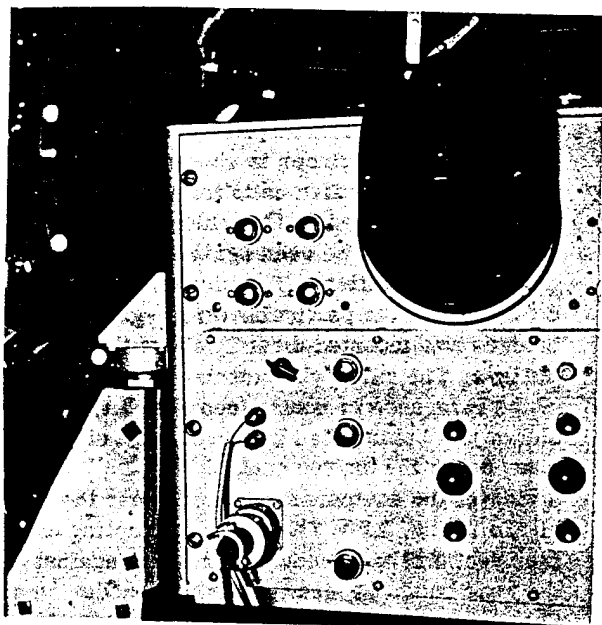
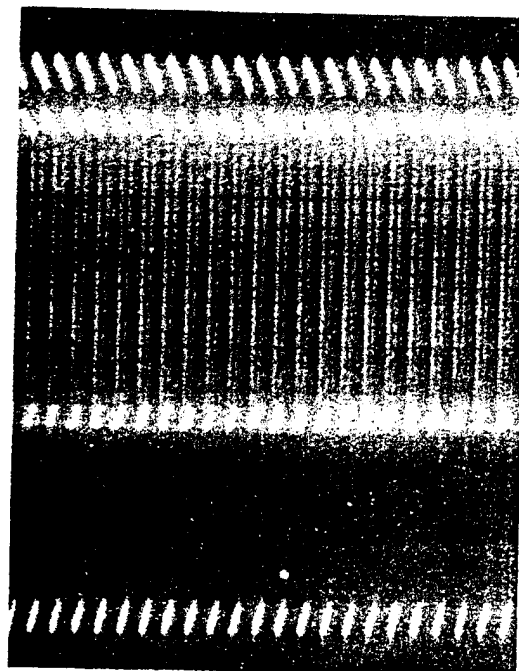
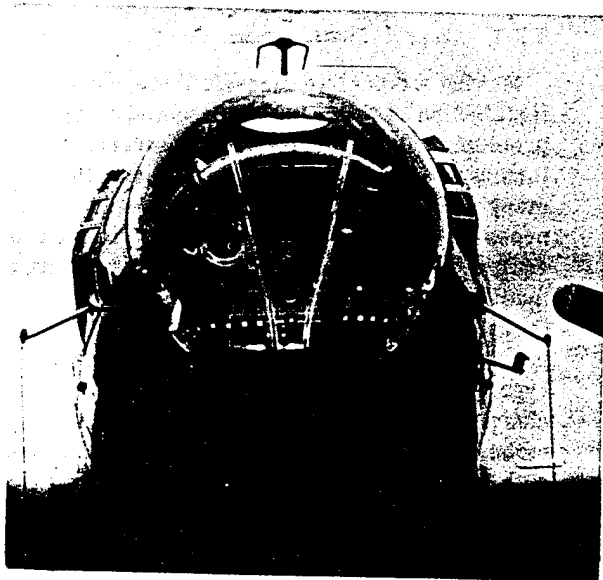


Fig. 2.26 High-frequency-pressure-recorder Installation and Sample Records. (Upper left) probe installation. (Lower left) recorder installation. (Upper right) sample record of calibration. (Lower right) sample record of high-frequency-pressure variation.

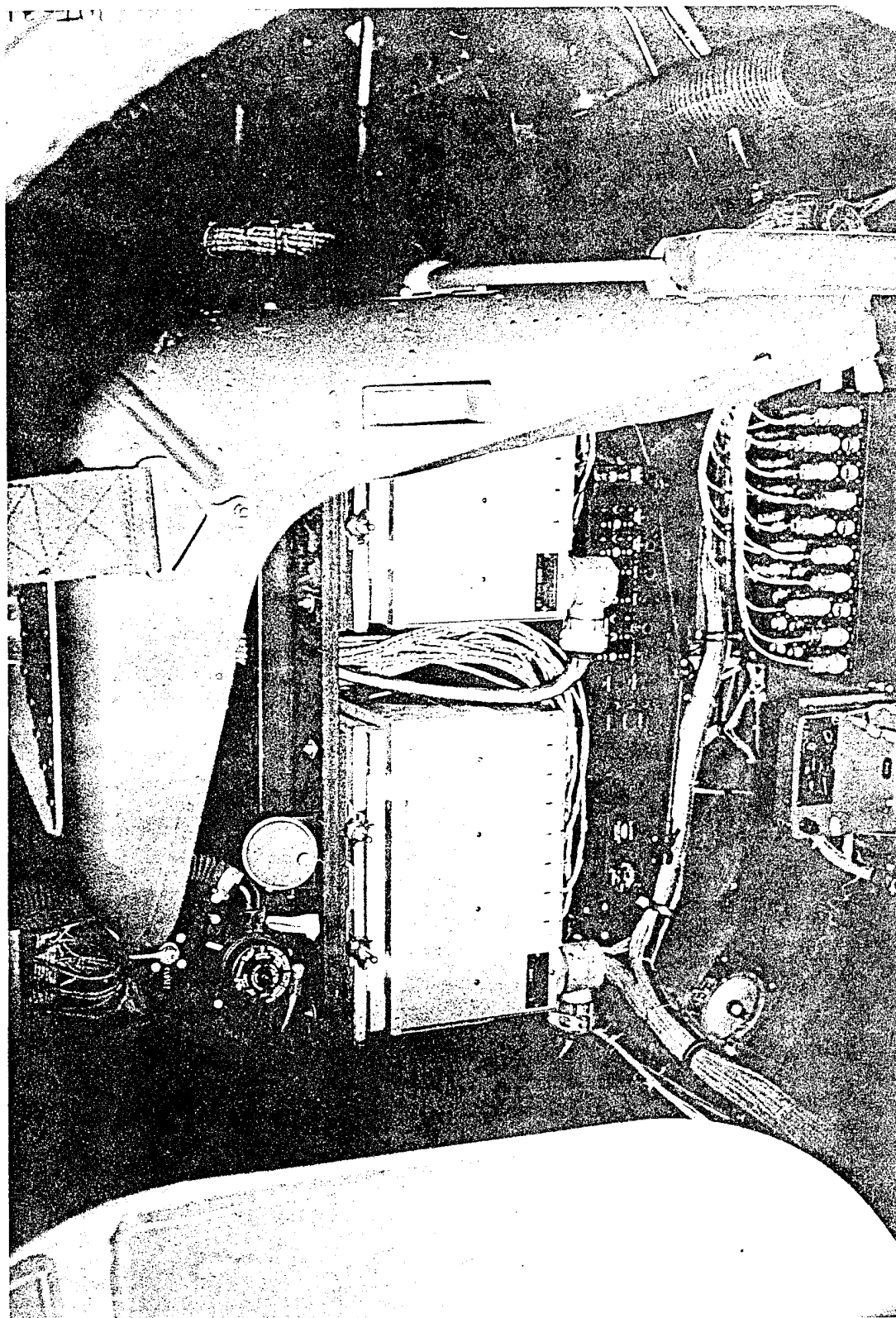


Fig. 2.27 Typical instrument-engineer's Control Station

SECRET

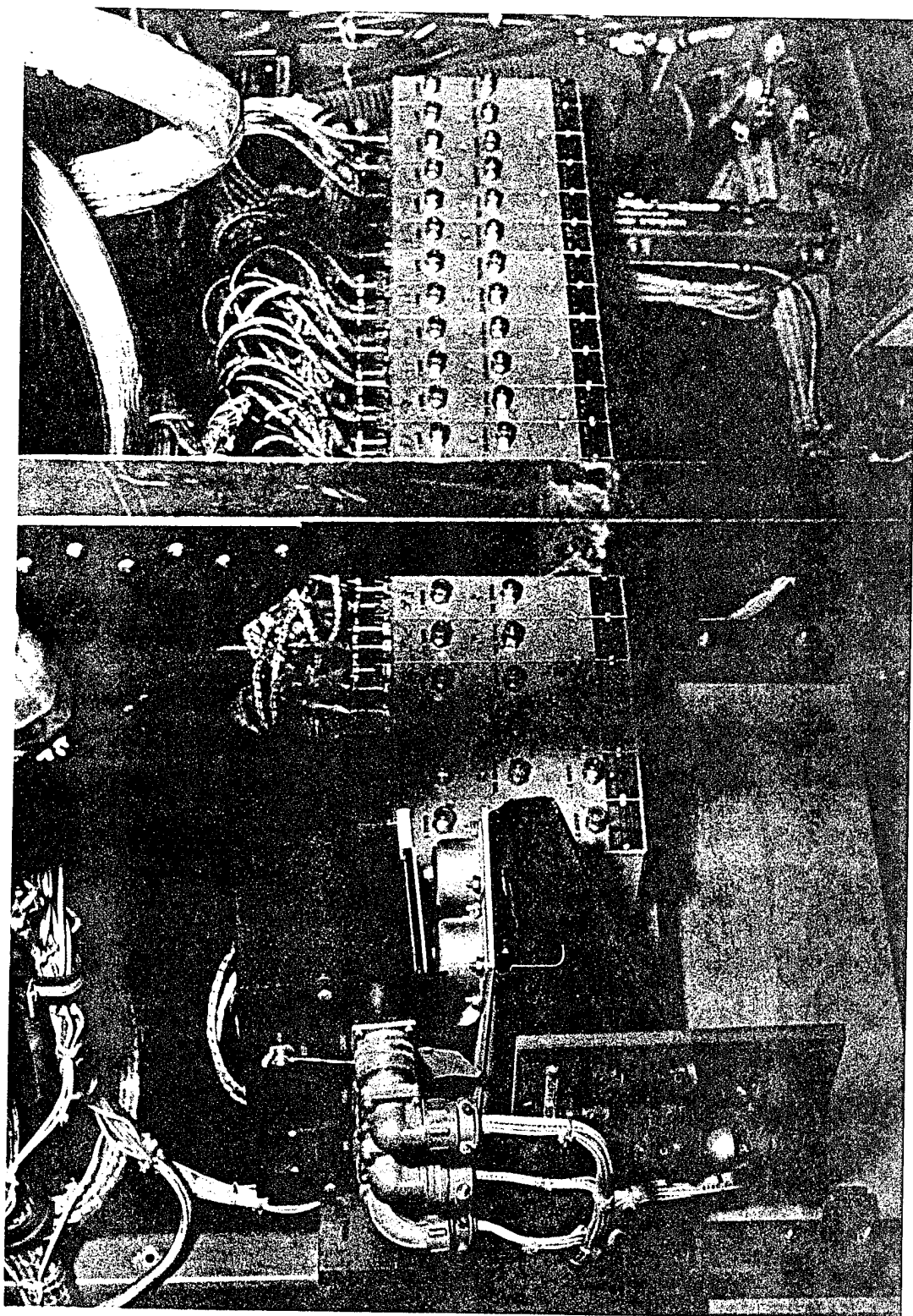


Fig. 2.28 Installation of Equipment below Table at Instrument-engineer's Station

Chapter 3

Airplane Preparations

3.1 INSTRUMENTATION

The preparation of the airplanes to accomplish the mission of Project 8.1 required the combined efforts of several Government agencies and private contractors. The selection and arrangement of the instrumentation, the supervision of the development of the recording equipment, and the detailed engineering on installation and interconnection of the instrumentation were performed at Headquarters Air Materiel Command (Hq AMC). The Class A instrumentation parts and provisions were installed in the test airplanes at either the Wright-Patterson Air Force Base, the Middletown Air Materiel Area (MAMA), the Sperry Gyroscope Co., or the Boeing Aircraft Co. The installation, maintenance, and operation of the instrumentation were performed by ATU 3.4.2.

The basic instrumentation plan concerned the measurement of flight parameters, airplane response, and structural and aerodynamic loads; establishment of a common time-reference point; and provision for chronological synchronization of all the measured data. The measurements were accomplished by standard-type strain gauges and transducers which converted the data into electrical energy and transmitted the information to the recording systems (local and telemetering). Timing and synchronization were accomplished by a specially developed timing decoder and a photoelectric-cell arrangement (blue box). A detailed description of this equipment is contained in Chap. 2.

The instrumented airplanes consisted of radio-controlled drones (QB-17 and QT-33) and manned aircraft (B-50D and XB-47). The instrumentation was essentially the same for both types of aircraft; however, the drones

were equipped with a telemetering system in addition to a local recorder. The initial instrumentation plan for the drones consisted in the installation of one set of transducers for air-speed, altitude, and accelerations; two sets of pressure transducers; and two sets of strain gauges. One set of pressure transducers was required for the telemetering, and the other set was required for the local recorder. The extra sets of strain gauges were to serve as spares in the event of gauge damage, since strain gauges were not so readily replaceable as the standard transducers. The two recording systems were to be supplied with intelligence from a single set of gauges which operated through an electronic filtering unit (see Sec. 2.3.3). The instrumentation plan for the manned aircraft was similar to that for the drones, except that a dual installation of pressure transducers was not required because telemetering was not installed, and more channels were used in order to obtain more-complete instrumentation.

Upon resumption of operations in the forward area, it was discovered that the filtering unit did not function properly (see Sec. 2.9.2). The initial plan was therefore abandoned for the drone aircraft, and individual gauges were installed for each recording channel wherever feasible. This new plan made use of the spare gauges and therefore necessitated the selection of a primary source of data recording and an alternate source. The primary source was to be completely equipped with operational gauges at test time. In case of last-minute gauge malfunctioning in the primary source, the alternate source was cannibalized. The decision to eliminate the filter unit did not affect the plans for the manned aircraft. A detailed description of the instrumentation in

each of the test airplanes is contained in the following sections. The general circuitry of the final instrumentation is contained in the schematic wiring diagram, Fig. 3.1.

The airplanes allocated for instrumentation purposes were delivered directly to the Government agency or contractor's plant for the installation of Class A instrumentation parts and provisions. This consisted in the following:

1. Fabrication and installation of mounting brackets for (a) 24-channel local recorder(s), (b) 24-channel recorder-amplifier(s), (c) AKT-6 multiplexer (telemetry),* (d) AKT-6 transmitter (telemetry),* (e) AKT-6 filter box,* (f) equipment control box, (g) accelerometers, (h) elevator-position indicator, (i) altitude transducer, (j) airspeed transducer, (k) timing decoder, (l) blue box, and (m) pressure transducers.
2. Fabrication of (a) control box, (b) strain-gauge junction panel, and (c) elevator-position indicator.
3. Installation of (a) interconnect wiring between sensing elements, recording systems, and associated equipment, and (b) additional pitot-static system.
4. Provisions of access holes and panels, where necessary, for instrument accessibility.
5. Modification of aircraft structure where required.

Upon completion of these installations the airplanes were delivered to Eglin Air Force Base for installation of the instrumentation by ATU 3.4.2 personnel. This consisted in installing the recording systems, strain gauges, transducers, timing decoder, and blue box and completing the electrical connections. Owing to the late delivery and malfunctioning of some of the equipment, sufficient time was not available to complete the installations at Eglin Air Force Base. The remaining tasks, including a considerable amount of rewiring necessitated by the elimination of the filter unit, were performed at the forward area. The relative location of the various items of equipment in the airplanes will be shown in the following sections pertaining to each airplane.

*Not required in the manned aircraft.

3.2 CALIBRATIONS

Both recording systems were originally planned to be calibrated simultaneously as one complete system (all component parts electrically interconnected in normal operating condition). This was to have been accomplished by subjecting the individual sensing elements to known representative values of their kinetic function and recording the measured data. The analysis of the records would determine a calibration curve in kinetic function versus trace deflection of the records. This plan was for use with a linear-output recording system such that relatively small calibration loads could be applied to a gauge for determination of a linear calibration curve, or slope, which was capable of accurate extrapolation to the maximum expected test load.

Field calibrations were attempted at Eglin Air Force Base in the afore-mentioned manner but were discontinued owing to the lack of adequate facilities for applying sufficiently large structural loads for calibration of the strain gauges. In order to accomplish these calibrations prior to departure for the forward area, one QB-17, one QT-33, the XB-47, and the two B-50D airplanes were ferried to Wright-Patterson Air Force Base and calibrated at the Structures Test Laboratory. The other sensing elements were scheduled to be calibrated at the forward area since no difficulty was experienced in applying calibration loads to these transducers. The strain-gauge calibrations of the QB-17 and QT-33 airplanes were to serve as master calibrations for the remaining airplanes of the same type. Inaccuracies due to differences in installations were kept to a minimum, and those due to differences in airplanes of a type were recognized and accepted. The final calibrations of the instrumentation of each QB-17 and QT-33 drone were completed in the forward area. The calibrations of the strain-gauge channels at Wright-Patterson Air Force Base were valuable in indicating the values and location of the loads to be used in field calibrations, in establishing the shapes of the calibration curves for each channel, and in proving the response of each gauge to the function which it was intended to measure. Also, since it was more convenient in the laboratory than in the field to apply pure

loads, the response of each gauge to extrinsic functions could be established. It was feasible, however, to calibrate the majority of the channels, including strain gauges, in the forward area, and, where applicable, these are the techniques described and the calibrations used.

3.2.1 Direct Method

It was possible to calibrate most of the channels directly by the application of the appropriate kinetic function in increments up to the full value expected during the test. Such functions as airspeed and aerodynamic pressure could be simulated readily, and the application of the function to the gauge was the basis of the direct calibration. In these instances it was necessary to have an accurate standard with which the functions were measured because the recorded data would be no more accurate than the reference standard. This method was the simplest and was used whenever possible.

3.2.2 Indirect Method

Upon resumption of operations at the forward area, considerable difficulty was experienced in maintaining linearity of the 12-channel playback system for the local recorder. The difficulty was caused by the malfunctioning of the playback tangent-compensating circuit (see Sec. 2.9). Since the discrepancy could not adequately be remedied in the field, the tangent-compensating circuit was disconnected. This modification necessitated a change in calibration technique for the local recorder since the reproduced data would no longer be a linear function in relation to applied loads but rather a tangent function. The recorder, the amplifier, and the transducers were not affected by this modification but maintained a linear output, as read on a vacuum-tube voltmeter (VTVM), to within ± 1 per cent. The initial calibration plan was satisfactory for use with the telemetering system, and excellent results were obtained; however, test data were not obtained from the telemetering. Consequently the calibration of that equipment will not be contained in this report.

An indirect calibration plan was devised for calibrating the local recorder whereby the major components of the system (gauge, amplifier, recorder, and playback) were individually calibrated. These calibrations were

correlated and combined into a single calibration curve. This plan made use of precision resistors which simulated 20, 35, 50, 70, and 100 per cent gauge unbalance of a nominal 350-ohm strain-gauge bridge. A calibration box was constructed with 10 such sets of resistors, in addition to a reversing switch which permitted simultaneous calibration, in the plus and minus sense, of 10 intelligence channels. The calibration box was connected into the electrical circuit of the sensing elements as shown by the schematic circuit, Fig. 3.2.

The sensing elements were calibrated in conjunction with the recorder-amplifier by the application of known loads. During this operation the recording system was operated normally, except that the amplified outputs of the gauges were measured by a VTVM connected to the amplifier output. This output, when plotted versus the applied load, represented the calibration of the sensing element. The value of amplified output with the recorder in the phase-balance position and with the sensing element in the no-load condition served as a datum point for correlation between the gauge calibration and the amplifier calibration. In order to illustrate the technique used in arriving at a calibration by the indirect method, the complete set of data and curves is shown for the calibration of channel 10 (outer wing bending, wing station 129) of QT-33 drone 2. The data for the calibration of the sensing element for the example are given in Table 3.1 and plotted in Fig. 3.3.

The amplifier was calibrated in conjunction with the sensing elements and the calibration box. The recording system was operated normally, as above, and the various calibration resistors were keyed into the circuit in both the plus and the minus sense. Millivolt measurements were taken in each position by means of a VTVM. The measured data represented a linear curve in relation to per cent of gauge unbalance. Prior to each calibration a value of the phase-balance position was determined for correlation purposes. The data thus measured for the example are contained in Table 3.2, and a graph of the data is shown in Fig. 3.4.

In the instance of this example, the value of phase balance remained the same for the calibration of the sensing element and the amplifier. However, if the values of voltage at phase-balance position differed, the millivolt meas-

SECRET

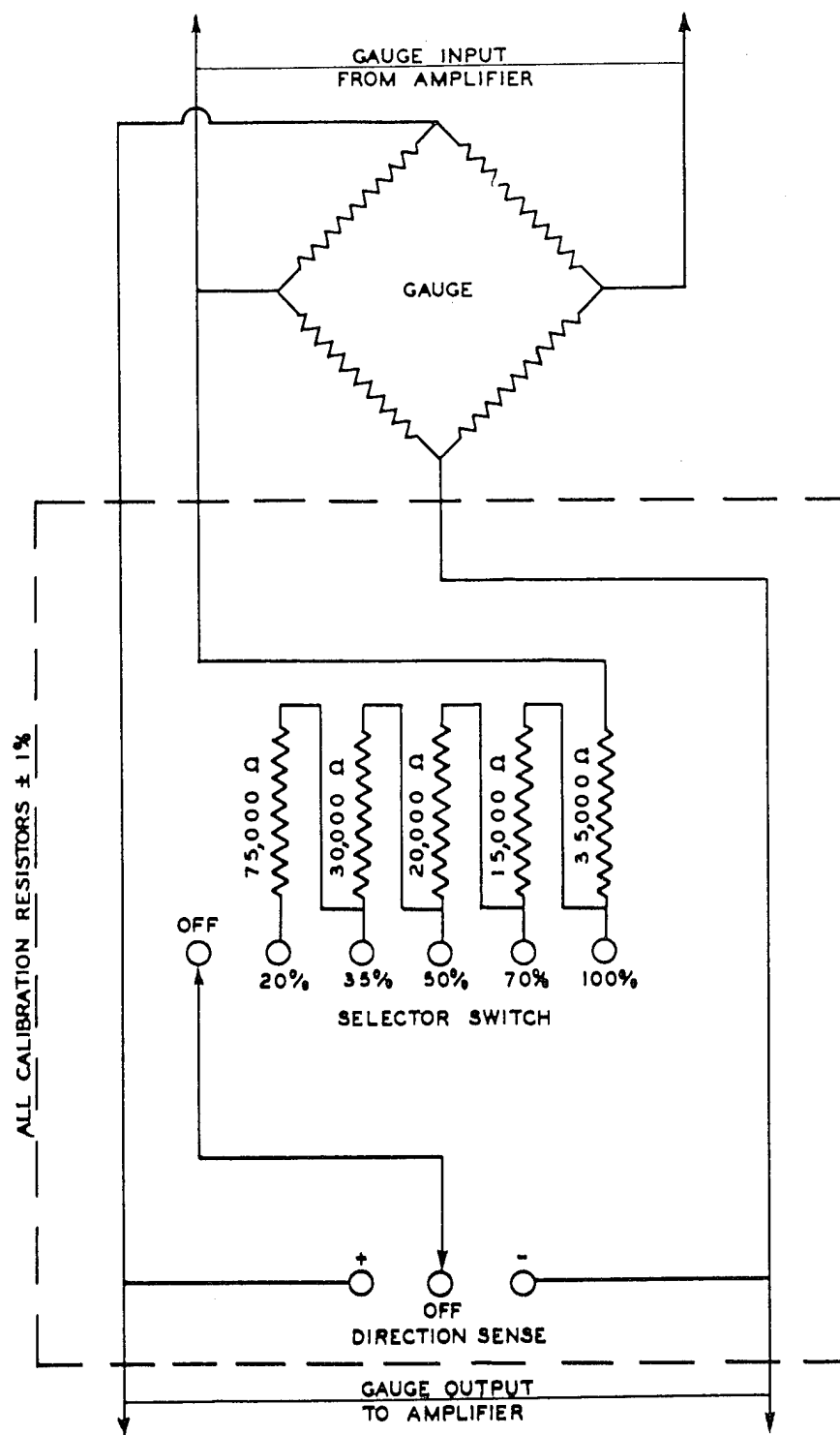


Fig. 3.2 Schematic Wiring Diagram for Connection of Calibration Box in Intelligence Channel

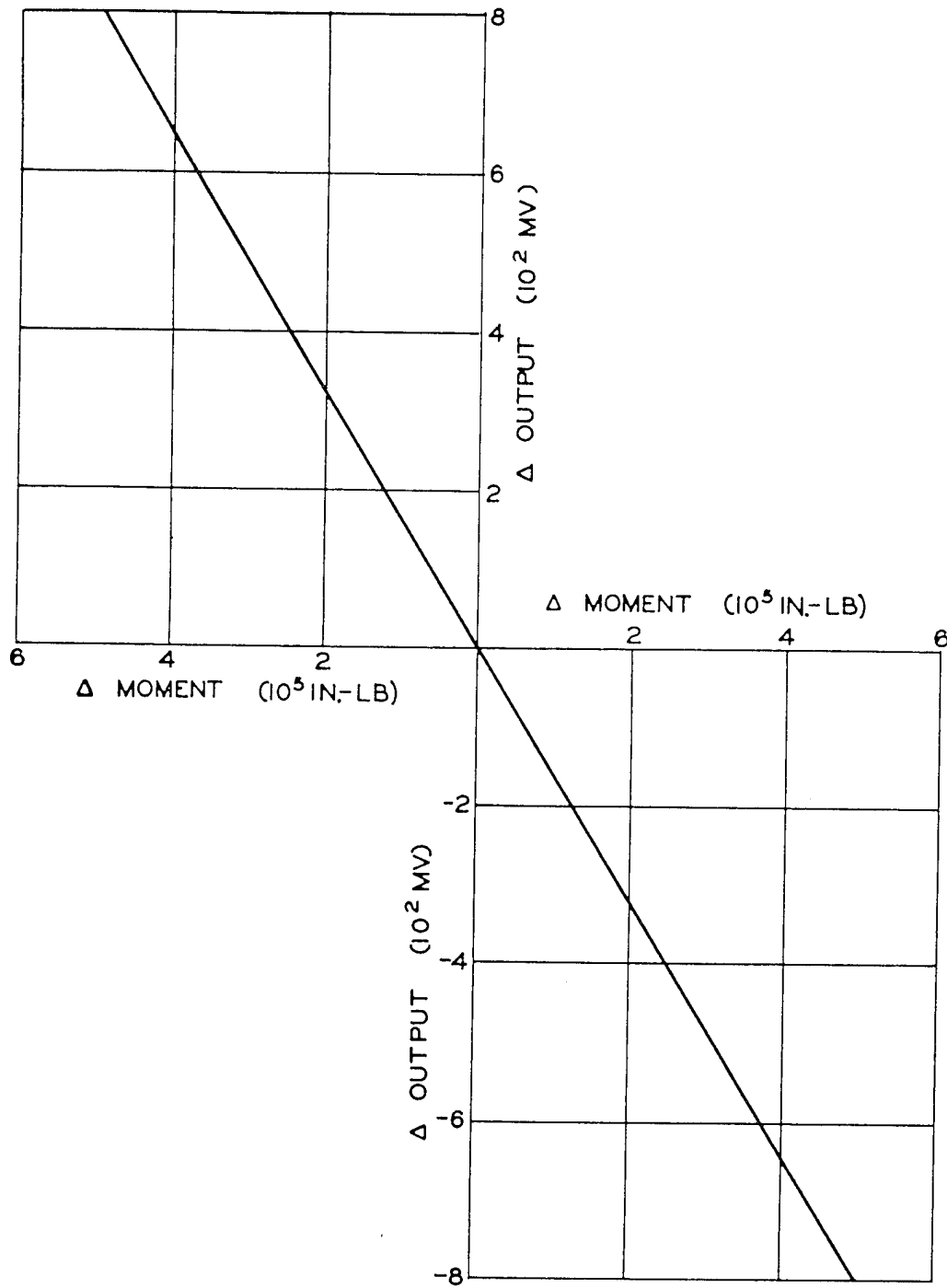


Fig. 3.3 Example Calibration of Sensing Element

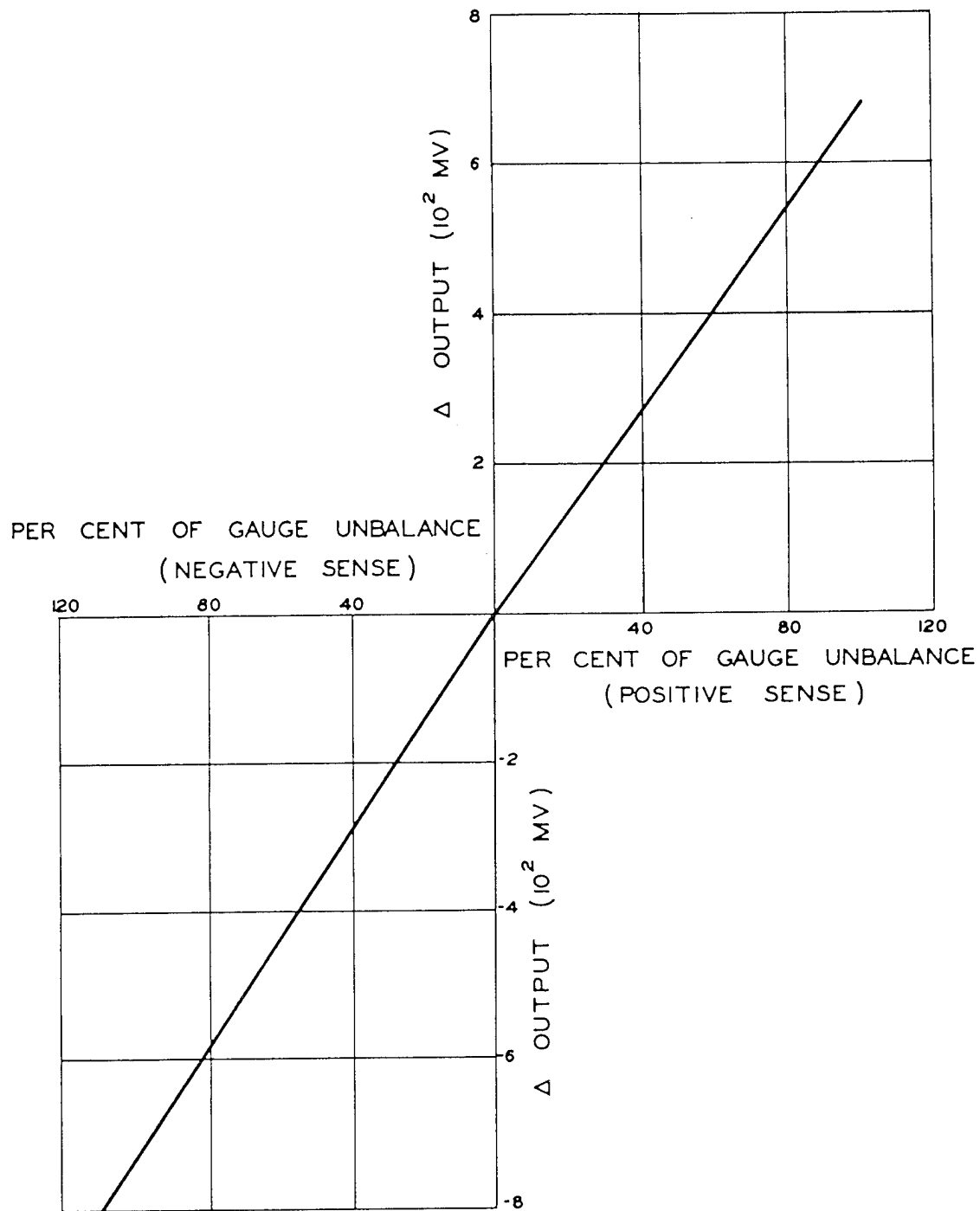


Fig. 3.4 Example Calibration of Recorder-Amplifier

TABLE 3.1 EXAMPLE DATA FOR CALIBRATION OF SENSING ELEMENT^a

Applied Load ^b (lb)	Bending Moment ^c (10 ⁵ in.-lb)	Δ Moment ^d (10 ⁵ in.-lb)	Amplified Output ^e (10 ² mv)	Δ Output ^f (10 ² mv)
+580	0.575	0	-0.05	0
+1,370	1.358	0.783	-1.35	-1.30
+2,315	2.290	1.715	-2.80	-2.75
+3,340	3.310	2.735	-4.40	-4.35
+4,365	4.320	3.745	-6.00	-5.95

^aPhase-balance position = 430 mv.

^bLoad applied to aircraft structure; up-load is plus sense.

^cLoad × moment arm (99 in.).

^dΔ moment (bending moment) - initial gauge-balance condition. For this example the gauge was balanced at the first load increment of 580 lb. The gauges were balanced with an initial applied load in order to remove any effect of structural looseness.

^eMinus sign indicates that the deflection of the corresponding recorder trace is in the cal-minus direction.

^fΔ output = amplified output - amplified output for the initial gauge-balance condition.

TABLE 3.2 EXAMPLE DATA FOR CALIBRATION OF RECORDER-AMPLIFIER*

Simulated Gauge Unbalance† (%)	Output (mv)	Δ Output (mv)
0	5	0
+20	135	130
+35	228	223
+50	340	335
+70	480	475
+100	695	690
-100	740	735
-70	520	515
-50	370	365
-35	245	240
-20	142	137
0	5	0

*Phase-balance position = 430 mv.

† Plus and minus signs indicate arbitrary-direction sense.

urements obtained for the amplifier calibration were corrected by multiplying the measurements by the ratio of the two phase-balance values. This correction correlated the two calibration curves by simulating adjustment of the equipment to identical conditions.

The recorder-playback combination was calibrated in a manner similar to that described for the amplifier, except that a tape recording was made for each calibration resistor rather than VTVM measurements. The phase-balance position of the recorder was not used in this procedure; however, the cal-plus and the cal-minus positions were recorded for correlation with the test data. The tape recordings were played back, and the trace deflections were determined for each resistor in the plus and the minus sense in addition to the trace deflections produced by the cal-plus and cal-minus positions. The trace deflection produced by each calibration resistor was compared to the trace deflection of either cal plus or cal minus (whichever applicable in direction sense) and expressed in terms of per cent of cal plus (or minus). An example of these data is contained in Table 3.3 and plotted in Fig. 3.5.

The final calibration curve was determined by correlation of the individual calibration curves to obtain units of applied load (pounds, inch-pounds, pounds per square inch, gravity units, feet, and miles per hour) compared to per cent of the applicable calibrate step. Values of applied load were selected in Fig. 3.3, and a corresponding amplified output was determined from the graph. This output was used with Fig. 3.4 to determine a simulated gauge unbalance. The gauge unbalance when used in conjunction with Fig. 3.5 determined the corresponding percentage of the calibrate position. The direction of sensing was determined by arbitrarily applying a load to the individual gauge and then recording the information. This determined the direction of trace deflection for the calibrate steps. In actual practice the individual calibration curves were consolidated into a single graph; however, in this report they are presented as individual graphs for the sake of clarity. The final calibration data for the example are contained in Table 3.4, and the calibration curve, comparable to those in the appendixes (reproduced elsewhere; see page iv), is contained in Fig. 3.6.

The detail calibration procedure used on

each type of airplane is contained in the following sections. The final calibration curves for those individual channels from which test data were obtained are contained in the appendixes to this report.

The indirect calibration method described here was used principally for calibration of the strain-gauge channels.

3.2.3 Analytical Method

For some of the Statham gauges (altimeters or accelerometers) it was not practicable or convenient to apply the actual function for the calibration. In these instances an analytical method of calibration was used.

With each gauge the manufacturer provides a certificate which gives certain parameters determined for that particular gauge. Along with accuracy guarantees, the certificate includes such parameters as input resistance, output resistance, and a gauge factor.

For the analytical calibration, Eq. 3.1 is used.

$$N = \frac{10^6 R_o R_i}{F(R_i + 100)(4R_c + R_o + R_i)} \quad (3.1)$$

where R_c = calibration resistance in ohms

R_o = gauge output resistance in ohms

R_i = gauge input resistance in ohms

F = calibration factor in millivolt output per volt input per unit (psi or g)

N = simulated function (pressure in psi or acceleration in g)

This equation was derived by Statham Laboratories, Inc., for use with their gauges. By means of Eq. 3.1 the equivalent value (pounds per square inch or gravity units) for each of the calibration resistors in the calibration box (Fig. 3.2) was established for a particular gauge. The insertion of the calibrating resistors across one arm of the gauge then simulated the application of the equivalent function for purposes of calibration.

3.2.4 Presentation

In order to avoid laborious repetitions in the discussion of the calibration of the individual channels of the various airplanes, a few comments on the technique used in presenting the calibrations are in order.

TABLE 3.3 EXAMPLE DATA FOR
CALIBRATION OF RECORDER-PLAYBACK
COMBINATION

Function*	Trace Defl. (in.)	Per Cent of Calibrate
Operate	0	
Cal +	+0.79	
Cal -	-1.00	
+20%	+0.27	34.2
+35%	+0.43	54.5
+50%	+0.60	76.0
+70%	+0.75	95.0
+100%	+0.94	119.0
-100%	-1.20	120.0
-70%	-1.03	103.0
-50%	-0.83	83.0
-35%	-0.60	60.0
-20%	-0.36	36.0

* Plus and minus signs indicate arbitrary-direction sense.

TABLE 3.4 EXAMPLE OF CORRELATED DATA FOR CHANNEL CALIBRATION

Δ Moment*	Δ Output†	Gauge Unbalance‡	Per Cent of Calibrate§
(10^5 in.-lb)	(10^2 mv)	(%)	
+1.0	-1.62	-23	-41.0
+2.0	-3.22	-45	-74.5
+3.0	-4.82	-67	-99.0
+4.0	-6.45	-89	-115.0
+4.52	-7.28	-100	-120.0
-1.0	+1.60	+23	+38.0
-2.0	+3.20	+48	+71.5
-3.0	+4.83	+71	+96.5
-4.0	+6.45	+94.5	+115.0
-4.2	+6.75	+100	+119.0

* Values of Δ moment were arbitrarily selected from Fig. 3.3.

† Values of Δ output were determined from Fig. 3.3 by the selection of the Δ moment.

‡ Gauge unbalance was determined from Fig. 3.4 by using the values of Δ output.

§ Per cent of calibrate was determined from Fig. 3.5 by using the values determined for gauge unbalance.

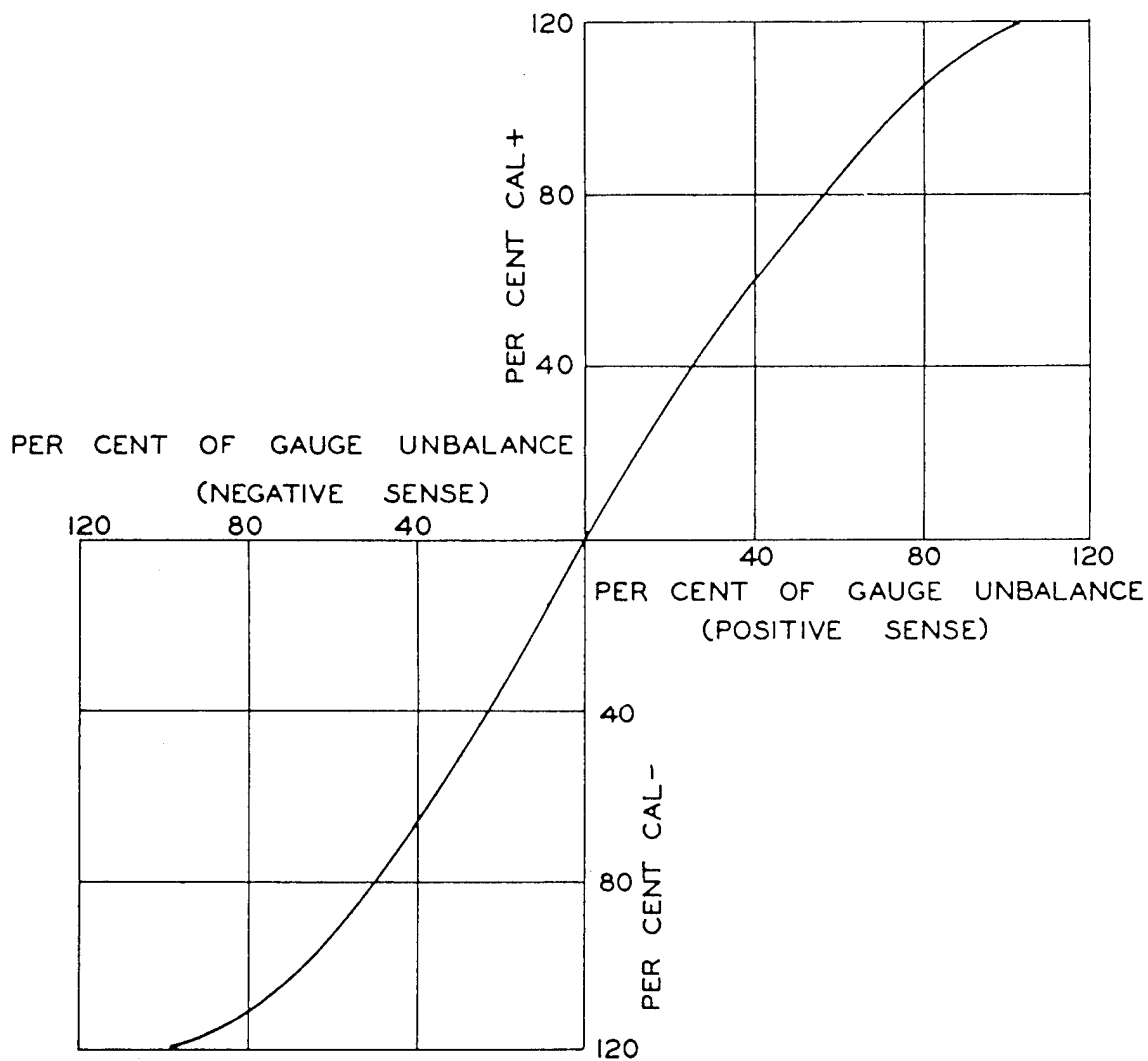


Fig. 3.5 Example Calibration of Recorder-Playback Combination

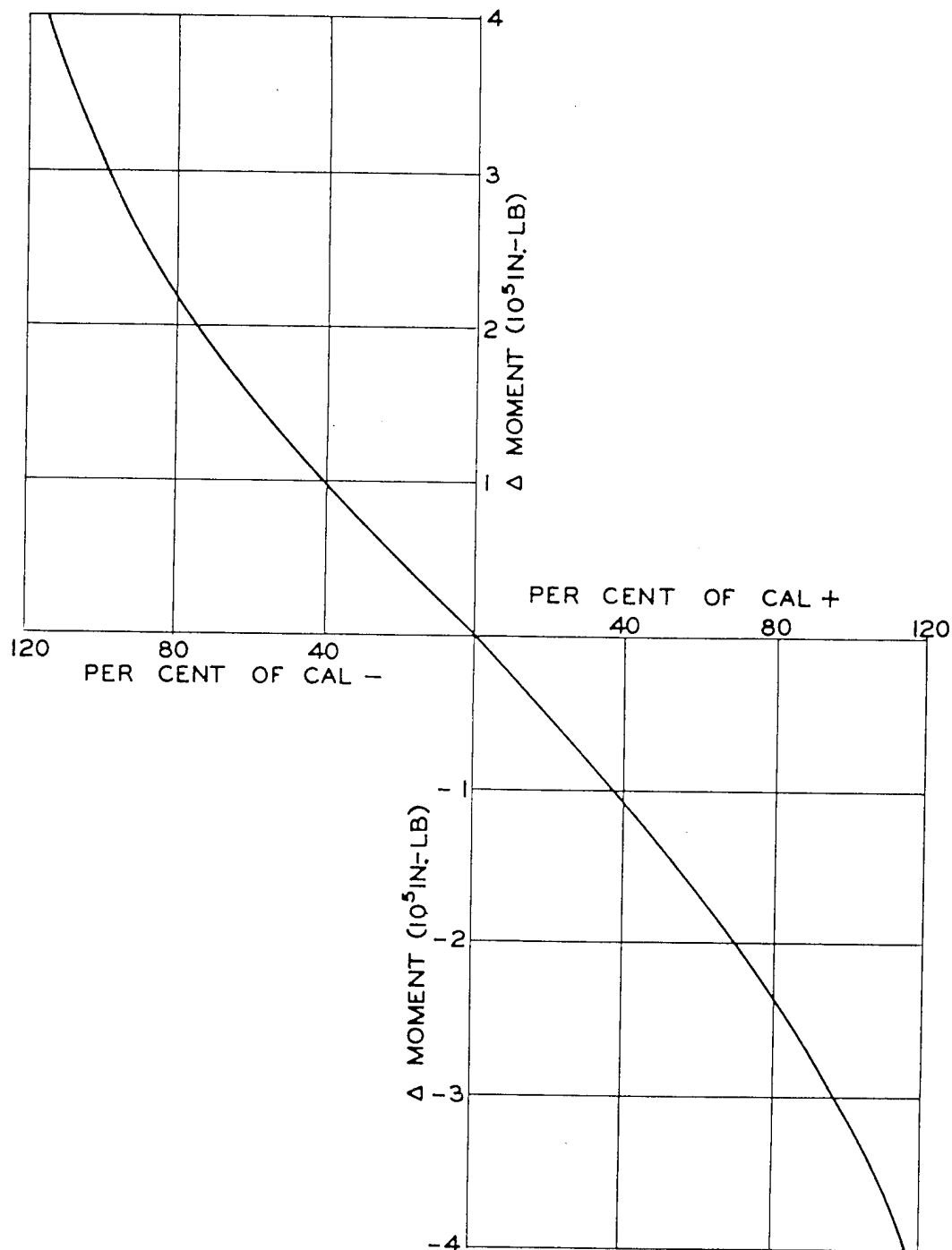


Fig. 3.6 Example Calibration of Complete Channel

It is apparent that the calibration of so many channels on so many airplanes is an involved process. The details of the calibration techniques used in each instance would probably only confuse the reader. The brief discussions presented in this chapter are then intended only to indicate the general techniques used in arriving at a calibration curve for each channel in order that the reader may justify (or doubt) the validity of the calibrations and thus the fidelity of the records. Details such as values of functions applied for calibration, computations, and intermediate curves have been omitted, except for the example in Sec. 3.2.2.

The calibration curves have been segregated into appendixes in order to be more readily identified and to avoid cluttering up the text of the report. It will be noted that each calibration curve contains as its abscissa the axis "per cent of cal plus" in one direction and/or "per cent of cal minus" in the other. The cal-plus (or cal-minus) trace deflection is generated by a fixed resistor built into the recorder for each channel. The absolute deflection caused by this resistor is a measure of the sensitivity of the channel under the conditions existing at that time. Using these trace deflections as bases for each measurement reduces, as much as possible, errors due to variations within a given channel. Each test record was first read in deflection as a per cent of the deflection caused by the calibrate (plus or minus) resistor. The calibration curves as presented in the appendixes are, therefore, shown as deflections in per cent of calibrate deflections versus the applied function for direct interpretation of the test records. The use of the known deflections (produced by a phase shift at the gauge, which is constant for a given gauge) effectively calibrates the various circuits of the recorder-playback channel for the conditions existing at the time each record (test or calibration) was made. The necessity for performing the cal steps as near as possible to the time the record is made and as frequently as possible is obvious. The term "per cent cal" as used in subsequent discussion refers, then, to the trace deflections produced by gauge unbalance expressed in terms of percentage of the deflections produced by cal plus or minus as appropriate.

Only calibrations of those channels from which data were collected are included in the

appendixes. Calibrations for the telemetering are not contained in this report since no usable data were obtained from this equipment.

3.3 QB-17 DRONES

The B-17 airplanes for Project 8.1 were drawn from storage along with the other B-17's for Operation Greenhouse and were sent to MAMA for modification and installation of the radio-control equipment. Since the facilities and personnel were available at MAMA, it was decided that the Class A instrumentation parts (brackets, wires, panels, etc.) should be installed in the drones at the same time. Upon completion of the installations at MAMA the airplanes were delivered to ATU 3.4.2 at Eglin Air Force Base. QB-17 airplanes lettered M, N, O, P, and Q were assigned to Project 8.1. Airplanes G, H, I, J, K, and L were assigned to Project 1.7, primarily, but were also modified so as to be used jointly by Project 8.1.

3.3.1 Instrumentation

The specific plan for the instrumentation was developed at Hq AMC, and instructions were issued to MAMA for the work to be performed there. The details of the installations are presented in Table 3.5 and shown diagrammatically in Fig. 3.7.

Channels 1 and 2 measured altitude and air-speed, respectively. The transducers were commercially standard, resistance type, and were mounted on the left-panel wall of the bombardier's compartment; they were connected into the pitot system normally installed for the navigator. The increase in volume in the system was kept as small as possible in order to minimize the lag between actual conditions and the indications of the transducers.

Channels 3, 4, 5, and 6 measured vertical accelerations. The accelerometers were resistance type, produced commercially by Statham Laboratories. The accelerometer for channel 3 was mounted in the bomb bay on a rigid bracket affixed to the cat-walk structure, which is a part of the primary structure of the fuselage. The accelerometer was located 43 in. aft of fuselage station 4 or at 22 per cent m.a.c. The vertical or sensitive axis of the accelerometer was located in the plane of symmetry

~~SECRET~~

TABLE 3.5 RECORDER-CHANNEL ASSIGNMENTS FOR QB-17 DRONES

Chan.	Intelligence Measured	Type	Model	Instrument Location
1	Pressure alt.	Satham press. gauge	P69-15A-350	Navigator's compt.
2	Airspeed	Satham press. gauge	P69-1D-350	Navigator's compt.
3	Normal accel.	Satham accel.	C-6-300	Bomb bay, airplane c.g.
4	Normal accel.	Satham accel.	C-6-300	Vertical stabilizer
5	Engine accel.	Satham accel.	A18-6-350	No. 3 engine access. sec.
6	Engine accel.	Satham accel.	A18-6-350	No. 4 engine access. sec.
7	Wing bending	SR-4 strain gauge	A13-350	Rt. wing station 1*
8	Wing bending	SR-4 strain gauge	A13-350	Lf. wing station 1
9	Stab. bending	SR-4 strain gauge	A13-350	Rt. hor. stabilizer
10	Wing bending	SR-4 strain gauge	A13-350	Rt. wing station 19
11	Wing torsion	SR-4 strain gauge	A13-350	Rt. wing station 8.8
12	Wing shear	SR-4 strain gauge	A13-350	Rt. wing station 1
13	Wing torsion	SR-4 strain gauge	A13-350	Rt. wing station 1
14	Wing bending	SR-4 strain gauge	A13-350	Rt. wing station 8.8
15	Elevator position	Shot fabricated	None	Elevator torque tube
16	Diff. aero. press.	Wiancko press. gauge	3PAD1OW	Rt. wing sta. 25.5, 5% chord
17	Diff. aero. press.	Wiancko press. gauge	3PAD1OW	Rt. wing sta. 25.5, 10% chord
18	Diff. aero. press.	Wiancko press. gauge	3PAD1OW	Rt. wing sta. 25.5, 20% chord
19	Diff. aero. press.	Wiancko press. gauge	3PAD1OW	Rt. wing sta. 25.5, 40% chord
20	Diff. aero. press.	Wiancko press. gauge	3PAD1OW	Rt. wing sta. 25.5, 60% chord
21	Diff. aero. press.	Wiancko press. gauge	3PAD1OW	Rt. wing sta. 25.5, 85% chord
22	Diff. aero. press.	Wiancko press. gauge	3PAD1OW	Rt. wing sta. 8.8, 40% chord
23	Diff. aero. press.	Wiancko press. gauge	3PAD1OW	Lf. wing sta. 25.5, 60% chord
24	Diff. aero. press.	Wiancko press. gauge	3PAD1OW	Rt. hor. stab., 40% chord

*Wing stations are arbitrarily assigned and bear no relation to distance.

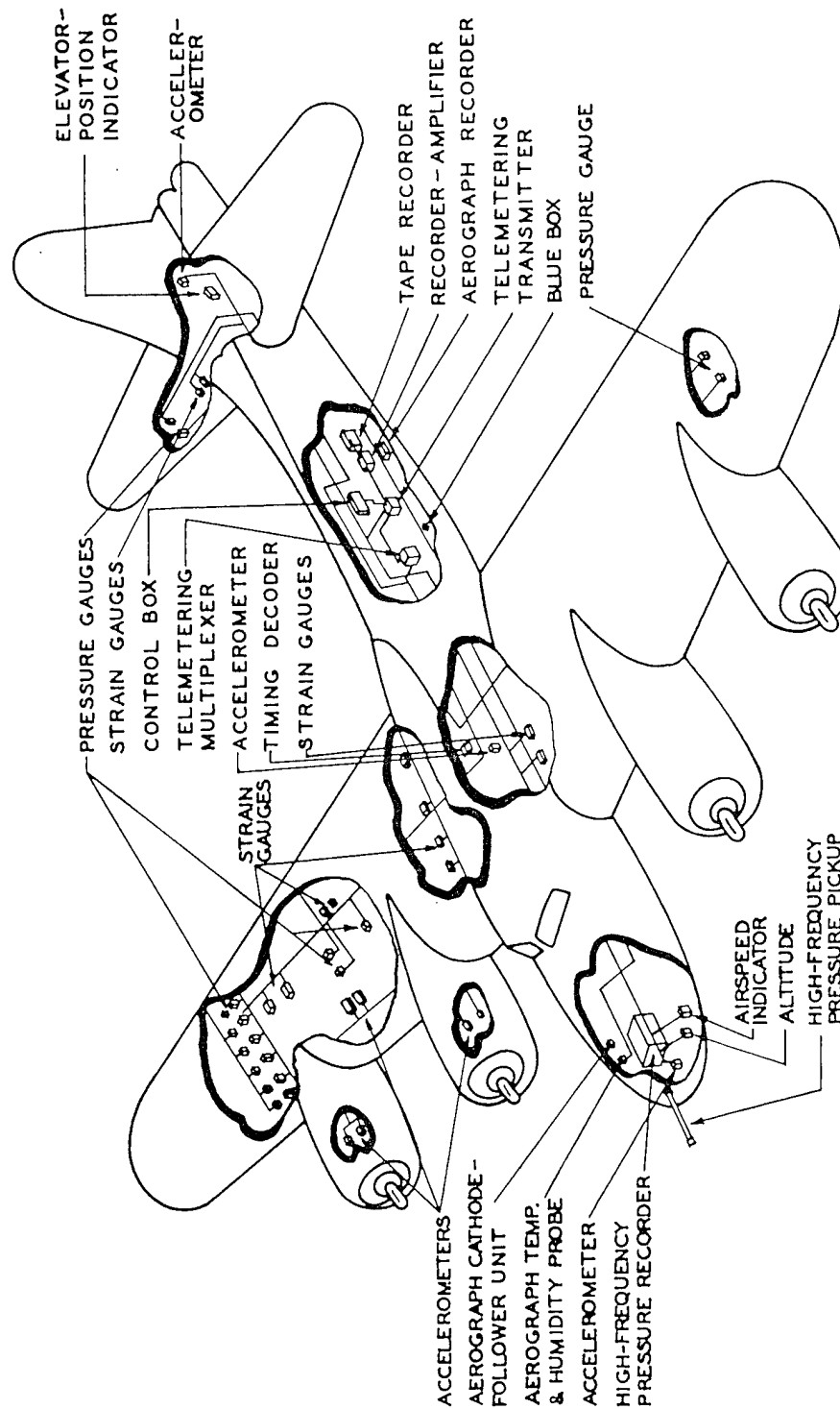


Fig. 3.7 Instrumentation of QB-17 Drones

~~SECRET~~

perpendicular to the level line of the airplane. The accelerometer for channel 4 was located within the fuselage and was affixed to a bracket on the main spar of the horizontal stabilizer. The accelerometer was located at fuselage station 9, or 472.42 in. aft of the normal c.g. position of 29 per cent m.a.c. Thus the acceleration measured by channel 4 when compared to that of channel 3 indicated the pitching acceleration of the airplane. The vertical or sensitive axis of the accelerometer was mounted parallel to the plane of symmetry and perpendicular to the level line of the airplane. The accelerometers for channels 4 and 5 were similarly mounted on engines 3 and 4, respectively. The brackets for the accelerometers were affixed to a pad on the accessory section of the engine. It was originally intended to determine the loads applied to the wing by the engine by means of strain gauges on the engine-mount structure. However, in tests at Hq AMC it was proved that the excess strength in the engine mounts reduced the output of the strain gauges below a readable level. A low-range (6-g) accelerometer was used in an attempt to filter mechanically the higher-frequency engine vibrations.

Channels 7, 8, 10, and 14 measured wing bending. Gauges for channels 7 and 8 were installed so as to measure the total bending in the root of each wing. Installations of these gauges either at wing station 1 or in the bomb bay on the carry-through structure were considered. It was decided to mount the gauges outboard of the root attachment points to avoid the losses that might occur at the wing-fuselage junction.

Channel 10 measured wing bending in the outer panel of the right wing. The gauges were mounted at wing station 19, which was just outboard of the wing-outer-panel attachment. Strain gauges were affixed to each of the spar-cap members and so connected as to measure the total bending moment in the outer panel. The right aileron was carried on this panel, and this channel indicated changes in load with aileron deflection.

Channel 14 measured bending in the right wing at station 8.8. Bending was measured by means of the compression or tension in the diagonal members of the spars.

From the B-17 stress analysis it was determined that the front spar of the wing carries

18 per cent more of the wing-bending moment than that carried by the rear spar. However, the upper and lower tubes of the front spar are spaced 15.8 per cent farther apart than tubes of the rear spar and are therefore stressed approximately equal to the tubes of the rear spar for any given load. The strain-gauge bridge attached to the upper and lower tubes of the front and rear spars is considered accurate for the purposes of the tests.

Channel 9 measured the bending at the root of the right horizontal stabilizer. The gauges were mounted directly on the spar-cap members, outboard of the fuselage attachment. The spars undoubtedly did not carry all the bending load in the stabilizer because of the rigidity of the elevator torque tube and the load which passed from the stabilizer through the hinges to the elevator torque tube. However, the strain gauges were calibrated in terms of bending moment by the application of known loads or moments so that, as long as a definite proportion of the load was carried by the spars, the measurements were still accurate. Deflection of the elevator during calibration had no effect on the gauge output.

Channel 11 was connected to measure the torsion in the right wing at wing station 8.8. This station is located approximately midway between engines 3 and 4. Torsion was measured by differential bending in the two spars. The gauges were mounted on the cap members of the two wing spars and so connected as to give an output when the spars were bent in opposite directions.

Channels 12 and 13 measured the shear and torsion in the right wing root at wing station 1. The torsion at this station was measured by differential shear in the two spars. The gauges were mounted on the diagonal members of the truss structure which formed the spars. The responses of the gauges to bending and other contingent loads were calibrated. The diagonal members were at 45° to the spar-cap members and were attached to the verticals and to the spar caps through gusset plates. The gauges were affixed to the sides (front and rear) of the square tubes which formed the diagonals in order to avoid bending stresses which may have been imposed by the end fixity of the gusset plates.

Channel 15 measured the position of the elevator. The measurement of position was ob-

tained by means of a cam affixed to the elevator torque tube which deflected a cantilever beam. The deflection of the beam was measured by means of strain gauges.

Channels 16 through 24 measured aerodynamic pressure. The pressure transducers (see Sec. 2.6.5) were fastened to the surface by means of an aluminum mount. In all the installations in the QB-17 airplanes the transducers were used in pairs, and the differential pressure was measured electrically. Each transducer was, in itself, a differential-pressure gauge. In order to measure the differential pressure across a section, the transducers were mounted one to each surface, and the reference sides of each transducer were connected with tubing. Thus each transducer measured the difference between the pressure at its surface and the reference pressure. Since the reference pressure was identical for each transducer, the algebraic difference between the two measurements, as taken electrically, measured the difference in pressure between the two surfaces. Channels 16 through 21 were located at a single chord of the right wing in order to measure the variation in chordwise lift distribution at that station. Channels 22, 23, and 24 were similar installations at another station on the right wing, at the same station on the left wing, and on the horizontal stabilizer. Wing station 25.5 was selected for the measurements of chordwise lift distribution because it was far enough out on the wing to be clear of the disturbance caused by the propeller slip stream and far enough inboard of the tip to be free from tip turbulence.

The sensing probe for the high-frequency pressure recorder (see Sec. 2.5) was installed in the lower nose section of the B-17 airplanes, anchored into the chin-turret well. The boom was aligned with the leveling lugs and projected ahead along the line of flight. The surface of the crystal sensing element was oriented vertically, parallel to the line of flight, about 6 ft ahead of the nose of the aircraft. The amplifier-recorder unit was mounted on top of the chin-turret-well cover in the bombardier's compartment. D-c power was taken from the aircraft's system, and a-c power was taken from a special-instrumentation inverter mounted in the waist of the drone. The recording cycle was started at T_0 by a signal from the blue box.

According to the original plan a total of

eleven QB-17's were modified and delivered to ATU 3.4.2 for the installation of Class B parts (recorders, telemetering equipment, timing decoders, sensing elements, and associated equipment) as required. Time did not permit the completion of the instrumentation of all the drones, so that emphasis was placed on the five USAF drones; the six AEC drones were not used for this program. Many problems arose in connection with the completion of the drones at Eglin Air Force Base. Of these, perhaps the most serious involved the wire used to interconnect the sensing elements and the recorder or telemeter. This wire was a newly developed type and had not been thoroughly tested. It was very difficult to install, and many faults were discovered from extraneous grounds, broken shielding, broken conductors, and faults in the insulation. Also, the wire was very susceptible to moisture, and shorts soon developed between conductors and between conductors and ground in otherwise satisfactory installations. It was necessary, therefore, to rewire the drones at Eglin Air Force Base just prior to their departure for the forward area.

3.3.2 Calibration

The calibrations of channels 1, 3, 4, 5, and 6 were performed by the analytical method described in Sec. 3.2.3. Various calibration resistors simulating calculated values of acceleration were keyed into the channel circuits, and records were taken of the resulting gauge-unbalance outputs.

Channel 2, indicated airspeed, was calibrated by the direct method of applying air pressure to the pitot line of the pressure transducer. The air pressure applied to the gauge, from bottled compressed air, simulated dynamic head which was measured by a calibrated airspeed indicator.

The strain-gauge channels used for measuring bending and shear of the wing, channels 7, 8, 10, 12, and 14, were calibrated by the indirect method (Sec. 3.2.2). The calibration was performed with the airplane in a straight-and-level-flight attitude supported at the tail jack point and the inboard wing jack points. By supporting the airplane in this manner, with the landing gear free of the ground, any side loads resulting from tire and landing-gear deformations were eliminated. The tail of the

airplane was raised onto an aircraft jack by a mobile crane. The front of the airplane was then raised by aircraft jacks placed at the in-board jack points. To obtain the basic weight of the airplane, each jack was provided with a weighing head from a calibrated Cox and Stevens aircraft weighing kit. The longitudinal axis of the airplane was placed in the level-flight position by raising or lowering the tail jack as required, and the lateral axis was maintained in the horizontal plane by raising or lowering either of the wing jacks. Special wing jigs, for applying up-loads to the wings, were placed on aircraft jacks under the outer panel of each wing at station 26. The jigs were constructed so as to apply loads to the front and rear spars as the jacks were raised. The loads applied to the wings were measured by a calibrated Cox and Stevens aircraft weighing kit. A basic up-load of 1,000 lb was applied to the wings, and the strain-gauge bridge circuits were electrically balanced. Four additional loads of 2,000 lb each were applied to the wings. The amplified millivolt output of the gauge was measured after each wing load was applied, and the output was compared to the applied load. This determined the calibration curve of the sensing element which, when correlated with the calibration-box data, resulted in the calibration curve for the complete channel.

Channel 9, bending in the right horizontal stabilizer, was calibrated by a method similar to that described in the preceding paragraph. With the tail of the airplane raised on an aircraft jack, dead-weight loads were applied at the tip of each horizontal stabilizer. Weights were placed on both stabilizer tips to prevent loading the fuselage in torsion.

Channels 11 and 13, wing torsion, were calibrated at Wright-Patterson Air Force Base on drone N. However, the records obtained during the test were not of sufficient magnitude to be read; therefore these data are not included, and the discussion of the calibration of these channels is omitted.

The elevator-position indicator, channel 15, was calibrated by the direct method. The unbalance of the strain-gauge bridge circuit was accomplished by downward travel of the elevator. The gauge was electrically balanced in the full-up position and then lowered in 10° increments until the full-down position was reached. A record was taken on the tape re-

corder after each 10° increment was applied. Elevator deflection was measured by a spirit-level-protractor combination.

Channels 16 through 24, differential aerodynamic pressure, were calibrated by the direct method. Air pressure obtained from bottled compressed air was applied to the top gauge of the channel, and the gain for the top gauge was set at the desired point. Pressure was then applied to the bottom gauge of the channel, and the gain for the bottom gauge was set to correspond to the gain setting of the top gauge. Pressure was then applied simultaneously to both the top and the bottom gauges of the channel, and any resulting gauge-unbalance output was measured by a VTVM and recorded by the tape recorder. Five increments of pressure ranging from 1 to 5 psi were applied to the top gauge of the channel, and the resulting unbalance output was recorded by the tape recorder. The same procedure was used for recording gauge unbalance when pressures were applied to the bottom gauges. This technique established the calibration for the channel through one sense (positive or negative), and, since it had been proved by laboratory tests that the calibration in the other sense was identical, the remainder of the curve was drawn.

3.4 QT-33 DRONES

The eleven T-33 airplanes for this program were obtained directly from the manufacturer and delivered to the Sperry Gyroscope Co., Great Neck, Long Island, N. Y., for modification and installation of the radio-control equipment. This particular company was chosen because of their design and development, under previous Government contracts, of the required radio-control and automatic flight-control equipment for high-speed fighter-type aircraft. Since the installation of this equipment required the partial dismantling and stripping of the aircraft, it was decided to have the contractor install the Class A instrumentation parts because maximum accessibility would then be available. In addition, any future damage to the control equipment during installation of Class A parts would be avoided. Five of the T-33 airplanes were equipped as instrumented drone aircraft, another five as director aircraft, and

the remaining one for radio-controlled-flight training purposes.

The installation of the Class A instrumentation parts in the five drone aircraft required considerable structural modification of the airplanes. In order to supply space provisions for the installation of differential-pressure gauges between the top and bottom surfaces of the right wing station 129, it was necessary to revise the fuel cell and to modify the wing structure. The required space was obtained by changing the shape of the inner-outboard and leading-edge fuel cells. In conjunction with these cell changes, it was necessary to fabricate and install an additional wing rib at wing station 132.75 to provide adequate cell support. In addition, proper interconnection, draining facilities, and access to the fuel cells as well as to the pressure transducers were provided. New inner-outboard and leading-edge fuel cells were fabricated by The Firestone Tire & Rubber Company. All the required modifications and installations at Sperry were accomplished under Contract No. AF 33(038)-8863. Upon completion of modifications the aircraft were delivered to ATU 3.4.2 at Eglin Air Force Base and were identified by numbers 1 through 5.

3.4.1 Instrumentation

The specific plan for the instrumentation was developed at Hq AMC, and instructions were issued to Sperry and to TU 3.4.2 for the work to be performed. The details of the installation are presented in Table 3.6, and the relative locations of the various items of equipment are shown in Fig. 3.8. Installation of equipment in the aft cockpit is shown in Fig. 3.9.

Channels 1 and 2 measured altitude and air-speed, respectively. The transducers were commercially standard, resistance type, and were mounted in the nose compartment just aft of fuselage station 22. These transducers were connected to the spare pitot-static system installed by the Sperry company. The increase in volume in the system was kept as small as possible in order to minimize the lag between actual conditions and the indications of the transducers. Only one set of these transducers was installed, and this set was intended for use with the telemetering system. Local recordings of the airspeed and altitude were taken from

the aerograph which was installed for another element of ATU 3.1.

Channels 3, 4, and 5 measured vertical accelerations in the plane of symmetry of the airplane, perpendicular to the level line of the airplane. The accelerometers used were a commercially standard, unbonded resistance-wire type. The accelerometer for channel 3 was mounted in the wheel well on a rigid bracket bolted to the lower *longeron* of the primary fuselage structure. The accelerometer was located at fuselage station 238.6 or 33.1 per cent m.a.c.* The accelerometer for channel 4 was mounted inside the vertical fin, at fin station 128, on a rigid bracket affixed to the main spar of the vertical fin. The accelerometer was mounted at fuselage station 443.0 or 204.4 in. aft of the accelerometer of channel 3. The accelerometer for channel 5 was mounted in the nose compartment at fuselage station 33.1. This transducer was mounted on a rigid bracket which was attached to the main fuselage bulkhead at that station. This instrument was 205.4 in. forward of the normal c.g. accelerometer (channel 3). When compared to the acceleration measured by channel 3, the acceleration measured by channels 4 and 5 indicated the pitching acceleration of the airplane in addition to any longitudinal deformation of the fuselage. Channels 3 and 5 had two sets of instruments installed (one each for telemetering and local recording). Channel 4, however, was not duplicated, owing to the space limitations and the inaccessibility of the gauge location and wire routing.

Channel 6 measured the torsion in the left wing at the wing root (station 34) by means of strain gauges. The gauges were installed and connected so as to measure torsion by means of differential shear. The gauges were connected into a bridge circuit with four active arms, two arms on each spar web at 90° to each other and 45° from the neutral axis of the spar. Duplicate gauges were installed at this location, one set for each recording system.

Channels 7 and 8 were strain gauges installed

*The m.a.c. for the QT-33 airplane is 80.6 in. in length, and the leading edge of the m.a.c. is 211.9 in. from the datum line of the airplane which is 16 in. forward of the nose of the airplane.

SECRET

TABLE 3.6 RECORDER-CHANNEL ASSIGNMENTS FOR QT-33 DRONES

Chan.	Intelligence Measured	Instrument		Model	Instrument Location*
		Type			
1	Press. altitude	Statham press. gauge	P69-15-350	Fus. sta. 37	
2	Airspeed	Statham press. gauge	P69-3-350	Fus. sta. 37	
3	Normal accel.	Statham accel.	A-18-12-350	Fus. sta. 238.6, approx. c.g.	
4	Normal accel.	Statham accel.	A-18-12-350	Fus. sta. 443, fin sta. 128	
5	Normal accel.	Statham accel.	A-18-12-350	Fus. sta. 33.1, nose	
6	Wing torsion	SR-4 strain gauge	A-13-350	Lf. wing sta. 34	
7	Wing bending	SR-4 strain gauge	A-13-350	Rt. wing sta. 33	
8	Wing bending	SR-4 strain gauge	A-13-350	Lf. wing sta. 33	
9	Stab. bending	SR-4 strain gauge	A-13-350	Rt. hor. stab. sta. 25	
10	Wing bending	SR-4 strain gauge	A-13-350	Rt. wing sta. 129	
11	Wing bending	SR-4 strain gauge	A-13-350	Rt. wing sta. 74	
12	Wing shear	SR-4 strain gauge	A-13-350	Rt. wing sta. 33	
13	Wing torsion	SR-4 strain gauge	A-13-350	Rt. wing sta. 33	
14	Wing torsion	SR-4 strain gauge	A-13-350	Rt. wing sta. 74	
15	Elevator position	SR-4 strain gauge	A-13-350	Rear beam hor. stab.	
16	Diff. aero. press.	Wiancko press. gauge	3PADIOS	Rt. wing sta. 128, 5% chord	
17	Diff. aero. press.	Wiancko press. gauge	3PADIOS	Rt. wing sta. 128, 10% chord	
18	Diff. aero. press.	Wiancko press. gauge	3PADIOS	Rt. wing sta. 128, 26% chord	
19	Diff. aero. press.	Wiancko press. gauge	3PADIOS	Rt. wing sta. 128, 42% chord	
20	Diff. aero. press.	Wiancko press. gauge	3PADIOS	Rt. wing sta. 128, 59% chord	
21	Diff. aero. press.	Wiancko press. gauge	3PADIOS	Rt. wing sta. 128, 79% chord	
22	Gauge aero. press.	Wiancko press. gauge	3PADIOS	Fuselage sta. 37	
23	Diff. aero. press.	Wiancko press. gauge	3PADIOS	Lf. wing sta. 128, 58% chord	
24	Diff. aero. press.	Wiancko press. gauge	3PADIOS	Rt. hor. stab., 49% span, 47% chord	

* All fuselage stations are in inches from a datum line 16 in. forward of the nose. All wing stations are in inches from the vertical plane of symmetry.

SECRET

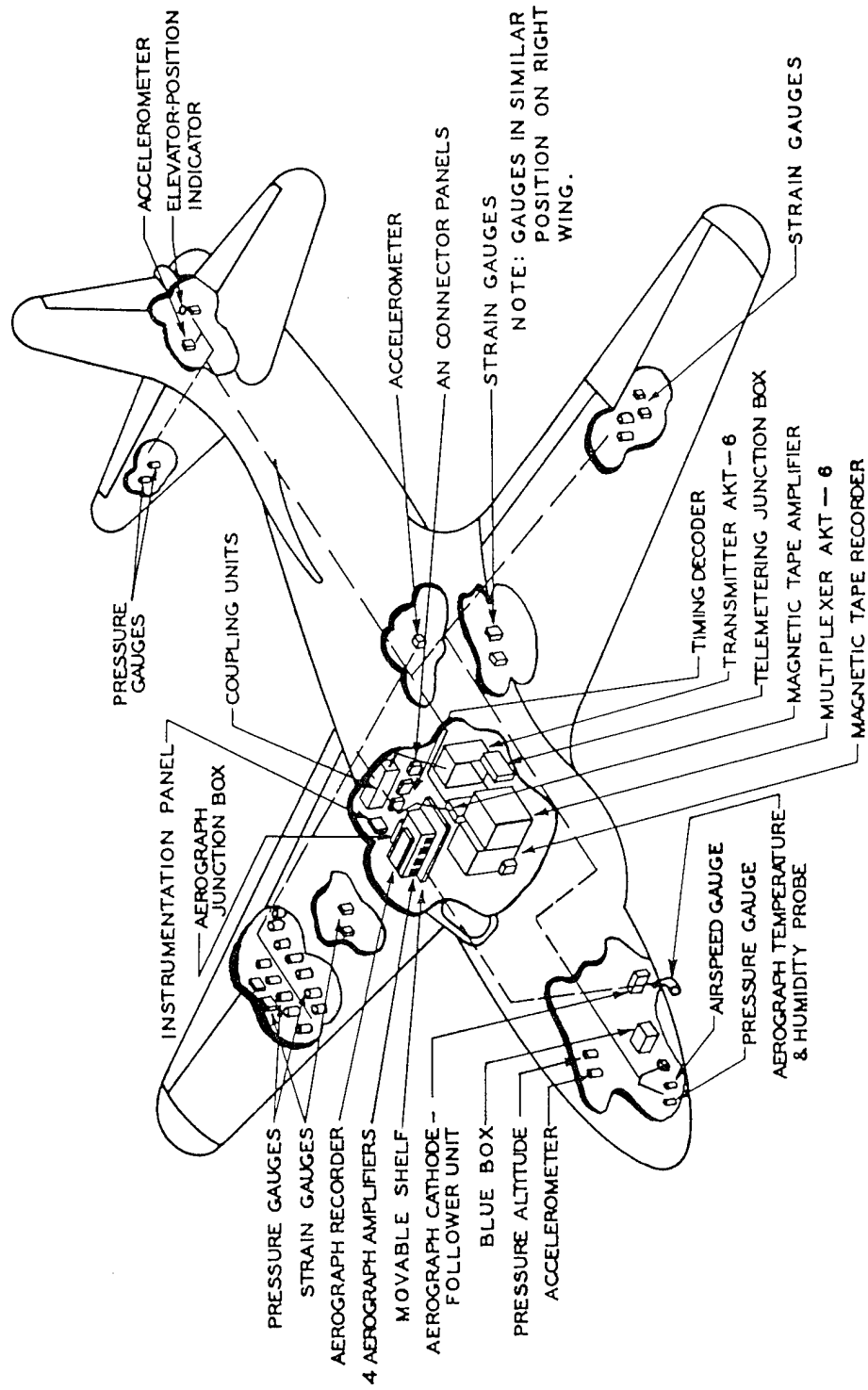


Fig. 3.8 Instrumentation of QT-33 Drones

SECRET

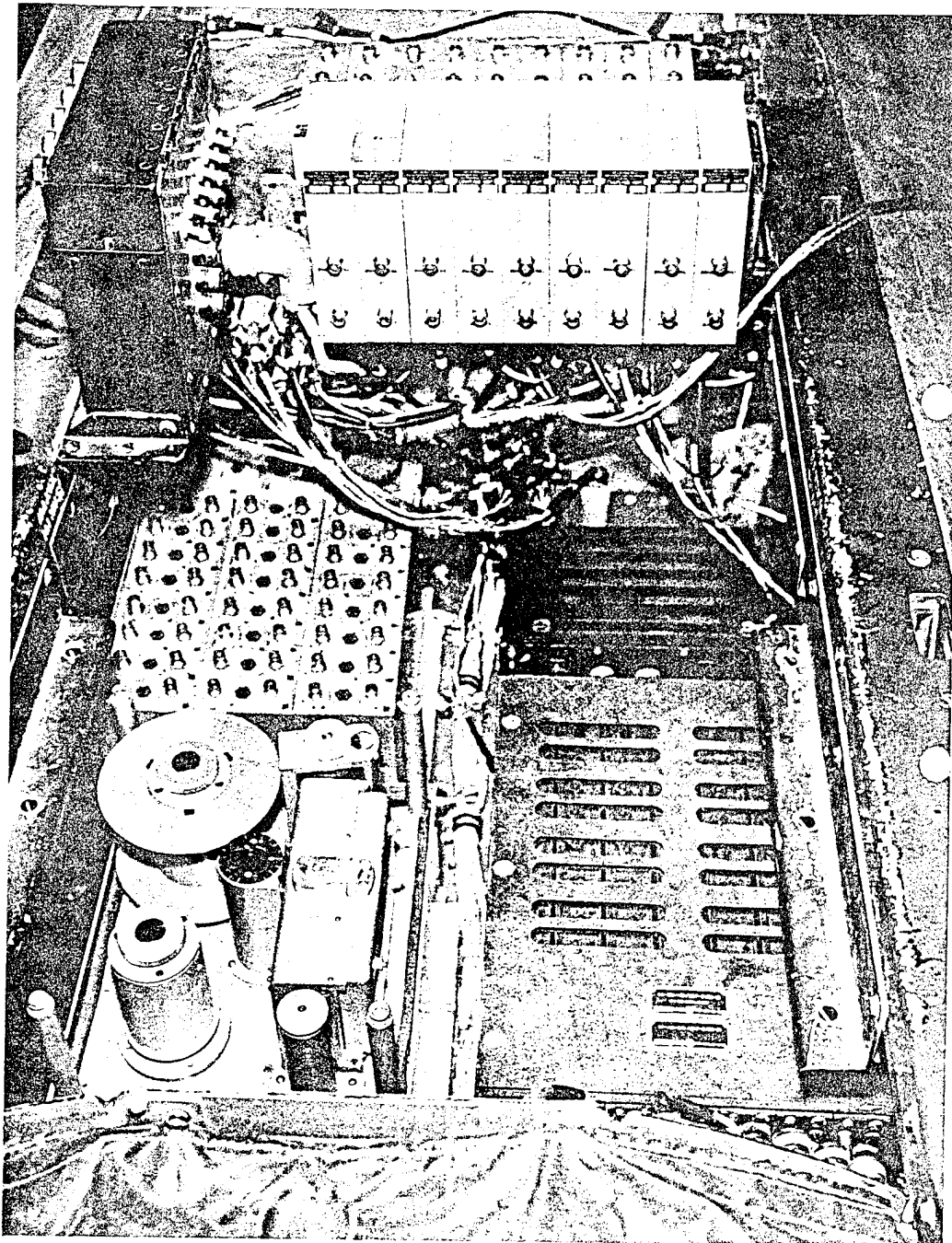


Fig. 3.9 Installation of Instrumentation in Aft Cockpit of QT-33 Drones

SECRET

to measure the total bending at the root of each wing (station 33). The gauges were mounted on the side of the spar cap of each spar just outboard of the attachment joints. These gauges were installed in duplicate for use with both recording systems.

Channel 9 measured the bending at the root of the right horizontal stabilizer. The gauges were mounted directly on the side of the spar webs at the extreme upper and lower edges outboard of the fuselage attachments. The spars undoubtedly did not carry all the bending load in the stabilizer because of the relative rigidity of the elevator torque tube and the load which passed from the stabilizer through the hinges to the elevator torque tube. Deflection of the elevator had no effect on the gauge output. Duplicate gauges were installed for use with both recording systems.

Channels 10 and 11 measured wing bending at right wing half-span (station 129) and quarter-span (station 74), respectively. The strain gauges were affixed to each of the spar-cap members and were connected so as to measure the total bending moment at the indicated wing stations. Both sets of gauges were installed in duplicate for use with both recorders. The gauges for channel 11 were located such that, in order to replace or repair any one of the gauges, it was necessary to remove the inner-outboard fuel tank. The removal of this tank represented considerable man-hours of labor in addition to presenting a replacement and resealing problem. It was therefore decided to delete the requirements for this channel in the event of gauge failure.

Channels 12 and 13 measured the shear and torsion, respectively, in the right wing root at wing station 33. The torsion at this station was measured by differential shear in the two spars. The gauges for channel 13 were installed and connected identically with those of channel 6. Both sets of gauges were installed in duplicate.

Channel 14 measured the wing torsion at station 74 (approximately quarter-span). These gauges were installed and connected in an identical manner to those of channels 6 and 13. These gauges were in the same general location as channel 11. The requirements for these gauges were, therefore, to be deleted in the event of gauge failure, for the same reasons as stated for channel 11.

Channel 15 measured the position of the elevator. The measurement of position was obtained by means of a cam affixed to the elevator torque tube which deflected a cantilever beam mounted to the horizontal-stabilizer structure. The deflection of the beam was measured by means of strain gauges. Only one set of gauges was provided because of space limitations.

Channels 16 through 24 measured aerodynamic pressure. The pressure transducers (see Sec. 2.6.5) were fastened to the surface by means of an aluminum mount such as shown in Fig. 3.10. Only one transducer was used in each location to measure the differential pressure between the upper and lower surfaces. The reference side of the transducers was vented to the lower surface of the wing or horizontal stabilizer (except channel 22) by means of a connecting tube $\frac{1}{2}$ in. in diameter. This tube was inserted in the reference side of the transducer, sealed with an O-ring, and secured with a cotter key. The vented end was positioned by an aluminum fitting attached to the lower surface and reamed for a slip fit with the connecting tube. This type of installation was utilized so that the pressure transducer would not act as a structural column and thereby damage the transducer during structural deflections. The transducer for channel 22 was mounted on the lower surface of the nose compartment at fuselage station 37 and was referenced to the interior of the nose compartment. Channels 16 through 21 were located, respectively, at 5, 10, 26, 42, 59, and 79 per cent of the chord at wing station 128 in order to measure the variation in chordwise distribution of lift at that station. Channel 23 was an installation on the left wing similar to that of channel 20 on the right wing. These two channels were used for comparative purposes in order to establish the symmetry (or asymmetry) of the load distributions on the two wings. Channel 24 was a similar installation on the right horizontal stabilizer. Duplicate pressure transducers were installed at all locations so that both recording systems would be furnished with information.

The installation of Class B parts (recorders, telemetering equipment, timing decoders, sensing elements, and associated equipment) could not be completed at Eglin Air Force Base because time did not permit. The installation of instruments was completed in the forward

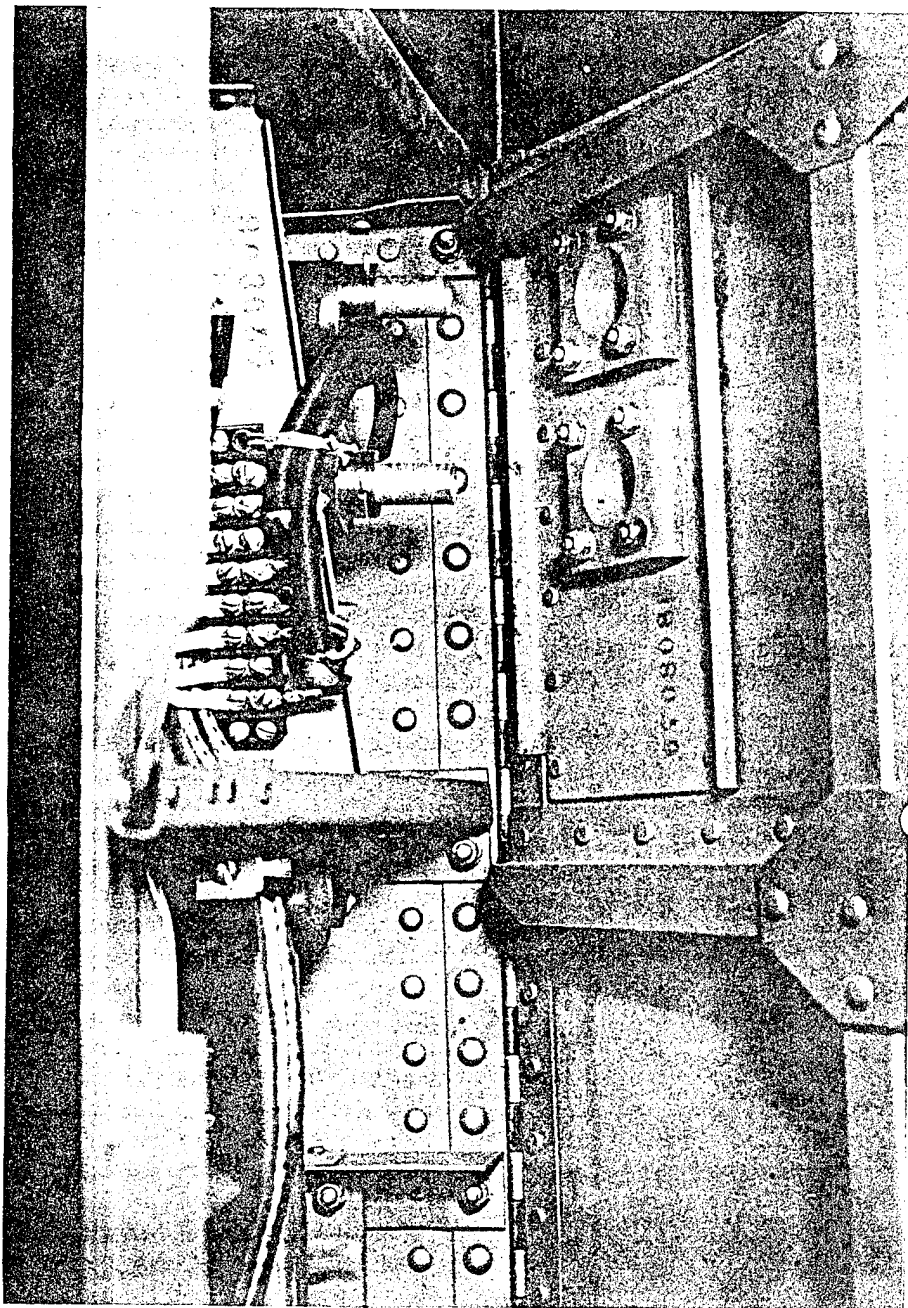


Fig. 3.10 Mounting of Pressure Transducers, QT-33

area. At this time, owing to the elimination of the filter unit, considerable rewiring was necessary. Many of the interconnecting cables between the sensing elements and recording systems required extensions in order to reach the proper attachment plugs. These extensions were the source of numerous short circuits, broken shielding, broken conductors, and mutilated insulation. These damages were incurred by excessive handling of the cabling in crowded quarters during "trouble shooting," removal and replacement of equipment, gauge checks, and similar operations.

3.4.2 Calibration

Channel 1, pressure altitude, was calibrated analytically. This method was used because a vacuum source to simulate change in altitude was not readily available.

Channel 2, indicated airspeed, was calibrated by the direct method since full-scale load could easily be applied for full-scale calibrations. Calibration loads were applied to the pitot system by means of bottled compressed air, and the values of the loads were measured by means of a calibrated airspeed indicator.

Channels 3, 4, and 5, normal accelerations, were also calibrated by the direct method since full-scale load could be applied by rigidly mounting the transducers to a sinusoidally oscillating table. The table was vibrated at various frequencies in increments equivalent to approximately 2 g. These approximate settings were determined by a tachometer graduated in g units. A record was obtained at each load increment. Since the tachometer readings were not sufficiently accurate for calibration purposes, the actual frequency was determined from the calibration record by counting the cycles per second. With this information it was possible to calculate the applied g loading by the equation (derived from $a = r^2$)

$$g = 0.0255N^2 \quad (3.2)$$

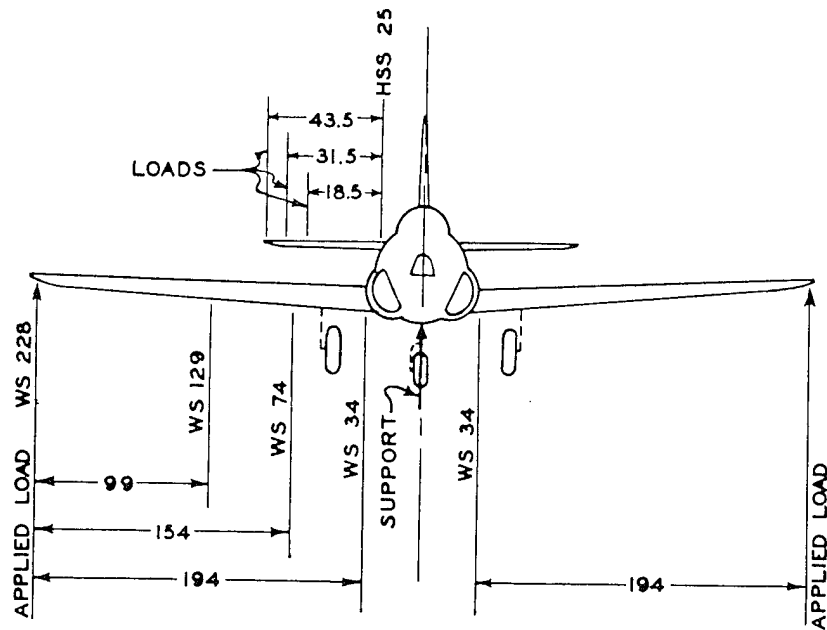
where N is in cycles per second.

Channels 6, 13, and 14 were strain-gauge channels for measuring wing torsion. Channel 13 was calibrated at the same time as the bending channels by applying the loads off the elastic axis. No test data were obtained from channels 6 and 14; therefore the calibrations of these channels are omitted. Because of the

short lever arm used to apply torque to the wing, the reliability of this calibration is somewhat questionable.

Channels 7, 8, 10, 11, and 12 were strain-gauge channels for measuring bending moments and shear of the wing panels. The indirect calibration method was used on these channels, as explained in Sec. 3.2.1. The gauges were calibrated by supporting the complete airplane on trestles and by applying loads at the wing tips (see Fig. 3.11). It was necessary to support the airplane from the principal fuselage structural members so that all loads and reactions could be accurately calculated. If the airplane remained on the landing gear, indeterminate side loads would result from deformation of the tires and landing gear. The airplanes were raised by aircraft jacks and lowered onto wooden trestles constructed to fit the bottom fuselage contour at fuselage stations 131 and 316.1. The trestles were constructed to support the total weight of the airplane and to position the longitudinal axis of the airplane in level-flight attitude. The lateral axis of the airplane was maintained in a horizontal plane by means of jacks located at the wing tips. The wing-tip jacks were seated on jack pads mounted on a bracket attached to the wing-tip fuel-tank supports. These brackets were fabricated from salvaged fuel tanks to ensure proper attachment and alignment. The calibration loads were applied to the wing-tip jack pads at a point midway between the spars (1.85 in. from the elastic axis) at wing station 216 to ensure proper stress distribution between the wing spars. The loads applied to the wing were measured by means of a calibrated Cox and Stevens aircraft weighing kit. Prior to the application of the calibration loads the wing panels were flexed four times by cycling the wing-tip load from minimum to maximum to minimum, in order to minimize the effects of structural looseness. The initial balancing load was maintained at approximately 500 lb, at which time the sensing elements were electrically balanced. Four additional loads were applied at approximate increments of 100 lb each. The amplified millivolt output of each gauge at each load increment was measured and compared to the applied load. This determined the calibration curve of the sensing element alone. This curve, when combined with the data obtained with the calibration box, determined the final calibration curves for the channels (see Sec. 3.2.1).

SECRET



NOTE: DIMENSIONS INDICATED ARE
MOMENT ARMS FROM LOAD
TO INDIVIDUAL GAUGES.

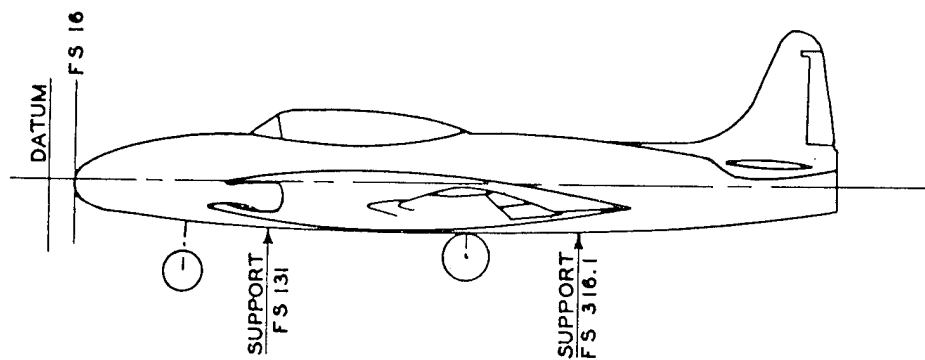


Fig. 3.11 Calibration of Bending and Shear Gauges, QT-33

SECRET

SECRET

Channel 9 was calibrated in the same manner as the bending channels; however, the calibration load increments were 200 lb rather than 100 lb each. These loads were applied by means of dead weights in a downward direction, owing to the difficulty of fabricating and attaching suitable jack pads on the horizontal stabilizers (see Fig. 3.11).

Channel 15, elevator position, was calibrated by the direct method since full-scale load was applied by the full-up travel of the elevator surface. The gauge was balanced in a full-down attitude, and loads were applied by deflecting the surfaces upward in 10° increments. The deflections were measured by means of a protractor-level combination.

Channels 16 through 24, aerodynamic pressure, were calibrated by the direct method since full-scale load could be applied on the pressure side of the gauge. Laboratory tests indicated that the output of the gauges was essentially the same for each positive and negative pressure. The anticipated loading on the pressure gauges was positive on the reference side and negative on the pressure side. The installation and construction of the gauges dictated the application of positive pressure on the pressure side for field calibration purposes. Pressure was applied by means of bottled compressed air and was measured by a calibrated airspeed indicator.

3.5 B-50D AIRPLANES

Two B-50D airplanes were obtained through regular Air Force commitments from the Boeing Aircraft Co. and were delivered to Wright-Patterson Air Force Base for installation of Class A instrumentation parts. Modification of both airplanes was necessary since sufficient space was not available for some installations. The changes accomplished at Wright-Patterson Air Force Base were the following:

1. Removal of rear sighting station and all necessary gunnery equipment to provide space for a control station for operation of instrumentation equipment.
2. Removal of forward gun turret to provide more space for personnel and to accommodate the blue box.
3. Cutting of access holes for installing sensing elements and brackets.

The airplanes underwent further modification at Kelly Air Force Base and Kirtland Air Force Base, preparing them as spares to replace the "drop" airplane being used by the 4925th Special Weapons Group at Kirtland Air Force Base. Approximately three weeks were spent modifying the airplanes and installing equipment as follows:

1. Modification of rear bomb-bay doors to permit protrusion of sensing antennas.
2. Removal of rear gun turret to accommodate brackets for installing A-11 camera mounts.
3. Installation of new bomb racks in the forward bomb bay for carrying an atomic bomb.
4. Provision of six instrument racks for mounting special test equipment in the aft part of the airplane.

Much of the equipment installed for this purpose was never utilized because of the cancellation of the scheduled King shot.

3.5.1 Instrumentation

The airplanes were flown to the Air Proving Ground, Eglin Air Force Base, where personnel of ATU 3.4.2 installed sensing elements and recording equipment. The relative locations of sensing elements, recording equipment, and related components are shown in Fig. 3.12. All sensing-element locations were accessible for field maintenance and replacement. Table 3.7 lists the function, location, type, and model of instrument used for each channel of the recorders.

The elevator-position indicator used in channel A1 was a thin cantilever beam with one end affixed to the fuselage and the other end attached to the elevator torque tube. Strain gauges were mounted on top and bottom surfaces and connected electrically to measure bending of the beam. The amount of bending in the beam was dependent on the travel of the elevator torque tube and was calibrated in terms of deflection of the elevator.

Channels A3 through A7, A15, and B3 contained Statham accelerometers with a range of ± 6 g for measuring vertical accelerations of different parts of the airplanes. The accelerometers used in channels A3, A4, and A15 were located on the accessory section of engines 2, 1, and 3, respectively, and were mounted with their sensitive axes perpendicular to the line of

SECRET

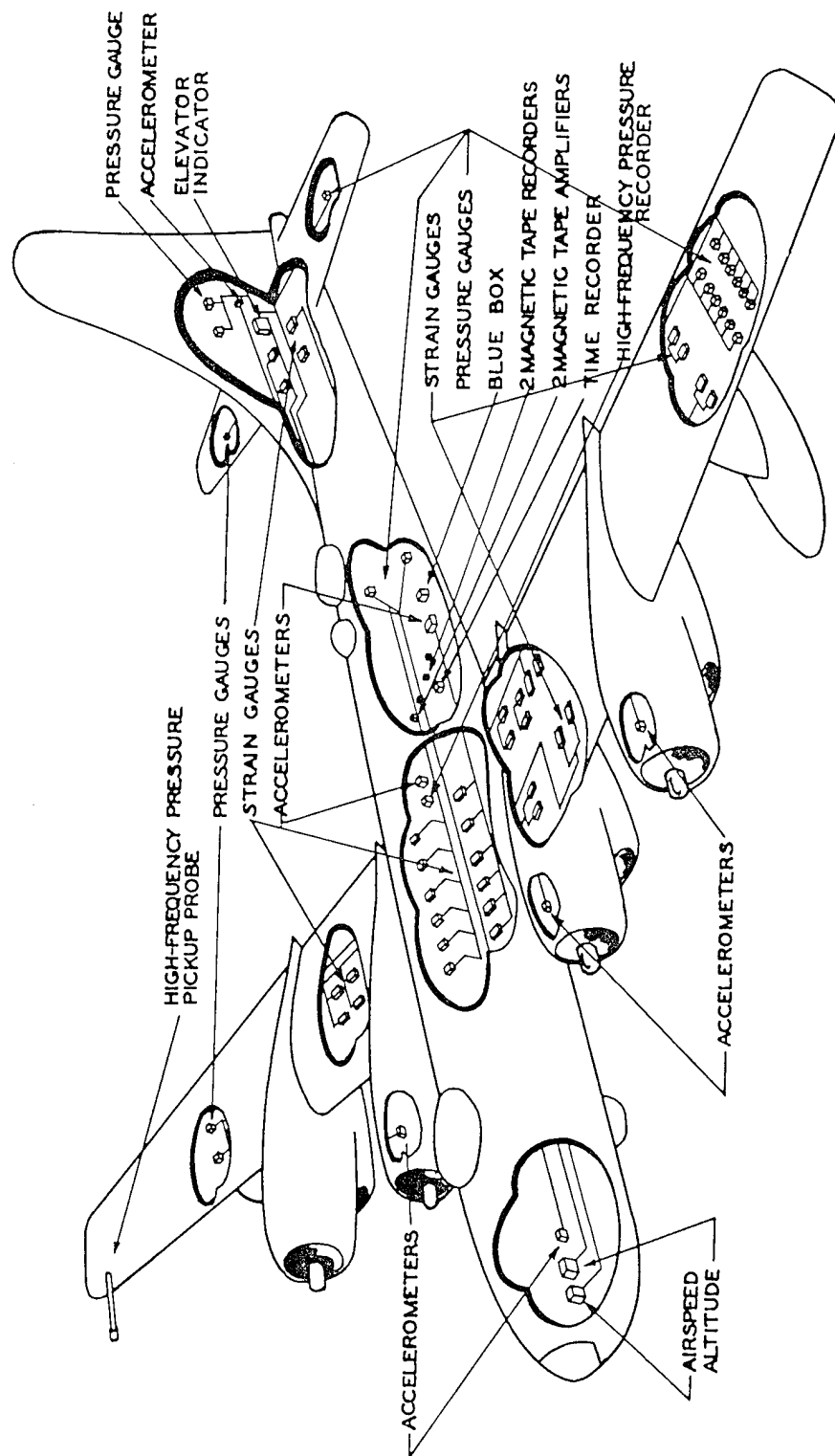


Fig. 3.12 Instrumentation of B-50D Airplanes

TABLE 3.7 RECORDER-CHANNEL ASSIGNMENTS FOR B-50D AIRPLANES

Chan.	Intelligence Measured	Instrument		Instrument Location*
		Type	Model	
A1	Elevator position	Shop fabricated	None	Elevator torque tube
A2	Wing bending	SR4 strain gauge	A18-6-350	Lf. wing sta. 505
A3	Vertical accel.	Statham accel.	A18-6-350	No. 2 engine access. sec.
A4	Vertical accel.	Statham accel.	A18-6-350	No. 1 engine access. sec.
A5	Vertical accel.	Statham accel.	A18-6-350	Forward bomb bay, sta. 370
A6	Vertical accel.	Statham accel.	A18-6-350	Nose-wheel well, sta. 149
A7	Vertical accel.	Statham accel.	A18-6-350	Tail-gunner comp., sta. 1141
A8	Stab. bending	SR4 strain gauge	A13-350	Rt. hor. stab., sta. 34
A9	Stab. bending	SR4 strain gauge	A13-350	Lf. hor. stab., sta. 34
A10	Wing bending	SR4 strain gauge	A13-350	Rt. wing sta. 266
A11	Wing bending	SR4 strain gauge	A13-350	Rt. wing sta. 79
A12	Wing bending	SR4 strain gauge	A13-350	Lf. wing sta. 79
A13	Wing bending	SR4 strain gauge	A13-350	Lf. wing sta. 120
A14	Wing bending	SR4 strain gauge	A13-350	Lf. wing sta. 266
A15	Vertical accel.	Statham accel.	A18-6-350	No. 3 engine access. sec.
A16	Wing shear	SR4 strain gauge	A13-350	Rt. wing sta. 269
A17	Wing shear	SR4 strain gauge	A13-350	Rt. wing sta. 78
A18	Wing shear	SR4 strain gauge	A13-350	Lf. wing sta. 78
A19	Wing shear	SR4 strain gauge	A13-350	Lf. wing sta. 122
A20	Wing shear	SR4 strain gauge	A13-350	Lf. wing sta. 269
A21	Wing shear	SR4 strain gauge	A13-350	Lf. wing sta. 506
A22	Wing torsion	SR4 strain gauge	A13-350	Rt. wing sta. 78
A23	Wing torsion	SR4 strain gauge	A13-350	Lf. wing sta. 78
A24	Wing torsion	SR4 strain gauge	A13-350	Lf. wing sta. 122
B1	Altitude	Statham press. gauge	P73-15A-350	Left-side radio compt.
B2	Airspeed	Statham press. gauge	P73-10-300	Left-side radio compt.
B3	Vertical accel.	Statham accel.	A18-6-350	Rear bomb bay, sta. 628
B4	Diff. aero. press.	Wiancko press. gauge	3PAD1OW	Rt. wing sta. 525, 23% chord
B5	Diff. aero. press.	Wiancko press. gauge	3PAD1OW	Rt. wing sta. 525, 60% chord
B6	Gauge aero. press.	Wiancko press. gauge	3PAD1OS	Fuselage sta. 26
B7	Gauge aero. press.	Wiancko press. gauge	3PAD1OS	Fuselage, rt. side, sta. 783
B8	Gauge aero. press.	Wiancko press. gauge	3PAD1OS	Fuselage, lf. side, sta. 783
B9	Gauge aero. press.	Wiancko press. gauge	3PAD1OS	Vert. fin, rt. side, sta. 974
B10	Gauge aero. press.	Wiancko press. gauge	3PAD1OS	Vert. fin, lf. side, sta. 974
B11	Gauge aero. press.	Wiancko press. gauge	3PAD1OS	Lf. wing, top, sta. 524, 5% chord
B12	Gauge aero. press.	Wiancko press. gauge	3PAD1OS	Lf. wing, top, sta. 524, 15% chord
B13	Gauge aero. press.	Wiancko press. gauge	3PAD1OS	Lf. wing, top, sta. 524, 23% chord
B14	Gauge aero. press.	Wiancko press. gauge	3PAD1OS	Lf. wing, top, sta. 524, 45% chord
B15	Gauge aero. press.	Wiancko press. gauge	3PAD1OS	Lf. wing, top, sta. 524, 60% chord
B16	Gauge aero. press.	Wiancko press. gauge	3PAD1OS	Lf. wing, top, sta. 524, 85% chord

*Wing stations in inches from plane of symmetry.

TABLE 3.7 (Continued)

Chan.	Intelligence Measured	Instrument		Instrument Location*
		Type	Model	
B17	Gauge aero. press.	Wiancko press. gauge	3PAD10S	Lf. wing, bottom, sta. 524, 5% chord
B18	Gauge aero. press.	Wiancko press. gauge	3PAD10S	Lf. wing, bottom, sta. 524, 15% chord
B19	Gauge aero. press.	Wiancko press. gauge	3PAD10S	Lf. wing, bottom, sta. 524, 23% chord
B20	Gauge aero. press.	Wiancko press. gauge	3PAD10S	Lf. wing, bottom, sta. 524, 43% chord
B21	Gauge aero. press.	Wiancko press. gauge	3PAD10S	Lf. wing, bottom, sta. 524, 60% chord
B22	Gauge aero. press.	Wiancko press. gauge	3PAD10S	Lf. wing, bottom, sta. 524, 85% chord
B23	Gauge aero. press.	Wiancko press. gauge	3PAD10S	Rt. hor. stab., bottom, sta. 170
B24	Gauge aero. press.	Wiancko press. gauge	3PAD10S	Lf. hor. stab., bottom, sta. 170

* Wing stations in inches from plane of symmetry.

flight. Acceleration measured at these points was to have been used to determine the loads imposed on the wings by the engines. Channels A5, A6, A7, and B3 contained accelerometers mounted vertically to measure normal acceleration, pitching, and deformations in the fuselage. The accelerometers were located in the fuselage at the following stations.

Channel A5, the c.g. accelerometer, was located at fuselage station 370 in the aft part of the forward bomb bay, 47 in. forward of the normal c.g. position of 24 per cent m.a.c.* The accelerometer for channel A6 was located in the aft part of the nose-wheel well at fuselage station 149, approximately 268 in. forward of the normal c.g. position. Data from this channel were intended to measure pitching of the airplane about the c.g. Channel A7 accelerometer was located in the tail-gunner's compartment of fuselage station 1141, approximately 724 in. aft of the normal c.g. position. Channel B3 accelerometer was located in the forward part of the rear bomb bay at fuselage station 628, approximately 211 in. aft of the normal c.g. position.

Bending, shear, or torsion was measured using Baldwin-Southwark resistance-type strain gauges. Four gauges were so connected

electrically that they formed a resistance bridge with opposite legs in either compression or tension and with all four arms of each bridge active. The measurement of either bending, shear, or torsion was dependent on the connection of the gauges. A double set of strain gauges was installed to ensure that each channel would have one bridge operative at all times. Owing to the location of the gauges, most installations were difficult to reach for replacement or repair.

Bending of the horizontal stabilizers was measured by channels A8 and A9 using strain gauges mounted on the rear spar caps, top and bottom, at stabilizer station 34. It was determined that the rear spar carried the greater proportion of loads imposed on the stabilizer and that this proportional amount was constant for all air loads.

Spanwise bending of the wings was measured by channels A2 and A10 through A14. Channel A2 measured the bending of the outer wing panel at the attachment points. The effect of the engines on wing bending was recorded by channels A10, A13, and A14. Wing-root bending was measured by channels A11 and A12. The strain gauges for these channels were mounted on front and rear spar caps, top and bottom. Channel A2 was located on the left wing at station 505 inboard of the outer-wing-panel attachment points. Channels A10 and A11 were located on the right wing at station 266 and 79, respectively. Station 266 was midway between

*The m.a.c. for the B-50 airplane is 151.41 in. in length, and the leading edge of the m.a.c. is 373.97 in. from the nose of the airplane (fuselage station 379.94).

engine nacelles, and station 79 was just outboard of wing-fuselage attachment points.

Channels A12, A13, and A14 were located on the left wing at stations 79, 120, and 266, respectively. Stations 266 and 79 were comparable to the same stations on the right wing, and station 120 was inboard of engine 2.

Wing shear was measured by channels A16 through A21. The gauges were installed on the front and rear surfaces of the spar web at 45° to the vertical. Channels A16 and A17 were located on the right wing at stations 269 and 78, respectively. Channels A18 through A21 were located on the left wing at stations 78, 122, 269, and 506, respectively.

Torsion was measured by differential shear between the front and rear spars. The gauges were mounted in an identical manner to those used in measuring shear but so connected as to measure torsion. Channel A22 measured torsion in the right wing at station 78, and channels A23 and A24 measured torsion in the left wing at station 78 and 122, respectively.

Channels B1 and B2 measured altitude and airspeed using Statham pressure transducers. The altitude transducer was connected to the lines of the static system used for the pilot's flight instruments, and the airspeed transducer was connected to the lines of both pitot and static systems. Each transducer contained a resistance-type bridge and was mounted on the left side of the fuselage just aft of the pilot's seat. The lag in both systems was kept at a minimum by using the shortest possible hoses connecting the transducers to the pitot and static lines.

Differential aerodynamic pressure was measured by channels B4 and B5 using two Wiancko pressure transducers for each channel. The transducers used in channels B4 and B5 were located in the right wing along station 525 at 23 and 60 per cent of wing chord, respectively. One transducer was mounted on top and one on the bottom surface of the wing, and these transducers were interconnected physically for reference pressure and electrically to measure pressure difference. Station 525 was chosen for the location of the transducers, since it was outside the propeller arc and thus clear of turbulent air in the propeller slip stream.

Channels B6 through B24 measured the overpressure experienced by the airplanes using

single Wiancko pressure transducers for each channel. The overpressure measured was actually the increase in pressure from a known reference pressure. A small tank was installed in the rear bomb bay, to which one side of each gauge was connected. The tank itself was vented to the bomb bay through a line extending via the control station, and a valve was installed at the control station to open or close the line. Opening the valve permitted the tank to assume the pressure in the bomb bay for any desired altitude, and closing the valve sealed the pressure in the tank to that of the particular altitude. In this manner the reference pressure was maintained at the same valve for all gauges, and, by using the pressure of the assigned test altitude, the full range of the pressure transducers was available for measuring pressure variations. Twenty-one Wiancko coupling units were used, one for each channel utilizing Wiancko pressure transducers. These units were installed on a rack at the control station. Channels B6, B7, and B8 measured pressure about the fuselage at fuselage stations 26 and 783. The transducer used in channel B6 was mounted on the underside of the fuselage forward of the nose-wheel well. The two transducers used in channels B7 and B8 were mounted on the right and left sides of the fuselage, respectively, midway between the top and bottom of the fuselage.

Two transducers were installed in the vertical fin at fuselage station 974, approximately 46 in. above the fuselage. The transducers for channels B9 and B10 were located, respectively, on the right and left sides of the vertical fin.

Channels B11 through B22 measured pressures on the left wing on top and bottom surfaces along wing station 524 at 5, 15, 23, 43, 60, and 85 per cent of the wing chord. The wing chord at station 524 was 134 in. in length. The transducers for channels B11 through B16 were mounted on the top surface, and those for channels B17 through B22 were mounted on the bottom surface.

The right and left horizontal stabilizer contained one transducer each, mounted on the bottom surface along stabilizer station 170 at 40 per cent of stabilizer chord. The length of the stabilizer chord at station 170 was 81 in. These transducers were connected into channels B23 and B24, respectively.

The sensing probe of the high-frequency

pressure recorder was installed under the left wing tip at the junction of the wing tip and the outer wing panel on B-50D No. 340. The probe clamps were mounted on the wing spars. The probe was aligned in a straight-ahead position in level-flight attitude. The crystal sensing element was located approximately 4 ft ahead of the leading edge of the wing. The surface of the sensing unit was oriented in the side of the boom parallel to the line of flight and parallel to the expected line of approach of the shock wave. The amplifier-recorder unit was mounted on a special platform in the after-section of the rear bomb bay. Both a-c and d-c power were taken from the electrical system of the airplane. The recording cycle was initiated by an electrical signal from the blue box at time T_0 .

3.5.2 Calibration

The B-50D airplanes were partially calibrated in the Z.I., and the remaining calibrations were performed at the forward area. In general, the strain-gauge channels were calibrated at the Structures Test Laboratory at Wright-Patterson Air Force Base, and the accelerometers and pressure transducers were calibrated at Eniwetok.

Channel A1, elevator position, was calibrated directly since full deflection of the elevator was possible during calibration. The gauge was balanced in the full-down position, and records were made at increments of 10° to the full-up position. The deflection increments were measured by means of a protractor-level combination.

Channels A2, A10, A11, A12, A13, and A14, wing bending, and channels A15, A17, A18, A19, A20, and A21, wing shear, were calibrated at Wright-Patterson Air Force Base by the actual application of known loads. The airplane was restrained by attachments at the bomb-rail fittings, and loads were applied by calibrated hydraulic struts. The points at which the loads were applied are indicated in Figs. 3.13 and 3.14. Figure 3.14 indicates the permissible level of bending moment from the stress analysis and the maximum level of bending as applied to the wings for calibration. Figure 3.13 indicates similar information with respect to shear: the maximum permissible shear from the stress analysis and the maxi-

mum shear applied for calibration. In order to reduce the extrapolation of the calibration curves, it was necessary to apply loads as large as possible. However, in view of the fact that the airplanes were to be manned during the test, it was even more important that the structure not be weakened by overloading.

Channels A3, A4, A5, A6, A7, A17, and B3, vertical acceleration, were calibrated by the analytical method as described in Sec. 3.2.3. Using Eq. 3.1, equivalent accelerations were established for the various calibration resistors for each accelerometer.

Channels A8 and A9, stabilizer bending, were not calibrated in the Z.I. Improper location and connection of the gauges reduced the output to such a point that no readings were obtained from the channels. This condition was corrected, and the stabilizers were calibrated in the forward area. The calibration was performed by applying up-loads (by means of jacks) near the tips. A third jack under the nose wheel reduced the vertical motion of the *empennage*.

Channels A22, A23, and A24, wing torsion, were calibrated in the Structures Test Laboratory by the application of pure torque. Five torque arms were installed on each wing at wing stations 780, 710, 650, 460, and 250. Bending loads were avoided by applying equal loads up and down at the proper ends of the torque arms.

Channel B1, pressure altitude, was calibrated analytically because of the difficulty of applying a vacuum to the system. Equation 3.1 and the technique described in Sec. 3.2.3 were used in this calibration, which was checked by actual flight tests against the pilot's altimeter and the radar altimeter.

Channel B2, airspeed, was calibrated directly by the application of pressures to the pitot side of the transducer equivalent to the dynamic heads corresponding to various airspeeds.

Channels B4 and B5, differential aerodynamic pressure, were very difficult to calibrate and to adjust because of the double transducer (top and bottom surfaces) installation. First, with an arbitrary gain setting for each transducer, a zero balance was achieved. Next, maximum pressure (2 psi) was applied to one transducer, and the gain for that transducer

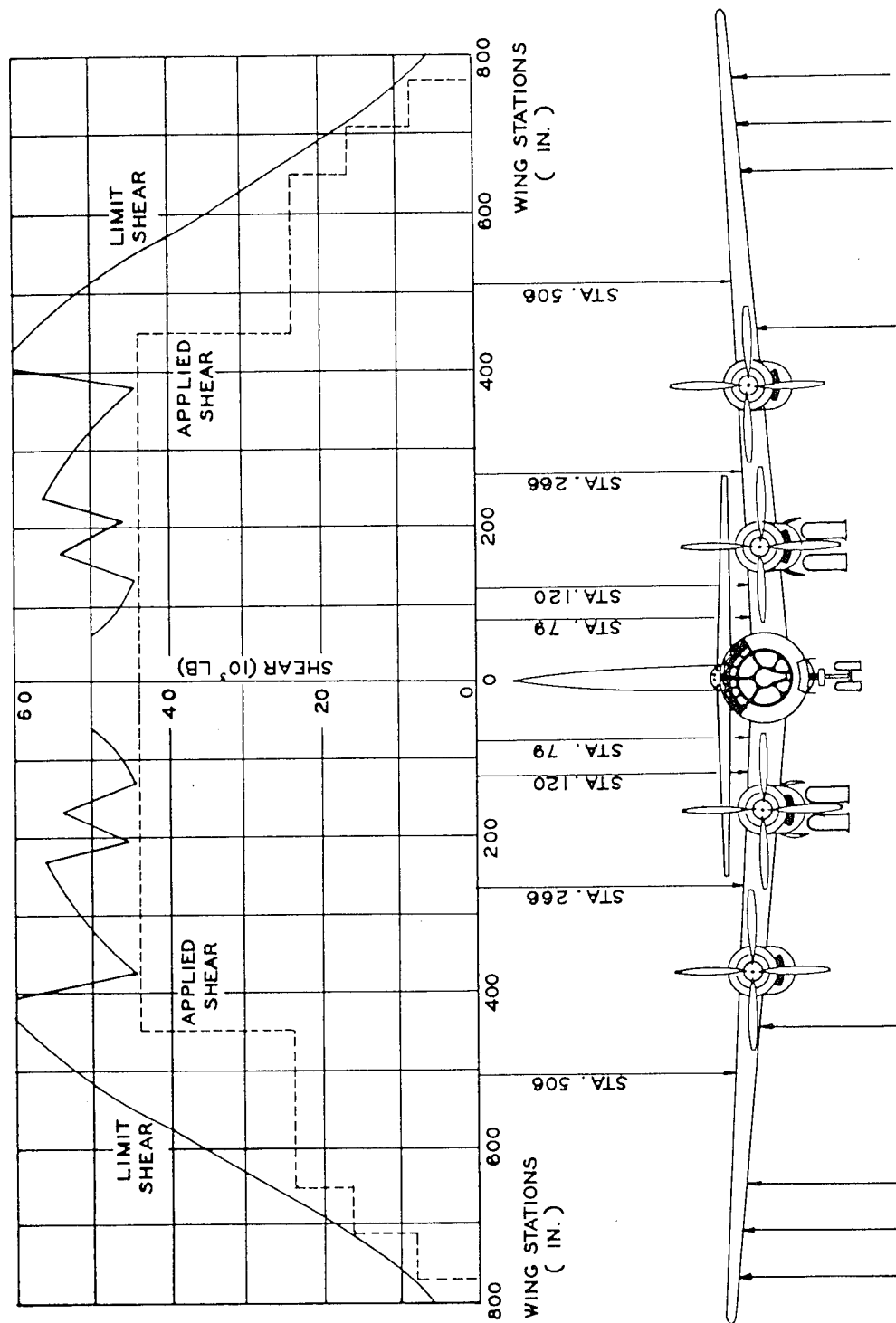


Fig. 3.13 Permissible and Maximum Applied Shear for Calibration of B-50D Wing Shear Gauges

SECRET

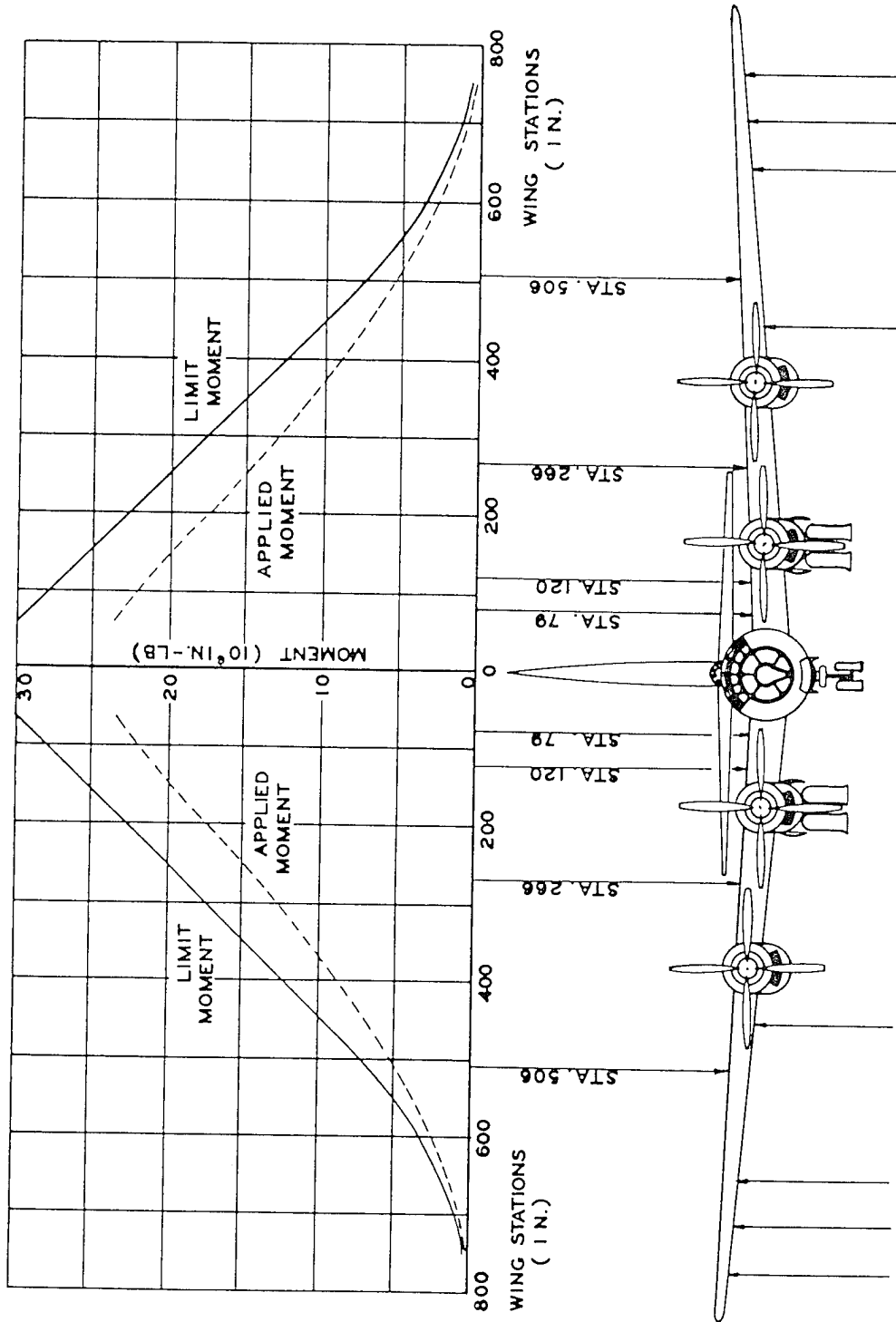


Fig. 3.14 Permissible and Maximum Applied Moments for Calibration of B-50D Wing-bending Gauges

was adjusted to a convenient value. The same pressure was then applied to the other transducer and that gain was adjusted to the same value. The check of the adjustment was the application of various pressures to each transducer simultaneously, and if the adjustment was correct no output was observed from the channel. The calibration was performed by the application of pressure increment, in turn, to each transducer. In order to have been complete, a series of pressure increments should have been applied to one transducer, with various pressures applied to the other transducer. However, this procedure would have required additional equipment and time; therefore the simplified technique was accepted. The graph of pressure on the lower transducer versus trace deflection was accepted as a calibration of positive pressure gradient, and on the upper transducer as a calibration in the negative direction.

Channels B6 through B24 were calibrated directly by the application of pressures up to full scale. Since laboratory tests had proved the calibration of the pressure transducers to be the same in the positive and negative senses, it was possible to improvise a quick and simple calibration of these channels. Each of the transducers in these channels had the reference side connected to a common reservoir. The calibration of the transducers was accomplished by the application of pressure increments to the reservoir. This was considered to be the equivalent of the application of a vacuum to the other side of each transducer, and it provided a calibration in the positive sense for those transducers on the upper surface of the wings and in the negative sense for those on the lower surface. Increments of pressure up to 3 psi were applied to the reservoir.

3.6 XB-47 AIRPLANE

The original request for the B-47 for this project was for a B-47A for reasons of modernity and logistic support. However, the B-47A's being built by Boeing Aircraft Co. were all assigned, and the second XB-47 had just completed its series of test flights. Being more readily available, the XB model was assigned to the project by higher authority.

The XB-47 underwent modification and installation of Class A instrumentation parts at the Boeing Aircraft Co., Wichita, Kans., under Contract W33-038-ac-22413. Modification of the airplane for a long-range operation under adverse conditions was quite extensive. The more important changes involved in preparing the airplane for its participation in Project 8.1 were the following:

1. Previously installed flight-test equipment and wiring were removed.
2. The APS-23 radar was overhauled so as to be operational for navigation.
3. The inboard and outboard nacelles, struts, J-35-GE-11 engines, and associated cowlings, fairing, etc., were removed and replaced by B-47A inboard nacelles, B-47B outboard nacelles, J-47-GE-11 engines, and associated items.
4. Bomb-bay doors and related components were modified to incorporate a 2,500-gal fuel tank in the bomb bay.
5. Main-landing-gear wheels and brakes were removed and replaced with a new type in order to provide an automatic antiskid braking system for the best possible landing performance on the limited runways of the forward area.
6. Type AM/APM-9 loran set was installed at the navigator's station.
7. The installation of Class A instrumentation parts at the time of modification by the contractor was considered the most expedient means of accomplishing the work in order that the airplane might meet the scheduled delivery date at Eglin Air Force Base.

3.6.1 Instrumentation

On completion of the work by the contractor, the airplane was flown to the Air Proving Ground, Eglin Air Force Base. Sensing elements and recording equipment were installed by personnel of ATU 3.4.2; however, the installations were not completed until the airplane reached the forward area. Figure 3.15 shows the relative locations of sensing elements, recording equipment, and related components. The locations of sensing elements were so chosen as to measure the information desired and to be readily accessible for installation and repair under field conditions where

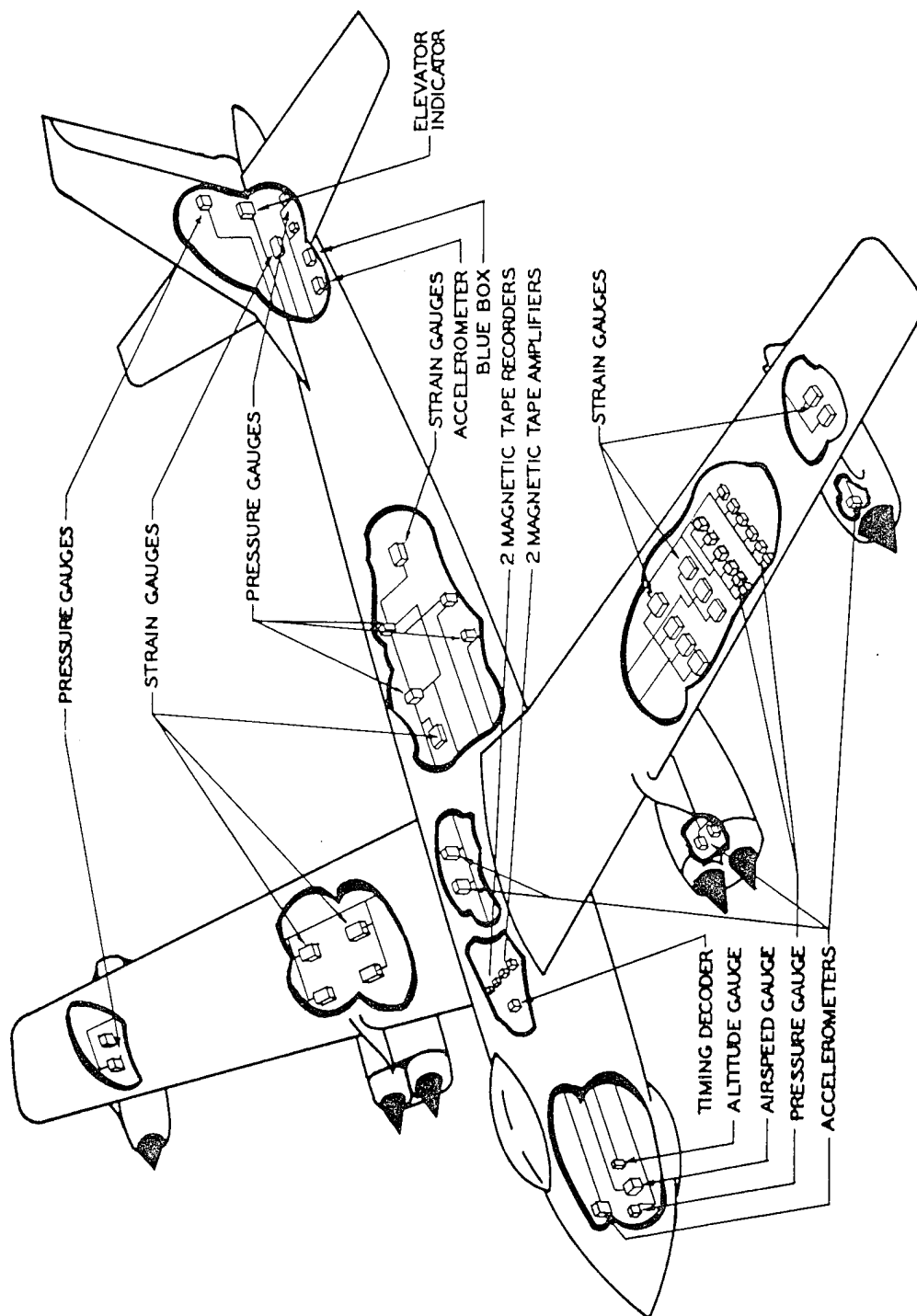


Fig. 3.15 Instrumentation of XB-47 Airplane

possible. Difficulty arose in satisfying desired information and readily accessible locations at the same time; hence some gauges were not easily replaced. Table 3.8 lists the function, location, type, and model of instrument used for each channel of the recorders.

The sensing element for channel A1, elevator-position indicator, was designed and installed by the contractor and was mounted in the vicinity of the elevator torque tube. Elevator movement was measured by a variable slide-wire potentiometer inserted at one corner of a resistance bridge and connected directly with the torque tube. The signal received from the resistance bridge was dependent on the travel of the torque tube.

Channels A2 through A8 contained resistance-type Statham accelerometers for measuring vertical and lateral acceleration at different stations of the fuselage. Channel A2 measured lateral acceleration of engine 3 by using a ± 6 -g accelerometer mounted on the "air-guide" section at the forward end of the engine with its vertical, or sensitive, axis perpendicular to the vertical plane of symmetry of the airplane. Channels A3 and A4 utilized ± 12 -g accelerometers for measuring vertical accelerations; these accelerometers were similarly mounted on the air-guide sections of engines 3 and 1, respectively, with their sensitive axes parallel to the vertical plane of symmetry of the airplane. Channels A5, A6, A7, and A8 measured vertical or normal acceleration, using ± 6 -g accelerometers mounted within the fuselage, with their sensitive axes perpendicular to the level line of the airplane. Comparison of these accelerations was intended to indicate the pitching of the airplane and the deformation of the fuselage. Channel A5 was located at fuselage station 210, approximately 403 in. forward of the normal c.g. position, which is taken as 18 per cent m.a.c.* Channel A6 was located at fuselage station 510, approximately 103 in. forward of the normal c.g. position. Channel A7 was located at fuselage station 612, or 18.5 per cent m.a.c., approximately $\frac{3}{4}$ in. aft of the normal c.g. position. Channel A8 was located at fuselage station

1166, approximately 553 in. aft of the normal c.g. position.

Channels A9 through A24 measured shear, torsion, or bending by using Baldwin-Southwark resistance-type strain gauges. Replacement or repair of the strain gauges was difficult and time-consuming. Many gauge installations were surrounded by equipment and were extremely hard to reach. A double set of strain gauges was initially installed to help alleviate this condition, one set for normal use and the other set for use as spares. Four gauges were connected electrically to form the four legs of a bridge and were installed so that opposite legs of the bridge measured compression or tension of the structure. Measurement of shear, torsion, or bending was dependent on the proper location of the various legs of the bridge.

The gauges used for channels A9 and A24 were mounted on four fuselage *longerons* at stations 985 and 718, respectively. The *longerons* chosen for these installations lay midway between the vertical plane and the horizontal plane of the fuselage. Thus the gauges at each station were located circularly about the fuselage with their axes of measurement along the line of flight. Gauges were installed so as to measure bending of the fuselage in the vertical plane at two stations aft of the normal c.g. position.

Channels A10 and A14 measured chordwise bending in the right and left wings, respectively, at wing station 307. Gauges installed at this station for wing-root measurements were outboard of any wing and fuselage junctions and fairing structure and were mounted on the front and rear spar cap, top and bottom.

Torsion in the right and left wings was measured by channels A11 and A15, respectively, at wing station 307 and by channel A20 at station 537 on the left wing. Torsion was measured by the differential shear between the front and rear spars. Two gauges were mounted on the front spar webbing and two gauges on the rear spar webbing between the top and bottom spar caps. Each gauge was mounted at 45° to the vertical.

Channels A12, A16, A19, and A21 measured shear on the right and left wings. Channels A12 and A17 were located in the right and left wings, respectively, at wing station 307. Channels A19 and A21 were located in the left wing

*The m.a.c. of the XB-47 is 155.9 in. long, and the leading edge of the m.a.c. is 540.2 in. from the nose of the airplane (fuselage station 584.7).

SECRET

TABLE 3.8 RECORDER-CHANNEL ASSIGNMENTS FOR XB-47 AIRPLANE

Chan.	Intelligence Measured	Instrument		Instrument Location*
		Type	Model	
A1	Elevator position	Shop fabricated	None	Elevator torque tube
A2	Lateral accel.	Satham accel.	A18-6-350	No. 3 engine
A3	Vertical accel.	Satham accel.	A18-12-350	No. 3 engine
A4	Vertical accel.	Satham accel.	A18-12-350	No. 1 engine
A5	Vertical accel.	Satham accel.	A18-6-350	Pilot's seat, fus. sta. 210
A6	Vertical accel.	Satham accel.	A18-6-350	Fwd. bomb bay, fus. sta. 510
A7	Vertical accel.	Satham accel.	A18-6-350	Near c.g., fus. sta. 616
A8	Vertical accel.	Satham accel.	A18-6-350	Radio compt., fus. sta. 1166
A9	Longeron bending	SR4 strain gauge	A13-350	Fuselage sta. 985
A10	Chordwise bending	SR4 strain gauge	A13-350	Rt. wing sta. 307
A11	Wing torsion	SR4 strain gauge	A13-350	Rt. wing sta. 307
A12	Wing shear	SR4 strain gauge	A13-350	Rt. wing sta. 307
A13	Wing bending	SR4 strain gauge	A13-350	Rt. wing sta. 307
A14	Chordwise bending	SR4 strain gauge	A13-350	Lf. wing sta. 307
A15	Wing torsion	SR4 strain gauge	A13-350	Lf. wing sta. 307
A16	Wing shear	SR4 strain gauge	A13-350	Lf. wing sta. 307
A17	Wing bending	SR4 strain gauge	A13-350	Lf. wing sta. 307
A18	Wing bending	SR4 strain gauge	A13-350	Lf. wing sta. 537
A19	Wing shear	SR4 strain gauge	A13-350	Lf. wing sta. 537
A20	Wing torsion	SR4 strain gauge	A13-350	Lf. wing sta. 537
A21	Wing shear	SR4 strain gauge	A13-350	Lf. wing sta. 660
A22	Wing bending	SR4 strain gauge	A13-350	Lf. wing sta. 664
A23	Stab. bending	SR4 strain gauge	A13-350	Lf. hor. stab., sta. 34
A24	Longeron bending	SR4 strain gauge	A13-350	Fus. sta. 718
B1	Altitude	Satham press. gauge	P69-15A-350	Pilot's compartment
B2	Airspeed	Satham press. gauge	P69-30-350	Pilot's compartment
B3	Diff. aero. press.	Wiancko press. gauge	3PAD1OW	Rt. wing, top, sta. 515, 11.7% chord
B4	Diff. aero. press.	Wiancko press. gauge	3PAD1OW	Rt. wing, top, sta. 515, 61.3% chord
B5	Gauge aero. press.	Wiancko press. gauge	3PAD1OS	Fuselage sta. 122
B6	Gauge aero. press.	Wiancko press. gauge	3PAD1OS	Lf. vertical fin, sta. 130
B7	Gauge aero. press.	Wiancko press. gauge	3PAD1OS	Lf. wing, bottom, sta. 515, 5% chord
B8	Gauge aero. press.	Wiancko press. gauge	3PAD1OS	Lf. wing, top, sta. 515, 11.7% chord
B9	Gauge aero. press.	Wiancko press. gauge	3PAD1OS	Lf. wing, bottom, sta. 515, 11.7% chord
B10	Gauge aero. press.	Wiancko press. gauge	3PAD1OS	Lf. wing, top, sta. 515, 20% chord
B11	Gauge aero. press.	Wiancko press. gauge	3PAD1OS	Lf. wing, bottom, sta. 515, 20% chord
B12	Gauge aero. press.	Wiancko press. gauge	3PAD1OS	Lf. wing, top, sta. 515, 27.3% chord
B13	Gauge aero. press.	Wiancko press. gauge	3PAD1OS	Lf. wing, bottom, sta. 515, 27.3% chord
B14	Gauge aero. press.	Wiancko press. gauge	3PAD1OS	Lf. wing, top, sta. 515, 40% chord
B15	Gauge aero. press.	Wiancko press. gauge	3PAD1OS	Lf. wing, bottom, sta. 515, 40% chord
B16	Gauge aero. press.	Wiancko press. gauge	3PAD1OS	Lf. wing, top, sta. 515, 61.3% chord
B17	Gauge aero. press.	Wiancko press. gauge	3PAD1OS	Lf. wing, bottom, sta. 515, 61.3% chord
B18	Gauge aero. press.	Wiancko press. gauge	3PAD1OS	Fus., right, sta. 740
B19	Gauge aero. press.	Wiancko press. gauge	3PAD1OS	Fus., left, sta. 740
B20	Gauge aero. press.	Wiancko press. gauge	3PAD1OS	Fus., bottom, sta. 744
B21	Gauge aero. press.	Wiancko press. gauge	3PAD1OS	Fus., top, sta. 744
B22	Gauge aero. press.	Wiancko press. gauge	3PAD1OS	Lf. hor. stab., bottom, sta. 110
B23	Gauge aero. press.	Wiancko press. gauge	3PAD1OS	Lf. hor. stab., bottom, sta. 110
B24	Gauge aero. press.	Wiancko press. gauge	3PAD1OS	Lf. wing, top, sta. 523, 5% chord

* Wing stations in inches from plane of symmetry.

SECRET

at wing stations 537 and 660, respectively. The gauges used for measuring shear were mounted on the front and rear spar webbing similar to the torsion gauges.

Spanwise bending was measured in the wings by channels A13, A17, A18, and A22. Channels A13 and A17 were located in the right and left wing, respectively, at wing station 307. Channels A18 and A22 were located in the left wing at stations 537 and 664, respectively. The gauges were mounted on the front and rear spar caps, top and bottom. Station 537 was approximately midway between engine nacelles, and station 664 was just inboard of engine 1 for measurement of loads imposed on the wing by the engine.

Stabilizer bending was measured by channel A23, and gauges were mounted on the rear spar caps, top and bottom, at stabilizer station 64. The greater proportion of loads imposed on the stabilizer was carried by the rear spar, and this proportion remained constant for all air loads. All four gauges were mounted on this spar.

Channels B1 and B2 contained Statham pressure transducers. The altitude transducer was connected to the lines of the static system for the pilot's flight instruments, and the airspeed transducer was connected to the lines of both the static and pitot system for the pilot's flight instruments. Both instruments contained resistance-type bridges and were mounted on the floor just forward of the pilot's compartment. This location kept the length of connecting hose used between the instruments and the static and pitot lines to a minimum. Consequently the possibility of sharp bends in the hose was eliminated, and the amount of lag of both systems was kept at a minimum.

Channels B3 through B24 contained Wiancko pressure transducers, Types 3PAD1OW and 3PAD1OS, installed by the contractor at the time of modification of the airplane. Both types were variable-inductance-type gauges and differed only in physical shape. It was necessary to cut the skin of the wings to provide orifices for the pressure transducers and access holes for their installation. Because of the stressed-skin construction, such cutting was kept to a minimum. These modifications were made at the contractor's plant while the airplane was already disassembled for the other modifications.

Channels B3 and B4 used the Type 3PAD1OW pressure transducer to measure differential aerodynamic pressure on the right wing along wing station 515 at 11.7 and 61.3 per cent of the wing chord, respectively. Differential aerodynamic pressure would normally be measured by interconnecting two pressure transducers, one on the upper surface of the wing and the other on the lower surface. In this case, however, owing to the thinness of the wing, only one transducer was used. The transducer was mounted to the upper surface of the wing at each chord location, and the reference side was vented through the wing to the lower surface. The pressure transducer installed for use in channel B3 was not readily accessible for replacement in the forward area. This situation existed since the transducer was located on the leading edge of the wing. Normal operation of the airplane involved extension of the leading edge for reducing landing speed; however, for this operation the slot was not needed and therefore was sealed closed.

Channels B5 through B24 used Type 3PAD1OS pressure transducers for measuring the pressure experienced by the airplane. The pressure measured was actually the increase in pressure as sensed by the transducers with respect to a known reference pressure. The reference pressure was available by using a small tank which was mounted in the bomb bay and vented through a small orifice to the bomb bay. With one side of each transducer connected to the tank, all gauges had a common reference pressure. A sudden change in pressure in the bomb bay would not affect the transducers over a short period of time because of the large lag in the system.

The transducer used in channel B5 was mounted on the underside of the fuselage at station 122, in the vertical plane of symmetry just forward of the radome compartment. Channel B6 used a transducer located on the left side of the vertical fin at fuselage station 1220 and fin station 130 just forward of the spar in the vertical fin. The transducers used in channels B7 through B17 were mounted in the left wing on top and bottom surfaces along wing station 515 at 5, 11.7, 20, 27.3, 40, and 61.3 per cent of wing chord. Channels B7, B8, and B9 were not readily accessible for replacement and repair because of their location on the leading edge of the wing.

SECRET

Channels B18 through B21 used transducers which were mounted circularly about the fuselage aft of the bomb bay. All four gauges were serviceable from the bomb bay or rear-wheel well. Channel B18 was mounted on the right side of the fuselage at station 740. Channel B19 was mounted on the left side of the fuselage at station 740. Channel B20 was mounted on the bottom side of the fuselage at station 744. Channel B21 was mounted on the top side of the fuselage at station 744.

The transducers used in channels B22 and B23 were mounted in the left horizontal stabilizer, bottom and top, respectively, at stabilizer station 110 just forward of the 50 per cent chord location.

Channel B24 used a transducer mounted in the left wing, top surface, along wing station 523 at 5 per cent of wing chord. This transducer was not readily accessible for replacement since it was installed on the leading edge of the wing which was sealed closed.

Wiancko coupling units were used in conjunction with the pressure transducers and were installed on the left side of the copilot's compartment.

3.6.2 Calibration

Calibrations of the strain-gauge channels on the XB-47 airplane were accomplished in the Structures Test Laboratory at Wright-Patterson Air Force Base prior to departure for the forward area. All the remaining channels were calibrated after the airplane reached the test site.

Channel A1, the elevator-position indicator, was calibrated using the direct method of calibration. The gauge was balanced electrically with the elevator in the full-down position. Loads were applied to the gauge by raising the elevator to the full-up position in increments of 5°, and elevator position was measured by using a spirit-level-protractor combination.

The accelerometers in channels A2 through A8 were calibrated analytically using Eq. 3.1 to determine equivalent values of acceleration.

Channels A9 and A24, longitudinal bending in the fuselage, were calibrated by the direct method. The airplane was restrained at the front- and rear-landing-gear positions. Loadmeters were inserted under the rear landing gear to measure the rear-gear reaction while

the aft section of the fuselage was bent down. I-beam jigs were erected about the left and right horizontal stabilizers. Oleo struts connected between the jigs and the stabilizers at stations 124 and 180 were rigged so as to apply down-loads when hydraulic pressure was applied. Stabilizer stations 124 and 180 were at the same longitudinal locations as fuselage stations 1220 and 1246. Bending moments were computed as though the loads had been applied to the fuselage at those stations. One oleo strut was attached between the floor and the drag-chute attachment point at fuselage station 1246 for applying down-loads.

Chordwise bending was to have been measured by channels A10 and A14. However, at the time of calibration it was determined that the loads which would be required to obtain a significant output from the strain gauges would be far greater than any anticipated during the tests. It was also agreed that the application of chordwise bending to the wings for calibration purposes would be difficult and would likely be injurious to the structure of the airplane. Hence the calibration of these channels was not performed, pending measurements from the tests. The gauges were maintained, and the indications on the channels proved the assumption of the low order of these data.

Calibration curves of wing torsion were to have been obtained for channels A11, A15, and A20, using the direct method of calibration. However, the output of the strain-gauge bridge circuits from the calibration loads was not sufficient to establish a calibration curve. Modifications of the circuit in the forward area so improved the gauge output that significant readings were obtained from the test. However, equipment was not available in the forward area to recalibrate the gauges in the more sensitive configuration. In order to make some use of the test data, an approximate calibration was achieved from the other data available on these channels.

Channels A12, A16, A19, and A21 measured wing shear, and channels A13, A17, A18, and A22 measured wing bending; all these channels were calibrated by the direct method. The airplane was restrained in level attitude by securing the front and rear landing gears in specially built jigs which were bolted to the floor. The right and left outrigger gears were retracted to ensure free movement of the wing and to

eliminate any possible gear reactions on the wings. I-beam jigs were constructed about both wings, and calibrated oleo struts were connected between the jigs and the wings at wing stations 307, 537, and 664. Loads were applied to both wings simultaneously using hydraulic pressure in the oleo struts in such a manner as to produce upward or positive wing bending. The strain-gauge bridge circuits were balanced electrically, with the first increment of load applied in order to remove structural looseness.

The calibration of channel A23, left-horizontal-stabilizer bending, was accomplished at the same time as that of longitudinal bending in the fuselage, mentioned previously. Equal loads were applied to each stabilizer to eliminate fuselage torsion. Down-loads were applied at stabilizer stations 124 and 180, and the bending moment at station 64 was computed.

Channel B1, pressure altitude, was calibrated analytically and checked by an actual flight test against the pilot's altimeter.

Channel B2, airspeed, was calibrated directly by means of pressure applied to the pitot side of the transducer. A calibrated airspeed indicator was used to measure the pressure applied to the transducer.

Channels B3 and B4, differential aerodynamic pressure, were calibrated directly by the application of known pressures on the transducers. The calibration of these channels was difficult because two transducers were interconnected for each channel, which necessitated the simultaneous calibration of both transducers. A pressure of 2 psi was applied to the upper transducer, and the gain was adjusted for a convenient millivolt output on the VTVM. Next, a pressure of 2 psi was applied to the lower transducer, and the other gain control was adjusted to produce the same millivolt output as the upper transducer. These steps were repeated several times until 2 psi applied to both transducers simultaneously produced no output. Both transducers were balanced electrically, and pressure was applied to each one separately in increments up to 2 psi. Laboratory tests on the transducers proved that, if either a positive pressure or a vacuum were applied to the gauge, the results obtained would be identical. Since this method of calibration of the transducers produced only half of the calibration curve, the other half was considered to be

identical, but in the opposite direction, and was plotted as such. The transducers mounted on the lower surfaces were calibrated to measure positive pressure, and those on the upper surfaces were calibrated to measure negative pressure.

Channels B5 through B24 were calibrated directly in much the same manner as were channels B3 and B4. Only one transducer was used for each channel, and all were manifolded to a common reservoir to which the pressure was applied. In this manner, all 20 channels were calibrated at once. The gain control for each transducer was arbitrarily set for maximum output, and each channel was then balanced electrically. Pressures were applied in increments up to 3 psi.

3.7 TEMP-TAPES

3.7.1 Installation

Areas were chosen for the installation of the temp-tapes so that various thicknesses of materials would be measured and so that various angles of incidence of the striking ray would be encountered. The temp-tapes were installed whenever possible in the center of large flat unsupported areas in order to ensure a minimum heat flow away from the immediate areas being studied. The surfaces were cleaned of dirt and grease but were not prepared in any other way. However, various colored blocks were painted on the under surfaces of the flaps of the B-17 drones for Easy shot, and temp-tapes were installed directly behind these colors (see Fig. 3.16).

The locations of the tapes are given in Tables 3.9 and 3.10, and the color code for the temp-tape locations is given in Table 3.11. Angles of incidence (defined as the angle between the incident ray and the surface normal) are listed in Table 3.12.

The formula for the determination of the angle of incidence, i , in terms of the three projection angles, α , β , and γ , of the surface normal and the angle, θ , between the incident ray and the vertical is as follows (see Fig. 3.17 for notations):

$$\tan \theta = \frac{a_x}{c_z + f}$$

SECRET

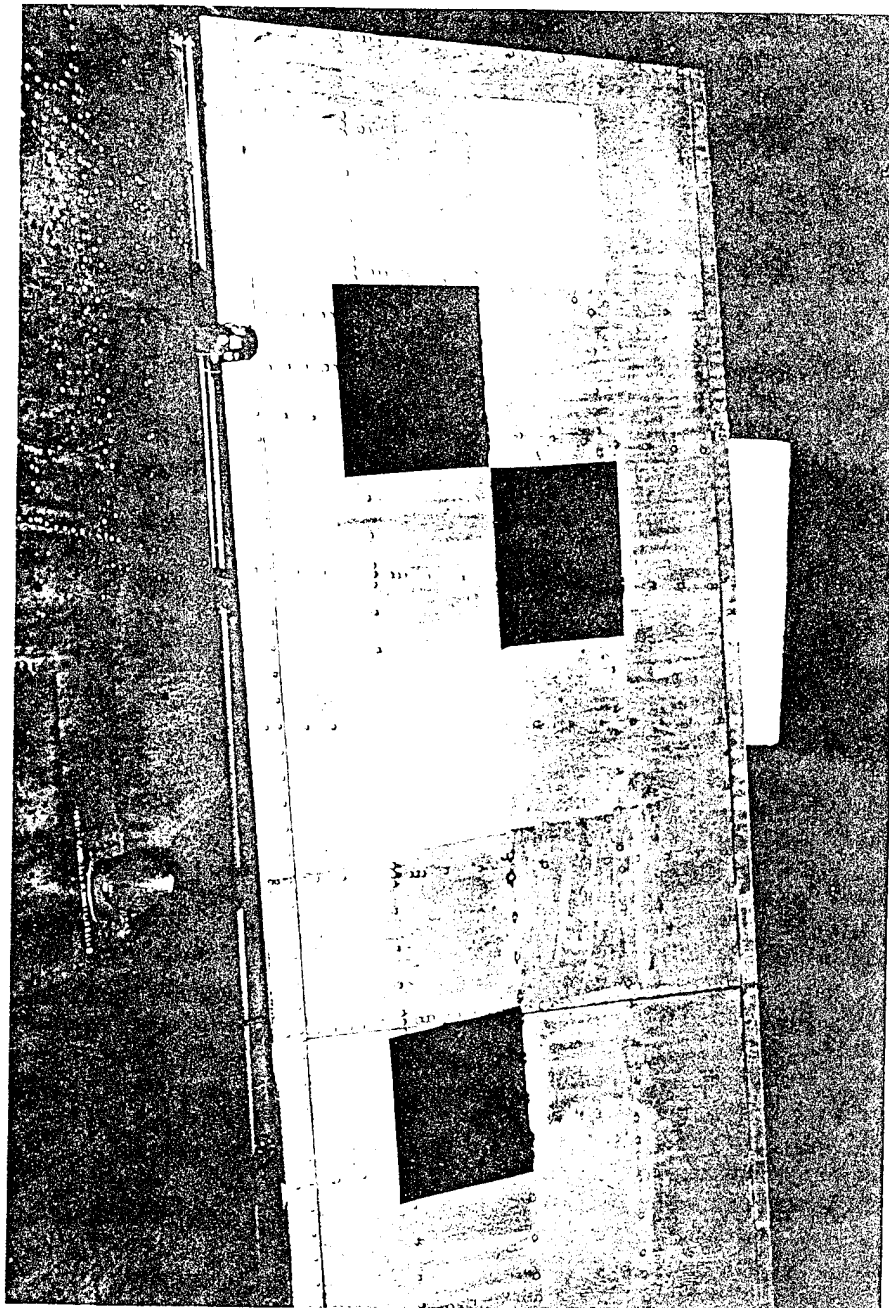


Fig. 3.16 Painted Areas on QB-17 Flaps

SECRET

TABLE 3.9 TEMP-TAPE LOCATIONS, QB-17 DRONES

Code	Location
1	Inside lower front edge of bombardier's plexiglas enclosure, just below floor level
2	Inside flap-control-inspection door, wing lower surface, second flap door from outboard, left-hand wing
3	Inside left bomb-bay door, 20° off airplane center line
4	Inside aft fuselage lower surface, by aft entry door, left side of airplane, 18° off bottom center line
5	Inside elevator hinge outboard door, elevator lower surface
6	Inside flap outboard lower surface, left wing, 50% flap chord, at 80% of flap span from inboard engine
7	Inside waist-gunner's window, lower edge of plexiglas surface, left-hand window
8	Inside side skin of fuselage, second bay aft of right-hand waist-gunner's window; bottom stringer of skin bay, level with window sill Inside bottom surface of flap
9	Opposite square painted black on flap outside lower surface
10	Opposite square painted white on flap outside lower surface
11	Opposite square painted red on flap outside lower surface
12	Opposite square painted yellow on flap outside lower surface
13	Opposite square painted blue on flap outside lower surface
14	Opposite square painted silver on flap outside lower surface
15	Opposite square that is clear aluminum on flap outside lower surface Inside upper surface of wing, just above flap surface and directly above colored squares on flap bottom
16	Opposite black square
17	Opposite blue square On flap rib webs, 2 in. above flap lower surface
18	Opposite black square
19	Opposite white square
20	Opposite red square
21	Opposite yellow square
22	Opposite blue square
23	Opposite silver square
24	Opposite clear aluminum square Inside of fuselage aft section, one skin bay aft of aft entry door, disposed around bottom half of fuselage every 22½°
25	Bottom center line of airplane
26	22½° up on right-hand side
27	45° up on right-hand side
28	67½° up on right-hand side
29	90° up on right-hand side
30	22½° up on left-hand side

TABLE 3.9 (Continued)

Code	Location
31	45° up on left-hand side
32	67½° up on left-hand side
33	90° up on left-hand side
34	Top surface of floor, just forward of right-hand control column, pilot's compartment
35	Inside of side skin, just below left-hand side window, pilot's compartment
36	Top aft right section of pilot's seat back
37	On vertical bulkhead, between pilot's compartment and bombardier's compartment

TABLE 3.10 TEMP-TAPE LOCATIONS, QT-33 DRONES

Code	Location
38	Inside flap lower surface, left-hand wing, third and fourth bay from outboard
39	Outside lower skin left stabilizer, 1 in. forward of center skin lap, one-third of span outboard
40	Inside left-hand camera-access door
41	Inside left-hand engine-access door
42	Outside lower left-hand wing surface, center
43	Outside lower skin, left elevator, just outboard center tab hinge
44	Inside bottom surface of left flap, outboard bay
45	Inside bottom surface of left flap, fifth bay outboard
46	Inside top skin left wing above flap outboard bay
47	Inside top skin left wing above fifth bay outboard
48	Upper flange of flap rib, outboard bay
49	Upper flange of flap rib, fifth bay outboard

TABLE 3.11 TEMP-TAPE COLOR CODE

Code	Color
A	Natural aluminum metal, unpainted
P	Plexiglas
AP	Aluminum paint
B	Dull black
W	White insignia paint
R	Red insignia paint
Y	Yellow-orange
BL	Blue insignia paint
LOG	Light olive green
DOG	Dark olive green
Subscript s	Shiny
Subscript d	Dull, unpolished

TABLE 3.12 TEMP-TAPE LOCATIONS, INCIDENCE ANGLES*

Airplane	Tape Location	α	β	γ	θ	i
B-17 M Dog	1	62°	0		336° 02'	83° 38'
	2	3° 30'	4° 30'		336° 02'	27° 48'
	3	337°	23°		336° 02'	21° 39'
	4	355°	22° 30'		336° 02'	29° 03'
	5	0	0	0	336° 02'	23° 58'
	6	3° 30'	4° 30'		336° 02'	27° 48'
	7	270°	90°	357°	336° 02'	88° 34'
	8	270°	270°	183°	336° 02'	88° 34'
T-33 No. 2 Dog	38	0	3° 50'		327° 35'	32° 37'
	39	1° 30'	0	90°	327° 35'	34° 18'
	40	90°	90°	10°	327° 35'	84° 41'
	41	0	15°	0	327° 35'	35° 22'
	42	0	3° 50'		327° 35'	32° 37'
	43	1° 30'	0	90°	327° 35'	34° 18'
B-17 M Easy	9	3° 30'	4° 30'		10° 46'	8° 32'
	10	3° 30'	4° 30'		10° 46'	8° 32'
	11	3° 30'	4° 30'		10° 46'	8° 32'
	12	3° 30'	4° 30'		10° 46'	8° 32'
	13	3° 30'	4° 30'		10° 46'	8° 32'
	14	3° 30'	4° 30'		10° 46'	8° 32'
	15	3° 30'	4° 30'		10° 46'	8° 32'
	25	355°	0	270°	10° 46'	15° 45'
	26	354° 36'	337° 30'		10° 46'	27° 23'
	27	352° 57'	315°		10° 46'	47° 29'
	28	347° 08'	292° 30'		10° 46'	68° 55'
	29	270°	270°	185°	10° 46'	89° 04'
	30	354° 36'	22° 30'		10° 46'	27° 23'
	31	352° 57'	45°		10° 46'	47° 29'
	32	347° 08'	67° 30'		10° 46'	68° 55'
	33	270°	90°	355°	10° 46'	89° 04'
B-17 N Easy	1	62°	0		52° 23'	9° 35'
	2	3° 30'	4° 30'		52° 23'	49° 02'
	3	337°	23°		52° 23'	76° 24'
	4	355°	22° 30'		52° 23'	60° 07'
	5	0	0	0	52° 23'	52° 23'
	6	3° 30'	4° 30'		52° 23'	49° 02'
	7	270°	90°	357°	52° 23'	87° 13'
	8	270°	270°	184°	52° 23'	87° 13'
	9	3° 30'	4° 30'		52° 23'	49° 02'
	10	3° 30'	4° 30'		52° 23'	49° 02'
	11	3° 30'	4° 30'		52° 23'	49° 02'
	12	3° 30'	4° 30'		52° 23'	49° 02'
	13	3° 30'	4° 30'		52° 23'	49° 02'
	14	3° 30'	4° 30'		52° 23'	49° 02'
	15	3° 30'	4° 30'		52° 23'	49° 02'

*See also Fig. 3.17.

TABLE 3.12 (Continued)

Airplane	Tape Location	α	β	γ	θ	i
B-17 N Easy	16	22°	4° 30'		52° 23'	30° 37'
	17	22°	4° 30'		52° 23'	30° 37'
	25	355°	0	270°	52° 23'	57° 23'
	26	354° 36'	337° 30'		52° 23'	60° 28'
	27	352° 57'	315°		52° 23'	68° 31'
	28	347° 08'	292° 30'		52° 23'	80° 32'
	29	270°	270°	185°	52° 23'	86° 02'
	30	354° 36'	22° 30'		52° 23'	60° 28'
	31	352° 57'	45°	185°	52° 23'	68° 31'
	32	347° 08'	67° 30'		52° 23'	80° 32'
	33	270°	90°	355°	52° 23'	86° 02'
T-33 No. 2 Easy	44	0	3° 50'		350° 32'	10° 47'
	45	0	3° 50'		350° 32'	10° 47'
	46	15°	3° 50'		350° 32'	24° 43'
	47	15°	3° 50'		350° 32'	24° 43'

or

$$f = a_x \cot \theta - c_z$$

but

$$c_z = a_x \cot \alpha$$

Therefore

$$f = a_x \cot \theta - a_x \cot \alpha = a_x (\cot \theta - \cot \alpha)$$

Then

$$\begin{aligned} e^2 &= f^2 + b_y^2 \\ &= a_x^2 (\cot \theta - \cot \alpha)^2 + b_y^2 \end{aligned}$$

but

$$b_y = c_z \tan \beta = a_x \cot \alpha \tan \beta$$

Then

$$\begin{aligned} e^2 &= a_x^2 (\cot \theta - \cot \alpha)^2 \\ &\quad + a_x^2 \cot^2 \alpha \tan^2 \beta \end{aligned} \quad (3.3)$$

Also

$$\frac{a_x}{R} = \sin \theta$$

or

$$R = a_x \csc \theta$$

and

$$R^2 = a_x^2 \csc^2 \theta \quad (3.4)$$

Also

$$\begin{aligned} N^2 &= b_y^2 + N_{xz}^2 = c_z^2 \tan^2 \beta + c_z^2 + a_x^2 \\ &= a_x^2 \tan^2 \beta \cot^2 \alpha + a_x^2 \cot^2 \alpha + a_x^2 \\ N^2 &= a_x^2 (\tan^2 \beta \cot^2 \alpha + \cot^2 \alpha + 1) \end{aligned} \quad (3.5)$$

Then

$$\cos i = \frac{N^2 + R^2 - e^2}{2NR} \quad (3.6)$$

Consequently

SECRET

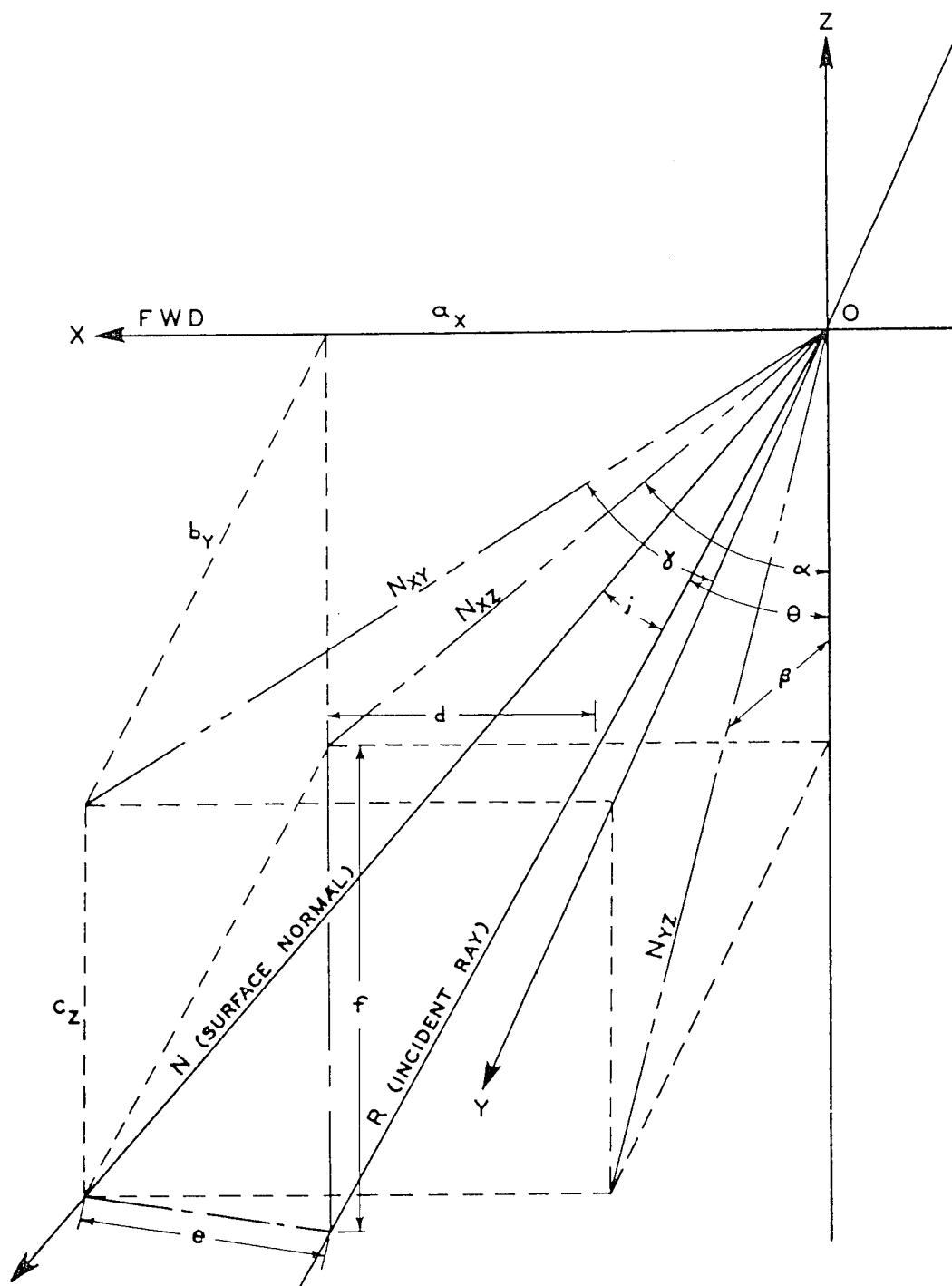


Fig. 3.17 Space Diagram for Computation of Angles of Incidence



~~SECRET~~

$$\cos i = \frac{a_x^2(\tan^2 \beta \cot^2 \alpha + \cot^2 \alpha + 1) + a_x^2 \csc^2 \theta - a_x^2(\cot \theta - \cot \alpha)^2 - a_x^2 \cot^2 \alpha \tan^2 \beta}{2a_x^2 \csc \theta \sqrt{\tan^2 \beta \cot^2 \alpha + \cot^2 \alpha + 1}}$$

From Eqs. 3.3 to 3.6,

$$\begin{aligned} \cos i &= \frac{\tan^2 \beta \cot^2 \alpha + \cot^2 \alpha + 1 + \csc^2 \theta - \cot^2 \theta + 2 \cot \theta \cot \alpha - \cot^2 \alpha - \cot^2 \alpha \tan^2 \beta}{2 \csc \theta \sqrt{\tan^2 \beta \cot^2 \alpha + \cot^2 \alpha + 1}} \\ &= \frac{1 + \csc^2 \theta - \cot^2 \theta + 2 \cot \theta \cot \alpha}{2 \csc \theta \sqrt{\tan^2 \beta \cot^2 \alpha + \cot^2 \alpha + 1}} = \frac{1 + 1 + \cot^2 \theta - \cot^2 \theta + 2 \cot \theta \cot \alpha}{2 \csc \theta \sqrt{\tan^2 \beta \cot^2 \alpha + \cot^2 \alpha + 1}} \\ &= \frac{2 + 2 \cot \theta \cot \alpha}{2 \csc \theta \sqrt{\tan^2 \beta \cot^2 \alpha + \cot^2 \alpha + 1}} = \frac{1 + \cot \theta \cot \alpha}{\csc \theta \sqrt{\tan^2 \beta \cot^2 \alpha + \cot^2 \alpha + 1}} \\ &= \frac{1 + \cot \theta \cot \alpha}{\csc \theta \sqrt{\cot^2 \alpha (\tan^2 \beta + 1) + 1}} = \frac{1 + \cot \theta \cot \alpha}{\csc \theta \sqrt{1 + \cot^2 \alpha \sec^2 \beta}} \end{aligned} \quad (3.7)$$

Equation 3.7 becomes indeterminate when $\alpha = 90^\circ$ or 270° and $\beta = 90^\circ$ or 270° and when $\alpha = 0^\circ$ or 180° . Then if $\cot \beta \cot \gamma = \cot \alpha$ is substituted in Eq. 3.7 the result is

$$\cos i = \frac{1 + \cot \theta \cot \gamma \cot \beta}{\csc \theta \sqrt{1 + \cot^2 \gamma \csc^2 \beta}} \quad (3.8)$$

Equation 3.8 again becomes indeterminate when both γ and $\alpha = 0$, but, if γ and $\alpha = 0$,

$$\cos \Psi = \cos \beta \cos \theta \quad (3.9)$$

from the law of cosines.

From Eqs. 3.7, 3.8, and 3.9, the angle of incidence, i , can be determined for any values of α , β , γ , and θ if the angles are measured as indicated on Fig. 3.17.

3.7.2 Calibration

During the development stage of the temp-tape temperature measuring devices, it was discovered that the melting points of the low-temperature alloys appeared not to correspond to the temperatures at which melting and fusion of the alloy foils occurred when mounted in the temp-tape. This indicated that a comprehensive calibration program would be necessary for accurate temperature determination. Accordingly, the Engineering Department of the University of California at Los Angeles contracted to undertake the task of calibrating the instruments. The complete calibration is contained in a UCLA report entitled "Calibration of a Temperature Measuring Device," by A. Am-

broso and B. Bussell, April 1951, which was prepared under Air Force Contract AF33(038)-14381.


Before the temp-tapes were calibrated, a determination of the actual melting points of the different alloys under consideration was made. It was found that each of the 14 alloys involved had sharp, although not precisely eutectic, melting points, the longest melting range being about 3°F .

The calibration was then made by affixing the temp-tape to a piece of sheet aluminum, irradiating the reverse side of the sheet with photoflood lamps, and checking the pieces of alloy foil for melting and fusion.

All temperature measurements in the calibration runs were made with the aid of thermocouples whose signals were amplified by d-c amplifiers and continuously recorded. The surface of the plate which was to be irradiated was blackened with dull-black brushing lacquer in order to increase its absorptivity. The radiating source was two special 750-watt photoflood lamps. A thermocouple was welded to the surface of the plate in order to record the plate temperature.

In general, successive runs for any one alloy were taken by increasing the maximum plate temperature in 5 to 10°F increments. At each run, the temp-tape was disassembled, and the amount of melting and fusion of the foils was noted. A calibration curve for each temp-tape was thus constructed, plotting per cent melting and per cent fusion against temperature in degrees Fahrenheit.

~~SECRET~~



Chapter 4

Operation Plans

4.1 GENERAL OPERATION OBJECTIVES

As described in Chap. 1, the principal objective of Project 8.1 was the collection of data at as many significant points in space as possible. Thus the arrangement of the airplanes in the airspace about the blast was specified originally on the basis of the predicted structural loading or the intensity of heat, and this arrangement was later modified to allow for operational consideration. The detailed calculations to establish the preliminary pattern of the arrangement of test airplanes is contained in Greenhouse Report, Annex 8.0. The importance of heat in the collocation of the test airplane was not realized until after Dog shot. The airplane arrangement for Easy and George shots included a careful consideration of the heat on the basis of the limited data available. In general, a safety limit of 8 miles or 0.32 psi overpressure was established for the director or "mother" airplanes.

It should be noticed that the various plans and arrays as described in this chapter are those actually used in the operations. The positions shown are those assigned and are not necessarily the ones attained by the airplanes. The data from the tests, including the positions attained, are presented in Chaps. 5, 6, and 7.

4.2 PLAN FOR DOG SHOT

The pattern for the test airplanes for Dog shot was based on a predicted shot strength of 90 kt. The original plan was established shortly after the final arrangements for the test shots with the predicted strengths had been announced to the project officers. The preliminary train-

ing by TU 3.4.2 was based on that plan. The pattern as actually used differed from the original plan in two details. The assigned altitudes for the B-50D airplanes, Frances and Grace positions, were changed from 35,000 to 29,000 ft, with corresponding changes in horizontal distances to maintain the 45° slant angle. This change was made at the request of the flight crews in order to improve the operation of the radar equipments. The other change was in the altitude of Carol position from 14,000 to 15,000 ft to avoid an altitude already assigned to one of the AEC drones. The plan as finally presented to the Task Unit for the preparation of operations orders is presented in Table 4.1. A sketch of the array of the airplanes according to the operations order, including the assigned courses, altitudes, and distances, is shown in Fig. 4.1. The plan was presented to the operating organizations in the form of a plan view, and the assignment of the specific courses was based on the possible locations of radar targets for the manned airplanes and on separation from other flight patterns for the drones.

4.3 PLAN FOR EASY SHOT

After the data from Dog shot indicated a correlation between theory and the actual structural loading on the aircraft, a bolder plan was established for Easy shot based on a predicted strength of 50 kt. Locations were prescribed on the basis of near-ultimate (destruction) loads for positions Alice and Carol and near-limit (permanent-set) loads for positions Betty and Doris. It was apparent, however, that heat would be a critical factor to be considered in

SECRET

TABLE 4.1 ASSIGNED AIRPLANE POSITIONS, DOG SHOT

Position Name	Airplane Type	At Time Zero			Shock Travel Time (sec)	At Shock Wave		Peak Over-press. (psi)	Peak Gust Vel. (ft/sec)
		True Altitude (ft)	Horiz. Range* (ft)	Slant Range* (ft)		Horiz. Range* (ft)	Slant Range* (ft)		
Alice	QT-33 drone 2	7,800	4,980	9,260	6.8	7,800	11,000	2.03	136
Betty	QT-33 drone 1	10,700	15,260	18,700	10.2	10,700	15,150	1.21	91
Carol	QB-17 drone M	15,000	6,690	16,150	13.3	10,500	18,310	0.86	75
Doris	QB-17 drone N	23,000	5,750	23,700	17.2	0	23,000	0.52	63
Elaine	XB-47 46-066	24,800	6,800	25,700	28.0	24,800	35,100	0.30	38
Frances	B-50D 49-340	29,000	43,600	52,100	33.8	29,000	40,900	0.23	34
Grace	B-50D 49-290	29,000	32,450	43,500	33.8	29,000†	40,900	0.23	34

*From blast.

†Grace headed alongside blast such that blast struck left wing first. Horizontal distance 0 in direction of flight, 29,000 ft from blast in direction perpendicular to line of flight.

SECRET

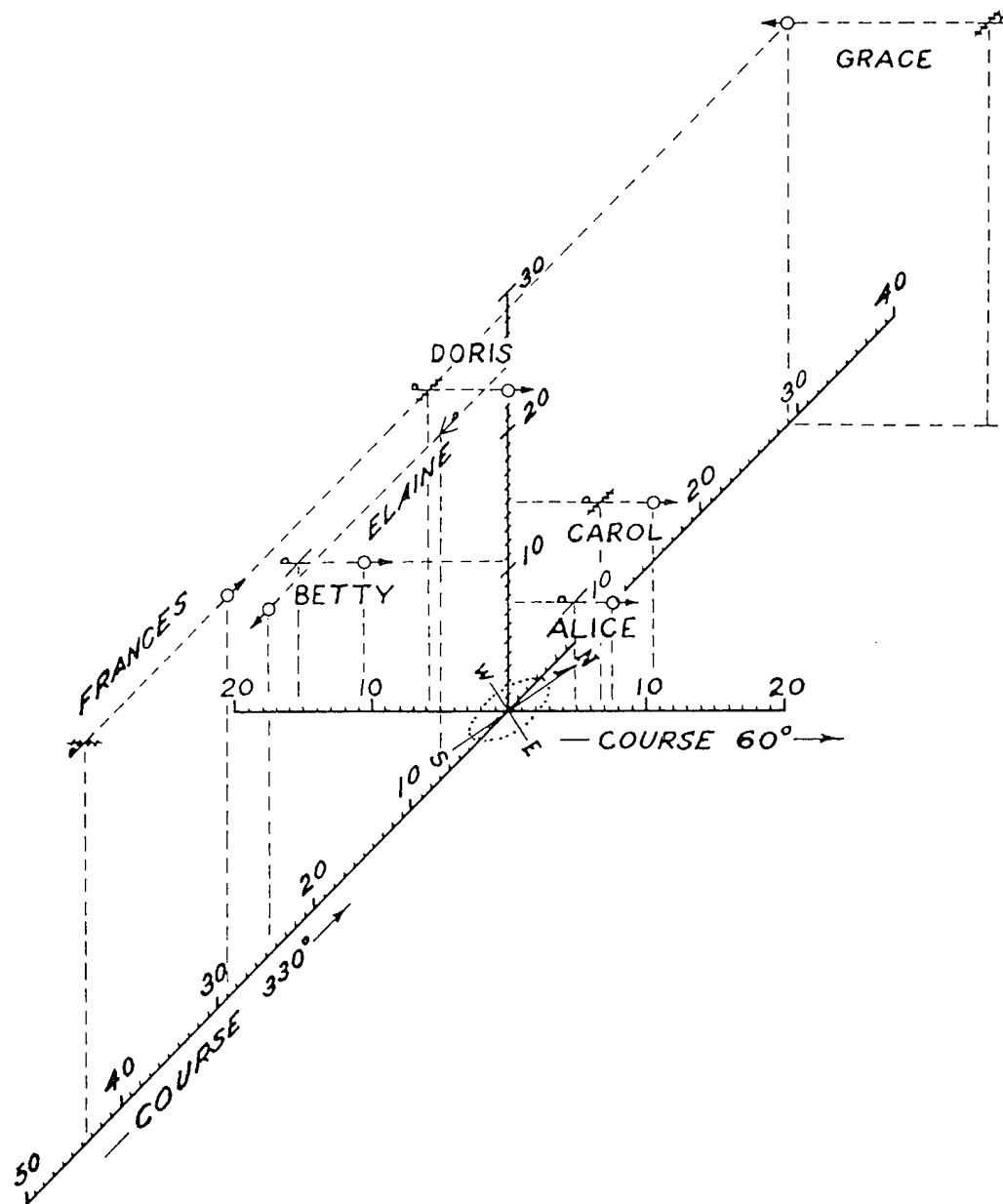


Fig. 4.1 Array of Test Airplanes for Dog Shot

~~SECRET~~

the conservation of the airplanes, especially those with fabric surfaces. The curve¹ in Fig. 4.2 plots the heat at the airplane, Q_t , versus the space parameter λ . The true expression for λ has been simplified for the purposes of this curve since only approximations of heat levels are intended and since other data on the curve are only estimates. The expression for λ as used is

$$\lambda = \frac{W \cos i e^{-kd}}{d^2} \times 10^{-9} \quad (4.1)$$

where W = yield of weapon in kt

i = angle of incidence at the airplane measured from the vertical

k = atmospheric attenuation factor in ft^{-1} (see bibliographic reference 2)

d = slant range at time of blast, T_0 , in ft

The slope $dQ_t/d\lambda$ for the experimental curve was primarily determined from the temperatures measured on the internal surface of the flap of QT-33 drone 2 in Alice position on Dog shot. The heat level at which doped fabric would burn was estimated to be between 18 and 19 Btu/sq ft. The heat level at which doped fabric, protected as described in Chap. 6, would burn was determined experimentally to be approximately twice as great or about 37 Btu/sq ft. These two heat levels, along with those at which black paper burns and at which slight skin burns occur,³ are indicated in Fig. 4.2.

The locations of the other airplanes on Dog shot were plotted on the curve to check correlation. For example, the λ for Carol position on Dog shot indicates that the heat level should have burned the fabric surfaces, which actually occurred (see Sec. 5.4). Also, the crew of the XB-47 in Elaine position on Dog shot reported intense heat on their skin, which is indicated by the location of that point on the curve.

Positions selected for the manned airplanes on Easy shot were investigated to be certain that the predicted heat level would not exceed 4 Btu/sq ft. The positions for the QB-17 drones were selected so as to be within the permissible heat limits. As indicated in Fig. 4.2, Carol position was close to the predicted limit as regards heat level. However, since this position was selected so as to involve near-ultimate structural loads, it was decided to accept the high heat level in order to evaluate

the technique of predicting heat levels. The positions of the QT-33 drones were subjected very briefly to this analysis, but, because of the metal surfaces, it was not expected that the absorbed heat would affect the structure of the airplanes. These points are not shown in Fig. 4.2 in order to expand the scale sufficiently to illustrate the computations for those airplanes which were considered to be critical as far as heat was concerned. It should be noted that the time for the position concerned in the heat analysis is T_0 , whereas that concerned in the structural analysis is the time of shock arrival at the airplane, T_0 plus a few seconds. Thus some control could be exercised over the relation between heat load and blast load by heading the airplanes toward or away from the blast.

An alternate plan, designated Plan B, was prepared because of the probability of failure of the telemetering equipment. The chance of loss of one of the aircraft in the Alice and Carol positions was rather high, and, in the event that the telemetering equipment did not operate satisfactorily, the data would be lost with the airplane. The alternate positions of Plan B then provided for additional safety for Alice and Carol and were intended for use in the event that the telemetering equipment appeared unreliable prior to shot time. Plan B was used, and the flight pattern is shown as Fig. 4.3. The data on the plan as presented to the operating organization are listed in Table 4.2.

4.4 PLAN FOR GEORGE SHOT

A plan similar to those used on the previous shots was prepared for George shot based on a predicted strength of 225 kt, and the appropriate operations orders were prepared by TU 3.4.2. However, severe weather conditions for the week prior to G-day soaked the radio-control equipment with water so that on G-1 day alternate positions were selected to permit the airplanes to be flown manned. These positions were hurriedly selected, with the safety of the crews as the primary consideration. The rain continued up through the time that the airplanes started their missions so that the test airplanes for this project were flown manned. A third B-17 airplane had been prepared as a spare

~~SECRET~~

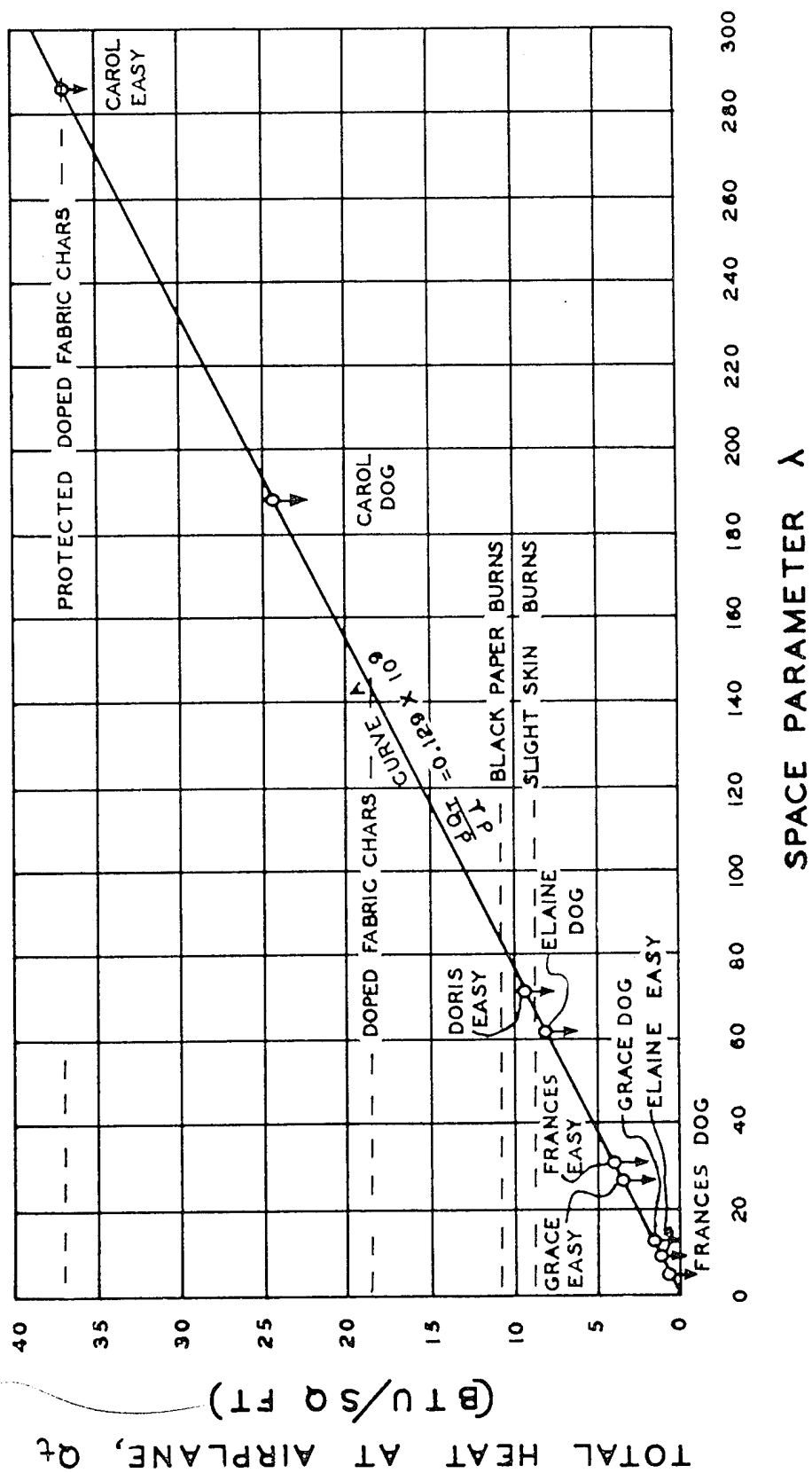


Fig. 4.2 Estimates of Heat Effects on Test Airplanes

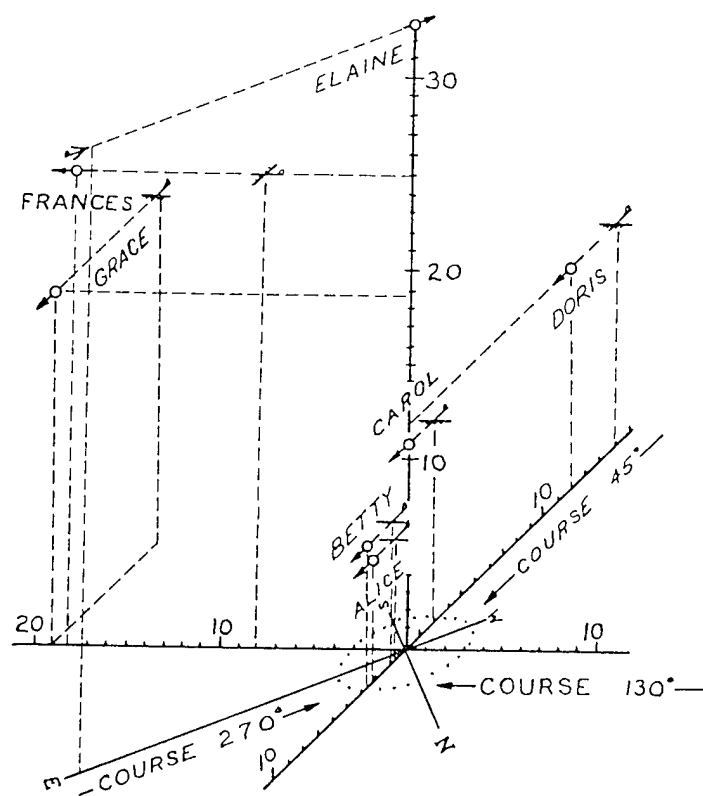


Fig. 4.3 Array of Test Airplanes for Easy Shot

TABLE 4.2 ASSIGNED AIRPLANE POSITIONS, EASY SHOT

Position Name	Airplane Type	True Altitude (ft)	At Time Zero		Shock Travel Time (sec)	At Shock Wave		Peak Over-press. (psi)	Peak Gust Vel. (ft/sec)
			Horiz. Range* (ft)	Slant Range* (ft)		Horiz. Range* (ft)	Slant Range* (ft)		
Alice	T-33 drone 3	6,500	866	6,540	3.8	2,367	6,920	3.06	195
Betty	T-33 drone 2	7,500	1,000	7,530	4.6	2,730	7,980	2.55	163
Carol	B-17 drone M	11,000	1,949	11,160	7.2	0	11,000	1.43	106
Doris	B-17 drone N	12,000	15,400	19,510	12.3	12,000	16,960	0.78	62
Elaine	XB-47 46-066	33,000	18,810	38,000	27.7	0	33,000	0.21	38
Frances	B-50D 49-290	25,000	7,940	26,210	24.9	18,000	30,800	0.28	36
Grace	B-50D 49-340	19,000	20,500	28,000	21.1	19,000†	26,870	0.37	39

*From blast.

†Grace headed alongside blast such that shock struck left wing first. Horizontal distance 0 in direction of flight, 19,000 ft from blast in direction perpendicular to line of flight.

SECRET

TABLE 4.3 ASSIGNED AIRPLANE POSITIONS, GEORGE SHOT

Position Name	Airplane Type	At Time Zero			Shock Travel Time (sec)	At Shock Wave		Peak Over-press. (psi)	Peak Gust Vel. (ft/sec)
		True Altitude (ft)	Horiz. Range* (ft)	Slant Range* (ft)		Horiz. Range* (ft)	Slant Range* (ft)		
Alice	QT-33 drone 5	29,000	58,500	65,300	39.4	39,000	48,600	0.26	50
Betty	QT-33 drone 4	32,000	59,580	67,600	38.4	35,000	47,400	0.25	42.5
Carol	QB-17 drone O	25,000	23,440	34,300	34.1	35,000	43,000	0.33	43
Doris	QB-17 drone N	27,000	21,340	34,500	33.8	33,000	42,600	0.32	45
Elaine	XB-47 46-066	35,000	45,500	57,400	40.5	35,000†	49,500	0.23	50
Frances	B-50D 49-290	31,000	59,420	67,000	41.5	40,000	50,600	0.24	39
Grace	B-50D 49-340	33,000	37,750	50,200	37.9	33,000†	46,700	0.25	44
Sally	QB-17 drone P	14,000	74,970	75,400	51.0	60,800	62,400	0.27	23.5

*From blast.

†Grace and Elaine headed alongside blast such that shock struck left wing first. Horizontal distances 0 in line of flight, 35,000 and 33,000 ft from blast in direct perpendicular to line of flight.

SECRET

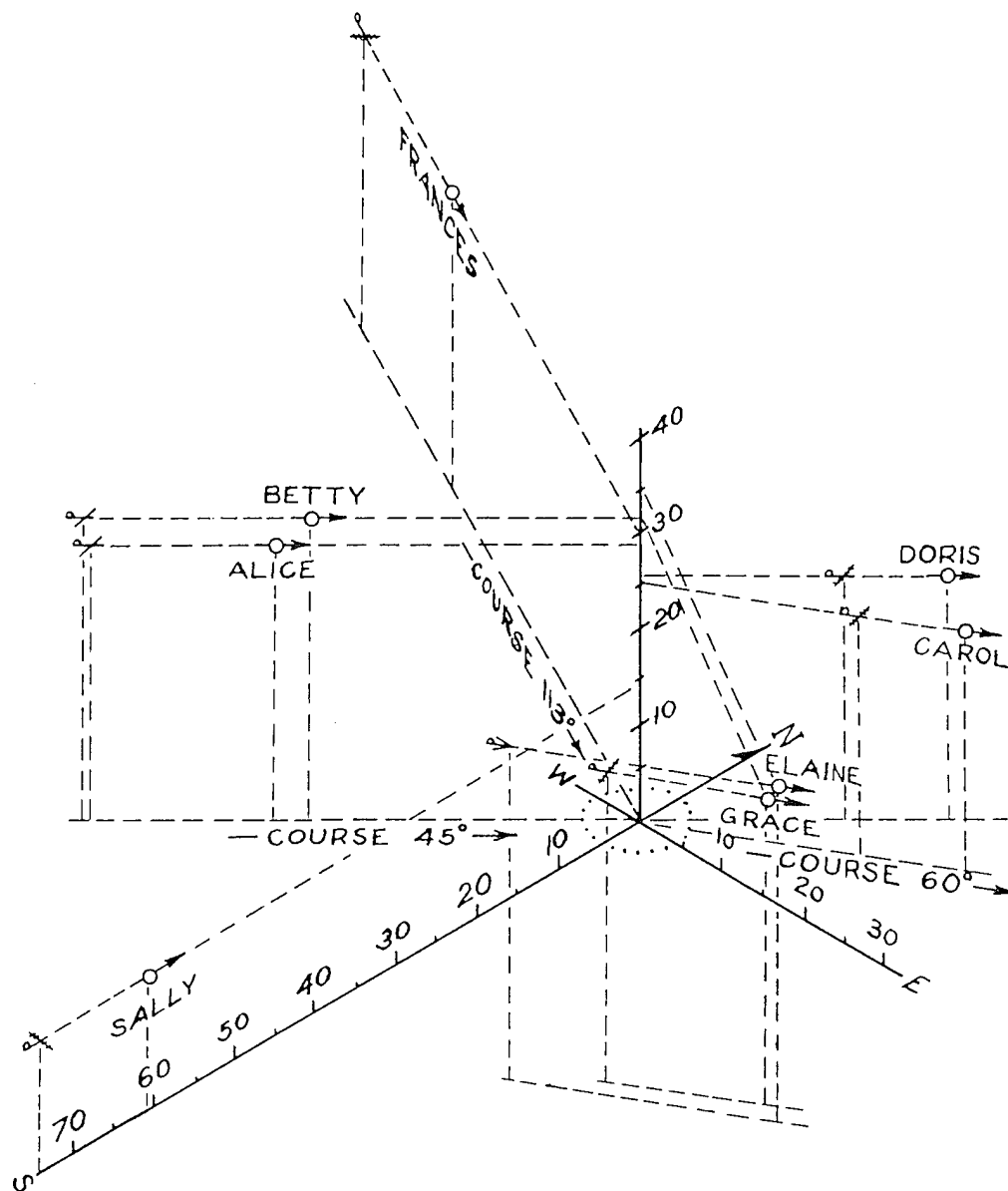


Fig. 4.4 Array of Test Airplanes for George Shot

~~SECRET~~

drone for use in the event that one of the assigned drones failed to "check out." When the decision was made to fly all the drones as manned airplanes, a crew was also assigned to that airplane, and it was assigned to position Sally. The data on the plan for George shot are listed in Table 4.3, and the array of test airplanes is pictured in Fig. 4.4.

4.5 STANDARD OPERATING PROCEDURE

In the days prior to each shot the time was spent in generally overhauling and calibrating the instrumentation in those airplanes assigned for the test. Where indicated by previous records, sensing elements were repaired or changed, telemeter or recorders were overhauled, or wiring was repaired as necessary. Check calibrations on equipment which had been previously installed or complete calibrations on new installations were performed as described in Chap. 3. Surveys of the data as collected indicated the emphasis to be placed on the maintenance of the various equipments between shots.

After about two days prior to each shot the number of changes in components was kept to a minimum. Daily checks were made on the systems to identify any weak points and to remedy as many of the operational failures as possible. Continual records were kept during this period of the operation of each item of the instrumentation, and detail plans for each shot were based on these performance records.

From the afternoon of shot day minus one until H-hour, the activities of the Instrumentation Section of ATU 3.4.2 were very closely scheduled. The final checkout of the system was made during the period H minus 16 hr and H minus 10 hr. At this time it was determined which gauges were operating and would be considered for the mission. One hour prior to take-off of the aircraft for the mission, a warm-up period for the equipment was started, and the final tuning of the telemetering was completed. One person from the instrumentation section was on the runway checkout crew to assure that all instrumentation equipment was functioning properly at take-off of the aircraft. A period from H plus 3 hr to H plus 12 hr was utilized in rechecking the equipment and gauge operation. The before- and after-mission checks were made in order to determine the zero drift or other changes in alignment which may have occurred during the mission.

REFERENCES

1. Preliminary Report on Temperature Response of an Aircraft Exposed to Short Time Radiant Heat Inputs, University of California at Los Angeles, 1950.
2. "The Effects of Atomic Weapons," p 192, Los Alamos Scientific Laboratory, Government Printing Office, Washington, D. C., 1950.
3. "The Effects of Atomic Weapons," p 201, Los Alamos Scientific Laboratory, Government Printing Office, Washington, D. C., 1950.

~~SECRET~~

SECRET

Chapter 5

Dog Shot

5.1 GENERAL INFORMATION

The weapons test designated "Dog" was fired at 0634 hours, local time, on Apr. 8, 1951. The maximum predicted strength as given by TG 3.1 was 90 kt, and the airplane positions had been computed on this basis with an added margin of safety to allow for errors in the unproved theory (see Sec. 4.2).

The days prior to shot time were spent in checking and rechecking the instrumentation. Because of the lack of service tests and flight checks on the instrumentation and on the application of the operation procedures, a condition of concern and of tenseness built up prior to shot time. This condition extended to the operating organization to some extent for quite similar reasons. The tension and lack of experience undoubtedly contributed to the misfortunes and equipment failures which plagued this mission.

QB-17 drones M and N and QT-33 drones 1 and 2 had been selected for this mission and were ready. Of the manned airplanes the XB-47 and one of the B-50D's (340) were ready. The other B-50D (290) was essentially complete in one recorder, but the other recorder was not ready because of the delay while a wing tip was replaced (see Sec. 5.8).

Just a few hours prior to take-off, during the final check, it was discovered that some interference existed in the controlling circuits to the instrumentation on the two QB-17 drones. On the chance that it might be due to the high-frequency pressure recorders, these equipments were disconnected so that no overpressure records were obtained.

5.2 ALICE POSITION, QT-33 DRONE 2

Assigned location (at shock)

True altitude, 7,800 ft

Horizontal distance, 7,800 ft beyond point zero

Predicted conditions

Peak overpressure, 2.03 psi

Peak gust velocity, 136 ft/sec (in direction of shock)

Time of travel (shock), 6.8 sec

5.2.1 Flight Log

QT-33 drone 2 took off approximately 6 min later than scheduled because of the excitement and confusion resulting from the loss of the other QT-33. The drone took a turn to the right during take-off and dragged the right wing-tip tank on the ground, causing slight damage to the tank. It appeared, at the time, as though considerable fuel had been lost from the right tank which might cause unbalance and hamper the flight characteristics or curtail the mission. However, the take-off and the mission were completed satisfactorily. The flight data as reported¹ by ATU 3.4.2 are as follows:

Time

Start engines, 0535

Take-off, 0545

At assigned altitude,* 0551

Shock arrival, 0634:09.2

Landing, 0720

Meteorological conditions at altitude

True altitude, 7,800 ft

*Approximate, not included in Navigator's Report, reference 1.

SECRET

Pressure altitude, 7,180 ft
Outside air temperature, +10°C
Wind direction (from), 025° (azimuth)
Wind velocity, 14 knots
Airplane parameters at shock arrival
Indicated airspeed, 222 knots
Ground speed, 241 ft/sec
Ground track azimuth, 060°
Horizontal angle from blast, 060° (azimuth)
Vertical angle from blast,* 42.3° (elevation)
Horizontal distance from blast, 8,580 ft
Slant distance from blast,* 11,600 ft
Shock struck drone from rear and below

5.2.2 Airplane Condition

Before take-off the telemetering equipment in QT-33 drone 2 was completely equipped with sensing channels. The recorder was equipped with sensing elements except for 10 channels as follows:

Channel 1—altitude
Channel 2—airspeed
Channel 4—acceleration, rear fuselage
Channel 6—torsion, right wing root
Channel 8—bending, left wing root
Channel 14—torsion, mid-span, right wing
Channel 15—elevator position
Channel 16—pressure, 5 per cent chord, right wing station 128
Channel 23—pressure, left wing station 128
Channel 24—pressure, horizontal stabilizer

For the most part, these gauges were removed from the recorder and connected to the telemeter. The fuel tanks were full at the time the engine was started for take-off. The take-off gross weight was computed to be 13,800 lb, with the c.g. at 31.1 per cent m.a.c. The airborne controller reported some tendency for the airplane to be heavy on the left wing due to loss of fuel from the right tip tank. However, this instability was easily overcome by the auto-pilot.

At the time that the shock wave struck the airplane, the gross weight was computed to have been 11,500 lb, with the c.g. at 29.2 per cent m.a.c. The fuel distribution at this time was 95 gal (637 lb) in the fuselage tank, 154 gal (1,032 lb) in the inboard wing tanks, and 90 gal (603 lb) in the wing leading-edge and outboard

*Computed from data in Navigator's Report, reference 1.

tanks. The airplane was not in sight of the airborne controlling crews at the time of shock, and consequently no visual observations of the reactions were made. The radar controller reported that the airplane took the shock in straight-and-level flight with a slight excess of airspeed over the scheduled 222 knots.

After the airplane landed, it was examined. The right tip tank had been scratched badly by dragging on the runway at take-off, but the damage appeared superficial and not so much fuel had been lost as had been estimated. No damage to the airplane was apparent other than scorching and blistering of the paint by heat from the explosion. Areas of the airplane surface that had been painted black, such as numbers and letters, were definitely blistered, and some of the areas of the flaps, wings, and elevators, which had been painted yellow, were scorched to a brownish tinge. A view of the underneath surface of the right wing and of the aft fuselage showing this scorching is presented in Fig. 5.1.

5.2.3 Radar Position Data

The film record from the radar-data recorder was not used because the range indicator on the recorder was inoperative. However, the track, as determined from the plotting board of the AN/MSQ-1, is presented in Fig. 5.2. In general, the correlation between the computed locations from the radar-data recorder and from the plotting board was very close as is indicated in other sections of this report.

The ground track of the drone, as plotted from information recorded by the AN/MSQ-1 plotting system, indicates that it was 860 ft beyond and 180 ft to the right of Alice position at the time the shock wave passed. This position was based on the time of shock-wave arrival ($T_0 + 9.15$ sec) that was indicated on the record of the master time signal as recorded in the airplane by the magnetic-tape recorder. The airplane passed ground zero 300 ft to the right on a course of 58.4°. The radar operator reported that the drone was flying directly on course at a true altitude of 7,800 ft and a heading of 58° at the time the shock wave passed. Based on the position indicated by the radar plotting board and on the heading and altitude as given by the radar operator, the shock wave

SECRET

SECRET

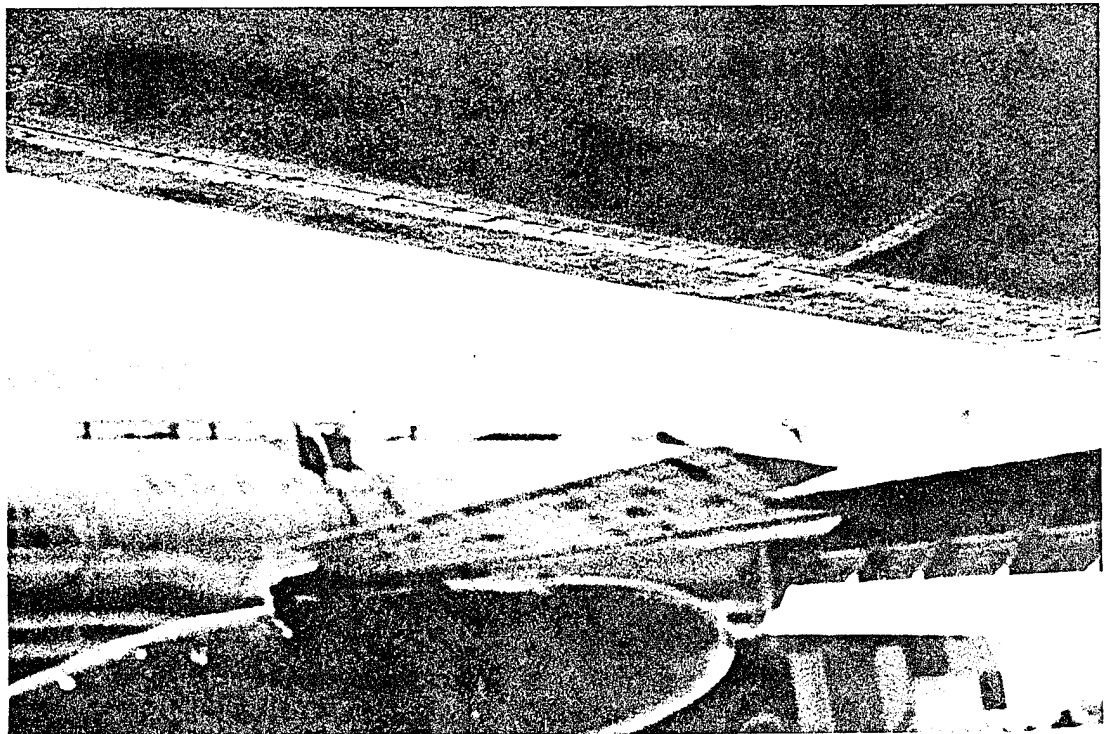
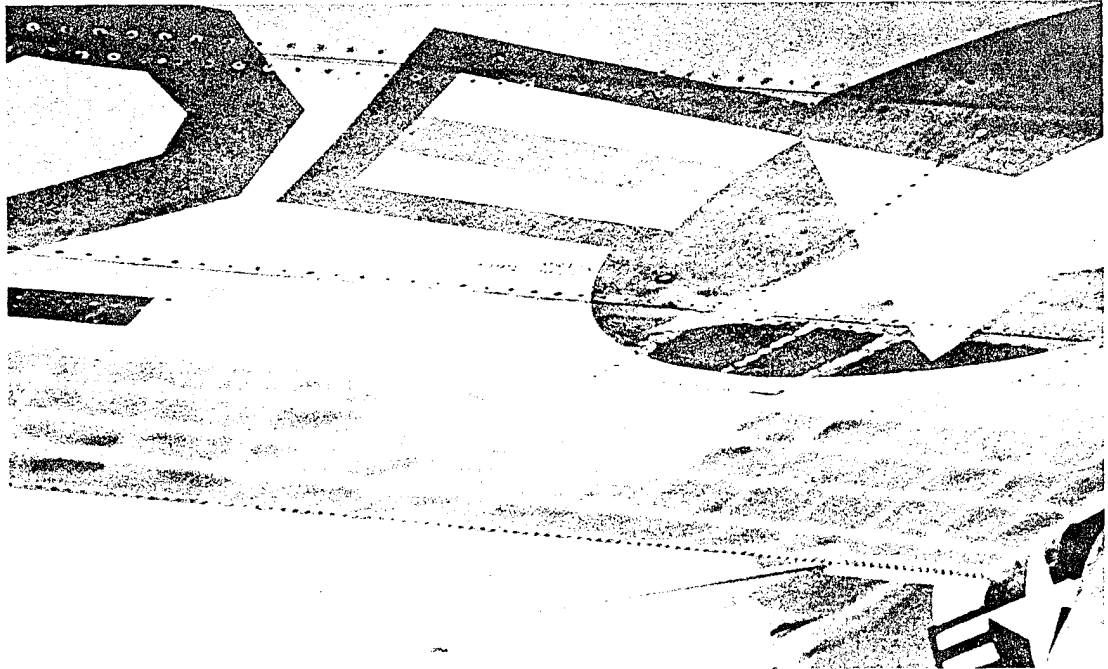


Fig. 5.1 Heat Damage to QT-33 No. 2, Dog Shot. (Above) right wing. (Below) aft fuselage.

SECRET

SECRET

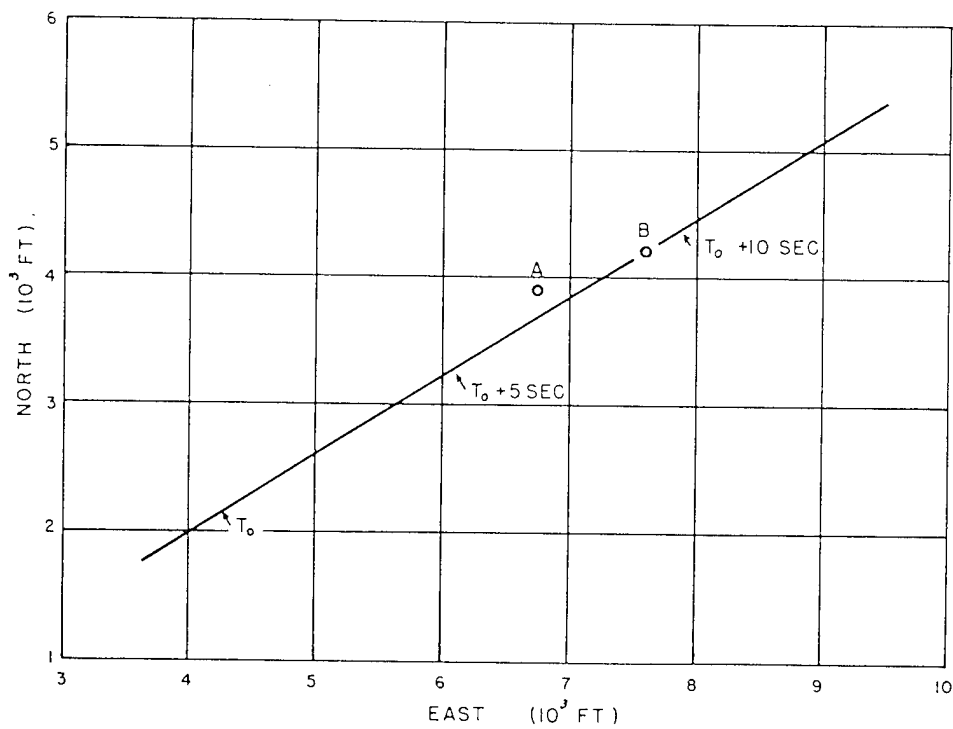


Fig. 5.2 Track of QT-33 Drone 2, Dog Shot. Point A indicates Alice position. Point B indicates actual location at shock.

SECRET

SECRET

struck the airplane from 3.0° left of the tail at a horizontal distance of 8,700 ft, an altitude of 7,800 ft, and a slant range of 11,680 ft at a vertical angle of 41.9° .

5.2.4 Load Data

The data as recorded on the tape recorder are presented in Figs. 5.3 through 5.15.

The reduction of the data from this drone was seriously complicated by the performance of channel 13. Although the data from this channel were not analyzed, the channel was reported as "in" before the mission and was connected to the recorder during the test. The record shows that the channel was intermittently "out." When the channel was out, the drain on the gauge source caused an artificial deflection, particularly of the pressure channels. It appears from the record that this artificial deflection was small and was a definite amount, for which compensation was made in preparation of the data graphs. Channel 13 was out until 9.27 sec after T_0 ; then it was in, except for a short period (0.24 sec) starting at 10.79 sec, until 11.31 sec when it went out to a lesser degree than it had been previously. The failure of this channel is indicated on the record by a violent "hash" or oscillation of the trace. It is believed that the data in the other channels have been properly compensated; however, any unusual or nonconformable data recorded during the times that channel 13 was out might reasonably be discounted. The gauge for channel 11 became open during the mission.

5.2.5 Heat Data

The temperatures as recorded on this drone are presented in Table 5.1.

5.2.6 Analysis

The location at which the shock struck the drone is identified as point B in Fig. 5.2 for measured time of shock travel, $T_0 + 9.15$ sec. The coordinates of this point are discussed in Sec. 5.2.3, and the theoretical values of peak overpressure and gust velocity are 1.75 psi and 122 ft/sec. Theoretically, the shock should have struck the drone at $T_0 + 7.5$ sec. Except for the possibility of slowing of the shock front by an unpredicted heterogeneous atmosphere, the discrepancy is unexplained.

Many cross-graphs to compare related data are possible, but only two of these are presented. Figure 5.16 illustrates the pressures over the chord of the right wing at station 128 at various times so as to show a pictorial representation of the lift variation caused by the shock wave. Figure 5.17 indicates the pitching acceleration* which should be readily comparable with tail load.

The load on the right-hand horizontal stabilizer, as measured in channel 9, is reported in the vicinity of T_0 (Fig. 5.6) as well as at the time of arrival of the shock wave (Fig. 5.7). The sharp rise in apparent stabilizer load from zero time to +0.95 sec was attributed to the radiant energy. The effect is assumed to be the expansion of the metal at or near the lower surface due to the heating of that metal by the radiant energy. This expansion would unbalance the strain-gauge bridge in exactly the same manner as an up-load on the stabilizer. The strain gauges for channel 9 were located on the inside surfaces of the spar caps (see Sec. 3.4.1) so that an approximate temperature of the inner surface of the lower spar cap was computed accepting the following assumptions:

1. No change in strain (due to either thermal expansion or change in load) occurred in the upper spar cap during this period.
2. The thermal expansion of the metal was 12.34×10^{-6} in. per degree Fahrenheit.
3. The gauge factor, $(\Delta R/R)/(\Delta L/L)$, for these gauges was 1.96.
4. The linear expansion at each of the gauges on the lower spar caps (front and rear spars) was equal.

According to Fig. 5.18 the maximum indicated increase in temperature was approximately 70°F above ambient. The maximum rate of temperature rise is shown to occur in the vicinity of T_0 and is about 118°F per second. The temperature rise is apparently complete in about 0.95 sec, and the further increase in load (after $T_0 + 1$ sec) is assumed to have been induced by the deformation of the stabilizer. The temperature of the metal appears to have remained constant until about $T_0 + 2.5$ sec, when the rate of cooling began to exceed the rate at which the heat was absorbed. The rate of cool-

*Pitching acceleration was obtained from the difference between c.g. and nose acceleration. This ignores fuselage deformation.

~~SECRET~~

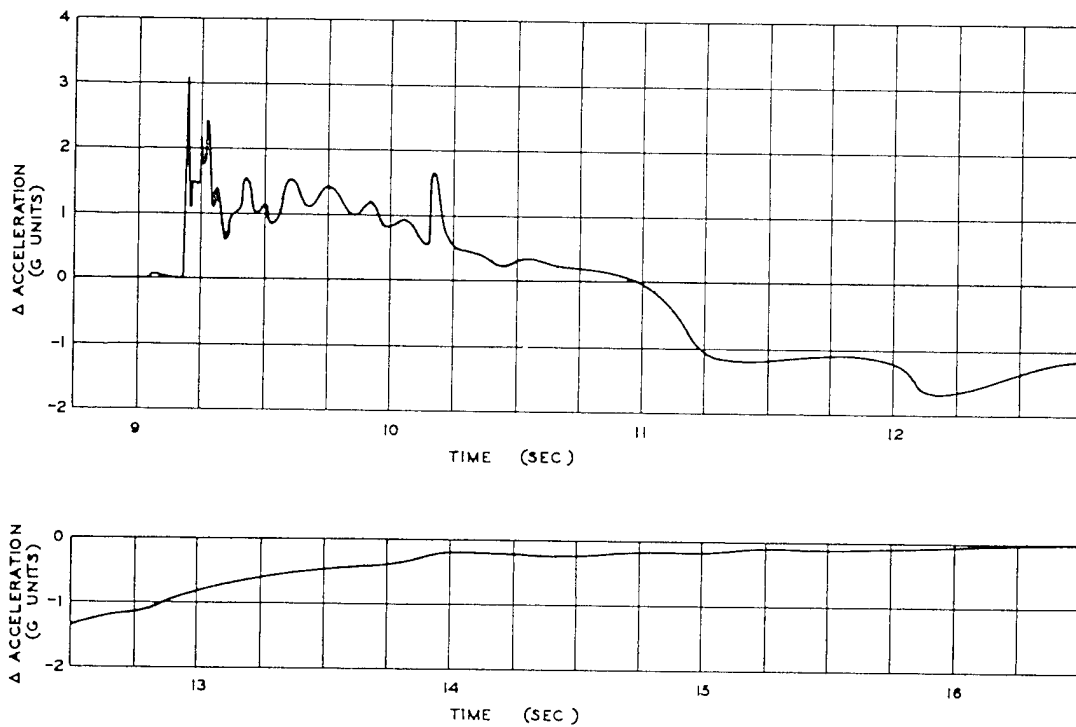


Fig. 5.3 Normal Acceleration, c.g., Channel 3, QT-33 No. 2, Dog Shot

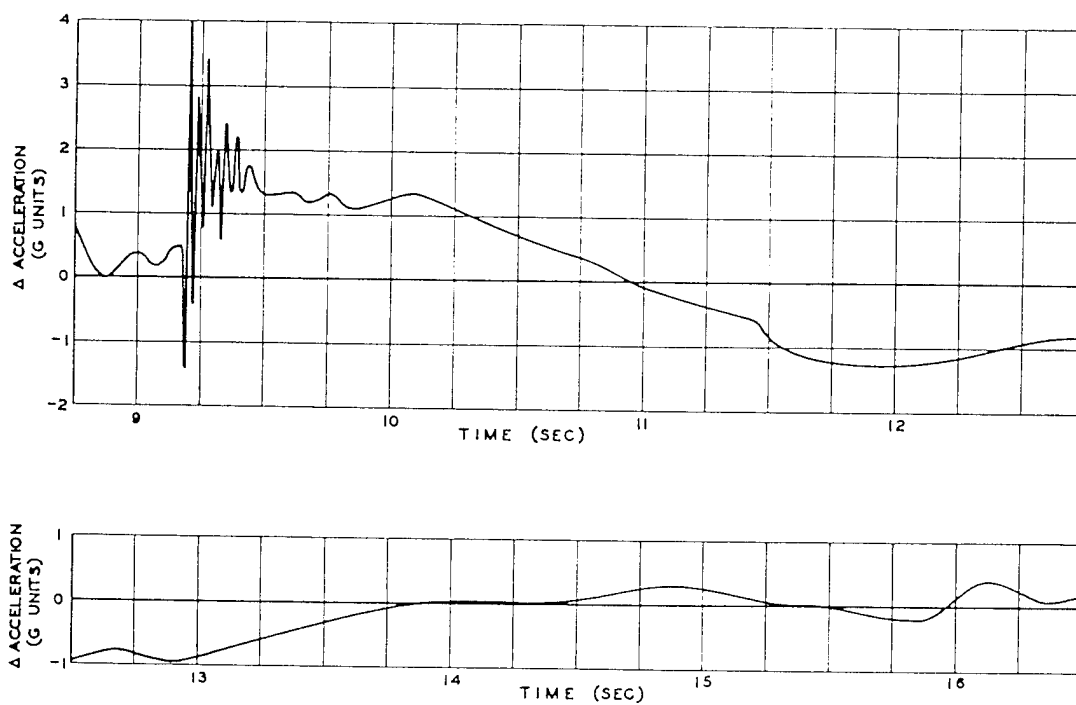


Fig. 5.4 Normal Acceleration, Nose, Channel 5, QT-33 No. 2, Dog Shot

~~SECRET~~

SECRET

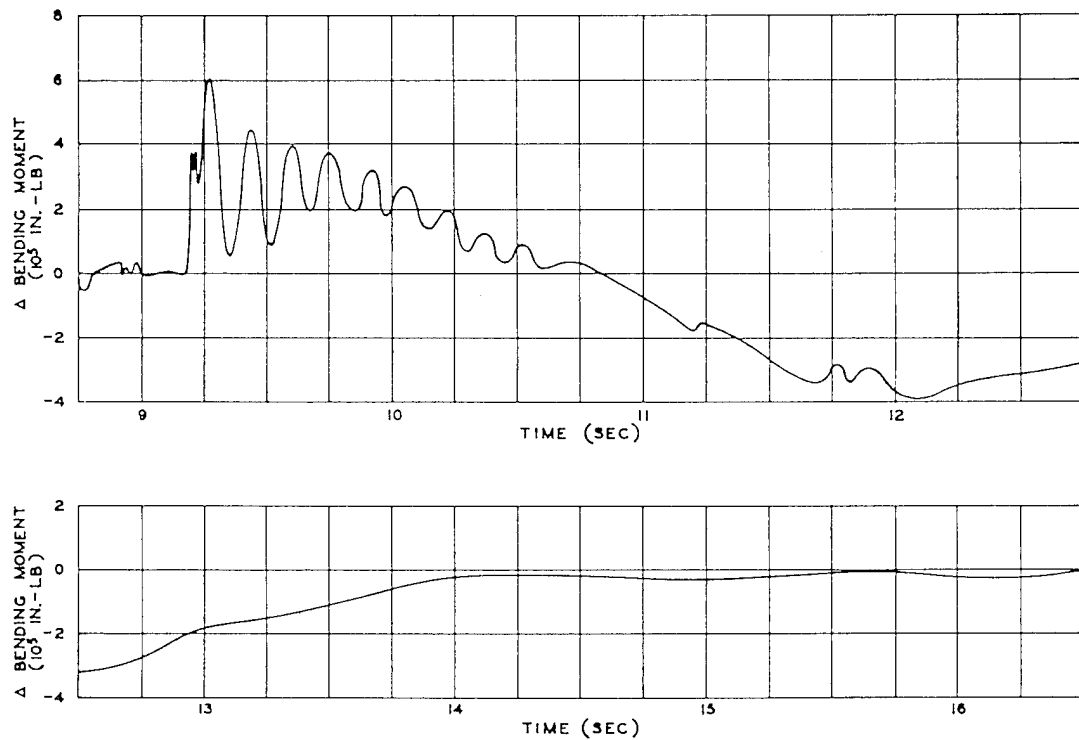


Fig. 5.5 Wing Bending, Right Root, Channel 7, QT-33 No. 2, Dog Shot

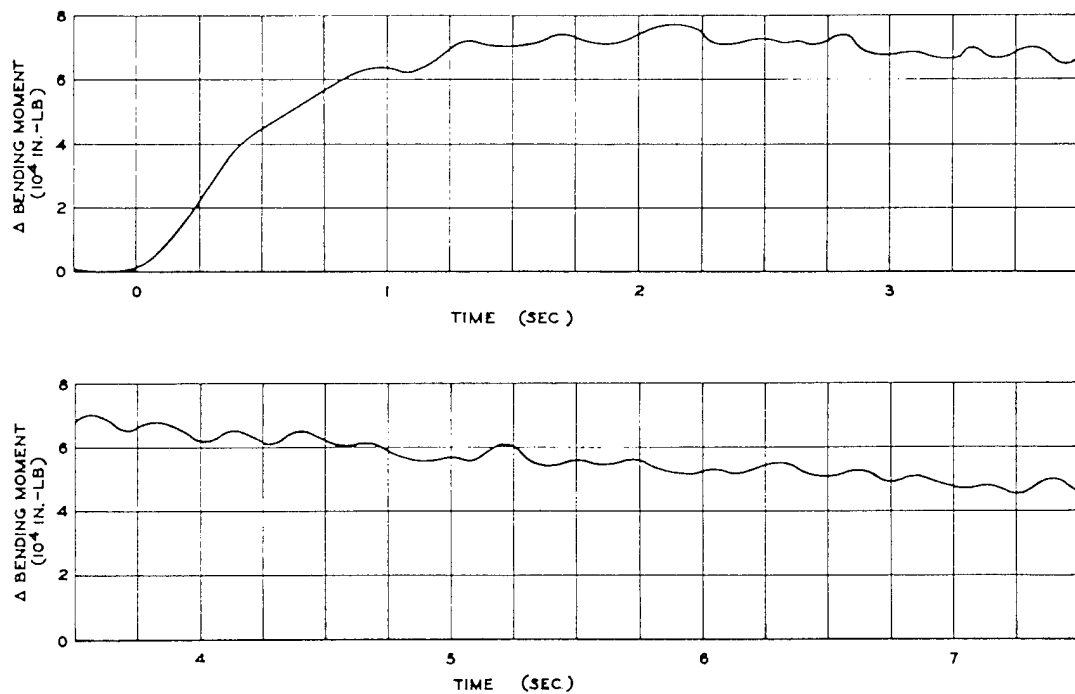


Fig. 5.6 Stabilizer Bending, Right Root, Channel 9, Before Shock Wave, QT-33 No. 2, Dog Shot

SECRET

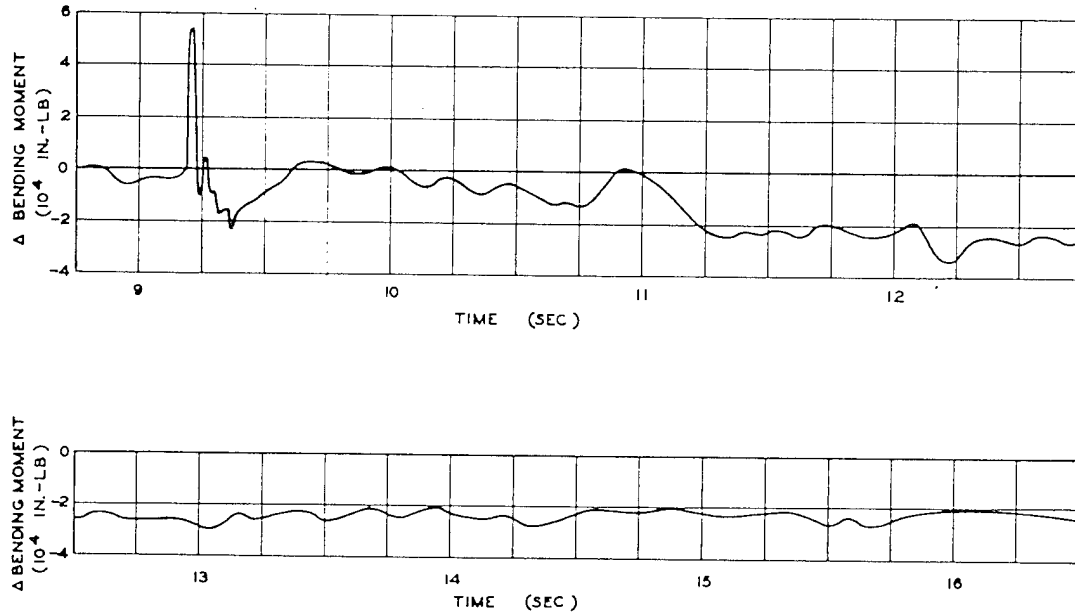


Fig. 5.7 Stabilizer Bending, Right Root, Channel 9, Shock Wave, QT-33 No. 2, Dog Shot

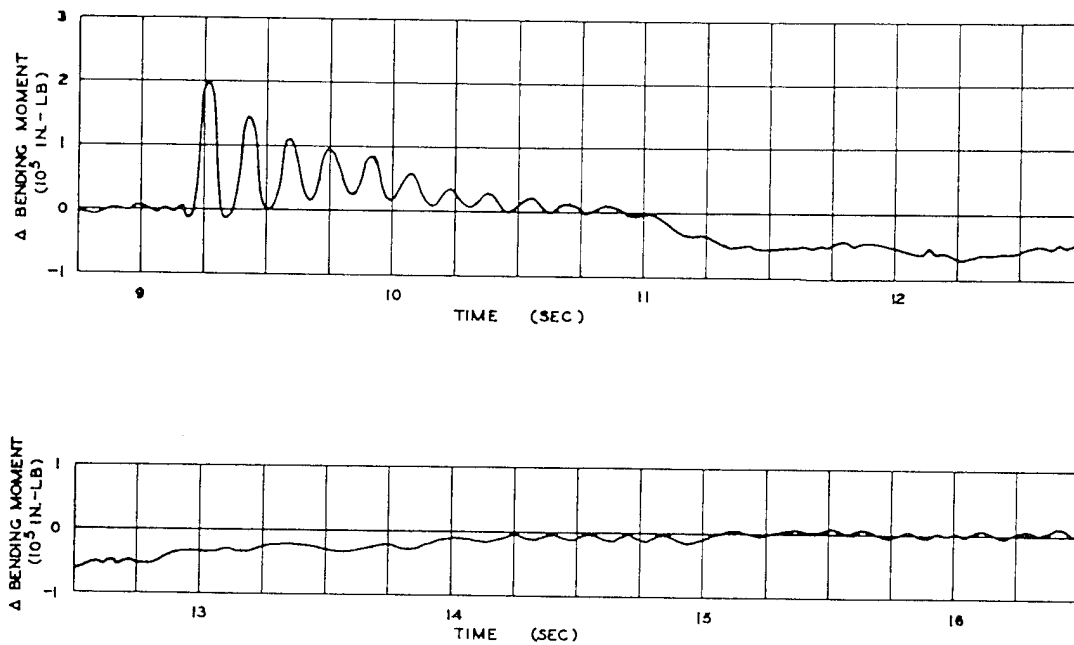


Fig. 5.8 Wing Bending, Outer Panel, Right Wing Station 129, Channel 10, QT-33 No. 2, Dog Shot

SECRET

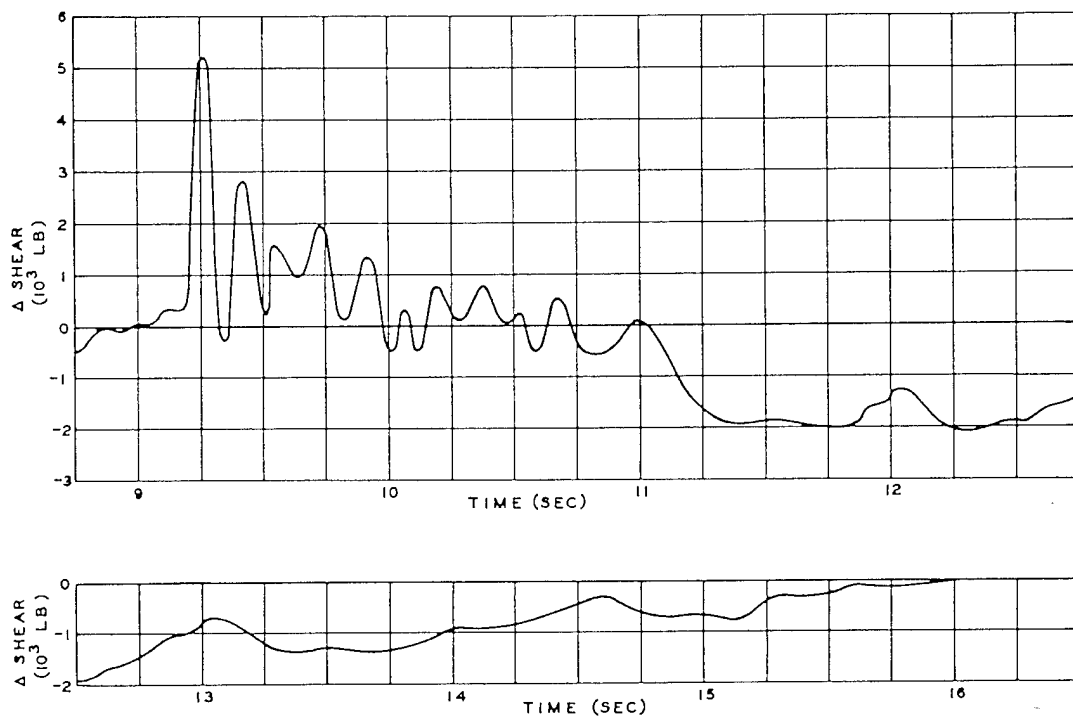


Fig. 5.9 Wing Shear, Right Root, Channel 12, QT-33 No. 2, Dog Shot

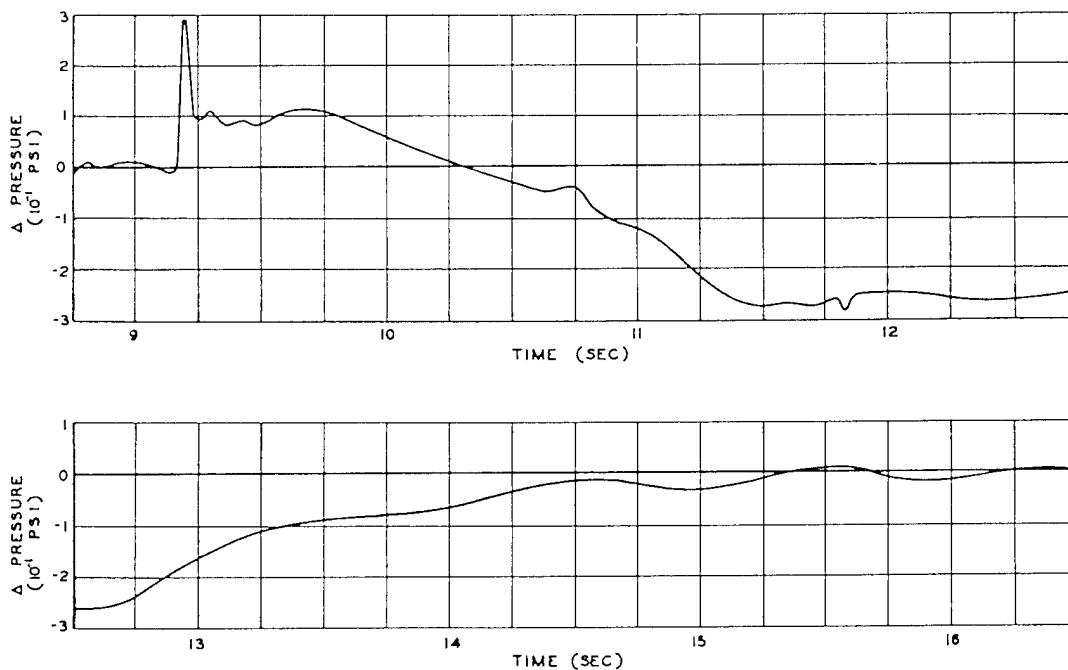


Fig. 5.10 Differential Pressure, 10% Chord, Right Wing Station 128, Channel 17, QT-33 No. 2, Dog Shot

~~SECRET~~

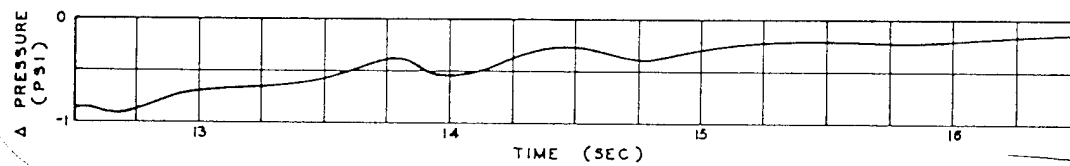
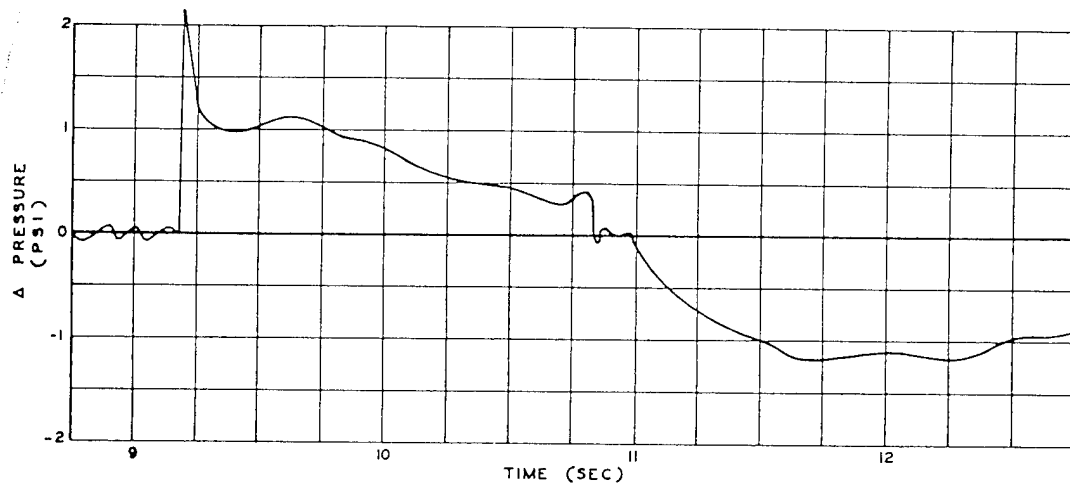


Fig. 5.11 Differential Pressure, 26% Chord, Right Wing Station 128, Channel 18, QT-33 No. 2, Dog Shot

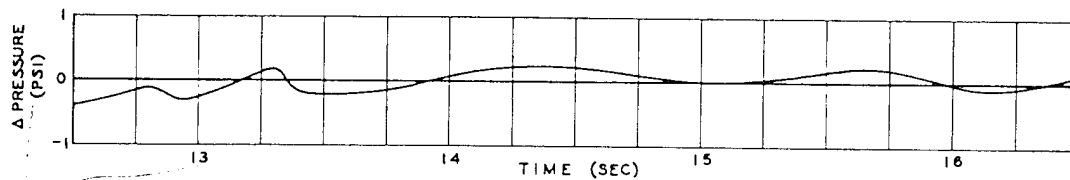
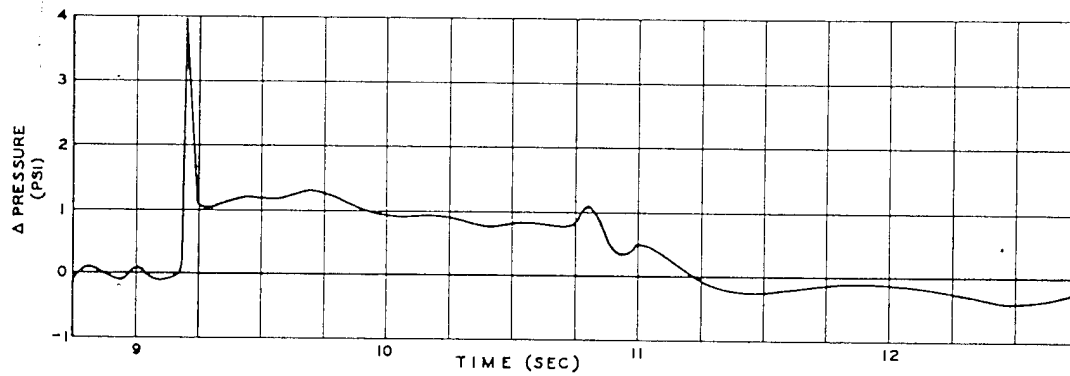


Fig. 5.12 Differential Pressure, 42% Chord, Right Wing Station 128, Channel 19, QT-33 No. 2, Dog Shot

~~SECRET~~

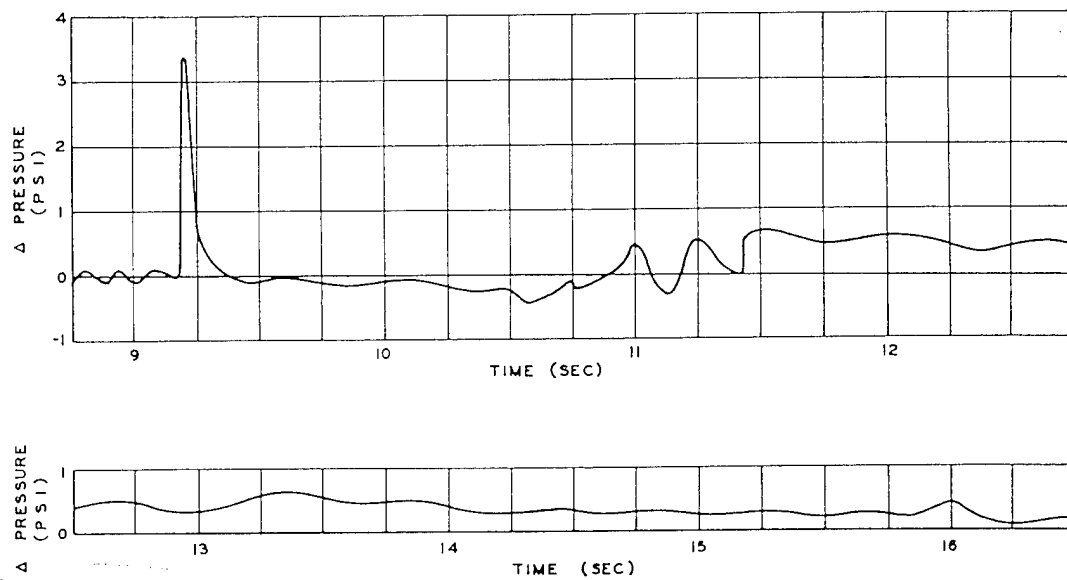


Fig. 5.13 Differential Pressure, 58% Chord, Right Wing Station 128, Channel 20, QT-33 No. 2, Dog Shot

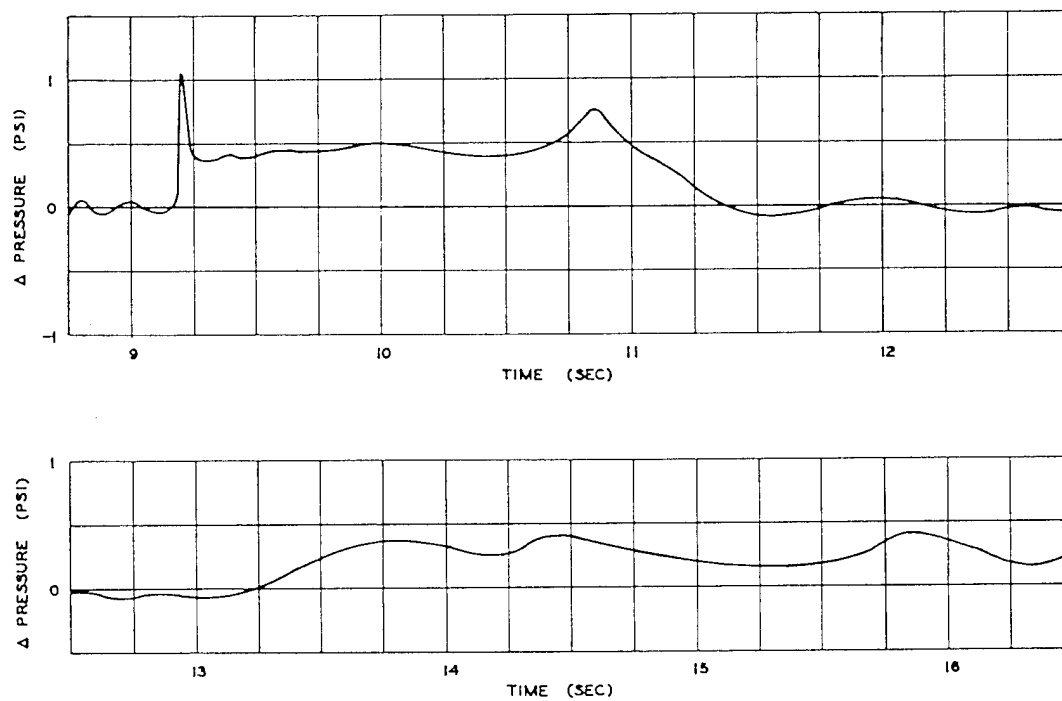


Fig. 5.14 Differential Pressure, 80% Chord, Right Wing Station 124, Channel 21, QT-33 No. 2, Dog Shot

~~SECRET~~

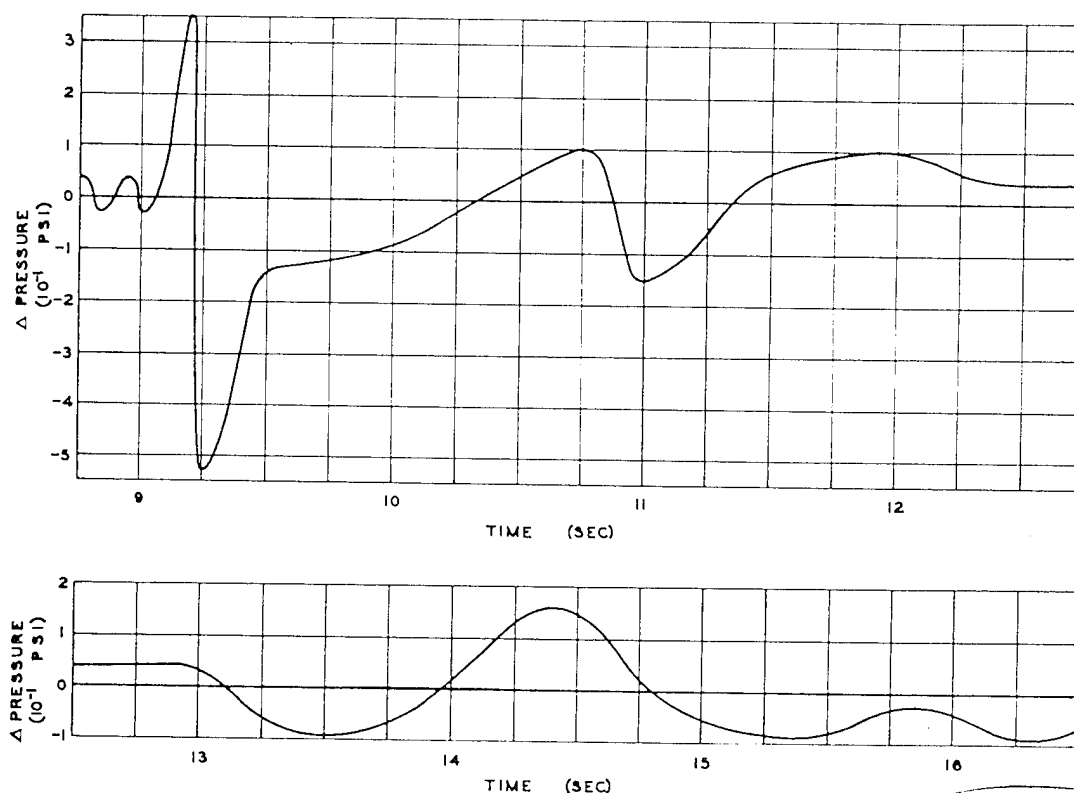


Fig. 5.15 Aerodynamic Pressure, Nose, Channel 22, QT-33 No. 2, Dog Shot

TABLE 5.1 HEAT MEASUREMENTS AT ALICE POSITION, DOG SHOT

Tape Location*	Material Thickness† (in.)	Color‡		Angle of Incidence	Max. Temp. (°F)	Ambient Temp. (°F)	Δ Temp. (°F)
		In	Out				
38	0.040	AP	A _s	32° 37'	275	58.6	216.4
39	0.040	AP	Y	34° 18'	330	58.6	271.4
40	0.032	B	A _s	84° 41'	130	58.6	71.4
41	0.040	A _s	A _d	35° 22'	240	58.6	81.4
42		LOG	Y	32° 37'	Burned off and lost		
43	0.040	LOG	Y	34° 18'	330	58.6	271.4

*See Table 3.10.

†Material is aluminum sheet.

‡See Table 3.11.

~~SECRET~~

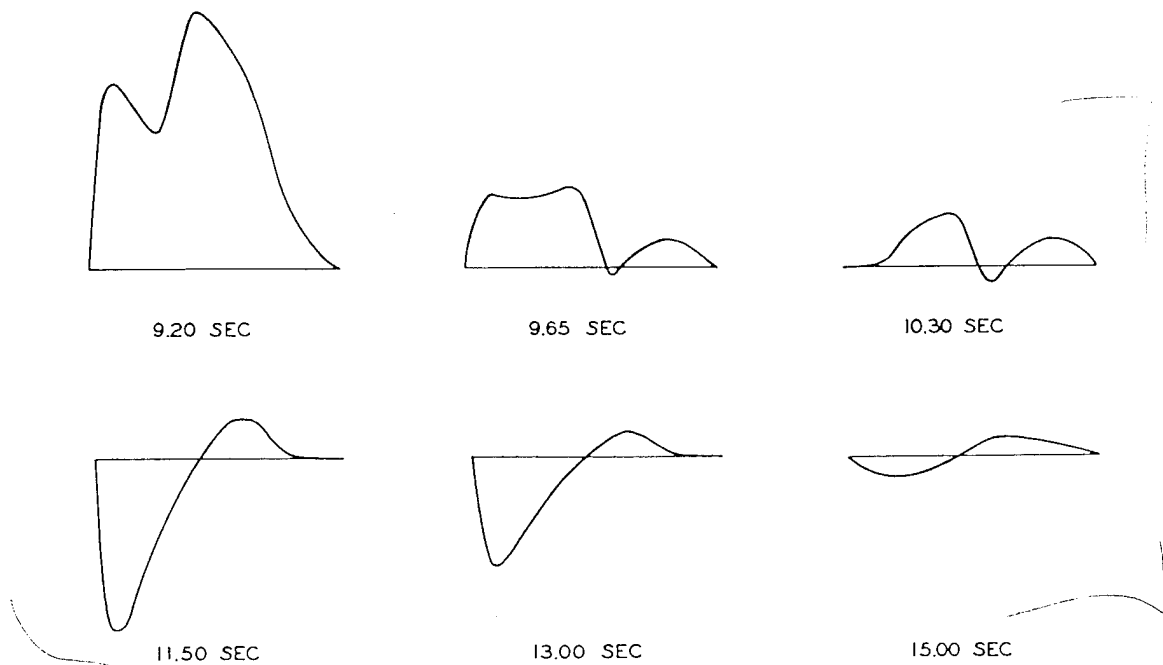


Fig. 5.16 Summary of Differential Pressures at Wing Station 128, QT-33 No. 2, Dog Shot

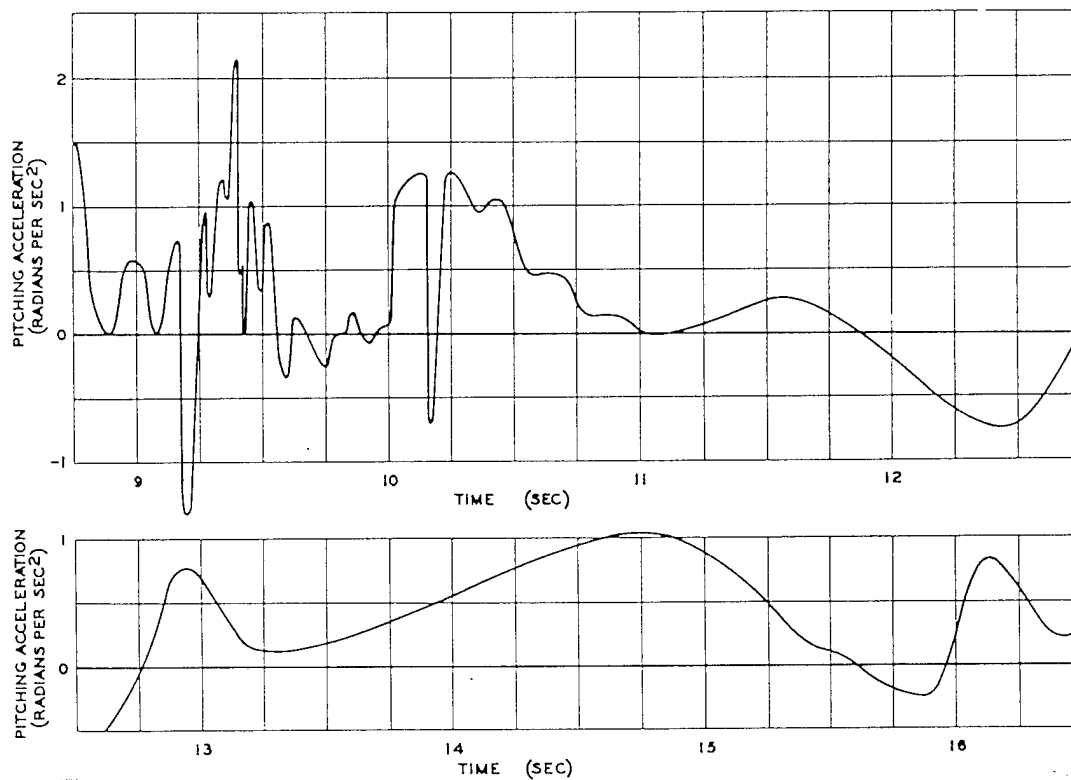


Fig. 5.17 Pitching Acceleration, QT-33 No. 2, Dog Shot

~~SECRET~~

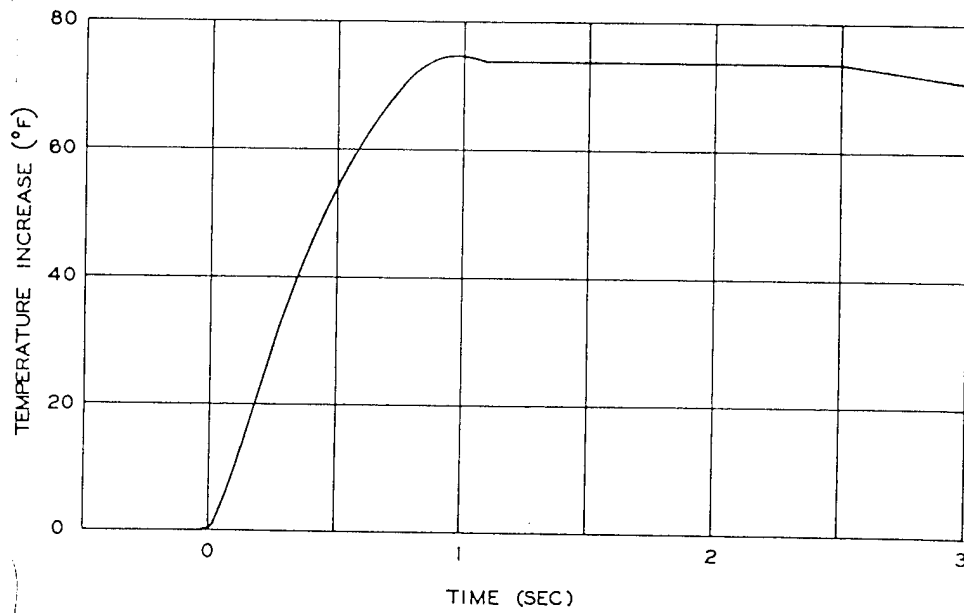


Fig. 5.18 Apparent Temperature Variation in Horizontal Stabilizer, QT-33 No. 2, Dog Shot

~~SECRET~~

ing appears to vary from about 6°F per second at $T_0 + 3$ sec to 4.4°F per second at the time the shock wave struck the airplane. In accordance with the afore-mentioned line of reasoning, the temperature of the metal within the stabilizer had only dropped to approximately 40°F above ambient by the time the shock wave struck, so that the loads due to the shock wave are superimposed on the thermal loads still present in the stabilizer.

5.3 BETTY POSITION, QT-33 DRONE 1

QT-33 drone 1 took off on schedule. However, during take-off the airplane drifted toward the left side of the runway, and after several large bounces the airplane hit the water in the lagoon. Fortunately, the airplane did not strike personnel, equipment, or installations, so that no damage was done except the loss of the airplane and its equipment. Examination of the wreckage showed that the airplane struck the water nose down at about 110 knots with full-up elevator. No spare drone was available as a replacement, and consequently Betty position was not occupied for Dog shot.

5.4 CAROL POSITION, QB-17 DRONE M

Assigned location (at shock)
True altitude, 15,000 ft
Horizontal distance, 10,500 ft beyond point zero

Predicted conditions

Peak overpressure, 0.86 psi
Peak gust velocity, 75 ft/sec (in direction of shock)
Time of travel (shock), 13.3 sec

5.4.1 Flight Log

QB-17 drone M took off essentially on schedule. The airplane made a normal take-off and completed the mission satisfactorily. The flight data as reported¹ by ATU 3.4.2 are as follows:

Time
Start engines, 0119
Take-off, 0204
At assigned altitude, 0414
Shock arrival, 0634:10.7
Landing, 0943

Meteorological conditions at altitude

True altitude, 15,000 ft
Pressure altitude, 14,000 ft
Outside air temperature, +5°C
Wind direction (from), 045° (azimuth)
Wind velocity, 28 knots

Airplane parameters at shock arrival

Indicated airspeed, 138 knots
Ground speed, 254 ft/sec
Ground track azimuth, 060°
Horizontal angle from blast, 060° (azimuth)
Vertical angle from blast, * 57.2° (elevation)
Horizontal distance from blast, 9,670 ft
Slant distance from blast, * 17,830 ft
Shock struck drone from rear and below

5.4.2 Airplane Condition

Before take-off the telemetering equipment in QB-17 drone M was completely equipped with sensing channels. The recorder was equipped with sensing elements, except for seven channels, as follows:

Channel 3—acceleration at c.g.
Channel 4—acceleration at aft fuselage
Channel 5—acceleration at No. 3 engine
Channel 6—acceleration at No. 4 engine
Channel 11—torsion in right-wing outer panel
Channel 20—pressure, 60 per cent chord, right wing station 25.5
Channel 23—pressure, 60 per cent chord, left wing station 25.5

The majority of these gauges were removed from the recorder and connected to the telemeter.

At the time the engines were started, the fuel tanks were filled to 2,100 gal—1,700 gal (10,200 lb) in the main tanks and 400 gal (2,400 lb) in the Tokyo tanks. The take-off gross weight was computed to be 51,290 lb with the c.g. at 29.6 per cent m.a.c. This weight and balance computation is based on the weighing of the airplane in the take-off configuration at the time of calibration of the strain gauges.

The director reported normal operation of the drone, and it was released on a 060° heading for the test run with an indicated airspeed of 138 knots. The gross weight at the time the shock wave struck the airplane was computed to have been 45,560 lb, with the c.g. at 28.5

*Computed from data in Navigator's Report, reference 1.

~~SECRET~~

per cent m.a.c. The fuel at the time of shock consisted of 1,145 gal (6,870 lb) in the main tanks and none in the Tokyo tanks. The director reported that the airplane "...bounded about 300 to 400 ft with a nose-high attitude dropping IAS (indicated airspeed) to 89 knots and changing direction 30°. Lost down-elevator control at this time." It was apparent from later observation that the loss of elevator control must have occurred approximately 10 to 14 sec earlier than reported (at T_0) since the elevator control should have been affected by the loss of the lower surface of the elevator which was due to radiant heat from the blast. Either the director may not have noticed the change in control effectiveness until the violent motion of the airplane or a few seconds may have been required for the fabric to be torn off the elevator after it had been charred by the heat.

Some difficulty was encountered in landing the drone owing to the loss of elevator effectiveness. The instability of the airplane and its tendency to stall caused several anxious moments just before and during the landing. After the airplane landed, it was examined, and considerably more damage was revealed than had been estimated while the airplane was in flight. In fact, it is believed that, had the extent of the damage been known, a normal landing on the island of Eniwetok would not have been attempted. Figure 5.19 shows the damage to the elevators. The strips of fabric were still intact along the ribs where the heat either was conducted away by the metal or was insufficient to char the extra thickness of fabric. On the upper surface of the right elevator, about mid-span, is a light spot where the heat, after the lower surface was burned away, was still sufficient to blister the dope and leave only the threads of the fabric remaining. Figure 5.20 shows a view of the left wing and aileron and a close-up of the right aileron. The damage to the surfaces is apparent. Other minor evidences of heat, such as blistering of paint on the black letters and the black surfaces and on the black compass-antenna housing and charring of a wooden plug, were found by careful examination of the airplane. No significant structural damage was evident.

5.4.3. Radar Position Data

According to the radar director, drone M was directly on course, straight and level, and 0.3

sec or 78 ft short of Carol position at the time that the shock wave struck the drone. The graph of the data from the radar-data recorder, Fig. 5.21, verifies the slight error in horizontal distance, but, owing to the difference in time for shock travel, the drone is shown to be slightly to the right and beyond its assigned position. The position error could be verified by examining the pattern of paint blisters on the compass-antenna housing. The blisters extended slightly higher on the left than on the right. According to the track as plotted in Fig. 5.21, the airplane passed 215 ft southeast of the point of the explosion, and the true course was 59°. If the course corrections were 1° for wind and 1° to compensate for missing the point of blast and if there was no sudden change in direction just at shock arrival, the shock struck the airplane from 2° to the left of rear at a horizontal distance of 10,600 ft. A true altitude of 15,000 ft gives a slant range of 18,380 ft and a vertical angle of 54.8°.

5.4.4 Load Data

The data as recorded on the tape recorder are presented in Figs. 5.22 through 5.35. The data are, for the most part, very erratic. This is attributed to the general instability which was caused by the damage to the surfaces. Channel 13 is not presented because of the lack of a suitable torsion calibration, and channels 12 and 21 failed during the mission.

The recorder was started by the blue box, and the time marks on the record (from the radio) are very poor. In fact, only four identifiable time "pips" were found in the interval before the shock struck. The interval established by these marks is extrapolated to form the time axis.

There is a considerable change in loads (particularly bending) and in elevator position at T_0 . Because of the fact that the recorder started at T_0 , the change in loads was under way when the recorder started. The rate at which these loads change is relatively small, but the amount of the change indicates a long-period longitudinal oscillation which is only slightly disturbed by the effects of the shock. The time from the positive peaks of loads just after T_0 to the negative peak just after shock arrival is about 13 sec, whereas the time to the next positive peak is about 19 sec. The zero-load

~~SECRET~~

SECRET

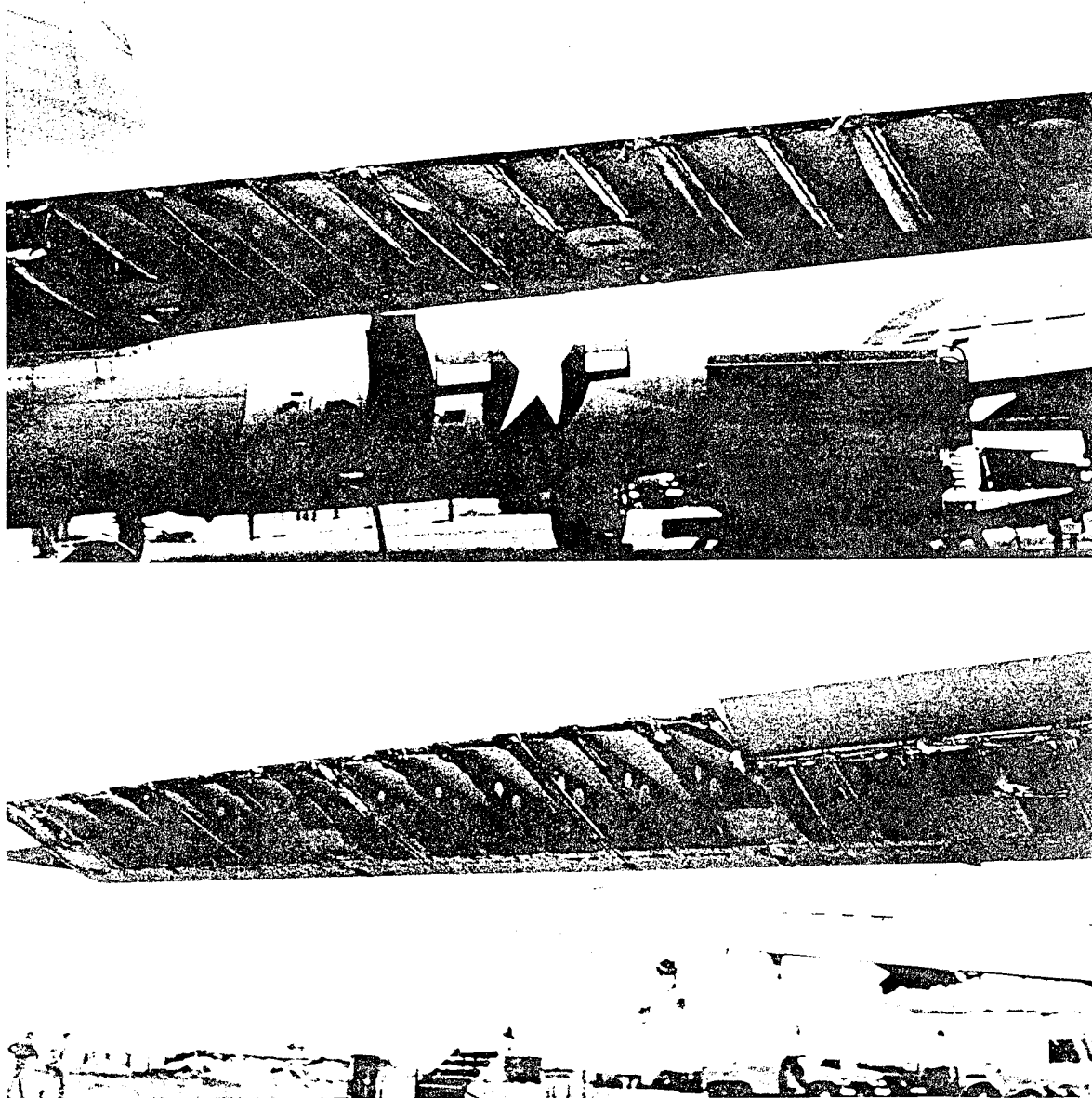


Fig. 5.19 Heat Damage to Elevators, QB-17 M, Dog Shot. (Above) right elevator. (Below) left elevator.

~~SECRET~~

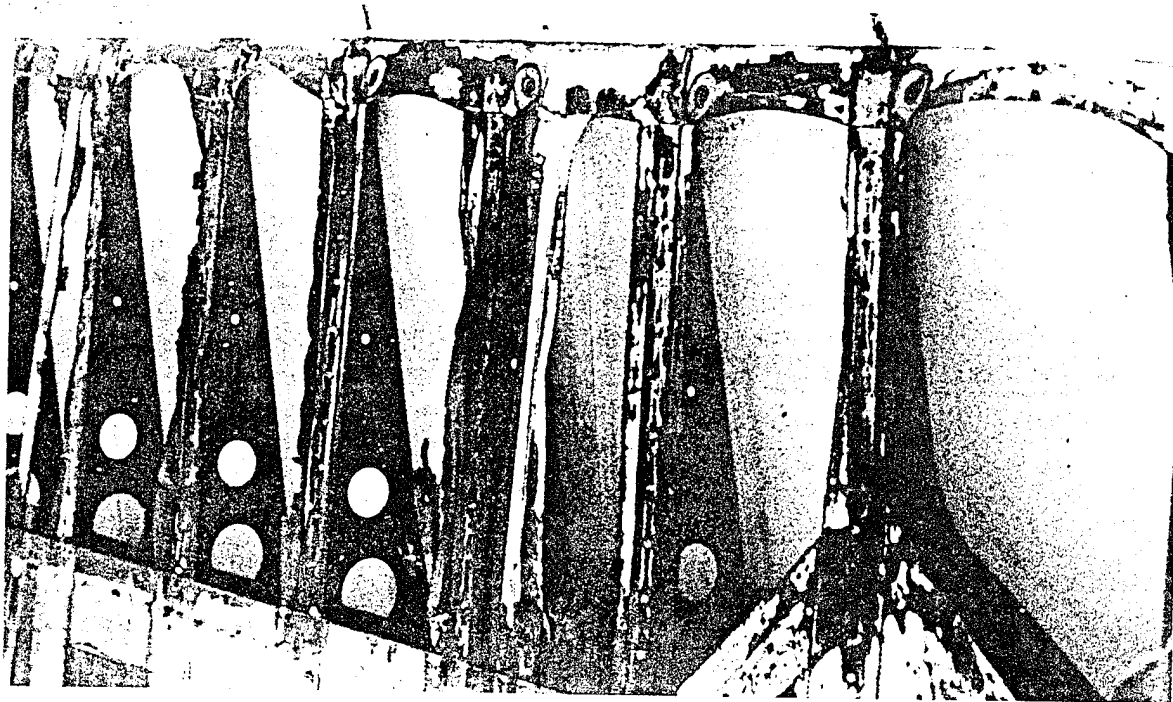
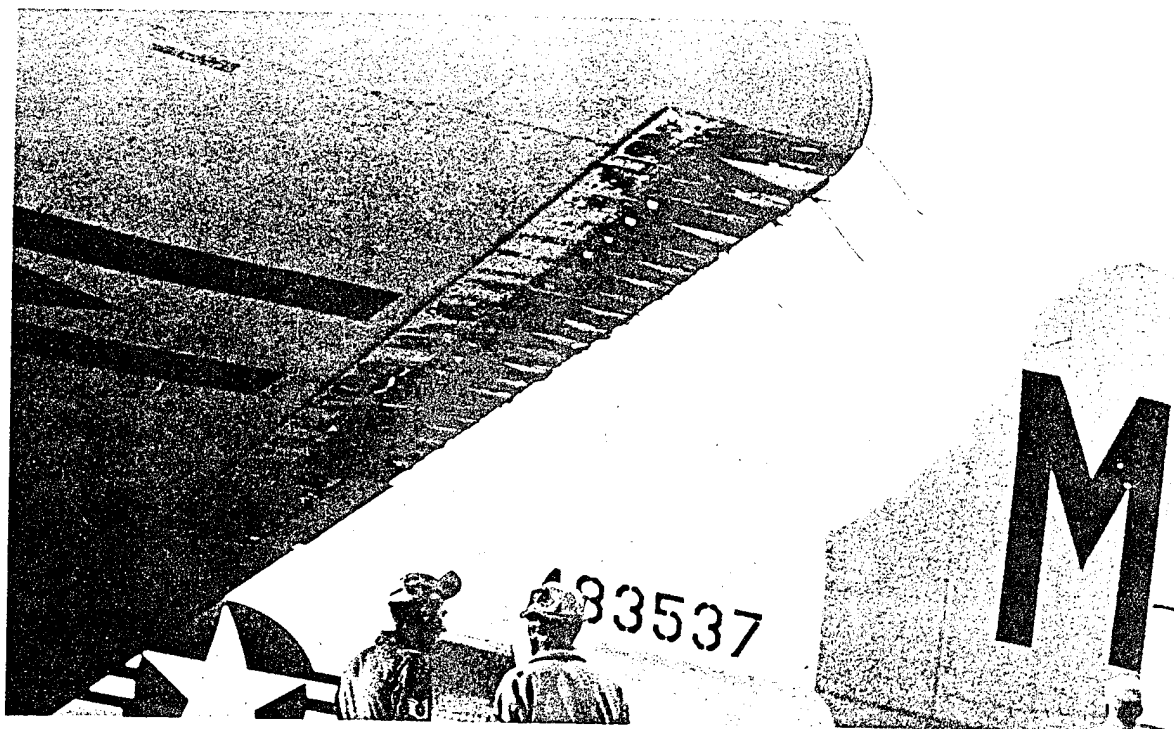


Fig. 5.20 Heat Damage to Ailerons, QB-17 M, Dog Shot. (Above) left wing and aileron. (Below) right aileron.

~~SECRET~~

SECRET

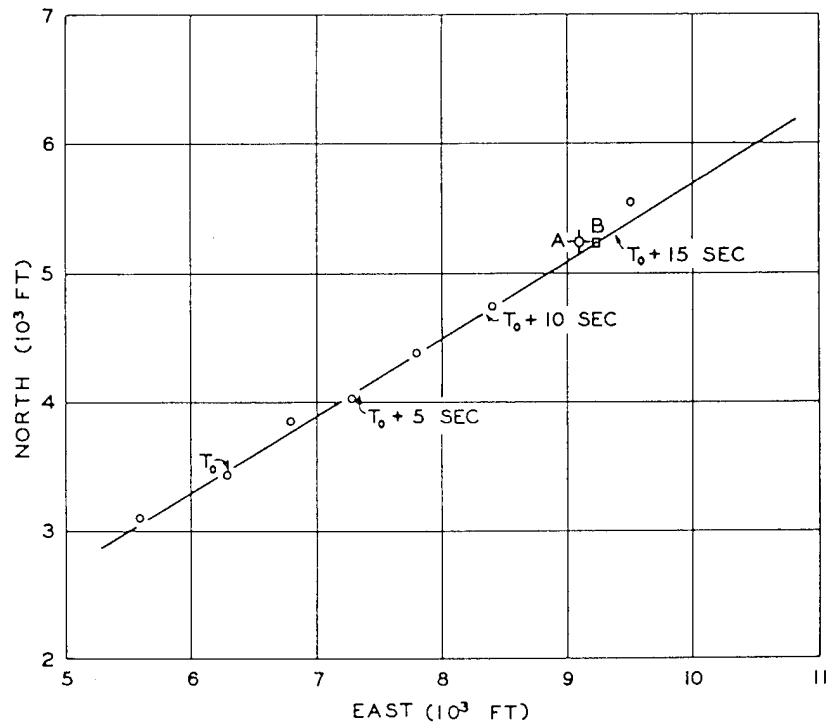


Fig. 5.21 Ground Track, Radar-data Recorder, Drone Carol, Dog Shot. Point A indicates Carol position. Point B indicates actual location at shock.

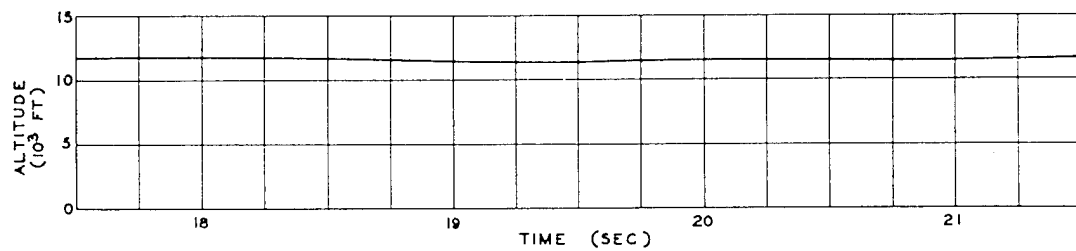
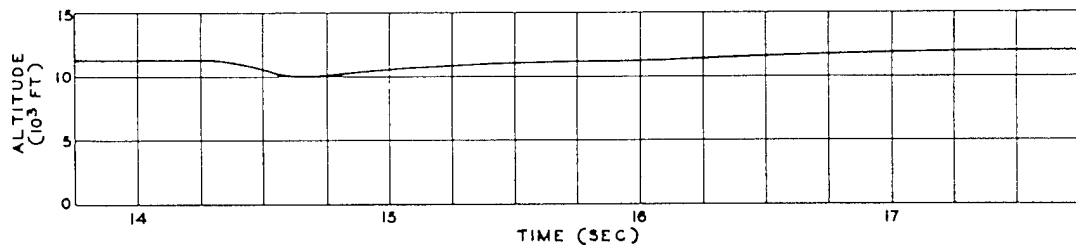


Fig. 5.22 Altitude, Channel 1, QB-17 M, Dog Shot

~~SECRET~~

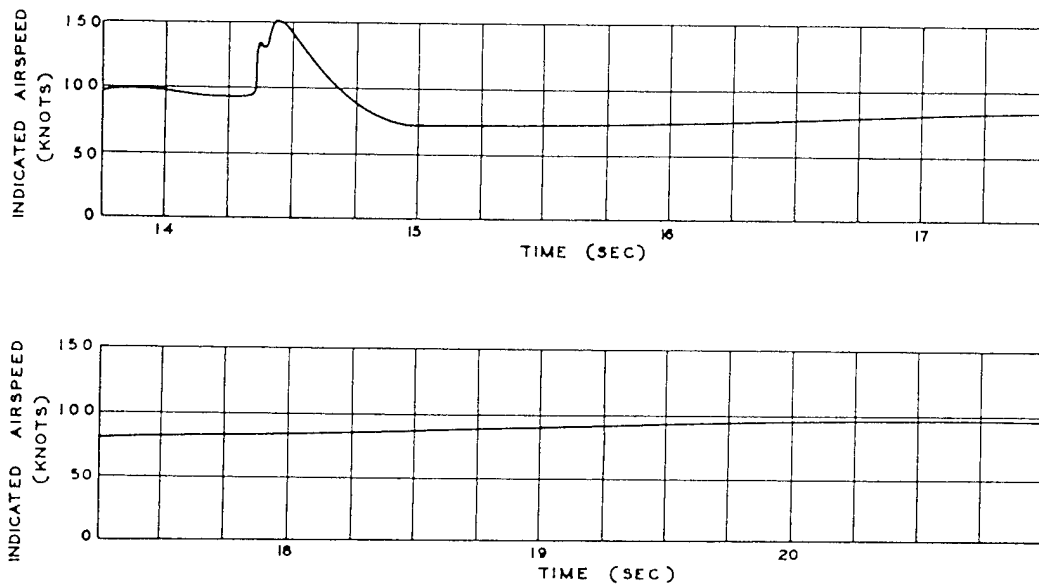


Fig. 5.23 Airspeed, Channel 2, QB-17 M, Dog Shot

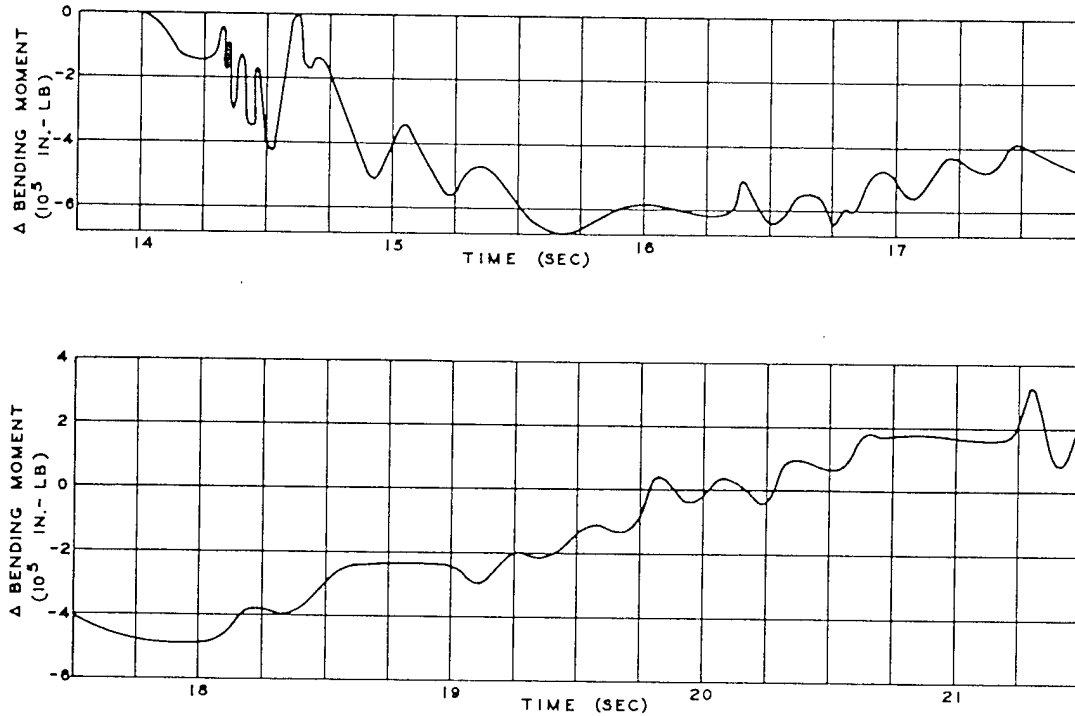


Fig. 5.24 Wing Bending, Right Wing Root, Channel 7, QB-17 M, Dog Shot

~~SECRET~~

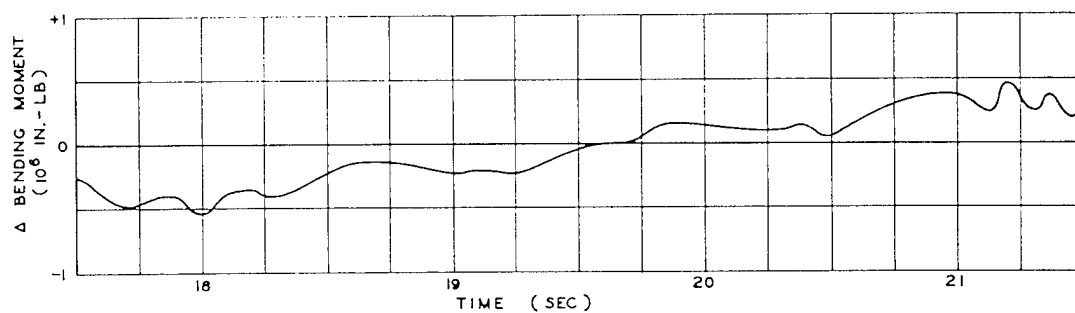
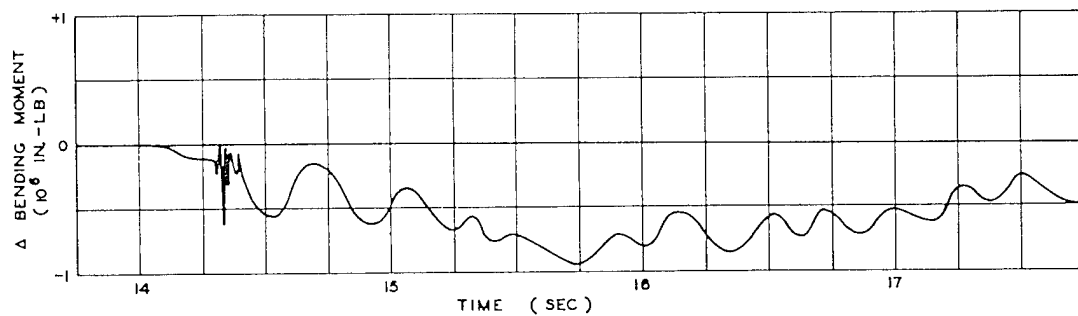


Fig. 5.25 Wing Bending, Left Wing Root, Channel 8, QB-17 M, Dog Shot

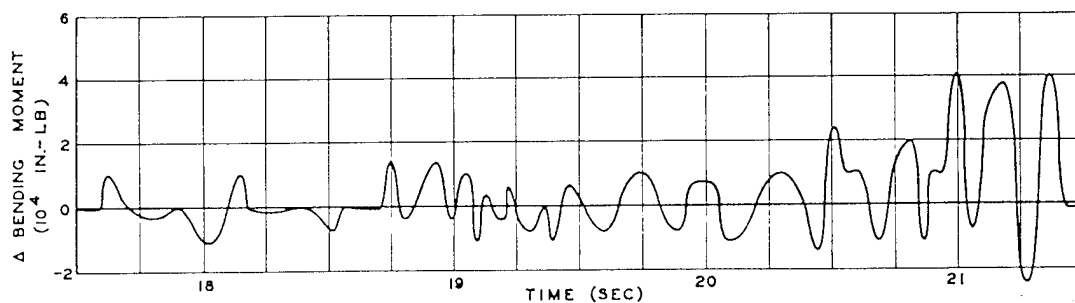
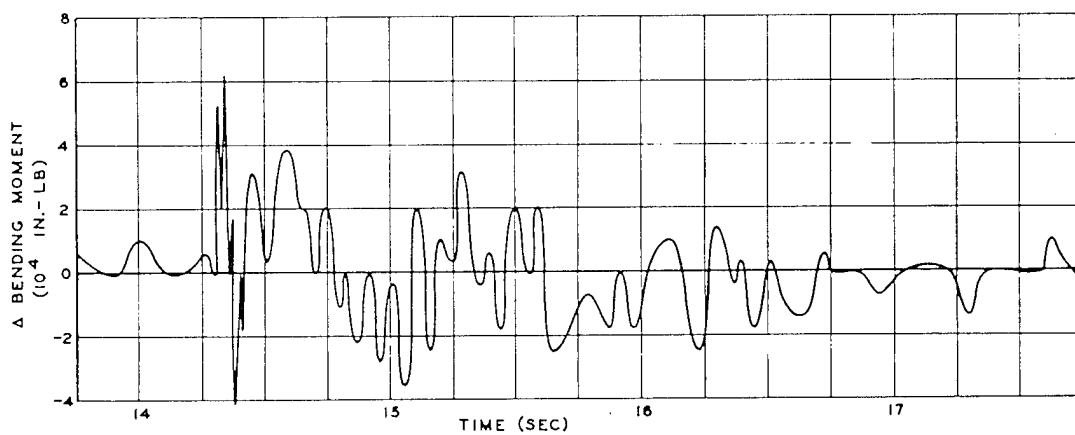


Fig. 5.26 Stabilizer Bending, Right Horizontal Stabilizer, Channel 9, QB-17 M, Dog Shot

~~SECRET~~

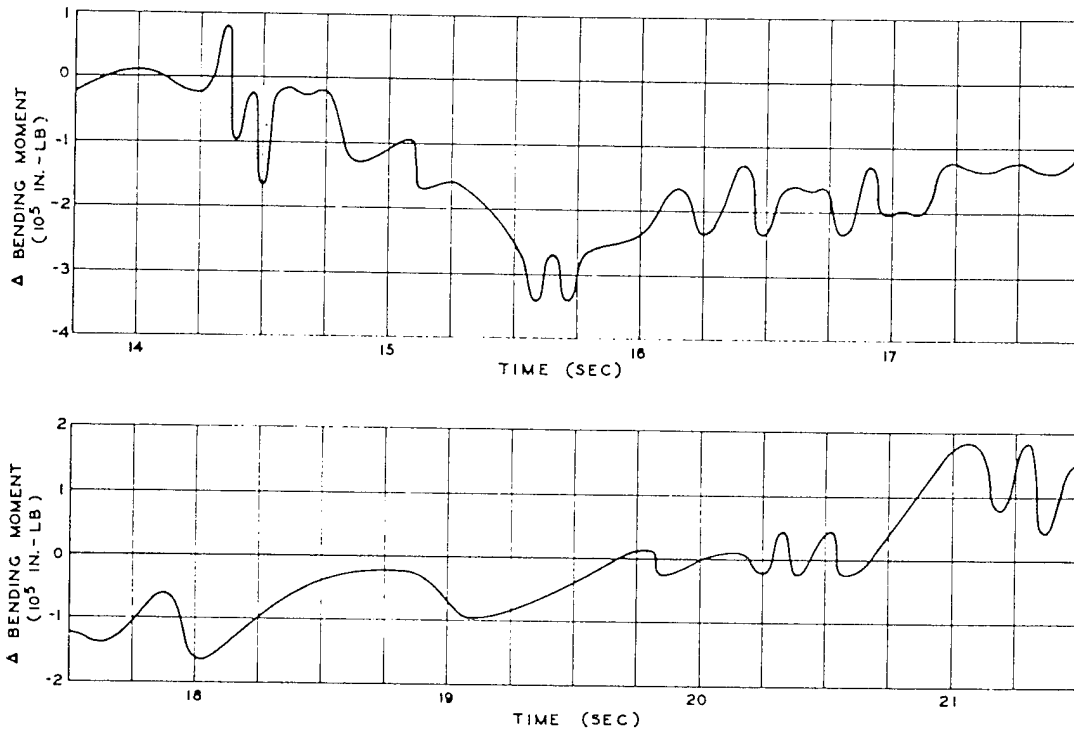


Fig. 5.27 Wing Bending, Outer Panel, Right Wing Station 19, Channel 10, QB-17 M, Dog Shot

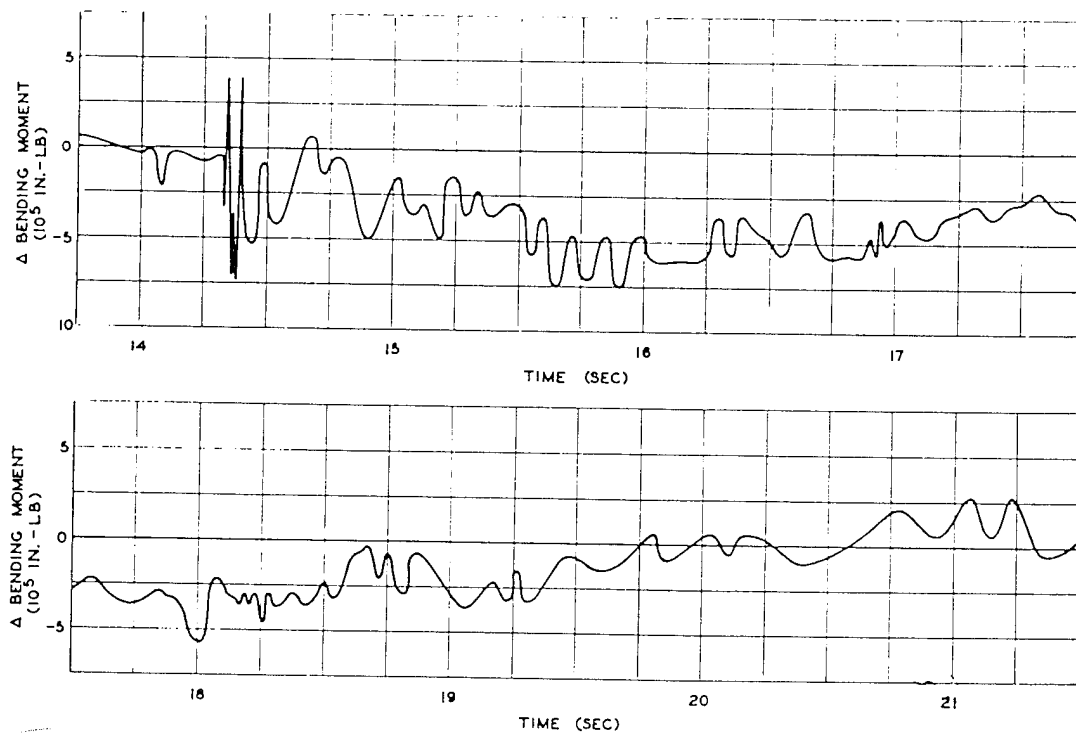


Fig. 5.28 Wing Bending, Mid-span, Right Wing Station 8.8, Channel 14, QB-17 M, Dog Shot

~~SECRET~~

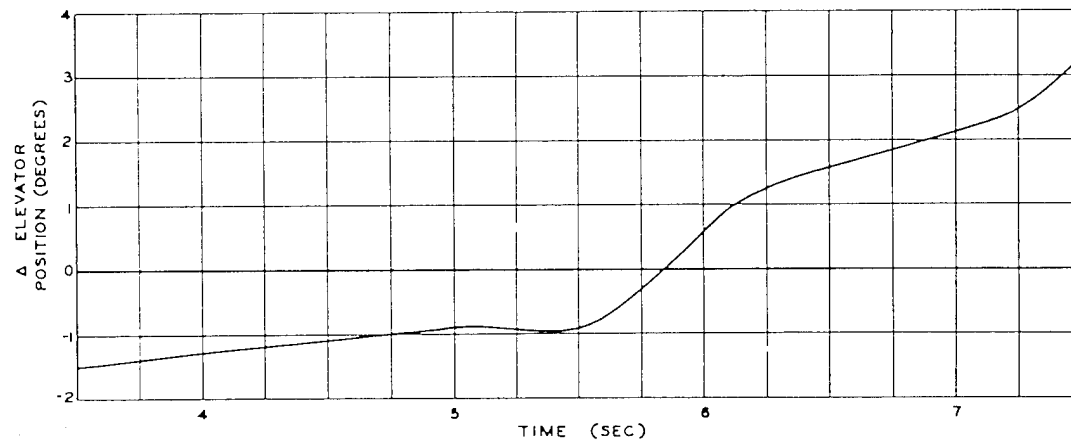
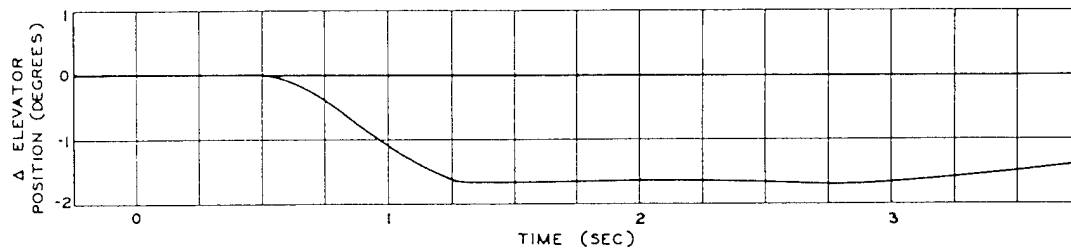


Fig. 5.29 Elevator Position, Channel 15, QB-17 M, Dog Shot

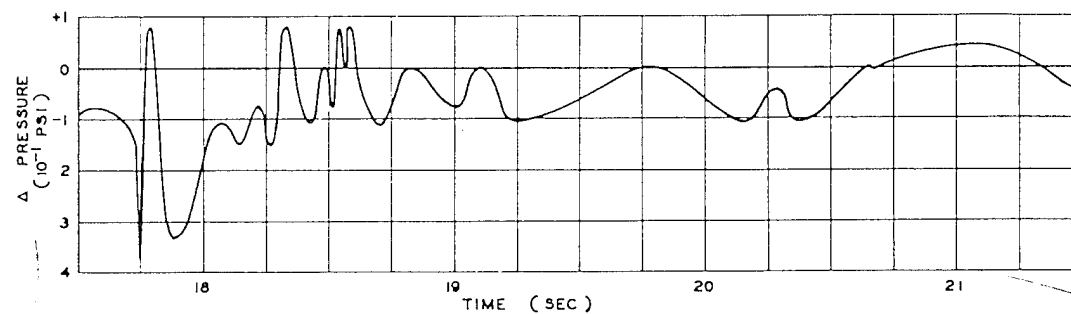
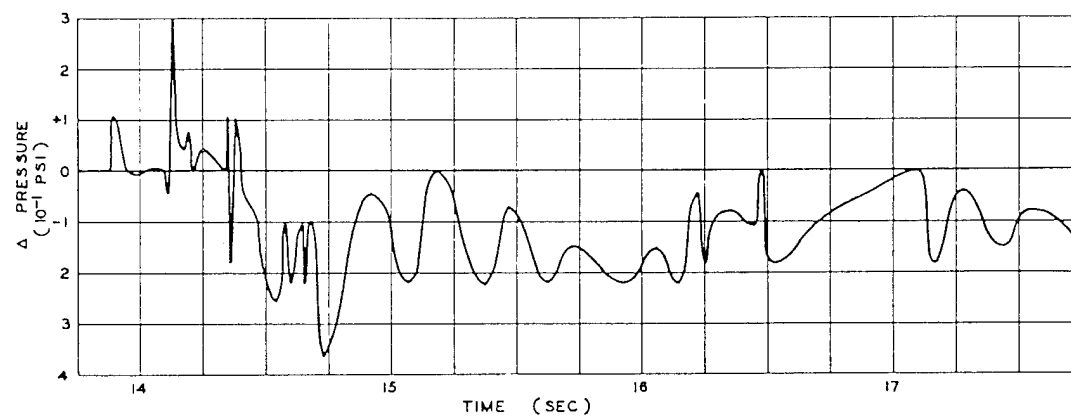


Fig. 5.30 Differential Pressure, 5% Chord, Right Wing Station 25.5, Channel 16, QB-17 M, Dog Shot

~~SECRET~~

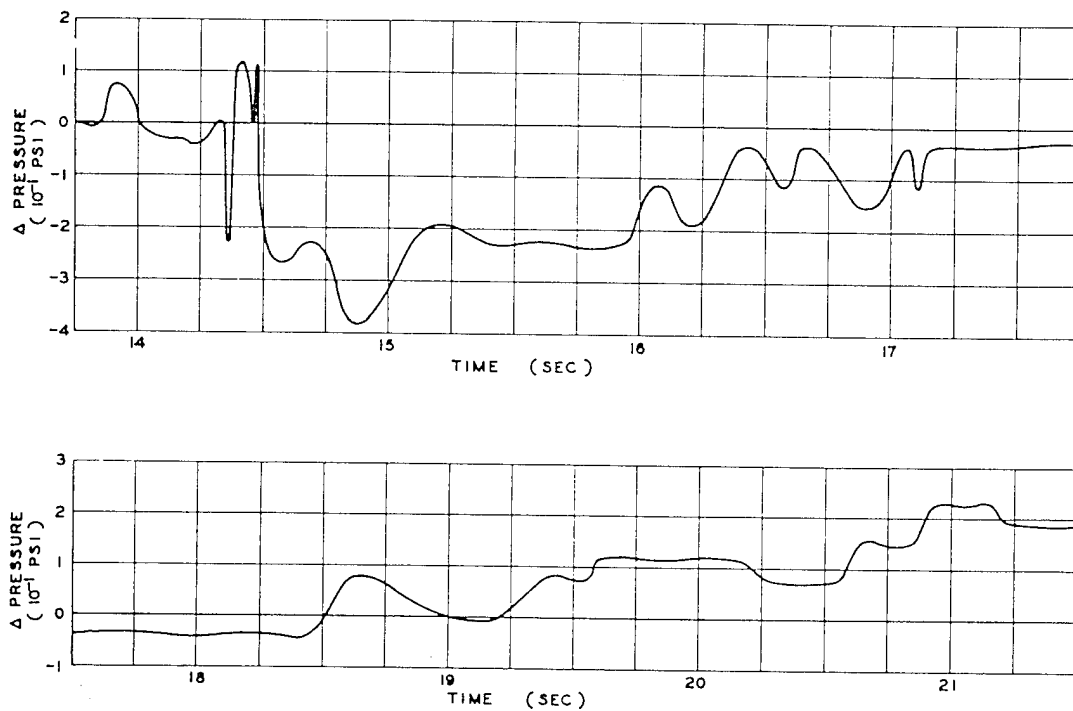


Fig. 5.31 Differential Pressure, 10% Chord, Right Wing Station 25.5, Channel 17, QB-17 M, Dog Shot

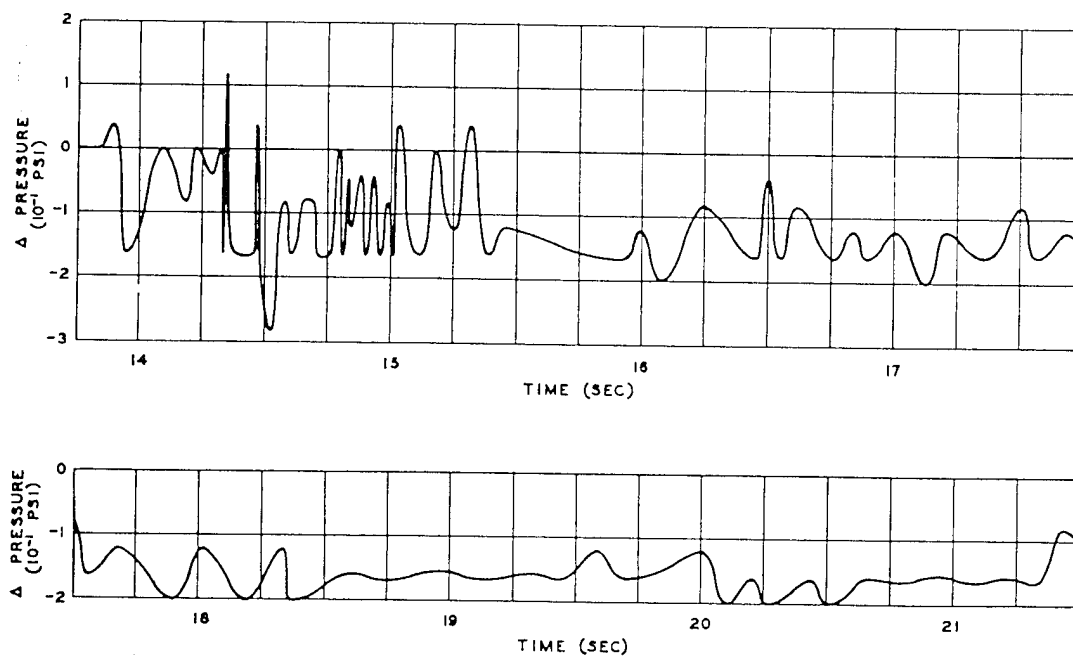


Fig. 5.32 Differential Pressure, 20% Chord, Right Wing Station 25.5, Channel 18, QB-17 M, Dog Shot

~~SECRET~~

SECRET

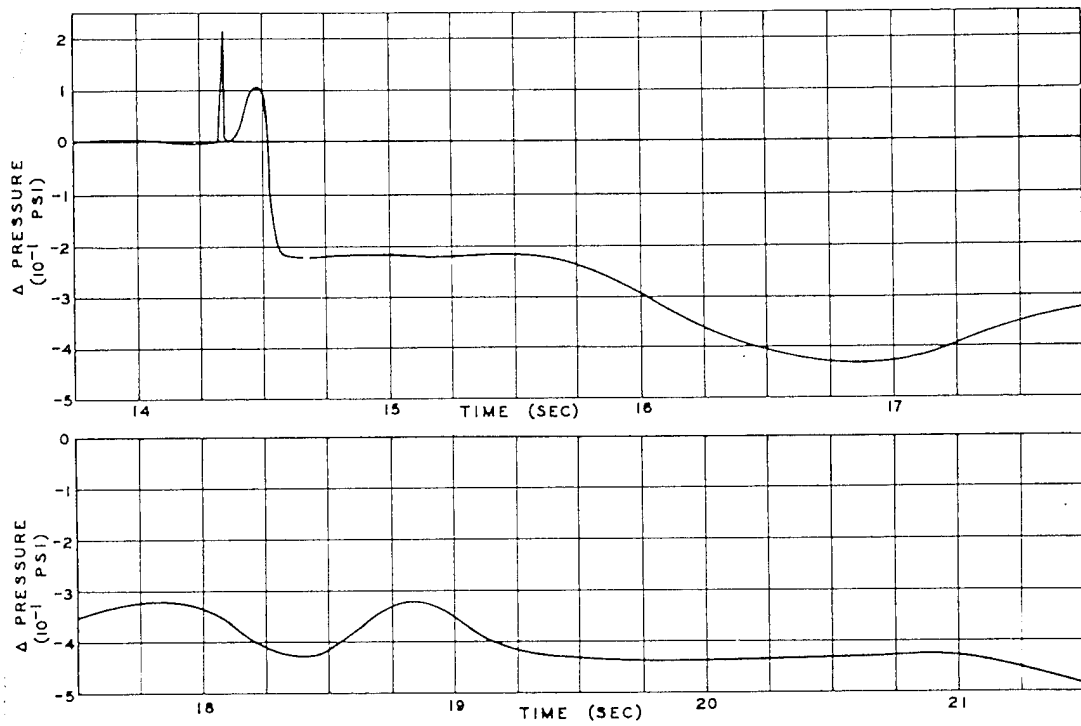


Fig. 5.33 Differential Pressure, 40% Chord, Right Wing Station 25.5, Channel 19, QB-17 M, Dog Shot

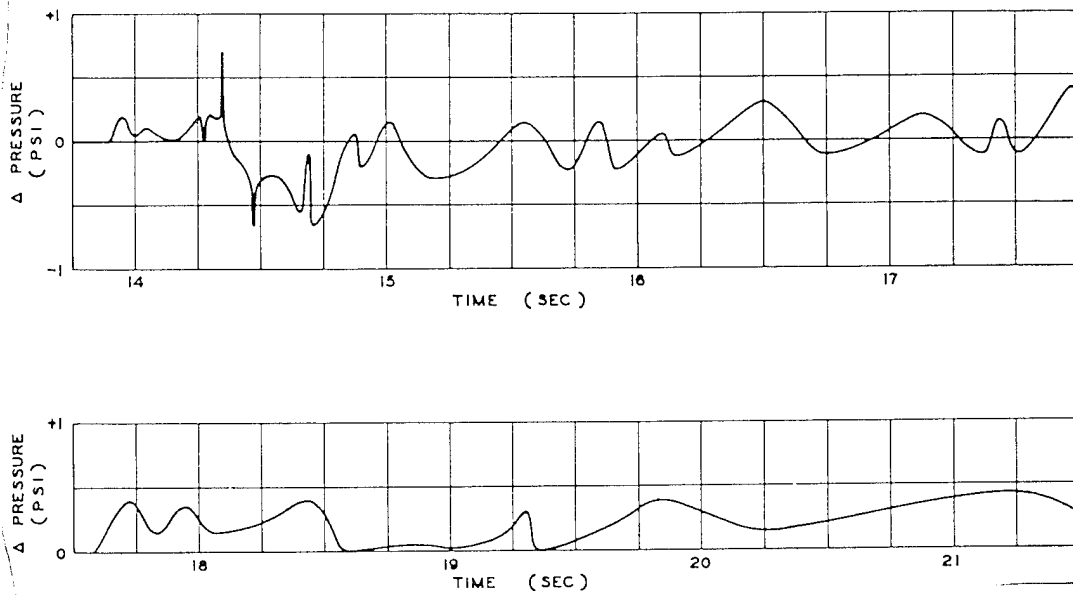


Fig. 5.34 Differential Pressure, 40% Chord, Right Wing Station 8.8, Channel 22, QB-17 M, Dog Shot

SECRET

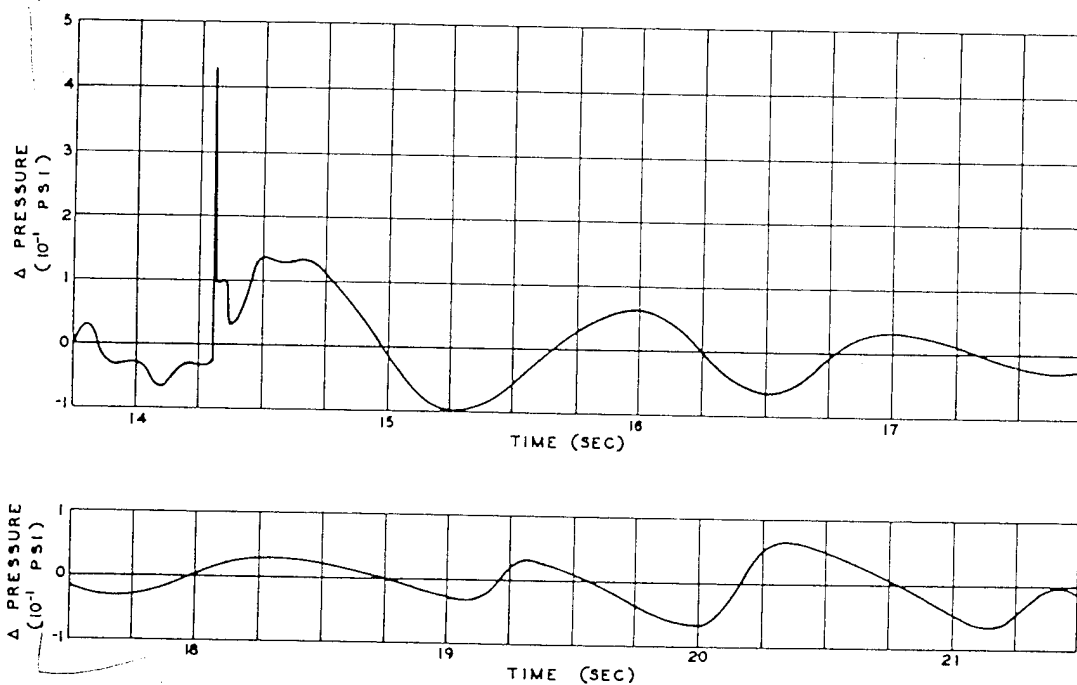


Fig. 5.35 Differential Pressure, 40% Chord, Right Horizontal Stabilizer, Channel 24, QB-17 M, Dog Shot

condition to which the incremental (Δ) loads are referred is arbitrarily chosen as that existing at $T_0 + 14$ sec. Because of the long-period oscillation, this does not represent level flight. However, if the loads due to the oscillations are recognized, the shock loads are identifiable. The continued maneuvering of the airplane makes the selection of a good, stable, level-flight attitude as zero condition impossible.

5.4.5 Heat Data

The temperatures as measured on drone M during its mission on Dog shot are given in Table 5.2.

5.4.6 Analysis

The location of the drone at the time the shock struck, as described in Sec. 5.4.3, was identified for the measured time for shock travel, $T_0 + 14.3$ sec. The theoretical values of peak overpressure and gust velocity for this point in space are 0.99 psi and 74 ft/sec. Theoretically the shock wave should have arrived at this location in 13.1 sec.

A comparison of the loads imposed by the long-period oscillations is given in Table 5.3. The first point in time ($T_0 + 3$ sec) represents the response to the instability caused by the loss of surfaces. As indicated in Table 5.3, the elevator and stabilizer responded quickly to the loss of the lower surface of the elevator. Because of the aft c.g., the drone was flying with an up tail load (positive stabilizer bending) with the elevator deflected down from the streamline position. When the heat struck the airplane it destroyed a part of the lift of the tail, which caused the tail to drop, increased the angle of attack of the wing, and increased the bending loads. In order to reestablish the lift on the tail it was necessary that the elevator be deflected almost to the full-down position, and the auto-pilot overcontrolled in attempting to regain equilibrium. This overcontrol apparently caused the long-period oscillation. Because the conditions were so unorthodox, it is really surprising that the auto-pilot was able to cope with the circumstances at all.

The oscillation continues through the period of passage of the shock wave, so that a part of the deflections shown in Figs. 5.22 through

5.34 may be attributable to this oscillation rather than to the shock.

The third time period ($T_0 + 35$ sec) represents the recovery from the stall that apparently occurred on the second positive peak of the oscillation. During this stall and the recovery, the airspeed dropped to about 72 knots and then rose to about 150 knots. Apparently, the drone lost about 1,300 ft during the recovery, most of which was regained by means of the automatic altitude control before the mother resumed its position. The oscillations continue throughout the record (about 3 min), but none are so violent as those described.

One aspect of the control of the drone is of interest and is confirmed by the report of the controlling pilots. Because of the large down-deflection of the elevator, the normal relation between throttle position and rate of climb was reversed. Normally, an increase in throttle setting (increased power) will cause increased lift on the wings and an increase in the rate of climb. However, in this instance the stabilizer was operating so near to a stall condition that it was very responsive to changes in power; a reduction in power (reduced air flow over the stabilizer) caused a greater relative reduction in stabilizer lift than in wing lift, and the tail dropped, thus increasing the angle of attack. This could have been disastrous except for the excellent performance of the controlling pilots.

The fact that the elevator went to the full-down position and was still not sufficient to keep the nose down so as to prevent the stall probably accounts for the controller's comment concerning the loss of elevator control. However, as previously deduced, the loss of control stems from the long-period oscillations which started at T_0 and not from the effect of the shock, as is intimated by the pilot's report.

5.5 DORIS POSITION, QB-17 DRONE N

QB-17 drone N made a satisfactory take-off, but the director lost turn control after the drone had been air-borne for about 4 hr. The mission was aborted, and the drone was orbited south of Eniwetok until daylight and then landed. No opportunity for substitution was available, so that Doris position was not occupied on Dog shot.

SECRET

TABLE 5.2 HEAT MEASUREMENTS AT CAROL POSITION,
DOG SHOT

Tape Location*	Material Thickness (in.)	Color†		Angle of Incidence	Max. Temp.‡ (°F)	Δ Temp. (°F)
		In	Out			
1	0.25§	P	P	83° 38'	130	89
2	0.032¶	LOG	Y	27° 48'	180	139
3	0.020¶	LOG	A	21° 39'	190	149
4	0.032¶	DOG	Y	29° 03'	150	109
5	0.032¶	A _d	A _s	23° 58'	230	189
6	0.020¶	LOG	AP	27° 48'	240	199
7	0.25§	P	P	88° 34'	130	89
8	0.032¶	DOG	BL	88° 34'	130	89

*See Table 3.9.

†See Table 3.11.

‡Ambient temperature, 41°F.

§Plexiglas.

¶Aluminum sheet.

TABLE 5.3 COMPARISON OF LOADS ON QB-17 DRONE M, DOG SHOT

	T ₀ + 3 sec	T ₀ + 16 sec	T ₀ + 35 sec
Bending, right wing root (channel 8), in.-lb	+2.8 × 10 ⁶	-0.94 × 10 ⁶	+4.23 × 10 ⁶
Bending, left wing root (channel 7), in.-lb	+2.1 × 10 ⁶	-0.68 × 10 ⁶	+3.1 × 10 ⁶
Bending, mid-span, right wing (channel 14), in.-lb	+2.8 × 10 ⁶	-0.73 × 10 ⁶	+4.2 × 10 ⁶
Bending, outer panel, right wing (channel 10), in.-lb	+1.8 × 10 ⁶	-0.34 × 10 ⁶	+1.5 × 10 ⁶
Elevator position (channel 15), degrees	8*	2.7	7.5†
Bending, right stabilizer (channel 9), in.-lb	+2.5 × 10 ⁴ *	+2.5 × 10 ⁴	+14.2 × 10 ⁴ †

*At T₀ + 0.7 sec (when the recorder started) the elevator was in the full-down position, and the stabilizer bending was -1.6 × 10⁴ in.-lb.

†The elevator was oscillating through a double amplitude of about 4°, and the stabilizer bending was varying from 0 to the maximum value of +14.2 × 10⁴ in.-lb.

SECRET

~~SECRET~~

5.6 ELAINE POSITION, XB-47 AIRPLANE, NO. 46-066

Assigned location (at shock)

True altitude, 24,800 ft

Horizontal distance, 24,800 ft beyond point
zero

Predicted conditions

Peak overpressure, 0.30 psi

Peak gust velocity, 38 ft/sec (in direction
of shock)

Time of travel (shock), 28.0 sec

5.6.1 Flight Log

The XB-47 took off from Kwajalein, flew to Eniwetok, and completed the mission satisfactorily. The flight data as reported¹ by ATU 3.4.2 are as follows:

Time

Take-off, 0349

At assigned altitude, 0412

Shock arrival, 0634:38.6

Landing, 0729

Meteorological conditions at altitude

True altitude, 25,150 ft

Pressure altitude, 23,300 ft

Outside air temperature, -12°C

Wind direction (from), 335° (azimuth)

Wind velocity, 26 knots

Airplane parameters at shock arrival

Indicated airspeed, 278 knots

Ground speed, 673 ft/sec

Ground track azimuth, 151°

Horizontal angle from blast, 150° (azimuth)

Vertical angle from blast,* 35.5° (elevation)

Horizontal distance from blast, 35,290 ft

Slant distance from blast,* 43,330 ft

Shock struck airplane from rear and below

5.6.2 Airplane Condition

Before take-off the two recorders were checked, and all channels were working except for two as follows:

Channel B4—pressure, right wing station
515, 61.3 per cent chord (defec-
tive transmitter)

*Computed from data in Navigator's Report, refer-
ence 1.

Channel B10—pressure, left wing station
515, 20 per cent chord (defec-
tive transmitter)

Since the amplifier in the recorder for chan-
nel A3 was defective and the sensing unit was
satisfactory, channel A3 was plugged into
amplifier A1, and channel A1 was plugged into
amplifier B10. It was necessary to switch
channel A1 because the cable length on channel
A3 was not sufficient to reach to the amplifier
for channel B10.

The take-off gross weight was computed to
have been 143,000 lb with the c.g. at 26 per
cent m.a.c. This weight included 7,680 gal
(52,200 lb) in the main tanks and 1,200 gal
(8,160 lb) in the bomb bay. The gross weight at
the time of shock was computed to have been
108,065 lb, with the c.g. at 18.0 per cent m.a.c.
This included 3,758 gal (25,550 lb) of fuel in
the main tanks. The pilot reported that in the
cockpit he felt intense heat which lasted
throughout the period of the glow. He contended
that the "... metal in the cockpit became al-
most too hot to touch." These observations of
heat are almost incredible. First, the cockpit
should have been shielded from the direct
radiant heat (through the plexiglas) by the
wings and fuselage since the blast was behind
and below the airplane. The only radiant heat
that should have been felt by the pilot was that
which had been reflected from atmospheric
particles, fog, etc., and this should not have
been intense. Second, the lower section of the
fuselage is constructed of two sheets separated
by a considerable airspace so that the inner
sheet should have been insulated, and the inci-
dence angle of the heat impinging on the sides
of the fuselage where the airspace is small
should have been great enough to prevent any
part of the fuselage from becoming too hot to
touch.

After the airplane landed, it was examined
and no damage was apparent.

5.6.3 Load Data

The data as recorded by the tape recorders
are presented in Figs. 5.36 through 5.55. All
the data from this mission are small in value,
and in approximately half the channels the data
were so low that noise obscured them. The
data from these channels are not reported. The
channels measuring chordwise bending and

~~SECRET~~

SECRET

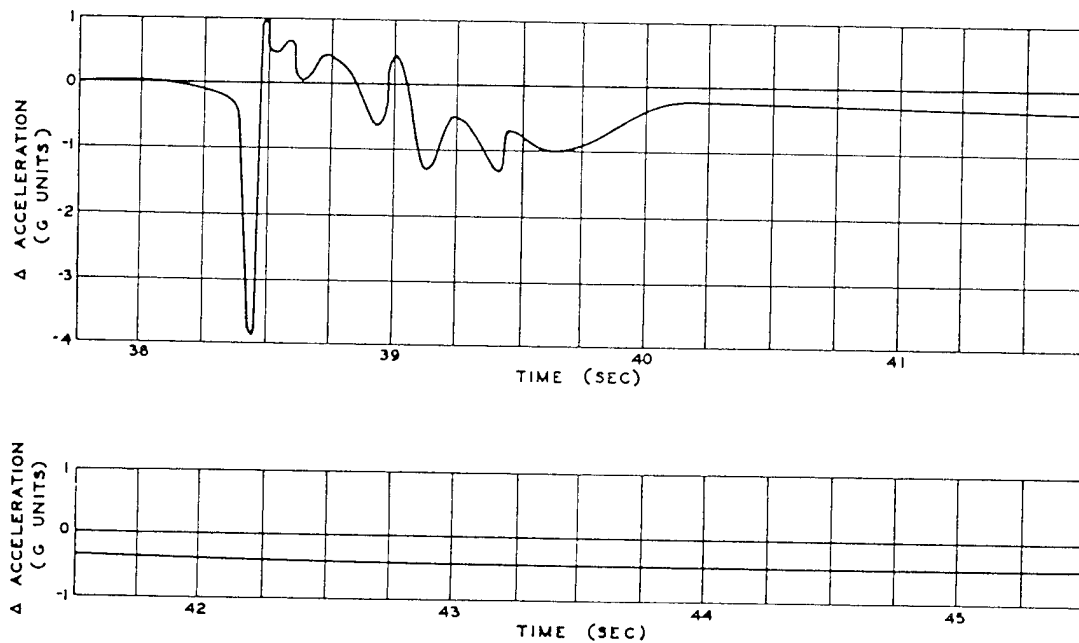


Fig. 5.36 Normal Acceleration, No. 3 Engine, Channel A3, XB-47, Dog Shot

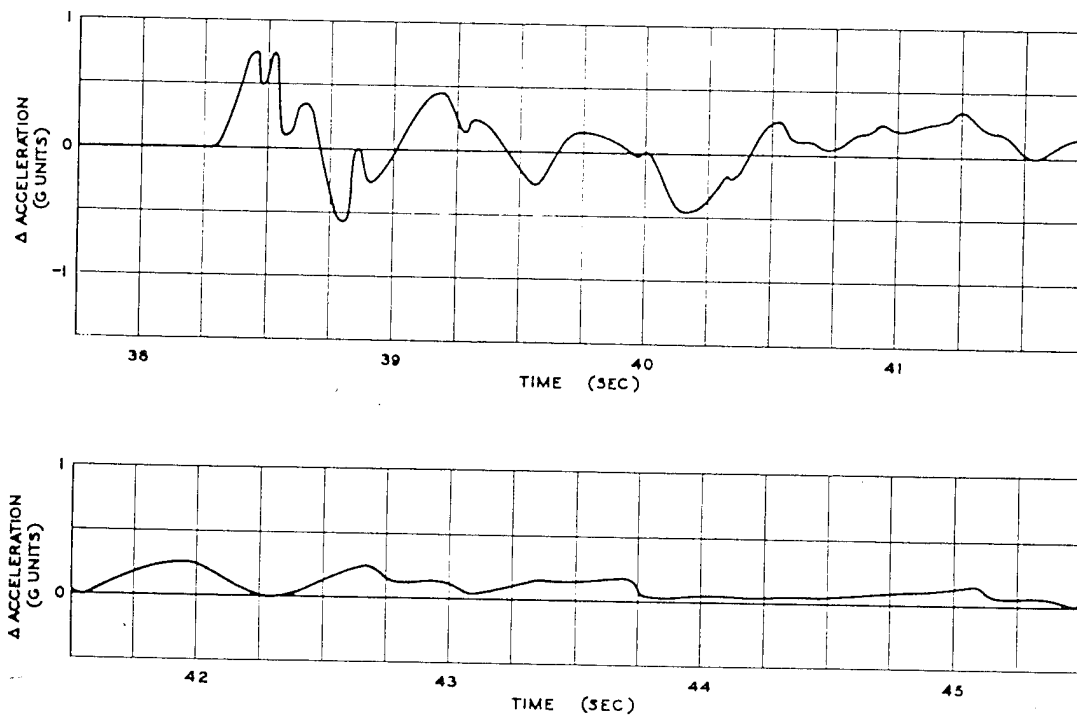


Fig. 5.37 Normal Acceleration, No. 1 Engine, Channel A4, XB-47, Dog Shot

SECRET

SECRET

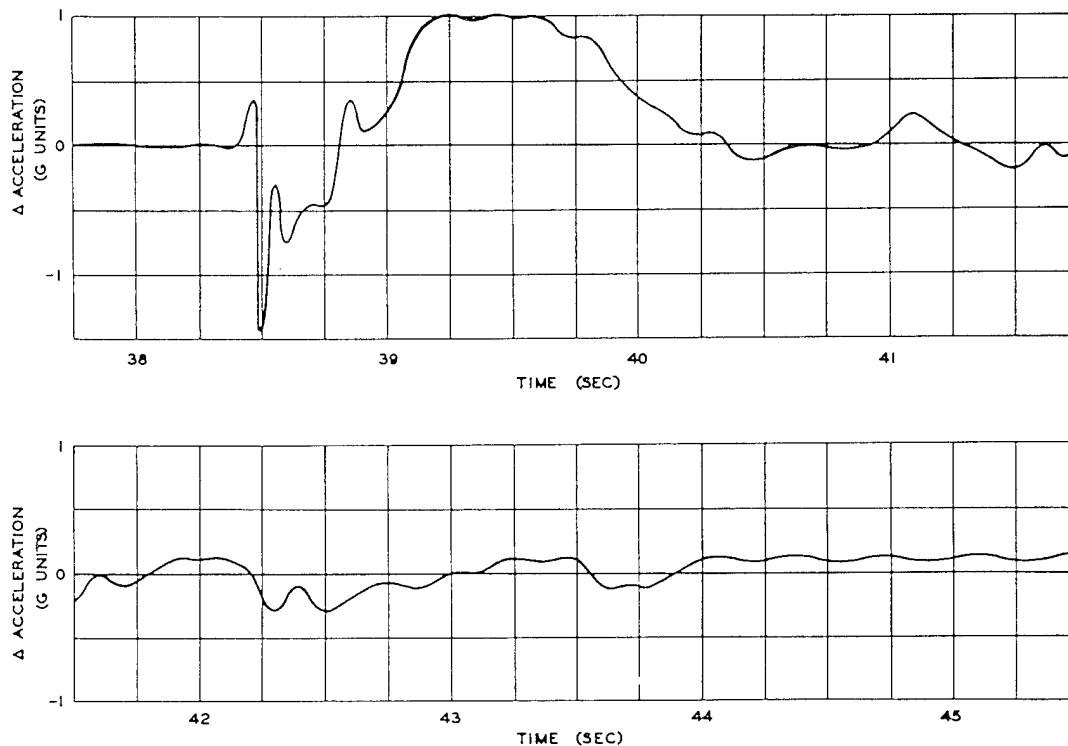


Fig. 5.38 Normal Acceleration, Bomb Bay, Forward, Channel A6, XB-47, Dog Shot

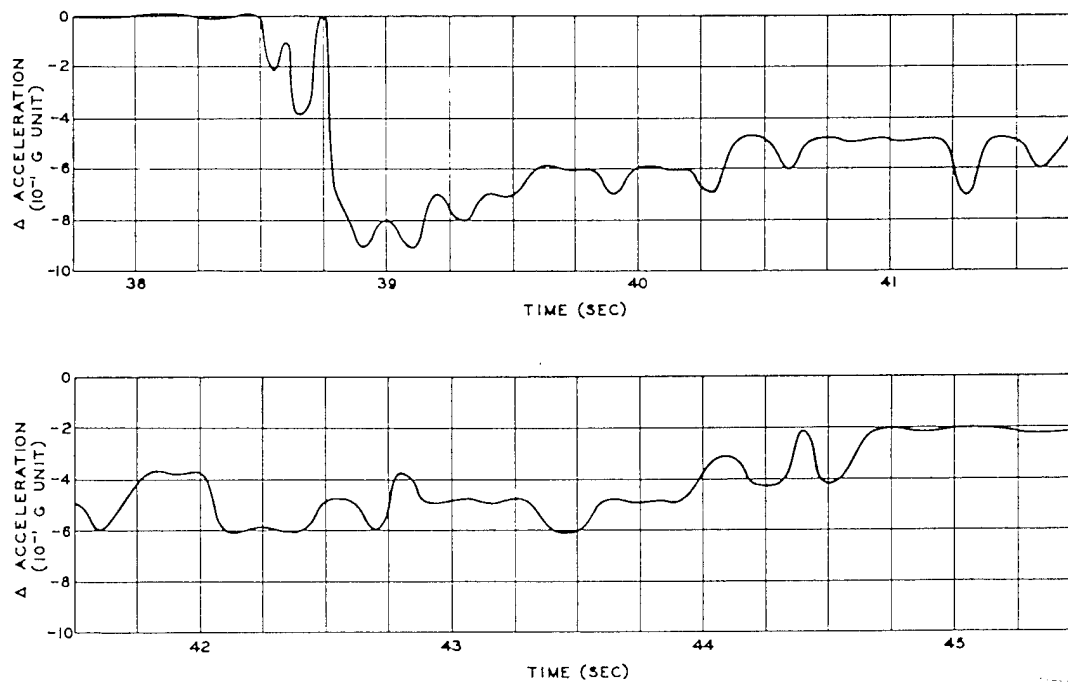


Fig. 5.39 Normal Acceleration, c.g., Channel A7, XB-47, Dog Shot

~~SECRET~~

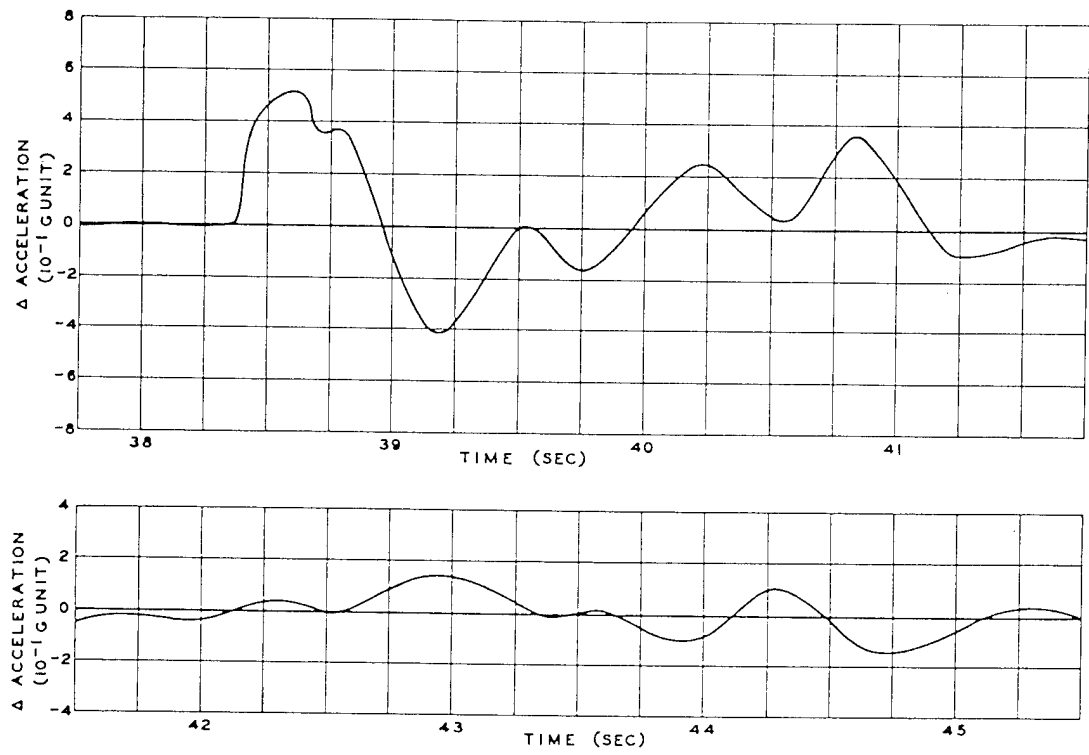


Fig. 5.40 Normal Acceleration, Aft Fuselage at Horizontal Stabilizer, Channel A8, XB-47, Dog Shot

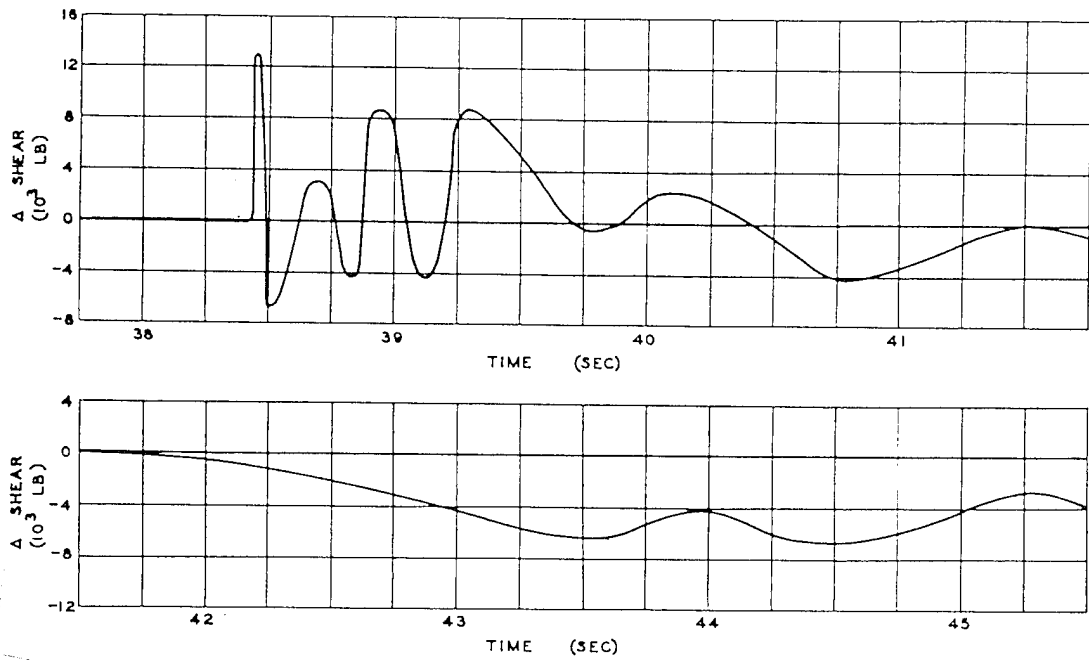


Fig. 5.41 Wing Shear, Right Wing Root, Wing Station 307, Channel A12, XB-47, Dog Shot

~~SECRET~~

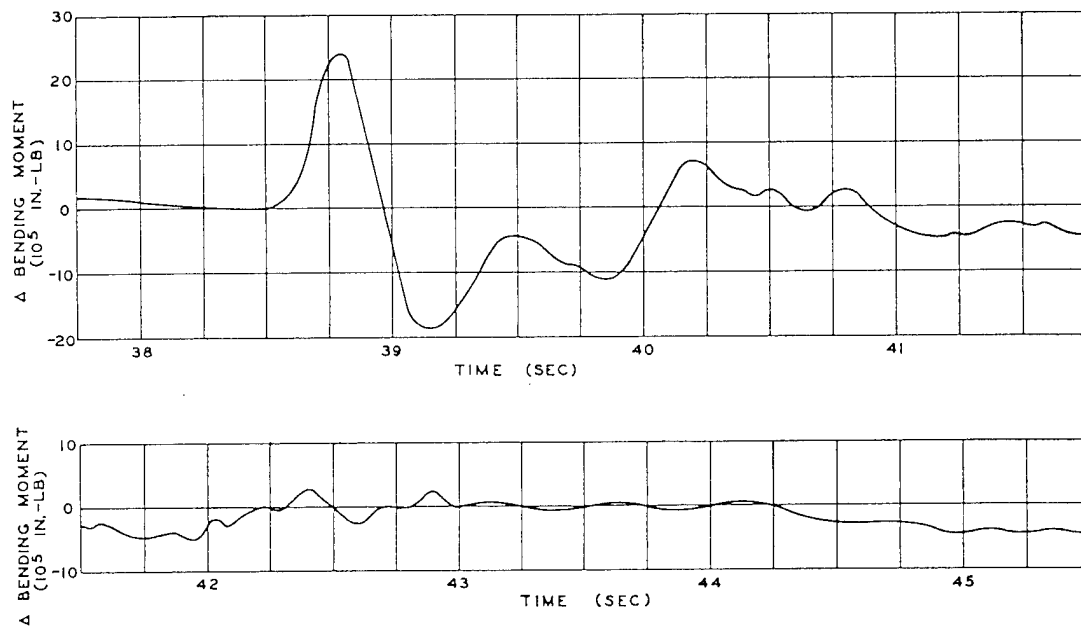


Fig. 5.42 Wing Bending, Right Wing Root, Wing Station 307, Channel A13, XB-47, Dog Shot

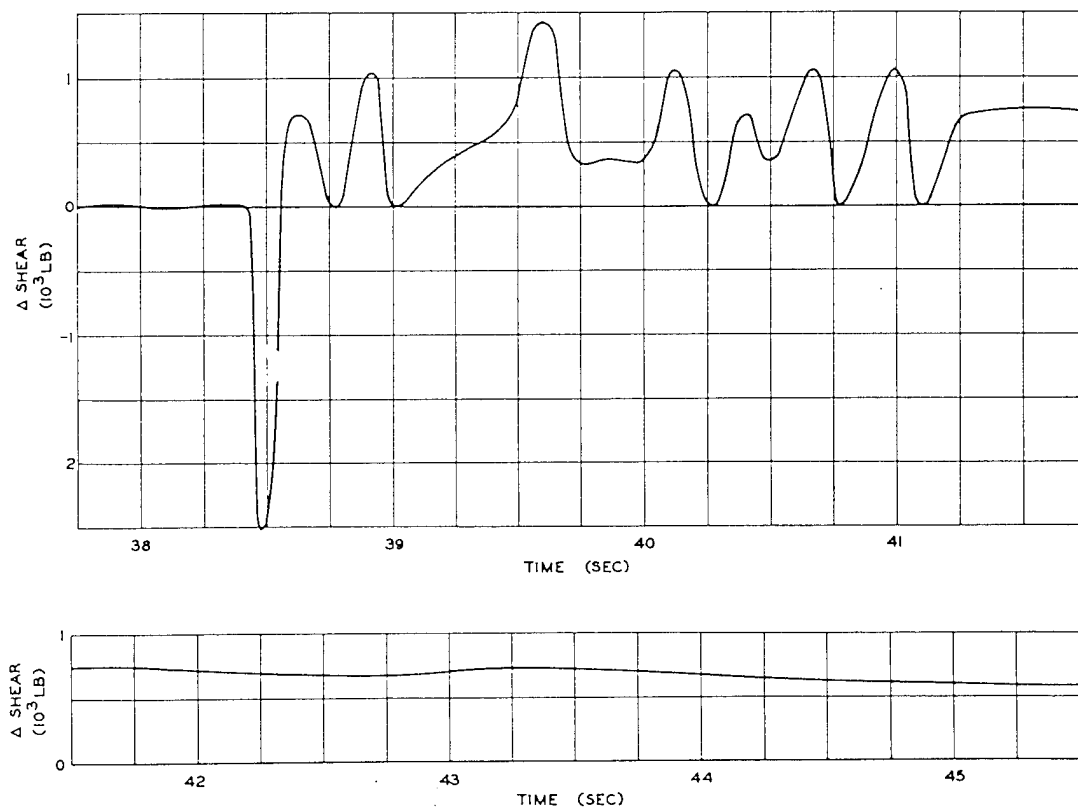


Fig. 5.43 Wing Shear, Left Wing Root, Wing Station 307, Channel A16, XB-47, Dog Shot

SECRET

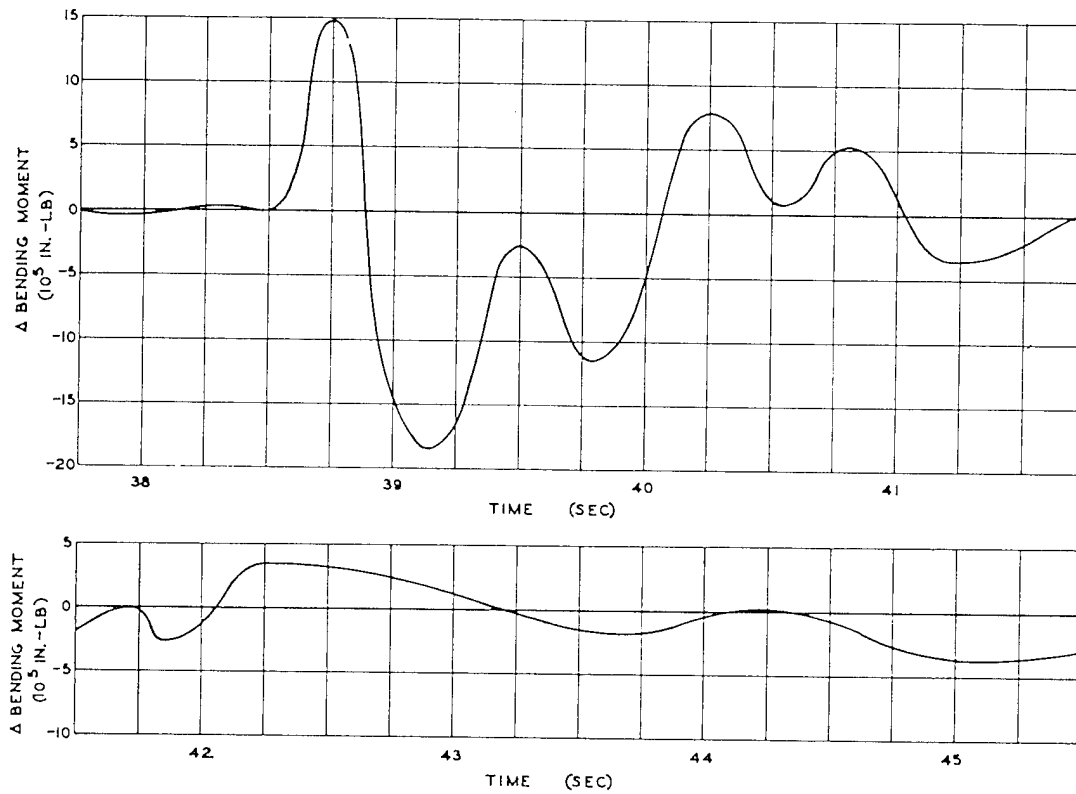


Fig. 5.44 Wing Bending, Left Wing Root, Wing Station 307, Channel A17, XB-47, Dog Shot

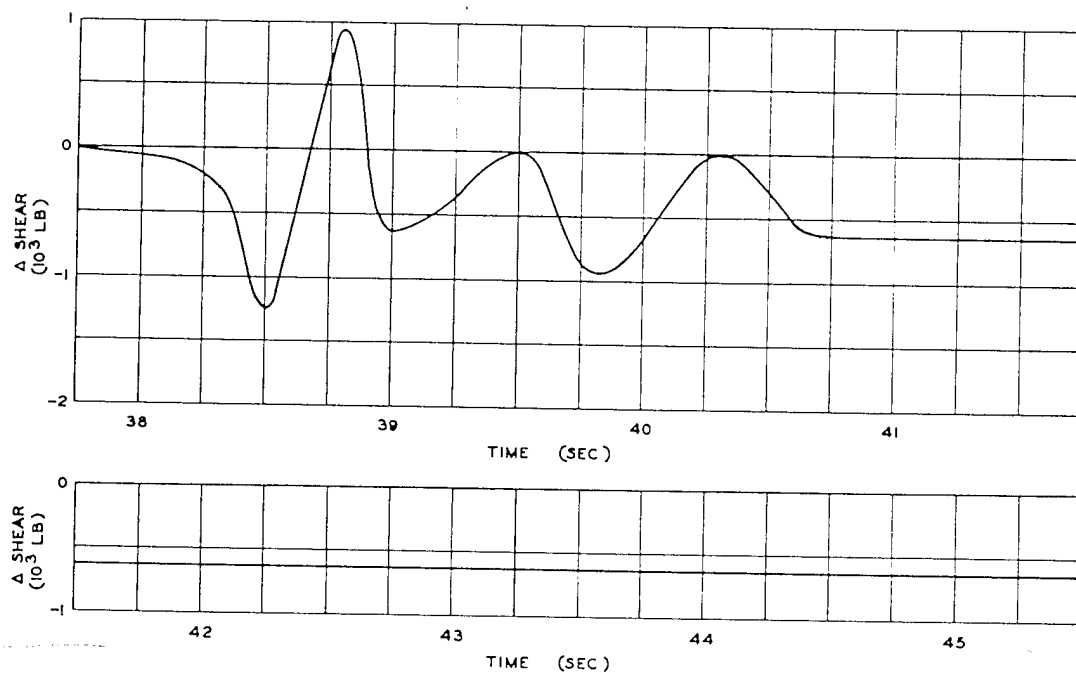


Fig. 5.45 Wing Shear, Left Wing Outboard, Wing Station 660, Channel A21, XB-47, Dog Shot

SECRET

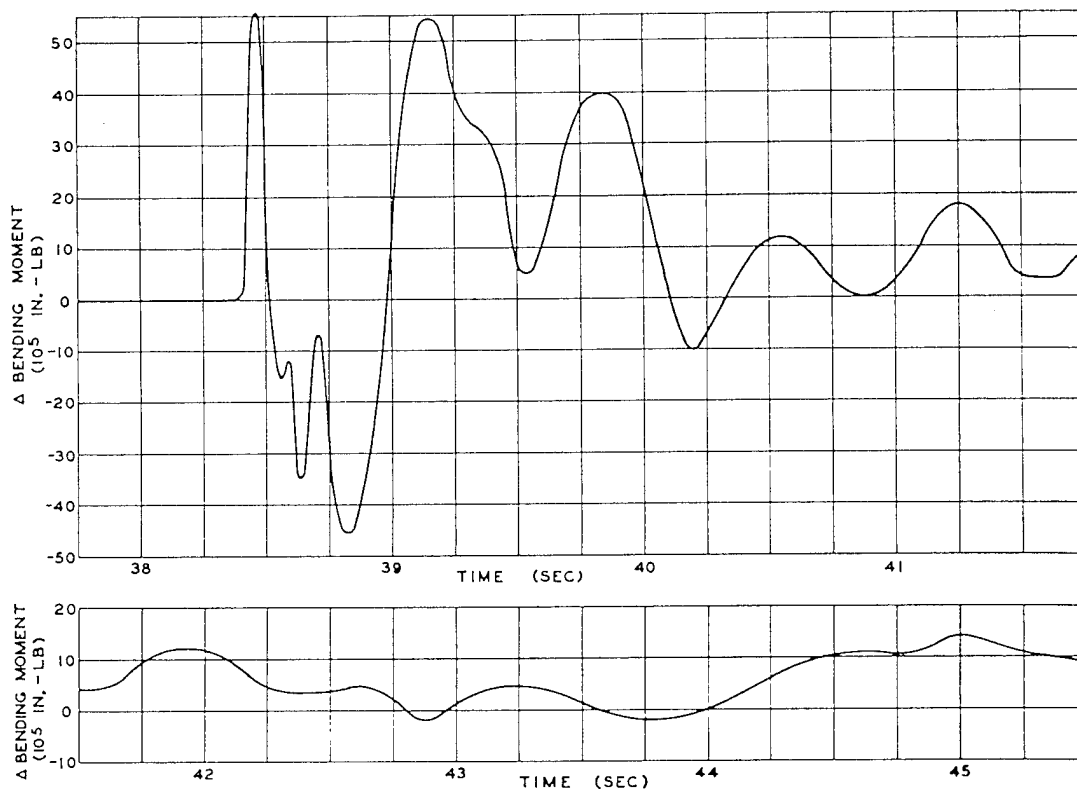


Fig. 5.46 Fuselage Bending, Aft End of Bomb Bay, Fuselage Station 718, Channel A24, XB-47, Dog Shot

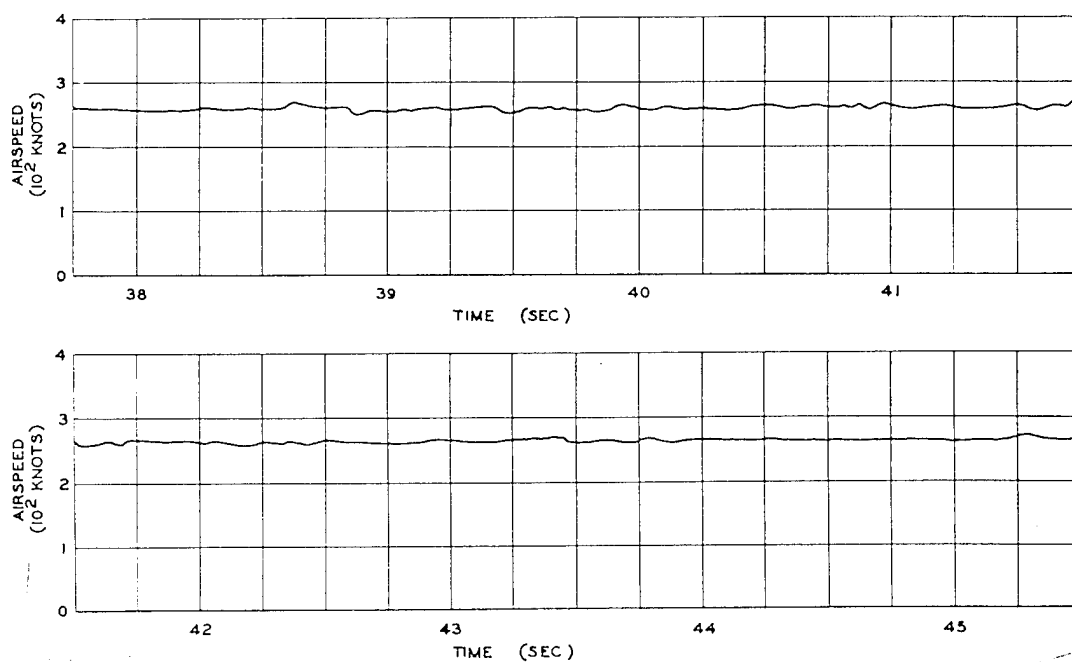


Fig. 5.47 Airspeed, Channel B2, XB-47, Dog Shot

~~SECRET~~

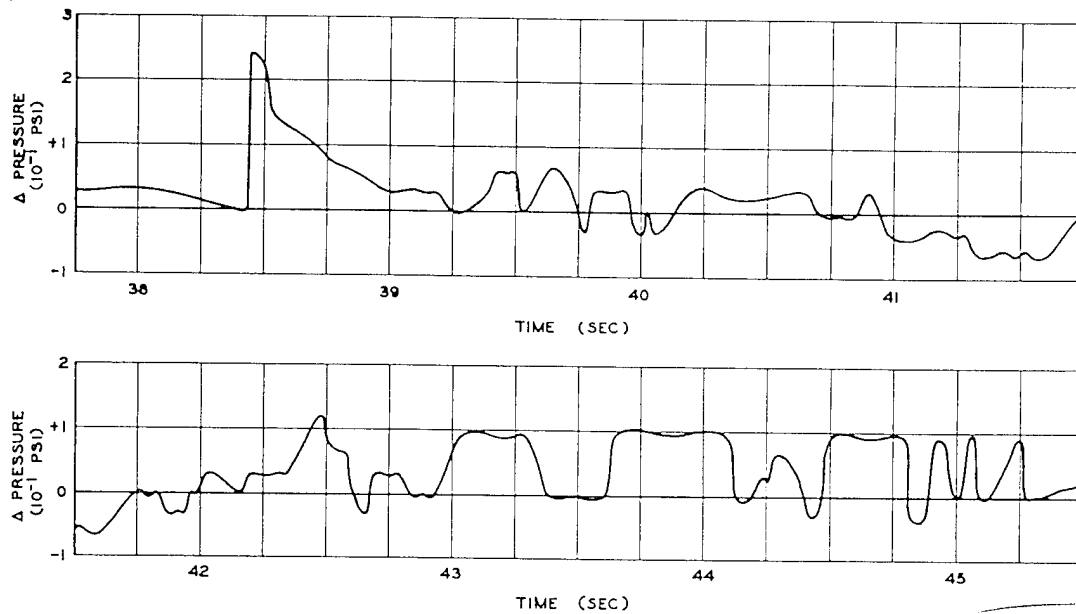


Fig. 5.48 Gauge Aerodynamic Pressure, Left-hand Side of Vertical Fin, Channel B6, XB-47, Dog Shot

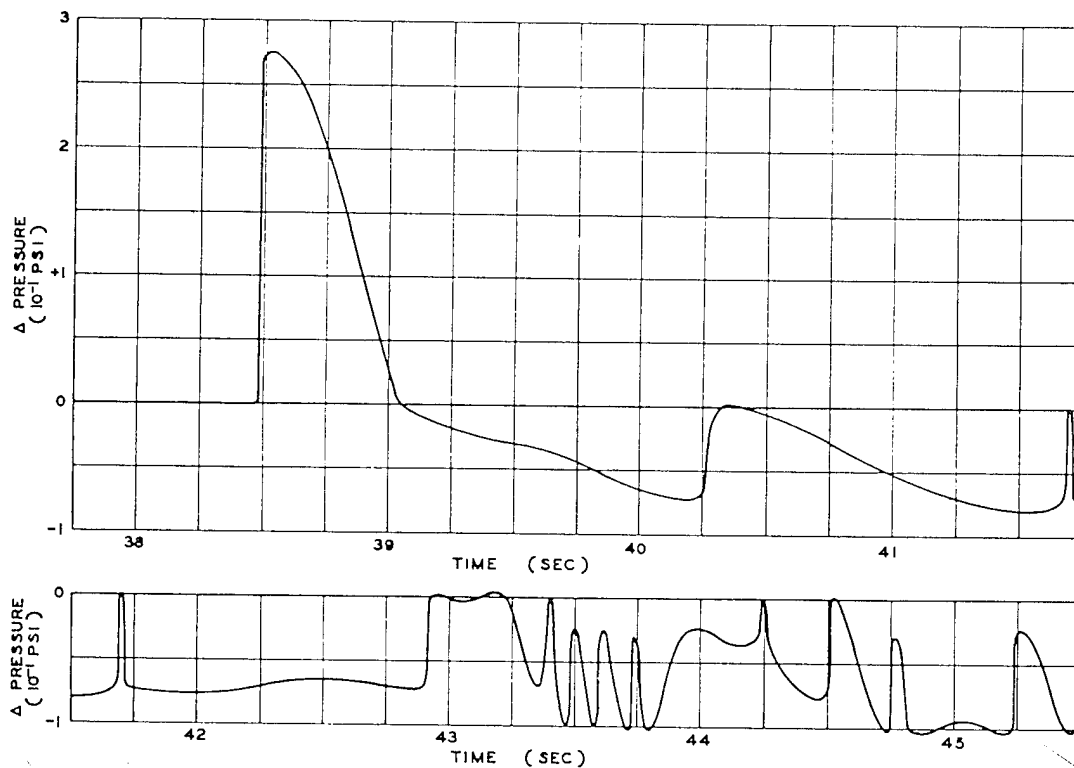


Fig. 5.49 Gauge Aerodynamic Pressure, 5% Chord, Bottom Left Wing Station 515, Channel B7, XB-47, Dog Shot

~~SECRET~~

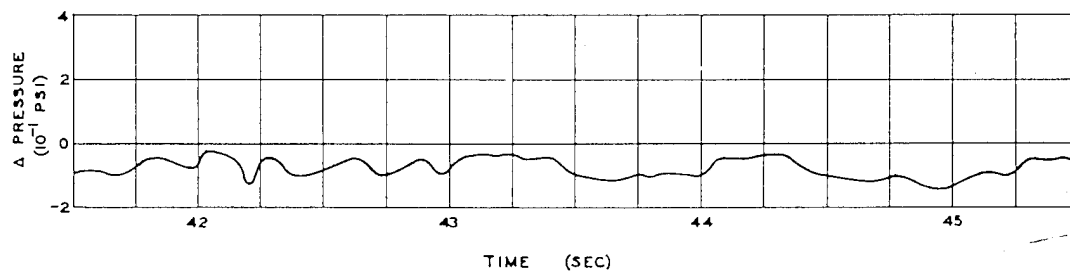
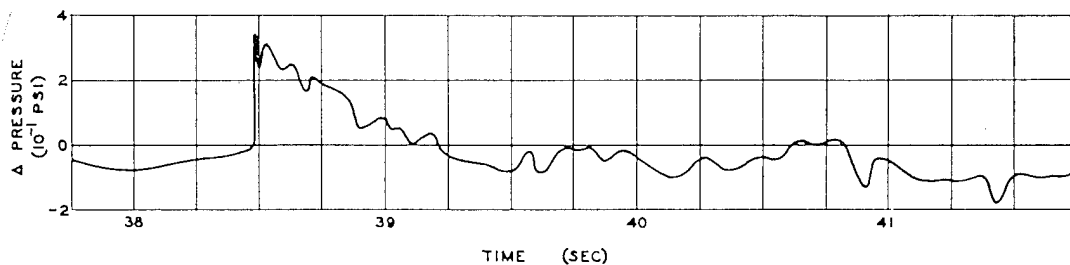


Fig. 5.50 Gauge Aerodynamic Pressure, 11.7% Chord, Bottom Left Wing Station 515, Channel B9, XB-47, Dog Shot

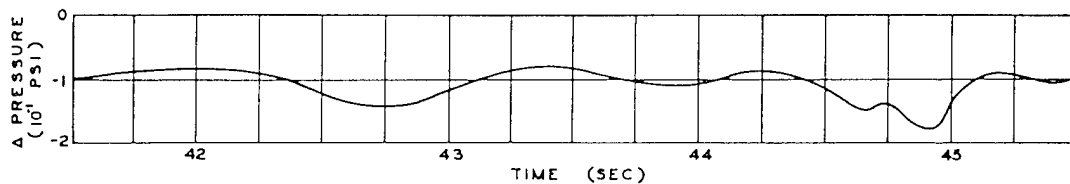
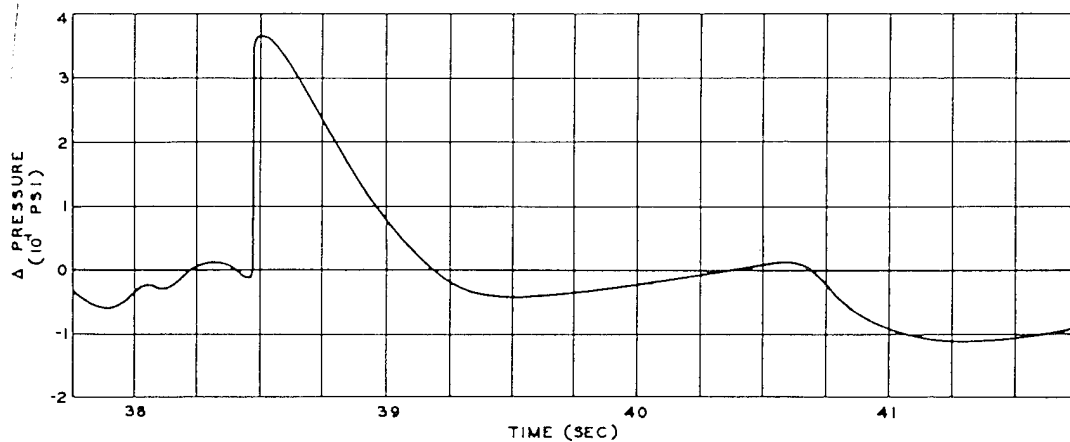


Fig. 5.51 Gauge Aerodynamic Pressure, 20% Chord, Bottom Left Wing Station 515, Channel B11, XB-47, Dog Shot

~~SECRET~~

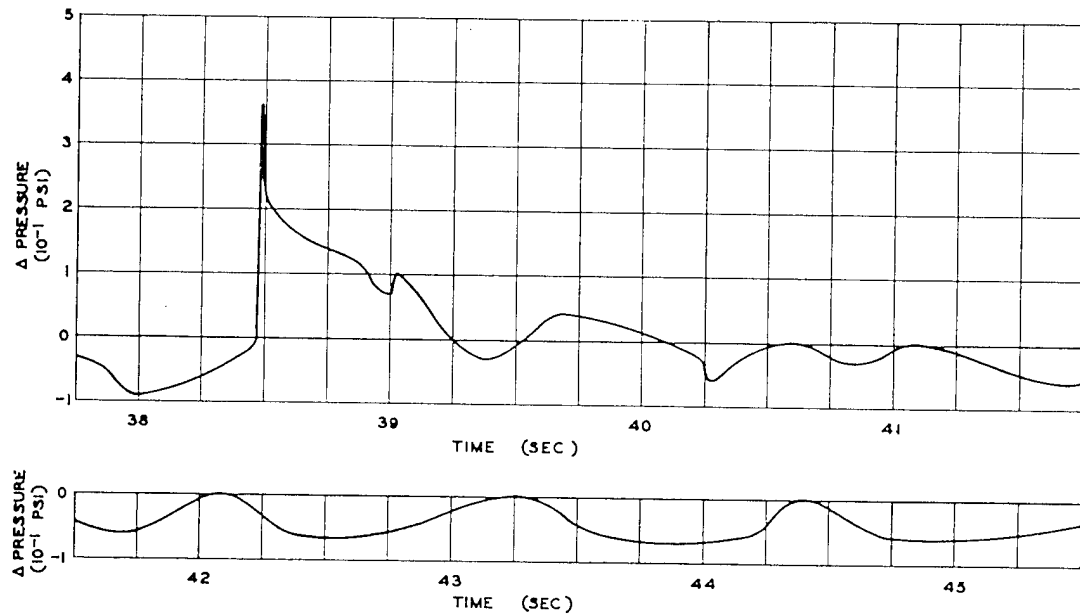


Fig. 5.52 Gauge Aerodynamic Pressure, 40% Chord, Bottom Left Wing Station 515, Channel B15, XB-47, Dog Shot

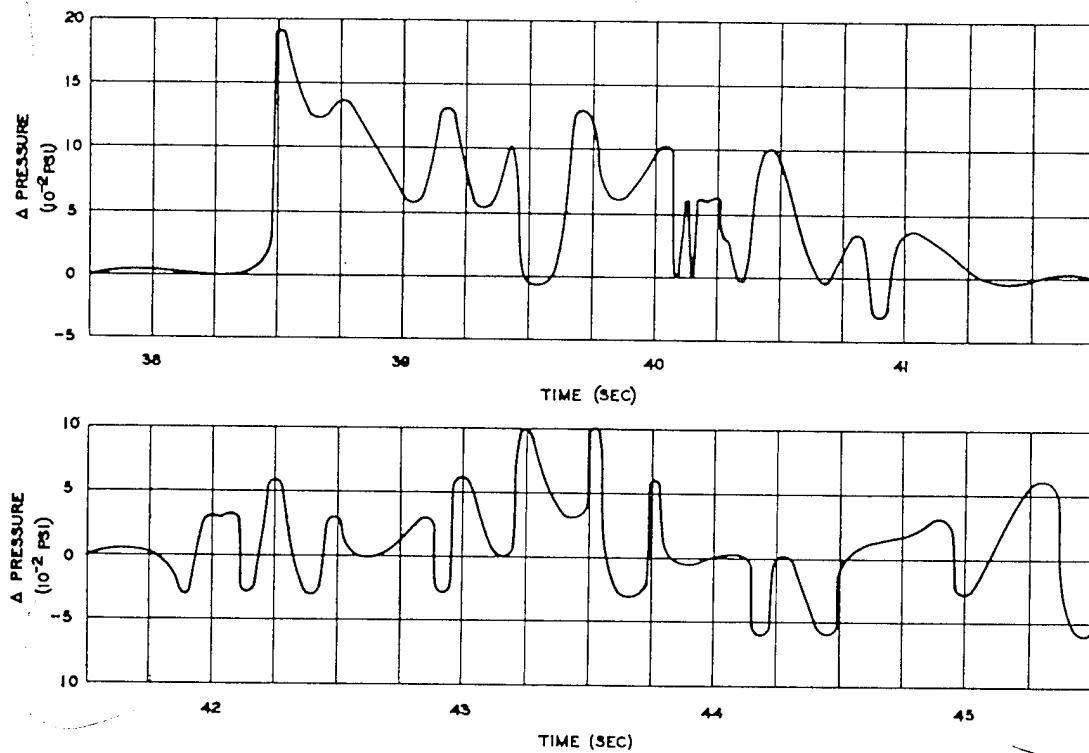


Fig. 5.53 Gauge Aerodynamic Pressure, 61.3% Chord, Top Left Wing Station 515, Channel B16, XB-47, Dog Shot

~~SECRET~~

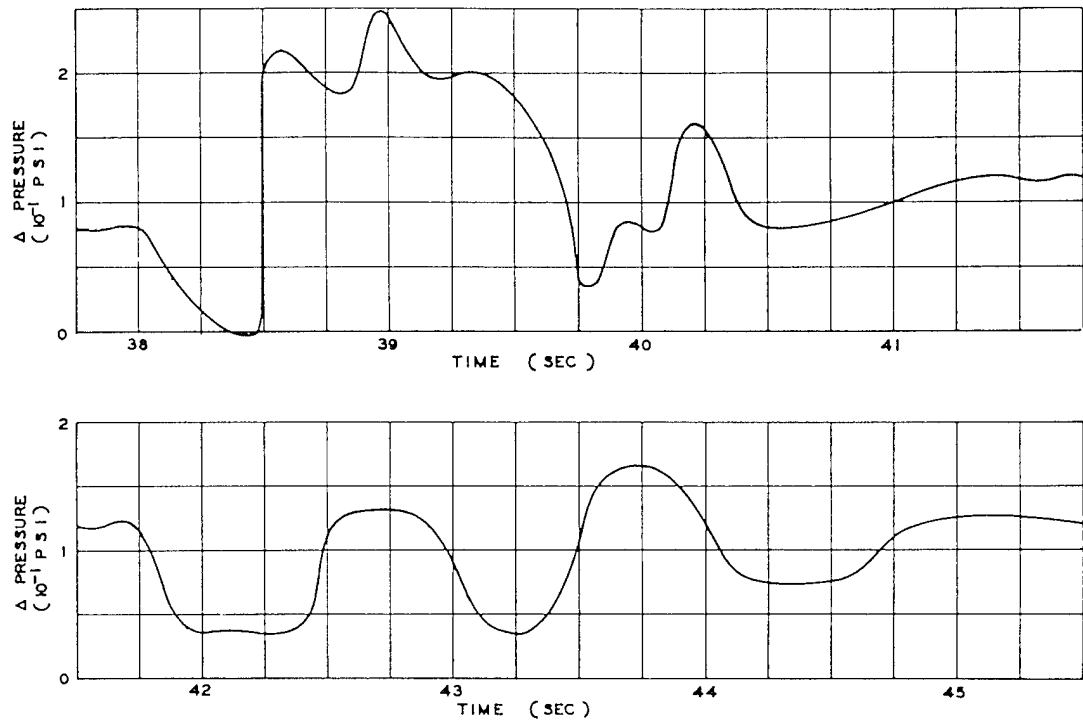


Fig. 5.54 Gauge Aerodynamic Pressure, Left-hand Side of Fuselage Aft of Bomb Bay, Channel B19, XB-47, Dog Shot

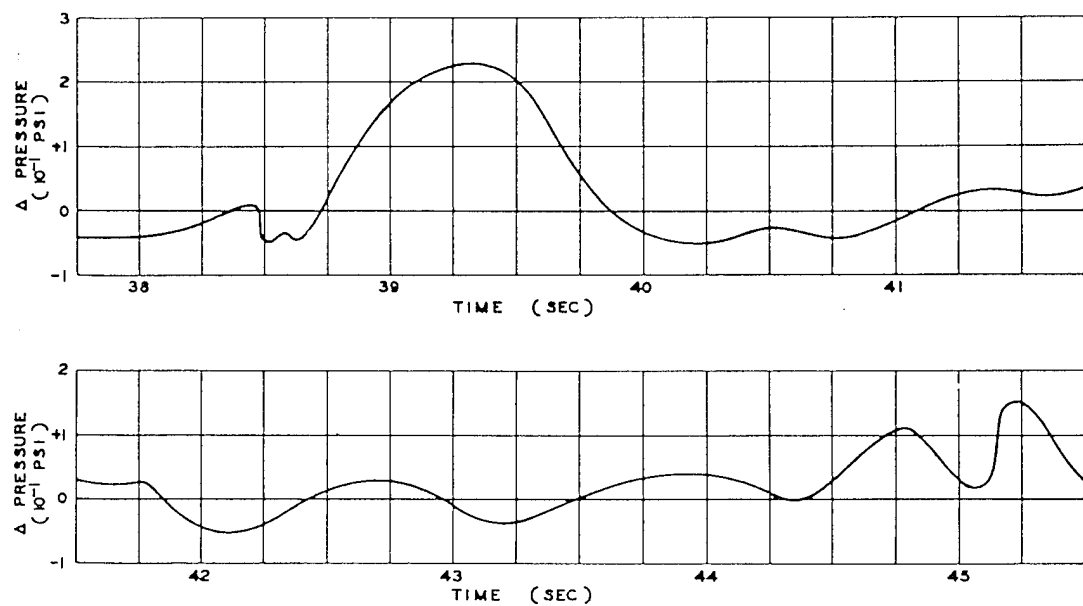


Fig. 5.55 Gauge Aerodynamic Pressure, 5% Chord, Top Left Wing Station 523, Channel B24, XB-47, Dog Shot

~~SECRET~~

outer panel bending in the wings measured data which are readable, but the calibration data are not satisfactory. Figure 5.39, c.g. acceleration, may be inaccurate because the noise level was almost as great as the trace deflections.

Figure 5.46, bending in the fuselage, may be inaccurate, especially in the large deflection, because it was necessary to extrapolate the calibration curve. The calibration of the fuselage-bending gauges was discontinued because of wrinkling and the possibility of permanent deformation of the fuselage.

5.6.4 Analysis

The theoretical conditions for the point in space at which the navigator reported that the shock struck the airplane are 0.24 psi peak overpressure, 30.8 ft/sec peak gust velocity, and 35.7 sec shock travel time. The actual time required for travel of the shock wave as measured by the tape recorder was 38.5 sec.

The pilot reported that shortly after the shock struck the airplane he made a turn to the left so that his crew could see the cloud and in order to set a course for Kwajalein. He described this turn as "a rather uncoordinated maneuver (because of his interest in the view) of no more than usual violence." However, the pressures, in particular, are at least as high in the turn as during the shock and in some instances higher. The accelerations are quite similar for both situations, and the strain-gauge measurements are, in general, higher in the shock.

Figure 5.56 summarizes the incremental pressures around left wing station 515 through the period of the shock. Figure 5.57 indicates the pitching accelerations of the airplane as derived from the three measured normal accelerations. The fact that the pitching accelerations are constantly positive is probably due to the errors in channel 6 (see Sec. 5.6.3).

5.7 FRANCES POSITION, B-50D AIRPLANE, NO. 49-340

Assigned location (at shock)

True altitude, 29,000 ft

Horizontal distance, 29,000 ft going toward point zero

Predicted conditions

Peak overpressure, 0.23 psi

Peak gust velocity, 34 ft/sec (in direction of shock)

Time of travel (shock), 33.8 sec

5.7.1 Flight Log

B-50D No. 340 took off on schedule and completed its mission satisfactorily. The flight data as reported¹ by ATU 3.4.2 are as follows:

Time

Take-off, 0315

At assigned altitude, 0355

Shock arrival, 0634:34.1

Landing, 0953

Meteorological conditions at altitude

True altitude, 29,000 ft

Pressure altitude, 27,800 ft

Outside air temperature, -21°C

Wind direction (from), 296° (azimuth)

Wind velocity, 26 knots

Airplane parameters at shock arrival

Indicated airspeed, 162 knots

Ground speed, 399 ft/sec

Ground track azimuth, 328°

Horizontal angle from blast, 150° (azimuth)

Vertical angle from blast, * 45.1° (elevation)

Horizontal distance from blast, 28,880 ft

Slant distance from blast, * 40,900 ft

Shock struck airplane from front and below

5.7.2 Airplane Condition

Before take-off the recording equipment was checked and balanced; it was found to be operating satisfactorily. However, during the mission, about 1 hr before H-hour, recorder B started smoking badly and was disconnected. No data were obtained from this recorder. The data from recorder A were complete except for channel 3, normal acceleration, No. 2 engine.

The gross weight at take-off was computed to have been 121,400 lb, with the c.g. at 23.7 per cent m.a.c. This condition included 1,050 gal (6,300 lb) in each of the four main wing tanks and 1,600 gal (9,600 lb) in the wing center-section tanks.

The pilot reported that the airplane was in straight-and-level flight at the time the shock

*Computed from data in Navigator's Report, reference 1.

~~SECRET~~

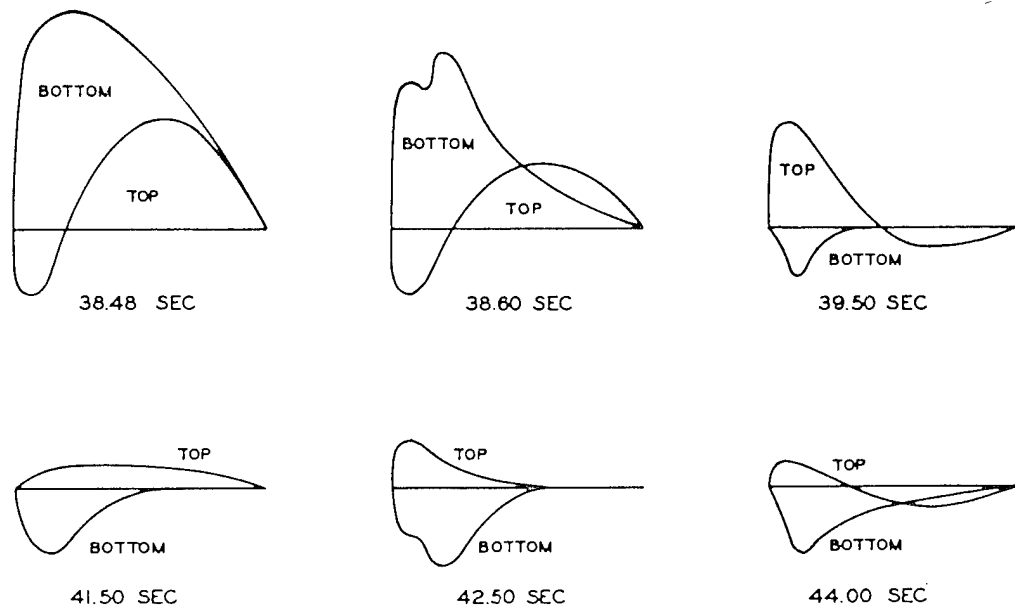


Fig. 5.56 Summary of Gauge Pressures at Left Wing Station 515, XB-47, Dog Shot

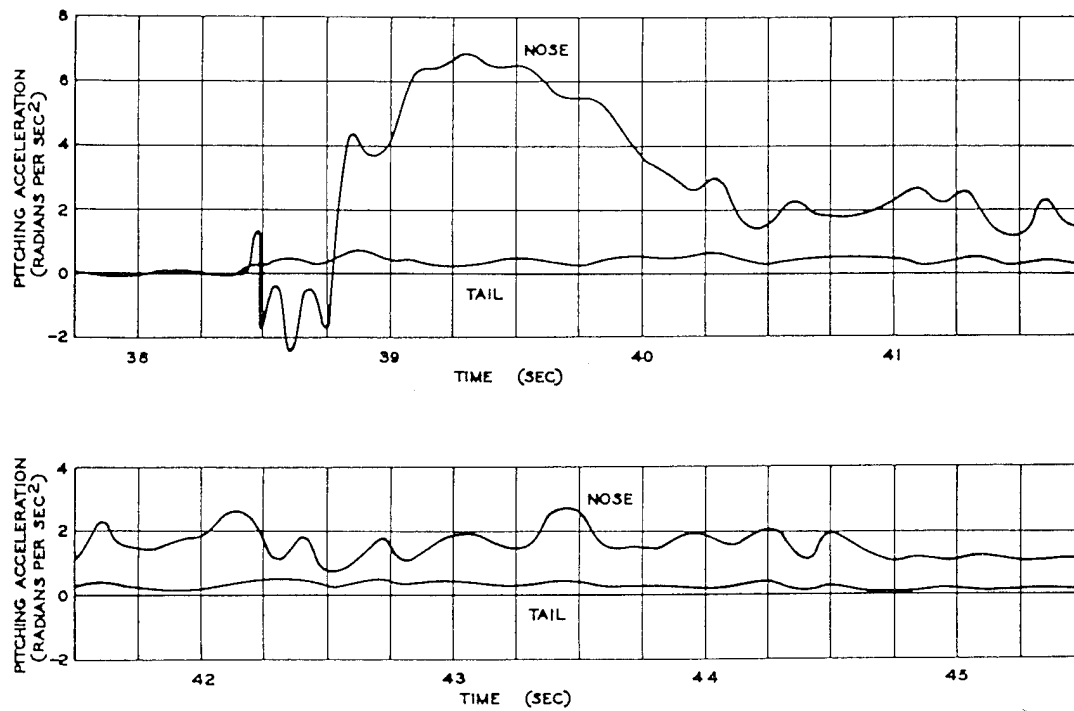


Fig. 5.57 Pitching Acceleration, XB-47, Dog Shot. Values determined from nose and c.g. accelerations (nose) and from tail and c.g. accelerations (tail).

SECRET

wave struck. The gross weight at this time was computed to have been 107,600 lb, with the c.g. at 23.0 per cent m.a.c. The fuel at this time consisted of 750 gal (4,500 lb) in each of the four main wing tanks and none in the center-section tanks.

The airplane performed a photographic mission after the test run. After the airplane landed, it was examined for damage. No damage was evident except for a very slight wrinkle along the edge of one of the bomb-bay doors, which looked as though the door had been tightly pressed against the frame. It was not definite whether this was the result of the test or of normal wear and tear, but it appeared that it might have been the result of overpressure.

5.7.3 Load Data

The data as recorded on the magnetic-tape recorder are presented in Figs. 5.58 through 5.74. The data from channels A4, A14, A15, and A24 are not presented because the low values of deflection were obscured by the level of noise on the channels. Data from channel A21 are not presented because this channel failed during calibration. It was discovered that the wiring in channels A8 and A9 was wrong, and consequently no data were obtained from these channels on Dog shot. The shear data in channels A16 and A17 are subject to question, especially in the higher values, because of the extrapolation that was necessary in the calibration curves.

5.7.4 Analysis

The navigator reported that his airplane was 120 ft short of Frances position when the shock struck. The theoretical conditions for his position are not significantly different from those predicted for Frances position. However, the measured time of shock arrival at the airplane was $T_0 + 34.7$ sec.

These data are not particularly unusual. The airplane returned to stabilized straight-and-level flight after the shock. There is indication that the pilot performed some sort of maneuver at about $T_0 + 50$ sec, but the loads from this maneuver are not significant and do not interfere with the shock data. No specific cross-graphs or comparisons of data are made. The

low magnitude of the measurements and the consequent expansion of the ordinates of the graphs make these data somewhat less reliable.

5.8 GRACE POSITION, B-50D AIRPLANE, NO. 49-290

Assigned location (at shock)

True altitude, 29,000 ft

Horizontal distance, 29,000 ft in direction perpendicular to the line of flight

Predicted conditions

Peak overpressure, 0.23 psi

Peak gust velocity, 34 ft/sec (in direction of shock)

Time of travel (shock), 33.8 sec

5.8.1 Flight Log

B-50D No. 290 took off on schedule and completed the mission without incident. The flight data as reported¹ by ATU 3.4.2 are as follows:

Time

Take-off, 0336

At assigned altitude, 0434

Shock arrival, 0634:36.0

Landing, 1000

Meteorological conditions at altitude

True altitude, 29,000 ft

Pressure altitude, 27,800 ft

Outside air temperature, -20°C

Wind direction (from), 314° (azimuth)

Wind velocity, 27 knots

Airplane parameters at shock arrival

Indicated airspeed, 162 knots

Ground speed, 439 ft/sec

Ground track azimuth, 239°

Horizontal angle from blast, 328° (azimuth)

Vertical angle from blast, 45° (elevation)

Horizontal distance from assigned position, 1,850 ft in direction of flight, 29,060 ft actual distance from blast

Slant distance from blast, $40,900$ ft

Shock struck airplane from the left and below

¹Computed from data in Navigator's Report, reference 1.

SECRET

SECRET

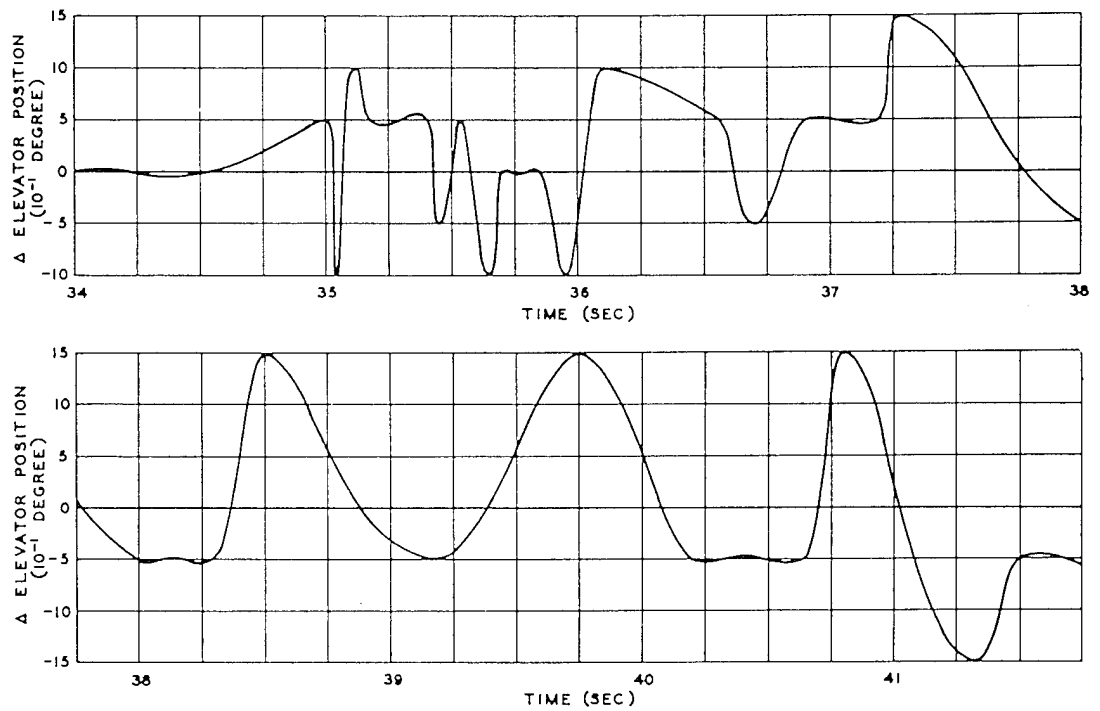


Fig. 5.58 Elevator Position, Elevator Torque Tube, Channel A1, B-50D (340), Dog Shot

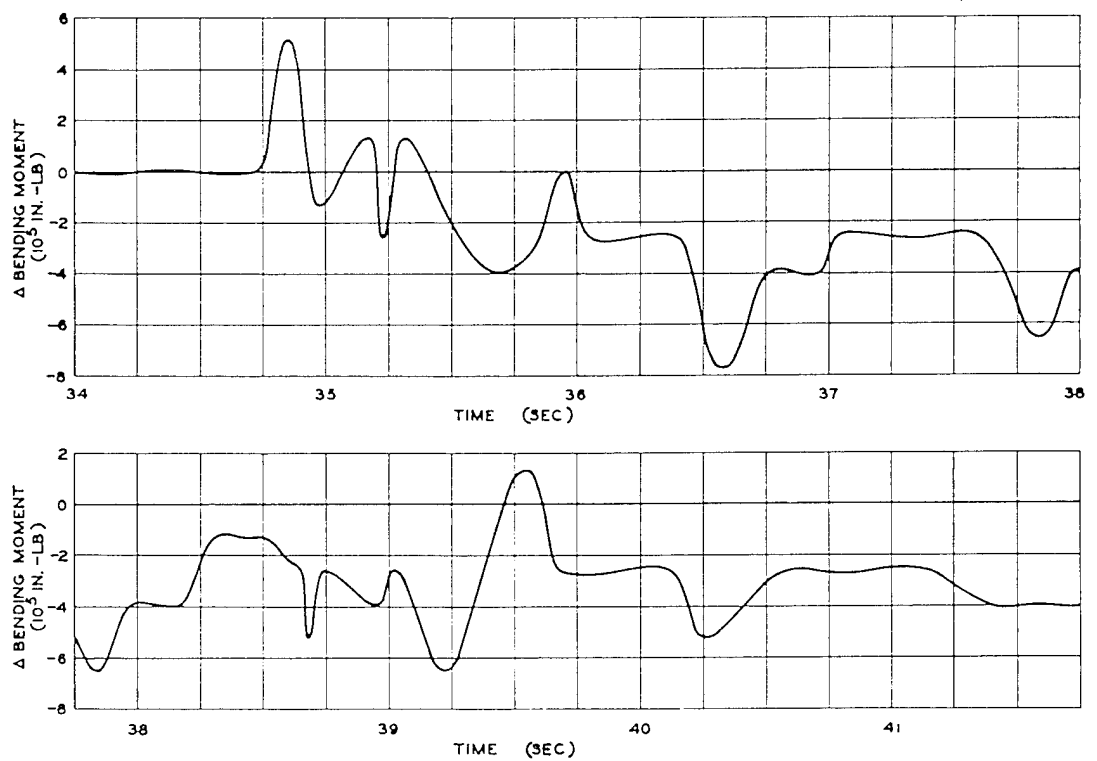


Fig. 5.59 Wing Bending, Left Wing Outboard, Wing Station 505, Channel A2, B-50D (340), Dog Shot

SECRET

SECRET

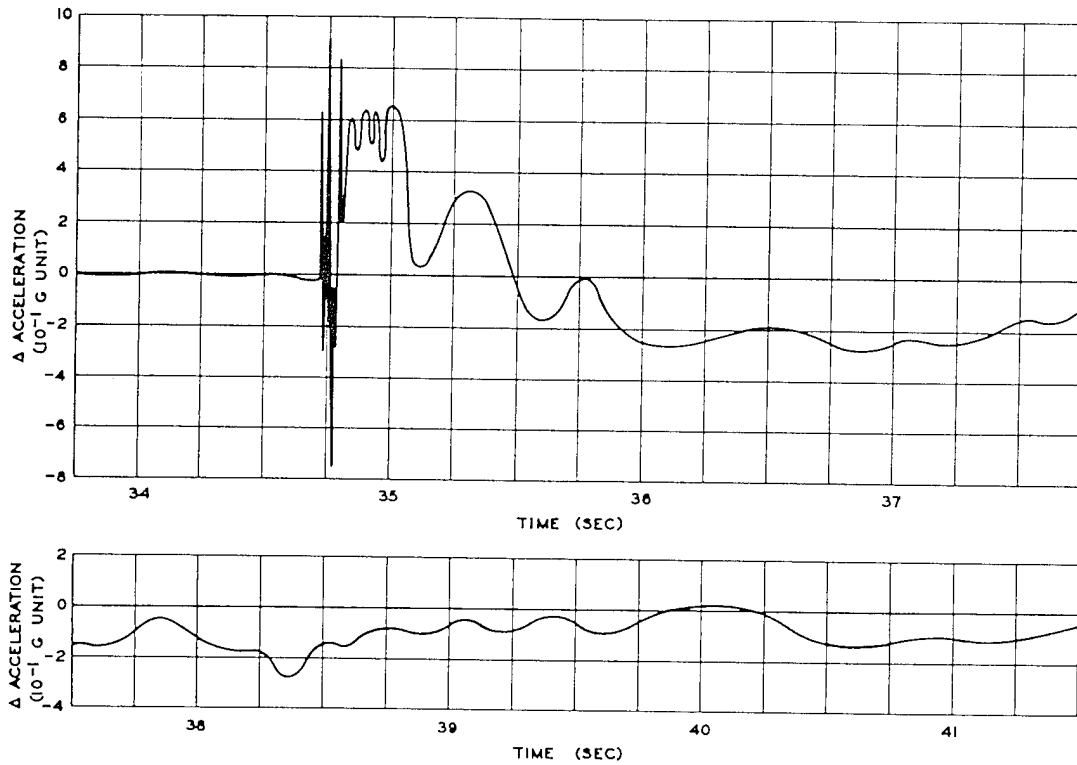


Fig. 5.60 Normal Acceleration, Forward Bomb Bay, Aft, Channel A5, B-50D (340), Dog Shot

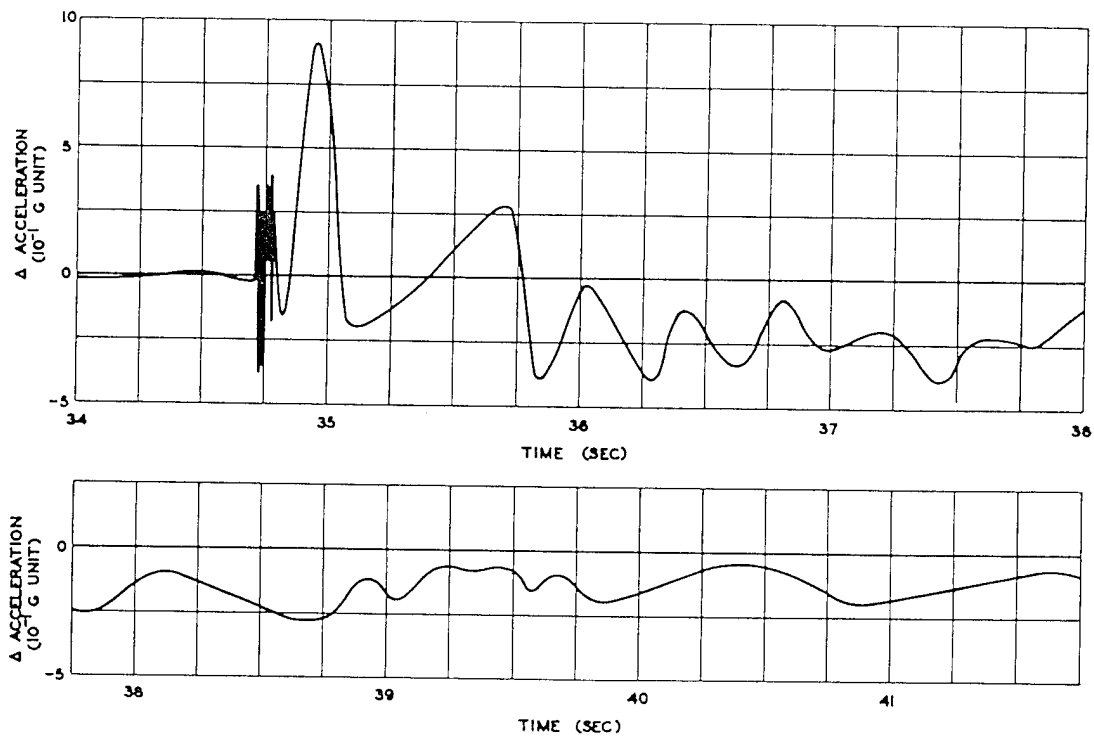


Fig. 5.61 Normal Acceleration, Nose-wheel Well, Aft, Channel A6, B-50D (340), Dog Shot

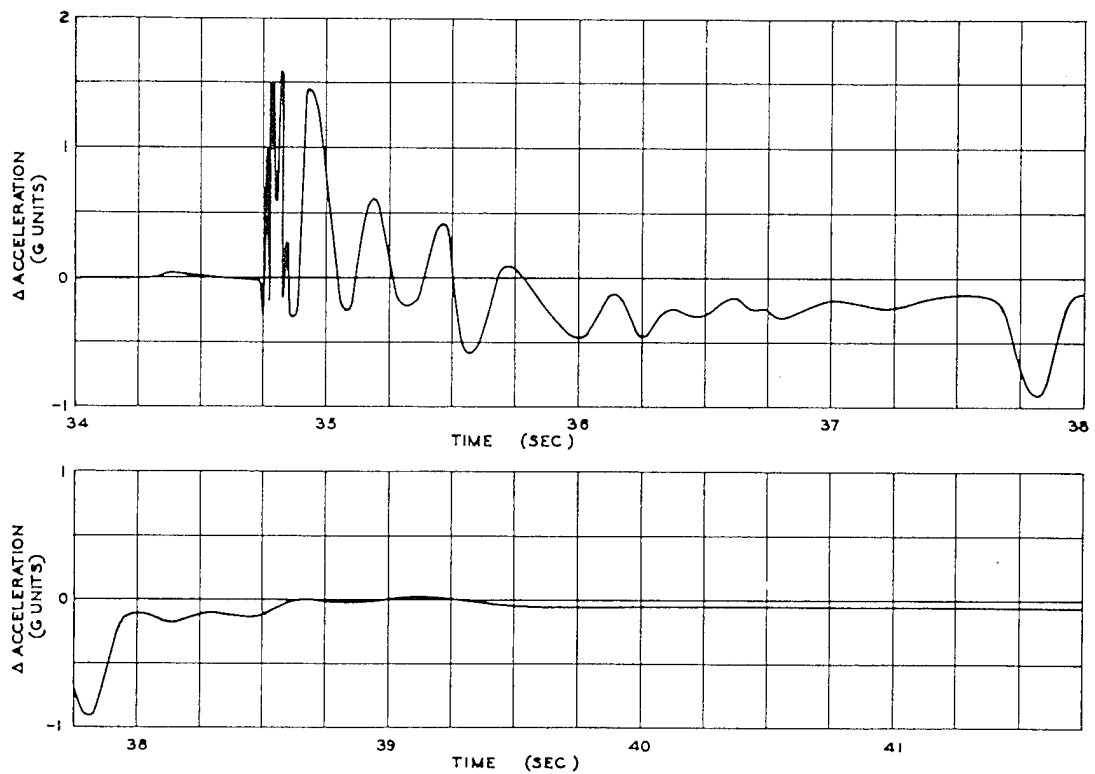


Fig. 5.62 Normal Acceleration, Aft Fuselage in Tail-gunner's Compartment, Channel A7, B-50D (340), Dog Shot

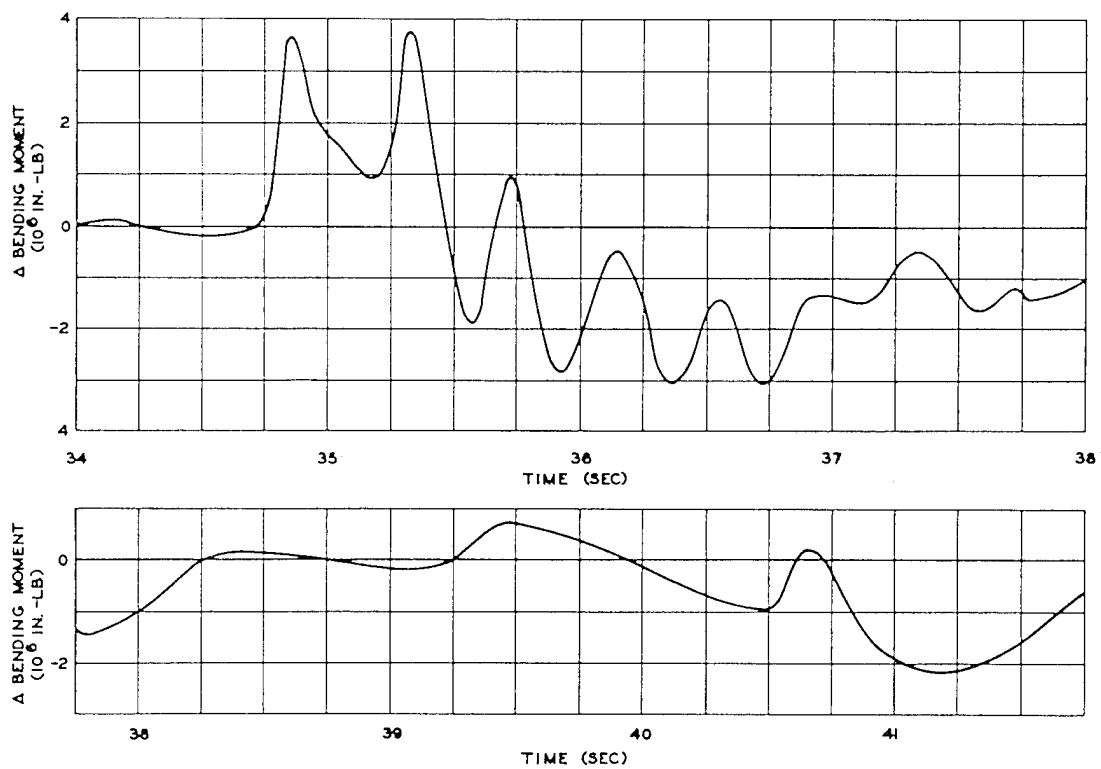


Fig. 5.63 Wing Bending, Right Wing Mid-span, Wing Station 266, Channel A10, B-50D (340), Dog Shot

SECRET

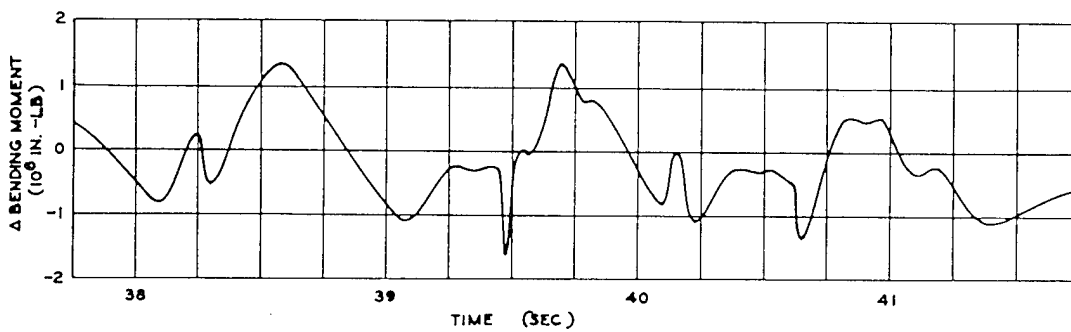
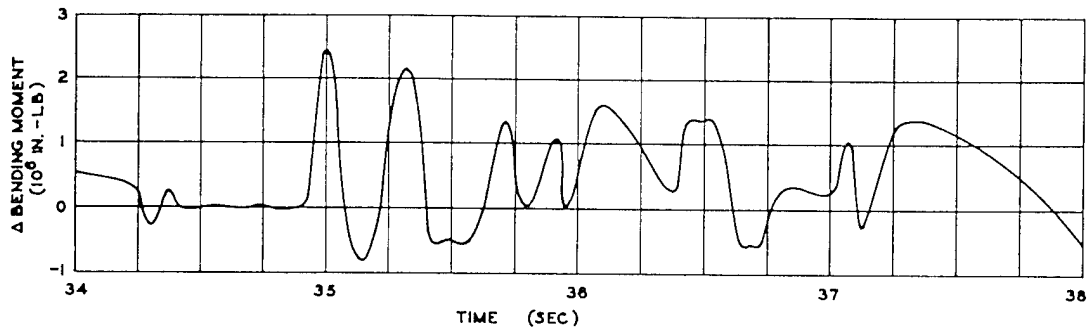


Fig. 5.64 Wing Bending, Right Wing Root, Wing Station 79, Channel A11, B-50D (340), Dog Shot

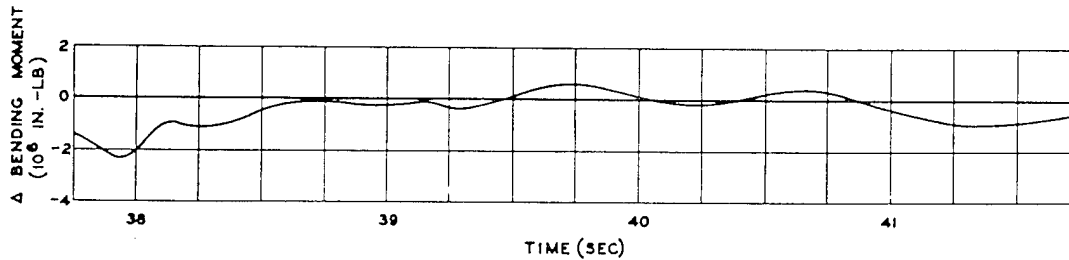
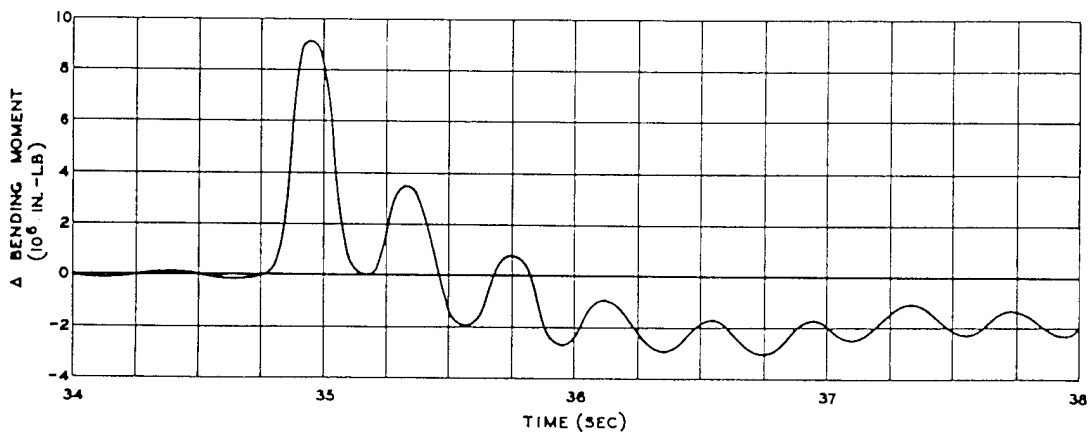


Fig. 5.65 Wing Bending, Left Wing Root, Wing Station 79, Channel A12, B-50D (340), Dog Shot

SECRET

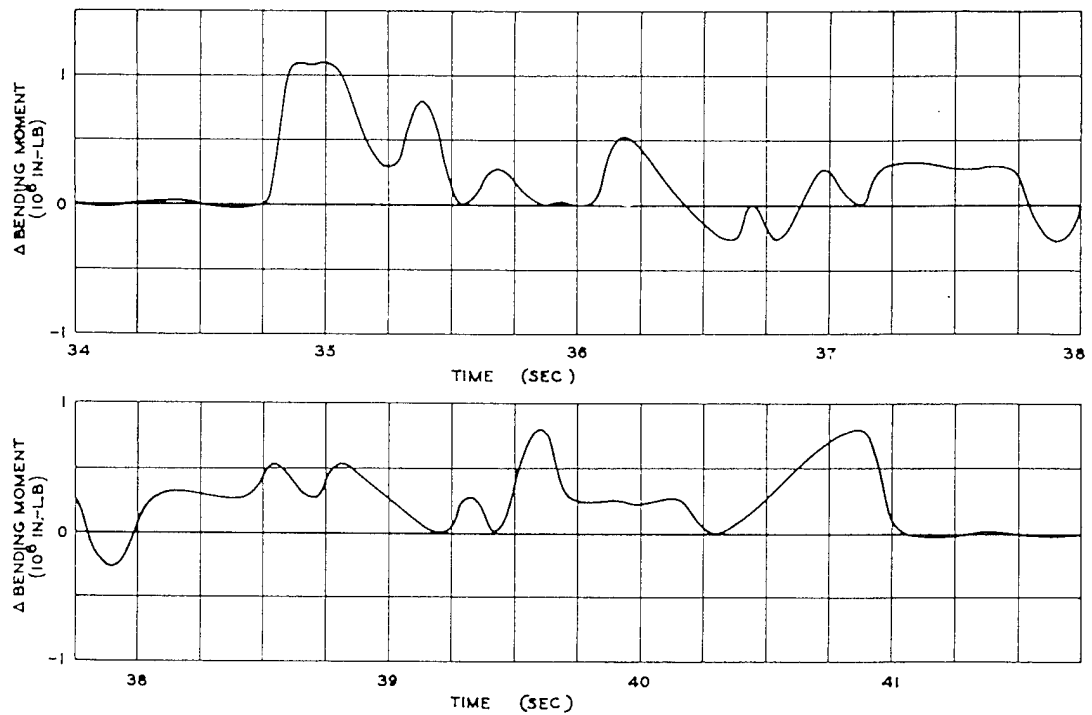


Fig. 5.66 Wing Bending, Left Wing Inboard, Wing Station 120, Channel A13, B-50D (340), Dog Shot

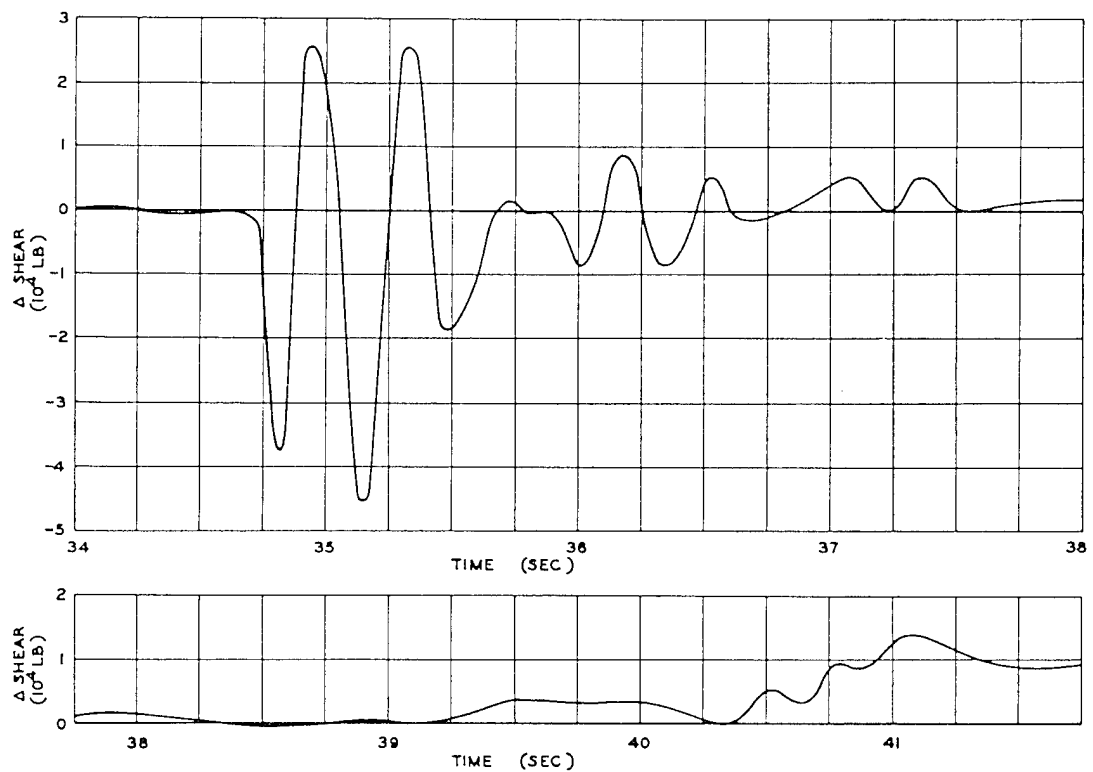


Fig. 5.67 Wing Shear, Right Wing Mid-span, Wing Station 269, Channel A16, B-50D (340), Dog Shot

SECRET

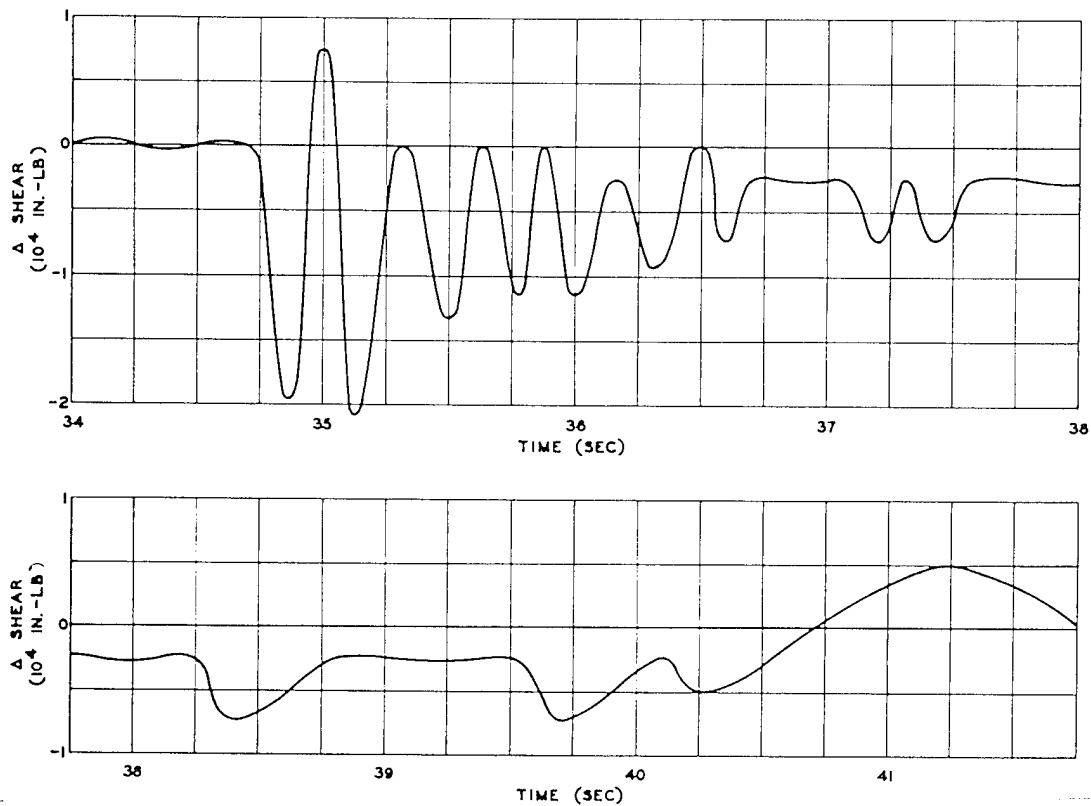


Fig. 5.68 Wing Shear, Right Wing Root, Wing Station 78, Channel A17, B-50D (340), Dog Shot

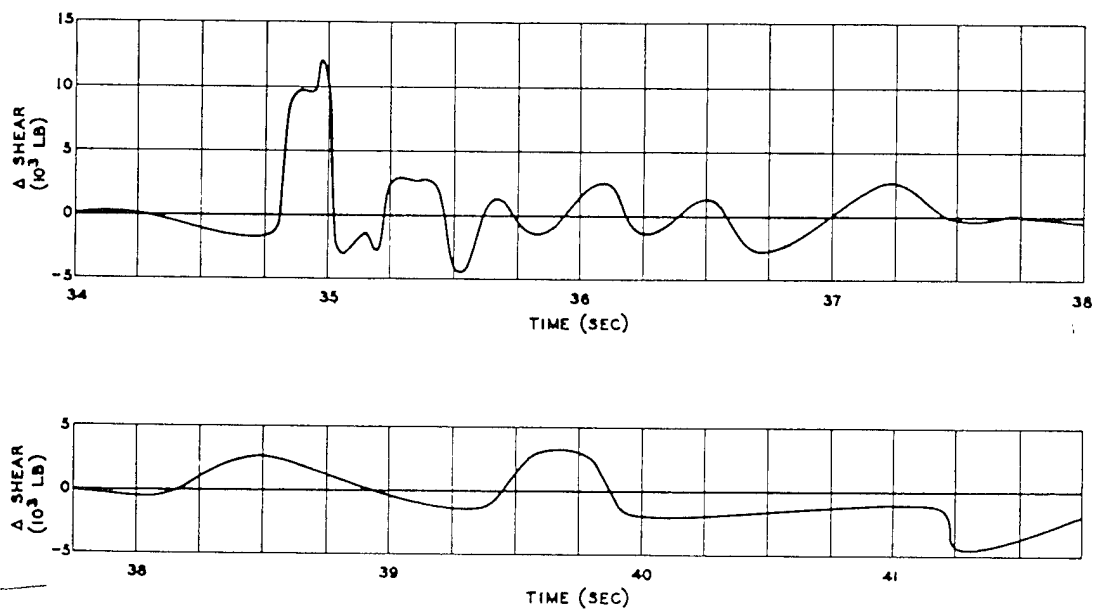


Fig. 5.69 Wing Shear, Left Wing Root, Wing Station 78, Channel A18, B-50D (340), Dog Shot

SECRET

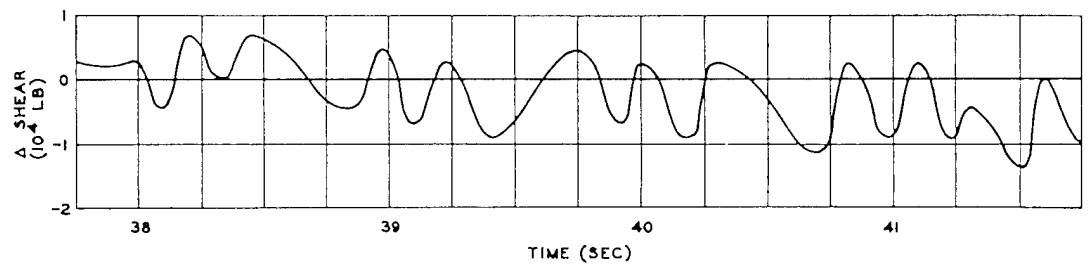
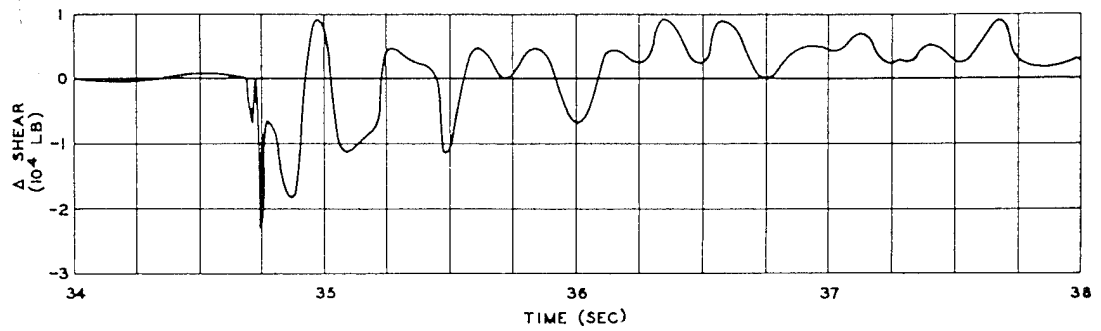


Fig. 5.70 Wing Shear, Left Wing Inboard, Wing Station 122, Channel A19, B-50D (340), Dog Shot

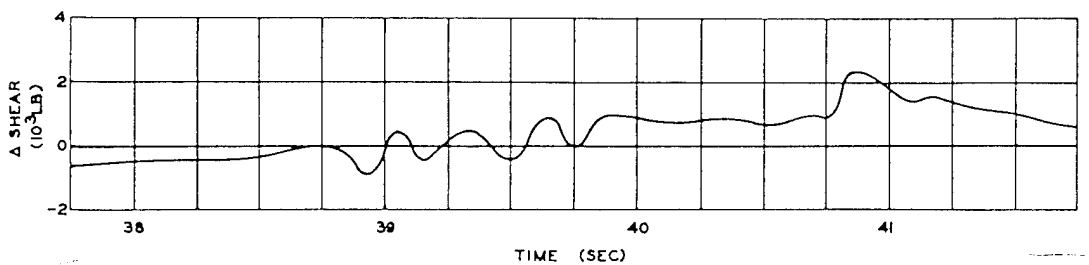
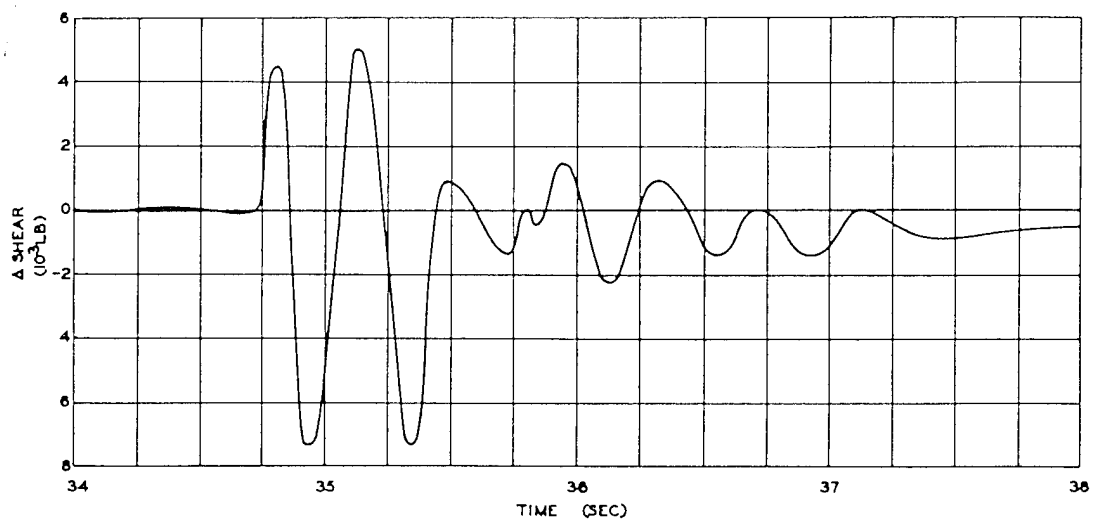


Fig. 5.71 Wing Shear, Left Wing Mid-span, Wing Station 269, Channel A20, B-50D (340), Dog Shot

~~SECRET~~

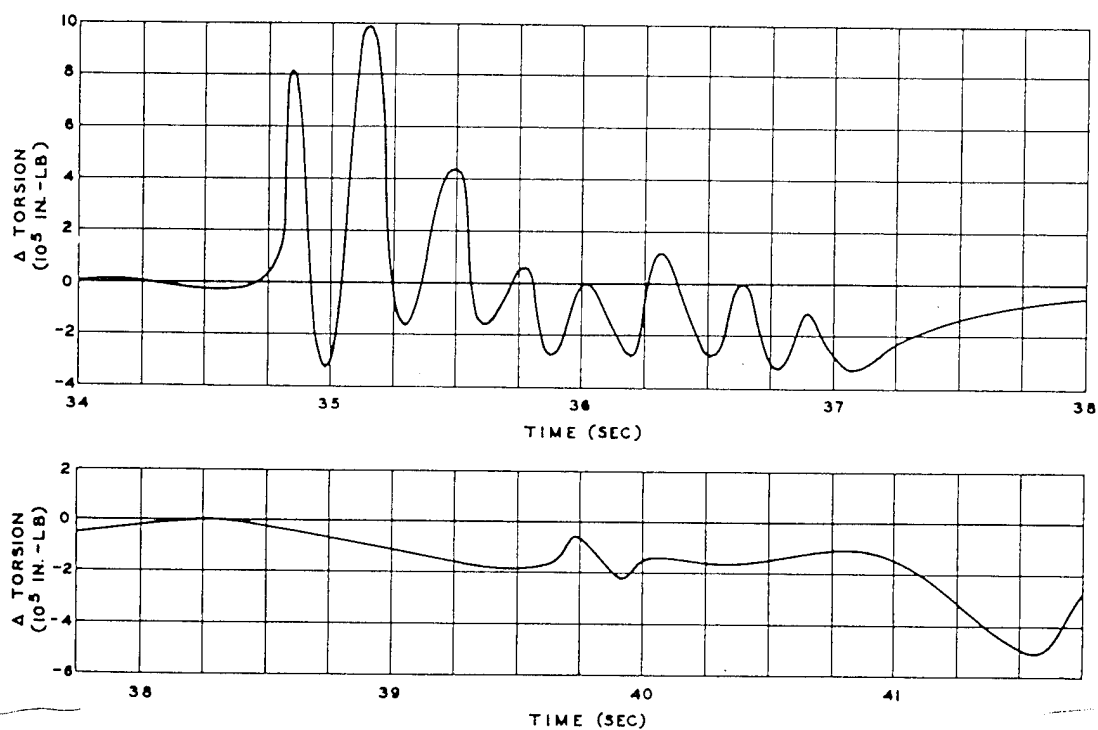


Fig. 5.72 Wing Torsion, Right Wing Root, Wing Station 78, Channel A22, B-50D (340), Dog Shot

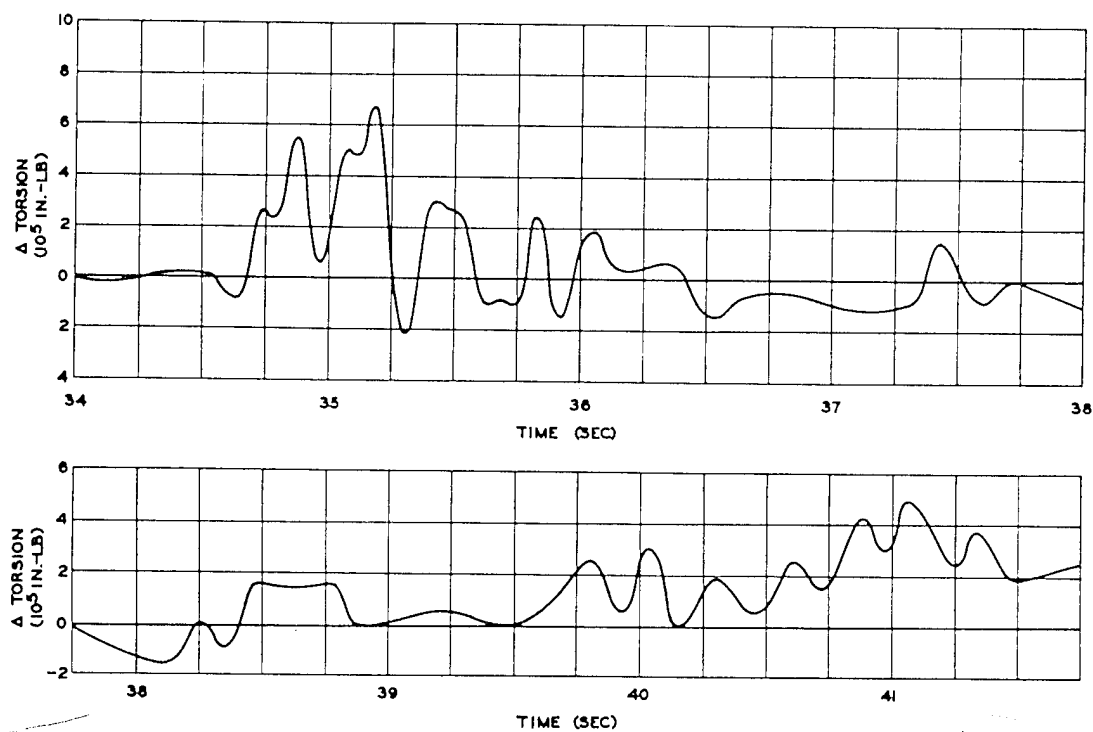


Fig. 5.73 Wing Torsion, Left Wing Root, Wing Station 78, Channel A23, B-50D (340), Dog Shot

~~SECRET~~

SECRET

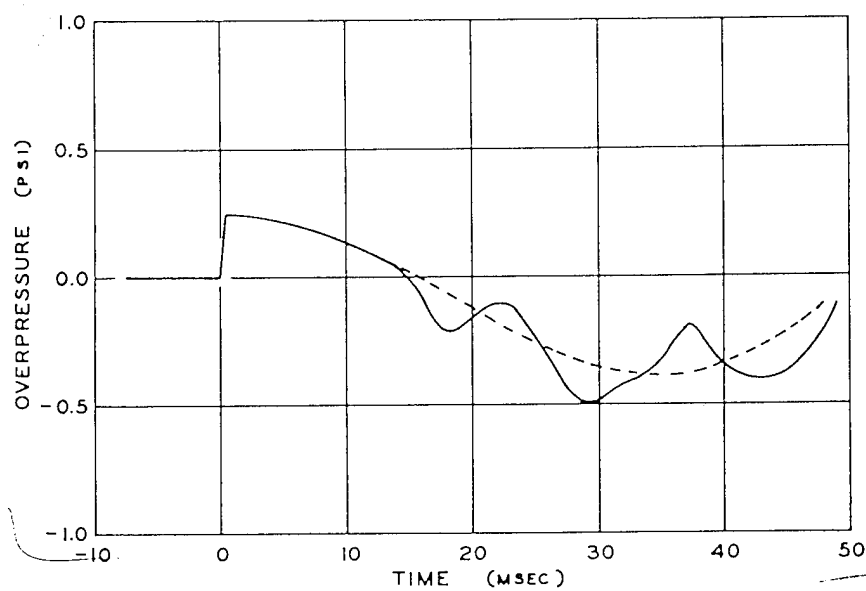


Fig. 5.74 Overpressure, High-frequency Recorder, B-50D (340), Dog Shot

SECRET

5.8.2 Airplane Condition

B-50D No. 290 had been damaged in a ground accident a few weeks prior to Dog shot. However, through considerable effort on the part of the supply and maintenance organizations, the airplane was made ready in time for the mission. The work on the right wing prevented the overhaul and calibration of the pressure transmitters in that wing; therefore only one recorder, recorder A, was used on this test. In this recorder all channels were operating except for seven channels as follows:

- Channel 9—bending, left stabilizer root
- Channel 11—bending, right wing root, station 79
- Channel 12—bending, left wing root, station 79
- Channel 13—bending, left wing mid-span, station 120
- Channel 14—bending, left wing outer panel, station 266
- Channel 19—shear, left wing station 122
- Channel 20—shear, left wing outer panel, station 269

Channels B2 and B3 from the other recorder were operable and were plugged into three of the vacant channels of recorder A. The gross weight at take-off was computed to have been 119,730 lb, with the c.g. at 24.0 per cent m.a.c. This weight included 1,005 gal (6,030 lb) of fuel in each of the four main tanks and 1,100 gal (6,600 lb) in the wing center-section tank.

The pilot reported that the aircraft was "in straight-and-level flight at time of shock wave (arrival)." The gross weight of the airplane at that time was computed to have been 106,700 lb, with the c.g. at 23.2 per cent m.a.c. No unusual circumstances were noted by the crew, and no damage was apparent from examination of the airplane.

5.8.3 Load Data

The data as recorded on the magnetic-tape recorder are presented in Figs. 5.75 through 5.82. The calibration of channel A16 was not acceptable, and the data from this channel are not shown. Channels A1, A2, A3, A4, A6, A10, A15, A16, A18, and A23 contained data that were low in value and consequently obscured by noise; the data from these channels are not presented. Channels A8 and A9 were wired

wrong. The deflections in channels A17 and A21 were such as to require considerable extrapolation of the calibration curves, and, as a result, the larger values of shear may be less accurate.

5.8.4 Analysis

The navigator reported that his airplane was 1,850 ft past Grace position when the shock struck his airplane. Because of the lateral position this amounts to only a 100-ft error in slant range; therefore the theoretical conditions are those predicted. The actual time of travel of the shock was not recorded; the reported time of $T_0 + 36$ sec is accepted.

These data are not particularly unusual, and no analysis is presented.

5.9 GENERAL CONCLUSIONS FROM DOG SHOT

Because of the necessity for caution on the first test, the structural loads attained on the test airplanes in this shot were all relatively low. However, the hazard from heat was shown to have been underestimated. This hazard in the QT-33 was in the form of damage to the control equipment and system and was only slightly apparent from the difficulty in recovering control of drone 2 after the mission. The hazard to the QB-17 was very apparent in the loss of the lower surface of the fabric-covered control surfaces. The hazard to the manned airplanes was in the form of radiant energy affecting the crew members and the danger to the fabric control surfaces.

The structural loads as recorded appear to be generally according to theory. The tendency for the shock, as an impulse function, to excite the natural frequencies of the structure is very apparent.

The low values of the data from the manned airplanes indicated a need for greater sensitivity in those recorders. A thorough reexamination and check of the starting and timing circuits were also indicated.

The discrepancy between the theoretical and actual shock travel time is greater on this test than on subsequent tests. This discrepancy indicates either (1) inadequacy of the theory, (2) unpredicted heterogeneity or discontinuity in the atmosphere, or (3) an unexplained pecu-

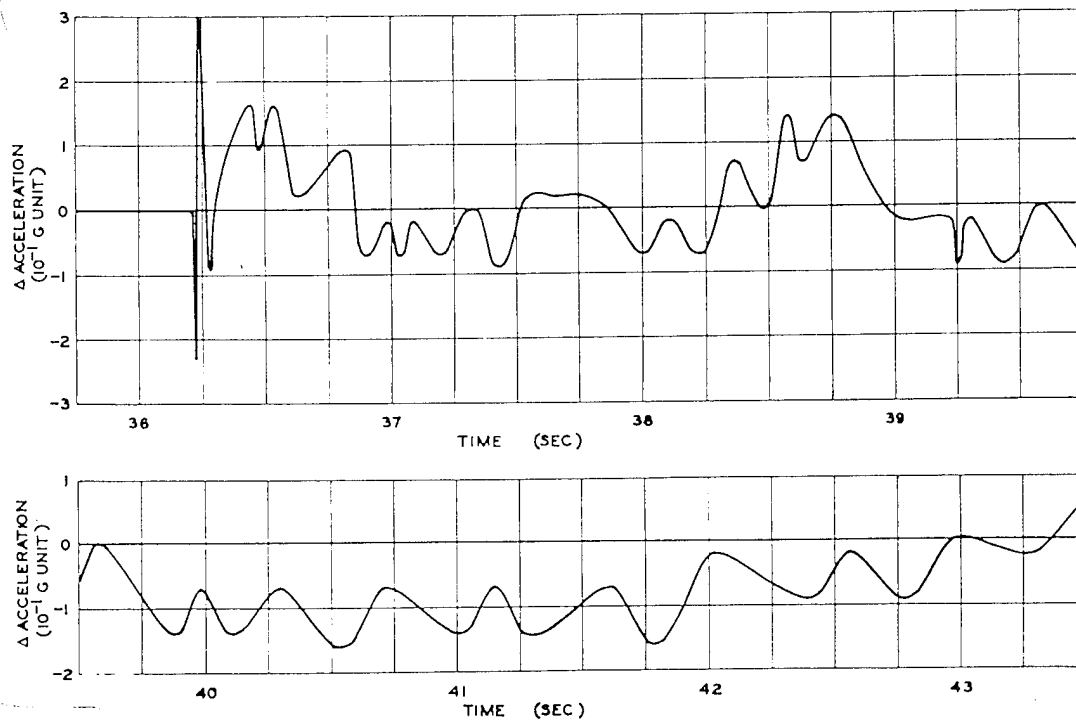


Fig. 5.75 Normal Acceleration, c.g., Channel A5, B-50D (290), Dog Shot

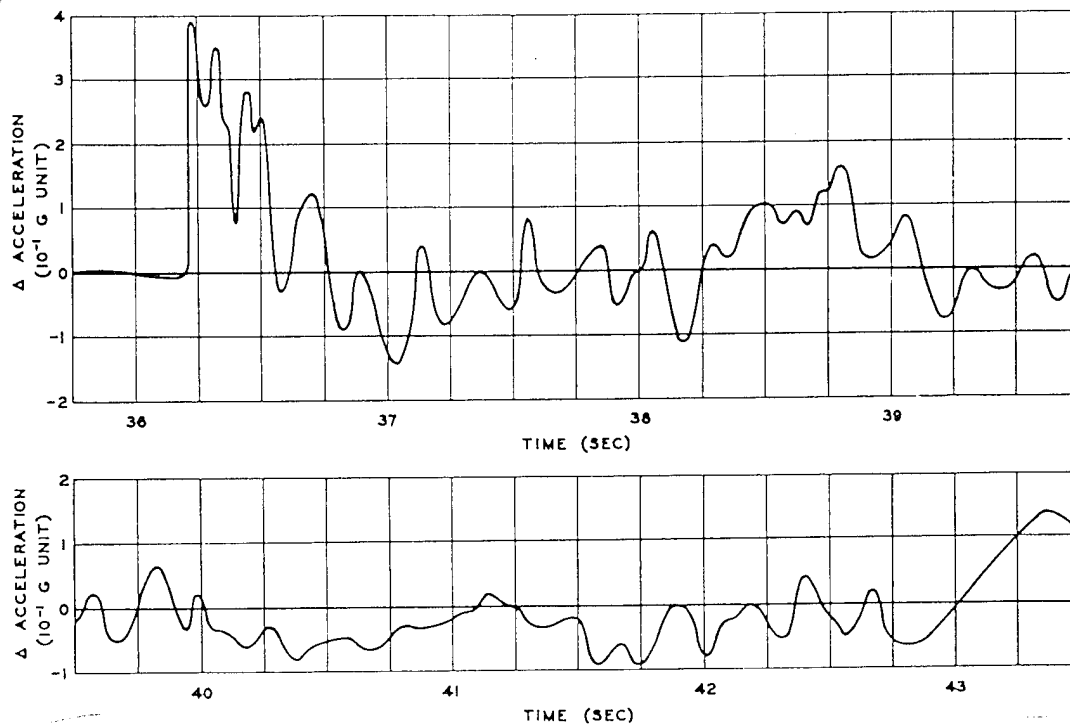


Fig. 5.76 Normal Acceleration, Aft Fuselage, in Tail-gunner's Compartment, Channel A7, B-50D (290), Dog Shot

SECRET

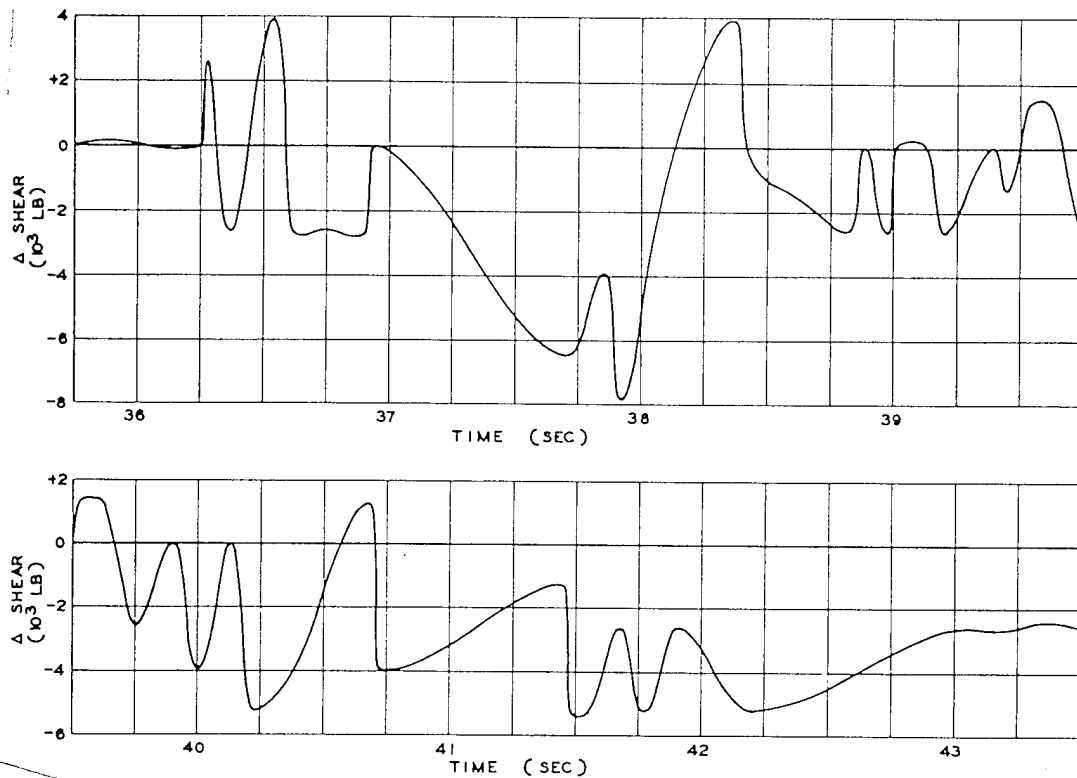


Fig. 5.77 Wing Shear, Right Wing Root, Wing Station 78, Channel A17, B-50D (290), Dog Shot

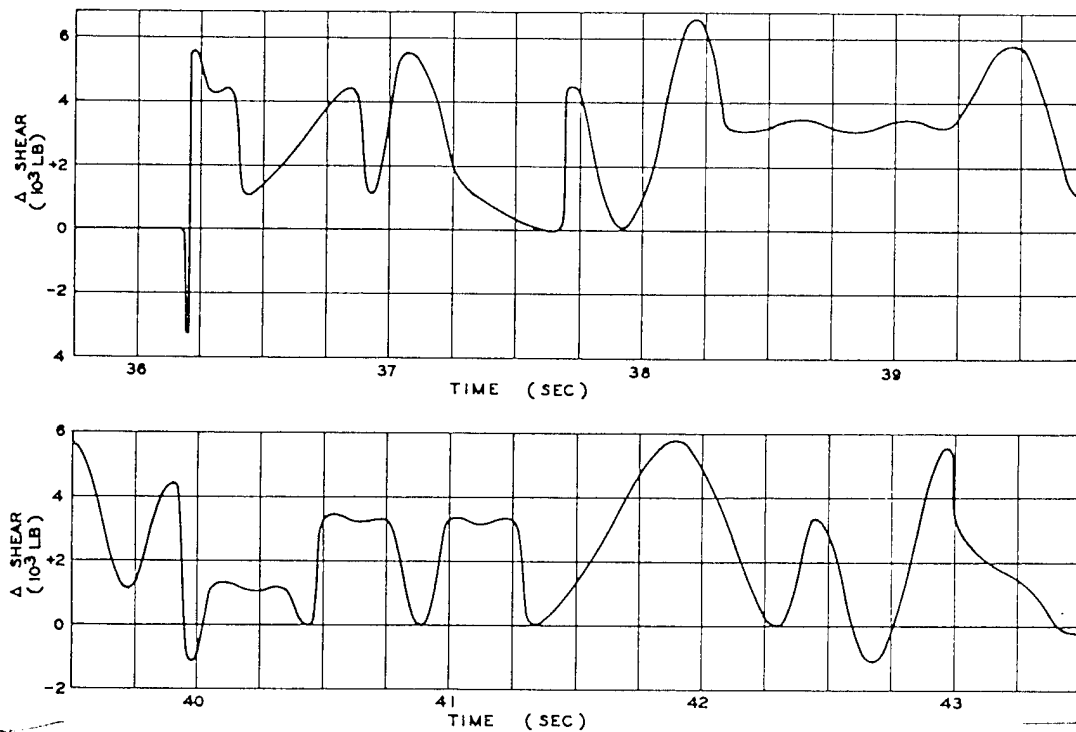


Fig. 5.78 Wing Shear, Left Wing Outboard, Wing Station 506, Channel A21, B-50D (290), Dog Shot

SECRET

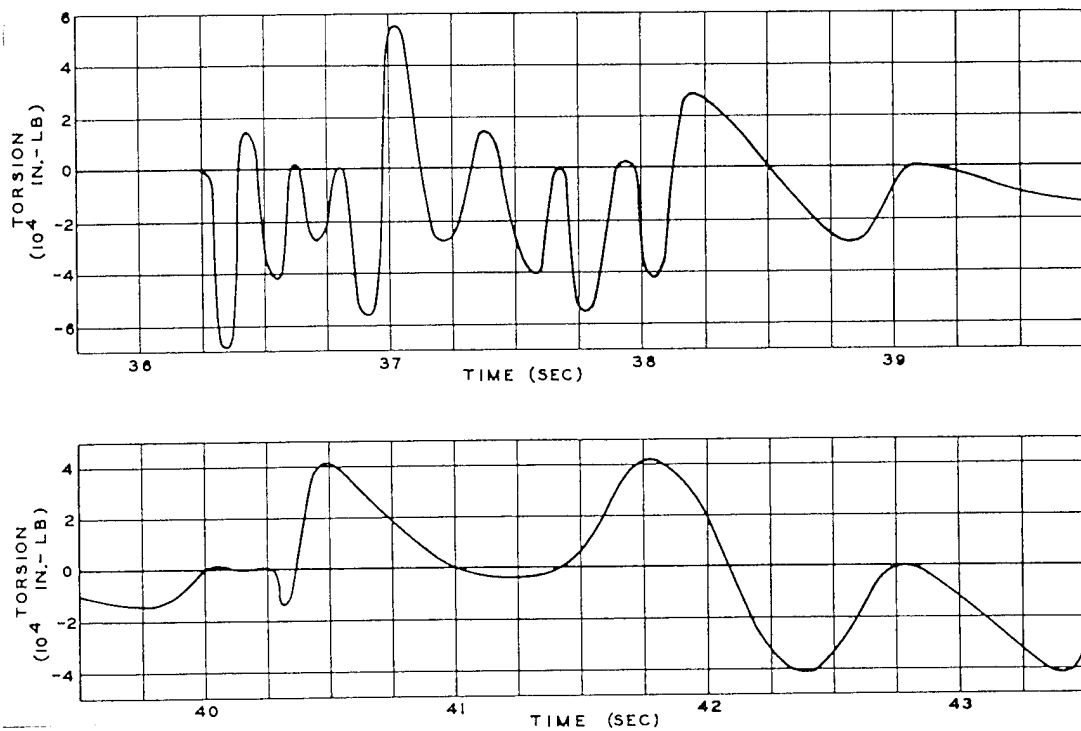


Fig. 5.79 Wing Torsion, Right Wing Root, Wing Station 78, Channel A22, B-50D (290), Dog Shot

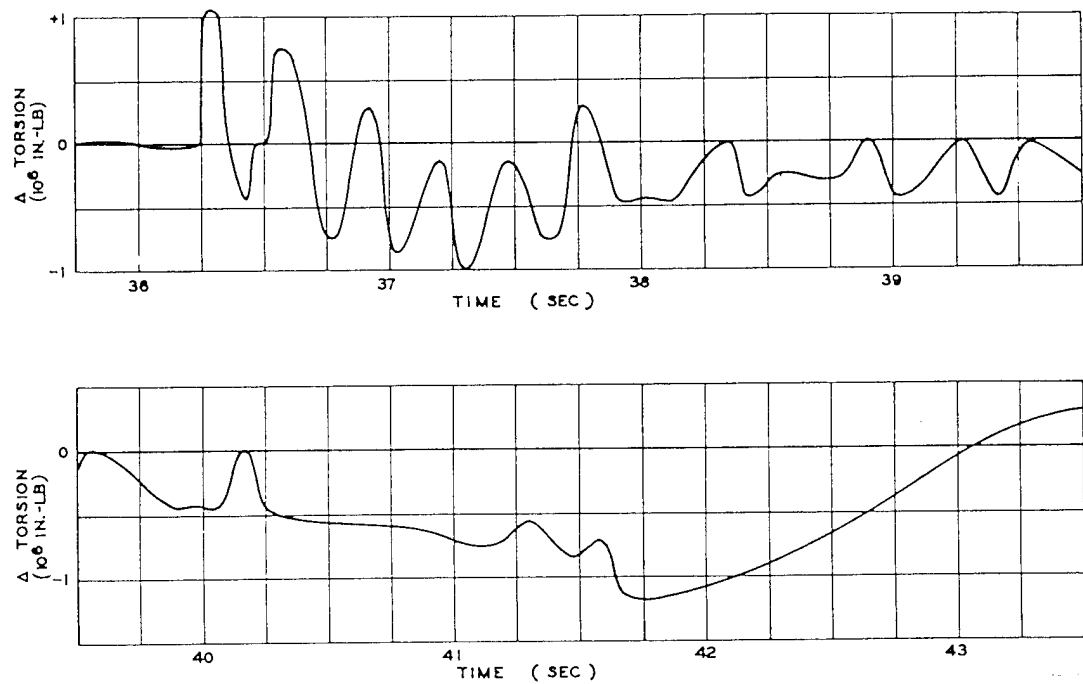


Fig. 5.80 Wing Torsion, Left Wing Inboard, Wing Station 122, Channel A24, B-50D (290), Dog Shot

~~SECRET~~

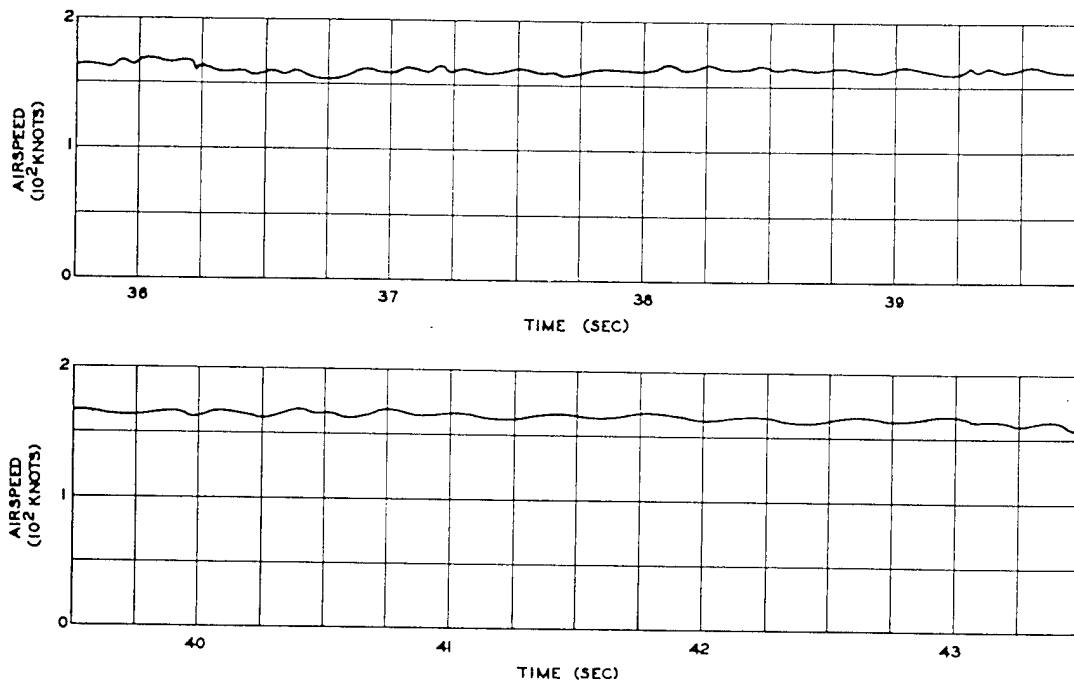


Fig. 5.81 Airspeed, Channel B2, B-50D (290), Dog Shot

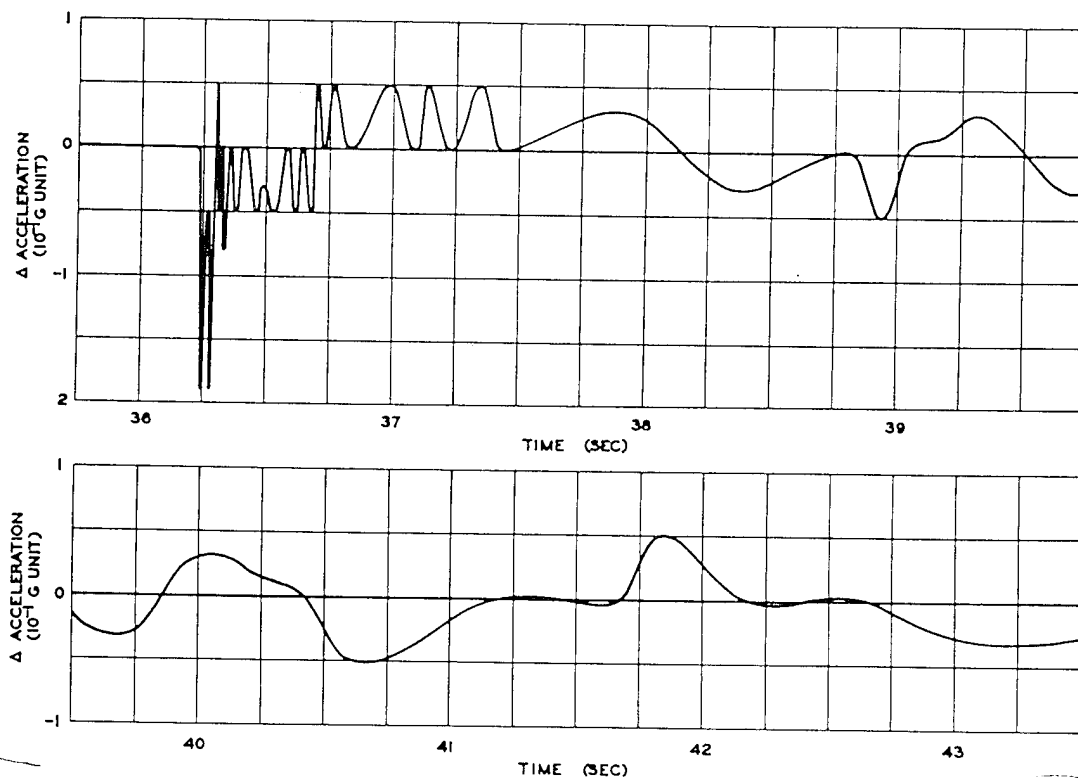



Fig. 5.82 Normal Acceleration, Rear Bomb Bay, Aft, Channel B3, B-50D (290), Dog Shot

~~SECRET~~



liarity in the shock wave itself. There appears to be little or no consistency of the discrepancies for the various points in space; they do not seem to vary reasonably with azimuth (which might be attributed to wind or local atmospheric conditions), horizontal distance, or slant range. An attempt to justify the differences by assuming appropriate errors in location proved unreasonable, especially in the instances of the radar locations and in Grace position. The magnitude of the errors required to justify the time of travel is not at all compatible with the accuracies which should be expected of the radar equipment. If it is assumed

that course and altitude are correct within the limits specified in the Navigator's Report, the range error necessary to justify the time of travel to B-50D No. 290 amounts to approximately 2 miles. The navigator should be capable of better accuracy than this, and observations by others aboard the airplane indicate that it was not that far from its assigned position.

REFERENCE

1. Navigator's Report, Dog Shot, prepared by ATU 3.4.2.

~~SECRET~~

Chapter 6

Easy Shot

6.1 GENERAL INFORMATION

The weapon test designated "Easy" was fired at 0627 hours local time, on Apr. 21, 1951. The predicted strength as given by TG 3.1 was 50 kt, and the airplane positions have been computed on this basis (see Sec. 4.3).

Because of the heat predictions based on the results of Dog shot (see Sec. 4.3), it was considered imperative that the fabric surfaces of the drone airplanes be protected. The materials on hand at Eniwetok were examined and considered for use as protective coats. Several materials, such as white paint, aluminum paint, wrapping paper, and two kinds of wrapping foil, were selected as most promising. Alternatives such as fabricating metal surfaces and covering the fabric surfaces with thin sheets of soft aluminum were considered and then discarded because they were too time-consuming or because they required unavailable material. A very crude comparative test was arranged using a heat-treating furnace as a source of heat. A section of old fabric (with dope and paint similar to that on the surfaces) was cut into test strips approximately $1\frac{1}{2}$ by 6 in. Some of the test strips were then covered with the various protective materials. The oven was treated to 1000°F, and the protected test strips were mounted to a sliding door along with a test strip of the unprotected fabric as a control. As the door was raised, the test strips were then in front of the hot oven, and the time required for each strip to char was measured. It was found that the strip protected with one of the foils took almost twice as long to char as the unprotected fabric. Admittedly this test was very crude and ignored such factors as edge charring, time of exposure to heat, and tem-

perature of and distance from the radiant source; but it was only intended to give approximate answers and was performed quickly with the equipment at hand. The foil selected consisted of laminated materials as follows: one layer of gauze impregnated with glue, one layer of brown wrapping paper, one layer of foil (apparently aluminum), and one layer of plastic (rather tough but very slightly heat resistant). The fabric horizontal surfaces (elevators and ailerons) of three B-17 drones (M, N, and O) were covered with this foil. The foil was doped to the fabric, and the edges of each sheet were sealed with a metal-foil-backed adhesive tape borrowed from Project 6.1. The surfaces were flight-tested before shot day to make sure that the protection was not likely to come off in flight.

As an afterthought, occasioned by the effects of heat on the airplanes, it was decided to check the amounts of radioactivity received by each test airplane. For this purpose a number of film badges were obtained from TG 3.1 and were affixed to various parts of the drones or given to crew members of the manned airplanes.

The results from Dog shot indicated a general need for greater sensitivity in the channels of the tape recorders in the manned airplanes. This increase in sensitivity was accomplished within the plug-in amplifiers by removing an input loading resistor, which increased the apparent impedance being fed by the sensing element, so that the scale presentation of the recorder was expanded. The resultant increase in sensitivity was about 1.75:1. The timing system within the recorders was improved by changing the indication from the blue box from a "pulse" to a "step" and by increasing the

height of the time pulses.

Since drone M did not appear to have been structurally damaged, it was scheduled to be reused for Easy shot along with drone N; drone O was prepared as a spare. Drones 2 and 3 were scheduled for Alice and Betty positions. The manned airplanes were all reported as being ready, but a few hours before take-off time one recorder of the XB-47 was reported "out" (see Sec. 6.6.2).

6.2 ALICE POSITION, QT-33 DRONE 3

Assigned location (shock)

True altitude, 6,500 ft

Horizontal distance, 2,367 ft beyond point zero

Predicted conditions

Peak overpressure, 3.06 psi

Peak gust velocity, 195 ft/sec (in direction of shock)

Time of travel (shock), 3.8 sec

6.2.1 Flight Log

QT-33 drone 3 made a normal take-off, and the air-borne controller reported good control; the mission, up to shot time, went as scheduled. The telemetering failed shortly after take-off and was never properly reestablished. The director crews reported that the "drone went in water at a very steep angle (estimated 80°) at approximately $H + 20$ sec... appeared to be spiraling." From further interrogation of the crews it was learned that the airplane was only very dimly seen because of distance and darkness. The conclusion that the drone was spiraling was based on the appearance of the lights. It was the stated opinion of the crews that whatever maneuvers were performed by the drone in its descent were controlled, i.e., caused by loss of control intelligence rather than by loss of surfaces. From the various discussions immediately after the accident, it was concluded that the loss of the drone was caused by heat damage to the controlling radio or auto-pilot systems rather than by damage to the airplane structure.

No data are available from this drone other than the radar data because the telemetering equipment was inoperative and the tape record was lost with the drone.

6.2.2 Radar Position Data

The graph of the data from the radar-data recorder, Fig. 6.1, indicates that the drone was flying on a course of 45.5° at a ground speed of 393 ft/sec during the time interval $T_0 - 5$ sec to T_0 and passed 212 ft southeast of point zero. The airplane then veered to the right (at T_0) to a course of 52° and nosed down to the extent that the ground speed increased to 450 ft/sec (average) from T_0 to $T_0 + 5$ sec. This increase in speed without change in power was calculated to have required an average nose-down attitude of approximately 20°. At T_0 the remote-flight-control system was apparently damaged by heat to the extent that control was partially lost, and the airplane veered 6.5° to the right and nosed down. If it is assumed that the ground track is correct and that the airplane did nose down at T_0 , the blast struck the airplane from 4.8° left of rear at a horizontal range of 2,200 ft, a true altitude of 5,750 ft, a slant range of 6,160 ft, and from a vertical angle of 69.1° (approximately 90° from the horizontal reference line of the drone). The assumption that the airplane nosed down at T_0 is substantiated by the air-borne-controller's report that the airplane was seen out of control in a steep dive prior to crashing into the sea at about 20 sec after T_0 . The radar data indicate that the drone was 170 ft short and 468 ft to the right of Alice position at the time the shock struck. The computed conditions for this position are approximately 30 per cent higher than those predicted for Alice position. The radar director reported that the drone was on course and 0.3 sec late (130 ft short) of Alice position when the shock struck. If the radar data and the afore-mentioned assumptions are correct, the drone might have been structurally damaged after it went into the dive because of the higher loads from being out of position combined with the higher airspeed from the dive.

6.3 BETTY POSITION, QT-33 DRONE 2

Assigned location (at shock)

True altitude, 7,500 ft

Horizontal distance, 2,730 ft beyond point zero

Predicted conditions

Peak overpressure, 2.55 psi

SECRET

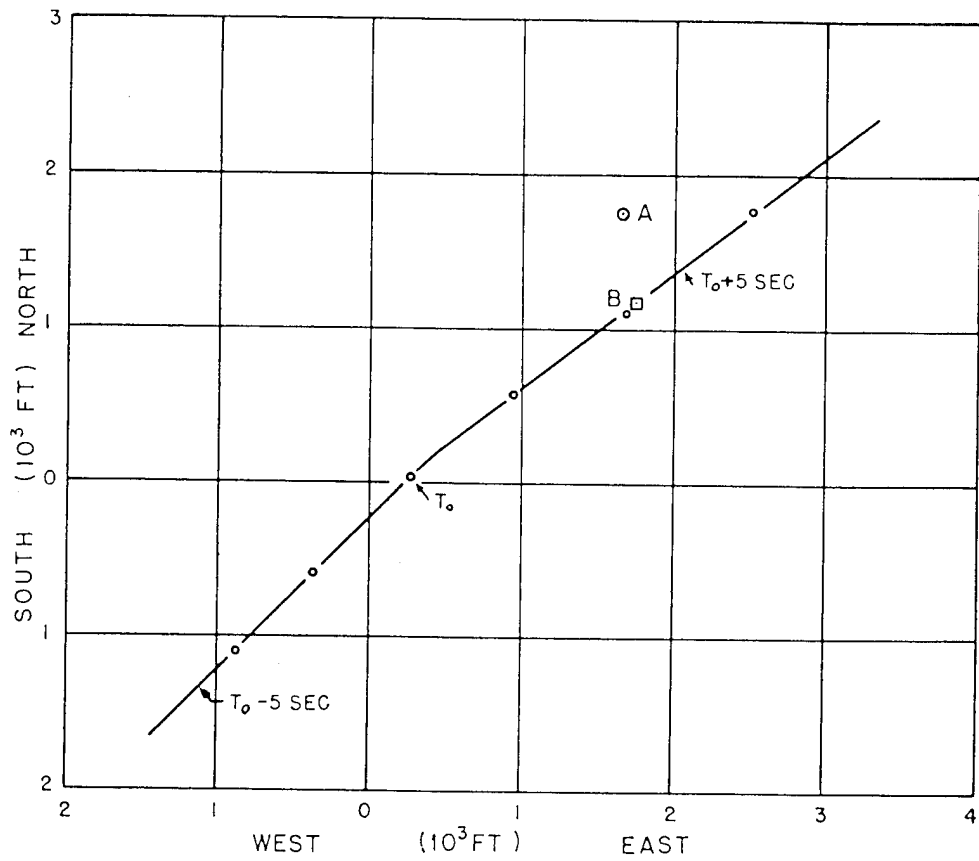


Fig. 6.1 Track, Radar-data Recorder, QT-33 Drone 3, Easy Shot.

SECRET

Peak gust velocity, 163 ft/sec (in direction of shock)

Time of travel (shock), 4.6 sec

6.3.1 Flight Log

QT-33 drone 2 took off 12 min later than scheduled. The mission was essentially without incident until shot time. Control was good, but telemetering failed on the final run. After the drone had completed its mission, the director was unable to regain proper control. It was impossible to turn off the AN/APW-11 which was used to control the drone by the radar director. Since it was also impossible for the radar director to land the drone and since the air-borne or ground director could not regain sufficient control to land the drone safely, the decision was made to crash-land the drone, according to a previously arranged plan, on Bogallua Island. The air-borne director attempted directional and altitude control while the radar director reduced power. The airplane crashed and burned. It was estimated that the airspeed at impact was approximately 225 knots (429 ft/sec). The flight data as reported¹ by ATU 3.4.2 are as follows:

Time

Start engines, 0541

Take-off, 0549

At assigned altitude, 0556

Shock arrival, 0627:04.6

Landing (crash), 0719

Meteorological conditions at altitude

True altitude, 7,500 ft

Pressure altitude, 7,200 ft

Outside air temperature, +16°C

Wind direction (from), 140° (azimuth)

Wind velocity, 9.5 knots

Airplane parameters at shock arrival

Indicated airspeed, 196 knots

Ground speed, 378 ft/sec

Ground track azimuth, 045°

Horizontal angle from blast, 045° (azimuth)

Vertical angle from blast, * 69.2° (elevation)

Horizontal distance from blast, 2,843 ft

Slant distance from blast, * 8,020 ft

Shock struck drone from rear and below

*Computed from data in Navigator's Report, reference 1.

6.3.2 Airplane Condition

Before take-off the telemetering equipment was selected as the primary recording medium (see Sec. 3.1). The local recorder, secondary medium, was equipped with sensing elements in all except 13 channels as follows:

Channel 1 — altitude

Channel 2 — airspeed

Channel 3 — acceleration, c.g.

Channel 4 — acceleration, aft fuselage

Channel 6 — torsion, left wing root

Channel 8 — bending, left wing root

Channel 11 — bending, right wing mid-span

Channel 14 — torsion right wing mid-span

Channel 15 — elevator position

Channel 16 — pressure, right wing, 5 per cent chord

Channel 22 — pressure, fuselage, nose

Channel 23 — pressure, left wing, 58 per cent chord

Channel 24 — pressure, stabilizer

Most of these gauges were removed from the recorder to make the telemetering system complete. The fuel tanks were full at the time the engine was started for take-off. With a take-off fuel load of 648 gal (4,340 lb) the gross weight was computed to have been 13,580 lb, with the c.g. at 31.05 per cent m.a.c.

The radar director reported that the drone took the shock while in a straight-and-level attitude. The gross weight was computed to have been 11,990 lb, with the c.g. at 30.2 per cent m.a.c. The fuel remaining at this time was 95 gal (637 lb) in the fuselage tank, 154 gal (1,032 lb) in the inboard wing tanks, 104 gal (696 lb) in the wing leading-edge and outboard tanks, and 57 gal (382 lb) in the tip tanks. The drone was not in sight of the air-borne directors at the time the shock struck, and no observations of the reaction were made.

As described previously, adequate control was not regained after the mission; consequently the drone was crash-landed on Bogallua Island. Because of the radioactivity on the island, it was not possible to examine the wreckage until D+1. The drone was destroyed to such an extent that it was impossible to identify the damage which might have been caused by the blast. The recorder was located underneath the cockpit section of the fuselage. Although the cockpit was badly burned and the amplifier unit of the recorder, which had re-

~~SECRET~~

mained in the cockpit, was destroyed, fortunately the recorder unit had been thrown outside the cockpit, and the tape was relatively unharmed. The film badges on this airplane were either destroyed by the fire or rendered useless by the extra radioactivity on the island.

6.3.3 Radar Position Data

The radar operator reported that drone 2 was flying at a true altitude of 7,500 ft, straight and level, directly on course, and 113 ft beyond the assigned Betty position at the time the shock wave arrived at the airplane. A graph of the data from the radar recorder, Fig. 6.2, indicated that the drone was 825 ft beyond, and 145 ft to the left of, the assigned Betty position when the shock wave struck and that it passed the point of explosion 180 ft to the northwest on a course of 45°. If it is assumed that the ground track as plotted and the altitude as reported were correct and that the airplane was flying a heading of 47° to compensate for wind drift to maintain a course of 45°, the blast struck the drone at an angle of 4.4° right of rear at a horizontal range of 3,550 ft, altitude of 7,500 ft, slant range of 8,200 ft, and vertical angle of 64.7°.

6.3.4 Load Data

The data as recorded from this mission are presented in Figs. 6.3 through 6.13. The record from which these data were taken was found in the wreckage of the drone (see Sec. 6.3.2); however, the data were not impaired in any way. In fact, except for the number of channels which had been removed to equip the telemeter, this is one of the better records collected from the operation.

The recorder was started by means of the blue box, but the time marks from the radio are very clear and distinct.

6.3.5 Heat Data

The temperature measurements as taken from this drone are presented in Table 6.1.

6.3.6 Analysis

The radar position (Sec. 6.3.3) is identified for the measured shock travel time of 5.3 sec. The theoretical peak overpressure and gust

velocity for that position is 2.38 psi and 155 ft/sec. However, the theoretical time for shock-wave travel to this position is 4.8 sec. The discrepancy is unexplained except that it might be attributed to unpredictable heterogeneous atmosphere.

Because the blue box started the recorder, the level-flight conditions before time zero are not identified, and the response data of the airplane, particularly of the stabilizer, are not so distinct as on Dog shot. However, if it is assumed that the conditions at the end of the record, $T_0 + 235$ sec, represent the level-flight conditions, the effect of the heat can be approximated in general terms. Using the four assumptions listed in Sec. 5.2.6, a total temperature rise of 103°F above ambient was computed. The highest temperature occurred at $T_0 + 1.10$ sec, and the temperature had only dropped about 20°F (to 80°F above ambient) when the shock struck. The rate of cooling at about $T_0 + 25$ sec is approximately 40°F per minute. Figure 6.14 illustrates the pressure over the chord of the right wing at station 128 at various times, so as to represent graphically the lift variations caused by the shock wave. These graphs follow the same general trend as those obtained from Dog shot.

6.4 CAROL POSITION, QB-17 DRONE M

Assigned location (at shock)

True altitude, 11,000 ft

Horizontal distance, 0 (directly over point zero)

Predicted conditions

Peak overpressure, 1.43 psi

Peak gust velocity, 106 ft/sec (in direction of shock)

Time of travel (shock), 7.2 sec

6.4.1 Flight Log

QB-17 drone M took off on schedule and completed the mission satisfactorily. The flight data as reported¹ by ATU 3.4.2 are as follows:

Time

Start engines, 0202

Take-off, 0232

At assigned altitude, 0407

Shock arrival, 0627:08.2

Landing, 0921

~~SECRET~~

SECRET

TABLE 6.1 HEAT MEASUREMENTS AT BETTY POSITION, EASY SHOT

Tape Location*	Material Thickness† (in.)	Color‡		Angle of Incidence	Max. Temp.§ (°F)	Temp. (°F)
		In	Out			
44	0.040	AP	A _s	10° 47'	295	235.6
45	0.040	AP	A _s	10° 47'	280	220.6
46	0.051	AP	A _s	24° 43'	145	85.6
47	0.051	AP	A _s	24° 43'	145	85.6
48	0.040	AP	AP		145	85.6
49	0.040	AP	AP		145	85.6

*See Table 3.10.

†Aluminum.

‡See Table 3.11.

§ Ambient temperature, 59.4°F. These temperature readings were taken from sections of the airplane that were thrown clear of the burning wreckage and were not affected by the fire.

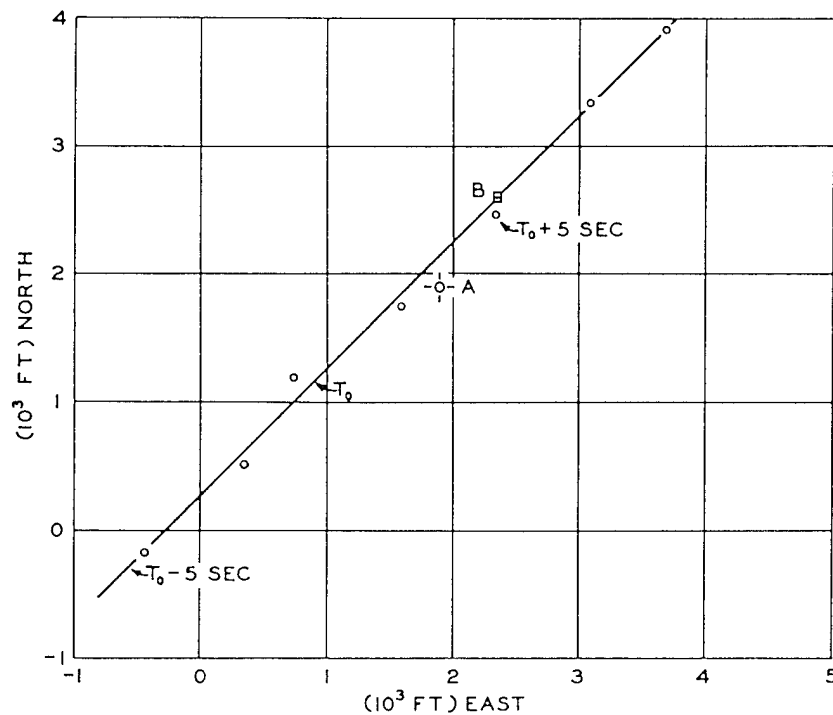


Fig. 6.2 Track, Radar-data Recorder, QT-33 Drone No. 2, Easy Shot

SECRET

~~SECRET~~

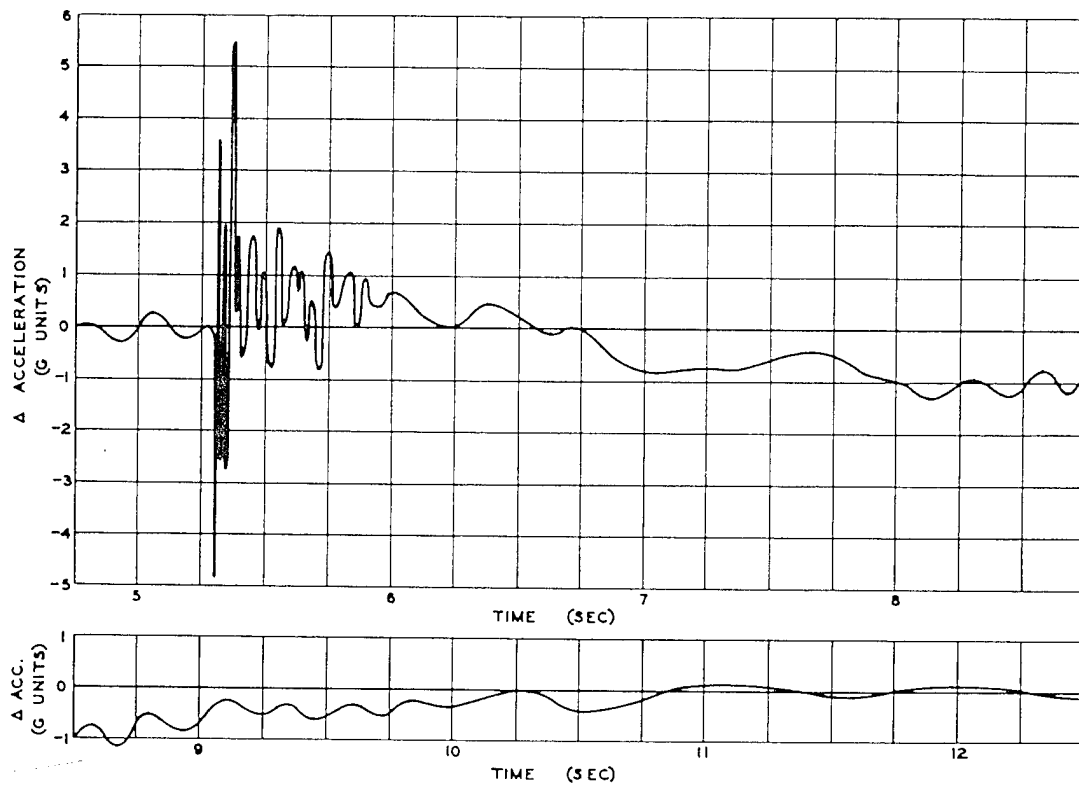


Fig. 6.3 Normal Acceleration, Nose, Channel 5, QT-33 No. 2, Easy Shot

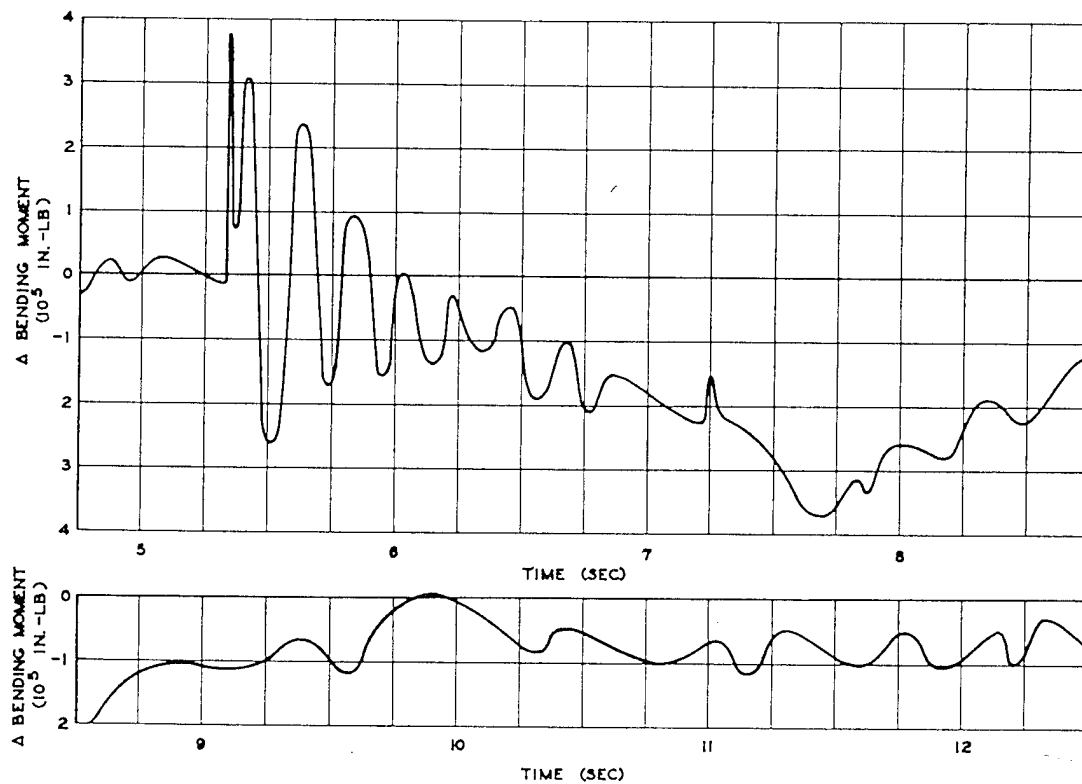


Fig. 6.4 Wing Bending, Right Root, Channel 7, QT-33 No. 2, Easy Shot

~~SECRET~~

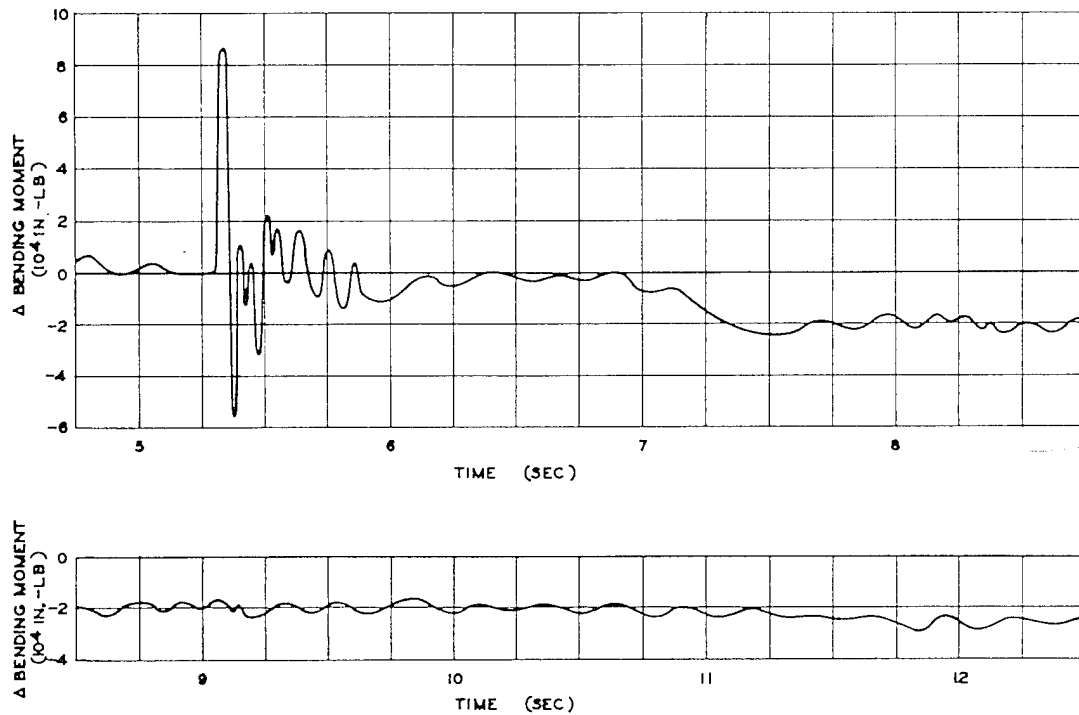


Fig. 6.5 Stabilizer Bending, Right Root, Channel 9, QT-33 No. 2, Easy Shot

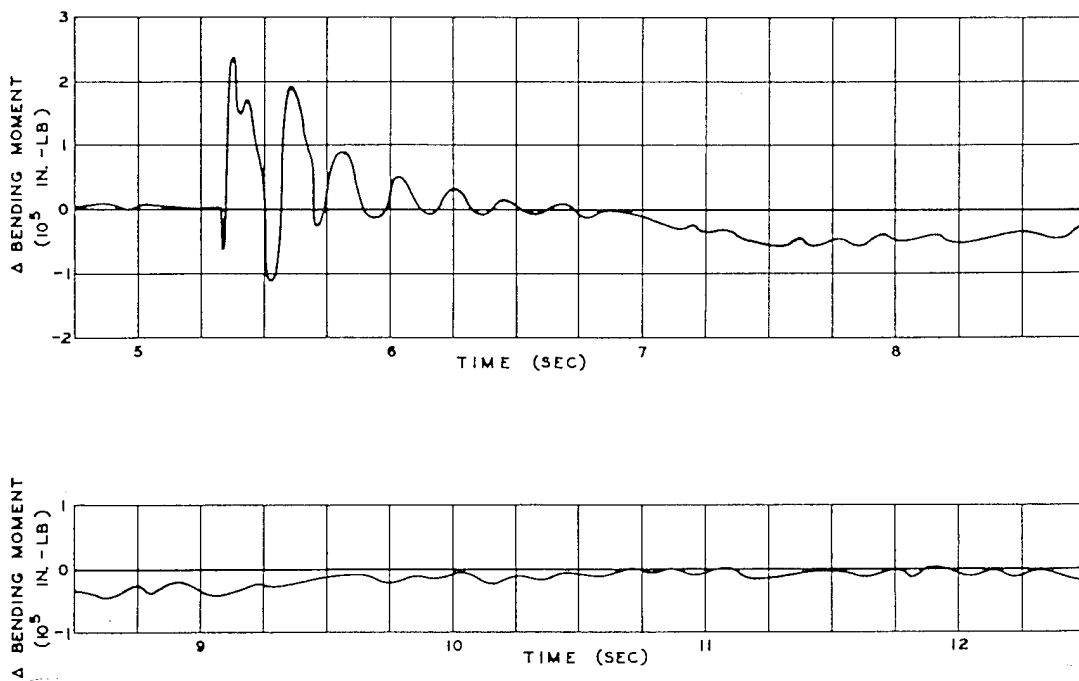


Fig. 6.6 Wing Bending, Outer Panel, Right Wing Station 129, Channel 10, QT-33 No. 2, Easy Shot

~~SECRET~~

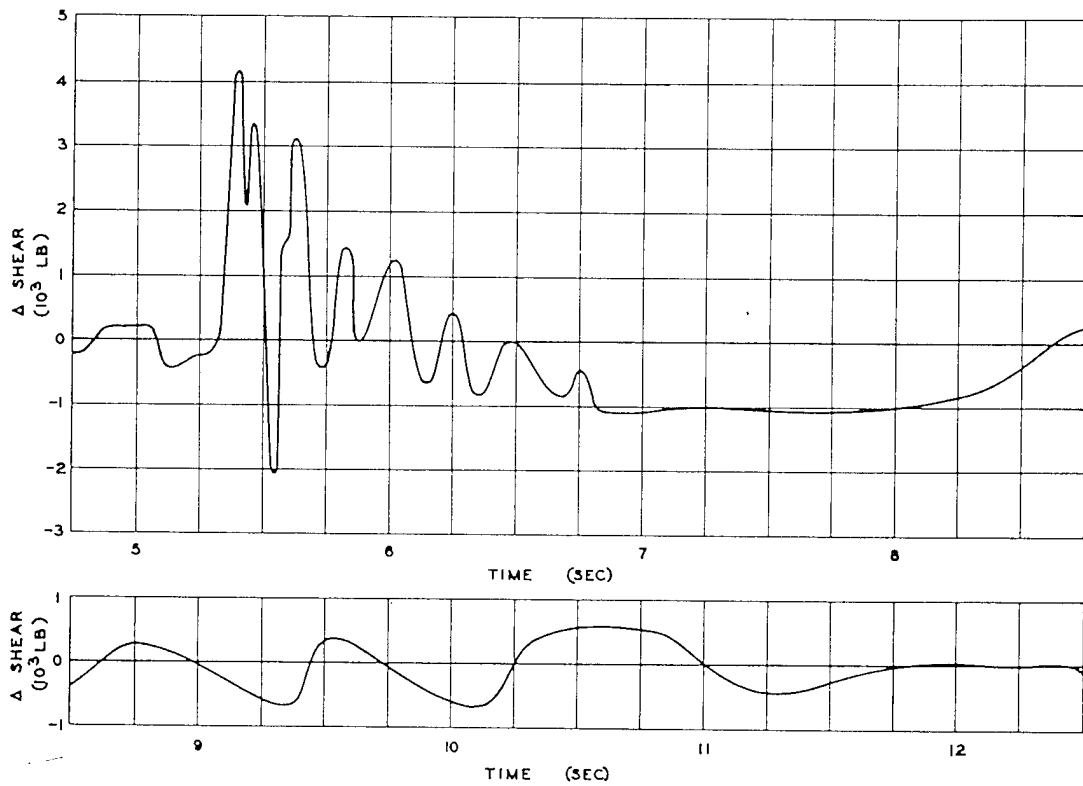


Fig. 6.7 Wing Shear, Right Root, Channel 12, QT-33 No. 2, Easy Shot

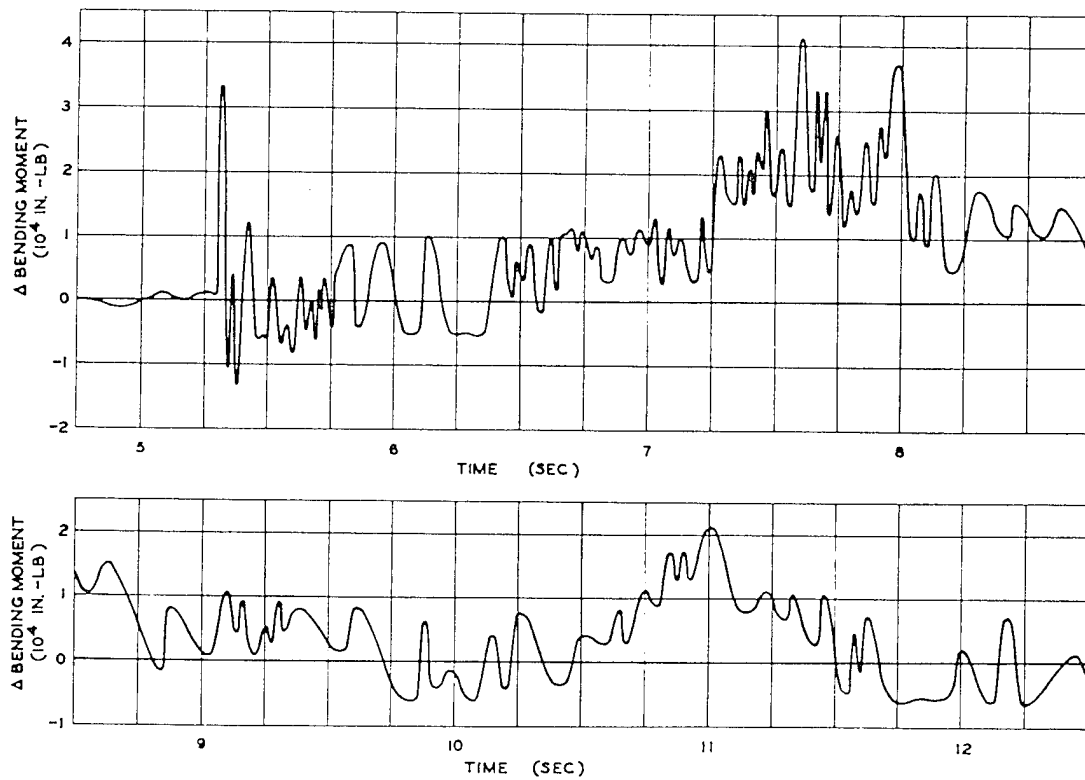


Fig. 6.8 Wing Torsion, Right Root, Channel 13, QT-33 No. 2, Easy Shot

~~SECRET~~

SECRET

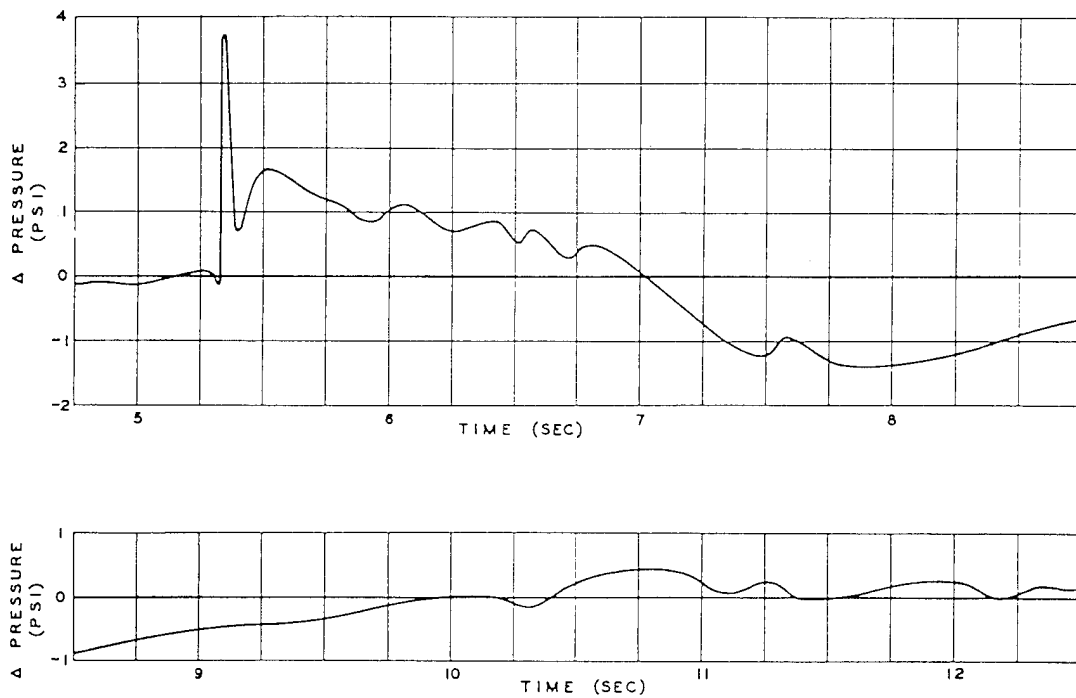


Fig. 6.9 Differential Pressure, 10% Chord, Right Wing Station 128, Channel 17, QT-33 No. 2, Easy Shot

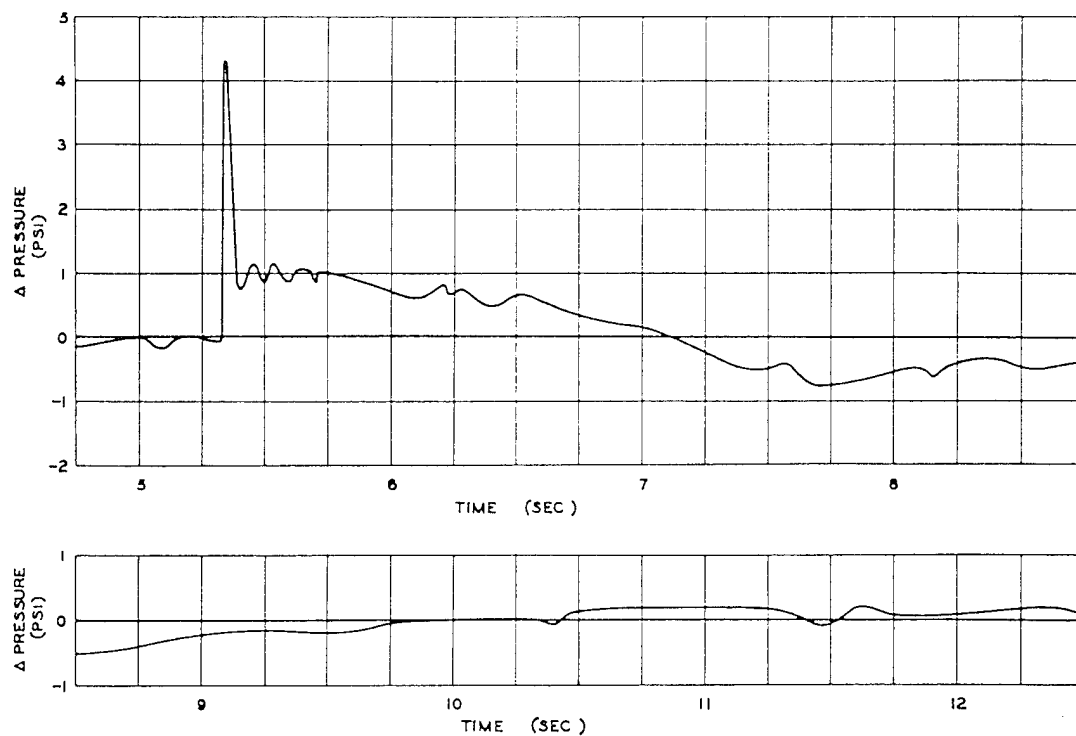


Fig. 6.10 Differential Pressure, 26% Chord, Right Wing Station 128, Channel 18, QT-33 No. 2, Easy Shot

SECRET

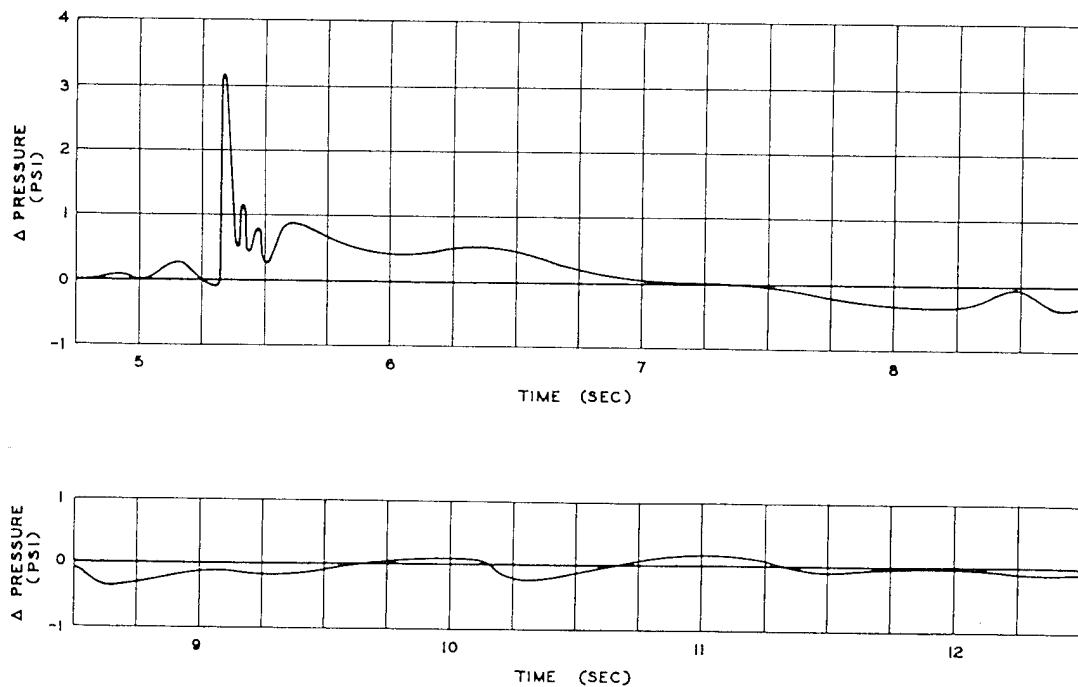


Fig. 6.11 Differential Pressure, 42% Chord, Right Wing Station 128, Channel 19, QT-33 No. 2, Easy Shot

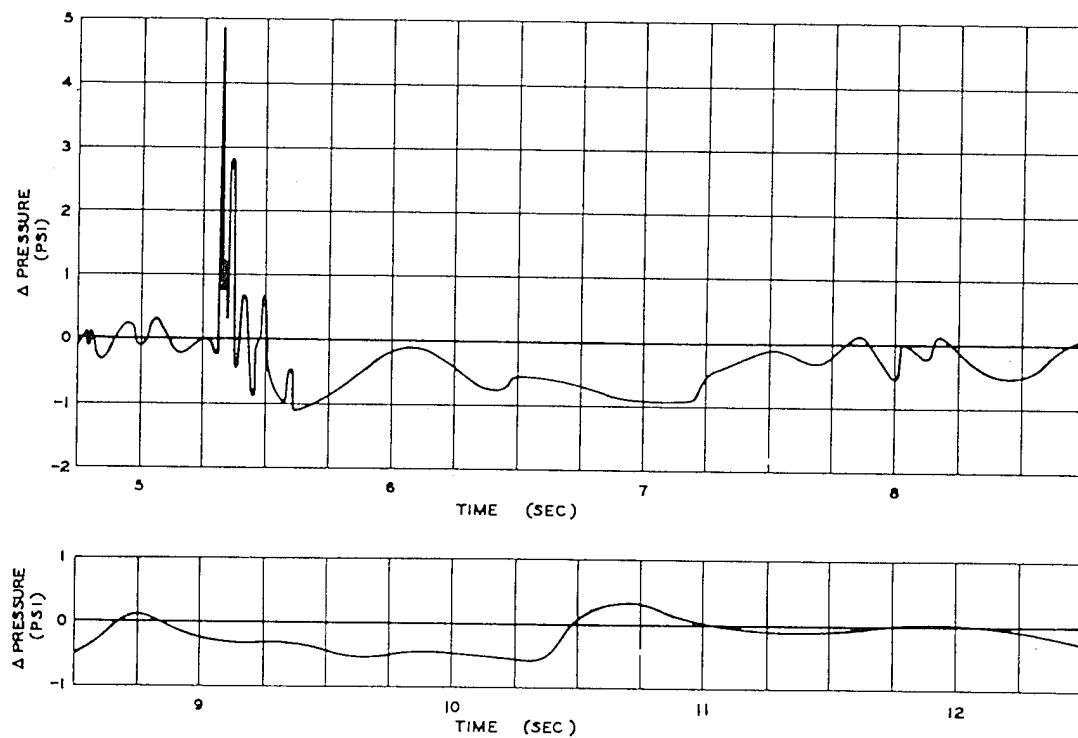


Fig. 6.12 Differential Pressure, 58% Chord, Right Wing Station 128, Channel 20, QT-33 No. 2, Easy Shot

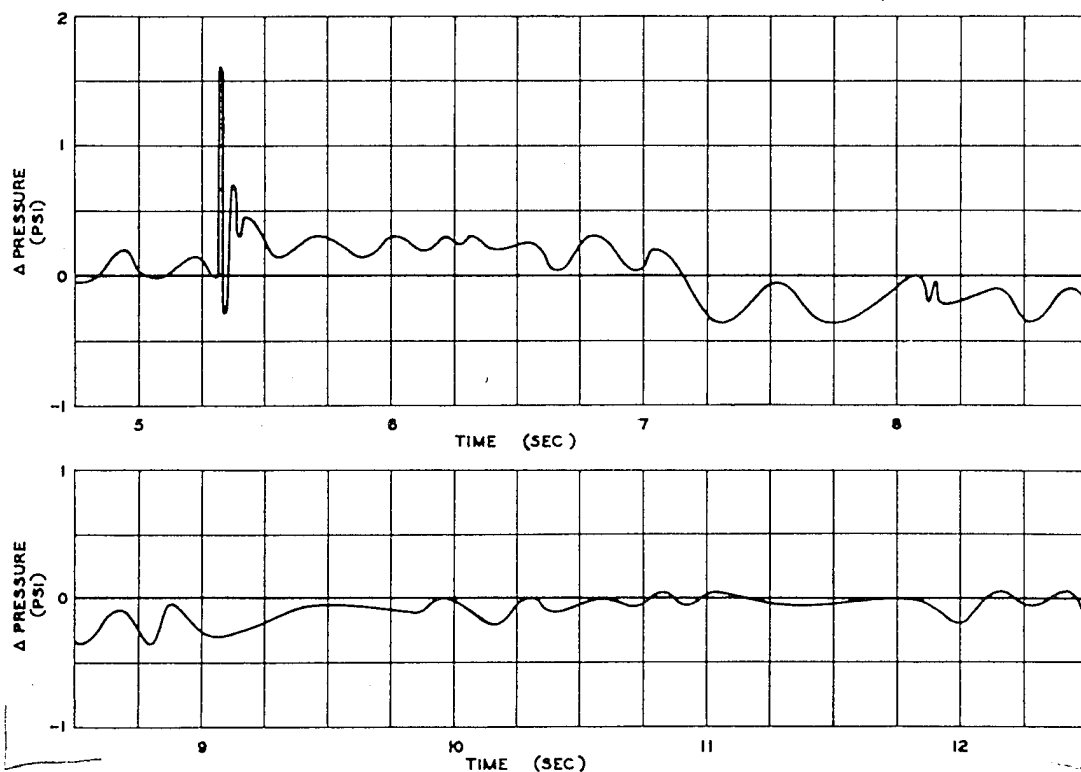


Fig. 6.13 Differential Pressure, 80% Chord, Right Wing Station 124, Channel 21, QT-33 No. 2, Easy Shot

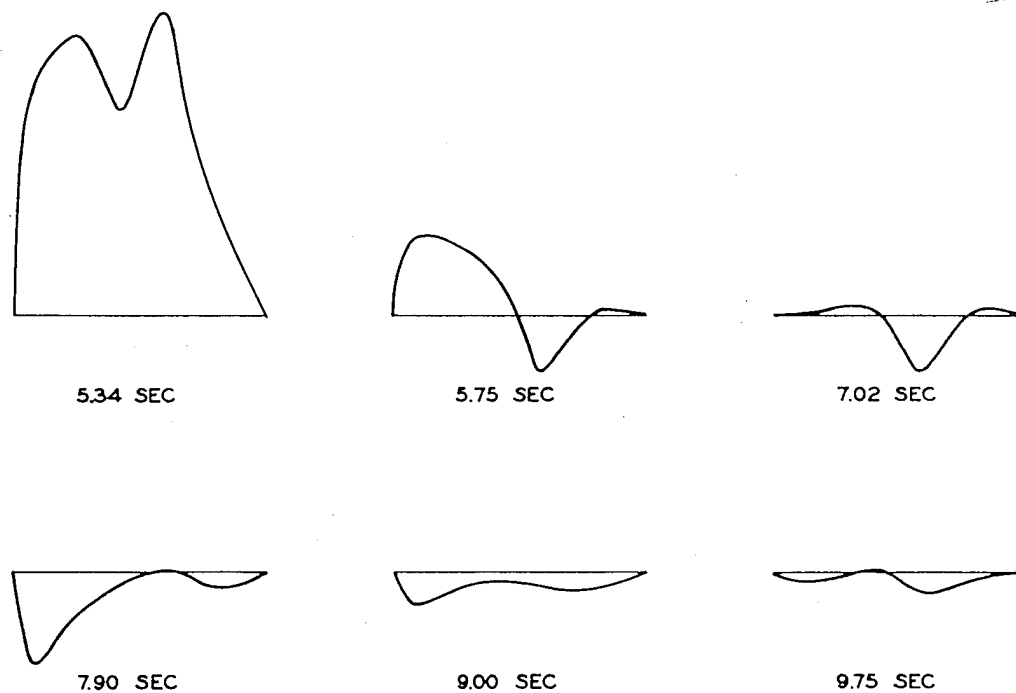


Fig. 6.14 Summary of Differential Pressures at Wing Station 128, QT-33 No. 2, Easy Shot

Meteorological conditions at altitude
True altitude, 11,000 ft
Pressure altitude, 10,500 ft
Outside air temperature, +13°C
Wind direction (from), 025° (azimuth)
Wind velocity, 22 knots

Airplane parameters at time of shock
Indicated airspeed, 139 knots
Ground speed, 235 ft/sec
Ground track azimuth, 045°
Horizontal angle from blast, 045°
Vertical angle from blast, * 88.2°
Horizontal distance from blast, 352 ft
Slant distance from blast, * 11,000 ft
Shock struck drone from below

6.4.2 Airplane Condition

Before take-off the telemetering equipment was again selected as the primary medium for data collection because of the possibility of loss of the drone. The recorder was equipped with the remaining available channels, which completed the installation except for the following six channels:

- Channel 3—acceleration at c.g.
- Channel 4—acceleration at aft fuselage
- Channel 5—acceleration at No. 3 engine
- Channel 6—acceleration at No. 4 engine
- Channel 15—elevator position
- Channel 18—pressure, 20 per cent chord, right wing station 25.5

The horizontal control surfaces had been protected as described in Sec. 6.1. The fuel tanks were filled to 2,100 gal—1,700 gal (10,200 lb) in the main tanks and 400 gal (2,400 lb) in the Tokyo tanks—at the time the engines were started. The take-off gross weight was computed at 51,330 lb, with the c.g. at 29.9 per cent m.a.c.

The director reported good control of the drone, and it was released on the test run on a 45° heading with an indicated airspeed of 139 knots. The gross weight at the time the shock wave struck the airplane was computed to be 46,270 lb, with the c.g. at 28.9 per cent m.a.c. The fuel at that time consisted of 1,256 gal (7,536 lb) in the main tanks and none in the Tokyo tanks. The radar director reported that the airplane was in straight-and-level flight at

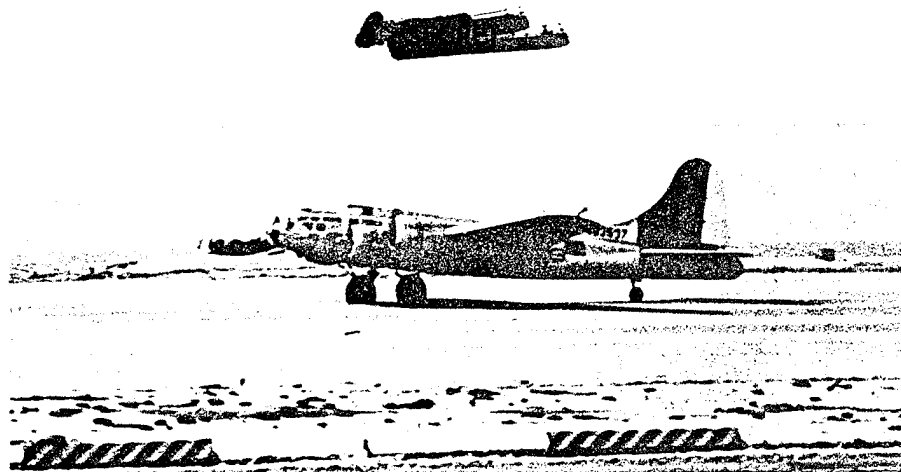
139 knots at the time the shock wave struck. The air-borne director reported that the television picture showed the pressure altitude to be 10,740 ft (slightly over 11,000 ft true altitude) and to be descending when the shock hit, and the airspeed indicator was not readable. When the director airplane returned to the drone, the right-hand tire on the drone was observed to be afire, but otherwise the airplane appeared to be undamaged and control was satisfactory. The gear was lowered in order to move the fire as far as possible from the nacelle, which contained inflammable fluids, and eventually the fire went out.

Because of the danger of a ground loop during the landing, this drone was landed last so that obstruction of the runway would not interfere with landing of other drones. The landing was normal, with the drone staying on the runway until just at the end of the landing roll, when it took a slight turn to the right. Pictures of the drone during landing and after stopping are presented in Fig. 6.15, and a close-up of the damage to the tire is shown in Fig. 6.16. The foil protection on the surfaces was burned, as can be seen in Fig. 6.15, but the surfaces themselves were not damaged. The structural damage to the airplane was apparently slight and was limited to pressure damage (rather than gust damage). All the inspection panels on the wings were popped open, as can be seen in Fig. 6.15. The damage to the bomb bay doors is shown in Fig. 6.17. The damage to the canvas cover over the tail-wheel opening, the rear entrance door, and the window in the tail-gunner's compartment, and the displacement of the floor boards in the radio compartment are shown in Fig. 6.18. Another interesting observation concerned damage to the exhaust duct on No. 2 engine, as shown in Fig. 6.19. The logical manner in which this damage could have occurred was for the engine to have been deflected up, with respect to the rest of the nacelle, in such a way that the end of the coupling slipped so far out of the rim of the exhaust duct that it did not return when the engine came back to its normal position. No other damage to the engine mount or nacelle was visible.

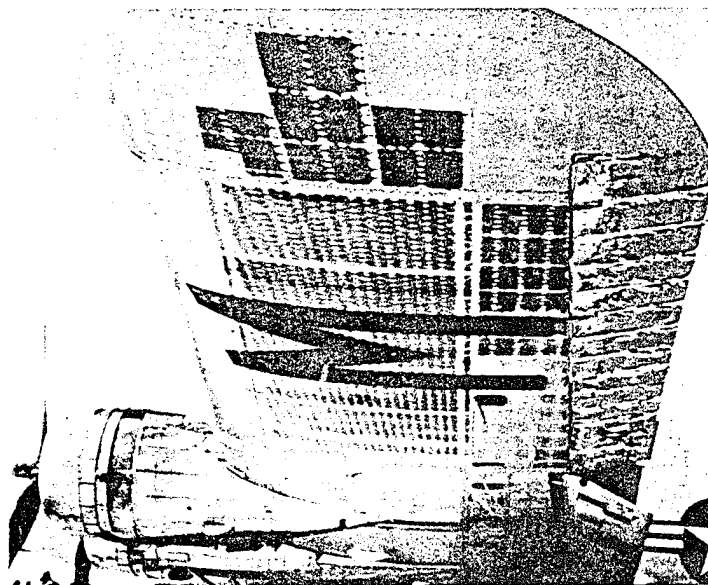
6.4.3 Radar Position Data

According to the radar-operator's report, drone M was flying at 11,000 ft directly on

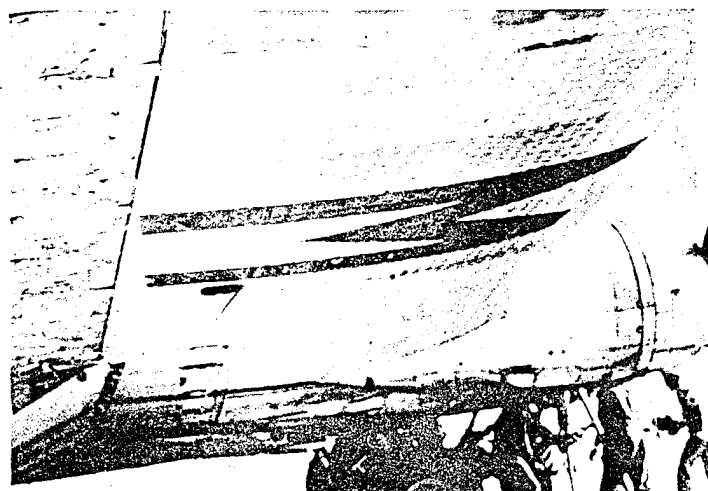
*Computed from data in Navigator's Report, reference 1.



A



B



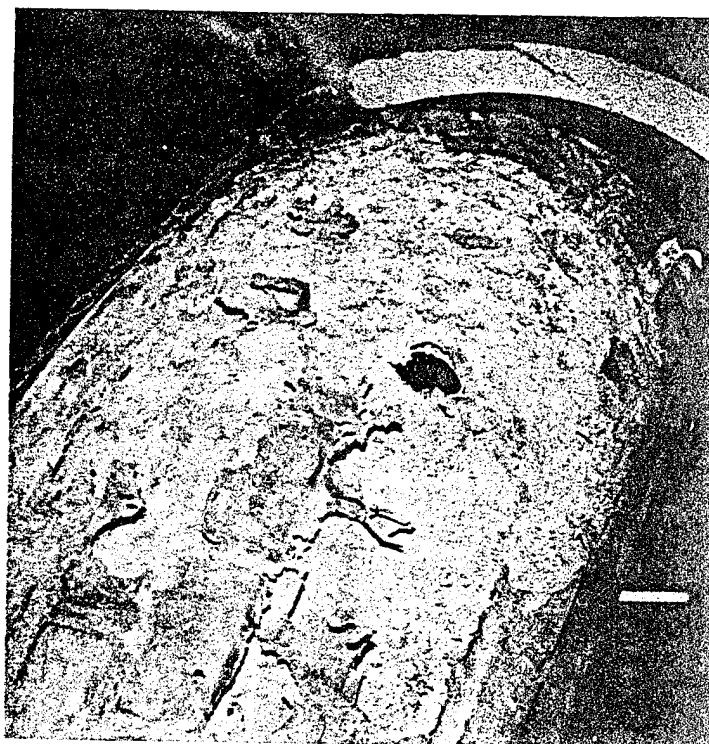
C

Fig. 6.15 Damage to QB-17 Drone M, Easy Shot. A, drone landing with flat tire. B, left wing. C, right wing.

~~SECRET~~



A



B

Fig. 6.16 Heat Damage to Tire, QB-17 Drone M, Easy Shot. A, tire and wheel. B, close-up of tire.

~~SECRET~~

SECRET

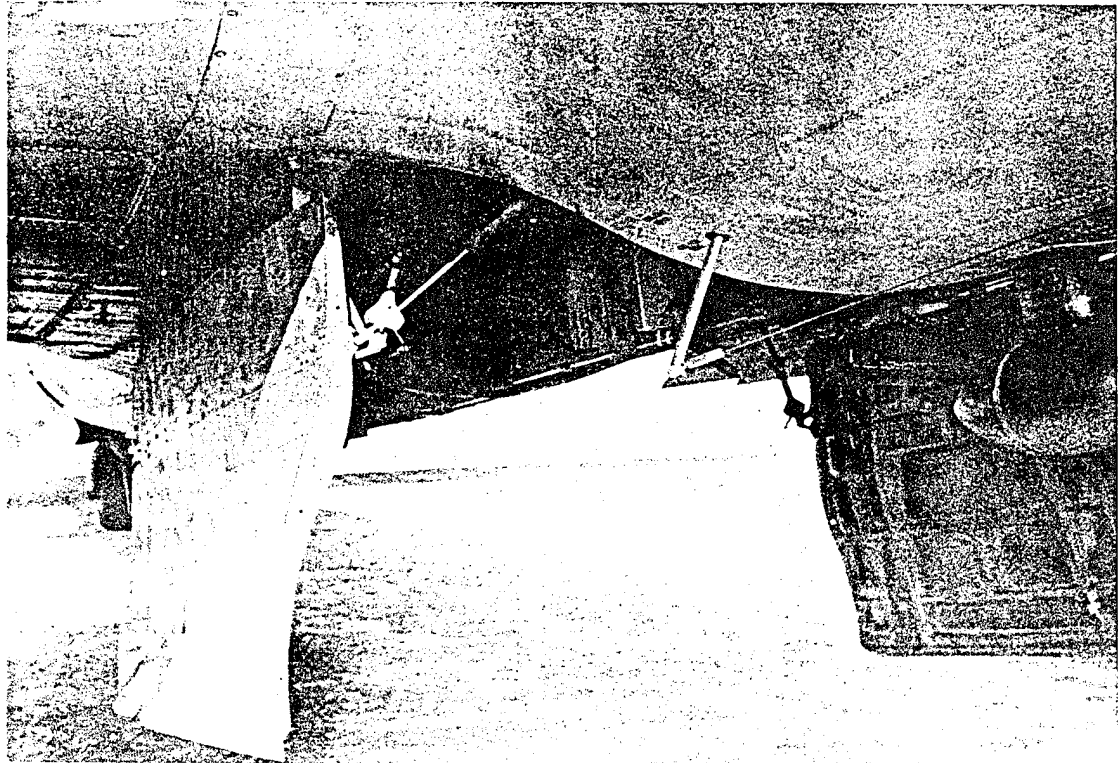
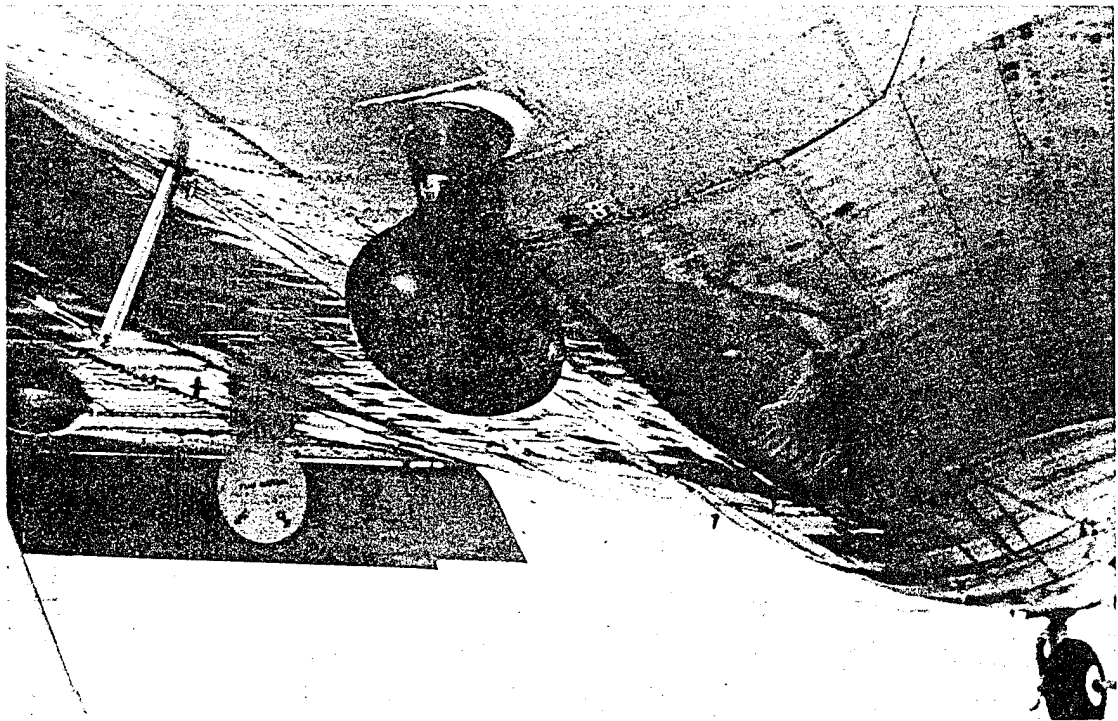


Fig. 6.17 Blast Damage to QB-17 Drone M, Easy Shot. (Above) bomb doors closed. (Below) bomb doors open.

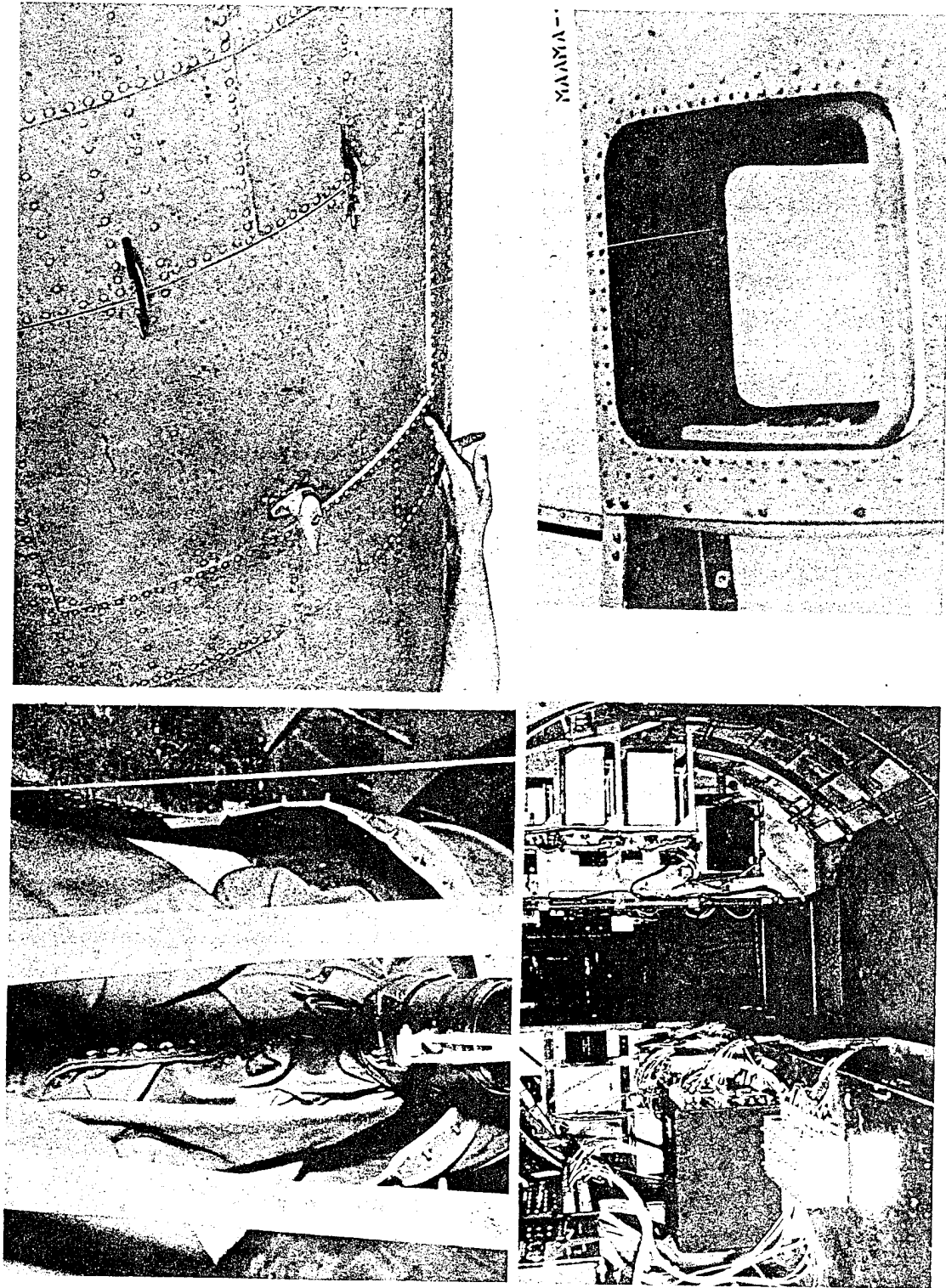


Fig. 6.18 Blast Damage to QB-17 Drone M, Easy Shot. (Upper left) tail-wheel-well cover blown out. (Upper right) entrance door sprung. (Lower left) radio-compartment floor boards blown in. (Lower right) tail-gunner's window blown in.

~~SECRET~~

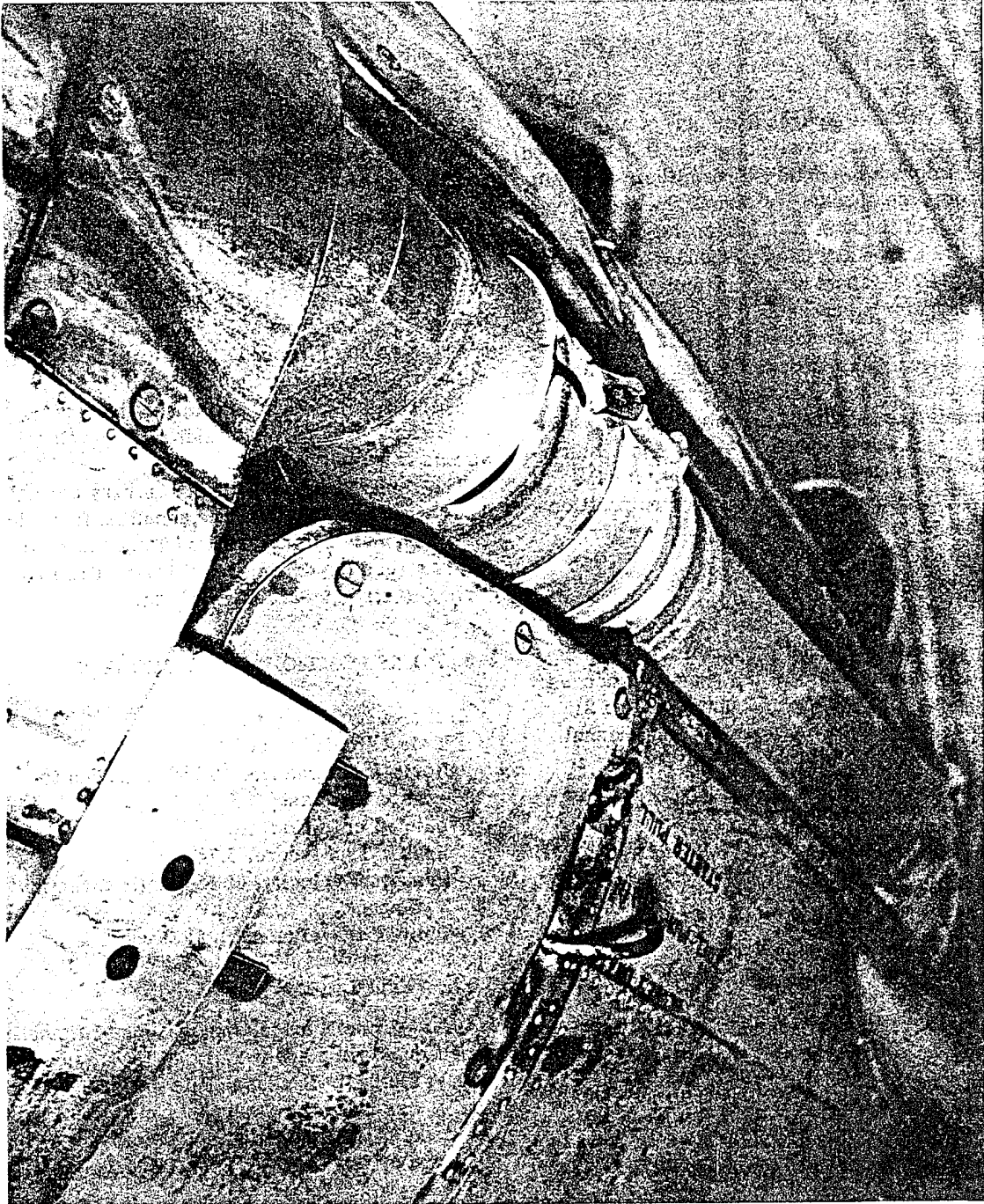


Fig. 6.19 Blast Damage to QB-17 Drone M, Easy Shot; Flexible Coupling of Exhaust Duct, No. 2 Engine

~~SECRET~~

course, straight and level, and 352 ft beyond the Carol position when the shock wave struck the airplane. The graph of the data from the radar-data recorder, Fig. 6.20, shows that the airplane was 230 ft short and 480 ft to the right of the assigned position when the shock wave passed and that it was flying a course of 44.75° . The navigator's report states that the heading was 42° . If these figures are correct and if the actual position of the airplane was that indicated by the information obtained from the radar-data recorder, the shock wave struck the drone from 64.2° left of the nose at a horizontal distance of 530 ft, at a true altitude of 11,000 ft, a vertical angle of 87.2° , and a slant range of 11,013 ft. The navigator's report indicated that the shock wave struck the airplane at $T_0 + 8.2$ sec. However, close examination of recordings made in the airplane, which included a recording of the master time signal, indicates that the shock wave struck the drone at $T_0 + 7.35$ sec. This difference in time partially accounts for the difference in the navigator's reported position and that shown by the radar-data recorder.

6.4.4 Load Data

The data from this mission are presented in Figs. 6.21 through 6.33. Channels 11, 13, and 23 were recorded but are not presented because of the lack of calibration. Channels 2 and 21 became open during the mission, and channel 22 was noisy; no data from these channels are presented.

The peak overpressure as recorded by the high-frequency recorder (Fig. 6.33) is very close to that predicted. Both channels of the recorder (high- and low-scale channels; see Sec. 2.5) are included to indicate the excellent correlation between the channels. Correction has not been made, however, for the time constant inherent in the recorder, so that neither the time durations nor the value of the slowly changing negative peak should be considered accurate as plotted.

The recorder was started by means of the blue box, so that the record starts a fraction of a second after time zero. The time marks from the radio are sharp and distinct on the record.

6.4.5 Heat Data

The temperatures as recorded on this drone are given in Table 6.2.

6.4.6 Radiological Data

The measurements of radiological dosage from the film badges in drone M are presented in Table 6.3.

6.4.7 Analysis

The radar position (Sec. 6.4.3) is chosen for the time as measured from the tape record (7.35 sec). The theoretical conditions for the actual position do not vary appreciably from those predicted. The theoretical time required for the shock wave to travel to this point in space is 7.1 sec.

There is some evidence of a change in the bending loads at time zero. However, there is too much possibility of change in loads or trim of the drone from the loss of the foil cover on the control surfaces to attempt to interpret these changes in terms of metal temperatures, as was done on the QT-33.

The remainder of the record is very normal. The long-period oscillations resulting from the shock are quickly damped, and 12 sec after the shock struck the drone ($T_0 + 19$ sec) it had returned to straight-and-level flight.

6.5 DORIS POSITION, QB-17 DRONE N

Assigned location (at shock)

True altitude, 12,000 ft

Horizontal distance, 12,758 ft headed toward the blast

Predicted condition

Peak overpressure, 0.78 psi

Peak gust velocity, 62 ft/sec (in direction of shock)

Time of travel (shock), 12.3 sec

6.5.1 Flight Log

QB-17 drone N made a normal take-off ahead of scheduled time and performed the mission without incident. Because of its assigned location, it was necessary that the drone go through the cloud. The flight data as reported¹ by ATU 3.4.2 are as follows:

Time

Start engines, 0216

Take-off, 0250

At assigned altitude, 0405

Shock arrival, 0627:10.2

Landing, 0740

~~SECRET~~

TABLE 6.2 HEAT MEASUREMENTS AT CAROL POSITION, EASY SHOT

Tape Location*	Material Thickness†	Color‡		Angle of Incidence	Max. Temp.§ (°F)	Temp. (°F)
		In	Out			
9	0.020	LOG	B	8° 32'	415 ± 25	
10	0.020	LOG	W	8° 32'	240	185.6
11	0.020	LOG	R	8° 32'	415 ± 25	
12	0.020	LOG	Y	8° 32'	320	265.6
13	0.020	LOG	BL	8° 32'	415 ± 25	
14	0.020	LOG	AP	8° 32'	350	295.6
15	0.020	LOG	A _s	8° 32'	300	245.6
18	0.040	LOG	LOG		135	80.6
19	0.040	LOG	LOG		130	75.6
20	0.040	LOG	LOG		130	75.6
21	0.040	LOG	LOG		130	75.6
22	0.040	LOG	LOG		130	75.6
23	0.040	LOG	LOG		130	75.6
24	0.040	LOG	LOG		130	75.6
25	0.032	DOG	Y	15° 45'	Not installed	
26	0.032	DOG	Y	27° 23'	240	185.6
27	0.032	DOG	Y	47° 29'	220	165.6
28	0.032	DOG	Y	68° 55'	170	115.6
29	0.032	DOG	Y	89° 04'	130	75.6
30	0.032	DOG	Y	27° 23'	280	225.6
31	0.032	DOG	Y	47° 29'	240	185.6
32	0.032	DOG	Y	68° 55'	210	155.6
33	0.032	DOG	Y	89° 04'	132	77.6
34	0.040	DOG	DOG		130	75.6
35	0.032	B	A _d		130	75.6
36	0.032	DOG	DOG		130	75.6
37	0.040	A _s	A _s		130	75.6

*See Table 3.9.

†Aluminum.

‡See Table 3.11.

§ Ambient temperature, 54.4°F.

~~SECRET~~

TABLE 6.3 RADIOLOGICAL DATA AT
CAROL POSITION, EASY SHOT

Location of Badge	Measured Exposure (roentgens)
Under pilot's seat	5.5 and 1.5
Under copilot's seat	5.5 and 5.5
Back of copilot's seat	6.5 and 5.5
Nose compartment	6.5 and 6.5

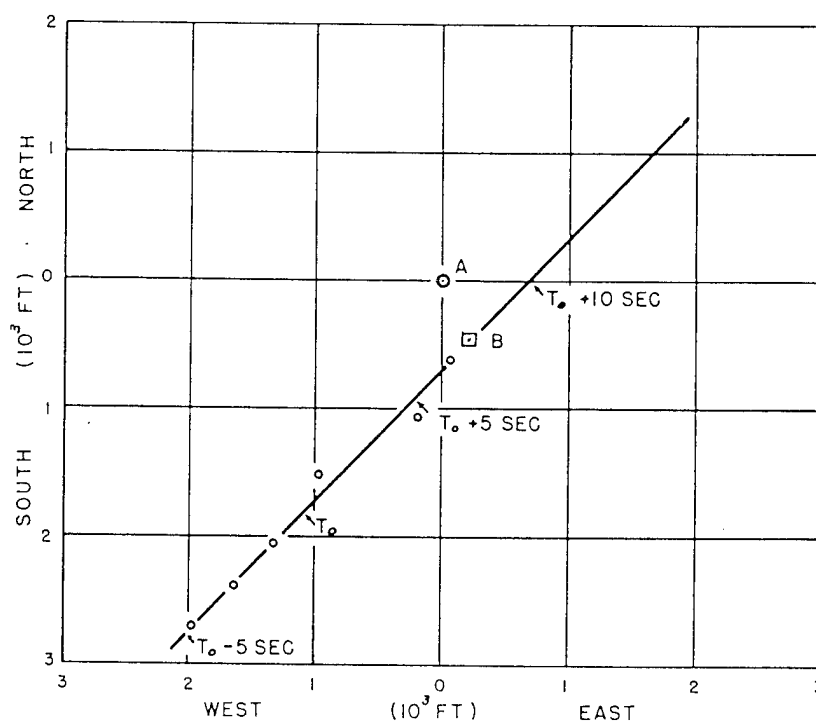


Fig. 6.20 Track, Radar-data Recorder, QB-17 Drone Carol, Easy Shot. Point A indicates Carol position.
Point B indicates actual location at shock.

SECRET

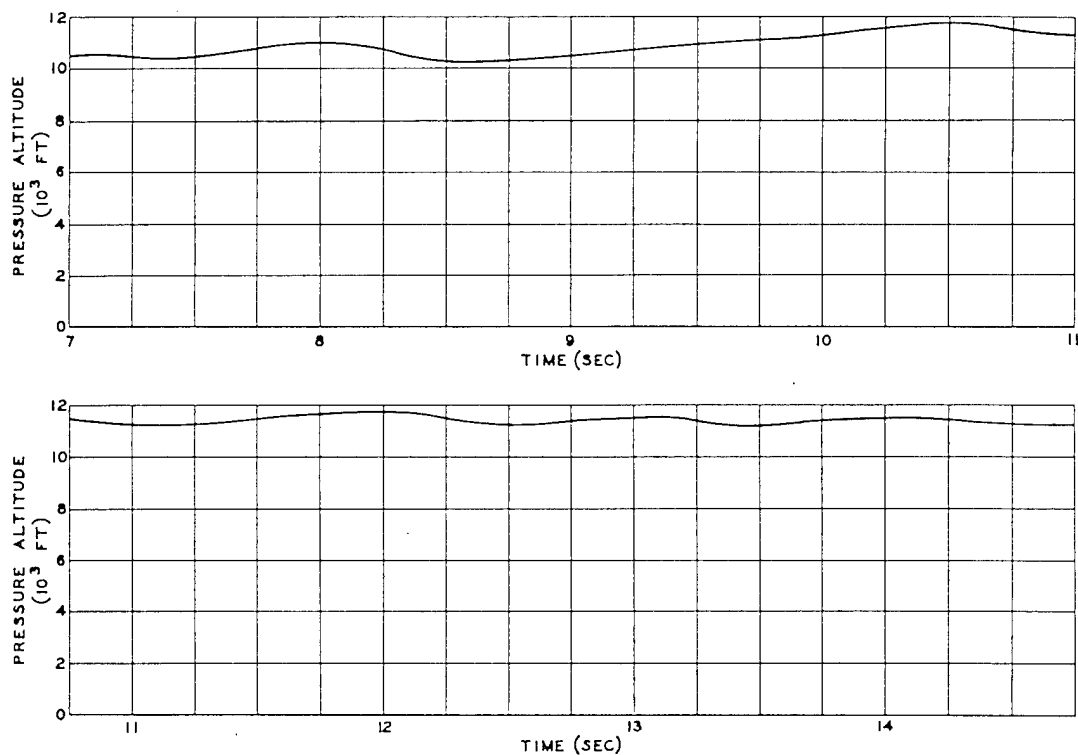


Fig. 6.21 Altitude, Channel 1, QB-17 M, Easy Shot

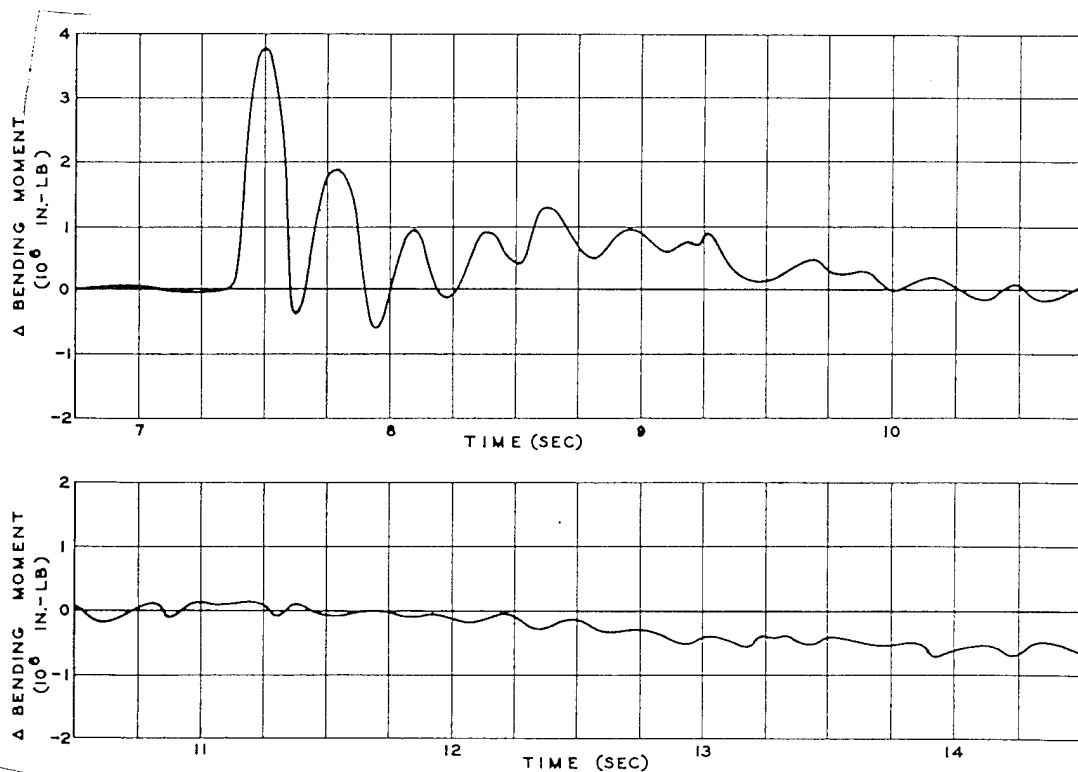


Fig. 6.22 Wing Bending, Right Wing Root, Channel 7, QB-17 M, Easy Shot

SECRET

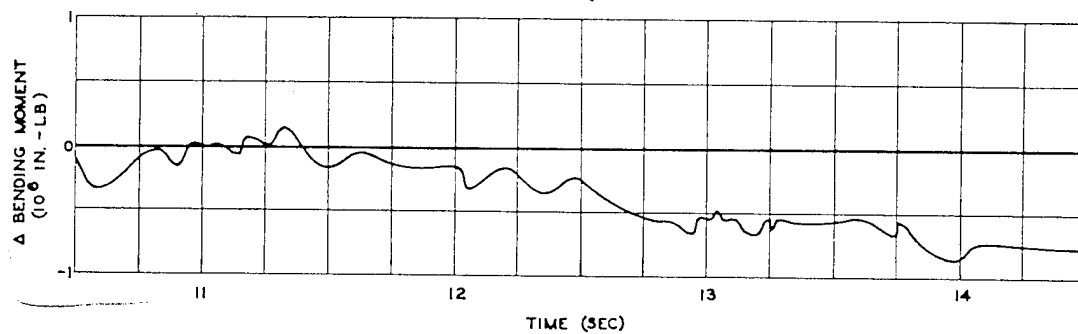
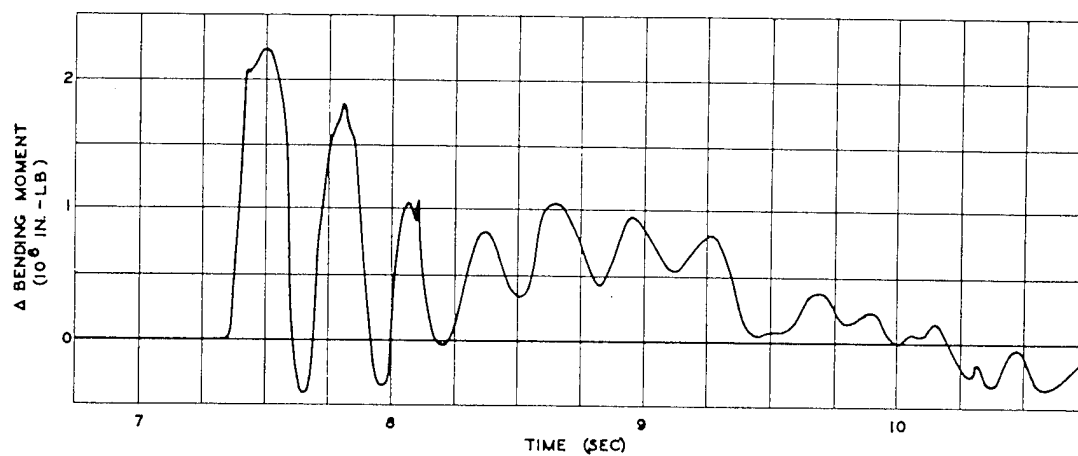


Fig. 6.23 Wing Bending, Left Wing Root, Channel 8, QB-17 M, Easy Shot

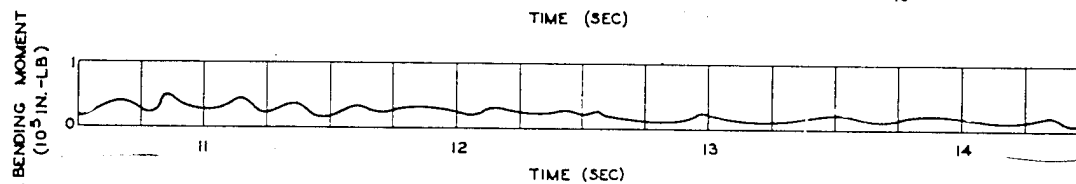
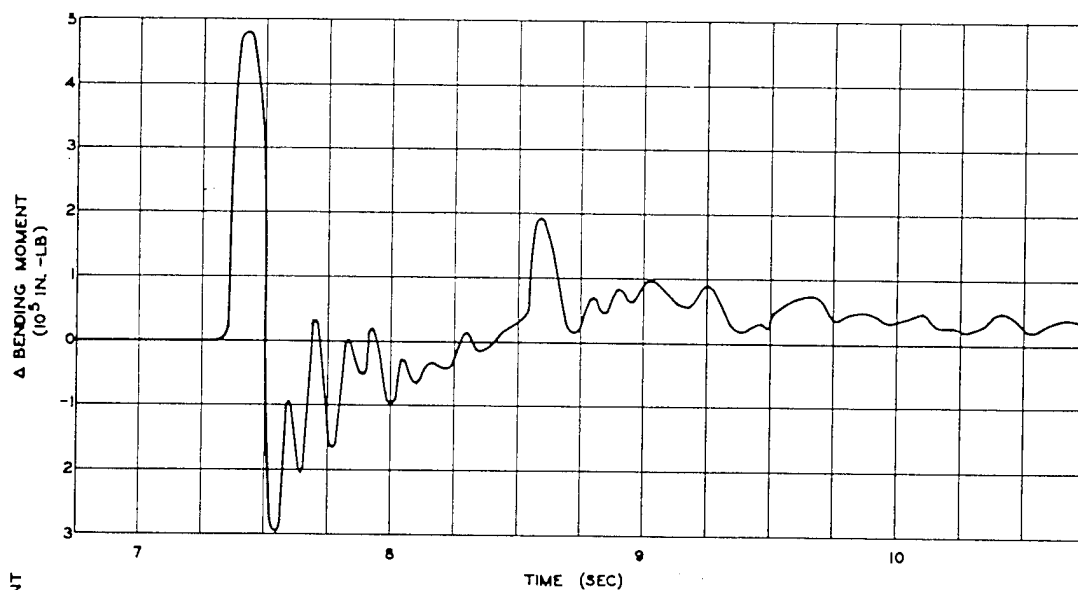


Fig. 6.24 Stabilizer Bending, Right Horizontal Stabilizer, Channel 9, QB-17 M, Easy Shot

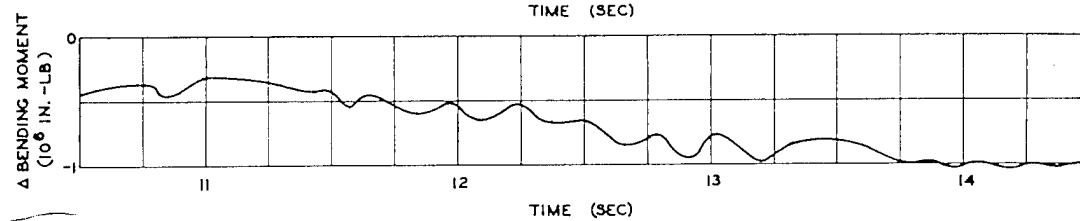
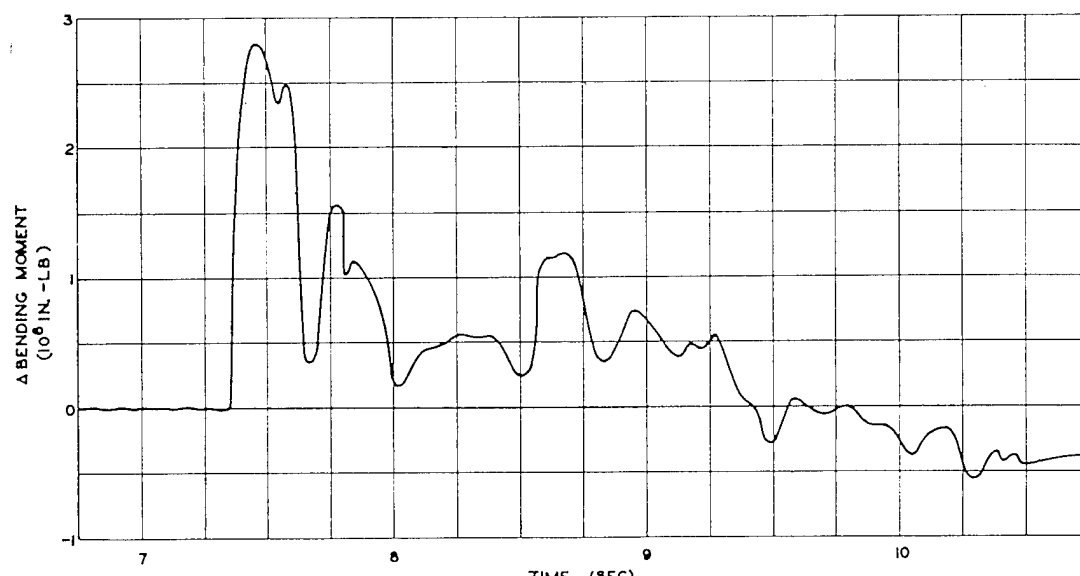


Fig. 6.25 Wing Bending, Outer Panel, Right Wing Station 19, Channel 10, QB-17 M, Easy Shot

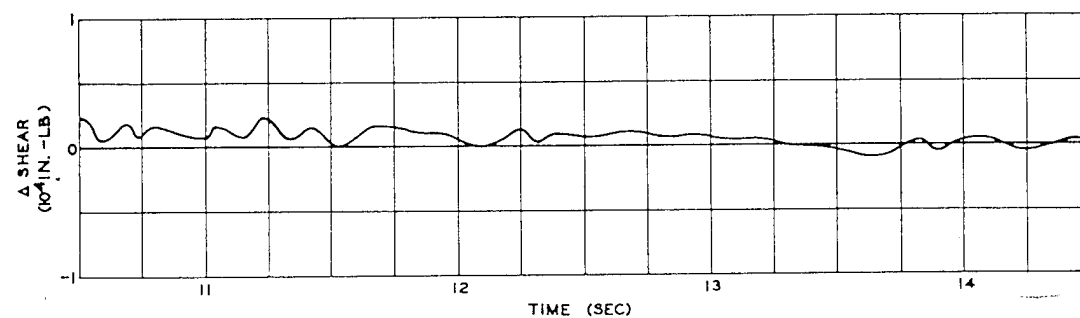
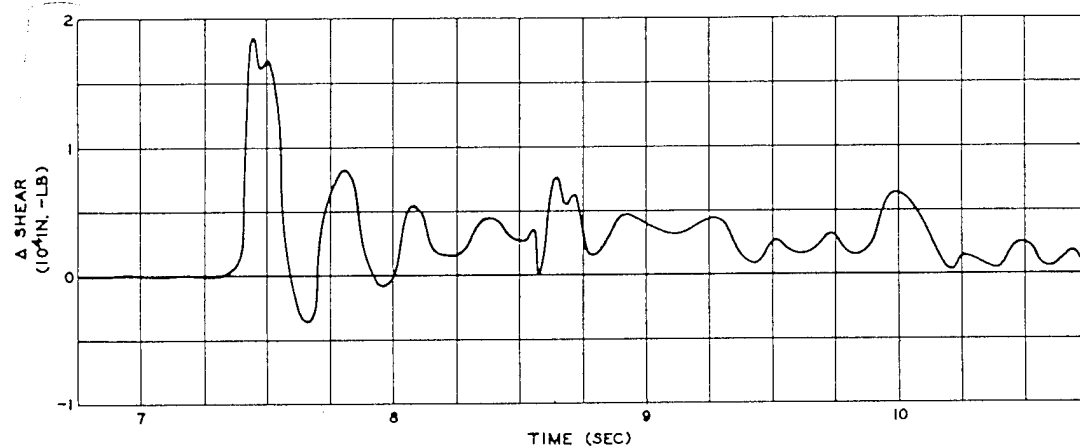


Fig. 6.26 Wing Shear, Right Wing Root, Channel 12, QB-17 M, Easy Shot

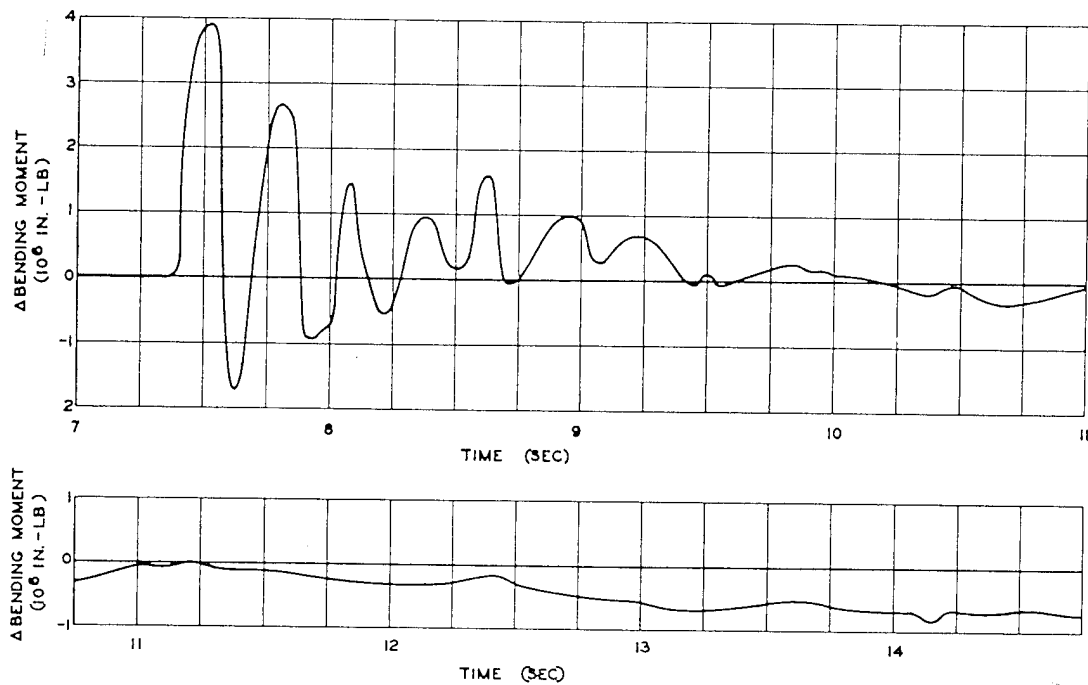


Fig. 6.27 Wing Bending, Mid-span, Right Wing Station 8.8, Channel 14, QB-17 M, Easy Shot

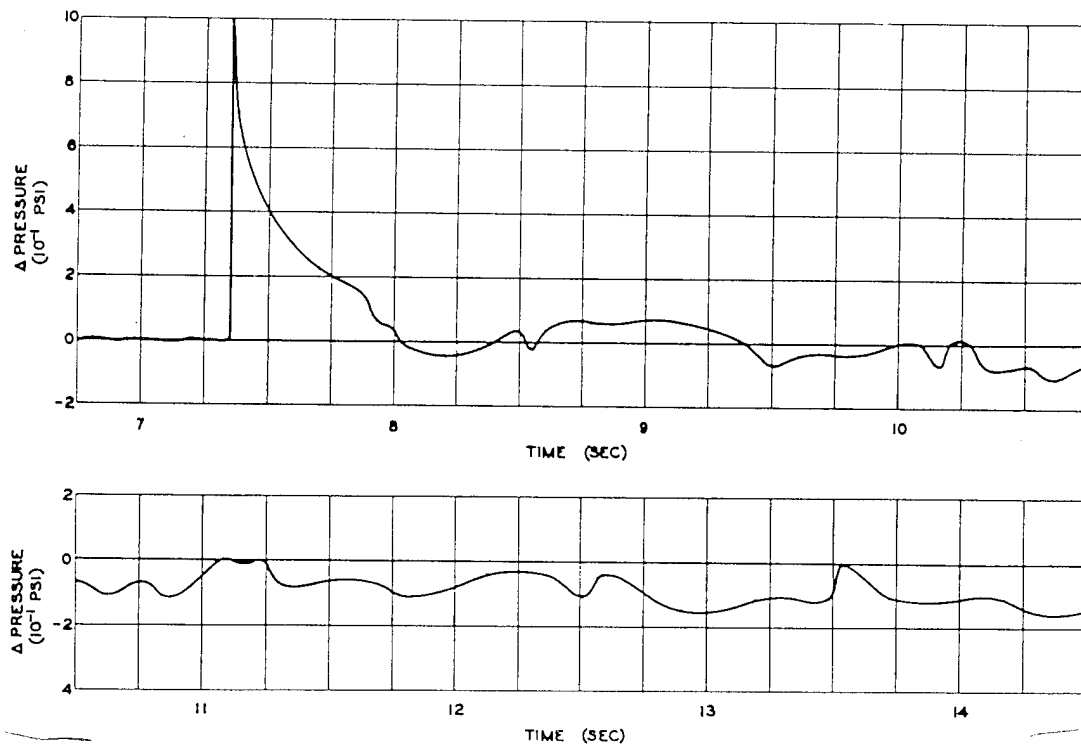


Fig. 6.28 Differential Pressure, 5% Chord, Right Wing Station 25.5, Channel 16, QB-17 M, Easy Shot

SECRET

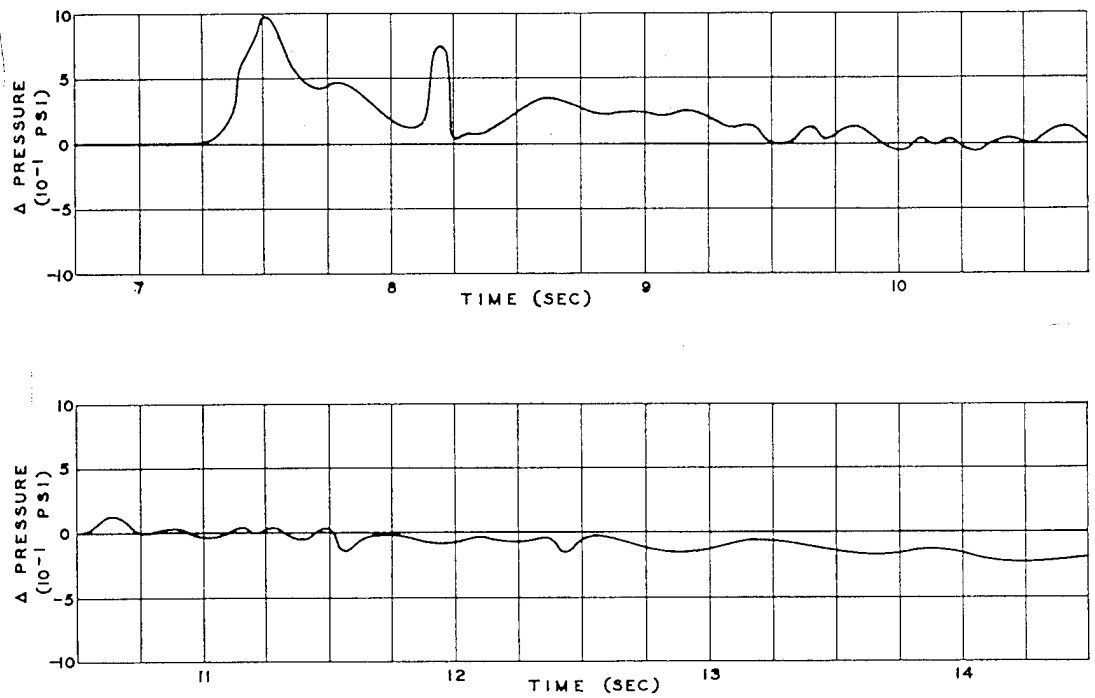


Fig. 6.29 Differential Pressure, 10% Chord, Right Wing Station 25.5, Channel 17, QB-17 M, Easy Shot

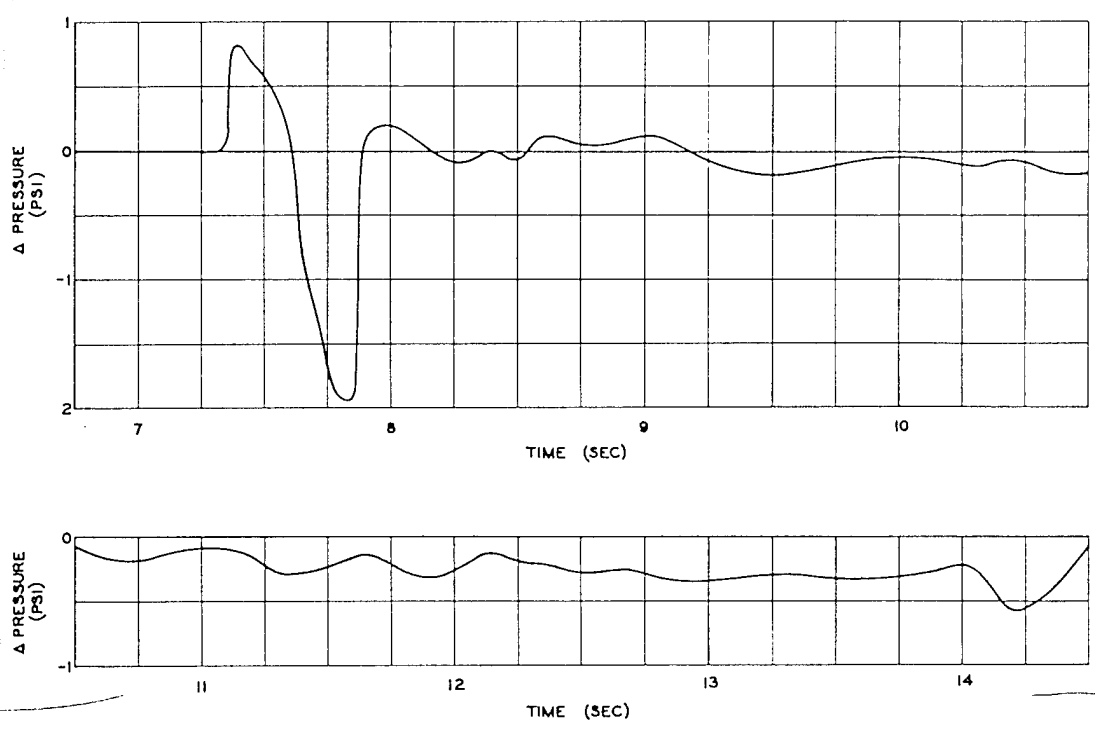


Fig. 6.30 Differential Pressure, 40% Chord, Right Wing Station 25.5, Channel 19, QB-17 M, Easy Shot

SECRET

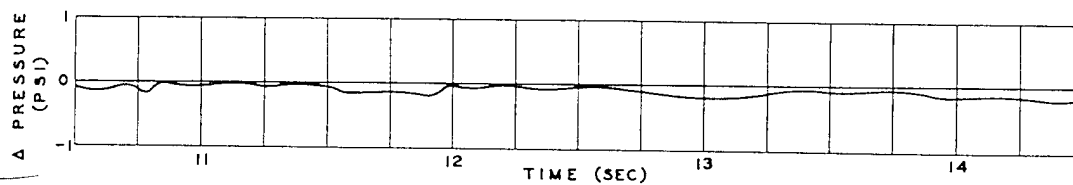
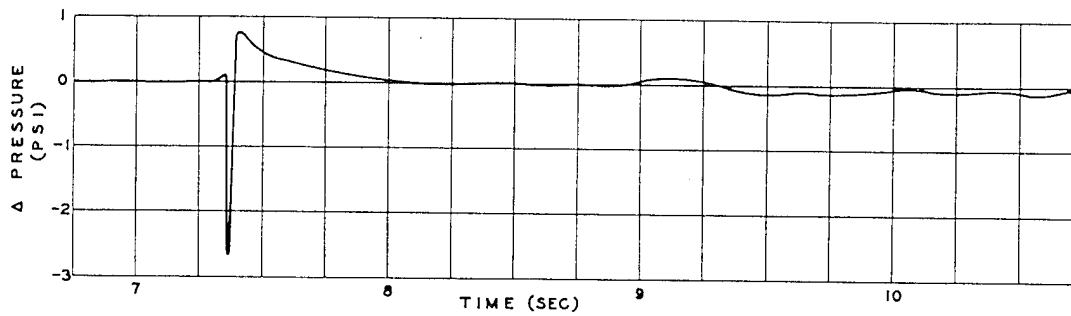


Fig. 6.31 Differential Pressure, 60% Chord, Right Wing Station 25.5, Channel 20, QB-17 M, Easy Shot

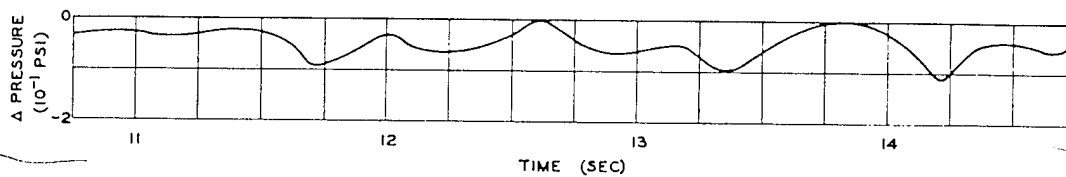
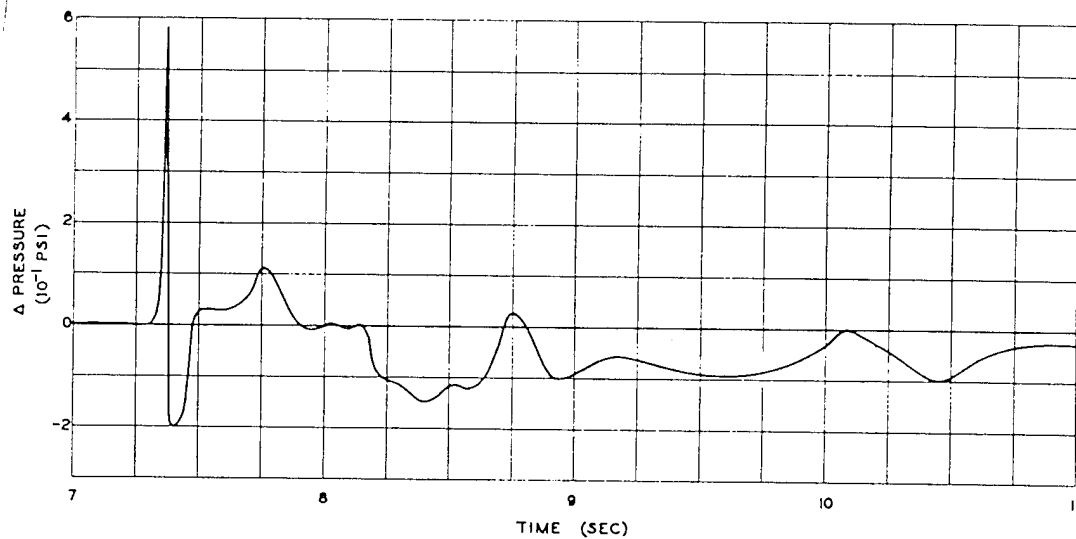


Fig. 6.32 Differential Pressure, 40% Chord, Right Horizontal Stabilizer, Channel 24, QB-17 M, Easy Shot

SECRET

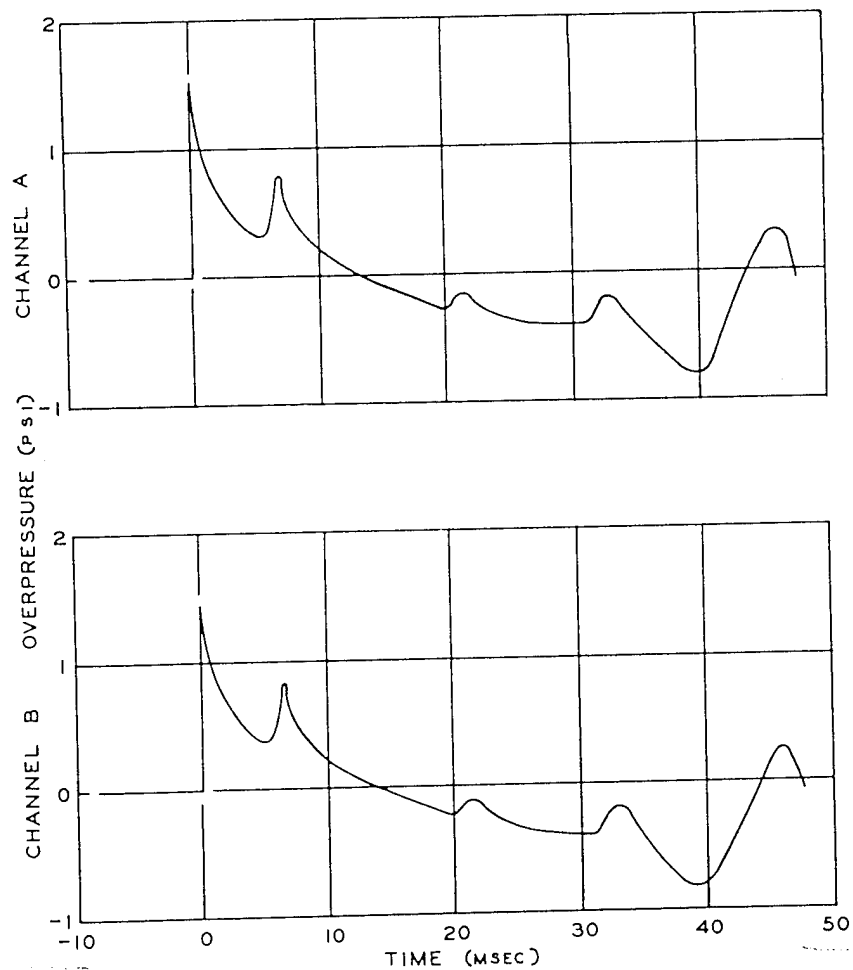


Fig. 6.33 Overpressure, High-frequency Pressure Recorder, QB-17 Drone M, Easy Shot

SECRET

Meteorological conditions at altitude

True altitude, 12,000 ft
Pressure altitude, 11,200 ft
Outside air temperature, +11°C
Wind direction (from), 080° (azimuth)
Wind velocity, 11 knots

Airplane parameters at shock arrival

Indicated airspeed, 132 knots
Ground speed, 254 ft/sec
Ground track azimuth, 045°
Horizontal angle from blast, 225° (azimuth)
Vertical angle from blast, * 43.3°
Horizontal distance from blast, 12,758 ft
Slant distance from blast, * 17,510 ft
Shock struck drone from front and below

6.5.2 Airplane Condition

Before take-off the instruments were given a final check. The telemetering was equipped with a complete set of sensing elements. The recorder system was complete except for five channels as follows:

Channel 3—acceleration, c.g.
Channel 4—acceleration, aft fuselage
Channel 5—acceleration, No. 3 engine
Channel 6—acceleration, No. 4 engine
Channel 20—pressure, 60 per cent chord, right wing station 25.5

The fuel tanks contained 2,100 gal at the time the engines were started—1,700 gal (10,200 lb) in the main tanks and 400 gal (2,400 lb) in the Tokyo tanks. The gross weight at take-off was 50,500 lb, with the c.g. at 28.7 per cent m.a.c.

The take-off was normal and the director reported good control. The gross weight at the time the shock wave struck the airplane was computed to have been 45,470 lb with the c.g. at 27.7 per cent m.a.c. The director reported that the airspeed (as viewed by television) "... jumped to 180 mph and (pressure) altitude from 11,300 to 12,100 indicated."

Because of the location assigned for this position, it was not feasible to maneuver the drone so as to miss the cloud. The airplane entered the turbulent area of the cloud approximately 54 sec after time zero.

The landing was normal and no damage to the airplane was apparent. It was impossible to

examine the airplane closely until after it had been decontaminated. The airplane had become radioactive from its pass through the cloud. After decontamination it was discovered that superficial damage had been done to the airplane; the fairing on the underneath of each wing root had been bent as shown in Fig. 6.34. It appeared that the wing had been deflected upward so far that the fairing had torn loose from the screws that attached it to the wing or to the fuselage and that, when the wing returned to its normal position, the fairing had buckled inward. Following this line of reasoning, the wing was examined carefully for other evidence of severe bending. No unusual wrinkles or permanent deformation was discovered on the wings; however, paint had flaked off around the heads of some of the rivets. The root fairing above the left wing was torn near the trailing edge as shown in Fig. 6.34. A close-up of the damage at the root of the trailing edge of the left wing and the pressure damage on the underside of the fuselage are shown in Fig. 6.35.

6.5.3 Radar Position Data

According to the radar-operator's report, drone N was flying straight and level at 12,000 ft on a course of 45°, 150 ft to the left and 250 ft short of the assigned Doris position when the shock wave struck the airplane. The graph of the data from the radar-data recorder, Fig. 6.36, shows that the airplane was 260 ft beyond and 95 ft to the left of the assigned position when the shock wave passed and that it was flying a course of 45.9°. The navigator's report states that the heading was 47°. If these figures are correct and if the actual position of the airplane was that indicated by the information obtained from the radar-data recorder, the shock wave struck the drone from 1.5° left of the nose at a horizontal distance of 11,740 ft, at a vertical angle of 45.6°, and at a slant range of 16,800 ft. The radar-operator's report indicated that the shock wave struck the airplane at $T_0 + 9.4$ sec. However, close examination of recordings made in the airplane, which included a recording of the master time signal, indicates that the shock wave struck the drone at $T_0 + 12.03$ sec. This difference in time partially accounts for the difference in the radar-operator's reported position and that shown by the radar-data recorder.

*Computed from data in Navigator's Report, reference 1.

SECRET

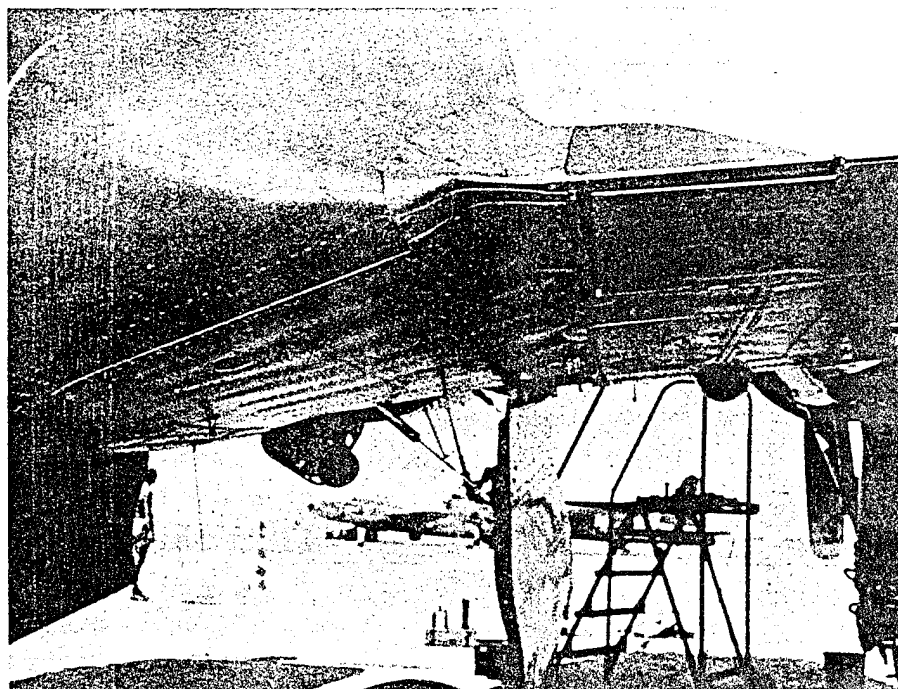
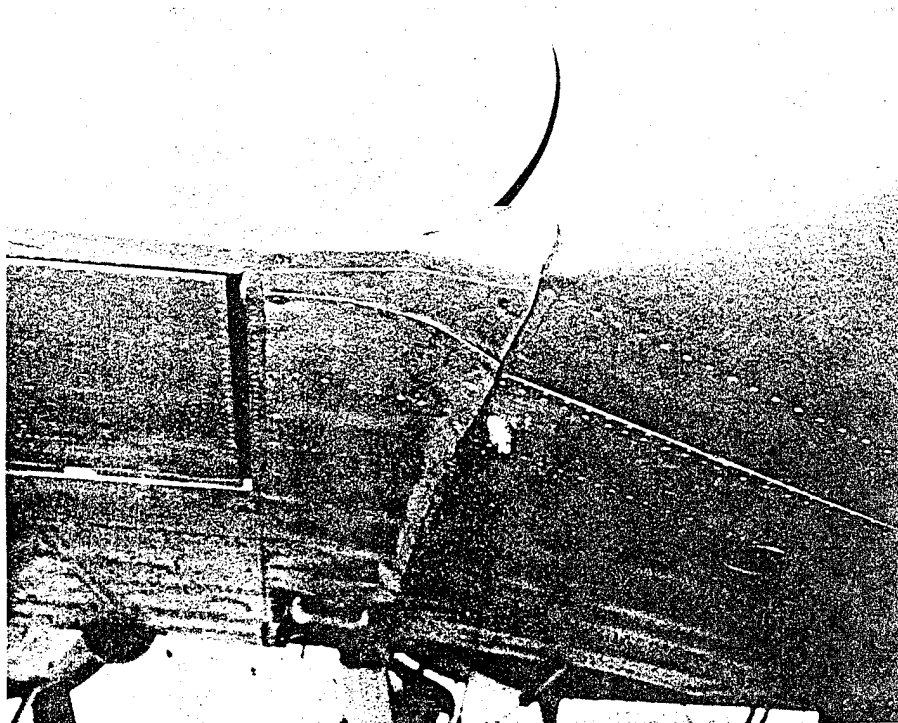
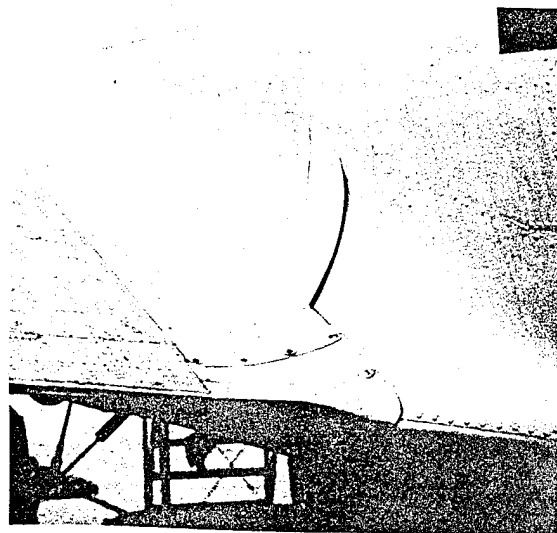


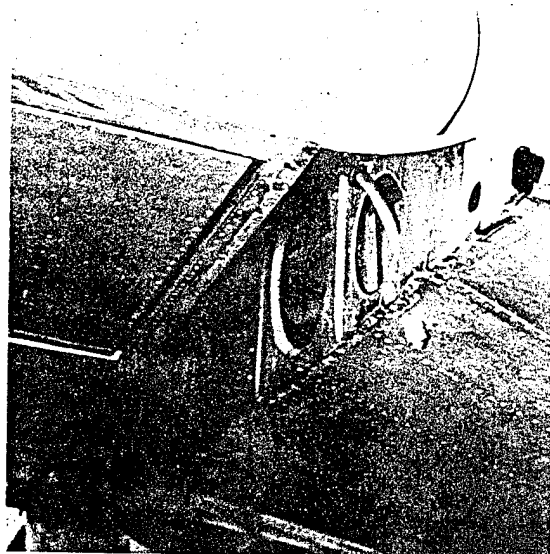
Fig. 6.34 Damage to QB-17 Drone N, Easy Shot. (Above) left wing root. (Below) right wing root.

SECRET

A



B



C

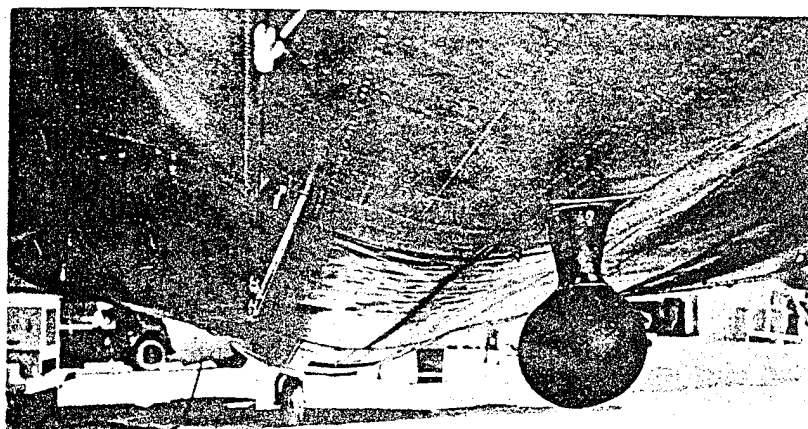


Fig. 6.35 Damage to QB-17 Drone N, Easy Shot. A, tear in wing-root fairing. B, close-up of wing-root fairing. C, damage to underside of fuselage.

~~SECRET~~

6.5.4 Load Data (Shock)

The data from this mission are presented in Figs. 6.37 through 6.48. Channels 1, 2, 7, 17, and 23 failed during the mission, and channels 11 and 13 had no calibrations; no data from these channels are included.

The tape record from this mission was severely affected by shrinkage due to humidity. It was necessary to play back the record a number of times, concentrating each time on aligning the track for one channel. Consequently the record was in rather poor shape at the end of playback. The graphs represent considerable effort and are believed to reproduce faithfully the loads experienced by the drone.

The record from the high-frequency pressure recorder was so badly fogged from the radiation in the cloud that it was unreadable.

6.5.5 Load Data (Cloud)

Although the strain-gauge data from the passage through the atomic cloud have no significance in a study of blast effects, the data are here presented as a matter of interest for comparison with the blast data and for explanation of the damage to the airplane.

In order to establish a convenient time axis for these graphs, a 9-sec interval was chosen. This interval does not include quite all the time in the cloud. Thus the drone was in the process of being loaded when the graphs start and had not quite emerged from the turbulence when the graphs stop. The zero reference for the incremental load is again the level-flight condition taken just before the loading occurred.

Although the channels measuring torsion are not shown because of insignificant calibration outputs, the failure of the wing fillets indicates a large torsional load. The torsion at the root (wing station 1) was recorded; however, calibration data are not available to reduce the measurements to actual numbers. The measurements indicate that an increment of torsion at the root of 60 per cent of cal plus occurred at 61.150 sec. The calibrating torsion of 420,000 in.-lb was not discernible on the record; therefore the cloud load must have been at least 10 times that load, or at least 4,200,000 in.-lb. This torsion is negative (leading edge down) and is superimposed on a peak of bending moment at the root of approximately 2,780,000 in.-lb as indicated by the measurements on the

opposite wing, Fig. 6.49. This combination of negative torsion and positive bending would have been additive on the rear spar and accounts for the failure in the fairing. Thus the bending at the rear spar amounted to about 3,900,000 in.-lb and that at the front spar amounted to about 380,000 in.-lb. This amounts to approximately 85 per cent of the limit load on the rear spar.

The pressures during the cloud passage are not considered significant and are not presented because the pressure changes could be associated with either changes in lift or changes in density of the air in the cloud. The data from this mission are presented in Figs. 6.49 through 6.54.

6.5.6 Heat Data

The temperatures as measured on this drone are presented in Table 6.4. The temperatures shown include the passage through the cloud.

6.5.7 Radiological Data

The measurements of radiological dosage from the film badges on drone N are presented in Table 6.5.

6.5.8 Analysis

The location of the drone at the time the shock wave struck at $T_0 + 12.1$ sec is described in Sec. 6.5.3. The theoretical conditions at this point in space are essentially those predicted for Doris position.

A comparison of the loads from the shock and from the cloud justifies the preliminary assumption that the structural damage was caused by the turbulence in the cloud. Obviously this drone was in the most turbulent area of the cloud, the "puff," at a very low altitude. A computation of the gust velocities has not been attempted, but they would probably exceed 150 to 200 ft/sec. One pertinent conclusion to be drawn from these data is that a rugged airframe is a necessity for any drone which is used to enter the cloud, where the drone is likely to encounter gusts of such velocities. These loads illustrate the conditions which, fortunately, have been avoided by the cloud-sampling drones in the past tests.

The recorder was started by means of the radio signal, and a clear stabilized record was obtained at time zero. There is no evidence of

~~SECRET~~

TABLE 6.4 HEAT MEASUREMENTS FROM QB-17 DRONE N, EASY SHOT

Tape Location*	Material Thickness† (in.)	Color‡		Angle of Incidence	Max. Temp.§ (°F)	Temp. (°F)
		In	Out			
1	0.25¶	P	P	9° 35'	130	83.6
2	0.032	LOG	Y	49° 02'	130	83.6
3	0.020	LOG	A	76° 24'	130	83.6
4	0.032	DOG	Y	60° 07'	130	83.6
5	0.032	A _d	A _s	52° 23'	130	83.6
6	0.020	LOG	AP	49° 02'	132	85.6
7	0.25¶	P	P	87° 13'	145	98.6
8	0.032	B	BL	87° 13'	145	98.6
9	0.020	LOG	B	49° 02'	145	98.6
10	0.020	LOG	W	49° 02'	130	83.6
11	0.020	LOG	R	49° 02'	132	85.6
12	0.020	LOG	Y	49° 02'	130	83.6
13	0.020	LOG	BL	49° 02'	143	96.6
14	0.020	LOG	AP	49° 02'	130	83.6
15	0.020	LOG	A	49° 02'	130	83.6
16	0.020	LOG	A	30° 37'	145	98.6
17	0.040	LOG	A	30° 37'	140	93.6
18	0.040	LOG	LOG		130	83.6
19	0.040	LOG	LOG		135	88.6
25	0.032	B	Y	57° 23'	130	83.6
26	0.032	B	Y	60° 28'	130	83.6
27	0.032	B	Y	68° 31'	130	83.6
28	0.032	B	Y	80° 32'	130	83.6
29	0.032	B	Y	86° 02'	130	83.6
30	0.032	B	Y	60° 28'	130	83.6
31	0.032	B	Y	68° 31'	130	83.6
32	0.032	B	Y	80° 32'	130	83.6
33	0.032	B	Y	86° 02'	130	83.6

* See Table 3.9.

† Aluminum except as marked.

‡ See Table 3.11.

§ Ambient temperature, 46.4°F.

¶ Plexiglas.

SECRET

TABLE 6.5 RADIOLOGICAL DATA FROM
QB-17 DRONE N, EASY SHOT
(Includes Pass through Atomic Cloud)

Location of Badge	Measured Exposure (roentgens)
Back of pilot's seat	1,100 and 1,100
Under copilot's seat	1,100 and 1,100
Under pilot's seat	1,100 and 1,100
Nose compartment	1,300 and 1,400

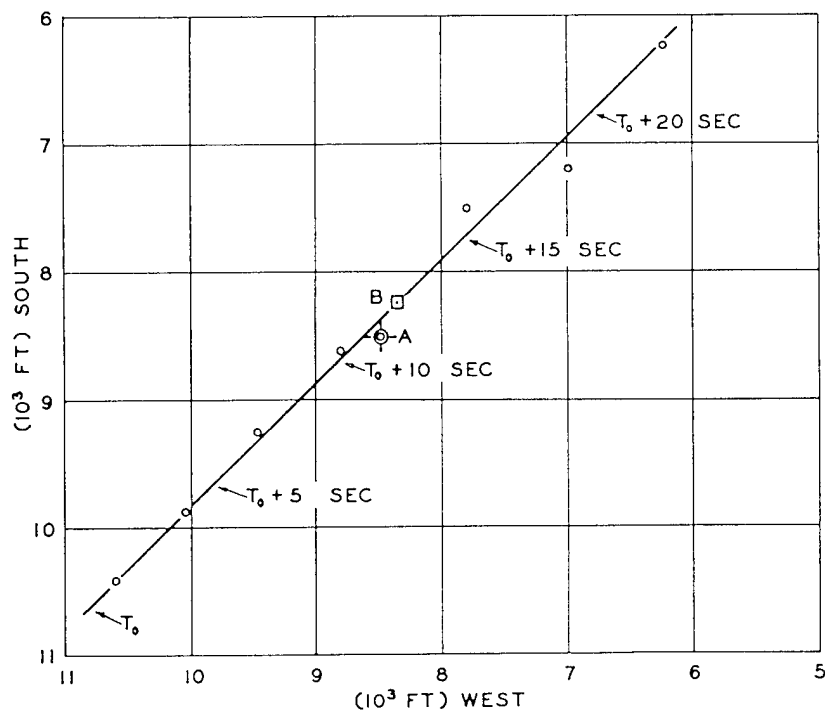


Fig. 6.36 Track, Radar-data Recorder, QB-17 Drone Doris, Easy Shot. Point A indicates Doris position. Point B indicates actual location at shock.

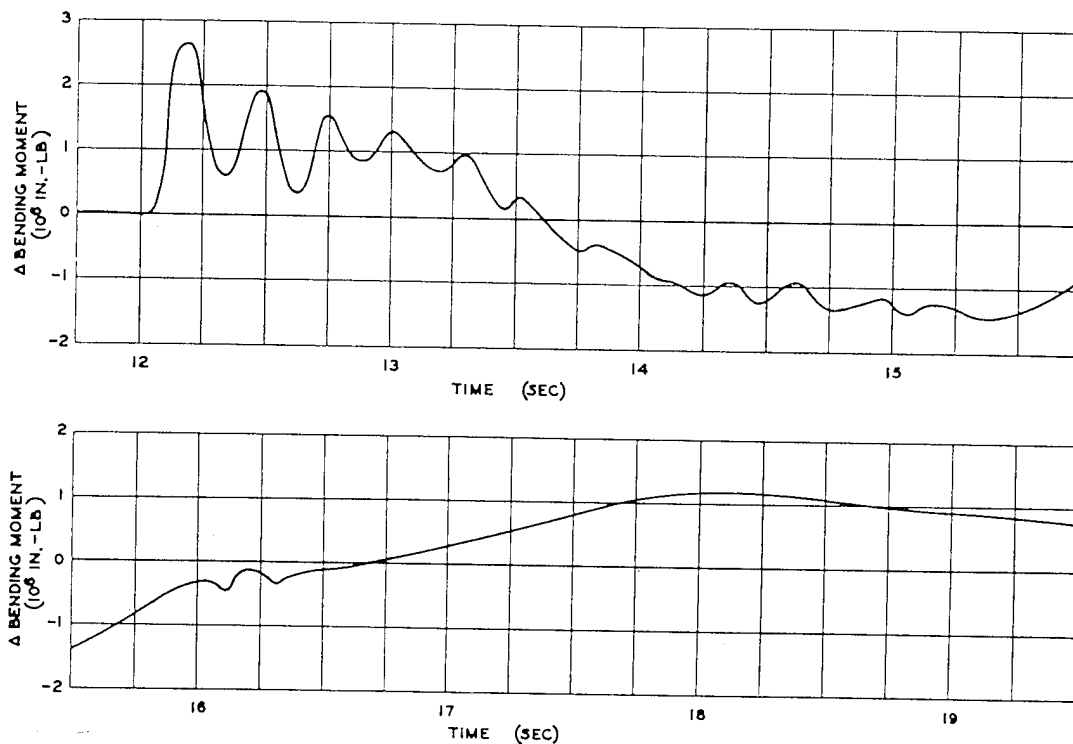


Fig. 6.37 Wing Bending, Left Wing Root, Channel 8, QB-17 N, Easy Shot

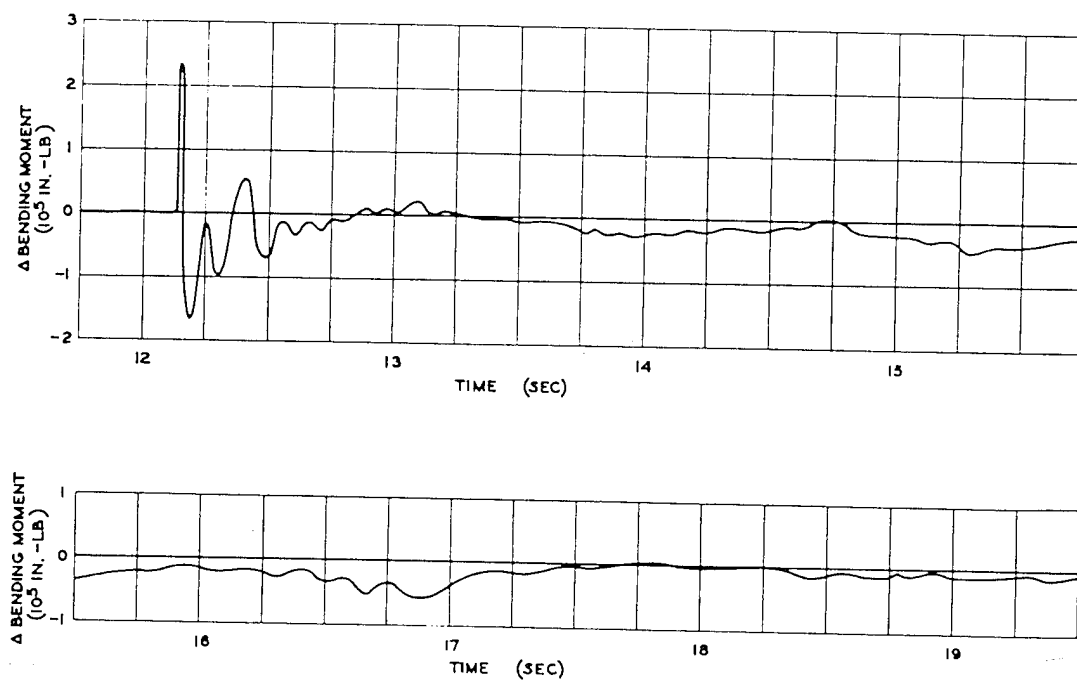


Fig. 6.38 Stabilizer Bending, Right Horizontal Stabilizer, Channel 9, QB-17 N, Easy Shot

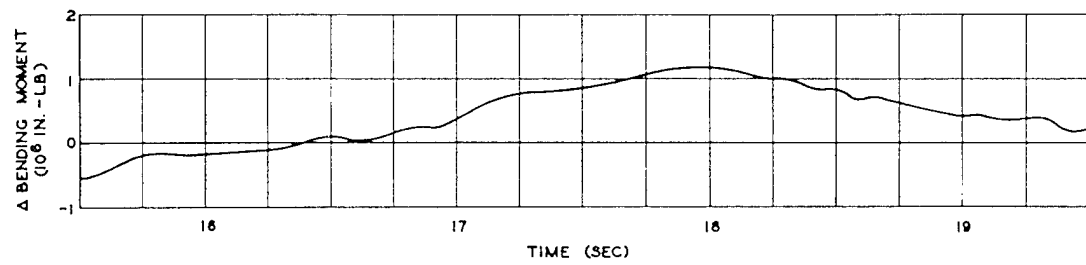
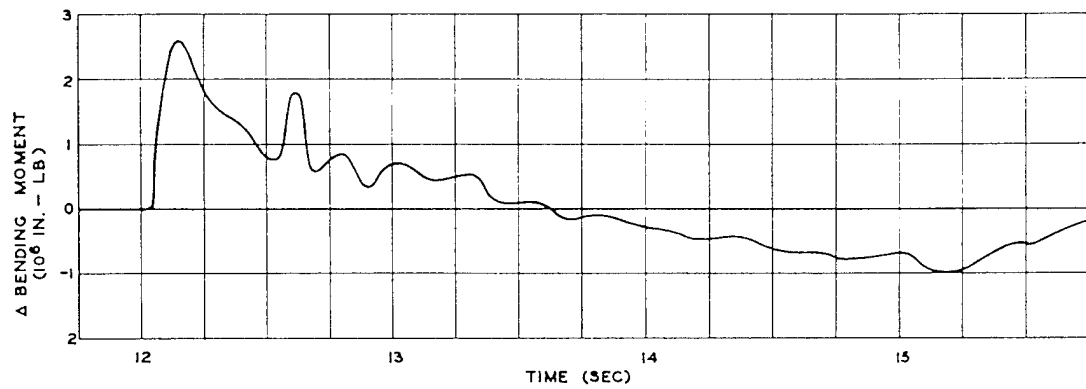


Fig. 6.39 Wing Bending, Outer Panel, Right Wing Station 19, Channel 10, QB-17 N, Easy Shot

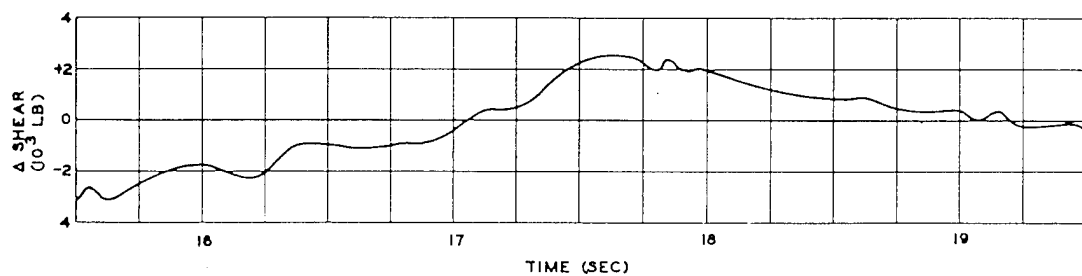
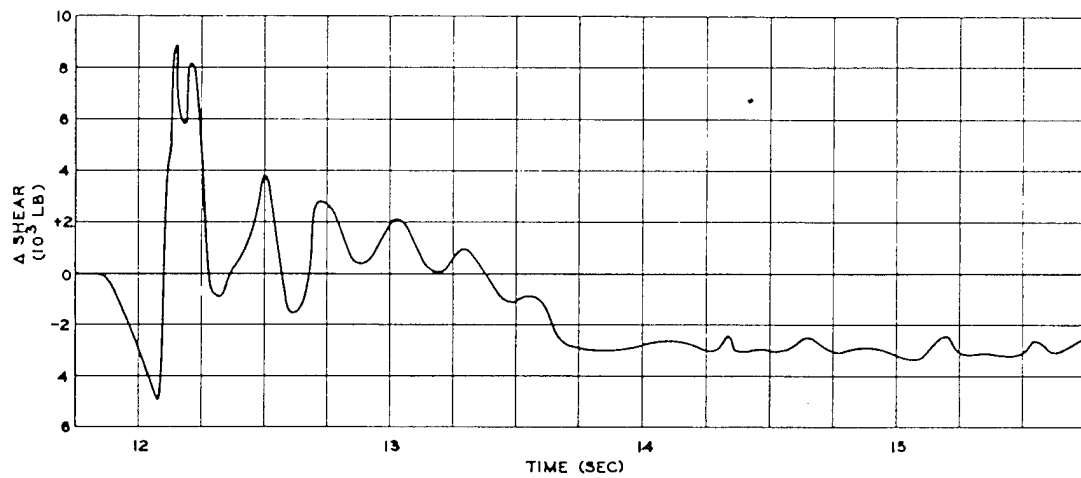


Fig. 6.40 Wing Shear, Right Wing Root, Channel 12, QB-17 N, Easy Shot

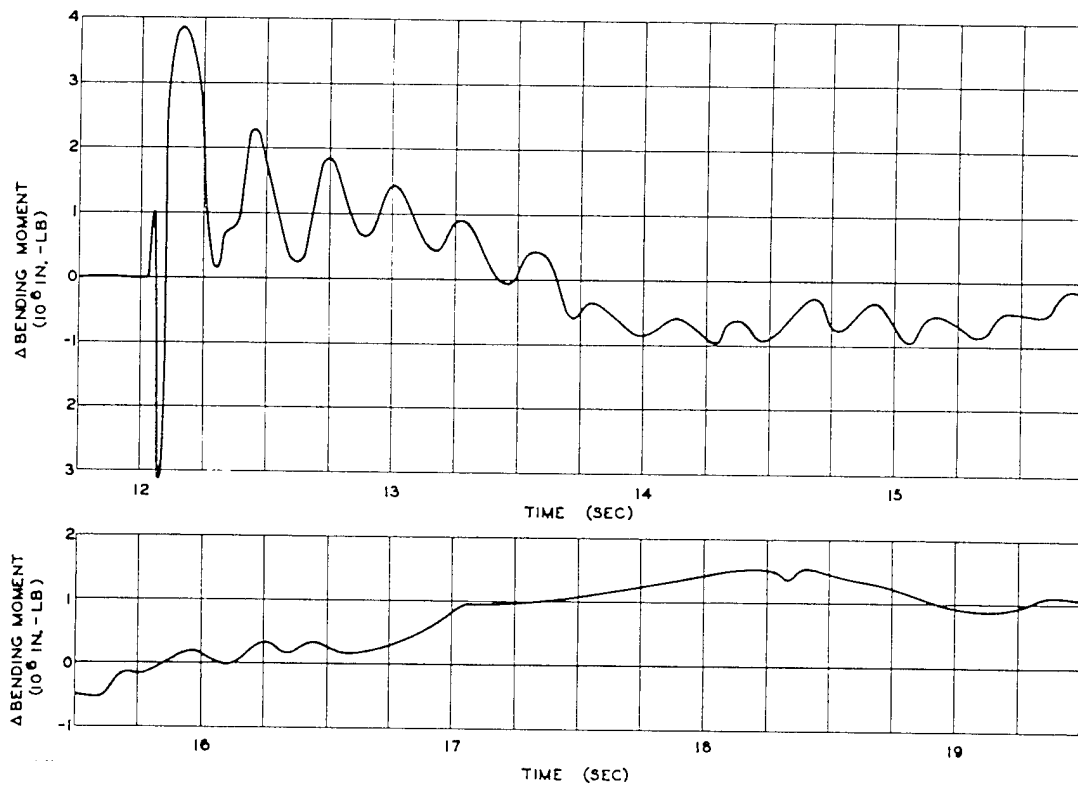


Fig. 6.41 Wing Bending, Mid-span, Right Wing Station 8.8, Channel 14, QB-17 N, Easy Shot

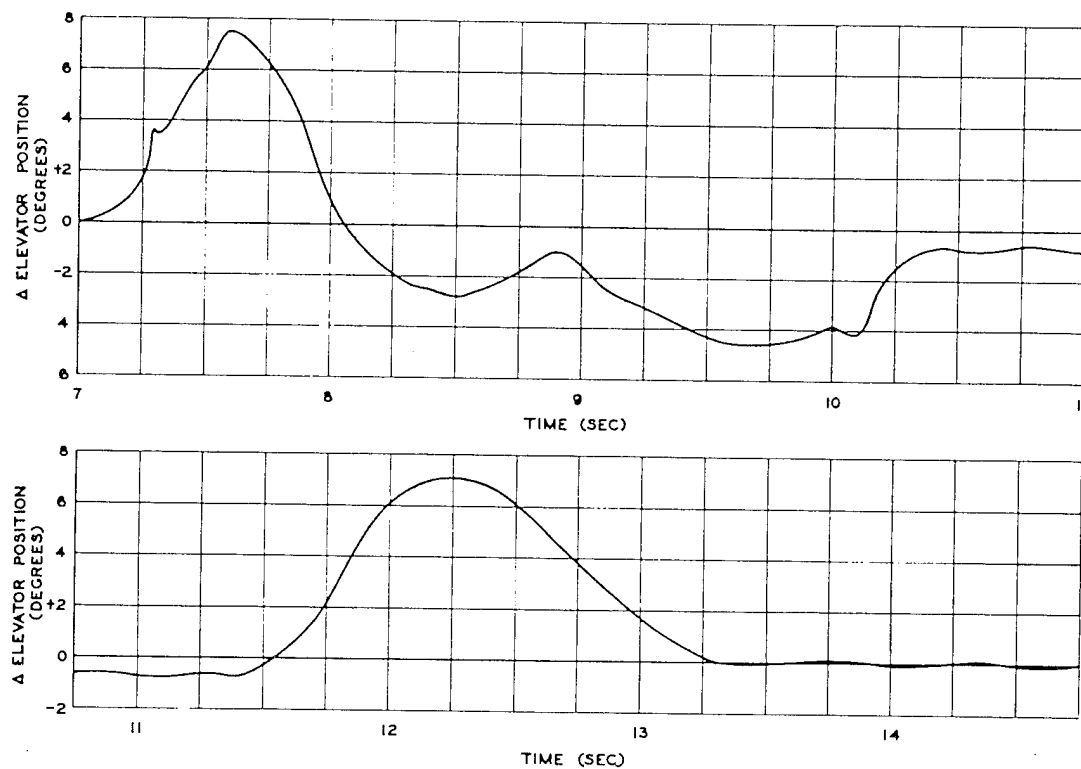


Fig. 6.42 Elevator Position, Channel 15, QB-17 N, Easy Shot

~~SECRET~~

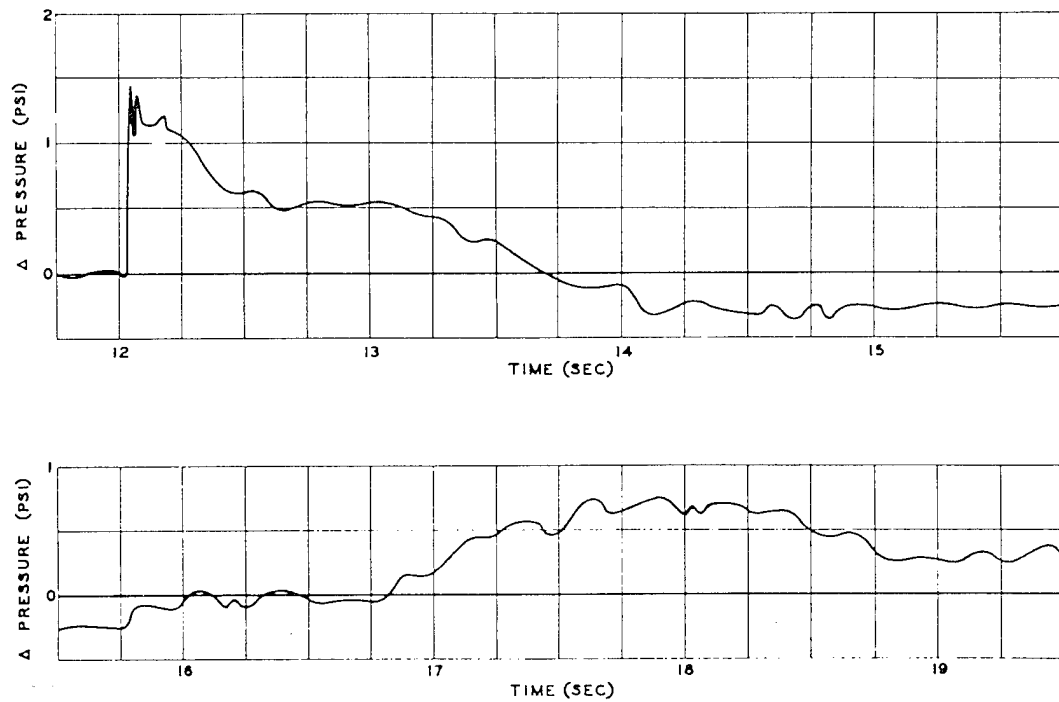


Fig. 6.43 Differential Pressure, 5% Chord, Right Wing Station 25.5, Channel 16, QB-17 N, Easy Shot

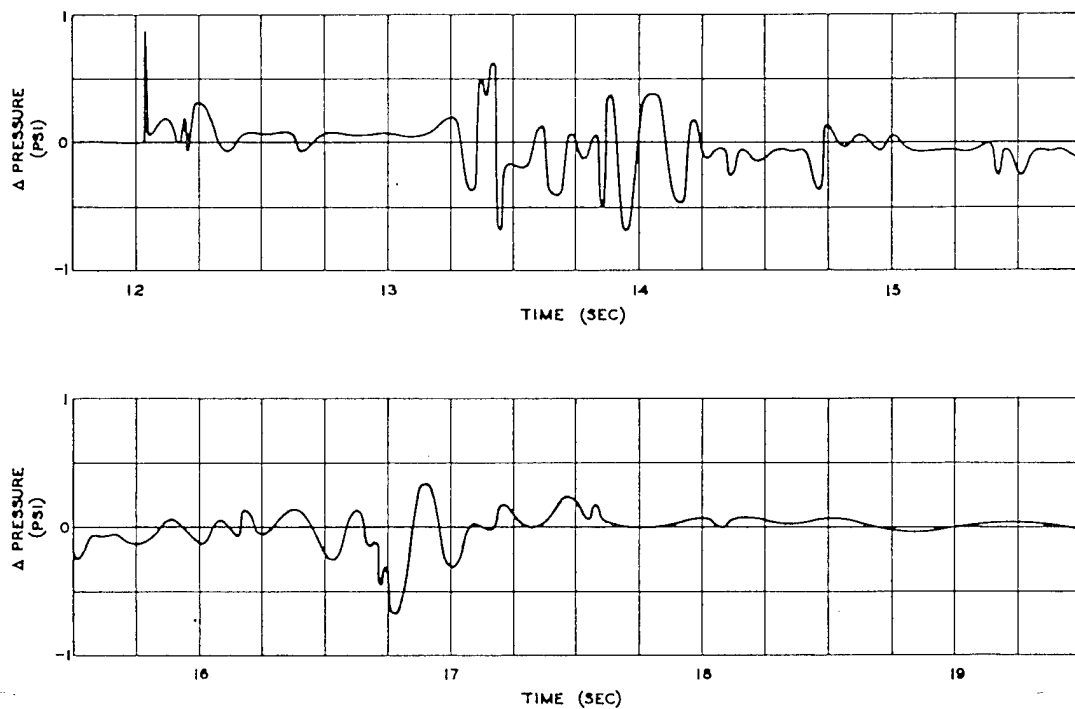


Fig. 6.44 Differential Pressure, 20% Chord, Right Wing Station 25.5, Channel 18, QB-17 N, Easy Shot

~~SECRET~~

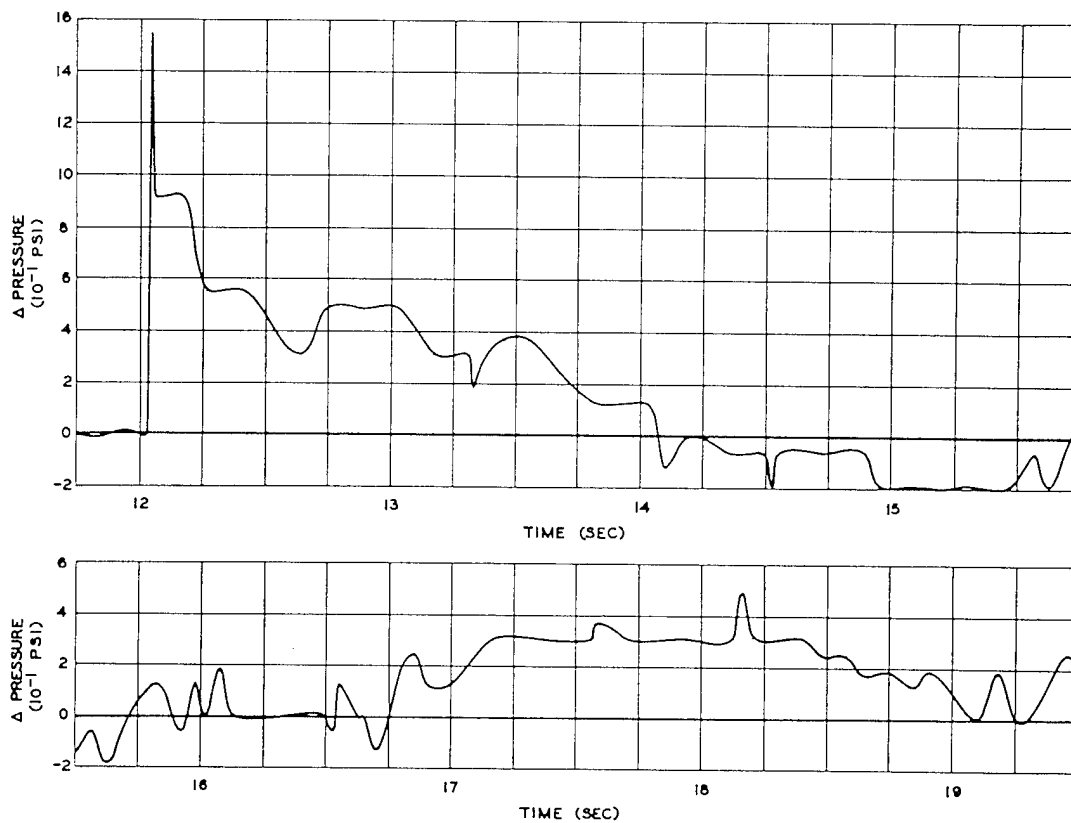


Fig. 6.45 Differential Pressure, 40% Chord, Right Wing Station 25.5, Channel 19, QB-17 N, Easy Shot

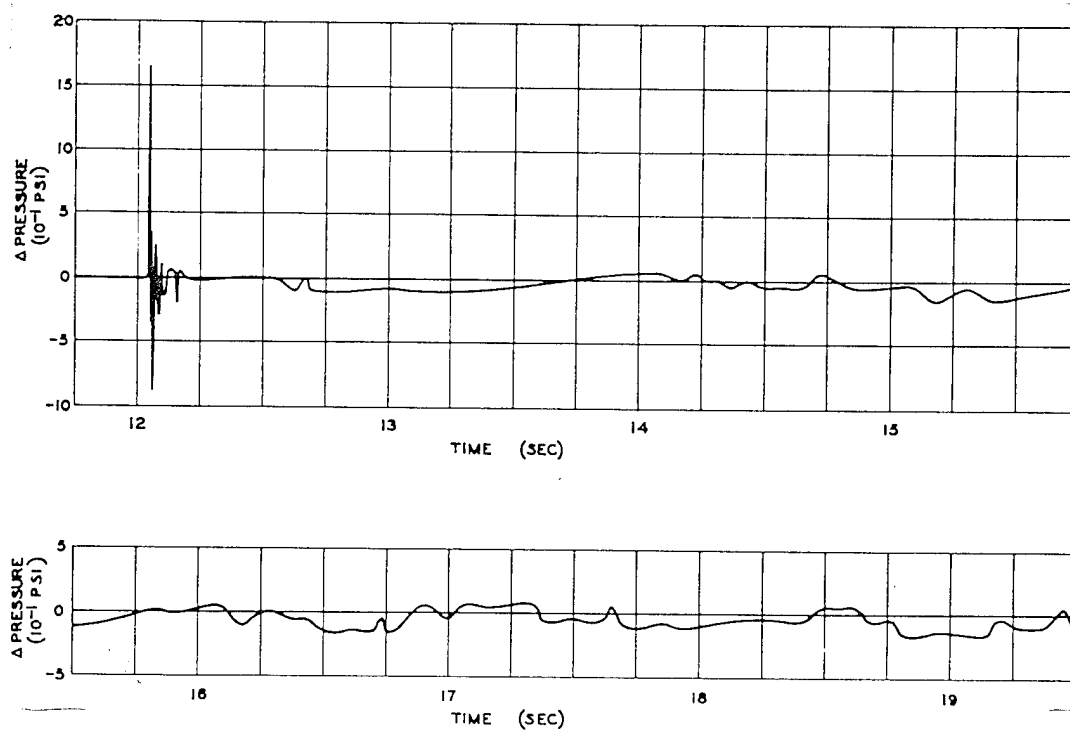


Fig. 6.46 Differential Pressure, 85% Chord, Right Wing Station 25.5, Channel 21, QB-17 N, Easy Shot

~~SECRET~~

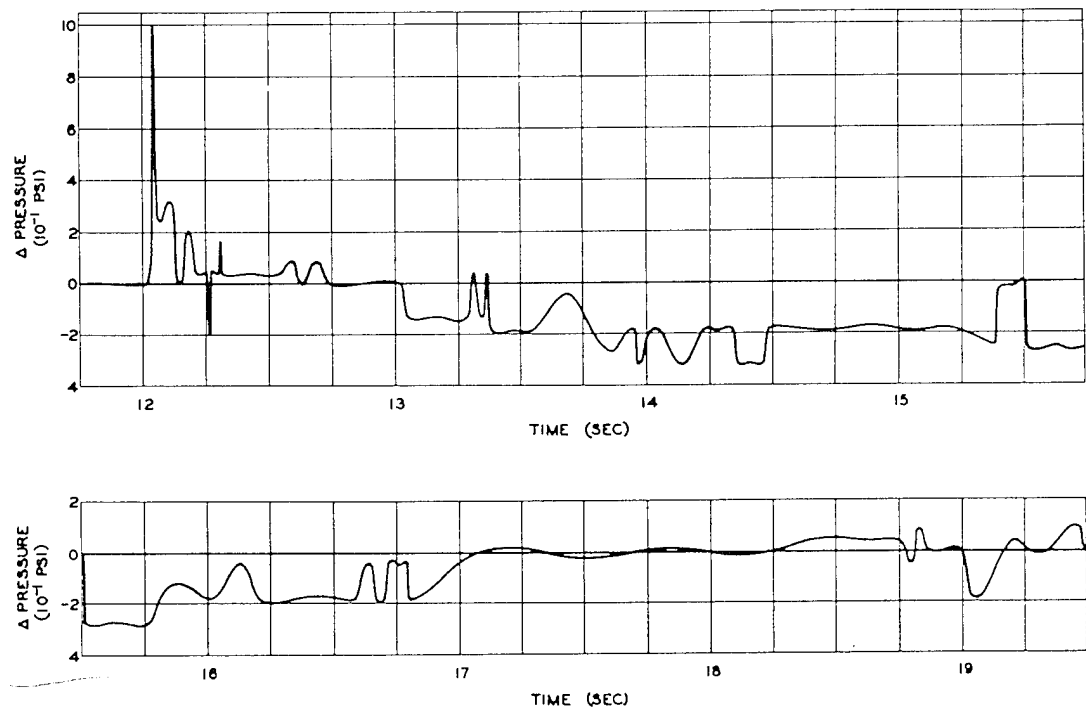


Fig. 6.47 Differential Pressure, 40% Chord, Right Wing Station 25.5, Channel 22, QB-17 N, Easy Shot

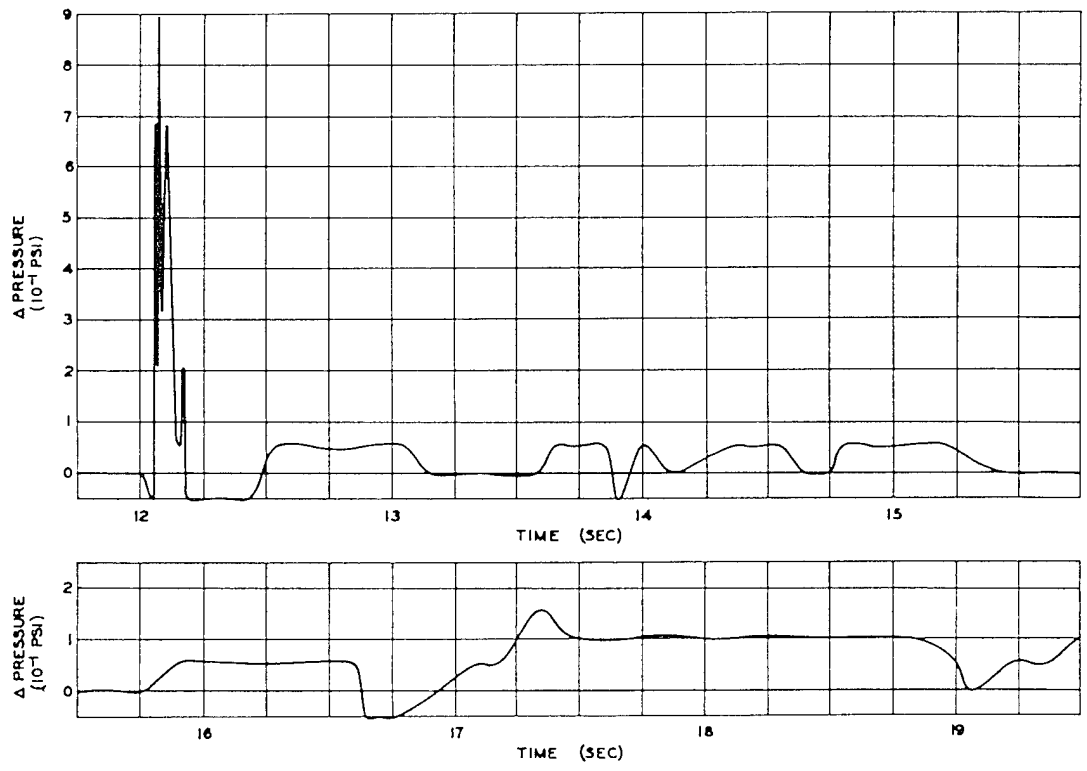


Fig. 6.48 Differential Pressure, 40% Chord, Right Horizontal Stabilizer, Channel 24, QB-17 N, Easy Shot

~~SECRET~~

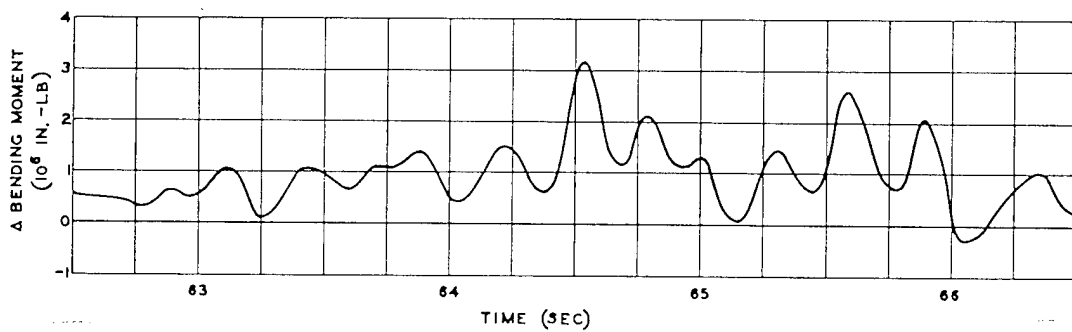
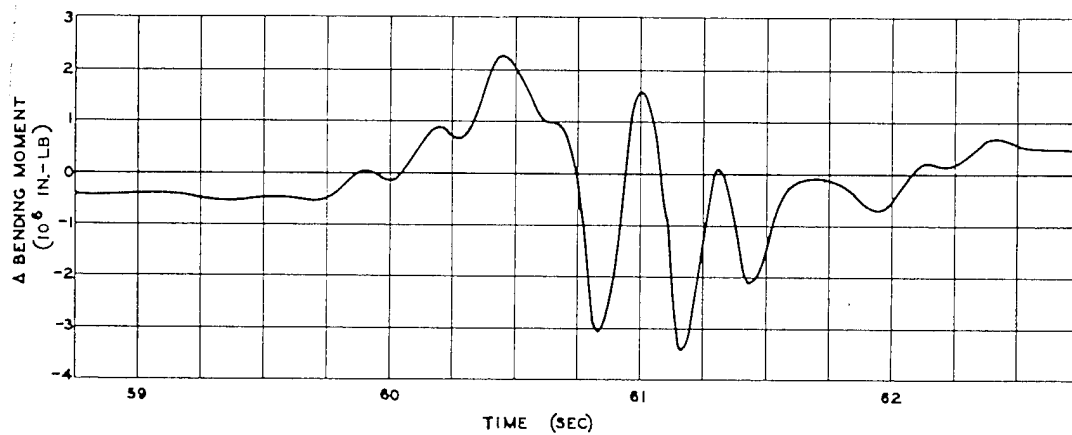


Fig. 6.49 Wing Bending, Left Wing Root, Channel 8, QB-17 N, Cloud Pass, Easy Shot

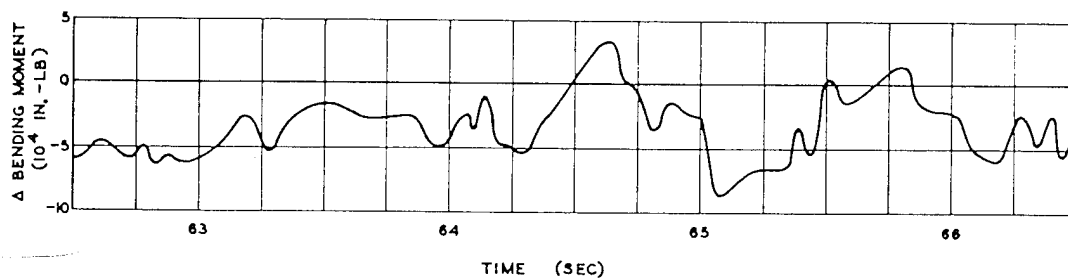
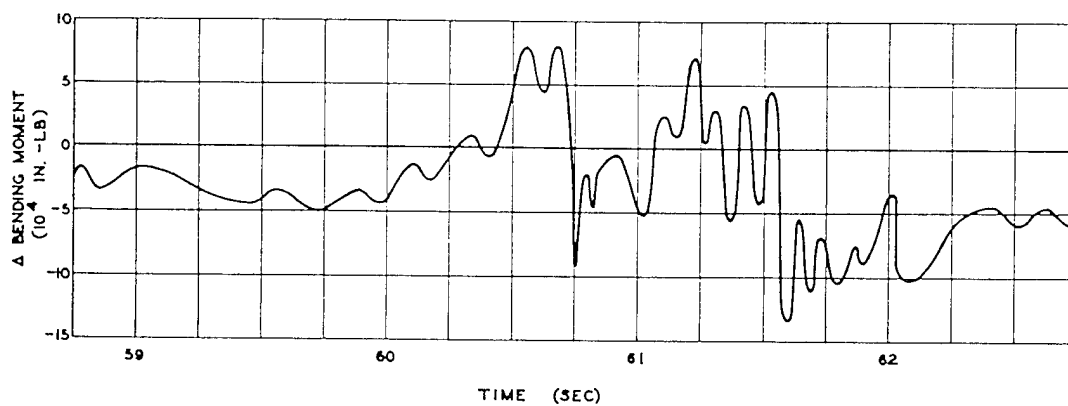


Fig. 6.50 Stabilizer Bending, Right Horizontal Stabilizer, Channel 9, QB-17 N, Cloud Pass, Easy Shot

SECRET

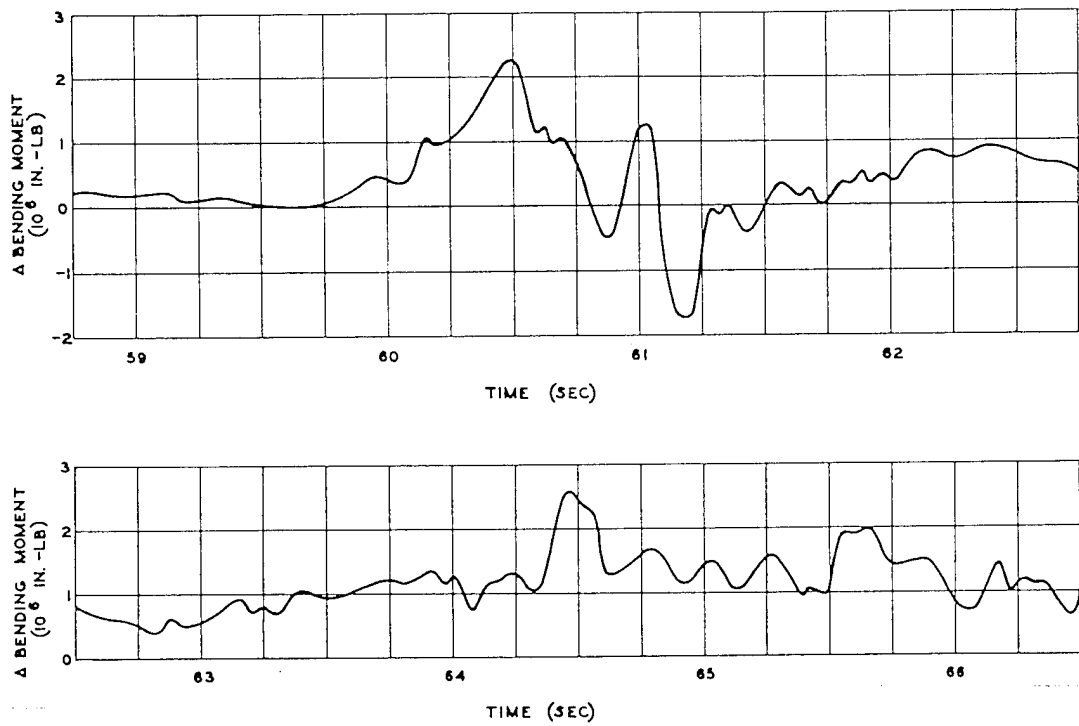


Fig. 6.51 Wing Bending, Outer Panel, Right Wing Station 19, Channel 10, QB-17 N, Cloud Pass, Easy Shot

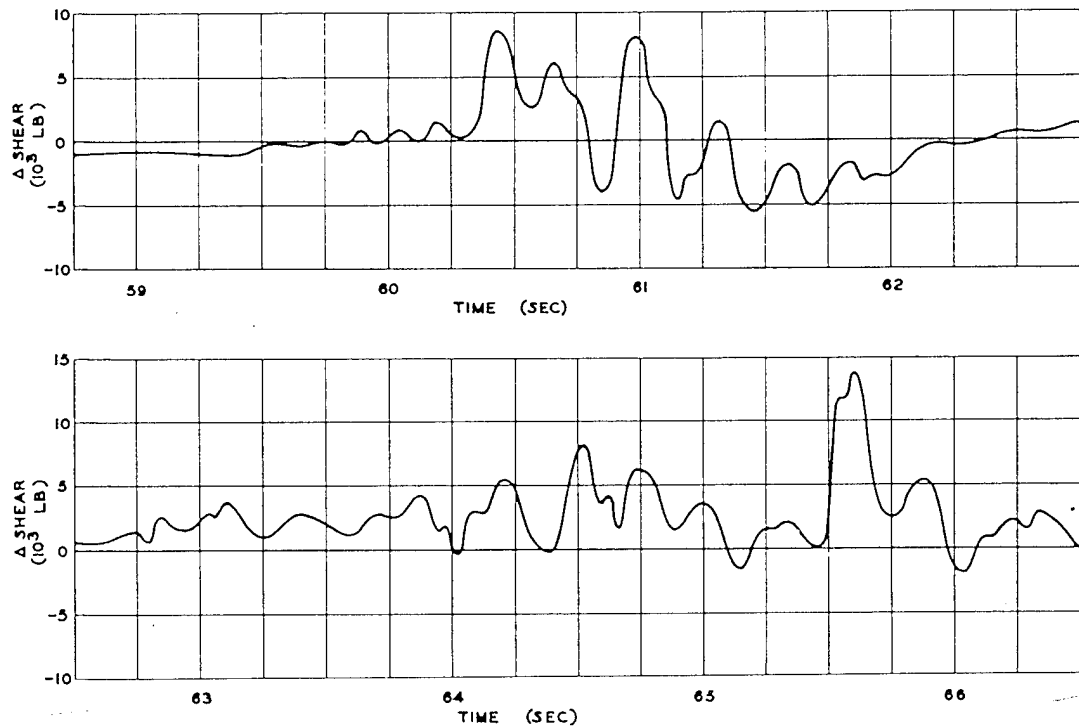


Fig. 6.52 Wing Shear, Right Wing Root, Channel 12, QB-17 N, Cloud Pass, Easy Shot

SECRET

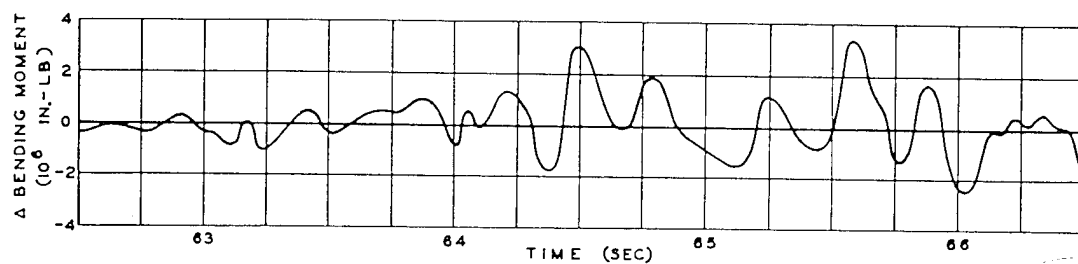
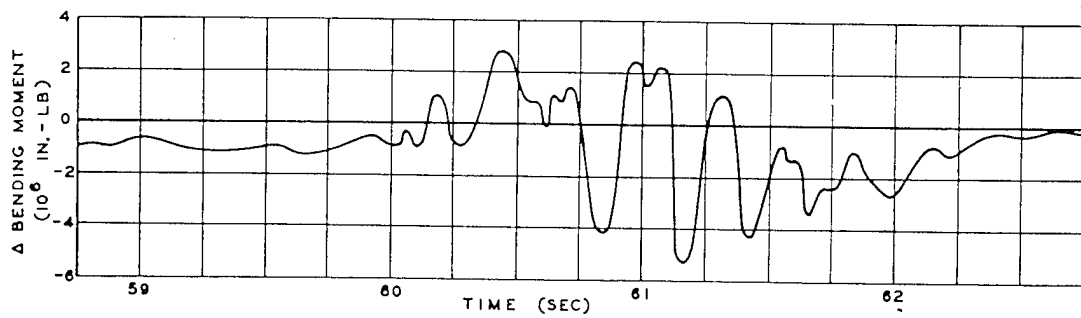


Fig. 6.53 Wing Bending, Mid-span, Right Wing Station 8.8, Channel 14, QB-17 N, Cloud Pass, Easy Shot

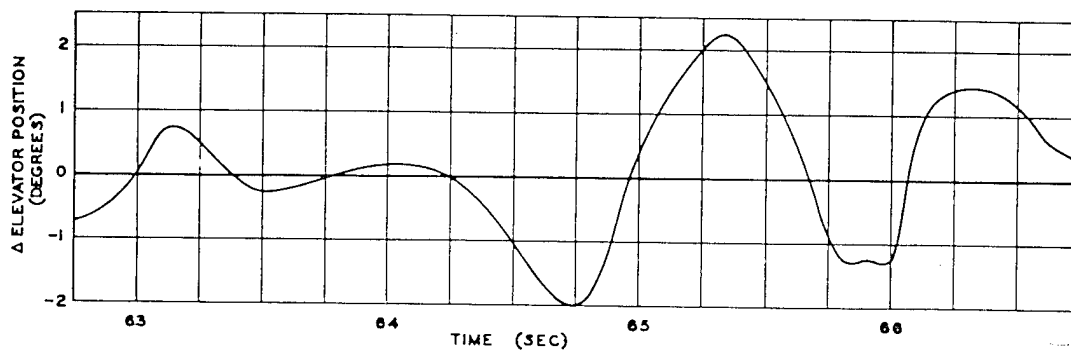
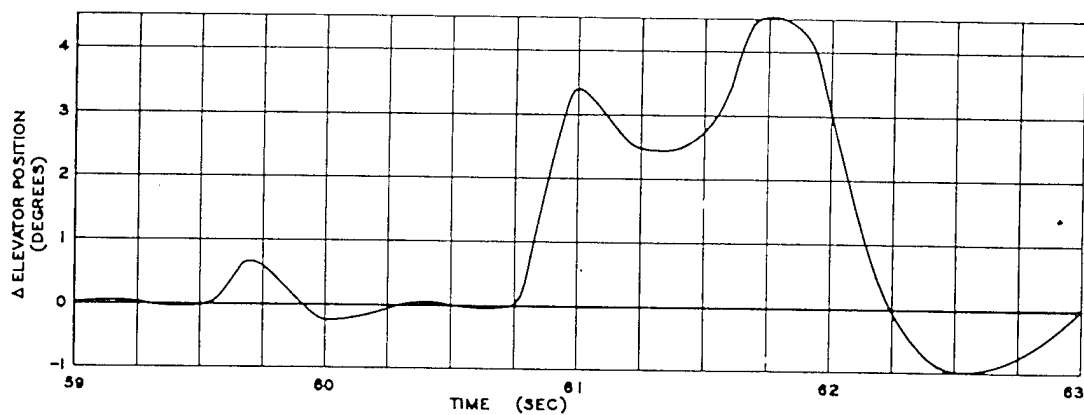


Fig. 6.54 Elevator Position, Channel 15, QB-17 N, Cloud Pass, Easy Shot

SECRET

any response to temperature rise in any of the gauges. The drone apparently returned to stabilized flight both after the shock and after the cloud, although there is evidence of a slight change in trim. There is evidence, although inconclusive, that the wing may have suffered a permanent set in bending from the gusts in the cloud. Careful measurements made on the drone after its return failed to show any unusual deformation or misalignment of any parts of the airplane.

6.6 ELAINE POSITION, XB-47 AIRPLANE, NO. 46-066

Assigned location (at shock)

True altitude, 33,000 ft

Horizontal distance, 0 (directly over)

Predicted conditions

Peak overpressure, 0.21 psi

Peak gust velocity, 38 ft/sec (in direction
of shock)

Time of travel (shock), 27.7 sec

6.6.1 Flight Log

The XB-47 took off from Kwajalein and performed its mission satisfactorily. The flight data as reported¹ by ATU 3.4.2 are as follows:

Time

Take-off, 0357

At assigned altitude, 0445

Shock arrival, 0627:28.4

Landing, 0733

Meteorological conditions at altitude

True altitude, 33,000 ft

Pressure altitude, 31,000 ft

Outside air temperature, -29°C

Wind direction (from), 320° (azimuth)

Wind velocity, 25 knots

Airplane parameters at shock arrival

Indicated airspeed, 244 knots

Ground speed, 641 ft/sec

Ground track azimuth, 265°

Horizontal angle from blast, 085° (azimuth)

Vertical angle from blast, * 84.8° (elevation)

Horizontal distance from blast, 3,005 ft

Slant distance from blast, * 33,140 ft

Shock struck airplane from below and ahead

*Computed from data in Navigator's Report, reference 1.

6.6.2 Airplane Condition

During the preflight check, all gauges were satisfactory, but one recorder, A, failed. The airplane was based at Kwajalein; the spare recorder had been cannibalized; and time was not available to get another recorder from Eniwetok. It was arranged by TWX that the instrumentation engineer would select the channels to be used in the B recorder so as to obtain the best general evaluation of the effect of the shock. For the most part, the selected channels were the strain-gauge measurements.

The take-off gross weight was approximately 140,000 lb. The pilot was prepared for a possible 15-min delay in H-hour in accordance with instructions from TG 3.4, so that the gross weight at the time of the shock wave was somewhat greater than on Dog shot. The gross weight at shock was 110,770 lb, with the c.g. at 18.0 per cent m.a.c. The fuel at shock time consisted of 4,124 gal (27,631 lb) so distributed among the main tanks as to maintain the c.g. position.

The pilot made no particular observations concerning the mission, and no damage was reported.

6.6.3 Load Data

Although channels A10, A11, A14, A15, and A22 were measured, no suitable calibrations are available for these channels, and they are not presented. The data for channels A1, A2, and B2 were obscured by noise and are not readable on the record, apparently because of failure during the flight. The data recorded from this mission are presented in Figs. 6.55 through 6.70.

6.6.4 Analysis

The navigator reported that he was out of position by a comparatively large amount (more than a half mile); but, since the airplane was in an overhead position, this error in range did not cause appreciable error in slant range, and the predicted theoretical conditions are still valid. The actual time of shock arrival was $T_0 + 28.5$ sec; the theoretical time was $T_0 + 27.7$ sec.

The strain-gauge channels are generally unsteady owing to the slight maneuvers or air turbulence of flight. The traces do, however,

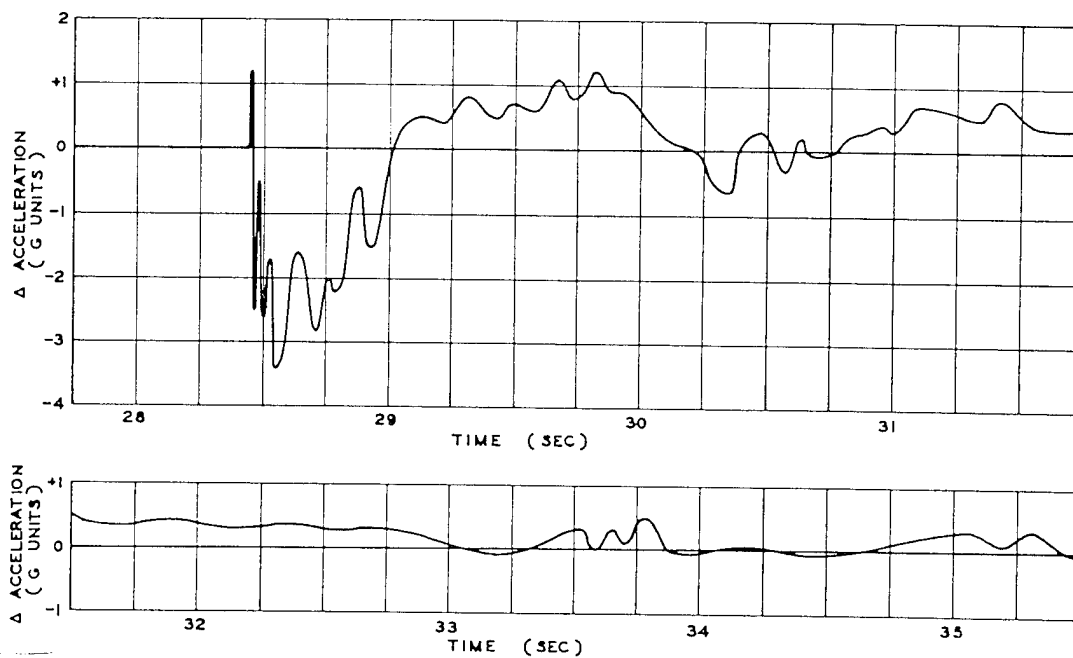


Fig. 6.55 Normal Acceleration, Bomb Bay, Forward, Channel A6, XB-47, Easy Shot

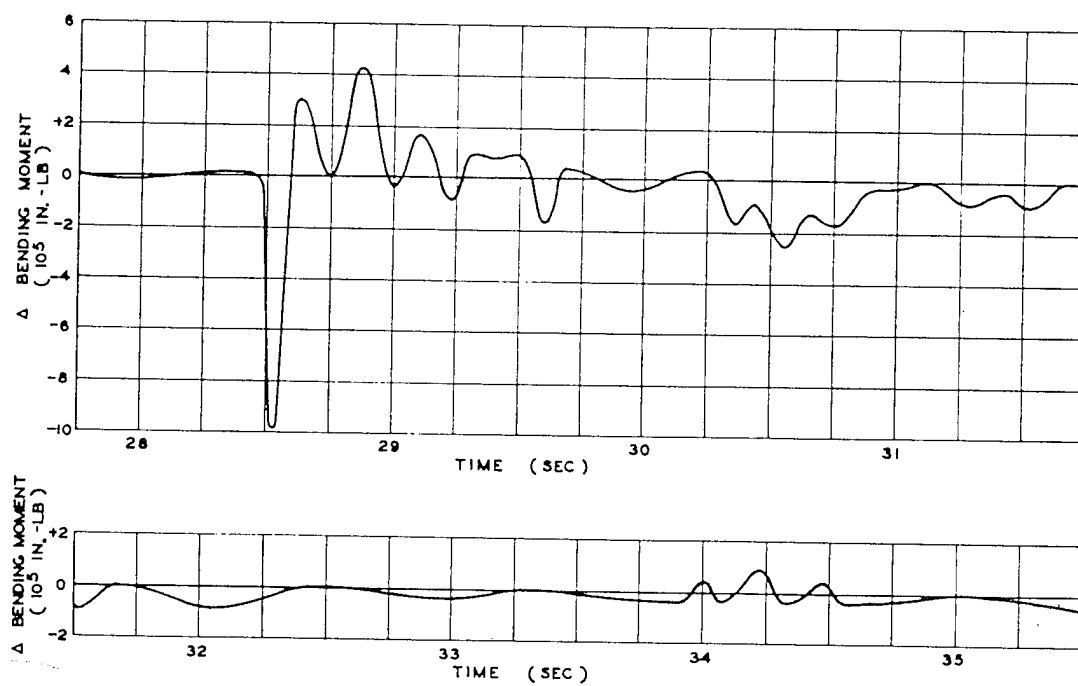


Fig. 6.56 Fuselage Bending, Forward of Vertical Fin, Fuselage Station 985, Channel A9, XB-47, Easy Shot

SECRET

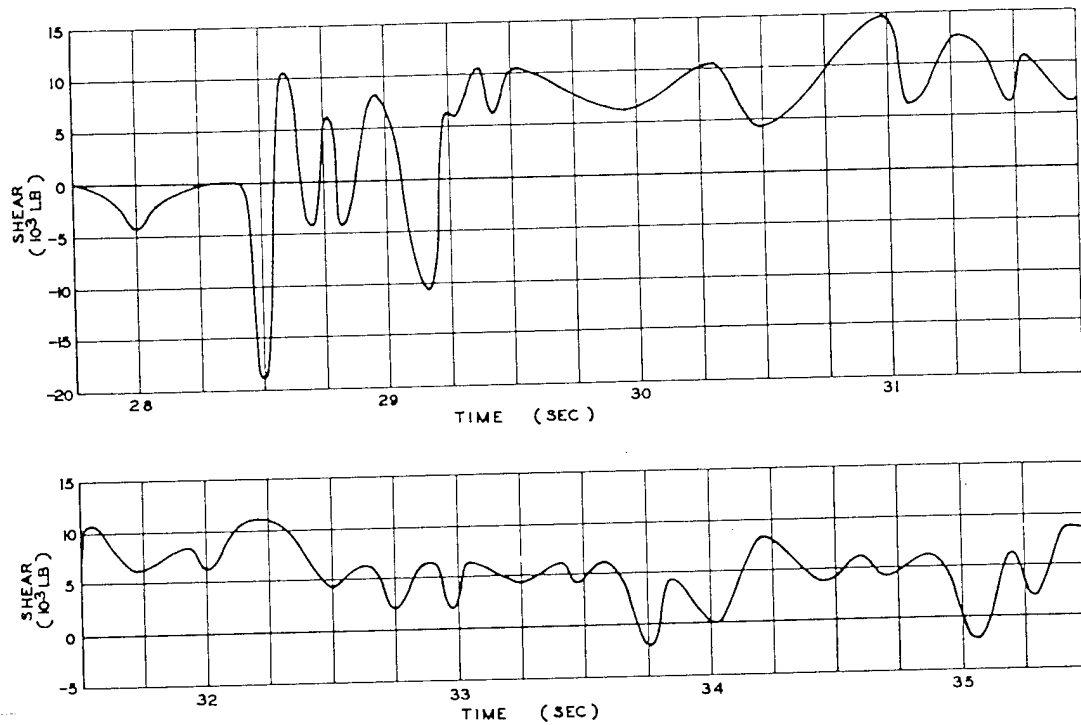


Fig. 6.57 Wing Shear, Right Wing Root, Wing Station 307, Channel A12, XB-47, Easy Shot

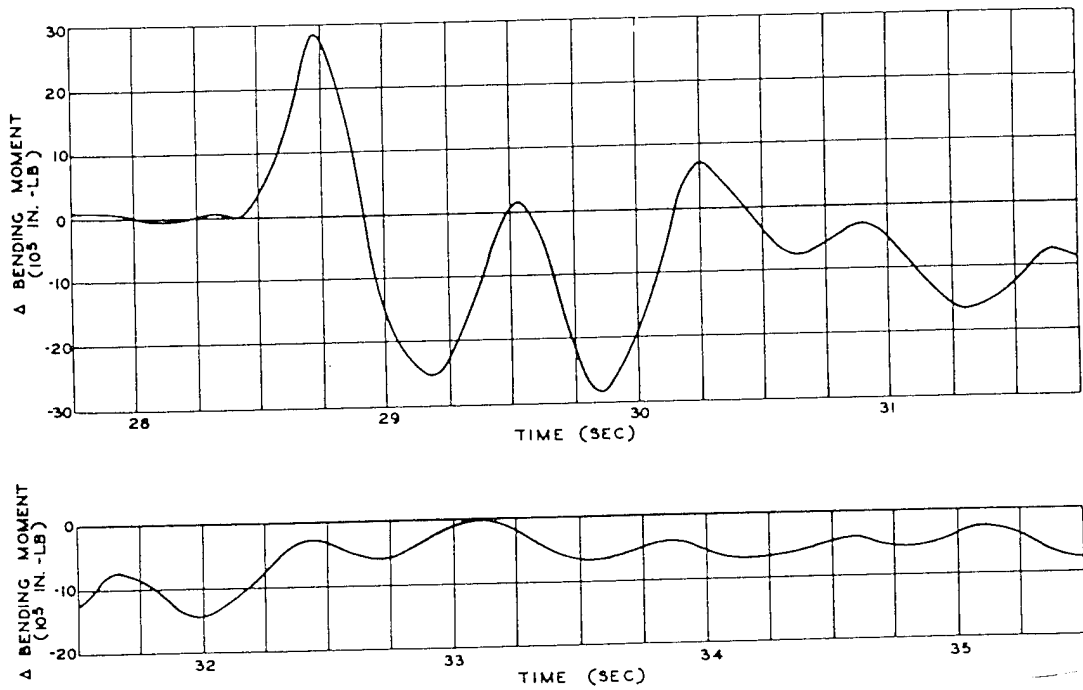


Fig. 6.58 Wing Bending, Right Wing Root, Wing Station 307, Channel A13, XB-47, Easy Shot

SECRET

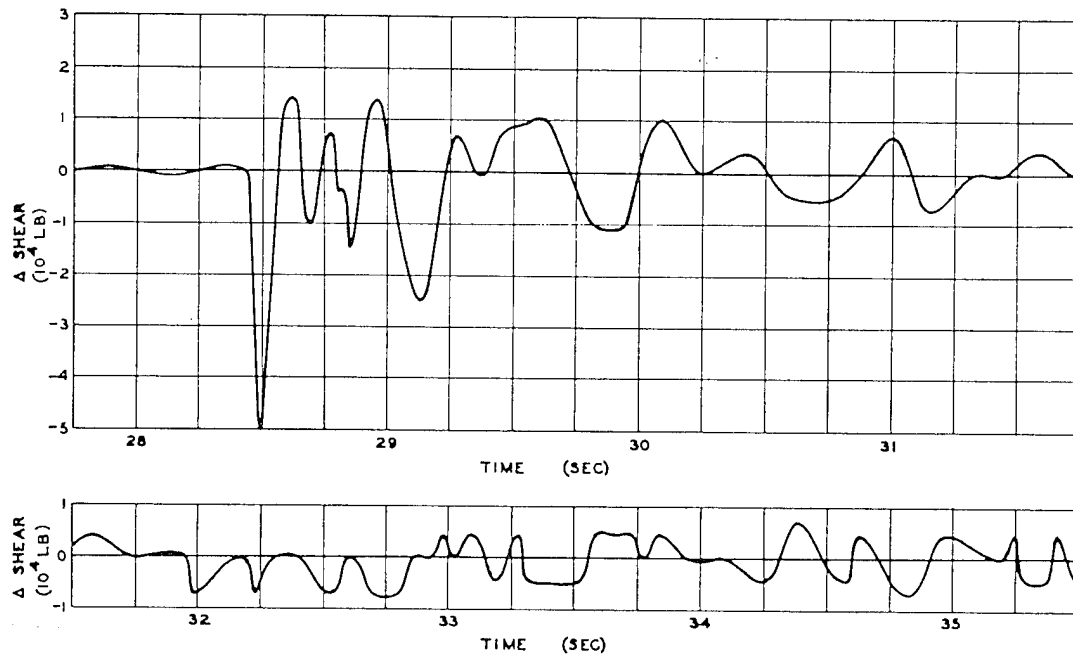


Fig. 6.59 Wing Shear, Left Wing Root, Wing Station 307, Channel A16, XB-47, Easy Shot

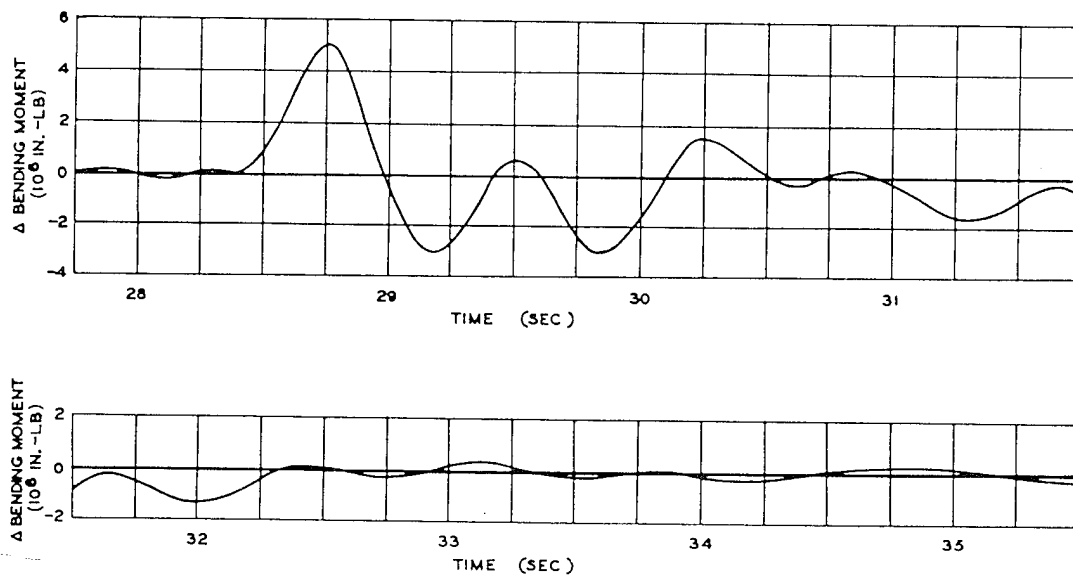


Fig. 6.60 Wing Bending, Left Wing Root, Wing Station 307, Channel A17, XB-47, Easy Shot

~~SECRET~~

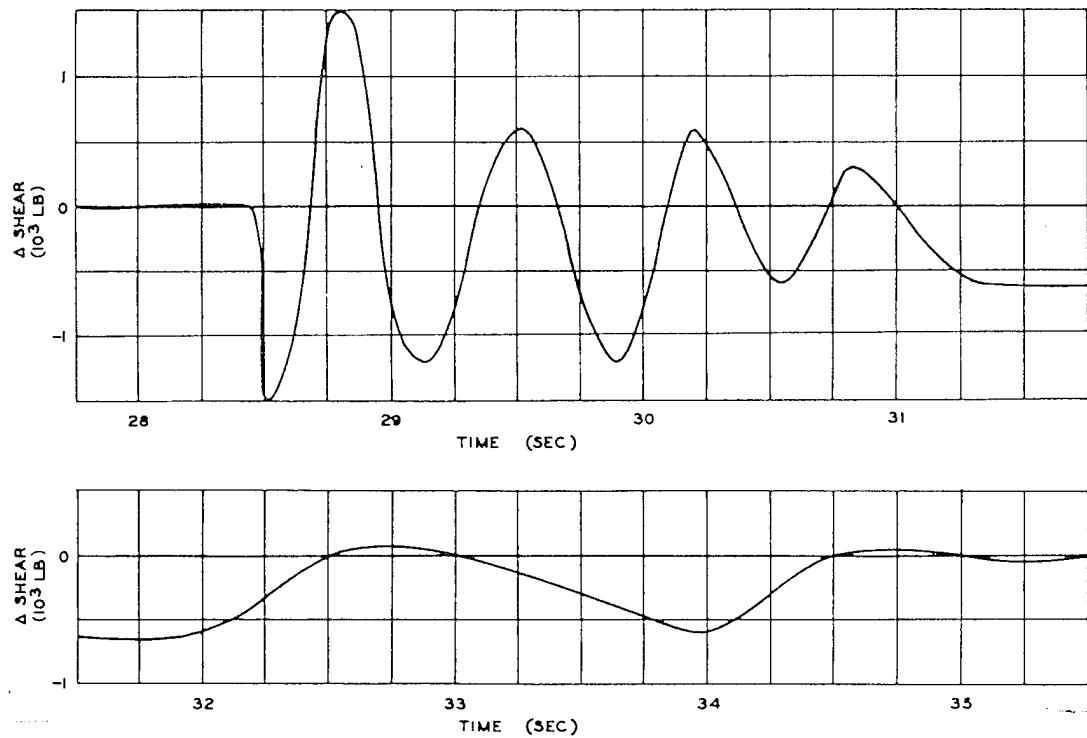


Fig. 6.61 Wing Shear, Left Wing Outboard, Wing Station 660, Channel A21, XB-47, Easy Shot

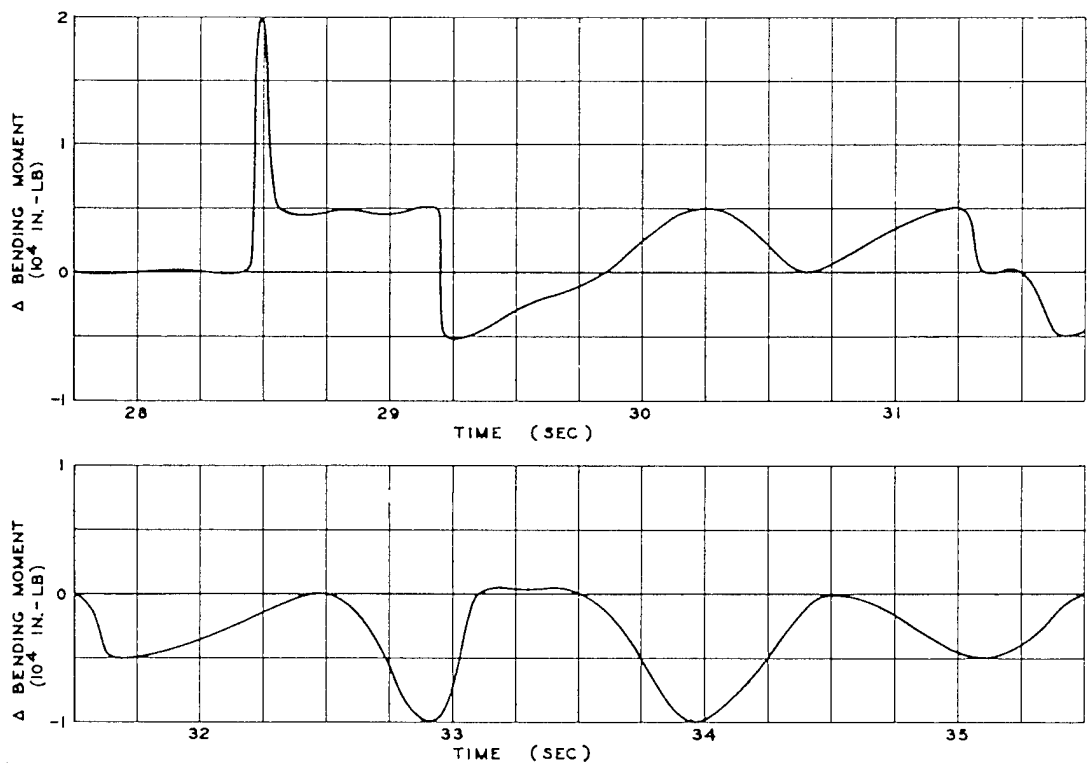


Fig. 6.62 Horizontal-stabilizer Bending, Left-horizontal-stabilizer Station 64, Channel A23, XB-47, Easy Shot

~~SECRET~~

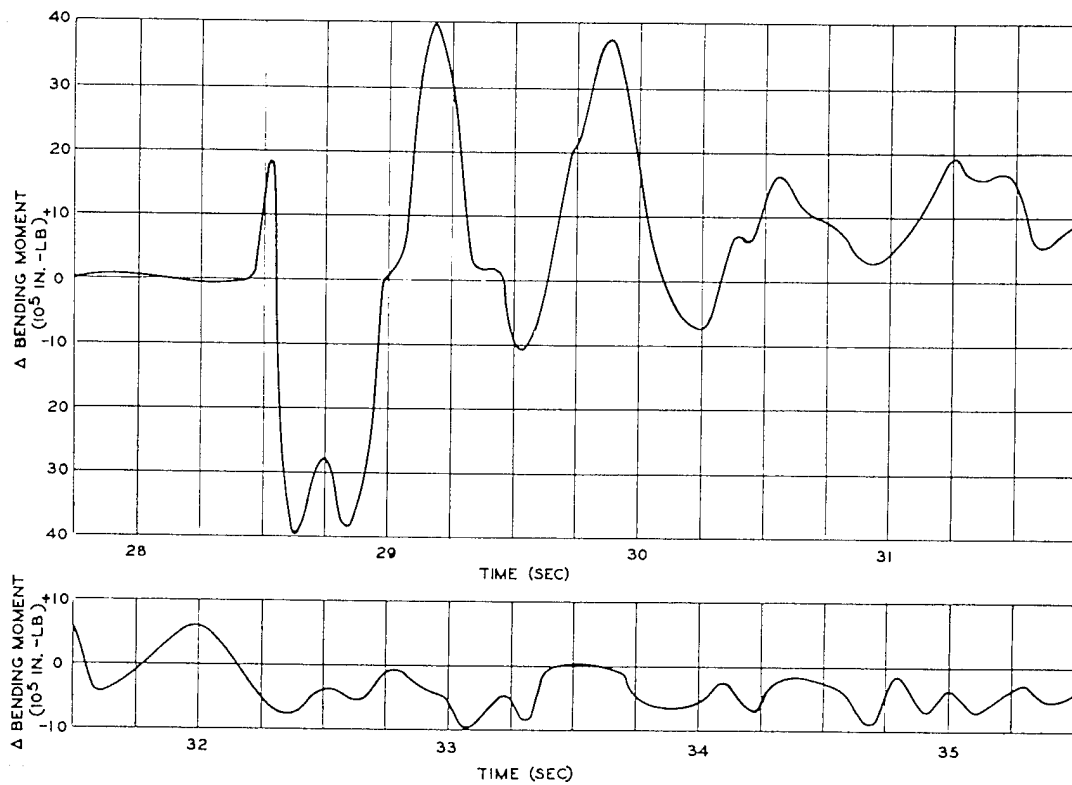


Fig. 6.63 Fuselage Bending, Aft End of Bomb Bay, Fuselage Station 718, Channel A24, XB-47, Easy Shot

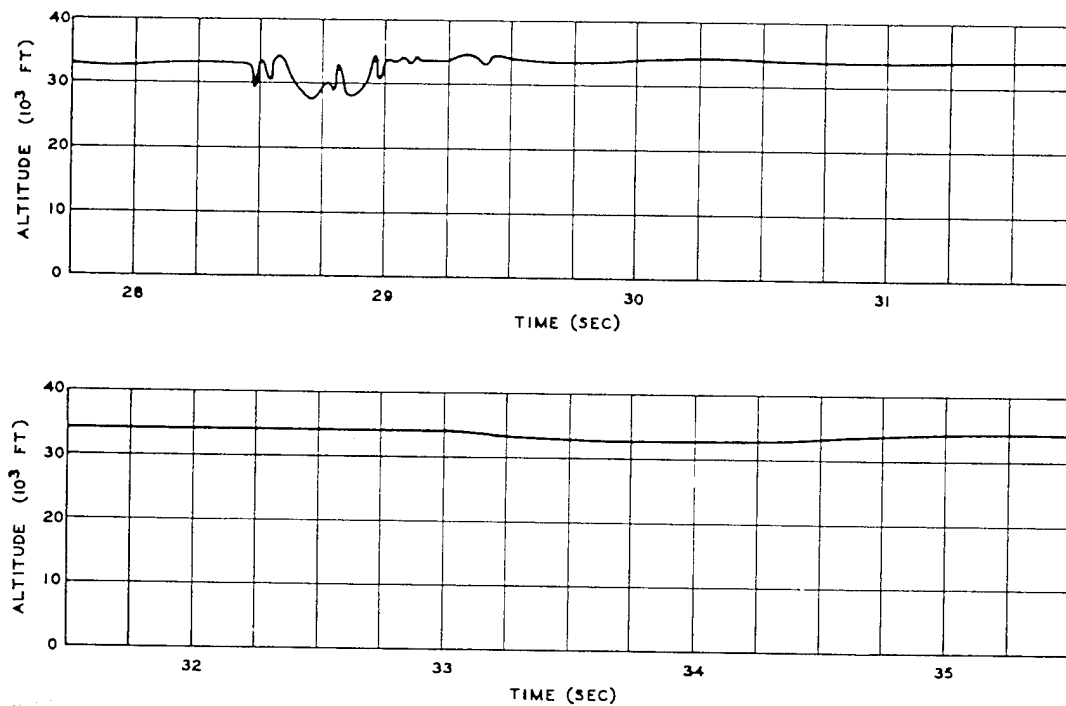


Fig. 6.64 Altitude, Channel B1, XB-47, Easy Shot

SECRET

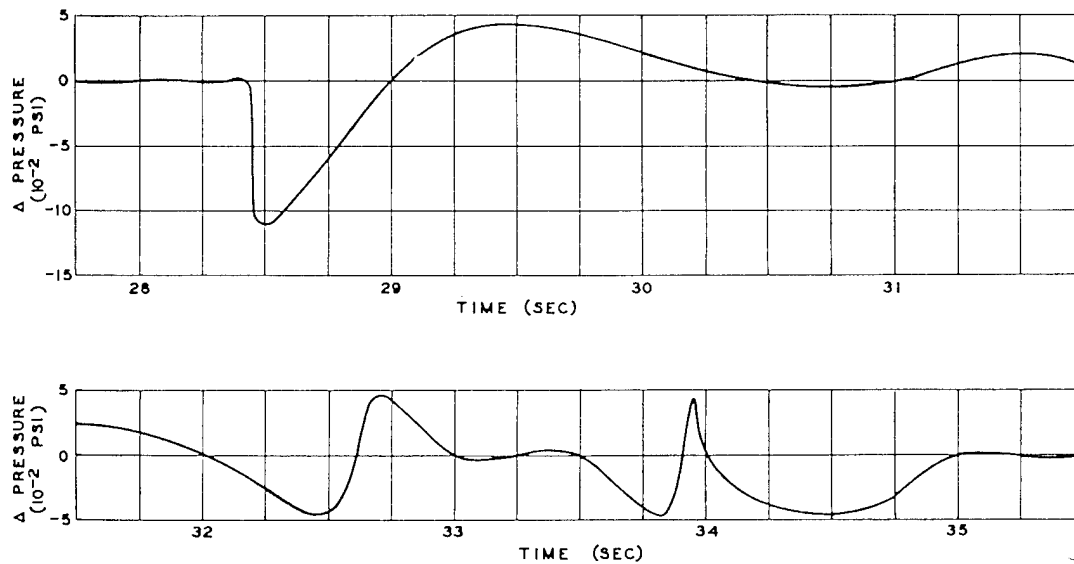


Fig. 6.65 Differential Aerodynamic Pressure, 61.3% Chord, Right Wing Station 515, Channel B4, XB-47, Easy Shot

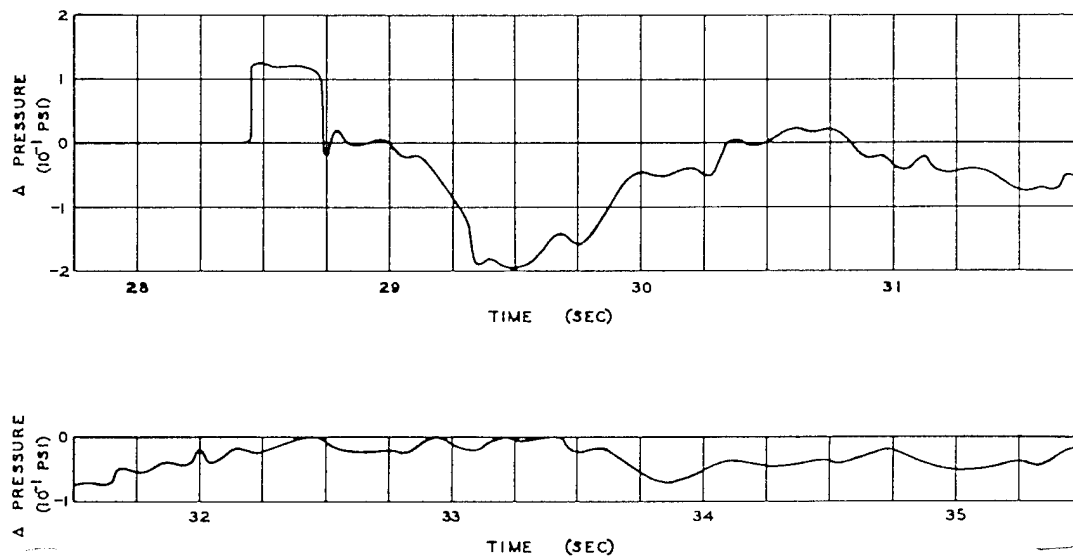


Fig. 6.66 Gauge Aerodynamic Pressure, 11.7% Chord, Top Left Wing Station 515, Channel B8, XB-47, Easy Shot

SECRET

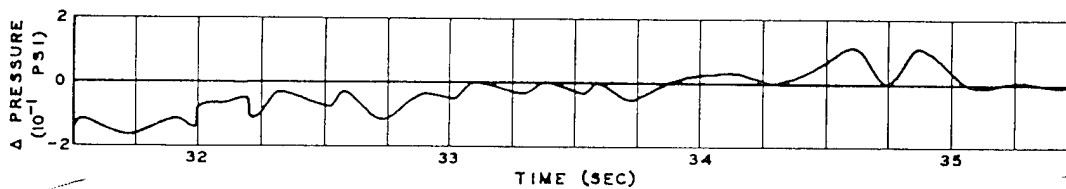
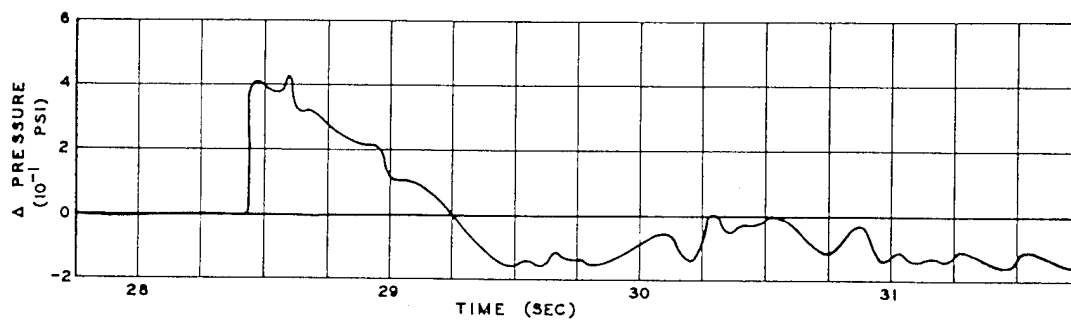


Fig. 6.67 Gauge Aerodynamic Pressure, 11.7% Chord, Bottom Left Wing Station 515, Channel B9, XB-47, Easy Shot

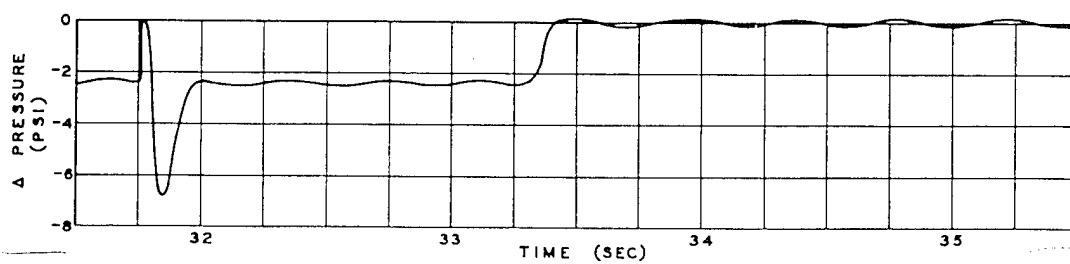
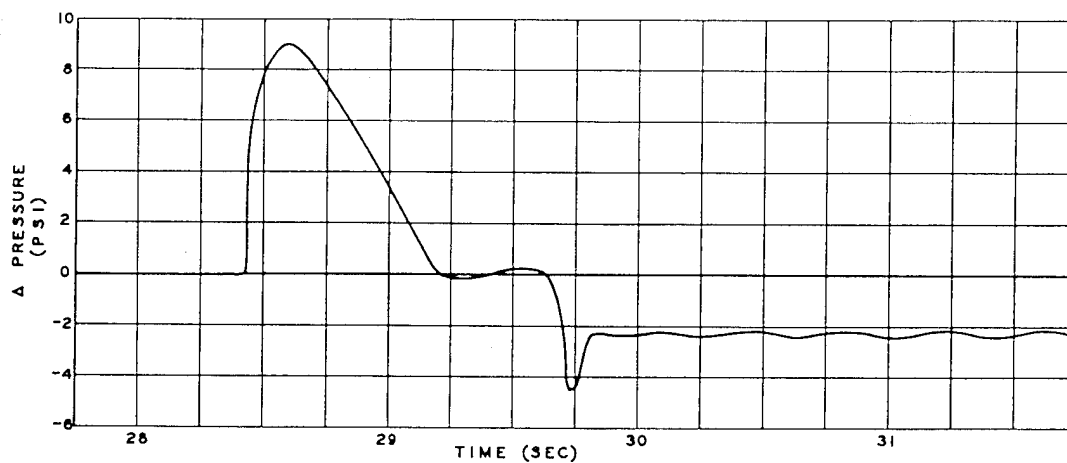


Fig. 6.68 Gauge Aerodynamic Pressure, 61.3% Chord, Bottom Left Wing Station 515, Channel B17, XB-47, Easy Shot

~~SECRET~~

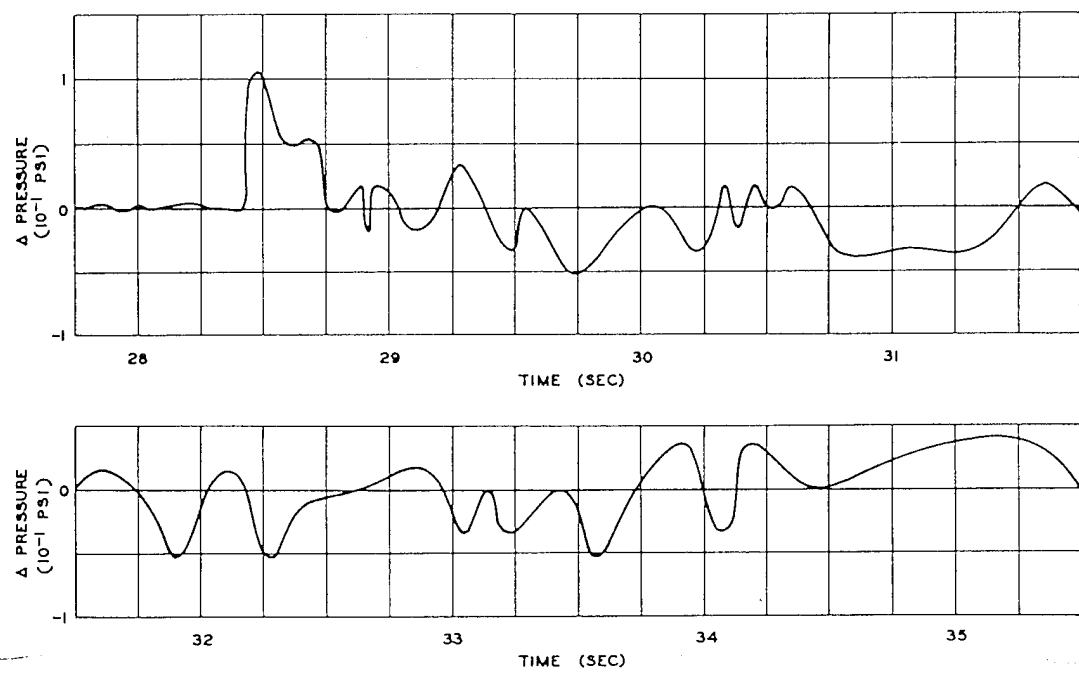


Fig. 6.69 Gauge Aerodynamic Pressure, Forward of 50% Chord, Bottom Left-horizontal-stabilizer Station 110, Channel B22, XB-47, Easy Shot

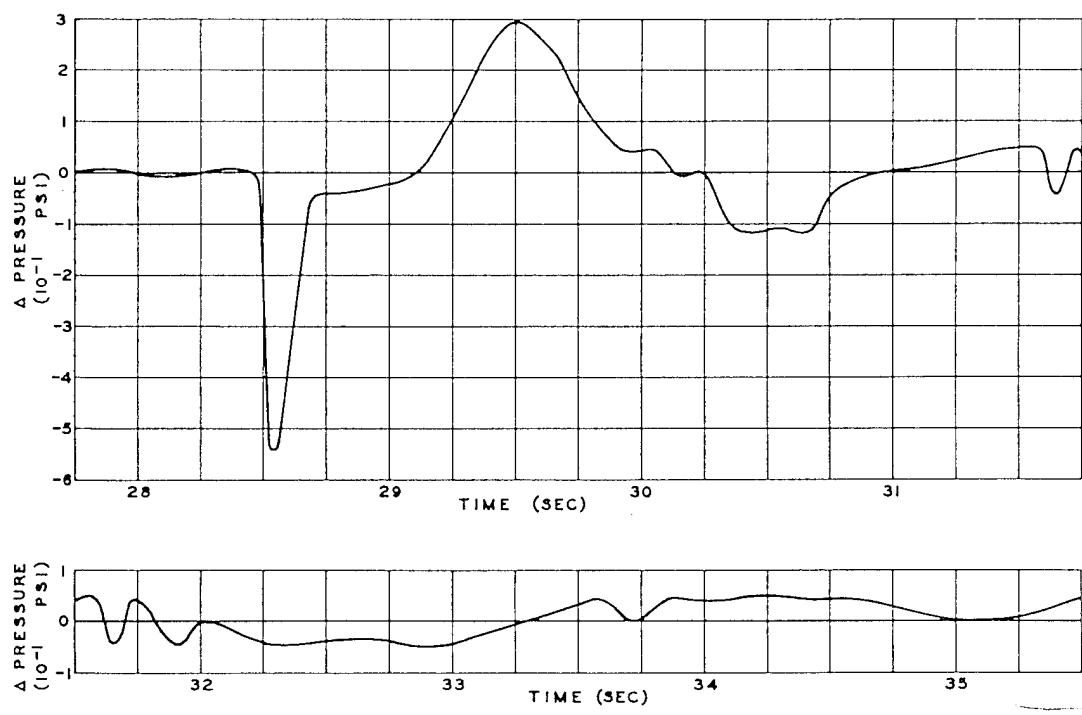


Fig. 6.70 Gauge Aerodynamic Pressure, 5% Chord, Top Left Wing Station 523, Channel B24, XB-47, Easy Shot

~~SECRET~~

remain steady for approximately 5 sec prior to shock. In general, the amplitude of the unsteadiness approaches that of the shock record. At about $T_0 + 41$ sec (13 sec after shock) there are four rather regular cycles of oscillation, the amplitude of which is about 500,000 in.-lb of wing-root bending in each direction from zero and the period of which is about 2 sec per cycle. The oscillation is quickly damped, however, and the traces return to the unsteadiness of normal flight.

6.7 FRANCES POSITION, B-50D AIRPLANE, NO. 49-290

Assigned location (at shock)

True altitude, 25,000 ft

Horizontal distance, 18,000 ft beyond point zero

Predicted conditions

Peak overpressure, 0.28 psi

Peak gust velocity, 36 ft/sec

Time of travel (shock), 24.9 sec

6.7.1 Flight Log

B-50D airplane No. 290 took off approximately 20 min ahead of schedule and completed the mission without incident. The flight data as reported¹ by ATU 3.4.2 are as follows:

Time

Take-off, 0308

At assigned altitude, 0340

Shock arrival, 0627:26.2

Landing, 0950

Meteorological conditions at altitude

True altitude, 25,000 ft

Pressure altitude, 23,400 ft

Outside air temperature, -14°C

Wind direction (from), 310° (azimuth)

Wind velocity, 19 knots

Airplane parameters at shock arrival

Indicated airspeed, 163 knots

Ground speed, 444 ft/sec

Ground track azimuth, 132°

Horizontal angle from blast, 129° (azimuth)

Vertical angle from blast, $* 52.7^{\circ}$ (elevation)

Horizontal distance from blast, 19,021 ft

Slant distance from blast, $* 31,430$ ft

Shock struck the airplane from the rear and below

^{*}Computed from data in Navigator's Report, reference 1.

6.7.2 Airplane Condition

Before take-off the channels of both recorders were checked and found to be satisfactory except for channel B14, which had a bad amplifier. However, during the mission (just before shot time) the recorders were accidentally tripped by an extraneous signal through the decoder circuit. The engineer caught the B recorder in time to save sufficient tape to record the mission, but the A recorder had expended most of its tape so that there was not enough for the mission.

The fuel at take-off consisted of 1,445 gal (8,670 lb) in each of the four main tanks. The take-off gross weight was computed to have been 124,700 lb, with the c.g. at 25.8 per cent m.a.c. The fuel remaining at the time of shock arrival was computed to have been 875 gal (5,250 lb) in each of the main tanks; the gross weight was 111,000 lb with the c.g. at 25.0 per cent m.a.c.

The pilot reported that "the shock was more severe than on Dog shot." Examination of the airplane after the mission showed a very slight deformation of the bomb-bay doors along the center line of the airplane. No other damage was noted.

6.7.3 Load Data

The data as recorded are presented in Figs. 6.71 through 6.86. The calibrate steps for channels B1, B18, and B22 are indistinguishable, and these data are not reported. The data in channels B5, B8, B11, and B12 are so low that they are obscured by noise.

6.7.4 Analysis

According to the navigator's report the airplane was 1,021 ft farther beyond point zero than the assigned position. However, the theoretical conditions are essentially those predicted. The actual time for travel of the shock wave was 25.9 sec; the theoretical time was 25.2 sec for the actual point in space.

Since the data collected from this mission are all pressures, it is impractical to draw conclusions from a brief analysis. Most of the pressures appear reasonable and should be informative when reduced to wing lifts and interpreted in terms of the results of other missions.

SECRET

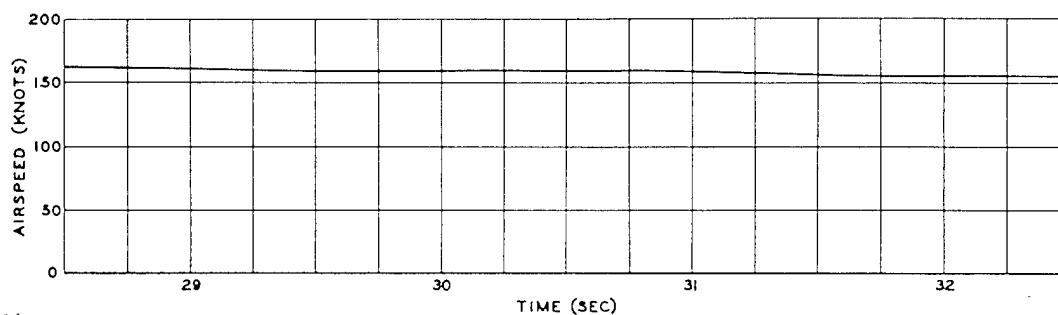
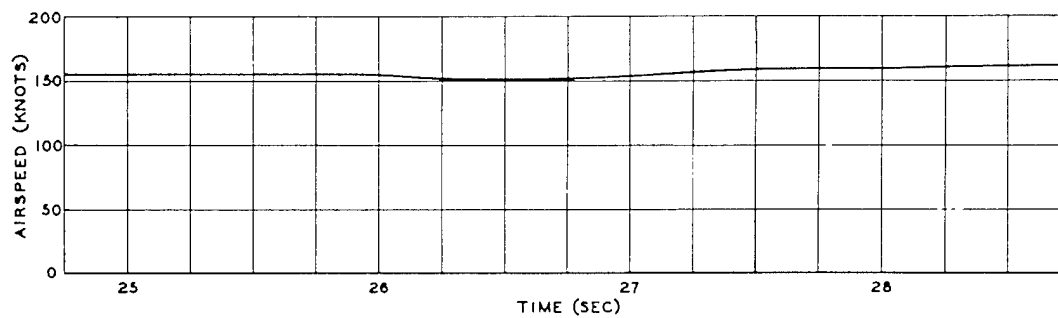


Fig. 6.71 Airspeed, Channel B2, B-50D (290), Easy Shot

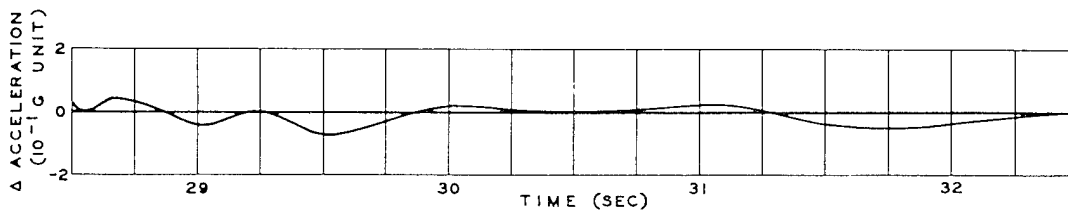
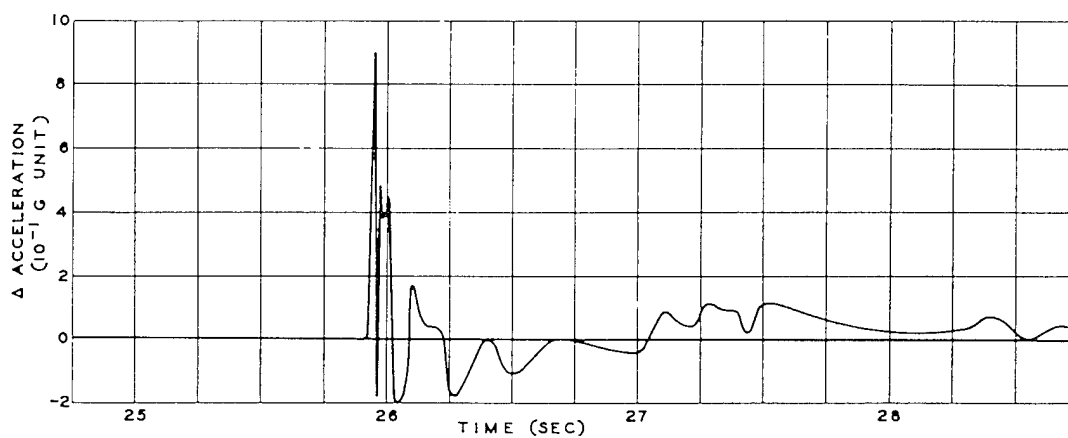


Fig. 6.72 Normal Acceleration, Aft Rear Bomb Bay, Fuselage Station 628, Channel B3, B-50D (290), Easy Shot

SECRET

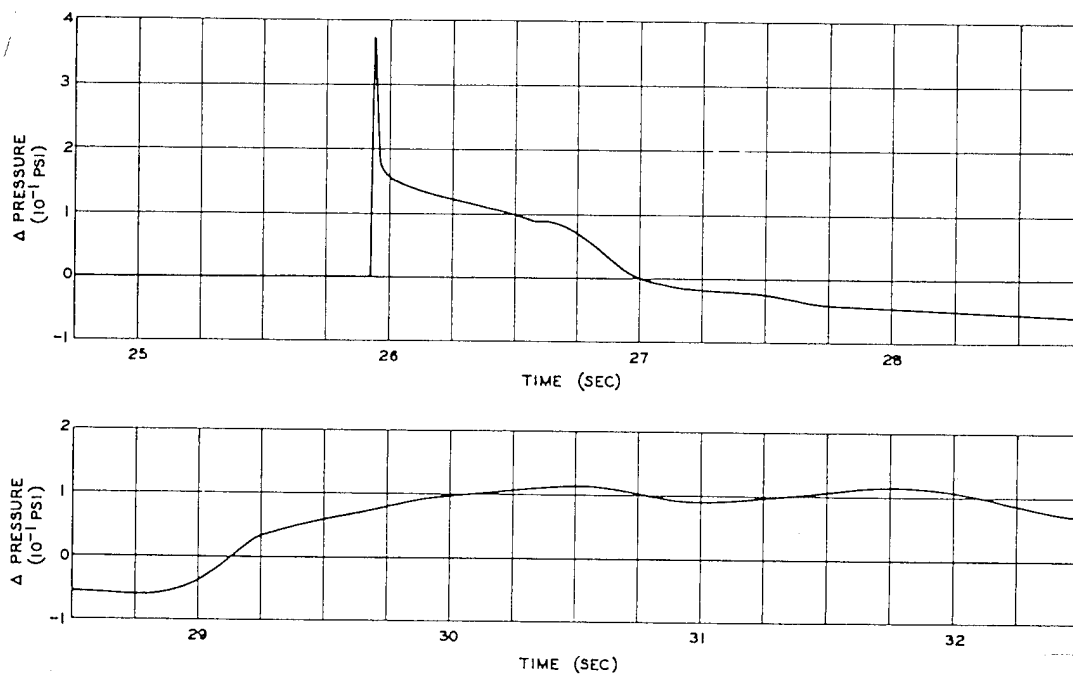


Fig. 6.73 Differential Aerodynamic Pressure, 23% Chord, Right Wing Station 525, Channel B4, B-50D (290), Easy Shot

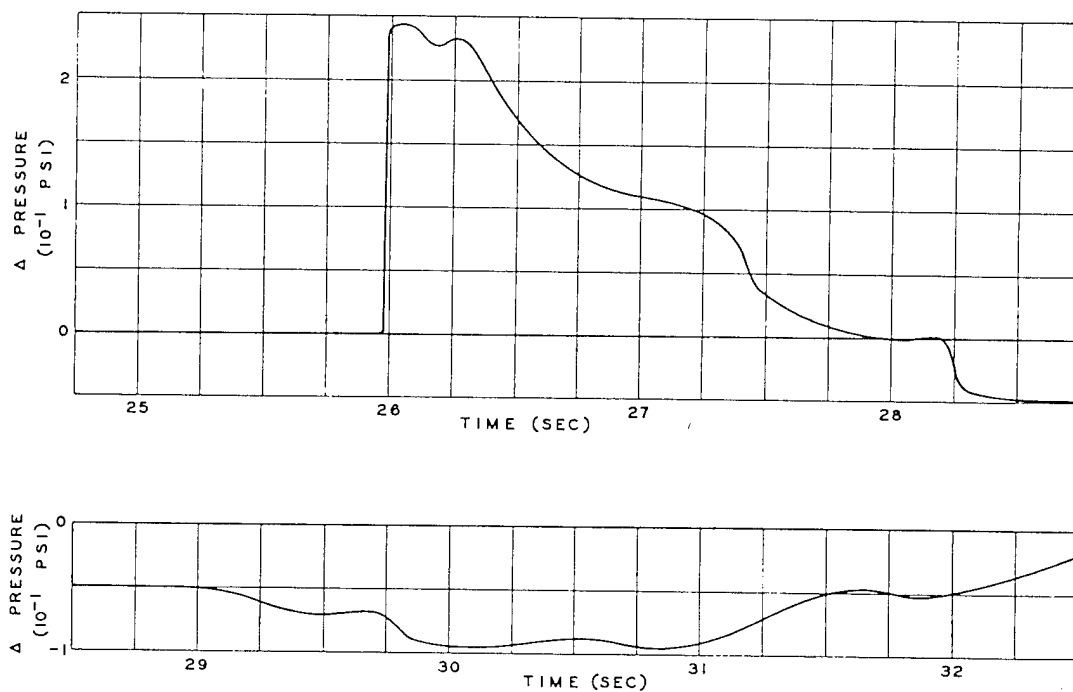


Fig. 6.74 Gauge Aerodynamic Pressure, Bottom Forward Fuselage, Fuselage Station 26, Channel B6, B-50D (290), Easy Shot

~~SECRET~~

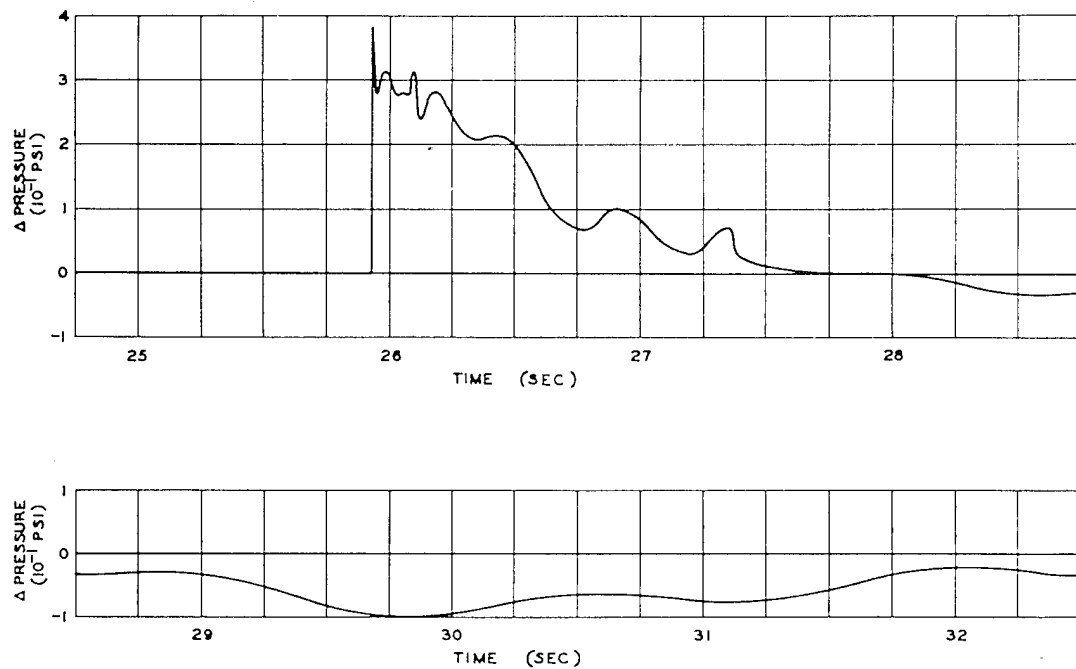


Fig. 6.75 Gauge Aerodynamic Pressure, Right Side of Fuselage, Fuselage Station 783, Channel B7, B-50D (290), Easy Shot

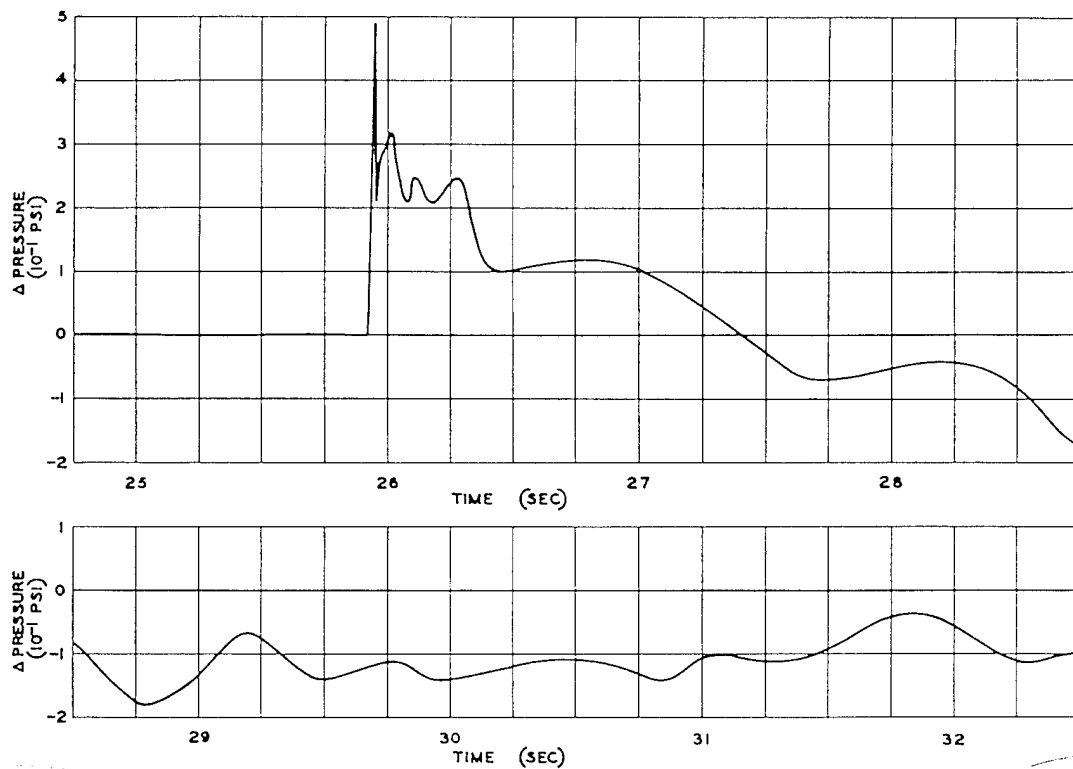


Fig. 6.76 Gauge Aerodynamic Pressure, Right Side of Vertical Fin, Fuselage Station 974, Channel B9, B-50D (290), Easy Shot

~~SECRET~~

~~SECRET~~

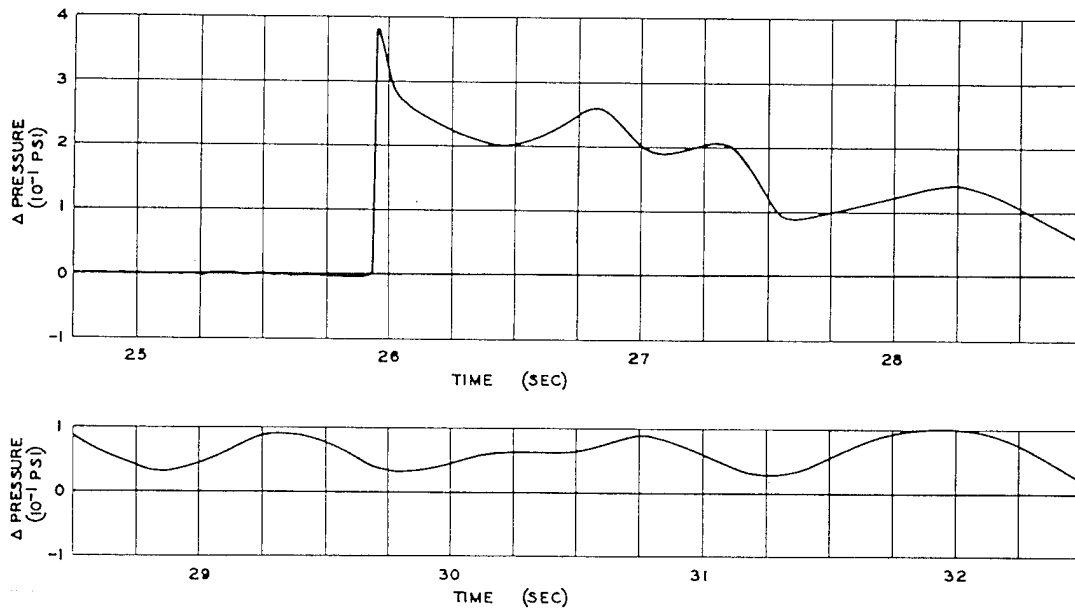


Fig. 6.77 Gauge Aerodynamic Pressure, Left Side of Vertical Fin, Fuselage Station 974, Channel B10, B-50D (290), Easy Shot

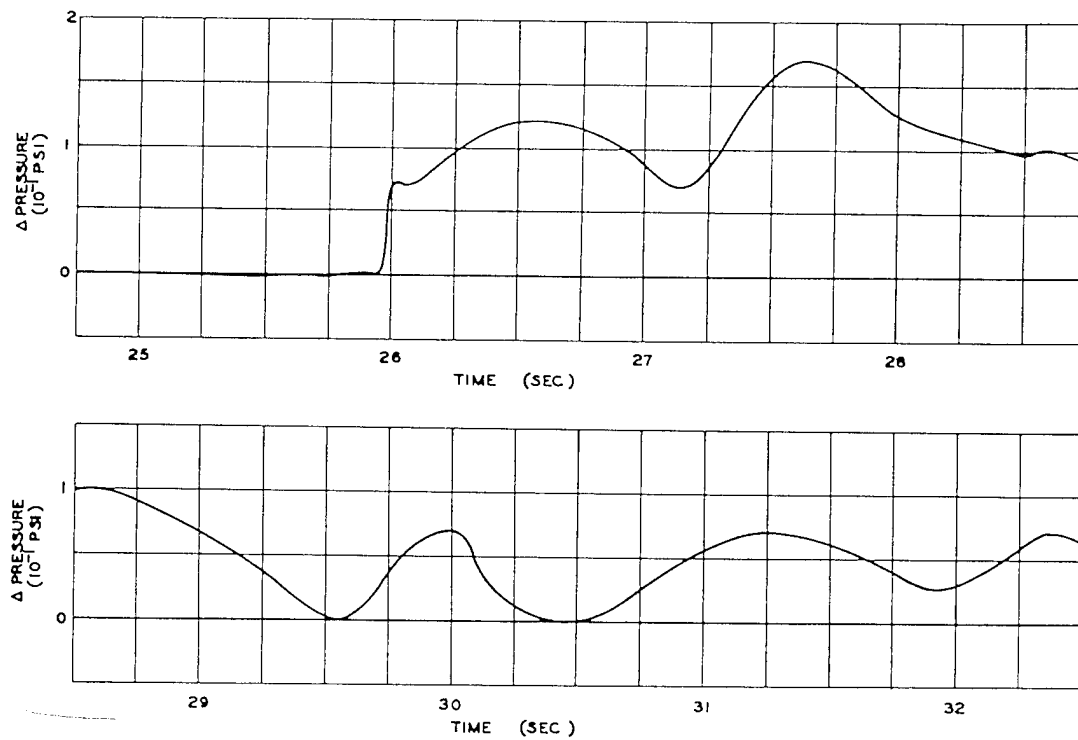


Fig. 6.78 Gauge Aerodynamic Pressure, 23% Chord, Top Left Wing Station 524, Channel B13, B-50D (290), Easy Shot

~~SECRET~~

~~SECRET~~

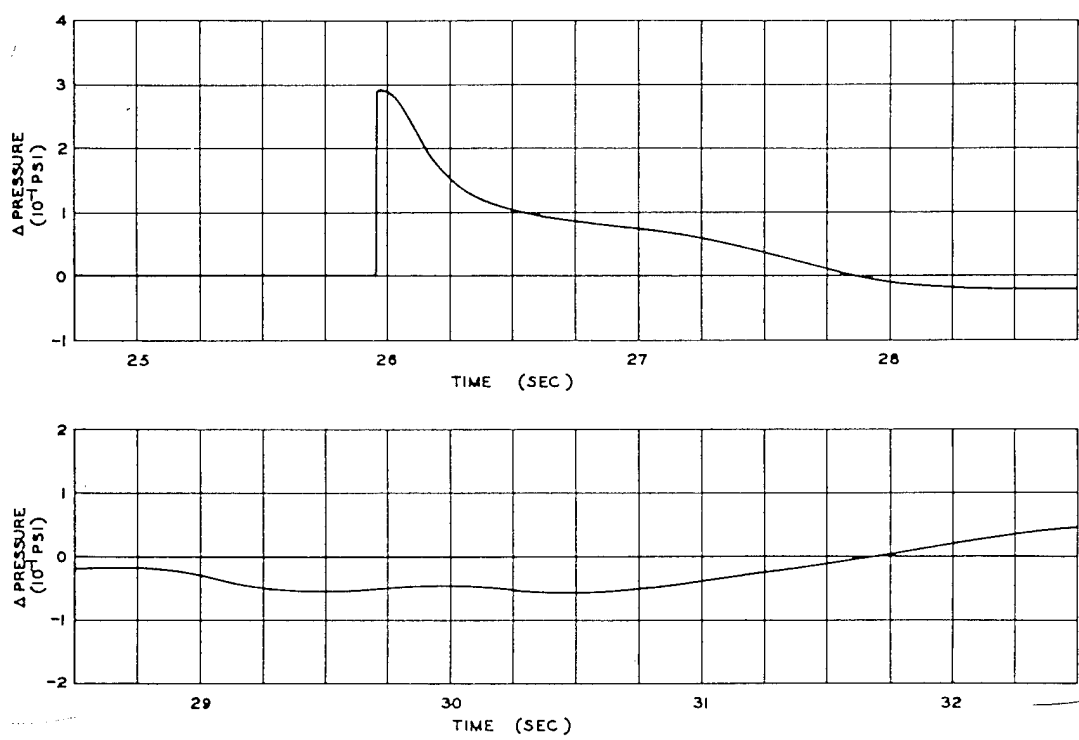


Fig. 6.79 Gauge Aerodynamic Pressure, 60% Chord, Top Left Wing Station 524, Channel B15, B-50D (290), Easy Shot

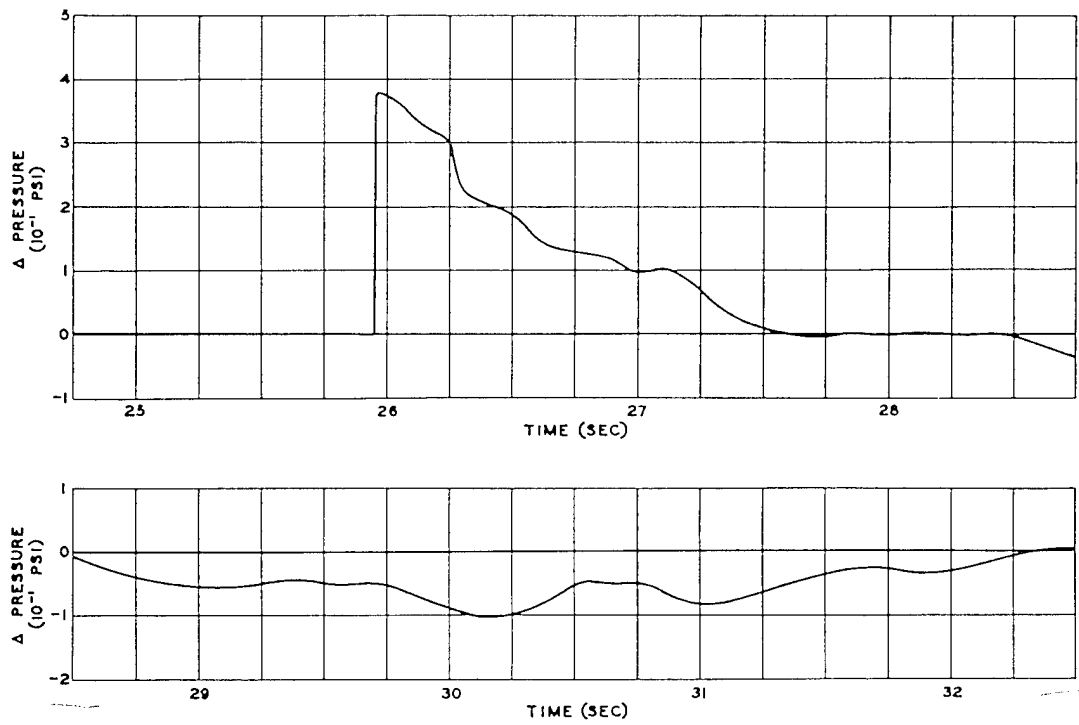


Fig. 6.80 Gauge Aerodynamic Pressure, 85% Chord, Top Left Wing Station 524, Channel B16, B-50D (290), Easy Shot

~~SECRET~~

~~SECRET~~

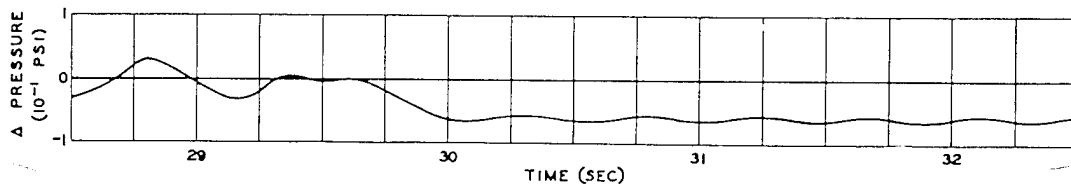
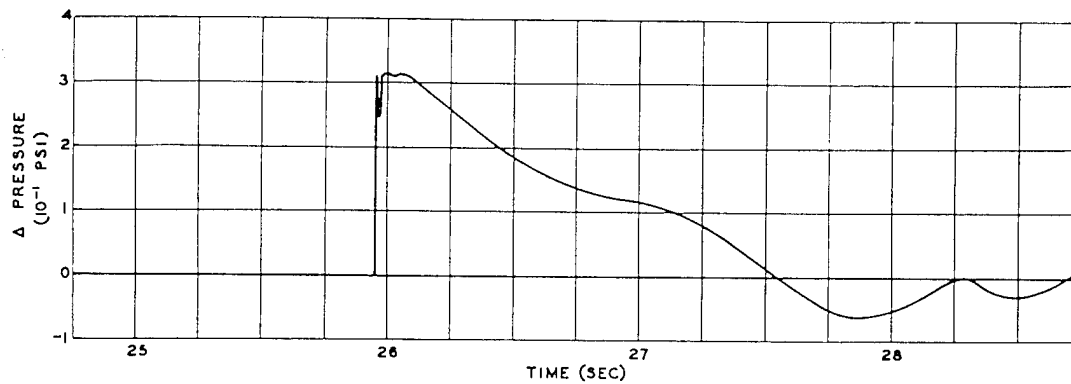


Fig. 6.81 Gauge Aerodynamic Pressure, 5% Chord, Bottom Left Wing Station 524, Channel B17, B-50D (290), Easy Shot

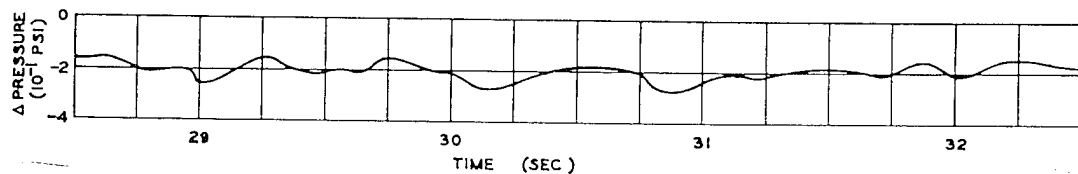
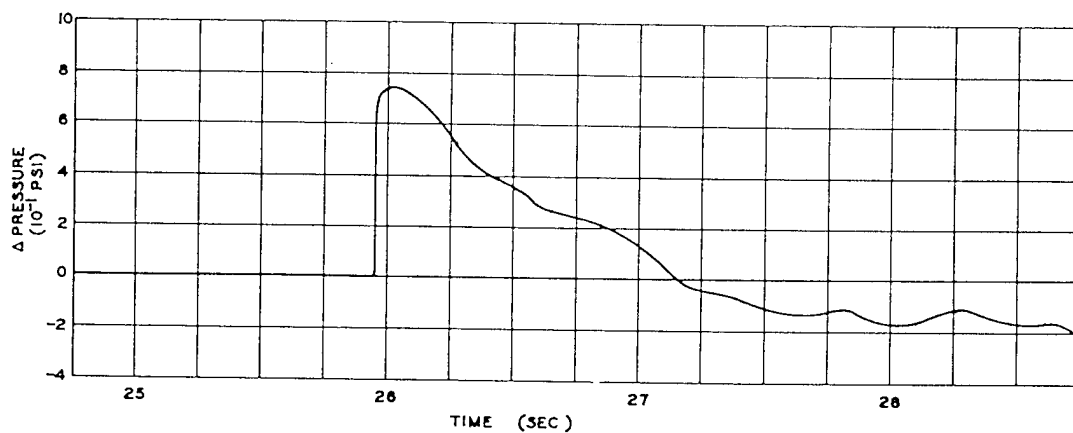


Fig. 6.82 Gauge Aerodynamic Pressure, 23% Chord, Bottom Left Wing Station 524, Channel B19, B-50D (290), Easy Shot

SECRET

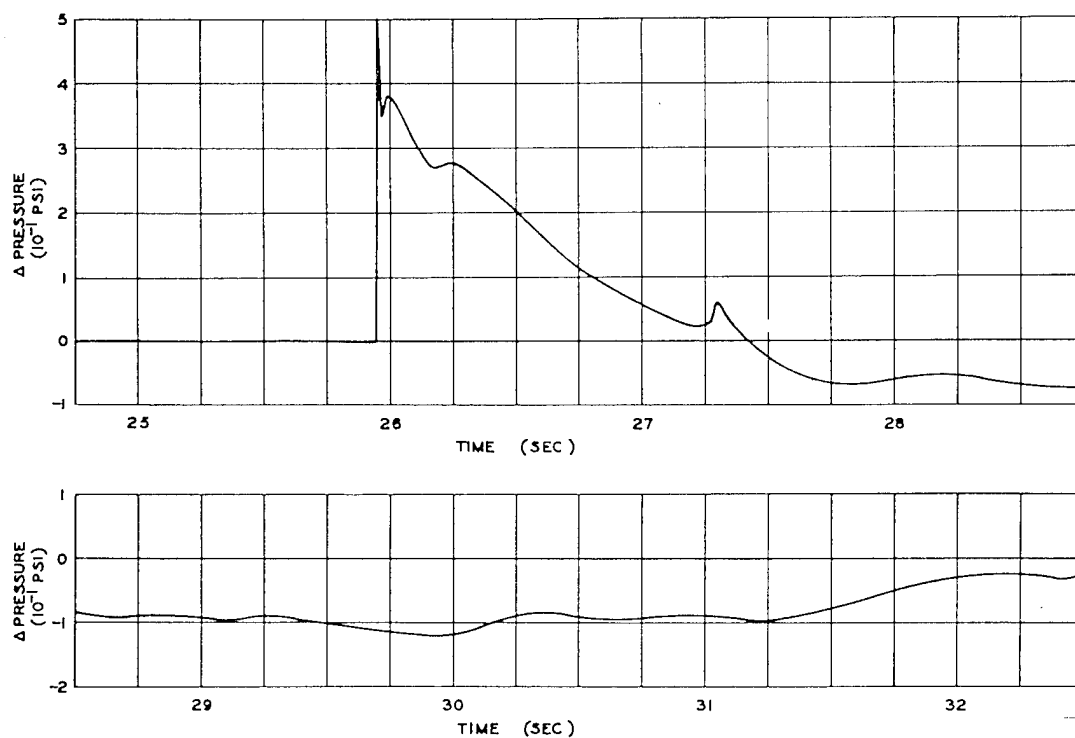


Fig. 6.83 Gauge Aerodynamic Pressure, 43% Chord, Bottom Left Wing Station 524, Channel B20, B-50D (290), Easy Shot

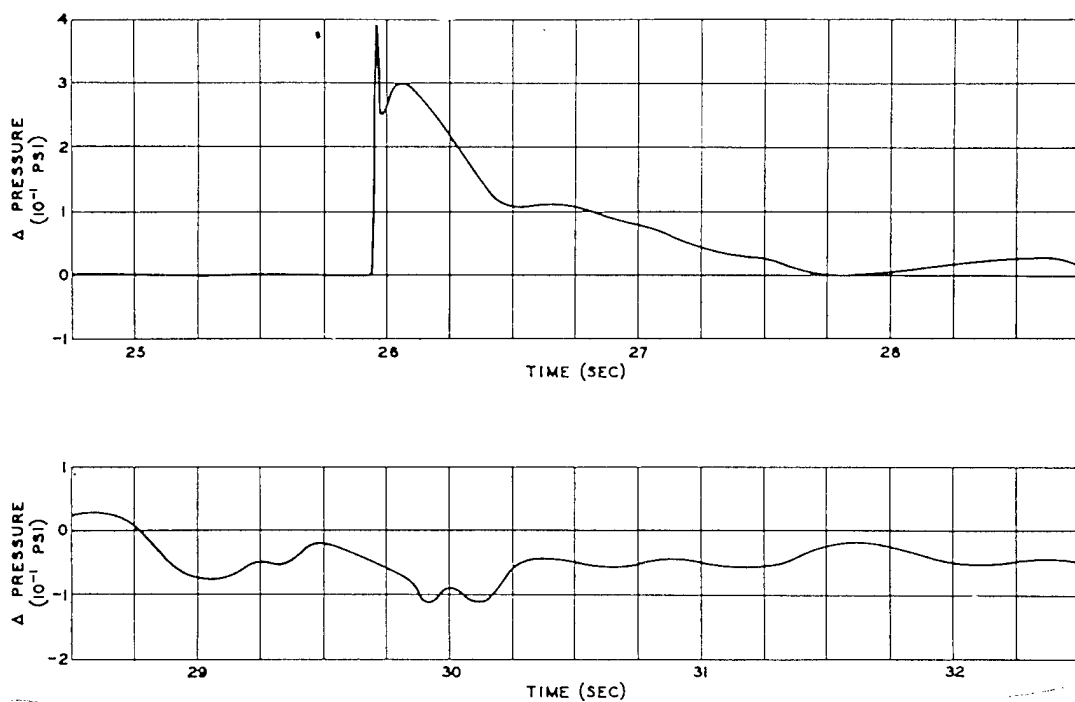


Fig. 6.84 Gauge Aerodynamic Pressure, 60% Chord, Bottom Left Wing Station 524, Channel B21, B-50D (290), Easy Shot

SECRET

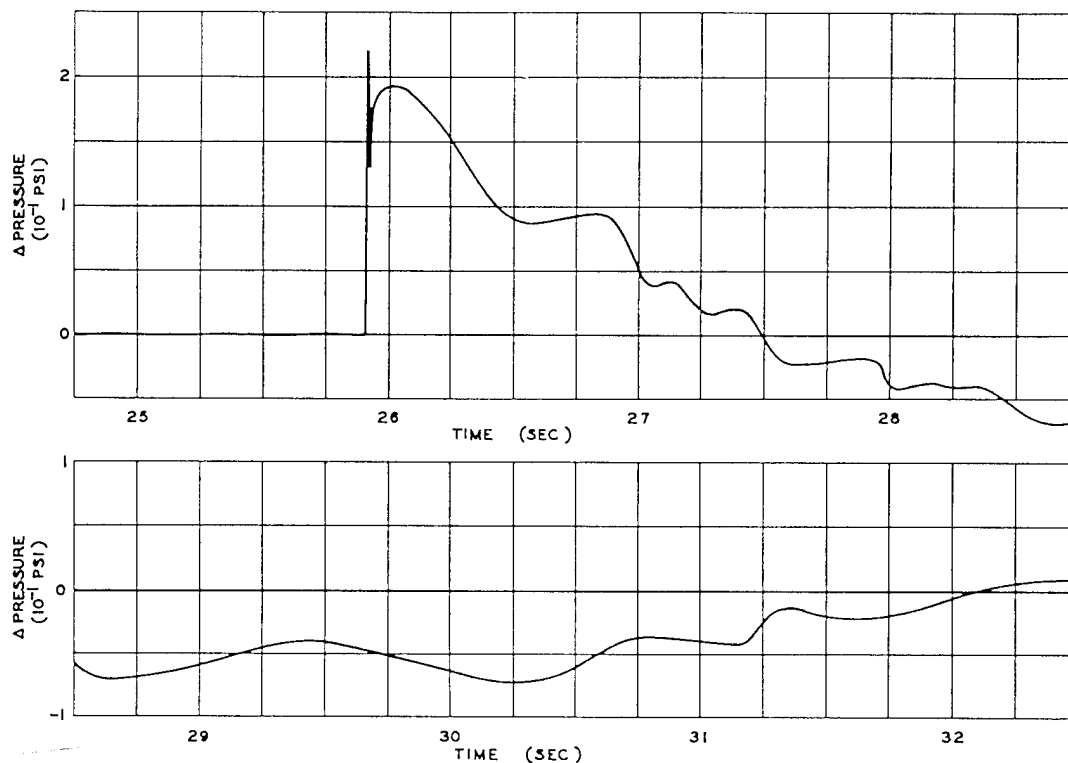


Fig. 6.85 Gauge Aerodynamic Pressure, Bottom Right-horizontal-stabilizer Station 170, Channel B23, B-50D (290), Easy Shot

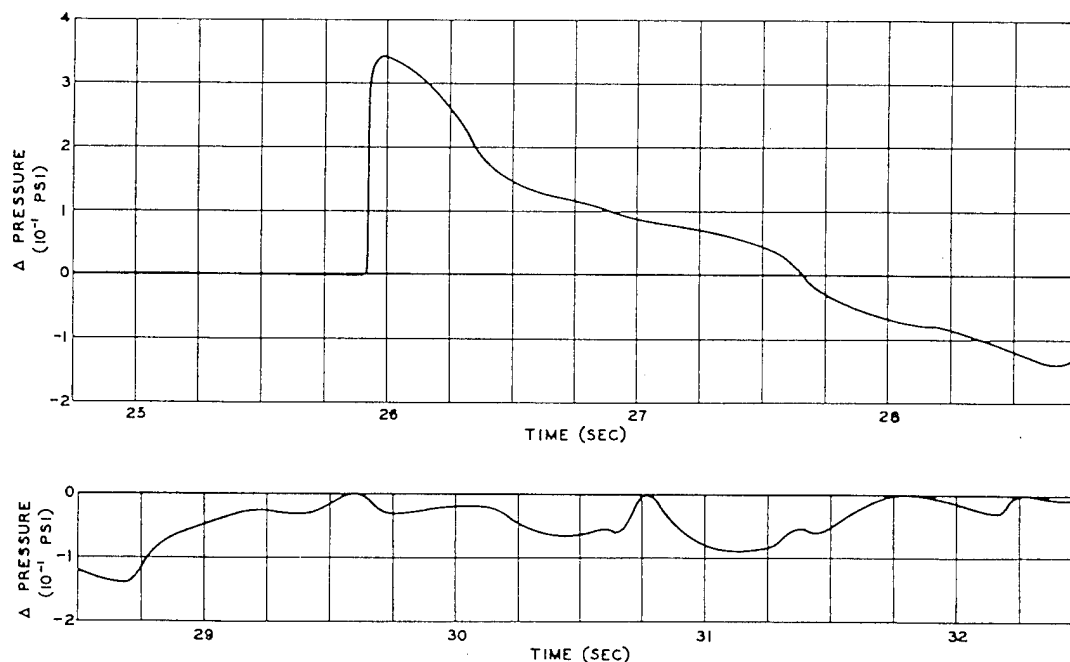


Fig. 6.86 Gauge Aerodynamic Pressure, Bottom Left-horizontal-stabilizer Station 170, Channel B24, B-50D (290), Easy Shot

~~SECRET~~

6.8 GRACE POSITION, B-50D AIRPLANE, NO. 49-340

Assigned location (at shock)

True altitude, 19,000 ft

Horizontal distance, 19,000 ft in direction
perpendicular to line of flight

Predicted conditions

Peak overpressure, 0.37 psi

Peak gust velocity, 39 ft/sec

Time of travel (shock), 21.1 sec

6.8.1 Flight Log

Because the whole sequence of take-off was ahead of schedule, B-50D (340) took off approximately 20 min before scheduled time and completed its mission without incident. The flight data as reported¹ by ATU 3.4.2 are as follows:

Time

Take-off, 0326

At assigned altitude, 0427

Shock arrival, 0627:22.2

Landing, 1000

Meteorological conditions at altitude

True altitude, 19,000 ft

Pressure altitude, 18,500 ft

Outside air temperature, -4°C

Wind direction (from), 270° (azimuth)

Wind velocity, 8 knots

Airplane parameters at shock arrival

Indicated airspeed, 162 knots

Ground speed, 389 ft/sec

Ground track azimuth, 040°

Horizontal angle from blast, 126.5° (azimuth)

Vertical angle from blast, * 45.0° (elevation)

Horizontal distance from blast, 19,030 ft

Slant distance from blast, * 26,900 ft

Shock struck the airplane from the left and below

6.8.2 Airplane Condition

Before take-off the channels of the recorders were balanced and aligned. All channels of both

*Computed from data in Navigator's Report, reference 1.

recorders checked satisfactorily except as follows:

Channels A3, A4, and A15—engine accelerometers had been disconnected (1) because of the noise which was imposed on the trace by the engine vibrations and (2) to prevent damage to these channels from destroying the record of the remaining channels of this recorder

Channel B13—had a bad amplifier

Channel B18—checked satisfactorily before take-off but failed and was disconnected during flight

The gross weight at take-off was computed to have been 120,400 lb, with the c.g. at 24.0 per cent m.a.c. This gross weight included 1,015 gal (6,090 lb) of fuel in each of the four main tanks, 970 gal (5,820 lb) in the center wing tank, and 100 gal (600 lb) in the skate tank. The fuel at the time of shock arrival was reported as 800 gal (4,800 lb) in each main tank, 100 gal (600 lb) in the center wing tank, and 100 gal (600 lb) in the skate tank; the gross weight was 109,950 lb, with the c.g. moving to 23.4 per cent m.a.c.

The pilot reported no particular observations, and no damage was discovered from examination of the airplane.

6.8.3 Load Data

The calibrate steps on channel B16 were not usable; the data on channels A2, A13, A14, A21, and B8 are obscured by noise; and no calibration is available for channel B21. As a consequence, the data from these channels are not presented. The data as recorded on this mission are presented in Figs. 6.87 through 6.122.

The record from the high-frequency recorder was lost because of an electrical failure. During the recording cycle a connection to a vacuum-tube socket became loose; this attenuated the signal to such an extent that it was not readable on the record.

6.8.4 Analysis

According to the navigator's report the airplane was essentially at its assigned position, and the theoretical predicted conditions are valid. The actual time for shock-wave travel was only 0.1 sec longer than the theoretical time.

~~SECRET~~

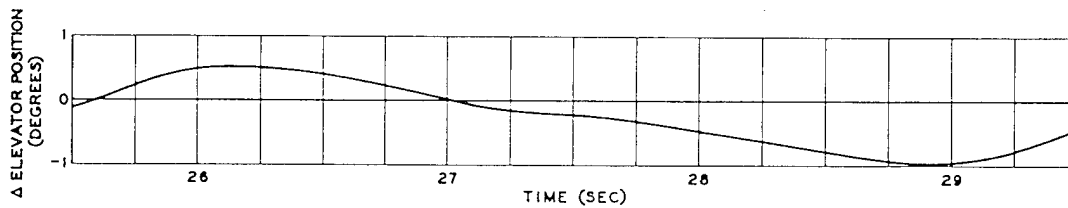
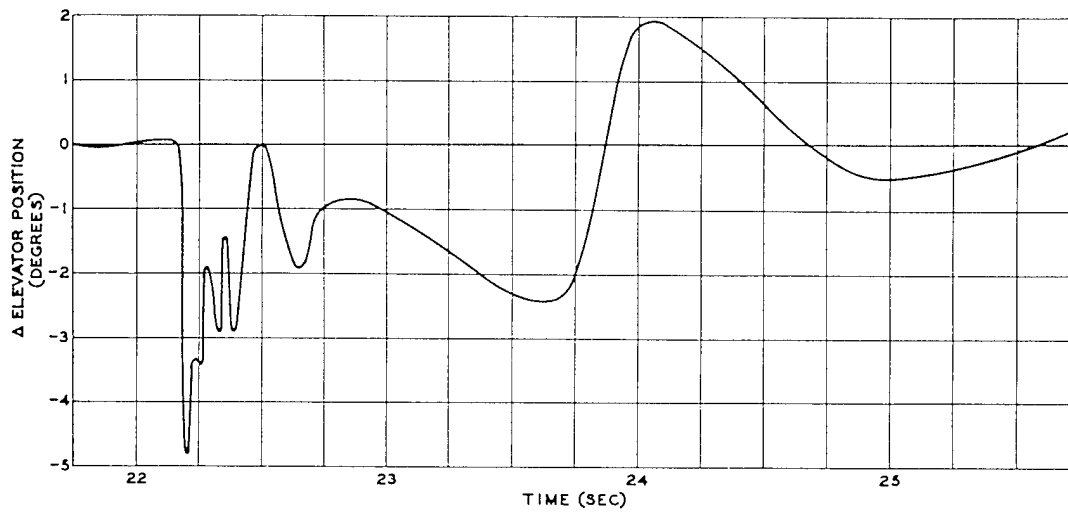


Fig. 6.87 Elevator Position, Elevator Torque Tube, Channel A1, B-50D (340), Easy Shot

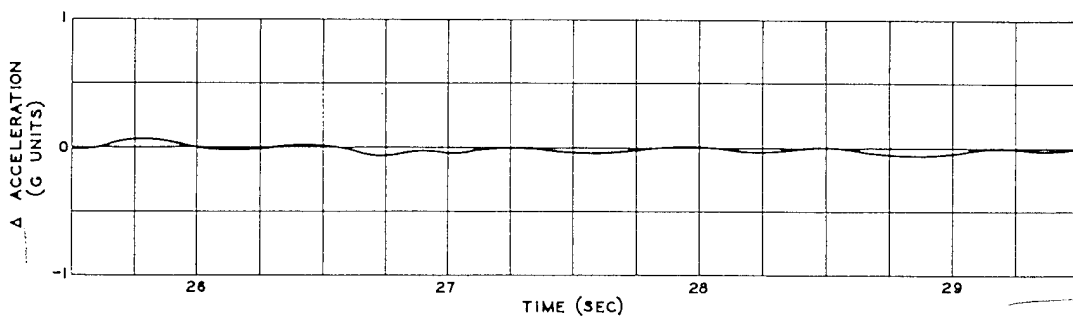
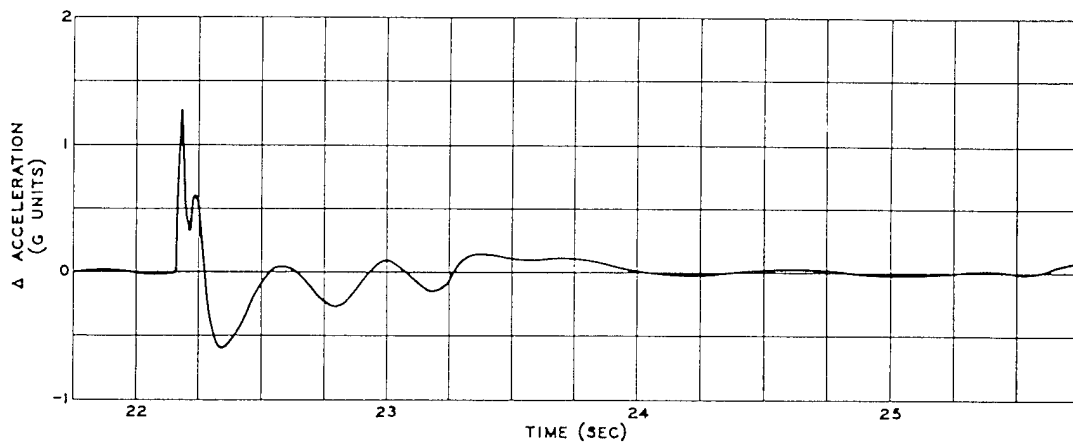


Fig. 6.88 Normal Acceleration, Forward Bomb Bay, Channel A5, B-50D (340), Easy Shot

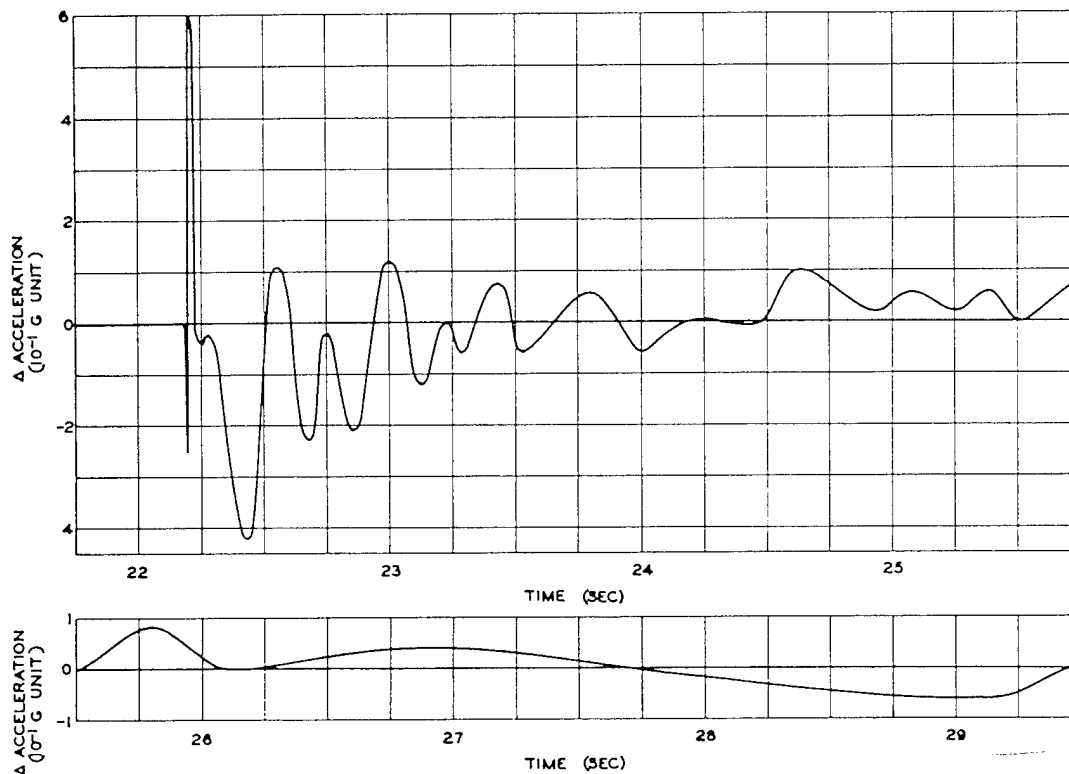


Fig. 6.89 Normal Acceleration, Nose-wheel Well, Channel A6, B-50D (340), Easy Shot

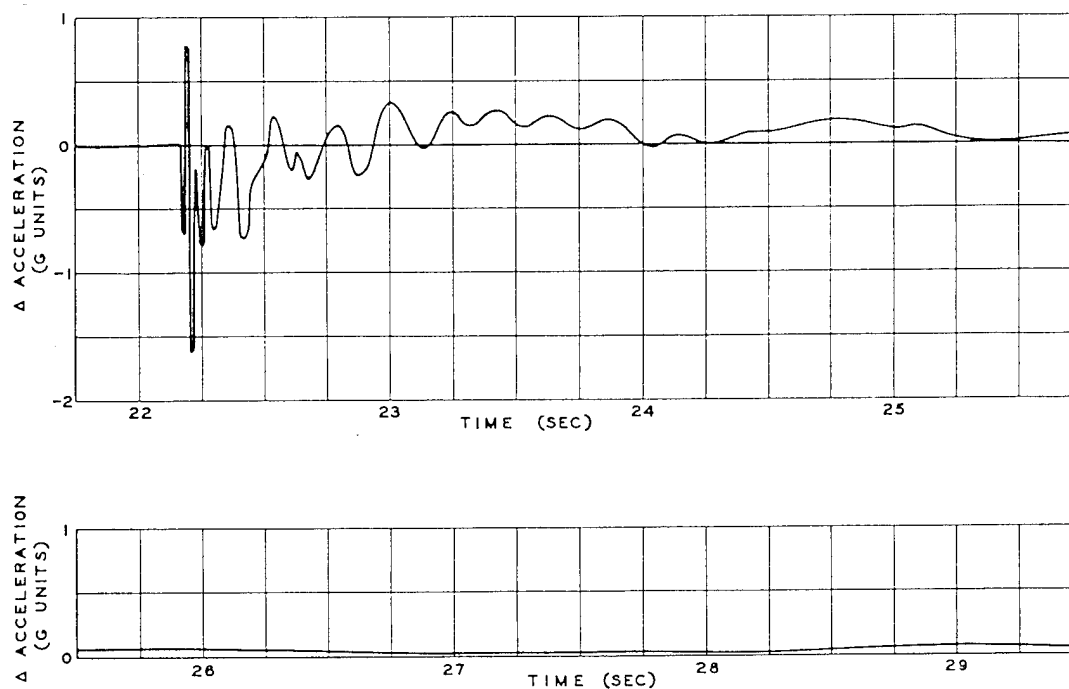


Fig. 6.90 Normal Acceleration, Aft Fuselage, in Tail-gunner's Compartment, Channel A7, B-50D (340), Easy Shot

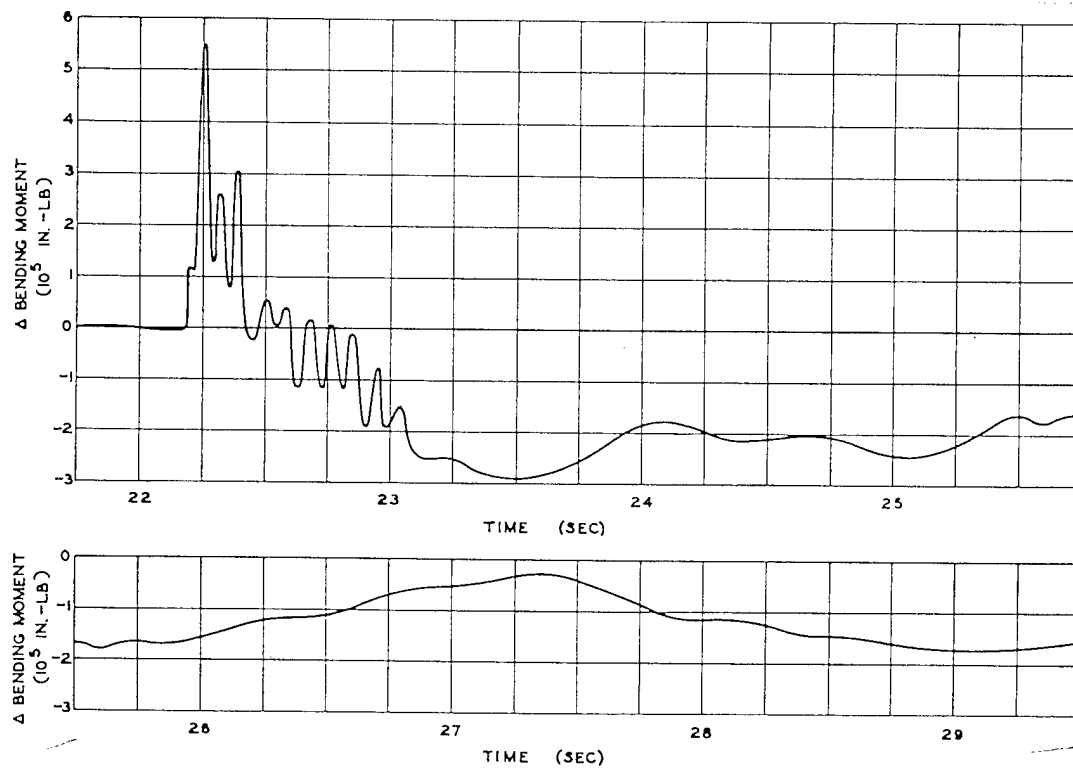


Fig. 6.91 Horizontal-stabilizer Bending, Right-horizontal-stabilizer Station 34, Channel A8, B-50D (340), Easy Shot

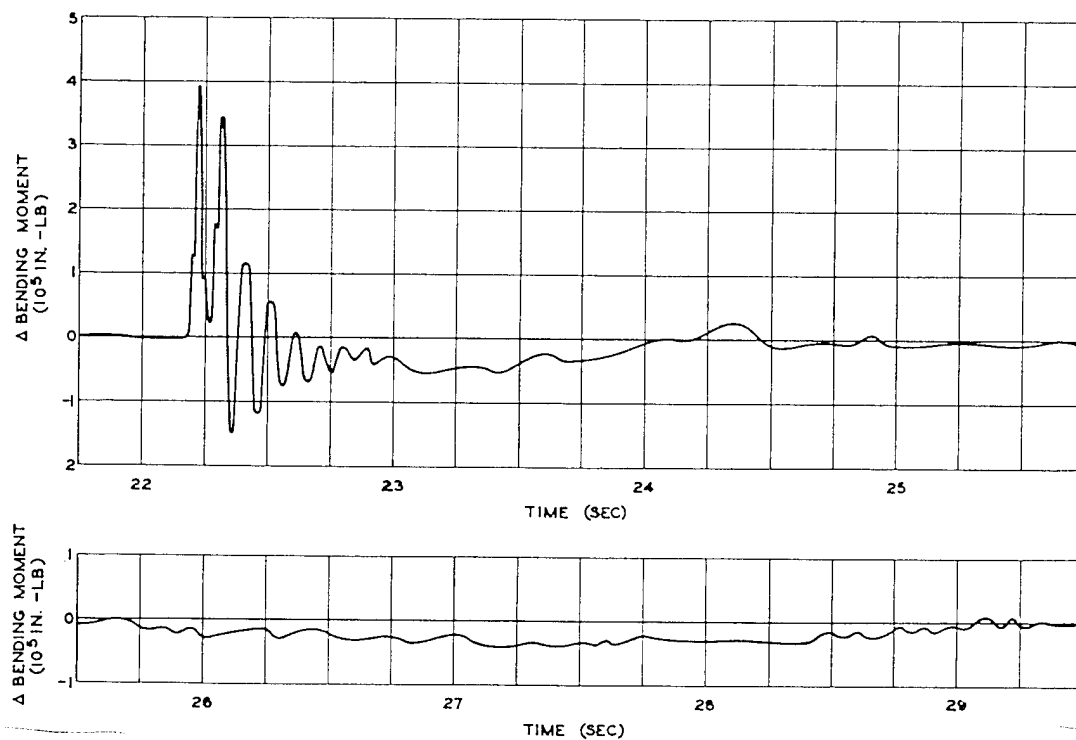


Fig. 6.92 Horizontal-stabilizer Bending, Left-horizontal-stabilizer Station 34, Channel A9, B-50D (340), Easy Shot

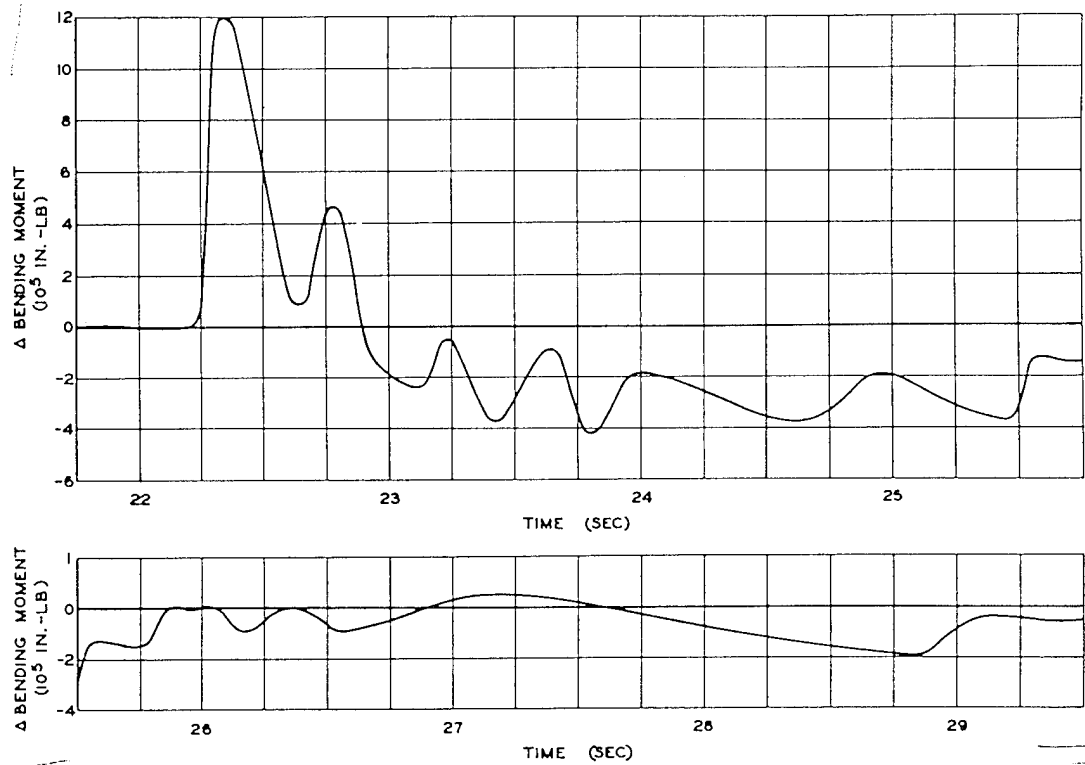


Fig. 6.93 Wing Bending, Right Wing Mid-span, Wing Station 266, Channel A10, B-50D (340), Easy Shot

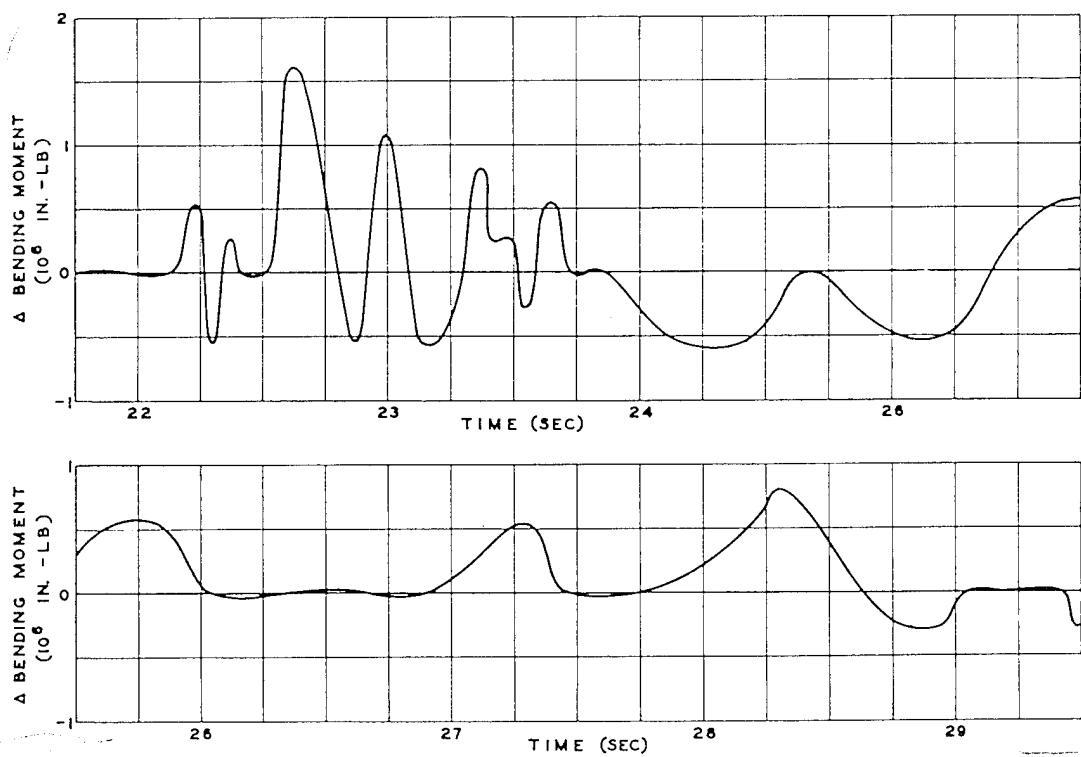


Fig. 6.94 Wing Bending, Right Wing Root, Wing Station 79, Channel A11, B-50D (340), Easy Shot

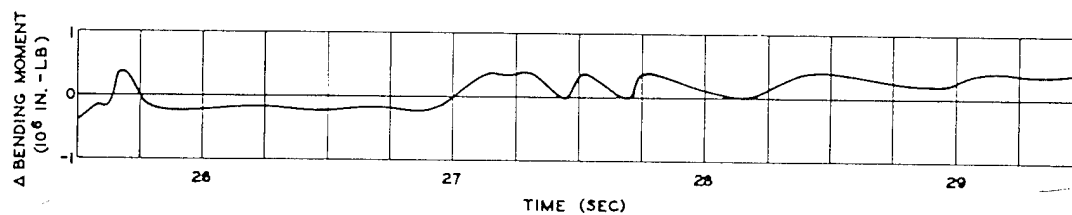
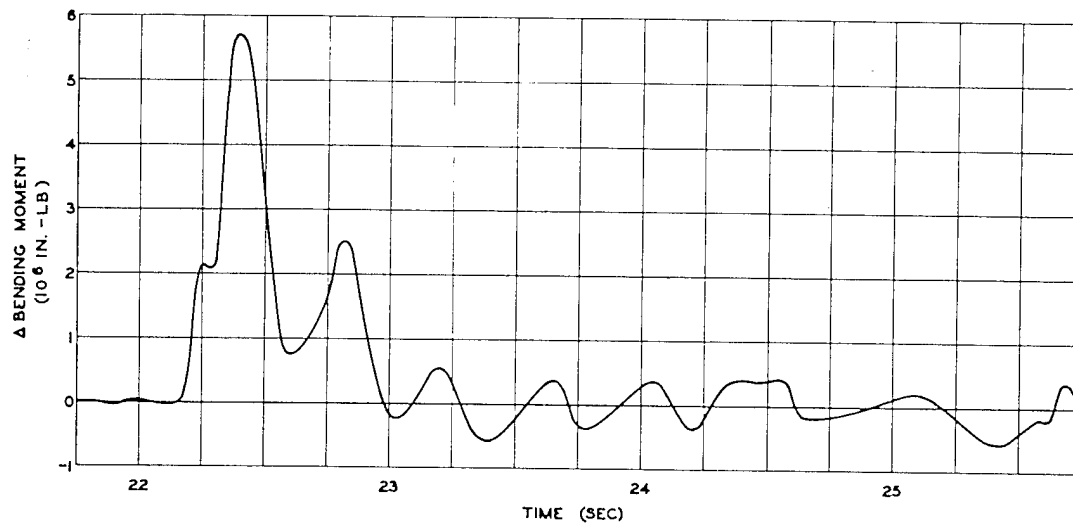


Fig. 6.95 Wing Bending, Left Wing Root, Wing Station 79, Channel A12, B-50D (340), Easy Shot

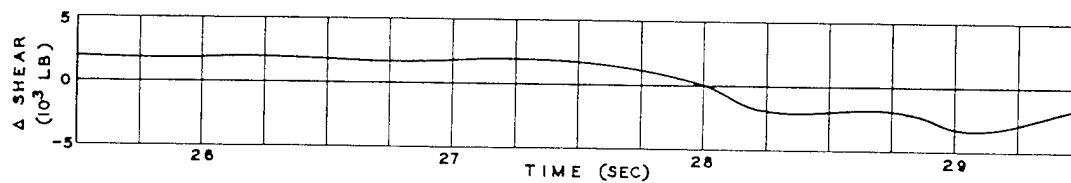
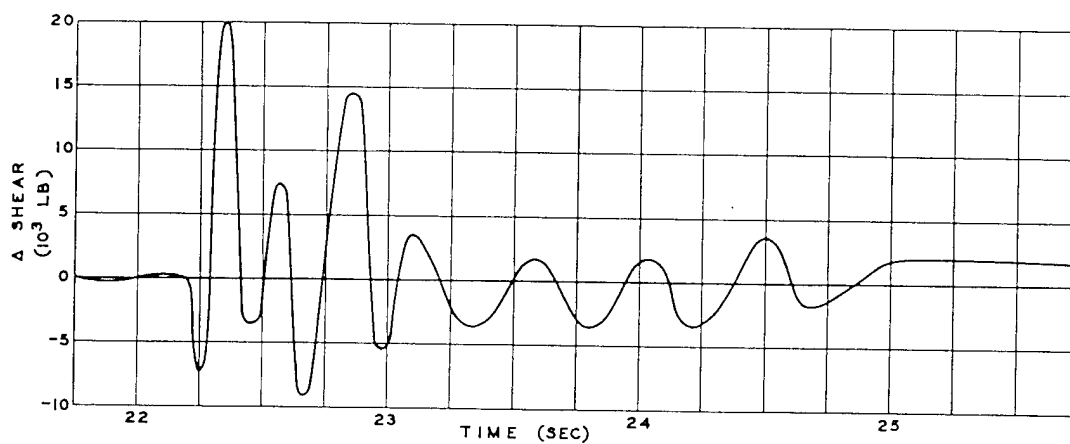


Fig. 6.96 Wing Shear, Right Wing Mid-span, Wing Station 269, Channel A16, B-50D (340), Easy Shot

SECRET

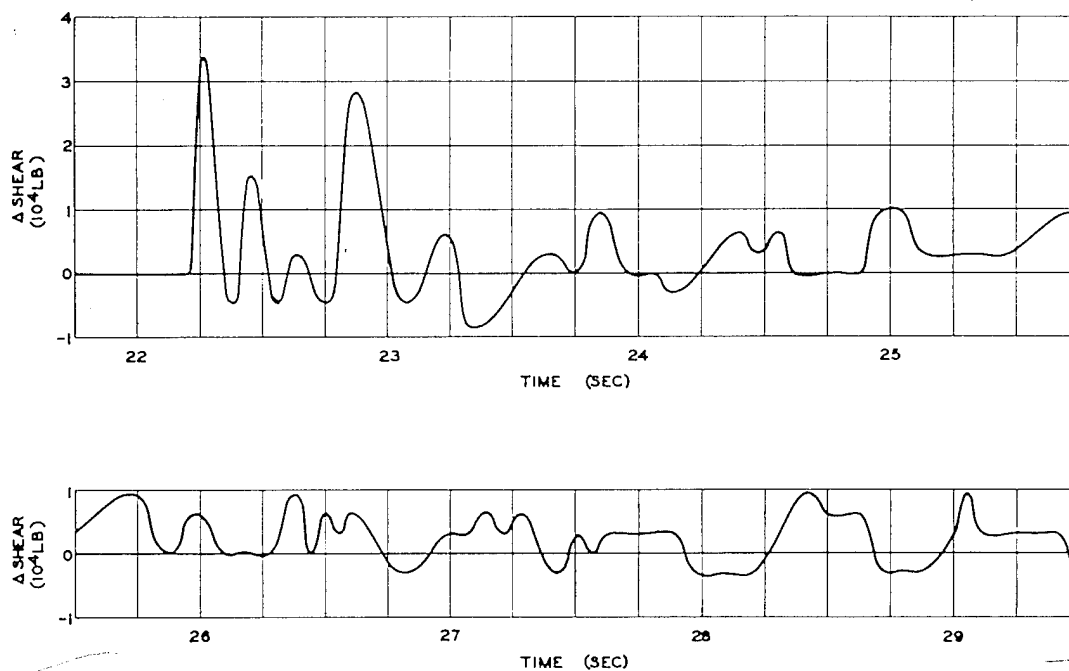


Fig. 6.97 Wing Shear, Right Wing Root, Wing Station 78, Channel A17, B-50D (340), Easy Shot

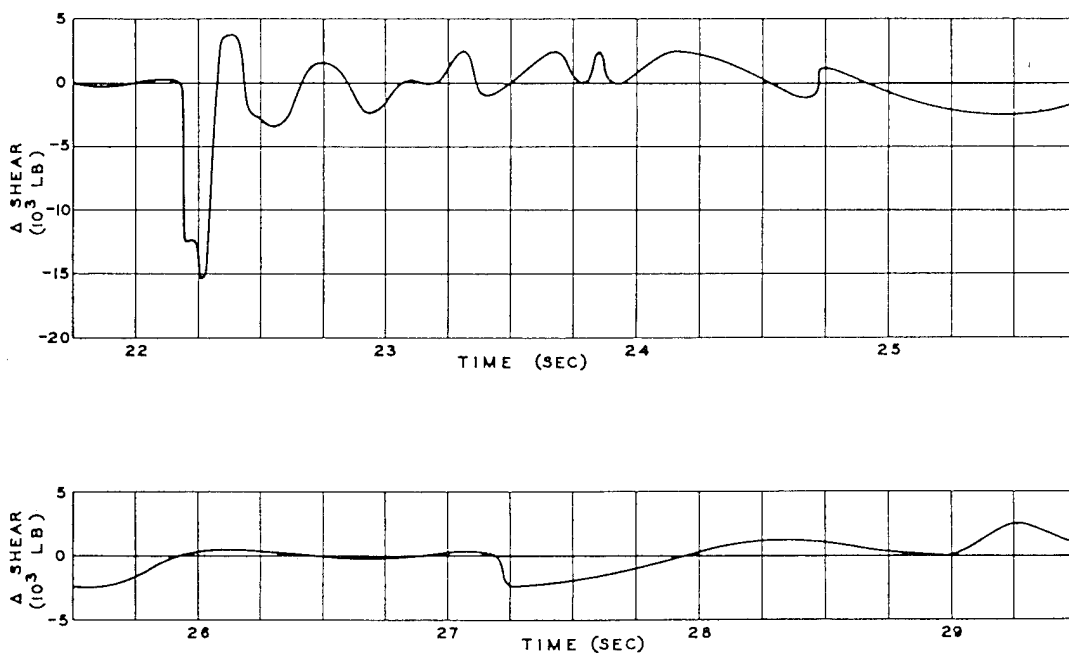


Fig. 6.98 Wing Shear, Left Wing Root, Wing Station 78, Channel A18, B-50D (340), Easy Shot

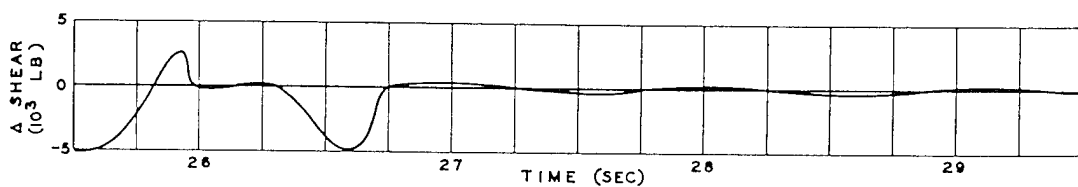
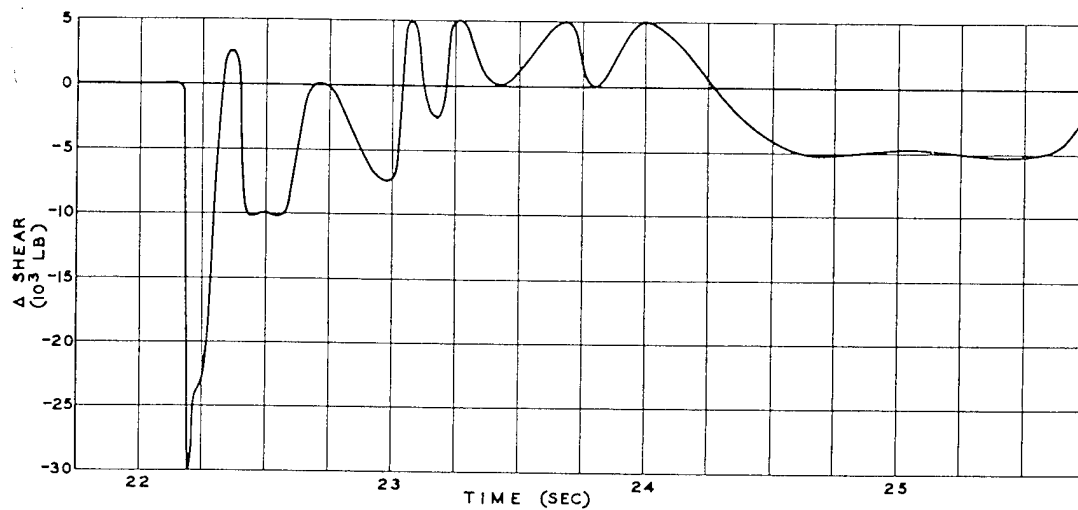


Fig. 6.99 Wing Shear, Left Wing Inboard, Wing Station 122, Channel A19, B-50D (340), Easy Shot

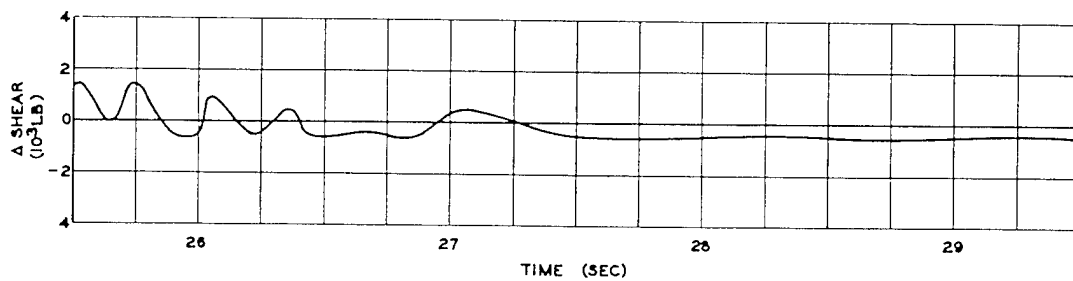
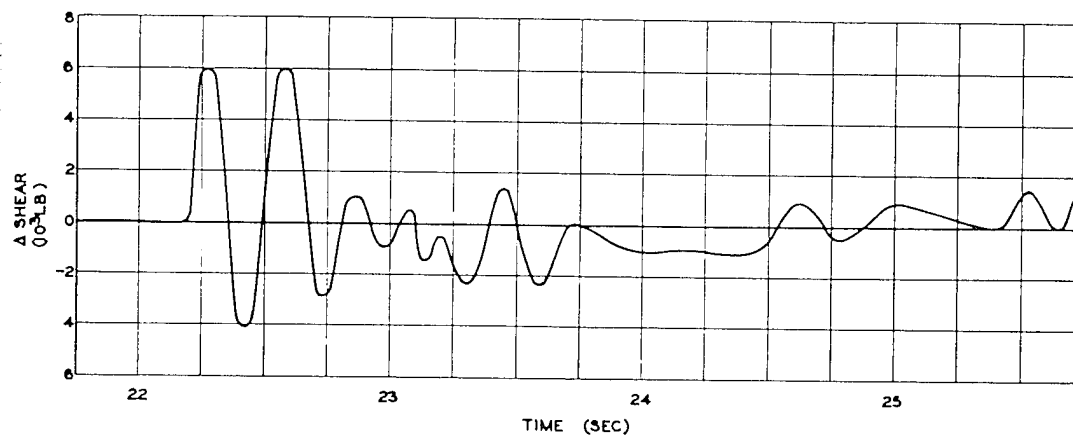


Fig. 6.100 Wing Shear, Left Wing Mid-span, Wing Station 269, Channel A20, B-50D (340), Easy Shot

SECRET

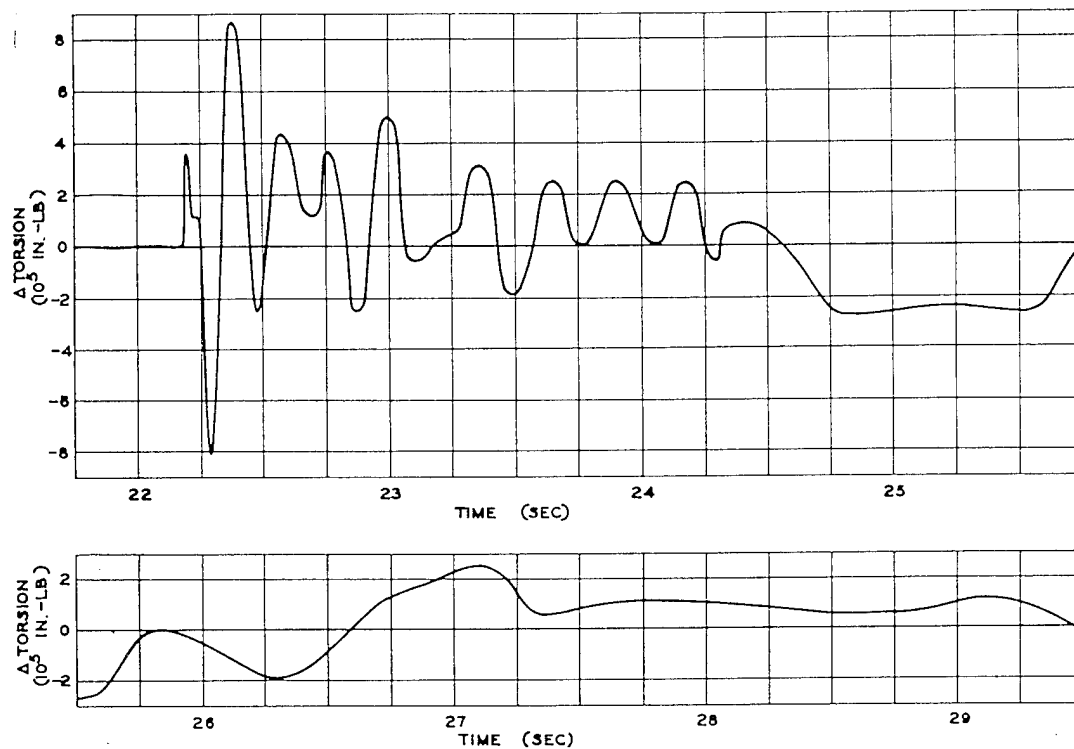


Fig. 6.101 Wing Torsion, Right Wing Root, Wing Station 78, Channel A22, B-50D (340), Easy Shot

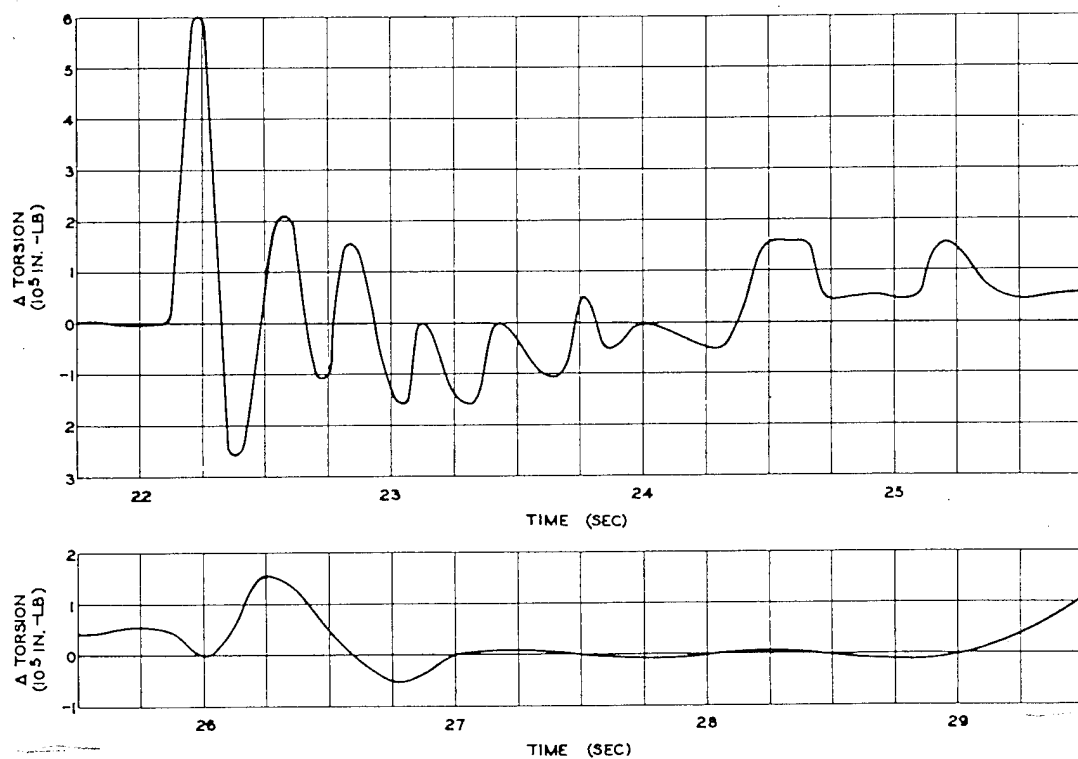


Fig. 6.102 Wing Torsion, Left Wing Root, Wing Station 78, Channel A23, B-50D (340), Easy Shot

SECRET

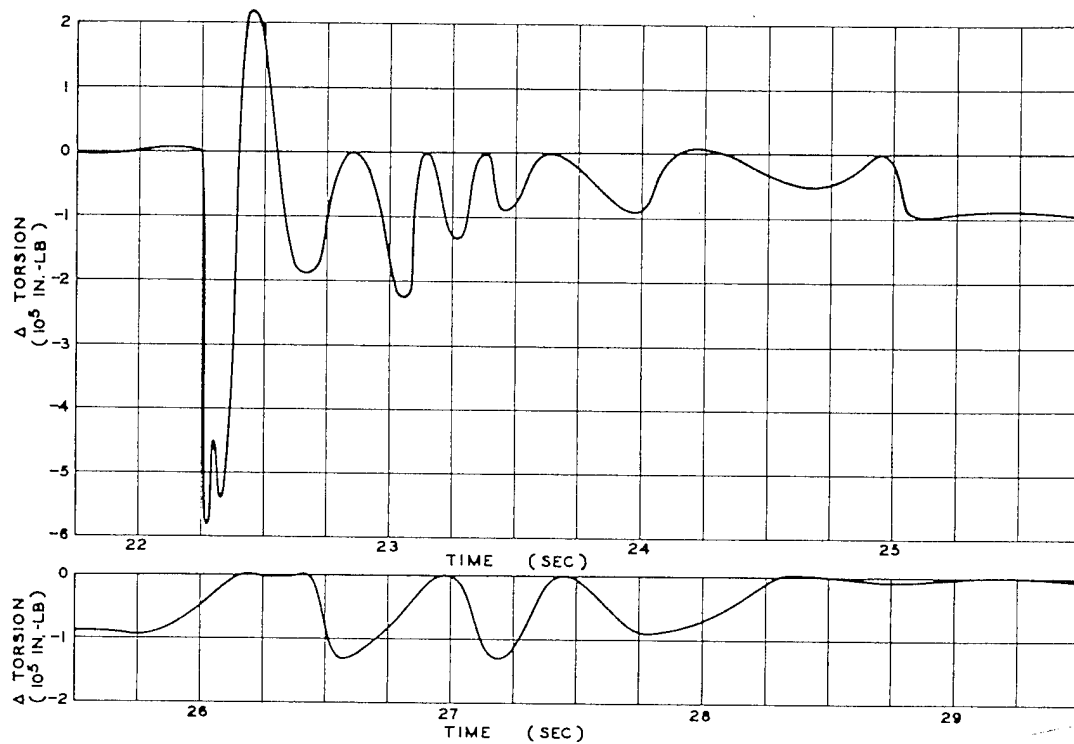


Fig. 6.103 Wing Torsion, Left Wing Inboard, Wing Station 122, Channel A24, B-50D (340), Easy Shot

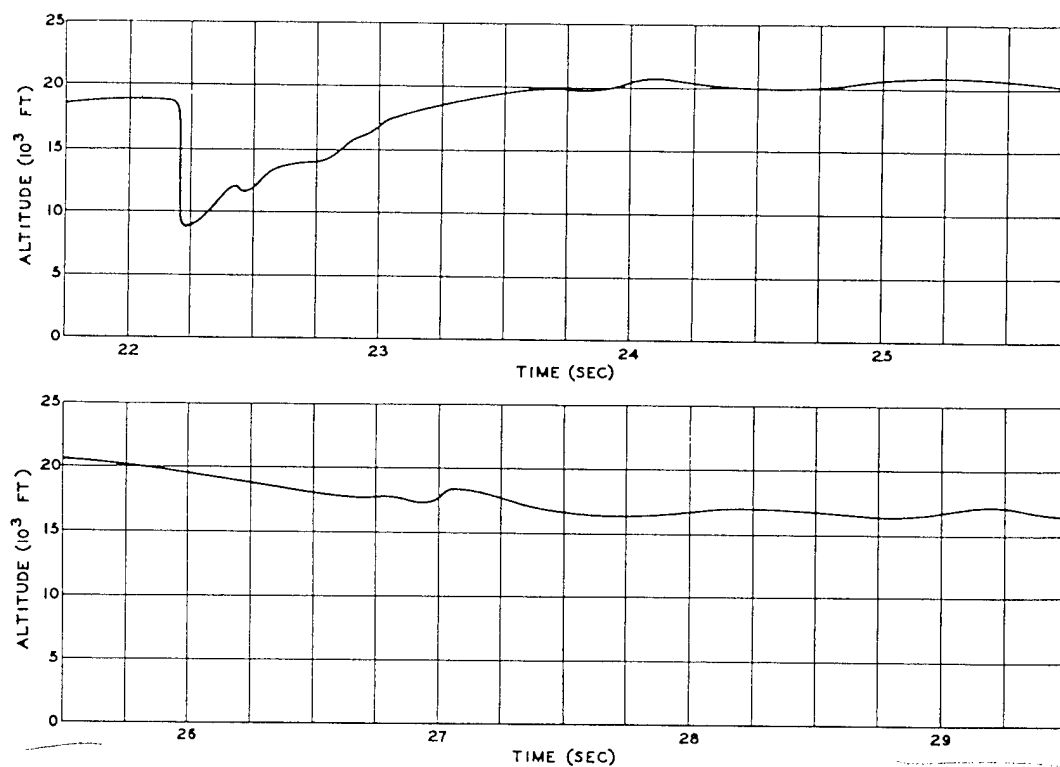


Fig. 6.104 Altitude, Channel B1, B-50D (340), Easy Shot

~~SECRET~~

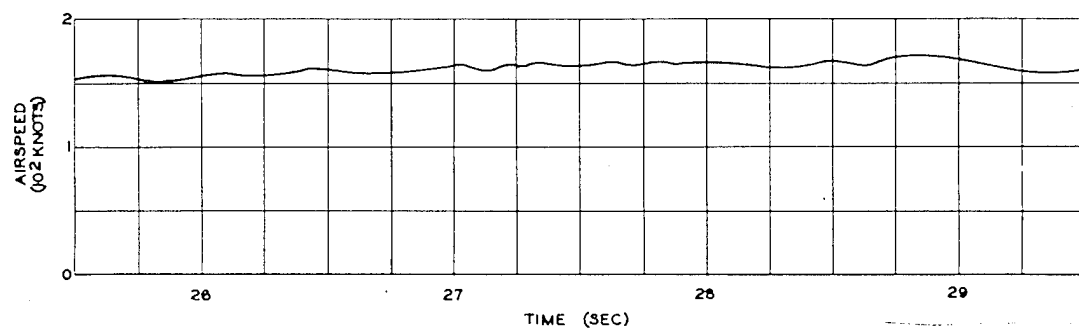
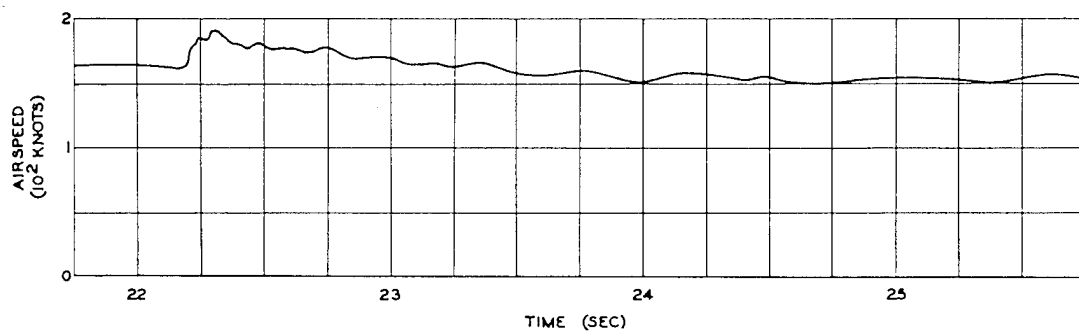


Fig. 6.105 Airspeed, Channel B2, B-50D (340), Easy Shot

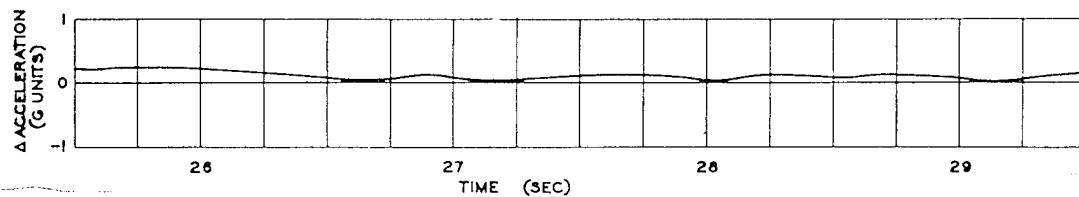
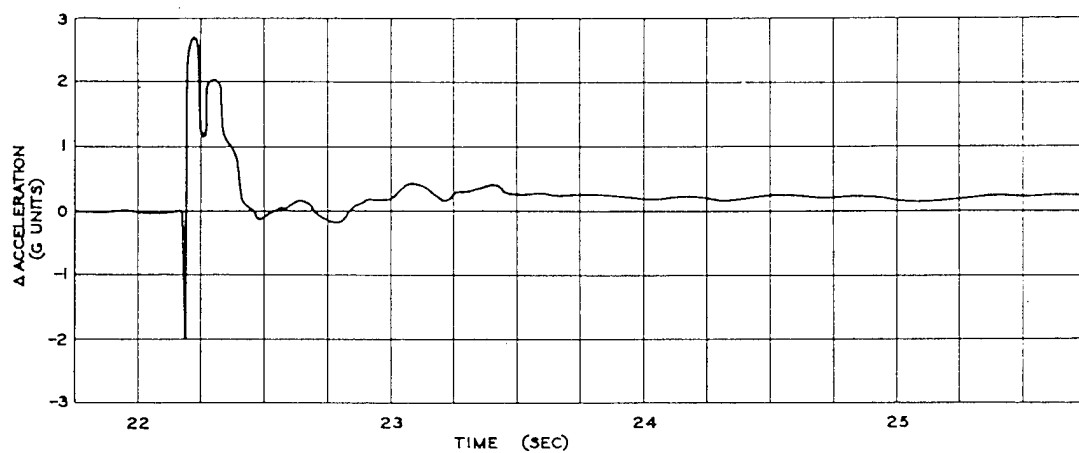


Fig. 6.106 Normal Acceleration, Aft Rear Bomb Bay, Fuselage Station 628, Channel B3, B-50D (340), Easy Shot

~~SECRET~~

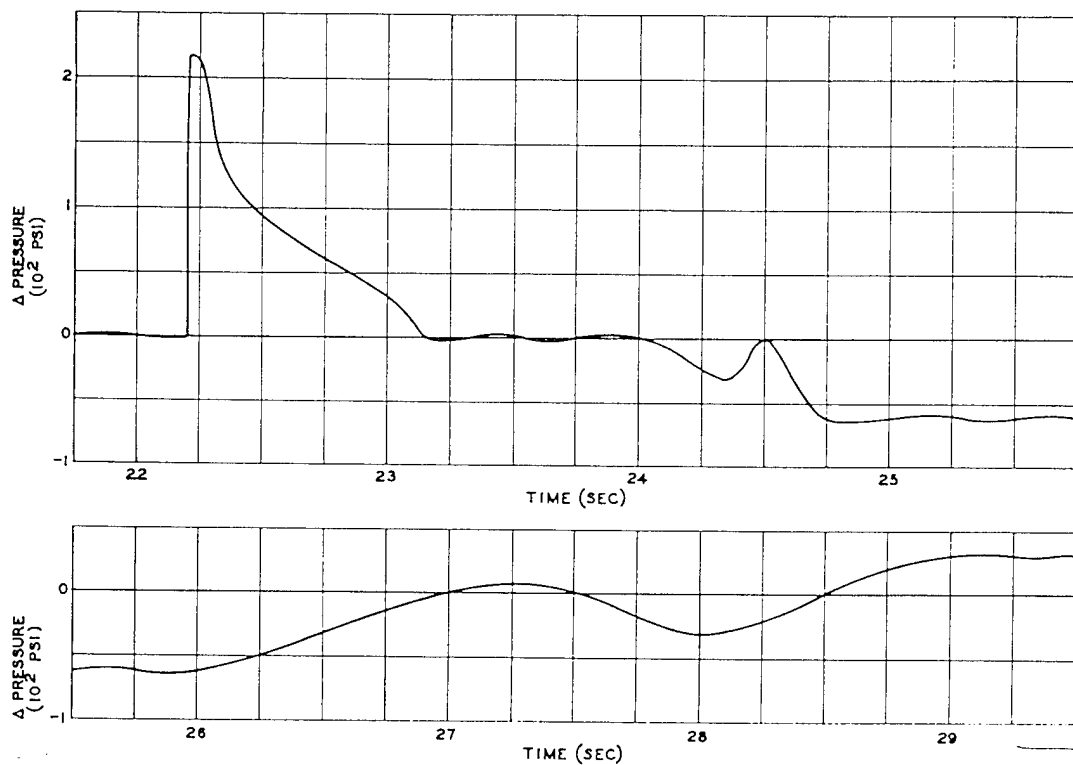


Fig. 6.107 Differential Aerodynamic Pressure, 23% Chord, Right Wing Station 525, Channel B4, B-50D (340), Easy Shot

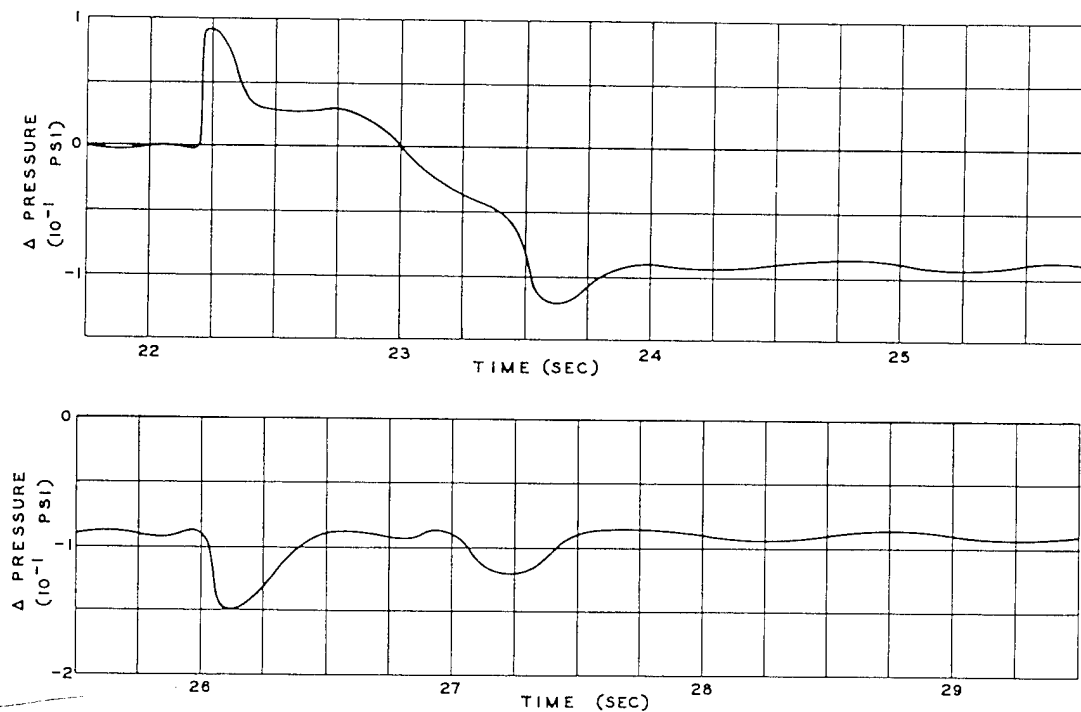


Fig. 6.108 Differential Aerodynamic Pressure, 60% Chord, Right Wing Station 525, Channel B5, B-50D (340), Easy Shot

SECRET

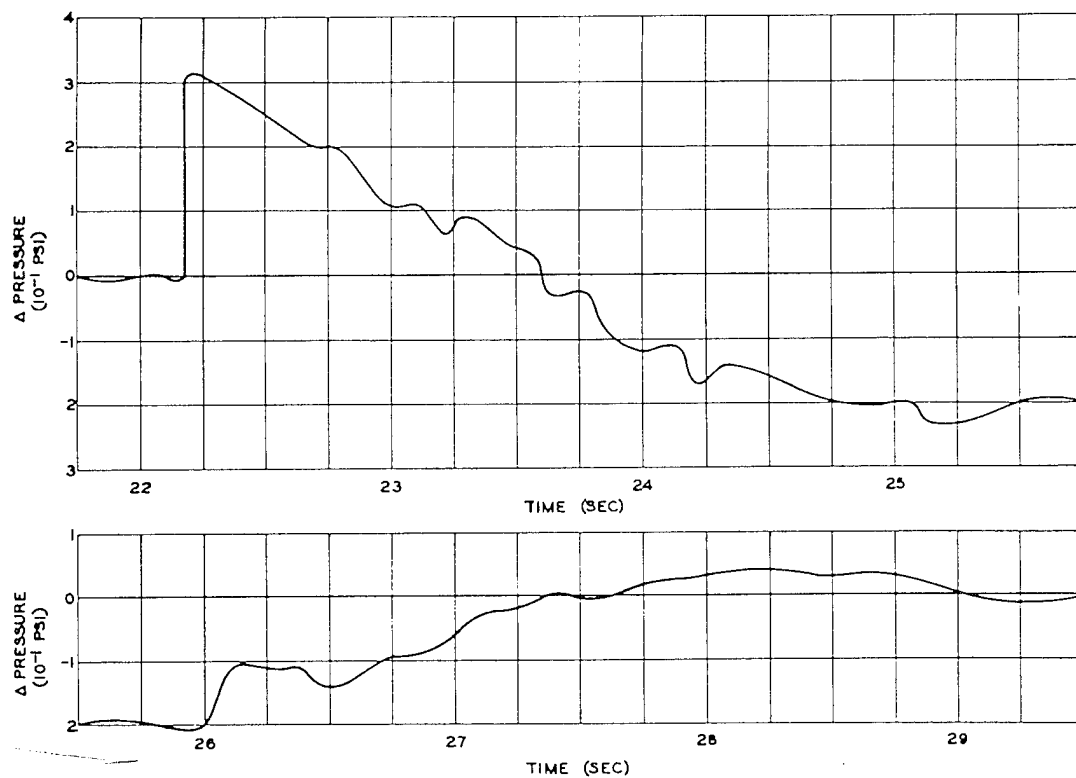


Fig. 6.109 Gauge Aerodynamic Pressure, Bottom Forward Fuselage, Fuselage Station 26, Channel B6, B-50D (340), Easy Shot

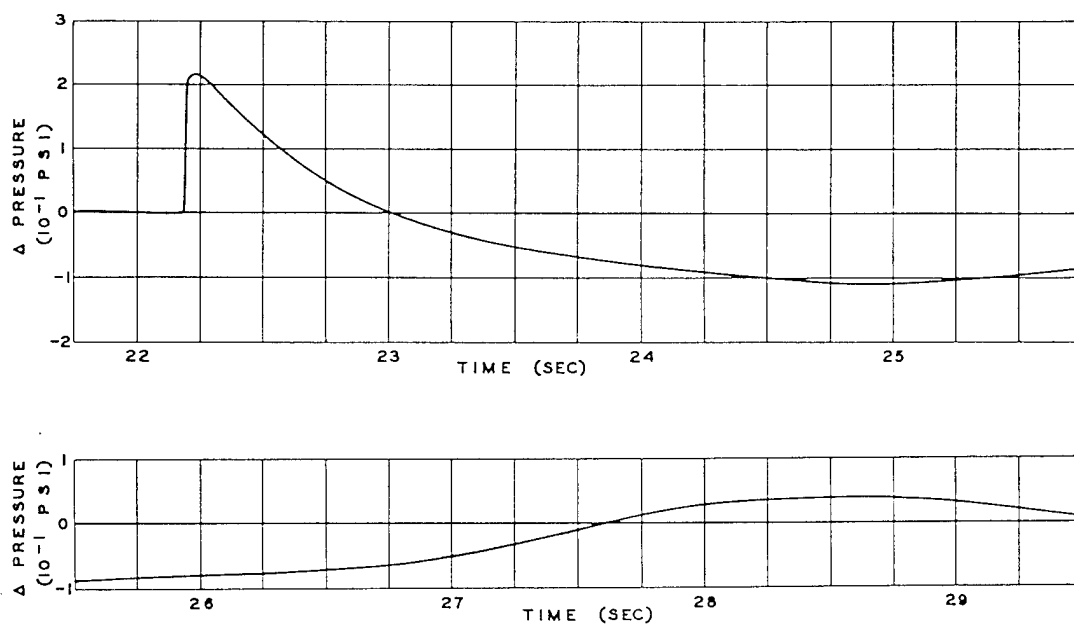


Fig. 6.110 Gauge Aerodynamic Pressure, Right Side of Fuselage, Fuselage Station 783, Channel B7, B-50D (340), Easy Shot

SECRET

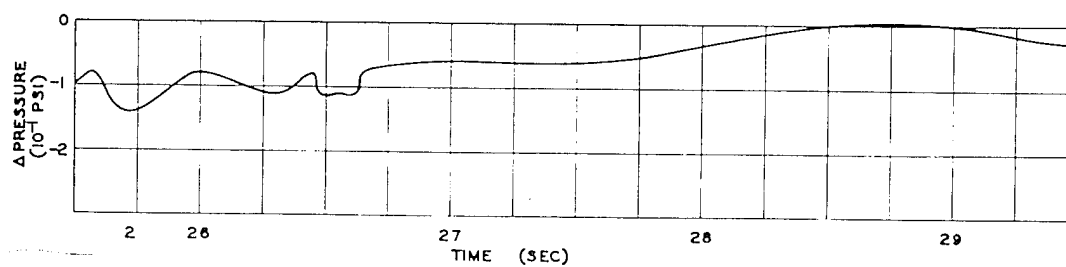
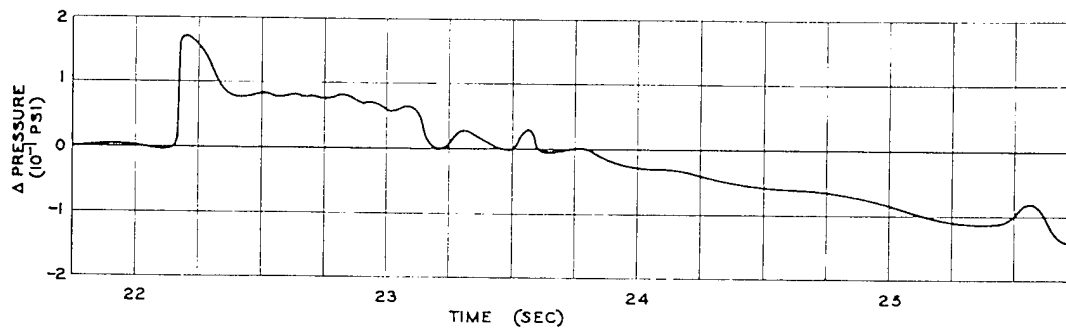


Fig. 6.111 Gauge Aerodynamic Pressure, Right Side of Vertical Fin, Fuselage Station 974, Channel B9, B-50D (340), Easy Shot

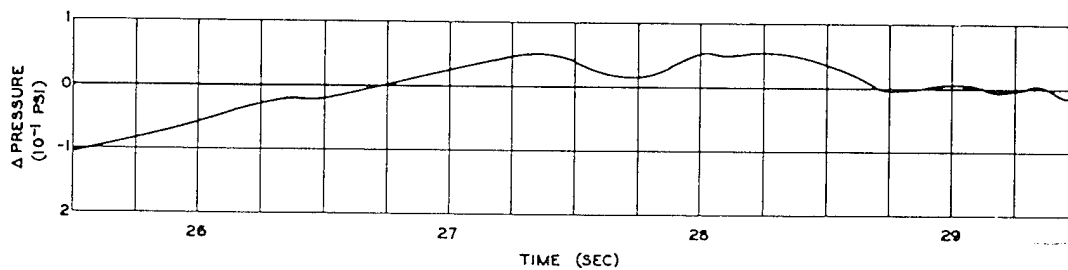
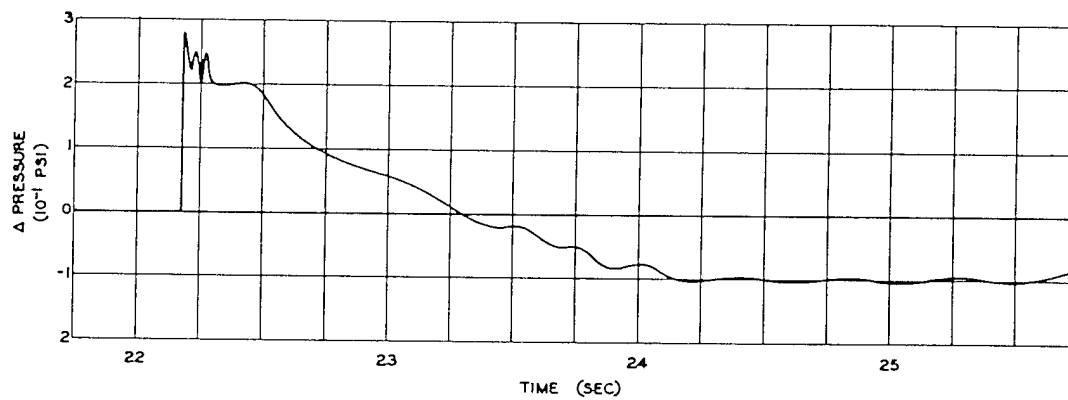


Fig. 6.112 Gauge Aerodynamic Pressure, Left Side of Vertical Fin, Fuselage Station 974, Channel B10, B-50D (340), Easy Shot

~~SECRET~~

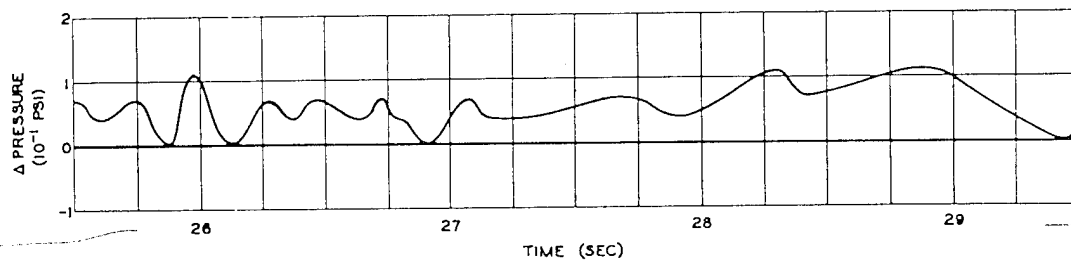
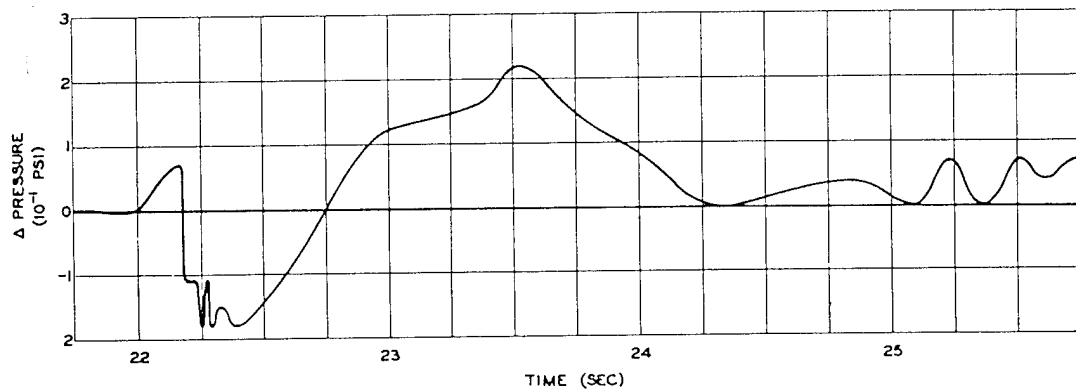


Fig. 6.113 Gauge Aerodynamic Pressure, 5% Chord, Top Left Wing Station 524, Channel B11, B-50D (340), Easy Shot

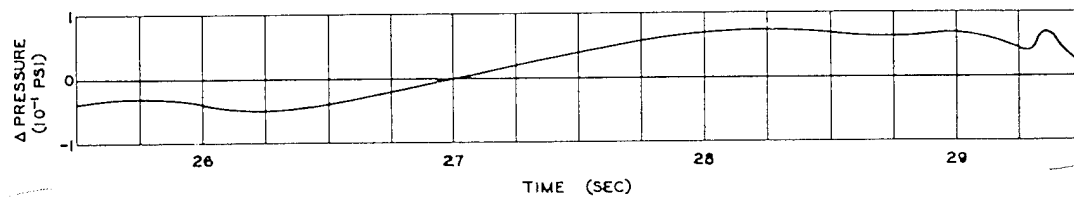
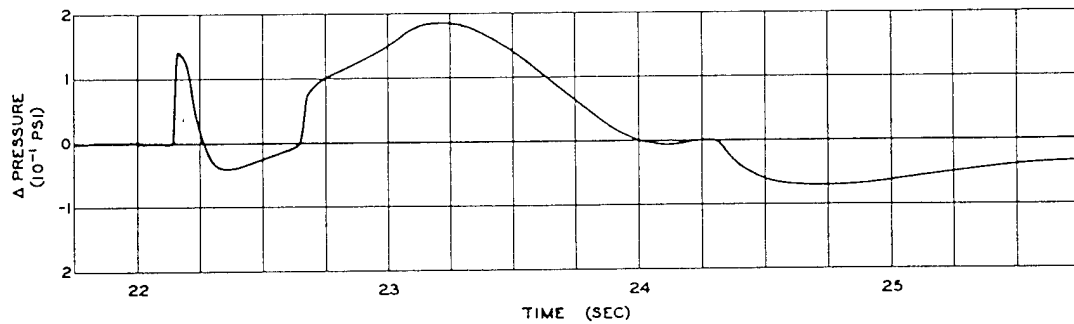


Fig. 6.114 Gauge Aerodynamic Pressure, 15% Chord, Top Left Wing Station 524, Channel B12, B-50D (340), Easy Shot

~~SECRET~~

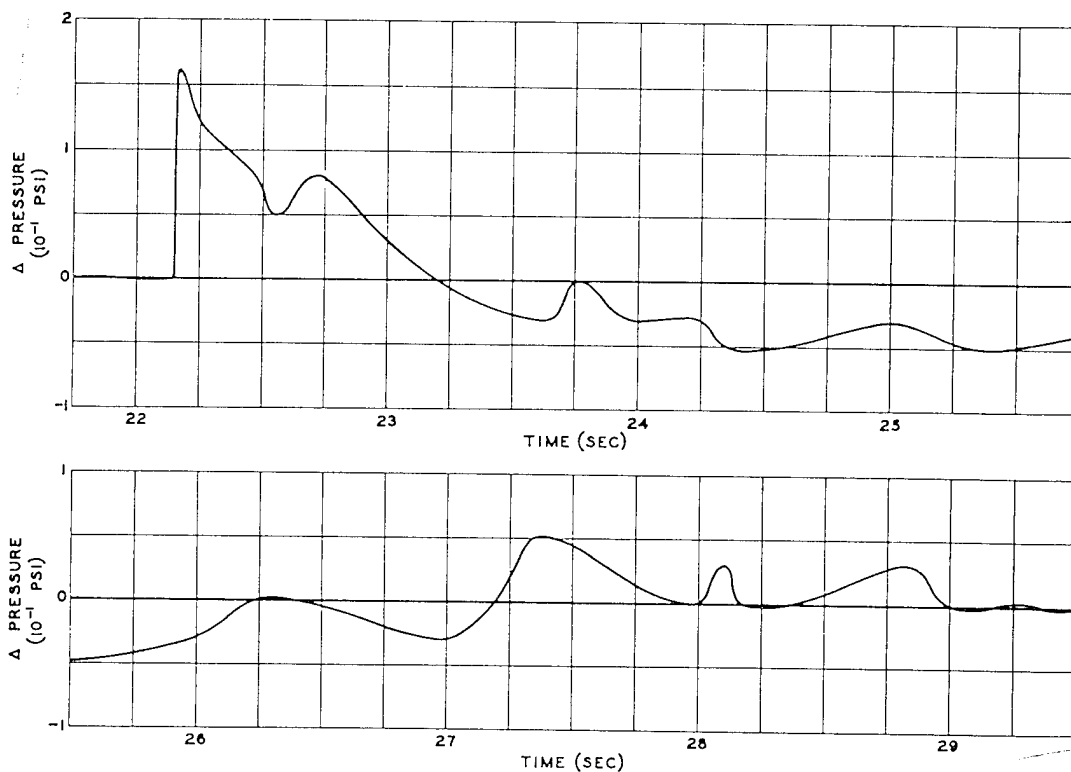


Fig. 6.115 Gauge Aerodynamic Pressure, 43% Chord, Top Left Wing Station 524, Channel B14, B-50D (340), Easy Shot

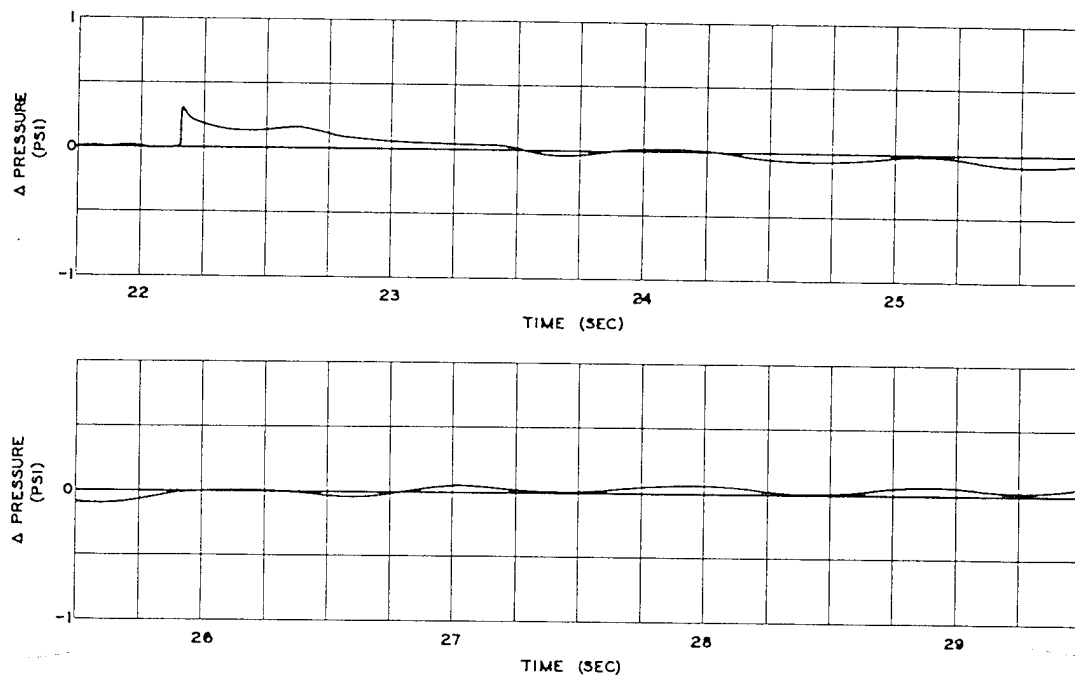


Fig. 6.116 Gauge Aerodynamic Pressure, 60% Chord, Top Left Wing Station 524, Channel B15, B-50D (340), Easy Shot

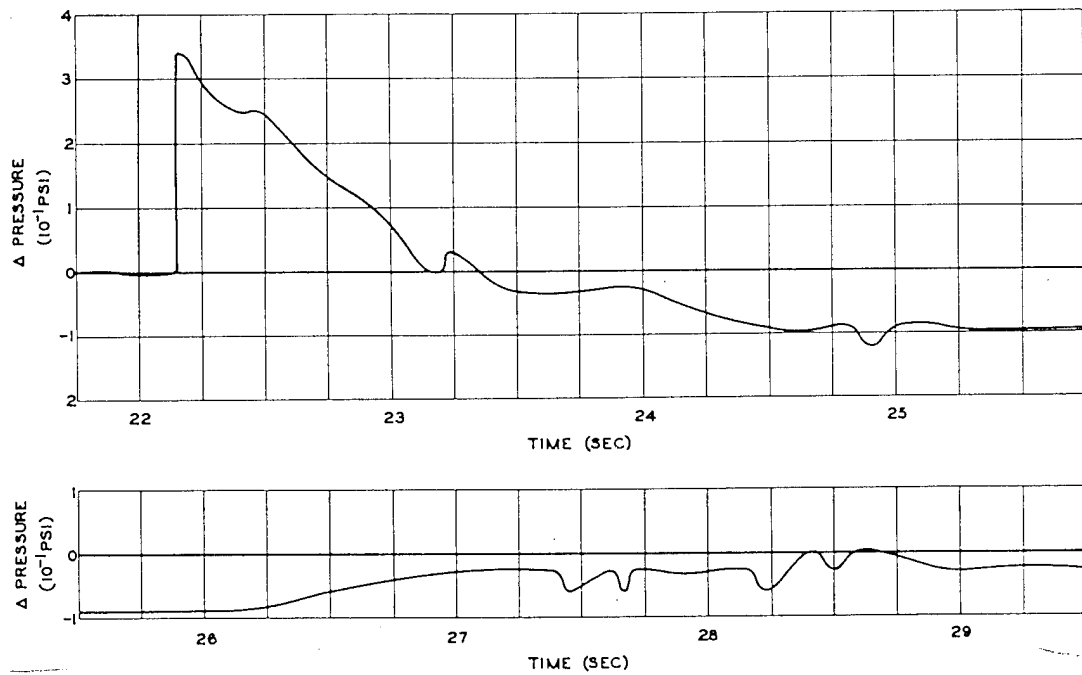


Fig. 6.117 Gauge Aerodynamic Pressure, 5% Chord, Bottom Left Wing Station 524, Channel B17, B-50D (340), Easy Shot

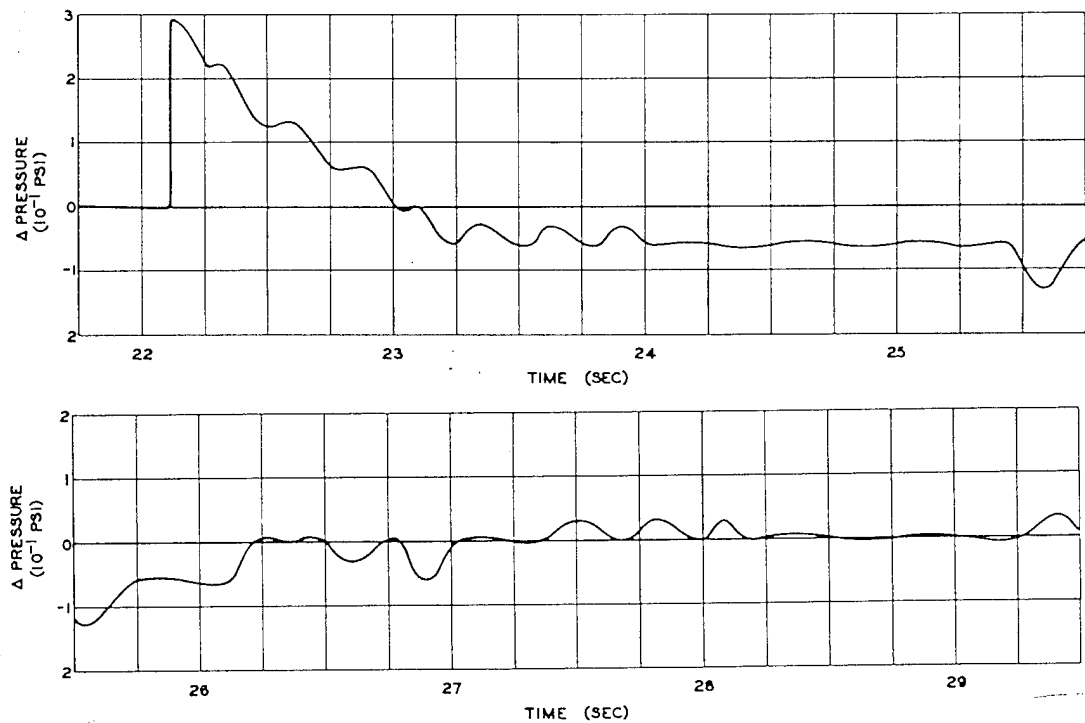


Fig. 6.118 Gauge Aerodynamic Pressure, 23% Chord, Bottom Left Wing Station 524, Channel B19, B-50D (340), Easy Shot

SECRET

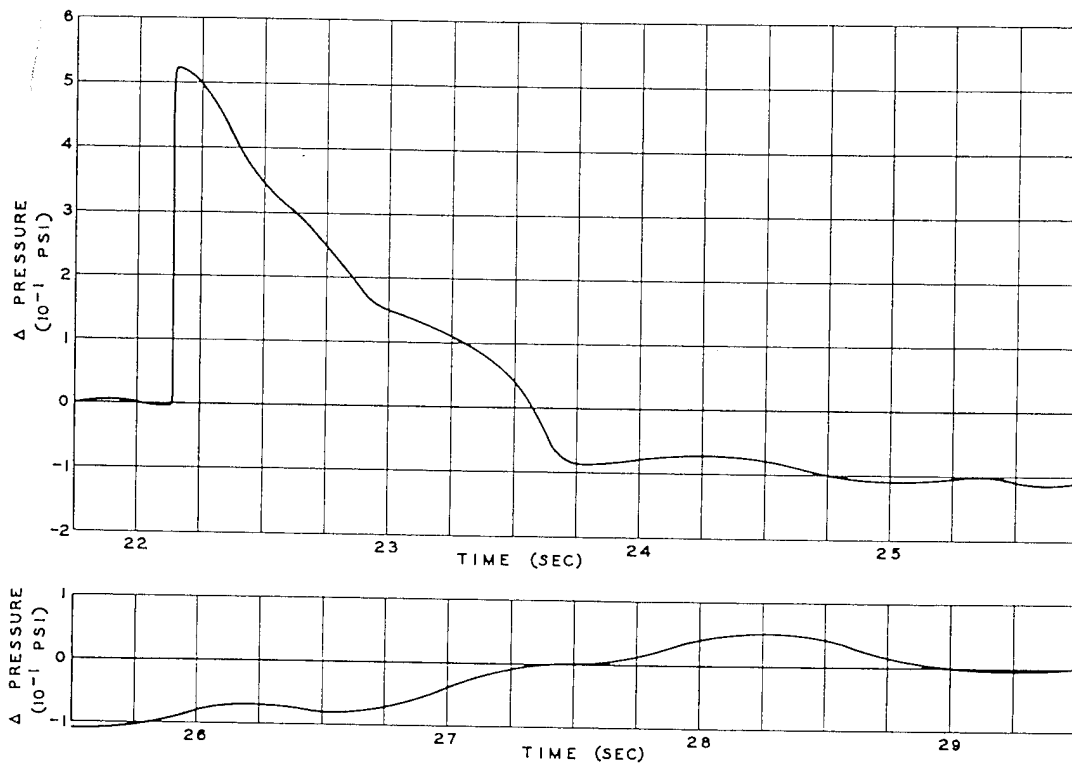


Fig. 6.119 Gauge Aerodynamic Pressure, 43% Chord, Bottom Left Wing Station 524, Channel B20, B-50D (340), Easy Shot

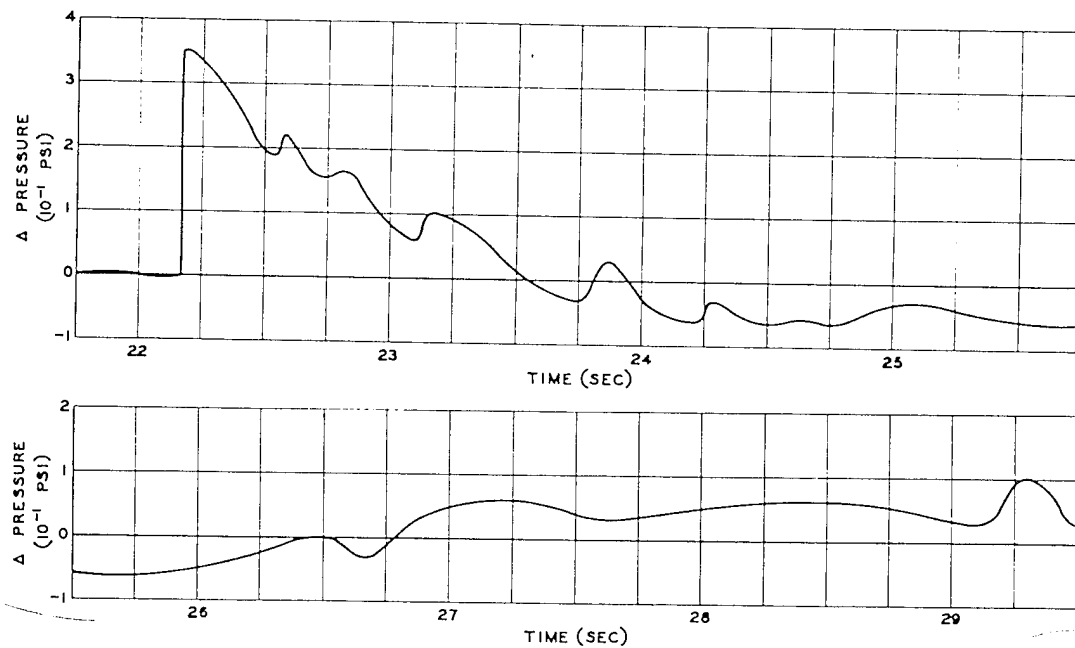


Fig. 6.120 Gauge Aerodynamic Pressure, 85% Chord, Bottom Left Wing Station 524, Channel B22, B-50D (340), Easy Shot

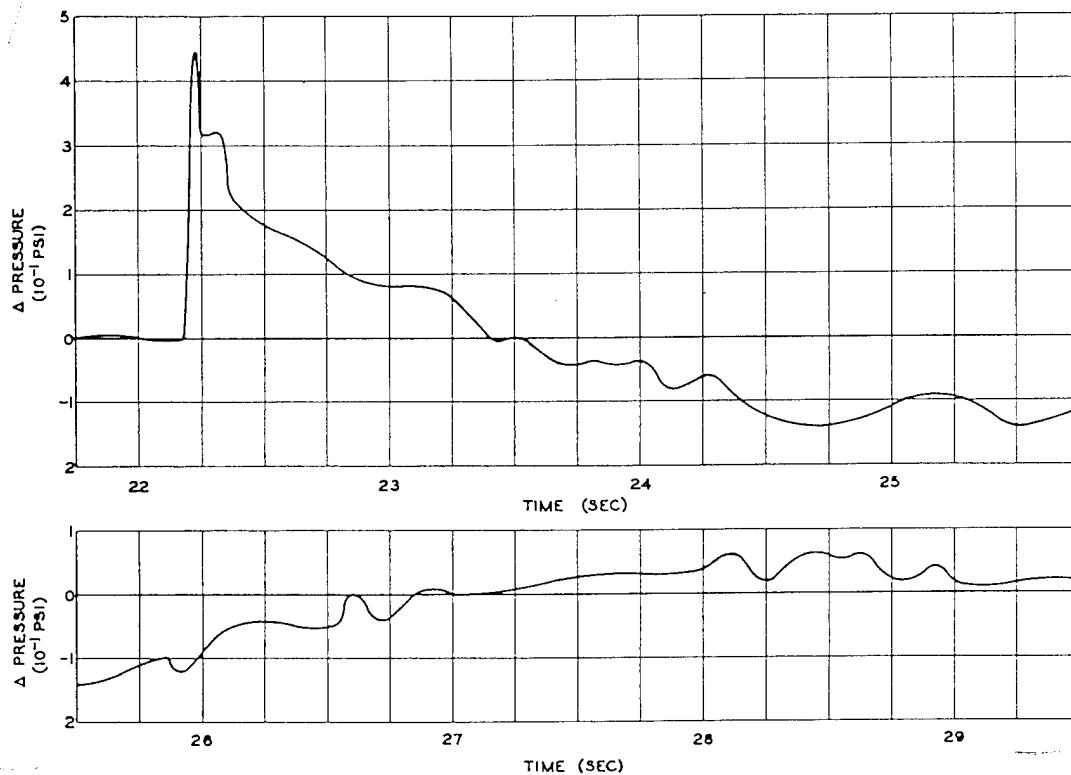


Fig. 6.121 Gauge Aerodynamic Pressure, Bottom Right-horizontal-stabilizer Station 170, Channel B23, B-50D (340), Easy Shot

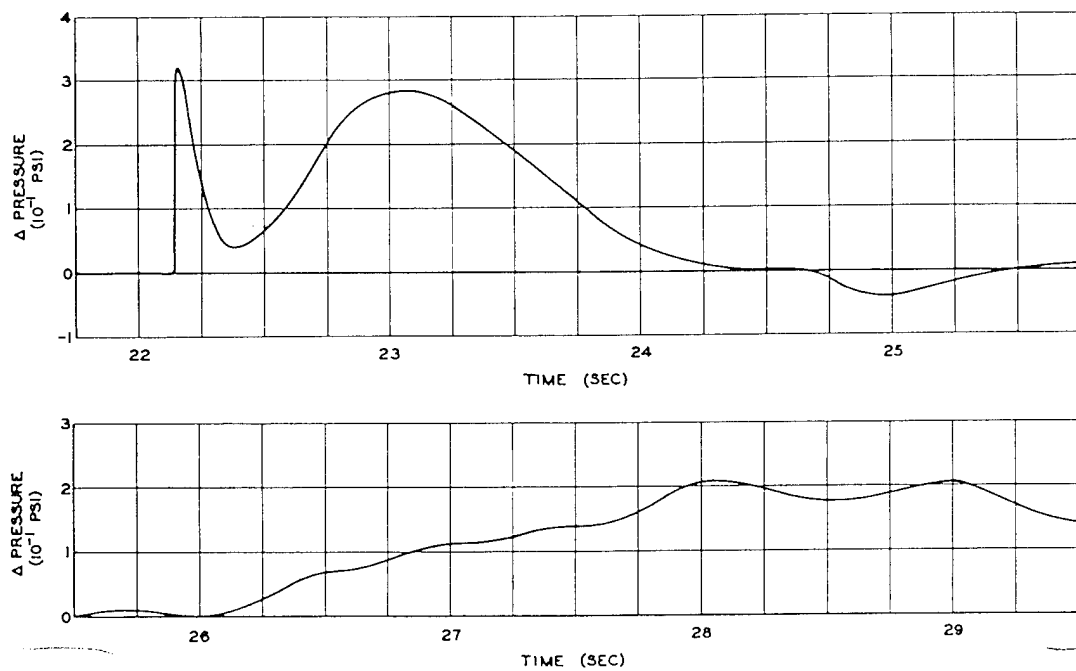


Fig. 6.122 Gauge Aerodynamic Pressure, Bottom Left-horizontal-stabilizer Station 170, Channel B24, B-50D (340), Easy Shot

[REDACTED]

No particular analysis is made of these data. The airplane appears to have been in steady flight just before the shock and to have returned to steady flight after the shock. There is some evidence of oscillation in some channels which appears to arise from "hunt" in the auto-pilot, but these oscillations are small and do not interfere with the data.

6.9 GENERAL CONCLUSIONS FROM EASY SHOT

Except for the XB-47 airplane, the actual location of the test airplanes and drones corresponded very closely to the assigned positions. The errors that did occur were, for the most part, due to the different time of travel of the shock wave. However, this difference on Easy shot was less than on the previous shot. Generally, the recorded loads are greater than on Dog shot and appear to correspond rather well to theory both in frequencies and magnitude. On one drone, N, the hazard of the cloud pass was added to those which were expected on other missions. The hazards from gusts and radioactivity were recognized before the mission but could not be avoided since a high-intensity shock from the front of the drone (at a 45° vertical angle) was desired.

The improved quality of the time marks and the increased sensitivity in the recorders of

the manned airplanes made the data from Easy shot generally more legible and more reliable than data from Dog shot.

If the loss of the QT-33 drone is discounted and if only the channels are counted that were, at the time of take-off, expected to be recorded on magnetic tape, data were obtained from approximately 70 per cent of the channels. The largest losses of data occurred in the destruction of the QT-33 and the premature triggering of the recorders in the B-50D. Radiological data were collected in addition to that on Dog shot, and the high-frequency pressure records and heat measurements were generally more successful.

The protection for the fabric surfaces appeared to have served the purpose rather well. The foil covering was destroyed, but it did succeed in protecting the fabric so that the surfaces were still intact. The damage to the tire of drone M indicated that other types of heat damage (other than to surfaces) would likely become important and would be more difficult to prevent if more critical positions were to be selected for tests or for tactical conditions.

REFERENCE

1. Navigator's Report, Easy Shot, prepared by ATU 3.4.2.

Chapter 7

George Shot

7.1 GENERAL INFORMATION

The weapon test designated "George" was fired at 0930 hours on May 9, 1951. The maximum predicted strength as given by TG 3.1 was 235 kt, and the airplane positions had been selected on this basis. The original positions were selected so as to produce reasonably large loads on the drones, but these positions were changed radically to provide for crew safety (particularly on the basis of heat) when it was decided to man the airplanes (see Sec. 4.4).

The rain and high humidity prior to George shot were very damaging to the instrumentation in the test airplanes. The rate of failure of sensing channels made it necessary to store at least the drones in the hangar for the few days prior to the shot. However, when the decision was made (about noon of G-1 day) to emphasize just a few of the sample-collecting drones, the Project 8.1 drones in the hangar were replaced by other drones. This replacement was necessary in order to ensure the reliability of the radio-control equipment in these drones. The high humidity and leaks in the hangar roof made the maintenance of the instrumentation difficult even in the hangar; after the drones were rolled out into the rain, maintenance became impossible. The decision to operate the Project 8.1 drones as manned airplanes and the resultant change in positions reduced further the amount of data collected from this test by reducing the level of the data on certain channels into the noise level. Such data as were collected and were acceptable are reported.

The heat and radiological measurements from this shot are not reported. The heat ex-

perienced by the drones was so low that it was below the range of the temp-tapes. The radiological data from the film badges vary from 0 to 0.1, which appears to be within the margin of error of this type of measurement.

7.2 ALICE POSITION, QT-33 AIRPLANE 5

This airplane was air-borne and was assigned a position. However, about 20 min prior to H-hour the radar equipment which was being used to position the airplane failed, and, rather than endanger the pilot, the mission was aborted. No data were collected from this mission.

7.3 BETTY POSITION, QT-33 AIRPLANE 4

This airplane was air-borne and performed its mission satisfactorily. However, failure of the tape recorder prevented the collection of data from the mission. The tape record actually becomes legible a few seconds after the shock wave has passed. This length of time is sufficient to obscure the peak loads and the greater part of the loads from the resultant disturbances. The cause of the malfunction is not certain, but it appears to have been a failure of the "calibrate-operate" switch on the amplifier unit. This record is available if further analysis proves the necessity for its reduction; however, the absence of a time reference, the lack of completeness of the record, and the low order of the data, as recorded, appear to justify the omission of these data from this report.

7.4 CAROL POSITION, QB-17 AIRPLANE O

Assigned location (at shock)

True altitude, 25,000 ft

Horizontal distance, 35,000 ft beyond point zero

Predicted conditions

Peak overpressure, 0.33 psi

Peak gust velocity, 43 ft/sec (in direction of shock)

Time of travel (shock), 34.1 sec

7.4.1 Flight Log

QB-17 airplane O took off approximately on schedule and completed its mission satisfactorily. The flight data as reported¹ are as follows:

Time

Take-off, 0522

At assigned altitude, 0715

Shock arrival, 0930:33

Landing, 0957

Meteorological conditions at altitude

True altitude, 25,000 ft

Pressure altitude, 23,500 ft

Outside air temperature, -10°C

Wind direction (from), 250° (azimuth)

Wind velocity, 31 knots

Airplane parameters at time of shock

Indicated airspeed, 135 knots

Ground speed, 339 ft/sec

Ground track azimuth, 060.5°

Horizontal angle from blast, 060° (azimuth)

Vertical angle from blast, * 35.8° (elevation)

Horizontal distance from blast, 34,660 ft

Slant distance from blast, * 42,700 ft

Shock struck airplane from rear and below

7.4.2 Airplane Condition

Before take-off the recorder was selected as the primary recording medium; therefore it was equipped with sensing elements even at the expense of the telemetering system. The following channels of the recorder were not equipped with sensing elements:

Channel 5—acceleration, No. 3 engine

Channel 6—acceleration, No. 4 engine

The balancing and final check of the instrumentation were made while the airplane was

*Computed from data in Navigator's Report, reference 1.

still in the hangar, and all gauges checked satisfactorily. However, although no formal check was made later, it is apparent that the strain-gauge channels were seriously affected by moisture.

The take-off gross weight was estimated at 50,300 lb, with the c.g. at 27.4 per cent m.a.c. This included the standard fuel load of 2,100 gal—1,700 gal (10,200 lb) in the main tanks and 400 gal (2,400 lb) in the Tokyo tanks. At the time the shock struck, the Tokyo tanks were empty and 1,140 gal (6,840 lb) remained in the main tanks; the gross weight was 44,520 lb, with the c.g. at 26.1 per cent m.a.c. This weight and balance estimate does not include allowance for the water that may have accumulated within the airplane.

The crew reported a "pitch-down of about 25° followed by a pitch-up at the time the shock struck." There was also a consensus of opinion that the airplane experienced a "bump" at T_0 .

7.4.3 Radar Position Data

According to the radar controller the airplane was 700 ft left of course and 0.2 sec early (330 ft short of the assigned position) when the shock struck. Further, the controller reported, "Drone over zero point so only one course correction made between zero point and target. Track at target time 060.5°."

According to the graph of the data from the radar-data recorder, Fig. 7.1, the airplane was 980 ft to the left of, and 100 ft beyond, Carol position when the shock struck. Also, the graph shows that the airplane passed within 20 ft of directly over point zero and that the azimuth of the track was 058.2°. The wind correction was negligible; therefore the shock must have struck the airplane from about 1° right of rear at a horizontal distance of 35,200 ft, true altitude of 27,000 ft, vertical angle of 37.5°, and slant range of 44,370 ft.

7.4.4 Load Data

Usable data were obtained only from channels 2, 3, 4, 7, 10, 14, and 15. These data are presented in Figs. 7.2 through 7.8. The elevator position, Fig. 7.8, is only approximate. The calibration of this channel was mostly unsatisfactory; a complete calibration curve could not be definitely plotted and had to be

SECRET

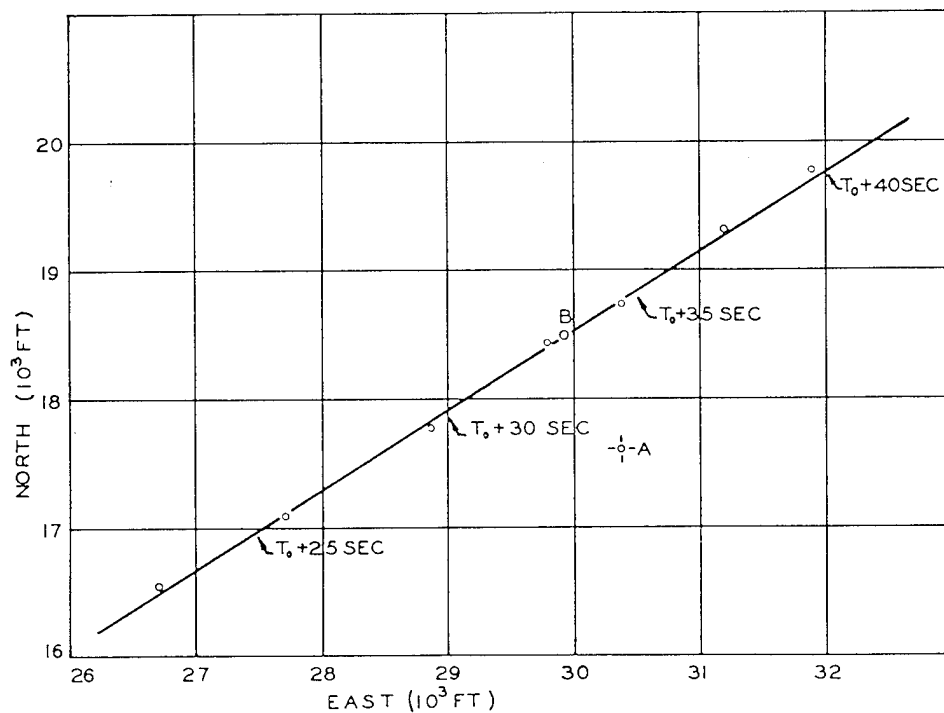


Fig. 7.1 Track, Radar-data Recorder, QB-17 Airplane O, Carol Position, George Shot

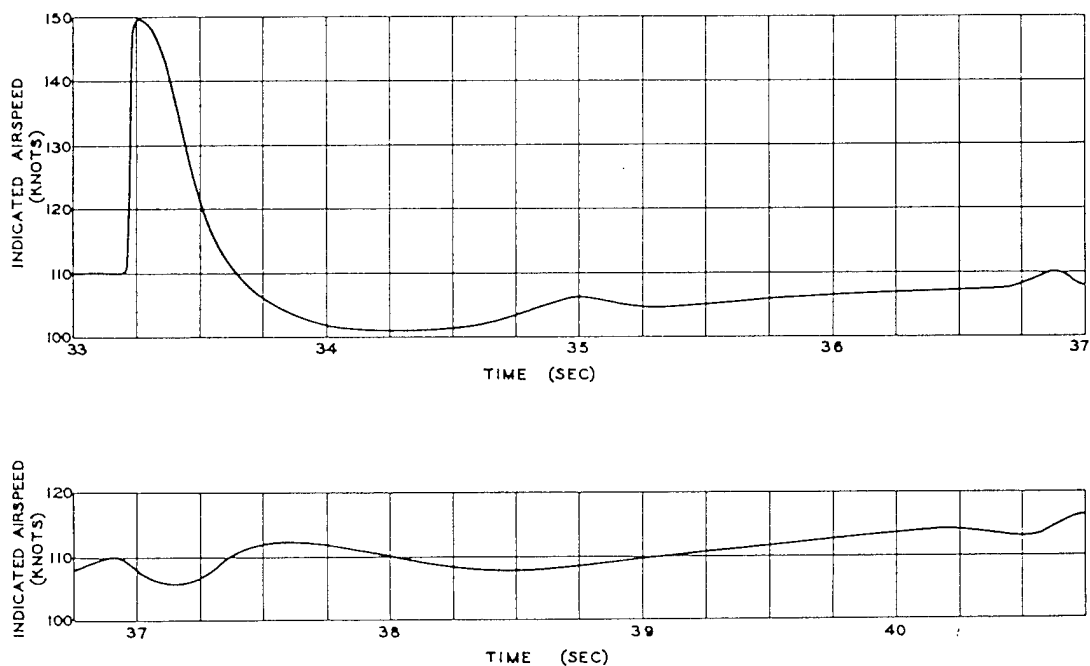


Fig. 7.2 Airspeed, Channel 2, QB-17 O, George Shot

SECRET

SECRET

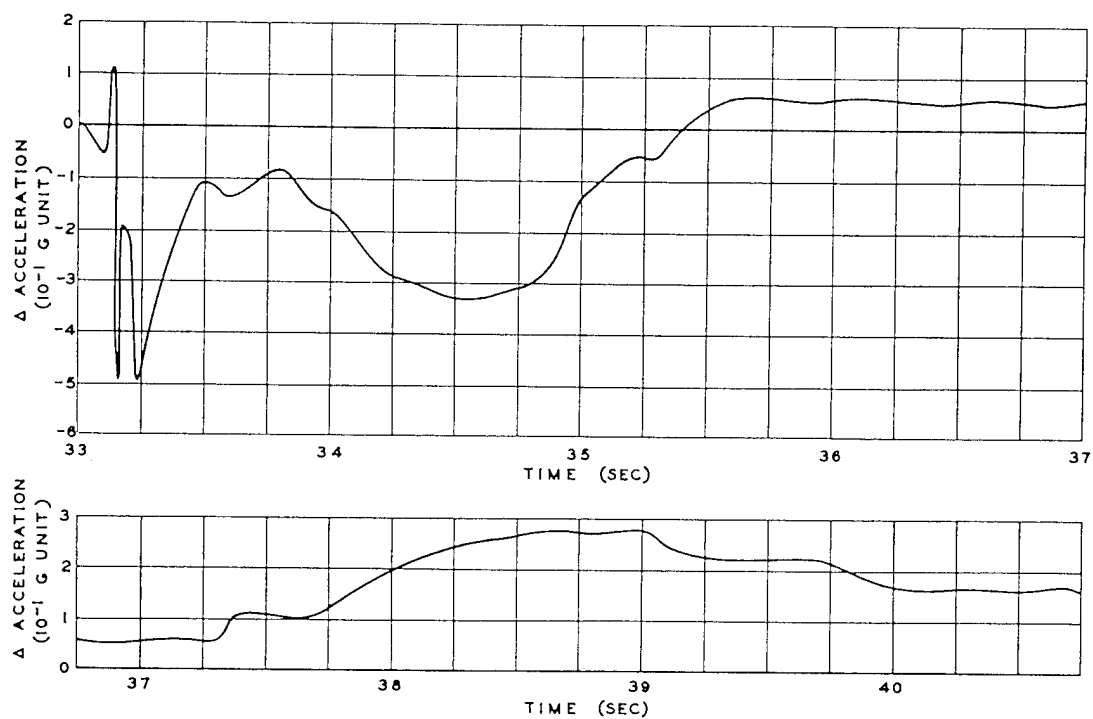


Fig. 7.3 Normal Acceleration, c.g., Channel 3, QB-17 O, George Shot

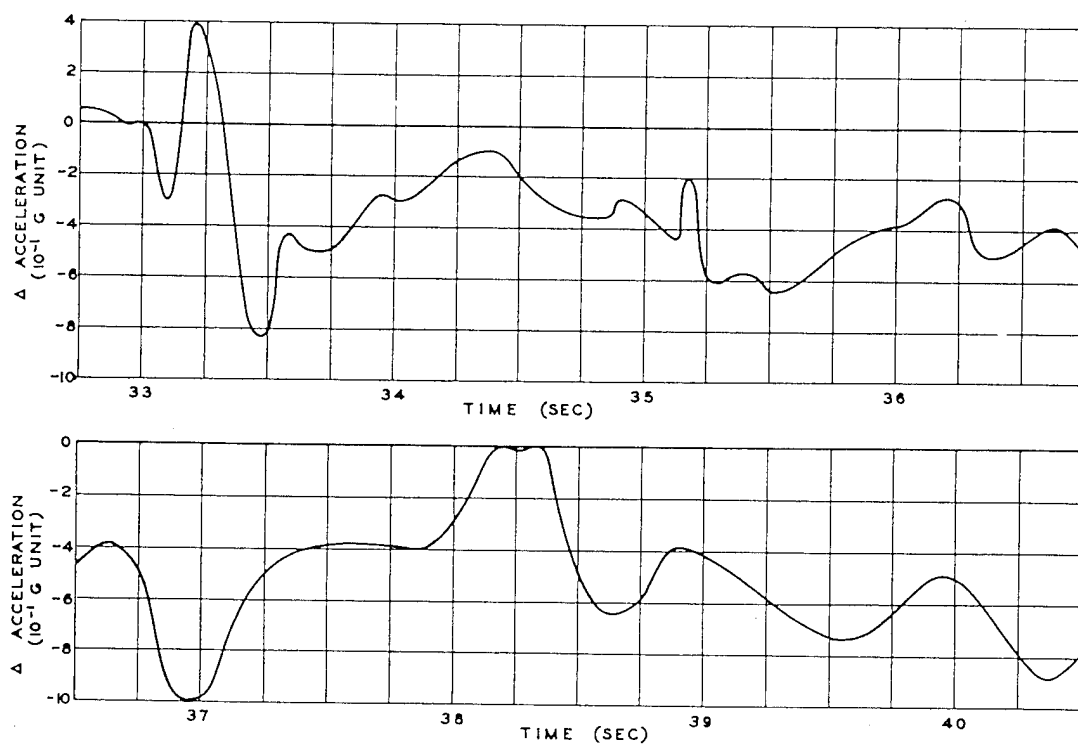


Fig. 7.4 Normal Acceleration, Aft Fuselage, Channel 4, QB-17 O, George Shot

SECRET

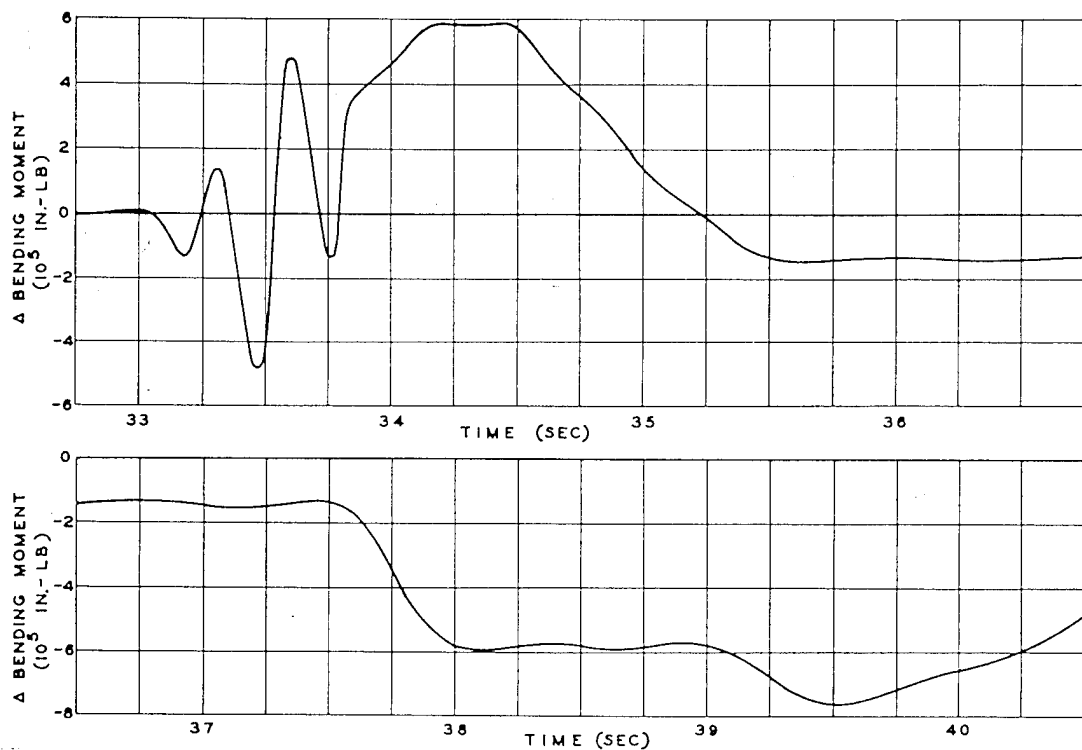


Fig. 7.5 Wing Bending, Right Wing Root, Channel 7, QB-17 O, George Shot

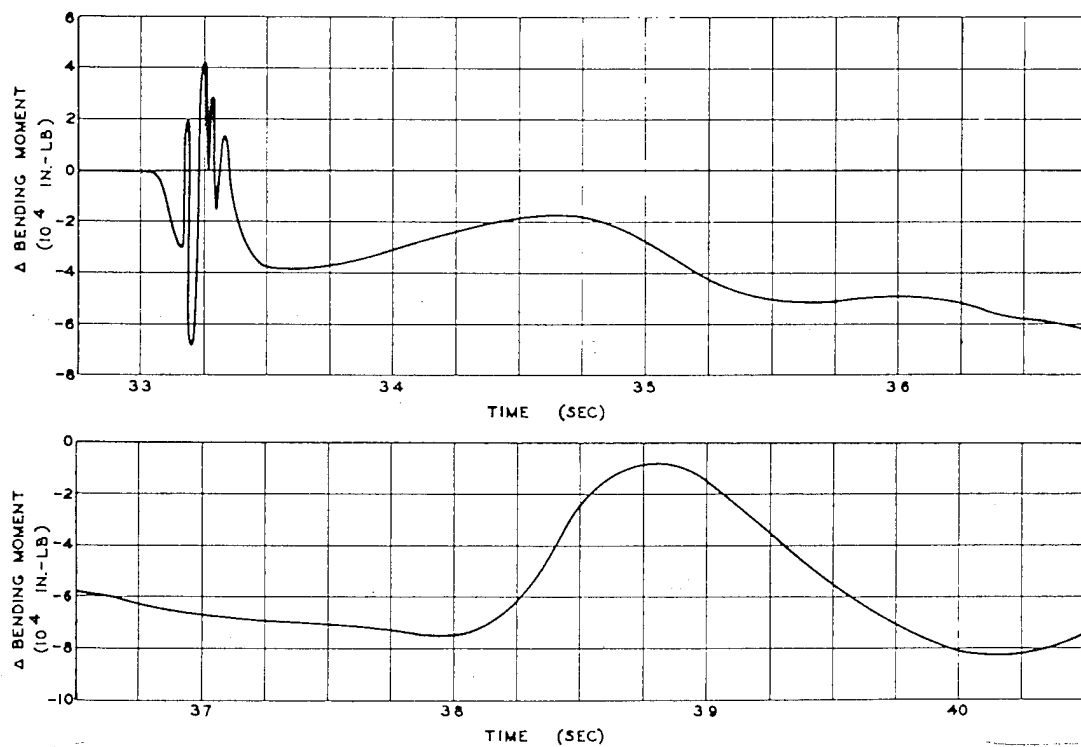


Fig. 7.6 Wing Bending, Outer Panel, Right Wing Station 19, Channel 10, QB-17 O, George Shot

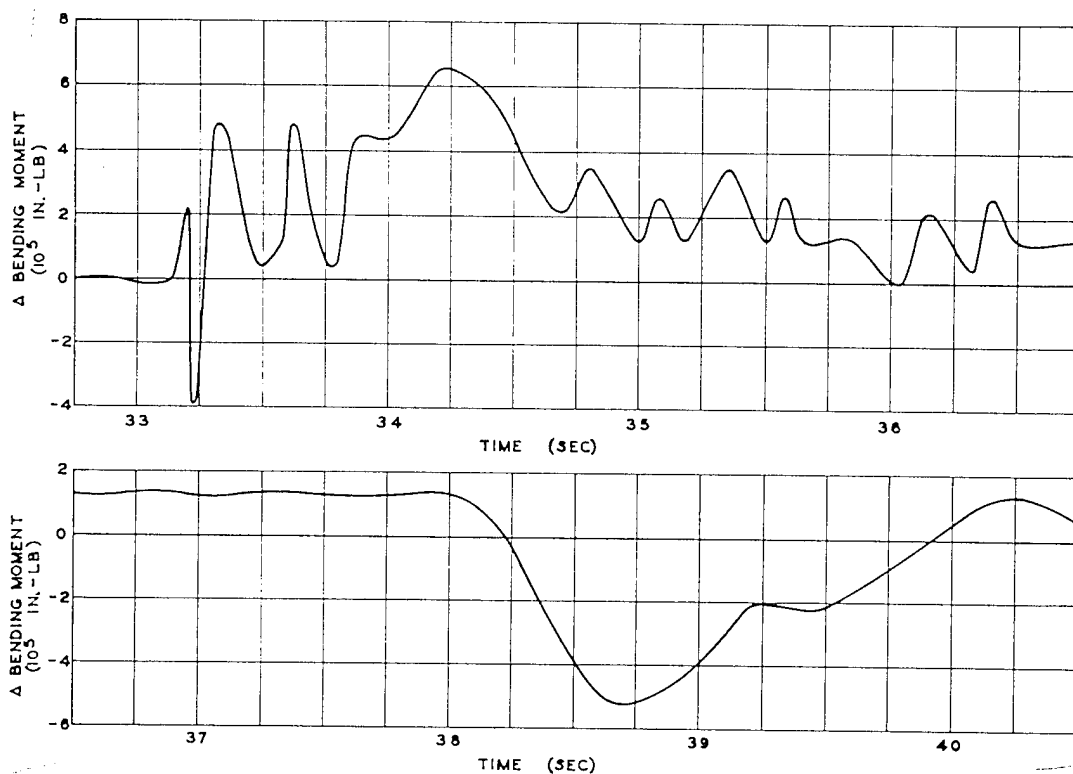


Fig. 7.7 Wing Bending, Mid-span, Right Wing Station 8.8, Channel 14, QB-17 O, George Shot

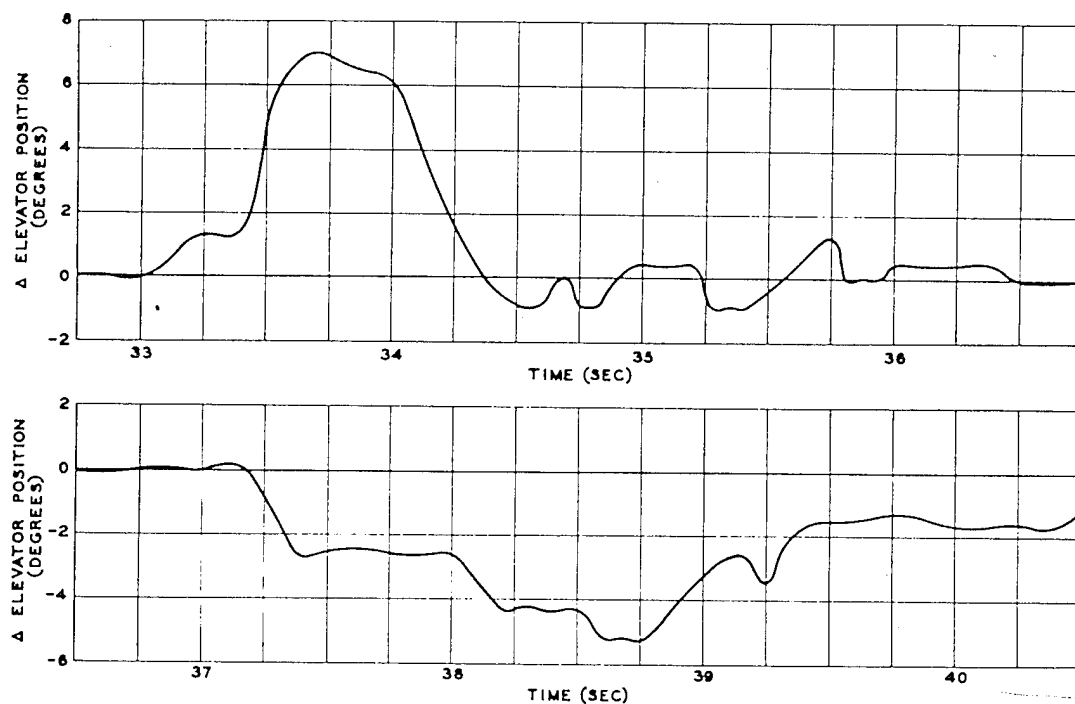


Fig. 7.8 Elevator Position, Channel 15, QB-17 O, George Shot

~~SECRET~~

approximated. A sinusoidal frequency of 180 cpm on the records from channels 3, 4, and 10 was faired out prior to plotting because it seemed to be present before and after the shock and did not appear on channel 7 for an appreciable length of time. The data from the pressure channels, 16 through 24, are undecipherable either because of the low pressures encountered or because of the presence of water in the tubes.

7.5 DORIS POSITION, QB-17 AIRPLANE N

Assigned location (at shock)

True altitude, 27,000 ft

Horizontal distance, 33,000 ft

Predicted conditions

Peak overpressure, 0.32 psi

Peak gust velocity, 45 ft/sec (in direction of shock)

Time of travel (shock), 33.8 sec

7.5.1 Flight Log

QB-17 airplane N took off on schedule and performed a satisfactory mission. The flight data as reported¹ are as follows:

Time

Take-off, 0512

At assigned altitude, 0720

Shock arrival, 0930:33

Landing, 1001

Meteorological conditions at altitude

True altitude, 27,000 ft

Pressure altitude, 25,100 ft

Outside air temperature, -20°C

Wind direction (from), 300° (azimuth)

Wind velocity, 20 knots

Airplane parameters at shock arrival

Indicated airspeed, 139 knots

Ground speed, 345 ft/sec

Ground track azimuth, 045°

Horizontal angle from blast, 045° (azimuth)

Vertical angle from blast, 39.3° (elevation)

Horizontal distance from blast, 33,000 ft

Slant distance from blast,* 42,600 ft

Shock struck airplane from rear and below

*Computed from data in Navigator's Report, reference 1.

7.5.2 Airplane Condition

Before take-off the recorder was selected as the primary recording medium. The recorder was, therefore, equipped with sensing elements even at the expense of the telemetering system. The following channels were not equipped with sensing elements:

Channel 5—acceleration, No. 3 engine

Channel 6—acceleration, No. 4 engine

The following channels were out because of dampness in the sensing elements before take-off:

Channel 7—bending, right wing root

Channel 12—shear, right wing root

Channel 17—pressure, right wing station 25.5, 10 per cent chord

It was almost certain that moisture would work into other gauges during the flight, and, since one shorted channel would load the recorder so as to ruin the entire record, it was very doubtful that any data would be collected.

The fuel tanks contained 2,100 gal at the time the engines were started—1,700 gal (10,200 lb) in the main tanks and 400 gal (2,400 lb) in the Tokyo tanks. The take-off gross weight was 51,700 lb, with the c.g. at 28.1 per cent m.a.c. This weight and balance condition may be in error because of the indeterminate amount of water collected by the airplane between the time of weighing and take-off. The fuel at the time of shock was estimated at 1,220 gal (7,320 lb) in the main tanks; the gross weight was 46,400 lb, with the c.g. at 27.0 per cent m.a.c.

The crews of the test airplane, the mother airplane, and the master-mother were interrogated after the mission. The three airplanes were flying in line-abreast formation at about 1,000-ft intervals. Observations of the crew members may be summarized as follows:

1. The heat of the flash was felt by those crew members in line with windows but not by others. The heat intensity was mild.

2. The airplanes felt a slight tail-up (negative) pitch as a result of the shock (estimated at 10°) which was corrected by the auto-pilot. The mother-airplane crew reported that the altimeter stabilized at 100 ft higher after the shock.

3. The doors of the camera hatch on the test airplane were blown open by the blast.

After the airplanes landed, they were examined, and no significant damage to any of

~~SECRET~~

them was noted. The time for shock travel as reported was 32 sec to the test airplane, 34 sec to the mother airplane, and 35 sec to the master-mother.

7.5.3 Load Data

Usable data were obtained from this mission by only five channels, 8, 9, 10, 14, and 15; these channels are presented in Figs. 7.9 through 7.13. The remainder of the channels were affected by moisture, and the data are not usable.

7.6 ELAINE POSITION, XB-47 AIRPLANE, NO. 46-066

The XB-47 airplane did not take off because bad weather conditions existed at Kwajalein at the time of the mission.

7.7 FRANCES POSITION, B-50D AIRPLANE, NO. 49-290

Assigned location (at shock)

True altitude, 31,000 ft

Horizontal distance, 40,000 ft short of point zero

Predicted conditions

Peak overpressure, 0.24 psi

Peak gust velocity, 39 ft/sec (in direction of shock)

Time of travel (shock), 41.5 sec

7.7.1 Flight Log

B-50D airplane 290 took off on schedule and completed its mission satisfactorily. The flight data as reported¹ are as follows:

Time

Take-off, 0602

At assigned altitude, 0655

Shock arrival, 0930:43.3

Landing, 1154

Meteorological conditions at altitude

True altitude, 31,000 ft

Pressure altitude, 29,100 ft

Outside air temperature, -23°C

Wind direction (blowing from), 270° (azimuth)

Wind velocity, 27 knots

Airplane parameters at shock arrival

Indicated airspeed, 151 knots

Ground speed, 468 ft/sec

Ground track azimuth, 116°

Horizontal angle from blast, 296° (azimuth)

Vertical angle from blast, * 37.8° (elevation)

Horizontal distance from blast, 40,000 ft

Slant distance from blast, * 50,600 ft

Shock struck airplane from ahead and below

7.7.2 Airplane Condition

From the instrument check just prior to take-off it was found that the B recorder was complete and operational except for three channels:

Channel B18—pressure, left wing bottom, station 524, 15 per cent chord

Channel B19—pressure, left wing bottom, station 524, 23 per cent chord

Channel B22—pressure, left wing bottom, station 524, 85 per cent chord

The A recorder failed during the mission and was disconnected; no data were obtained from that recorder.

The take-off gross weight was computed to have been 123,560 lb, which included 1,450 gal (8,700 lb) of fuel in each of the main tanks. The c.g. for take-off was at 25.0 per cent m.a.c. At shock time the fuel was estimated at 832 gal (4,992 lb) in each main tank, which would have made the gross weight 108,728 lb and would have placed the c.g. at 24.1 per cent m.a.c.

The pilot made no comment on the shock wave, and no damage was incurred by the airplane.

7.7.3 Load Data

Many of the channels which checked satisfactorily before take-off were bad at the time of the mission. This is attributed to the moisture, which had collected in the vicinity of the cables or sensing elements and had worked into critical spots during the flexures of flying. No data were obtained from channels B1, B5, B6, B7, B8, B11, B12, B13, B14, B16, or B23. The data which were considered acceptable are presented in Figs. 7.14 through 7.23.

*Computed from data in Navigator's Report, reference 1.

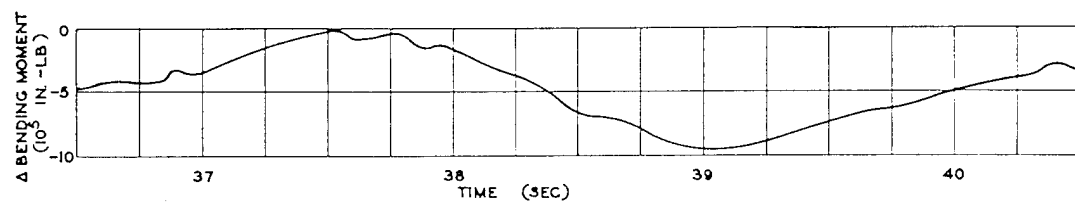
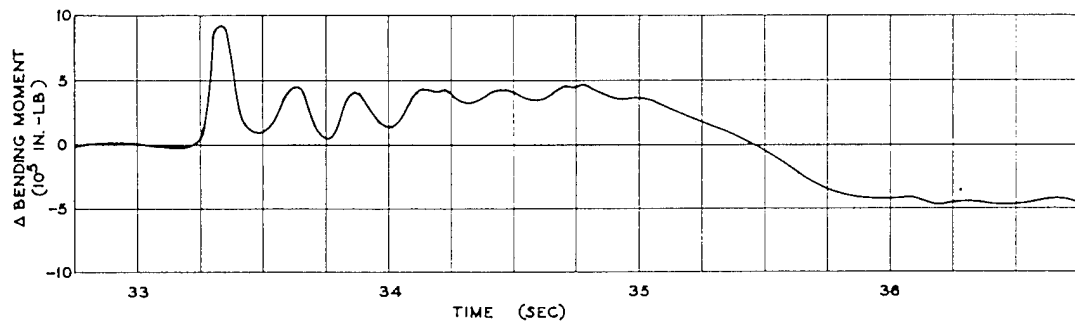


Fig. 7.9 Wing Bending, Left Wing Root, Channel 8, QB-17 N, George Shot

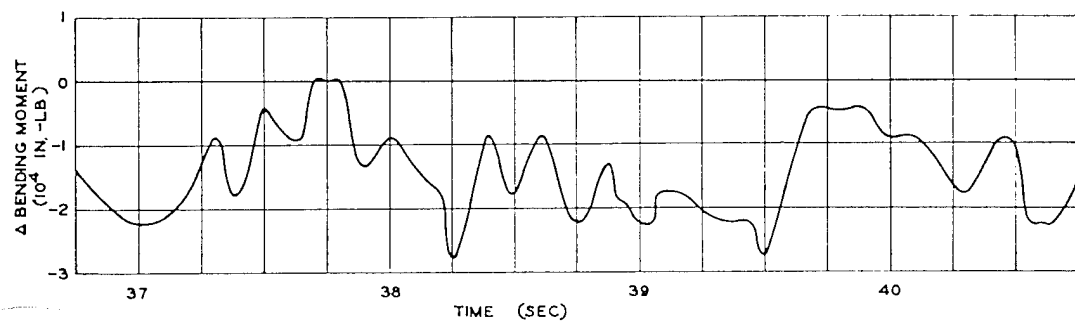
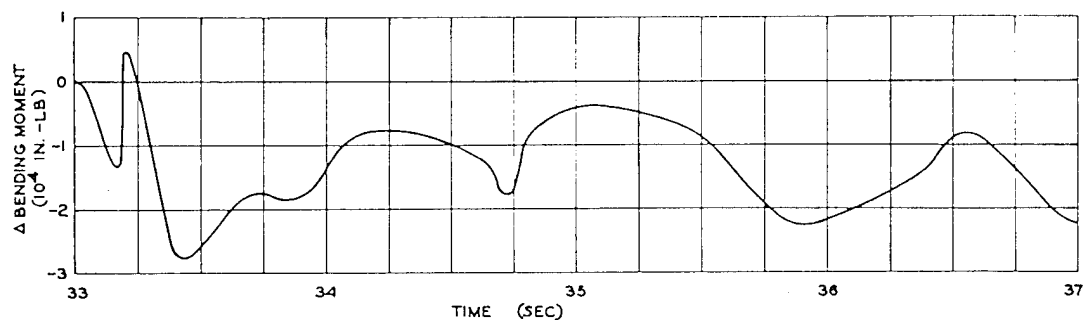


Fig. 7.10 Stabilizer Bending, Right Horizontal Stabilizer, Channel 9, QB-17 N, George Shot

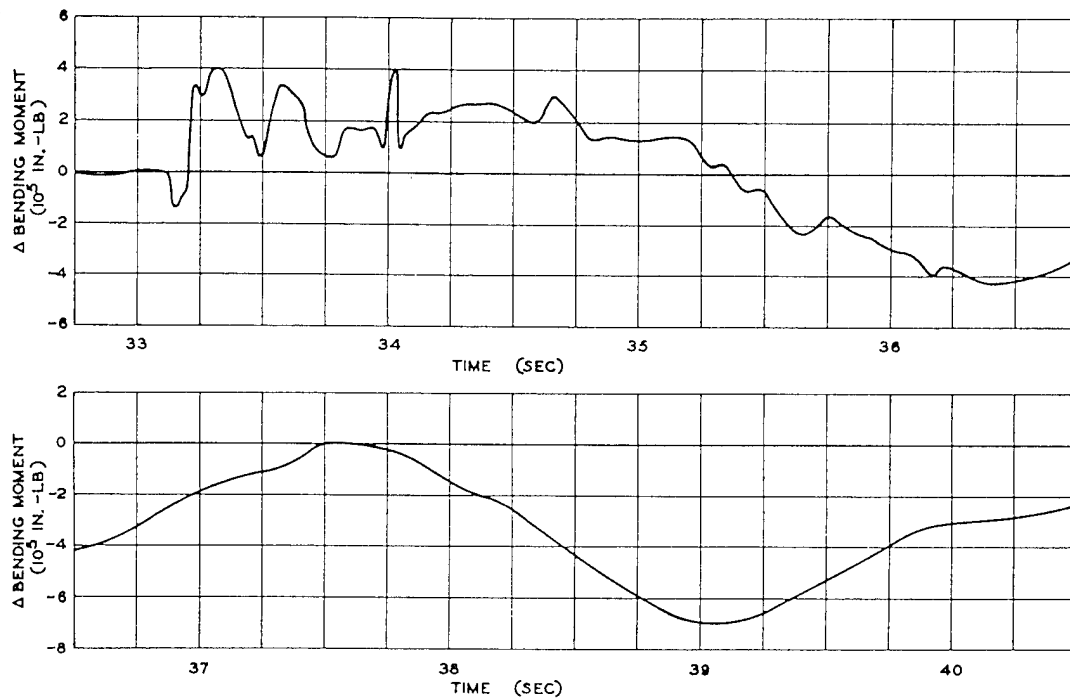


Fig. 7.11 Wing Bending, Outer Panel, Right Wing Station 19, Channel 10, QB-17 N, George Shot

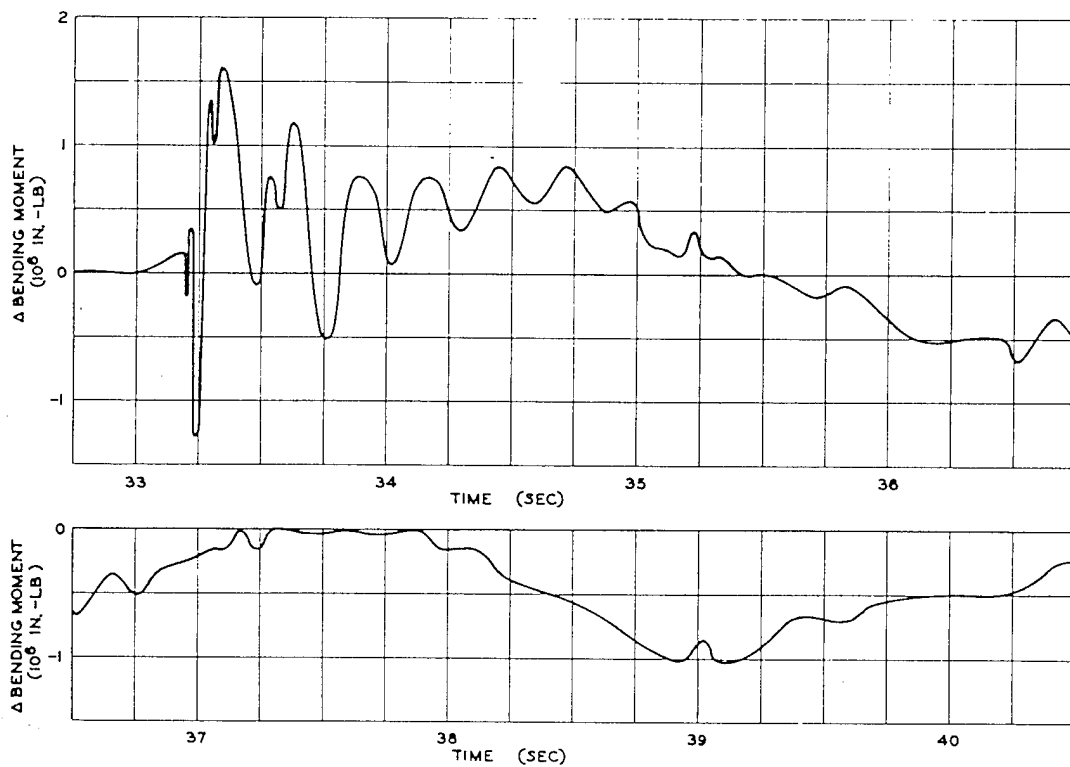


Fig. 7.12 Wing Bending, Mid-span, Right Wing Station 8.8, Channel 14, QB-17 N, George Shot

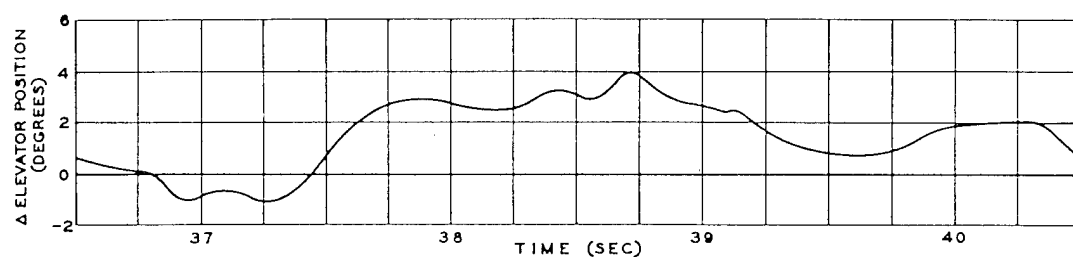
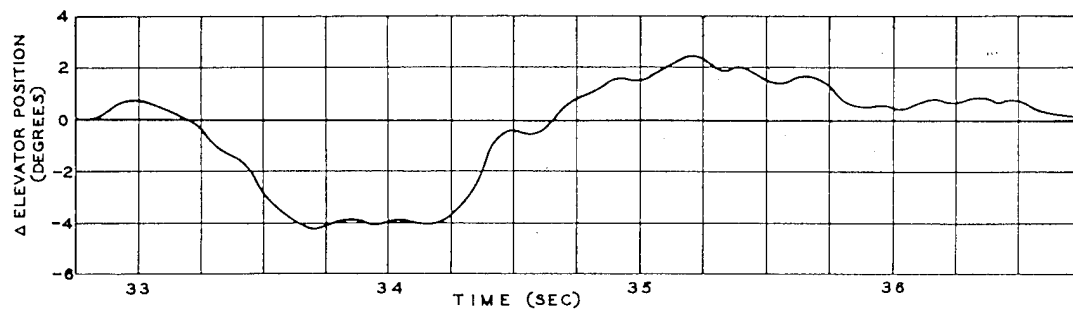


Fig. 7.13 Elevator Position, Channel 15, QB-17 N, George Shot

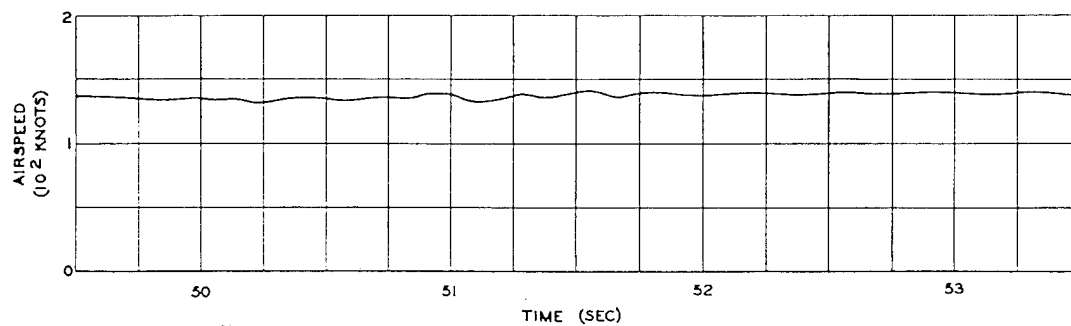
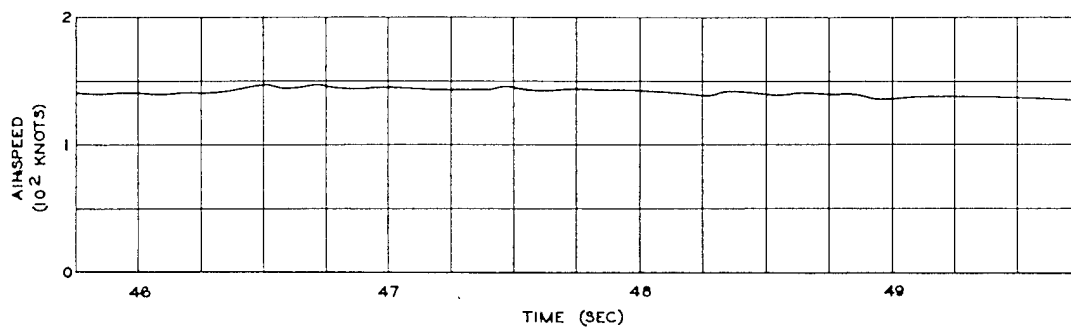


Fig. 7.14 Airspeed, Channel B2, B-50D (290), George Shot

SECRET

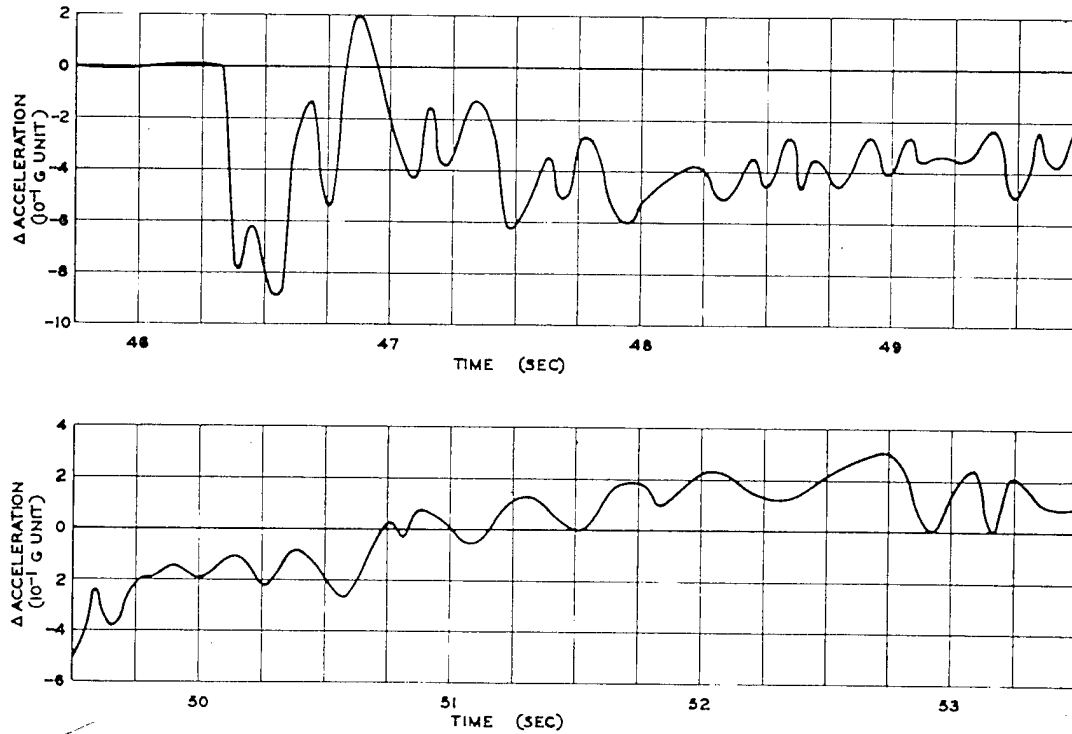


Fig. 7.15 Normal Acceleration, Rear Bomb Bay, Fuselage Station 628, Channel B3, B-50D (290), George Shot

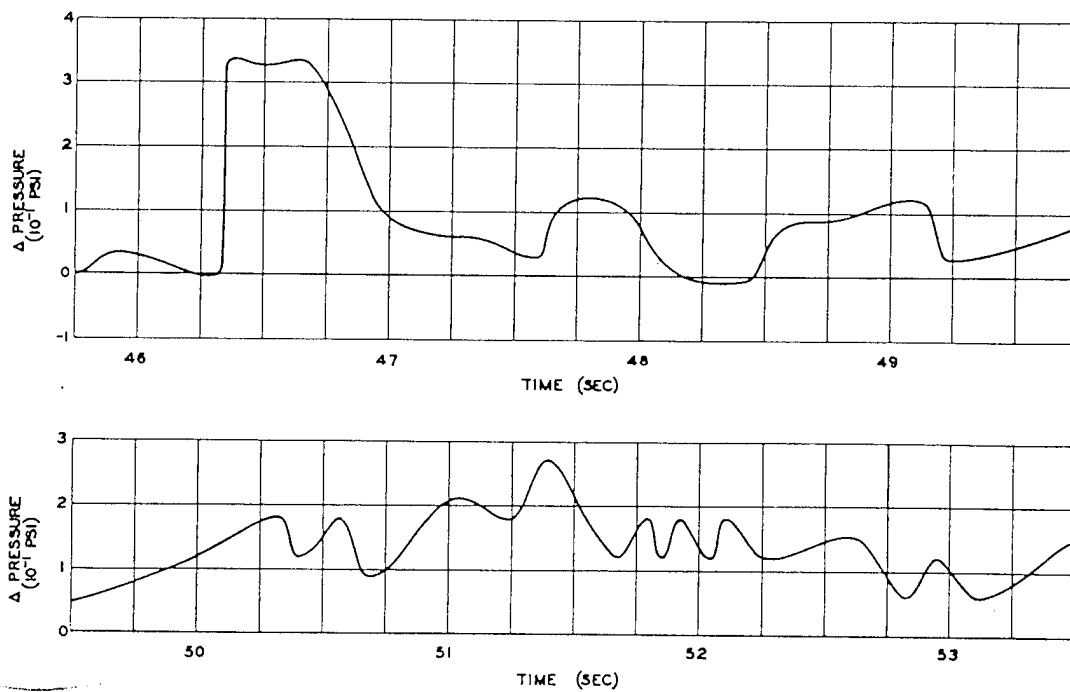


Fig. 7.16 Differential Aerodynamic Pressure, 23% Chord, Right Wing Station 525, Channel B4, B-50D (290), George Shot

SECRET

SECRET

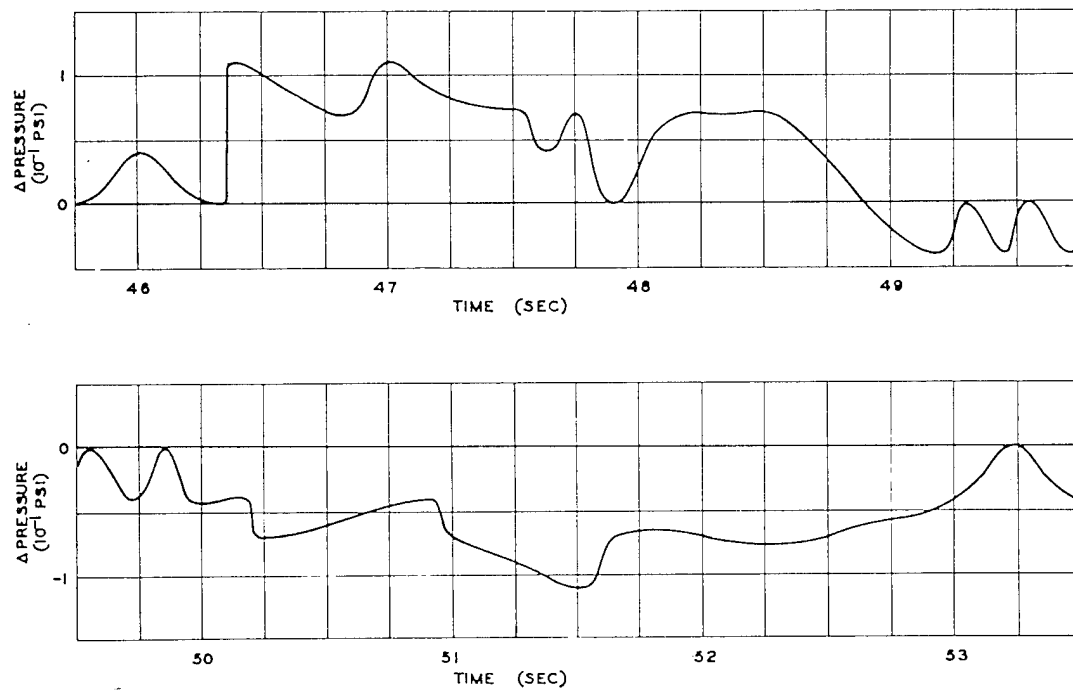


Fig. 7.17 Gauge Aerodynamic Pressure, Right Side of Vertical Fin, Fuselage Station 974, Channel B9, B-50D (290), George Shot

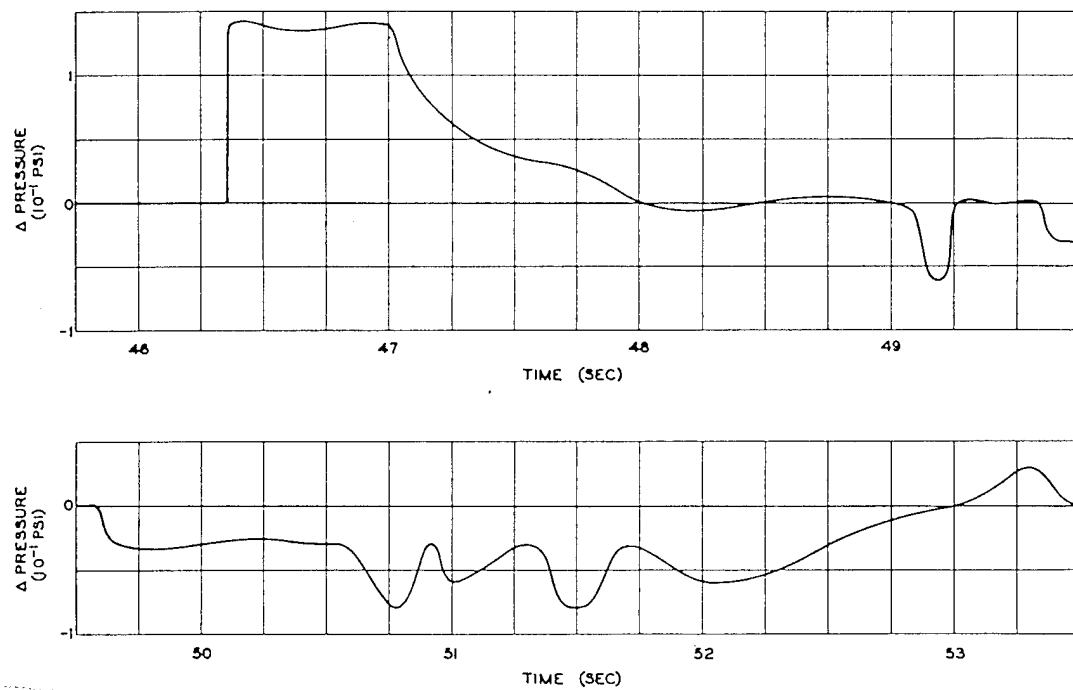


Fig. 7.18 Gauge Aerodynamic Pressure, Left Side of Vertical Fin, Fuselage Station 974, Channel B10, B-50D (290), George Shot

SECRET

SECRET

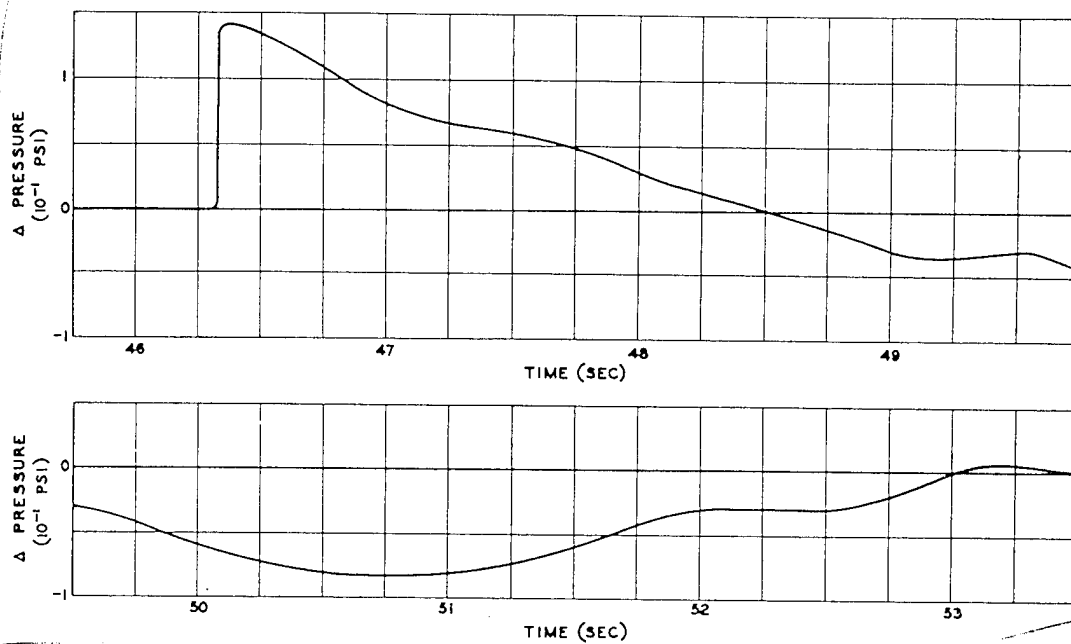


Fig. 7.19 Gauge Aerodynamic Pressure, 60% Chord, Top Left Wing Station 524, Channel B15, B-50D (290), George Shot

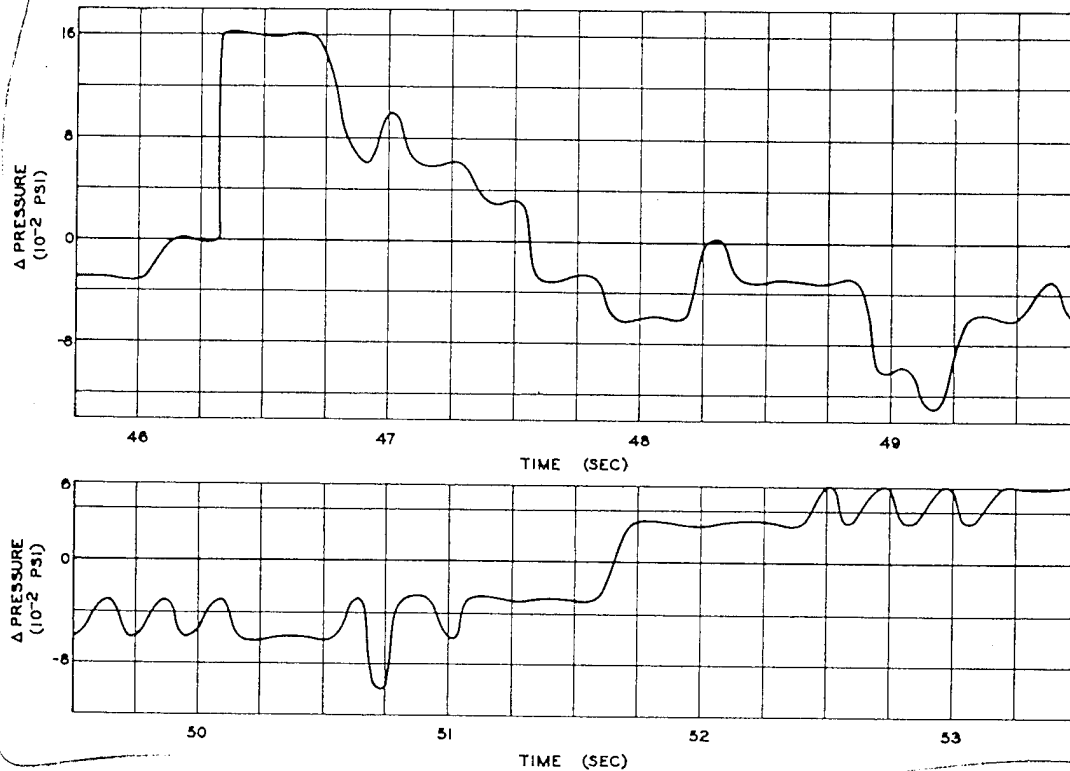


Fig. 7.20 Gauge Aerodynamic Pressure, 5% Chord, Bottom Left Wing Station 524, Channel B17, B-50D (290), George Shot

SECRET

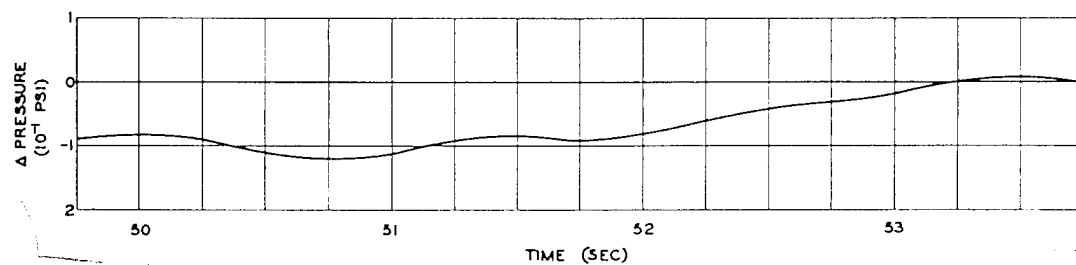
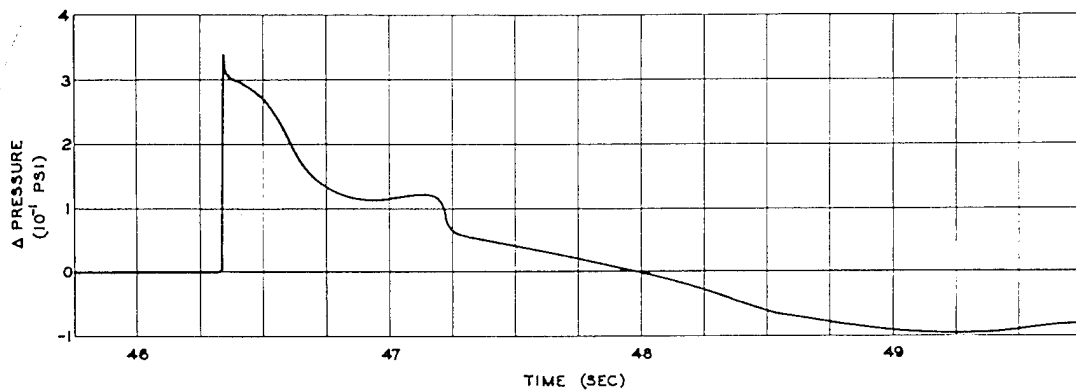


Fig. 7.21 Gauge Aerodynamic Pressure, 43% Chord, Bottom Left Wing Station 524, Channel B20, B-50D (290), George Shot

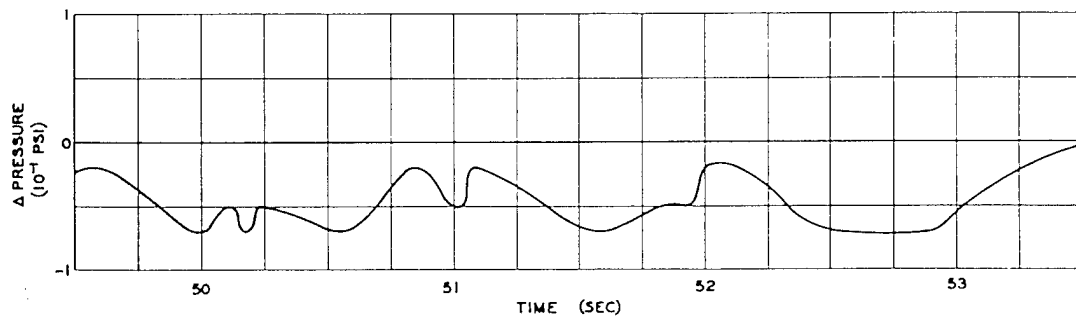
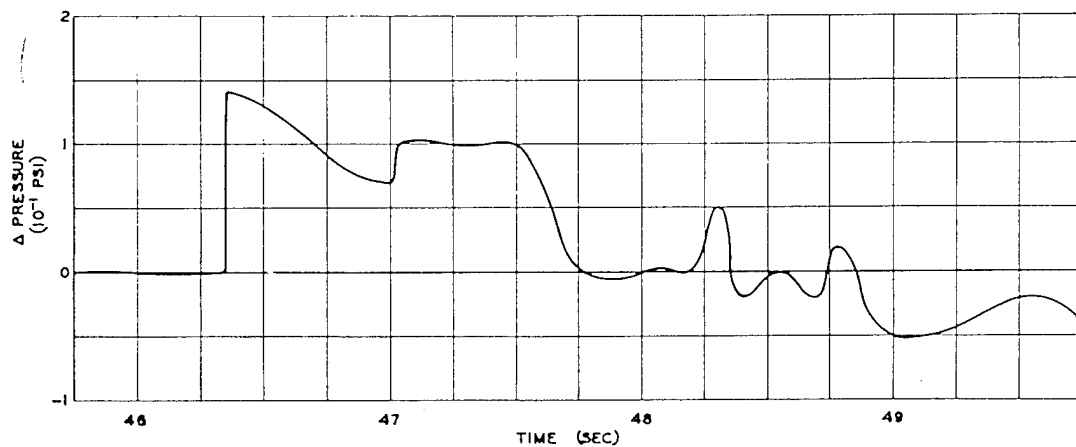


Fig. 7.22 Gauge Aerodynamic Pressure, 60% Chord, Bottom Left Wing Station 524, Channel B21, B-50D (290), George Shot

SECRET

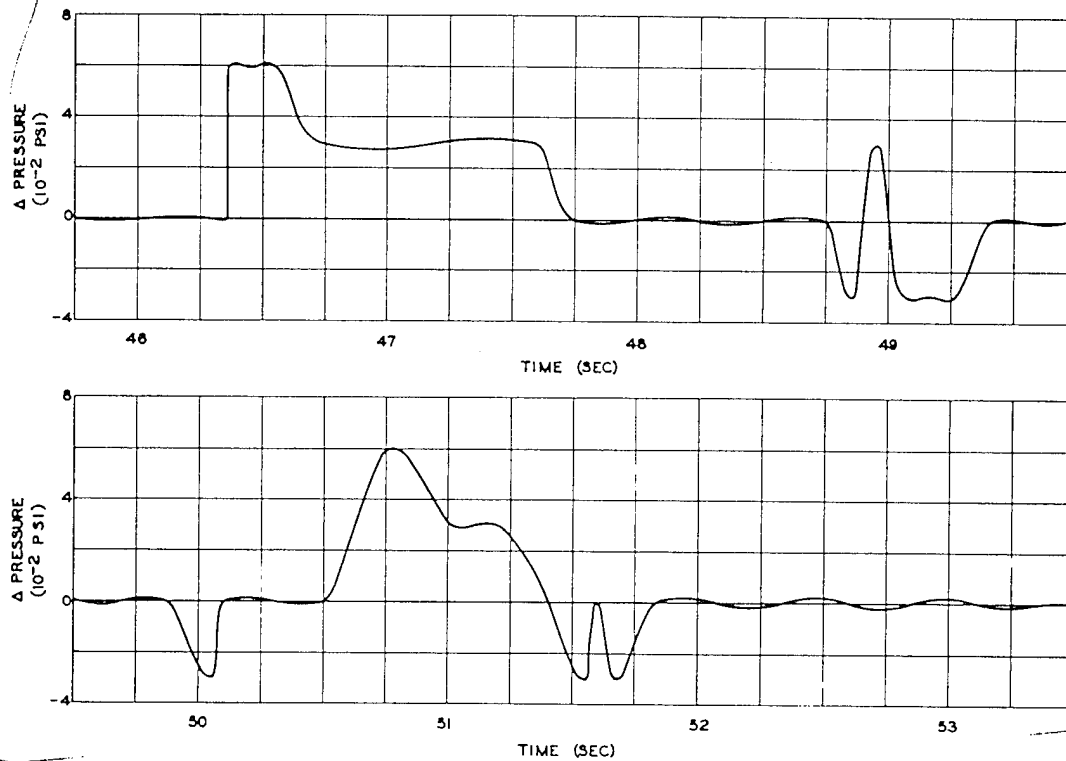


Fig. 7.23 Gauge Aerodynamic Pressure, Bottom Left-horizontal-stabilizer Station 170, Channel B24, B-50D (290), George Shot

SECRET

~~SECRET~~

7.8 GRACE POSITION, B-50D AIRPLANE, NO. 49-340

Assigned location (at shock)

True altitude, 33,000 ft

Horizontal distance, 33,000 ft

Predicted conditions

Peak overpressure, 0.25 psi

Peak gust velocity, 44 ft/sec (in direction
of shock)

Time of travel (shock), 37.9 sec

7.8.1 Flight Log

B-50D airplane 340 took off on schedule and performed its mission satisfactorily. The only incident was the feathering of No. 3 engine. The engine failed just as, or slightly after, the shock wave struck the airplane, but failure was apparently not related to that phenomenon. The flight data as reported¹ are as follows:

Time

Take-off, 0545

At assigned altitude, 0730

Shock arrival, 0930:37

Landing, 1045

Meteorological conditions at altitude

True altitude, 33,000 ft

Pressure altitude, 31,470 ft

Outside air temperature, -25°C

Wind direction (blowing from), 260°
(azimuth)

Wind velocity, 17 knots

Airplane parameters at shock arrival

Indicated airspeed, 162 knots

Ground speed, 484 ft/sec

Ground track azimuth, 059°

Horizontal angle from blast, 150° (azimuth)

Vertical angle from blast, * 45° (elevation)

Horizontal distance from blast, 33,050 ft

Slant distance from blast, * 46,700 ft

Shock struck airplane from left and below

7.8.2 Airplane Condition

Before take-off the recorders were checked, and all channels were satisfactory except for 11 channels as follows:

Channel A1—elevator position

Channel A3—normal acceleration, No. 2
engine

*Computed from data in Navigator's Report, reference 1.

Channel A4—normal acceleration, No. 1
engine

Channel A5—normal acceleration, forward
bomb bay

Channel A12—bending, left wing root

Channel A13—bending, left wing, inboard
station 120

Channel A15—normal acceleration, No. 3
engine

Channel B8—pressure, left side of aft
fuselage

Channel B13—pressure, top of left wing,
station 524, 23 per cent chord

Channel B20—pressure, bottom of left wing,
station 524, 43 per cent chord

Channel B21—pressure, bottom of left wing,
station 524, 60 per cent chord

The take-off gross weight for this airplane was computed to have been 122,450 lb, including 1,075 gal (6,450 lb) of fuel in each main tank and 1,100 gal (6,600 lb) in the center-section tank. The c.g. was at 25.1 per cent m.a.c. The gross weight at shock-wave arrival was estimated at 104,850 lb, which included 617 gal (3,700 lb) of fuel in each main tank. The c.g. position was at 24.0 per cent m.a.c. The pilot reported,¹ "definite roll and yaw as shock wave hit. Bomb-bay doors cut and caved in more than on Easy shot."

7.8.3 Load Data

The data as recorded from this mission are presented in Figs. 7.24 through 7.49. Channel B21 failed during flight, and the calibrate steps for channels A17 and A24 are not usable. Channels A14, B4, B6, B9, B14, B16, and B18 contain data which are so low that they are obscured by noise.

7.9 SALLY POSITION, QB-17 AIRPLANE P

Assigned location (at shock)

True altitude, 14,000 ft

Horizontal distance, 60,800 ft short of
point zero

Predicted conditions

Peak overpressure, 0.27 psi

Peak gust velocity, 23.5 ft/sec (in direction
of shock)

Time of travel (shock), 51.0 sec

~~SECRET~~

SECRET

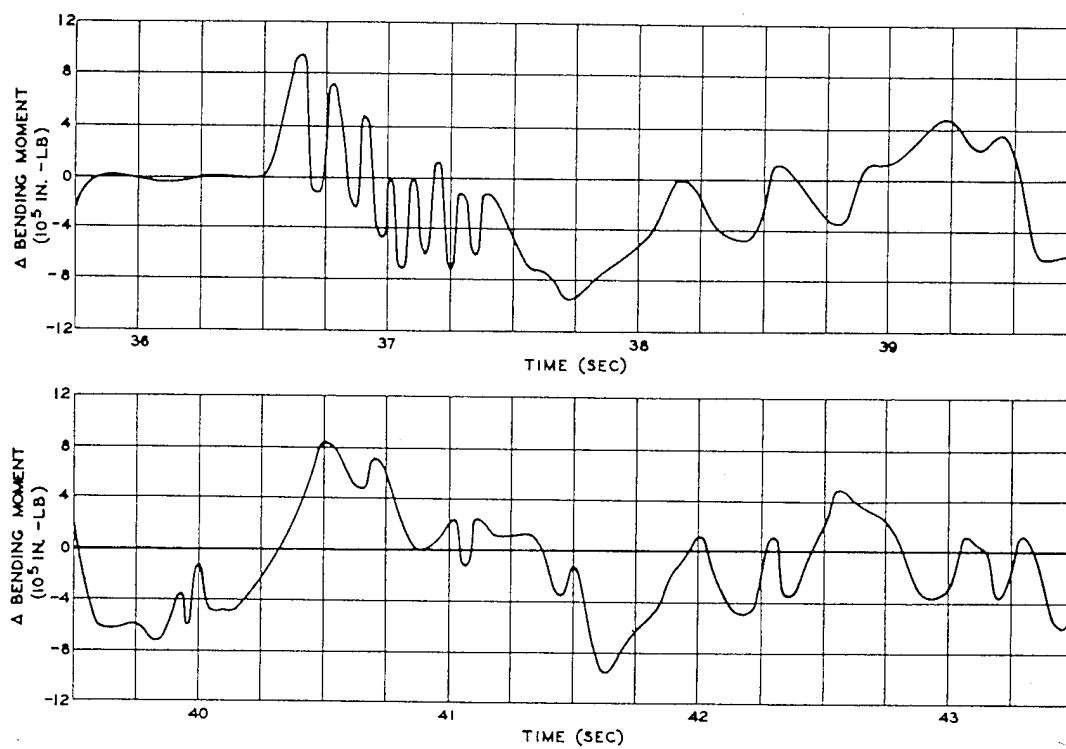


Fig. 7.24 Wing Bending, Left Wing Outboard, Wing Station 505, Channel A2, B-50D (340), George Shot

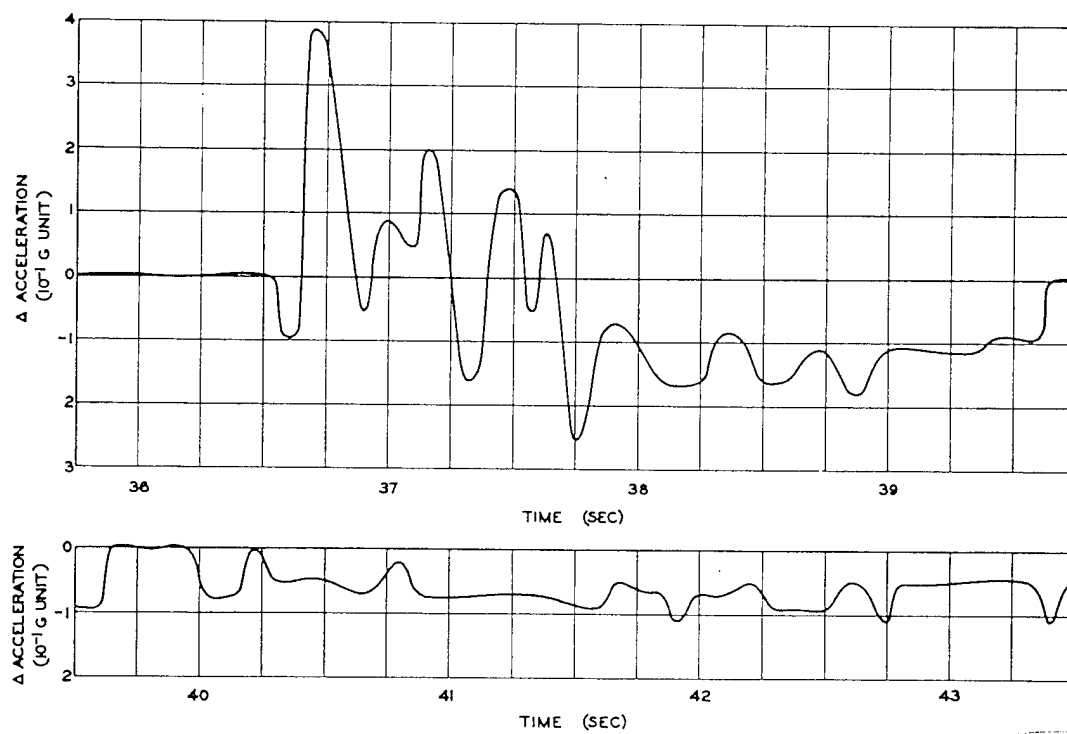


Fig. 7.25 Normal Acceleration, Nose-wheel Well, Channel A6, B-50D (340), George Shot

SECRET

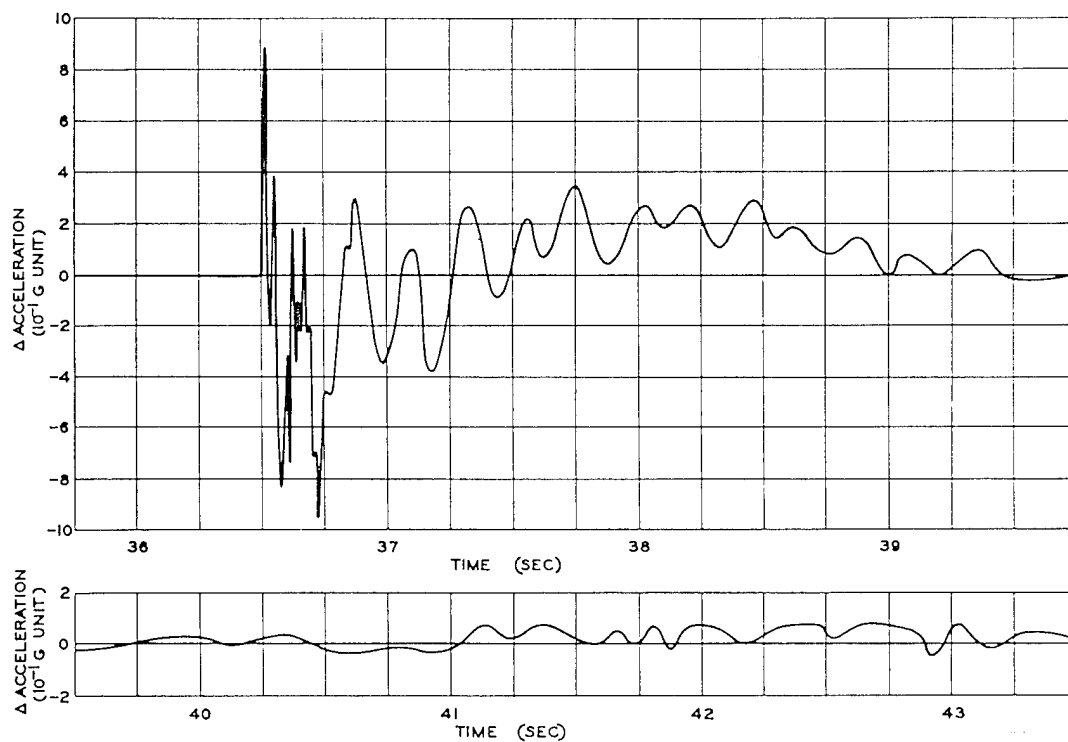


Fig. 7.26 Normal Acceleration, Aft Fuselage in Tail-gunner's Compartment, Channel A7, B-50D (340), George Shot

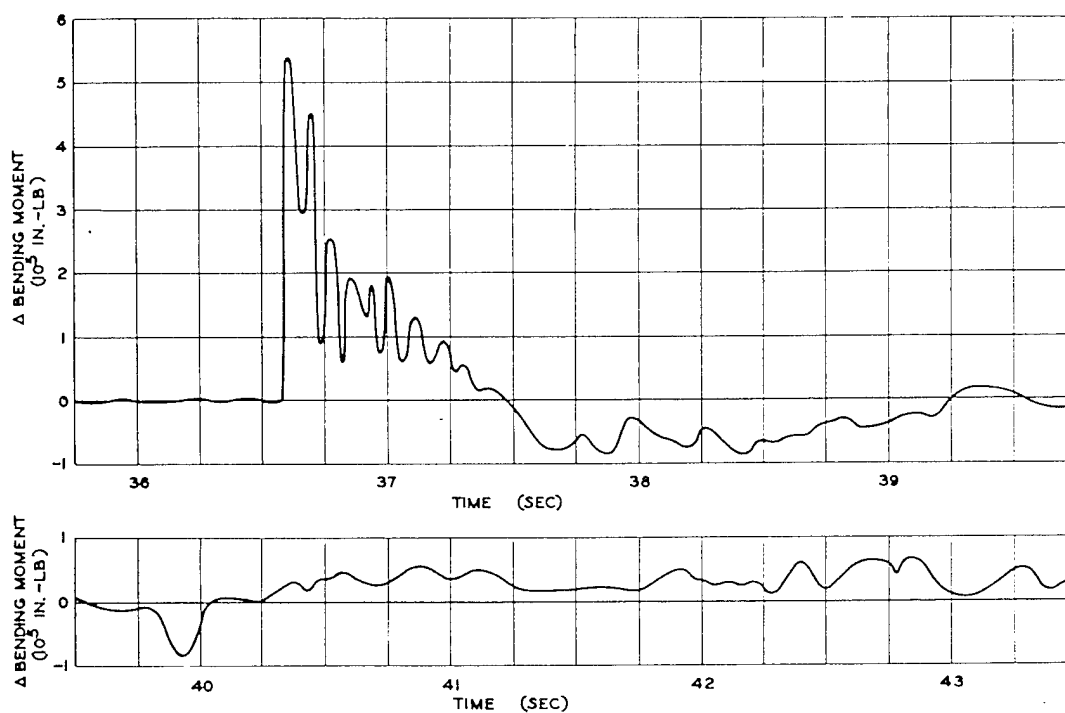


Fig. 7.27 Horizontal-stabilizer Bending, Right-horizontal-stabilizer Station 34, Channel A8, B-50D (340), George Shot

~~SECRET~~

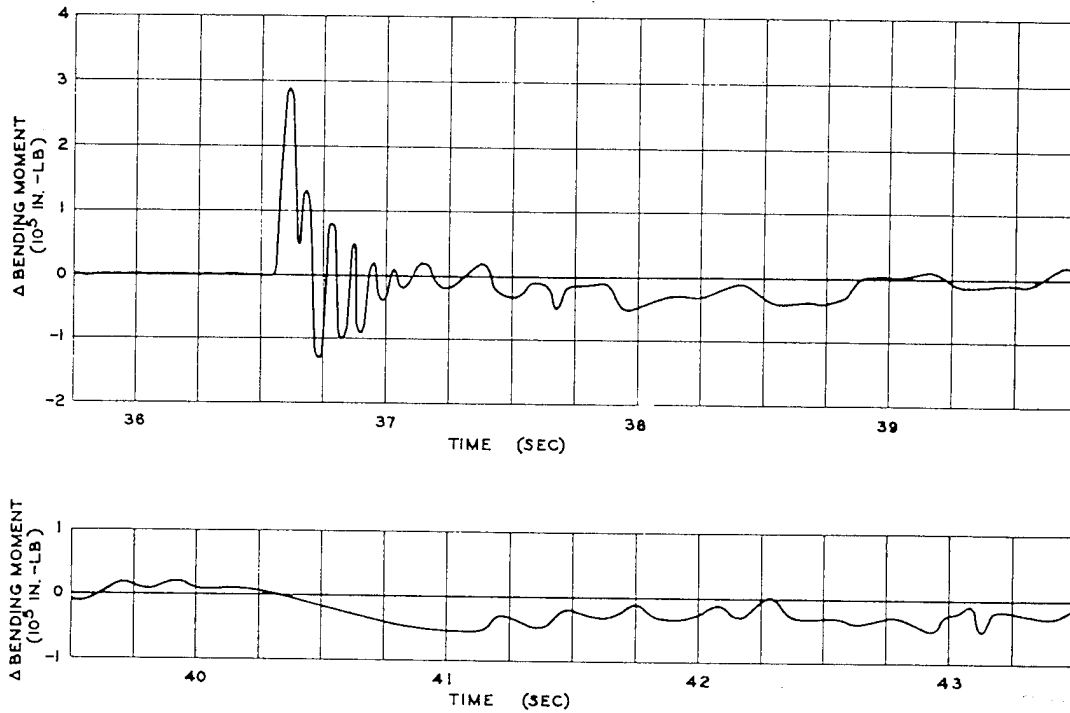


Fig. 7.28 Horizontal-stabilizer Bending, Left-horizontal-stabilizer Station 34, Channel A9, B-50D (340), George Shot

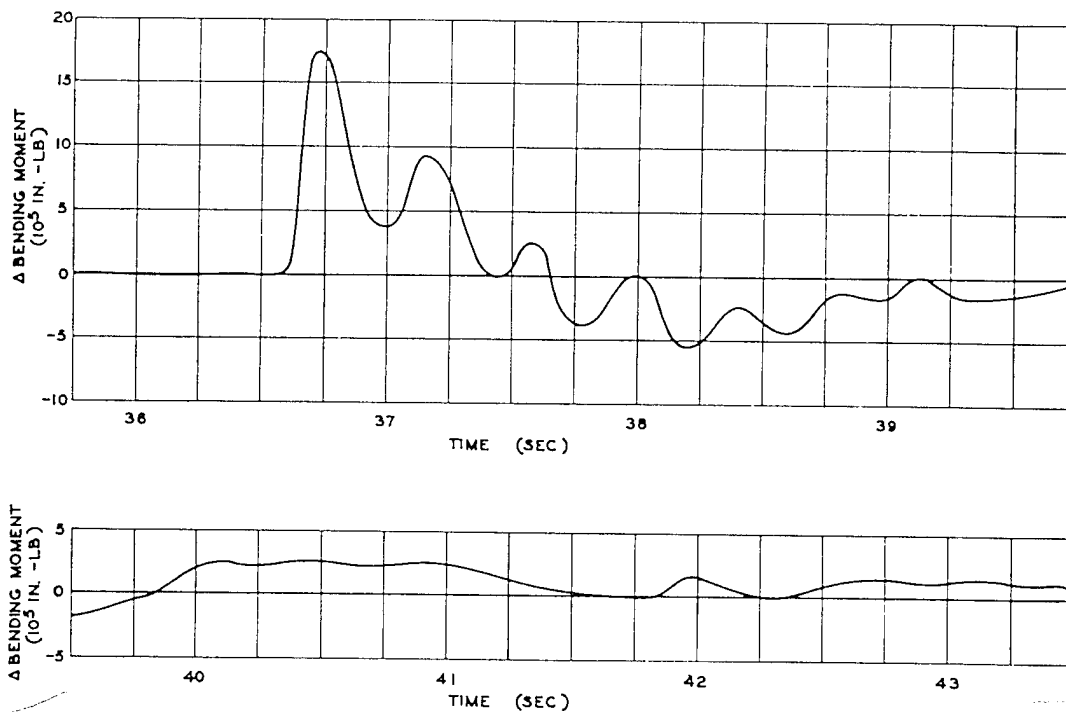


Fig. 7.29 Wing Bending, Right Wing Mid-span, Wing Station 266, Channel A10, B-50D (340), George Shot

~~SECRET~~

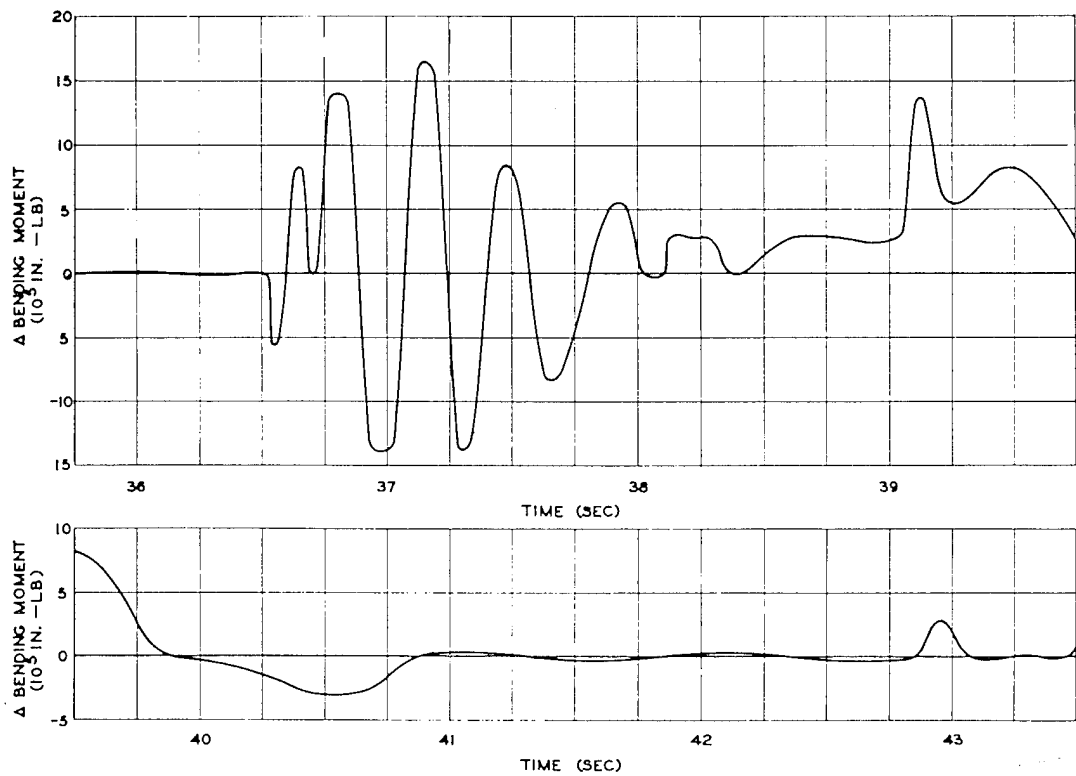


Fig. 7.30 Wing Bending, Right Wing Root, Wing Station 79, Channel A11, B-50D (340), George Shot

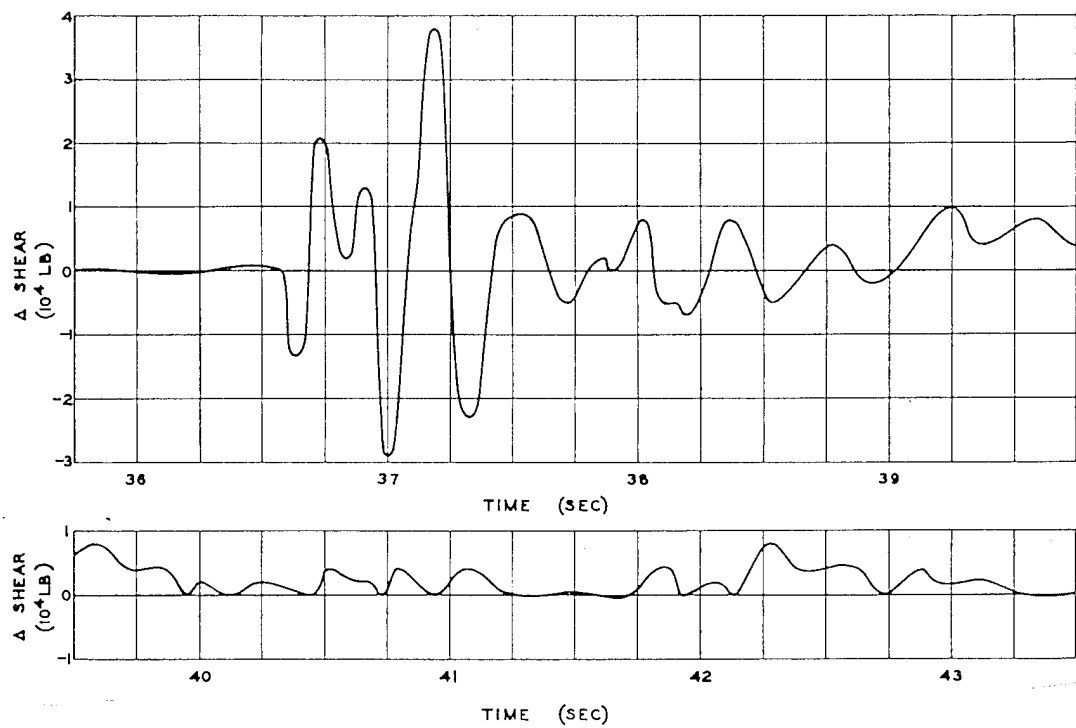


Fig. 7.31 Wing Shear, Right Wing Mid-span, Wing Station 269, Channel A16, B-50D (340), George Shot

~~SECRET~~

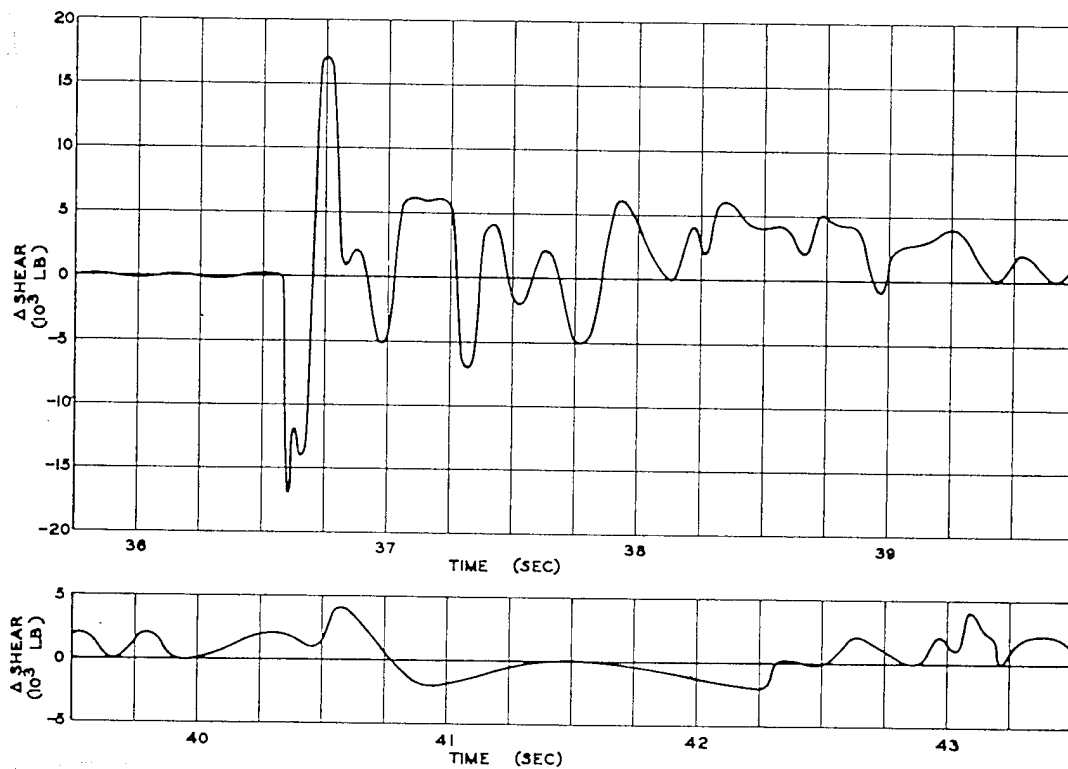


Fig. 7.32 Wing Shear, Left Wing Root, Wing Station 78, Channel A18, B-50D (340), George Shot

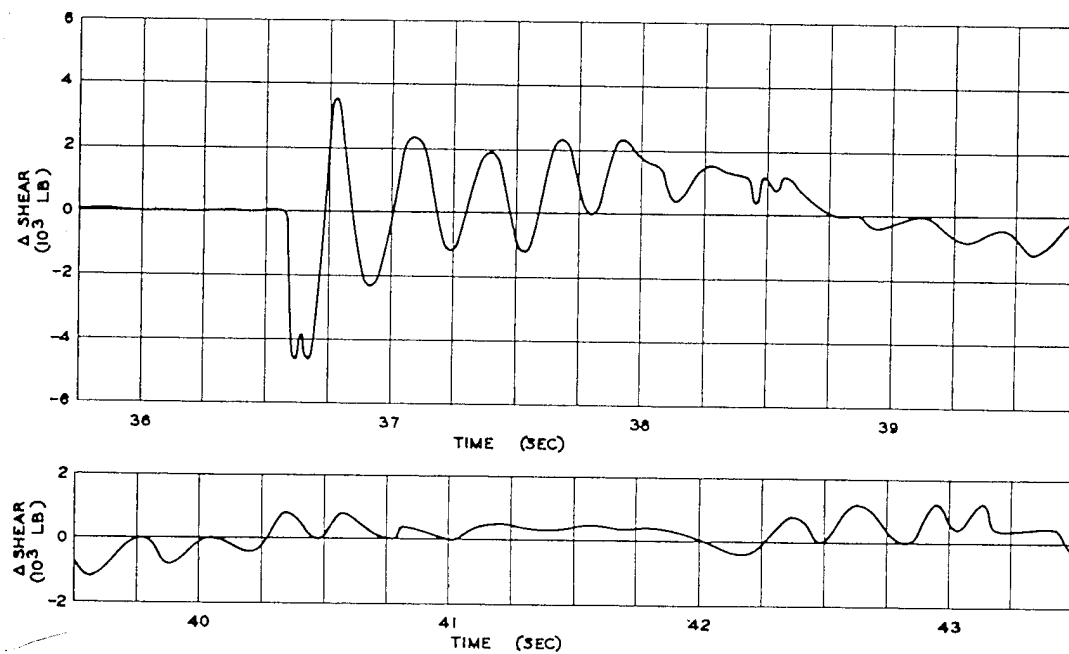


Fig. 7.33 Wing Shear, Left Wing Inboard, Wing Station 122, Channel A19, B-50D (340), George Shot

~~SECRET~~

~~SECRET~~

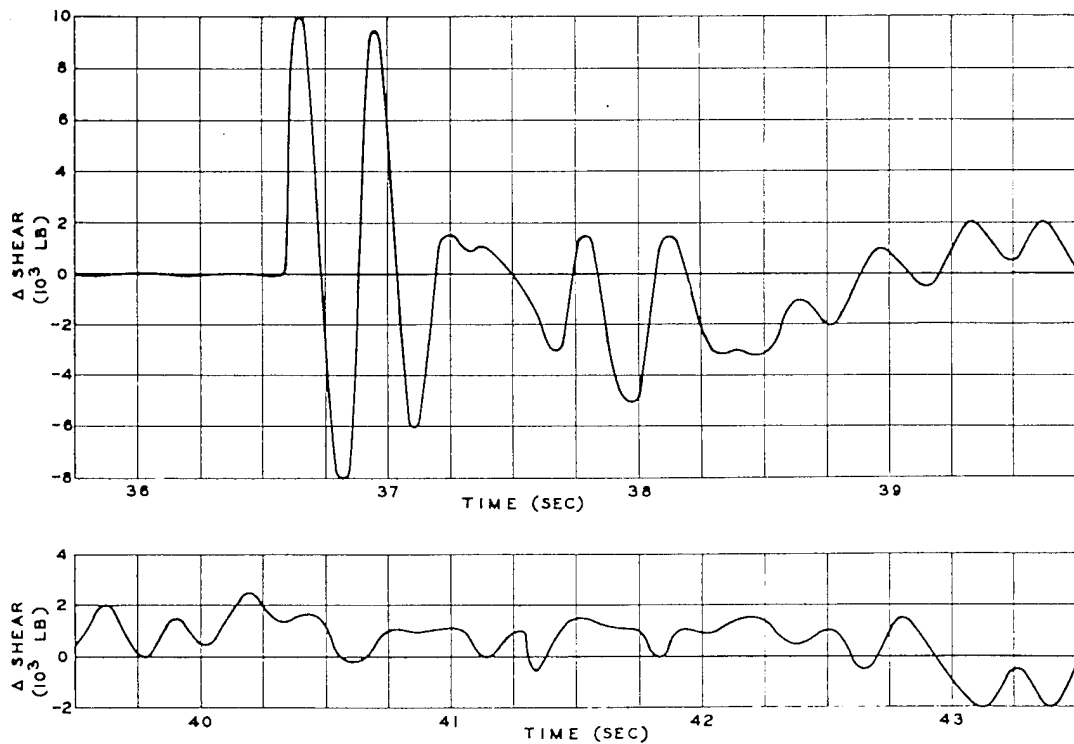


Fig. 7.34 Wing Shear, Left Wing Mid-span, Wing Station 269, Channel A20, B-50D (340), George Shot

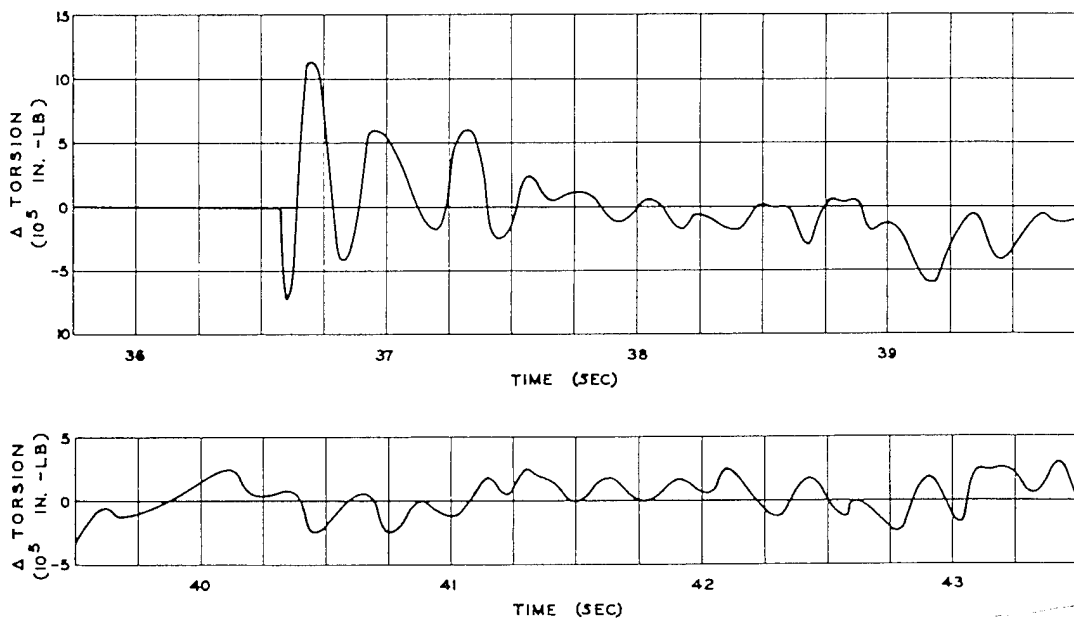


Fig. 7.35 Wing Torsion, Right Wing Root, Wing Station 78, Channel A22, B-50D (340), George Shot

~~SECRET~~

~~SECRET~~

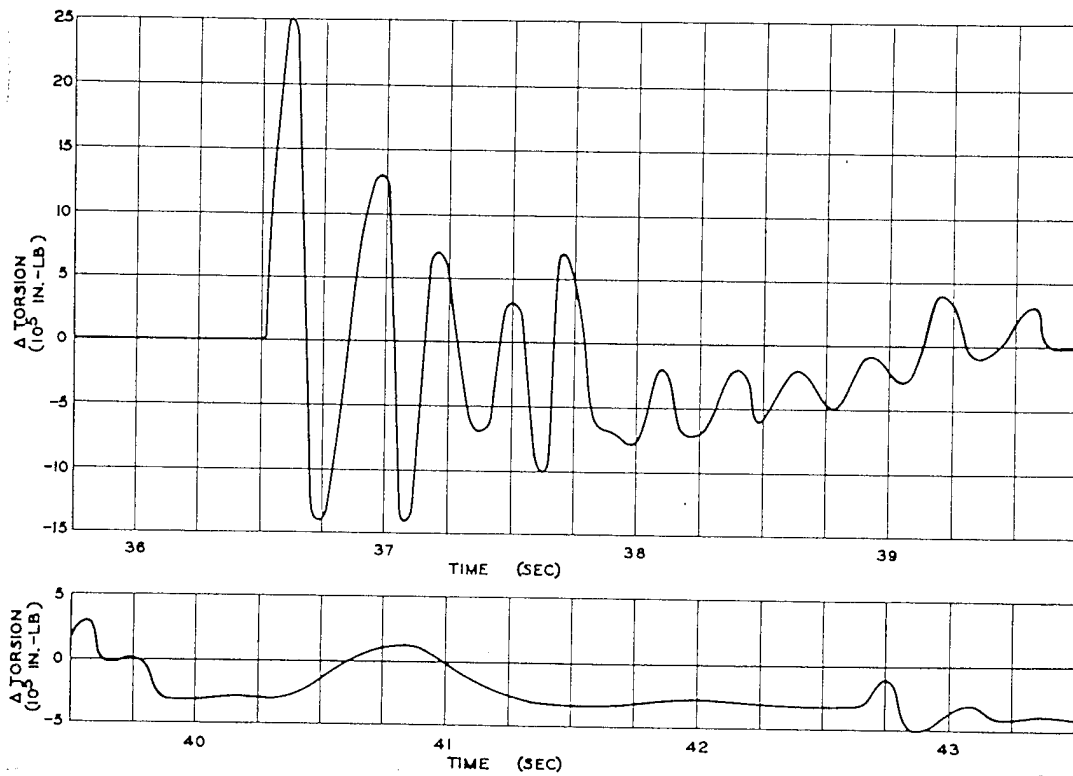


Fig. 7.36 Wing Torsion, Left Wing Root, Wing Station 78, Channel A23, B-50D (340), George Shot

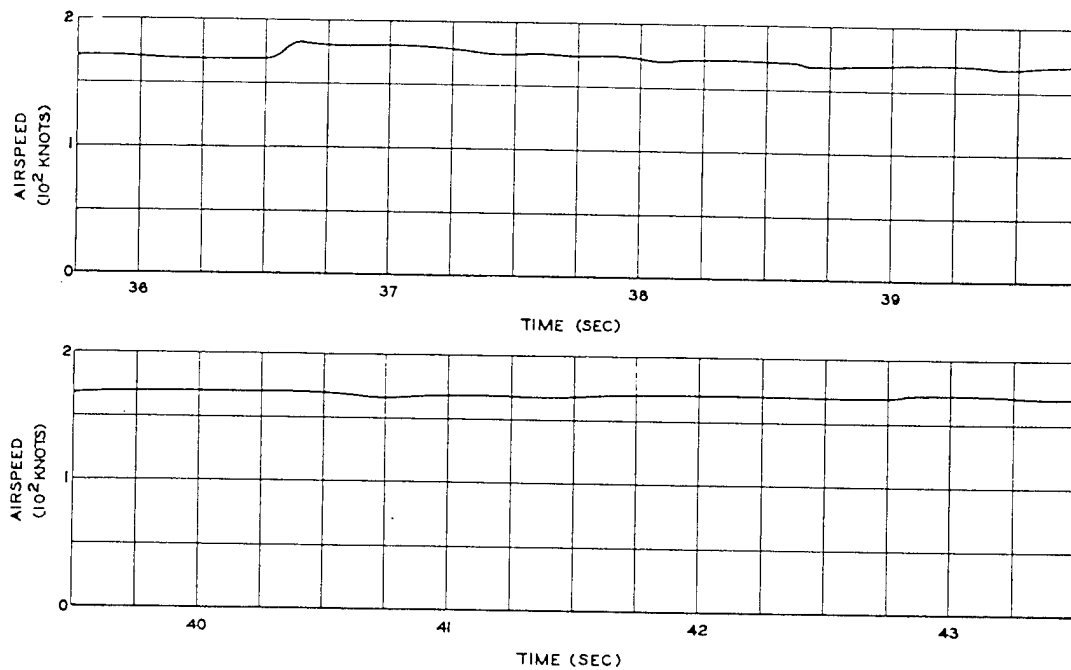


Fig. 7.37 Airspeed, Channel B2, B-50D (340), George Shot

~~SECRET~~

SECRET

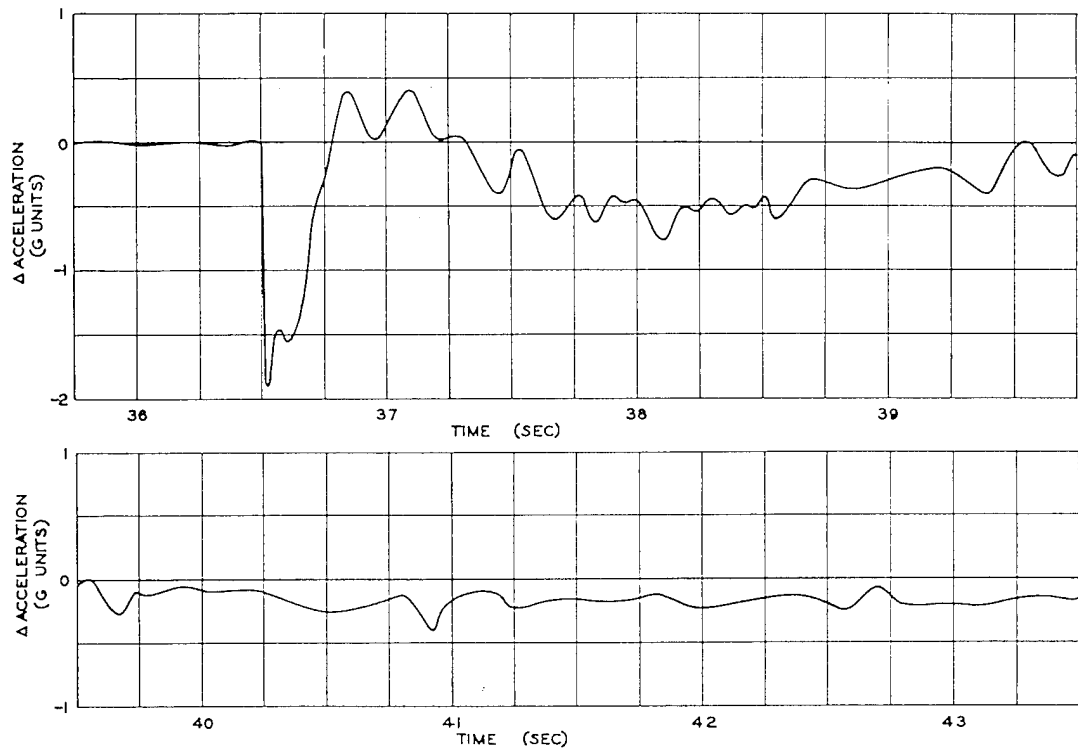


Fig. 7.38 Normal Acceleration, Aft Rear Bomb Bay, Fuselage Station 628, Channel B3, B-50D (340), George Shot

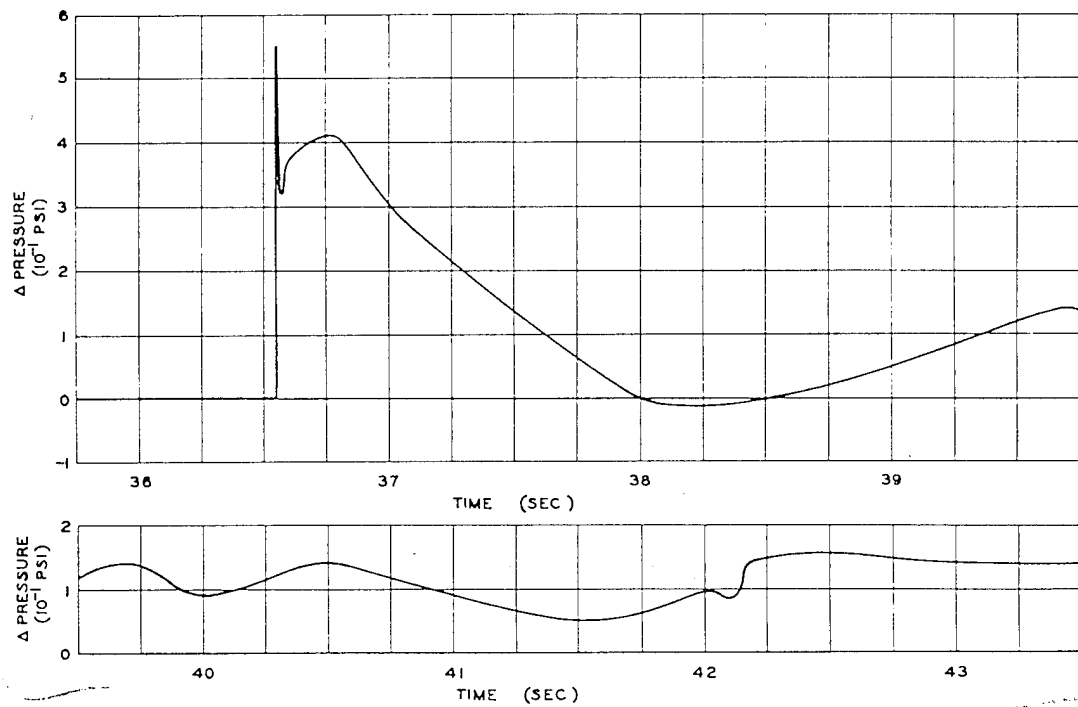


Fig. 7.39 Differential Aerodynamic Pressure, 60% Chord, Right Wing Station 525, Channel B5, B-50D (340), George Shot

SECRET

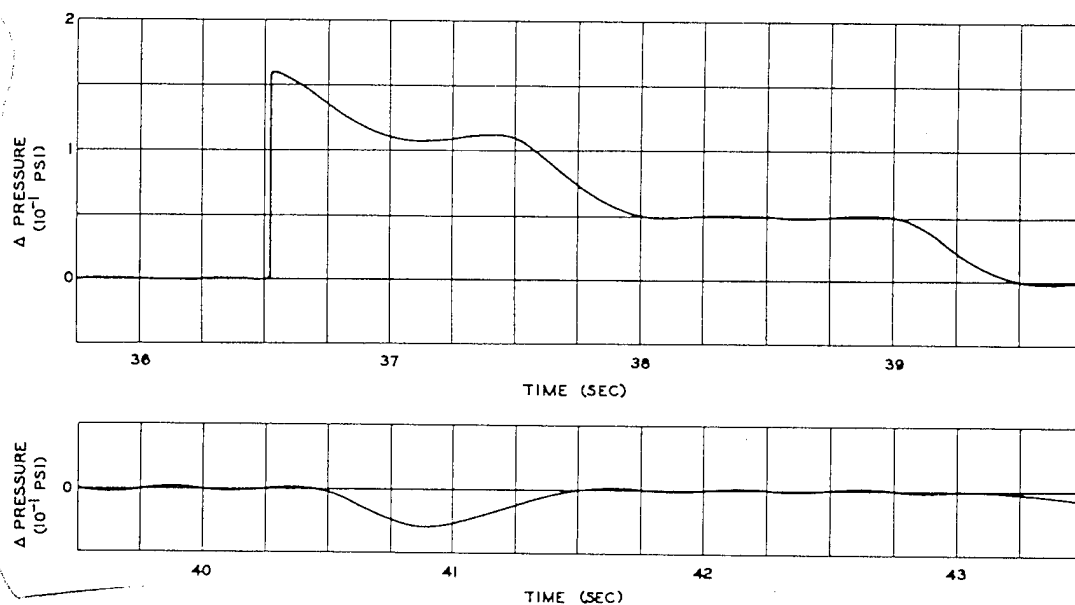


Fig. 7.40 Gauge Aerodynamic Pressure, Left Side of Vertical Fin, Fuselage Station 974, Channel B10, B-50D (340), George Shot

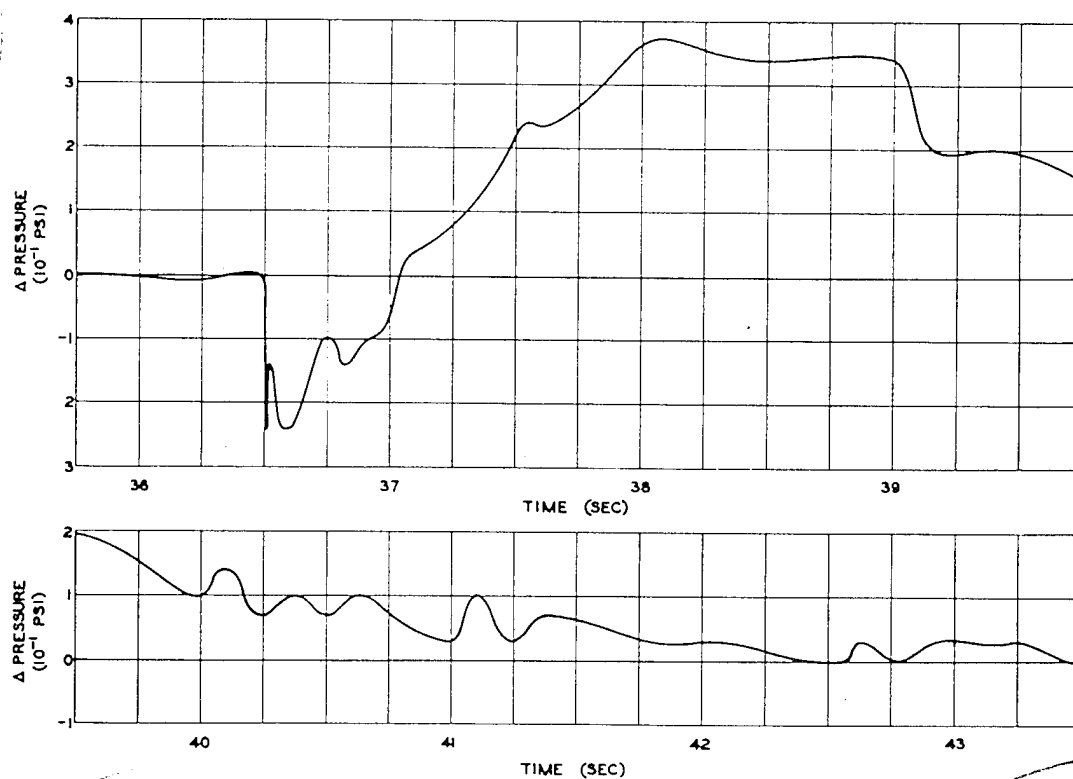


Fig. 7.41 Gauge Aerodynamic Pressure, 5% Chord, Top Left Wing Station 524, Channel B11, B-50D (340), George Shot

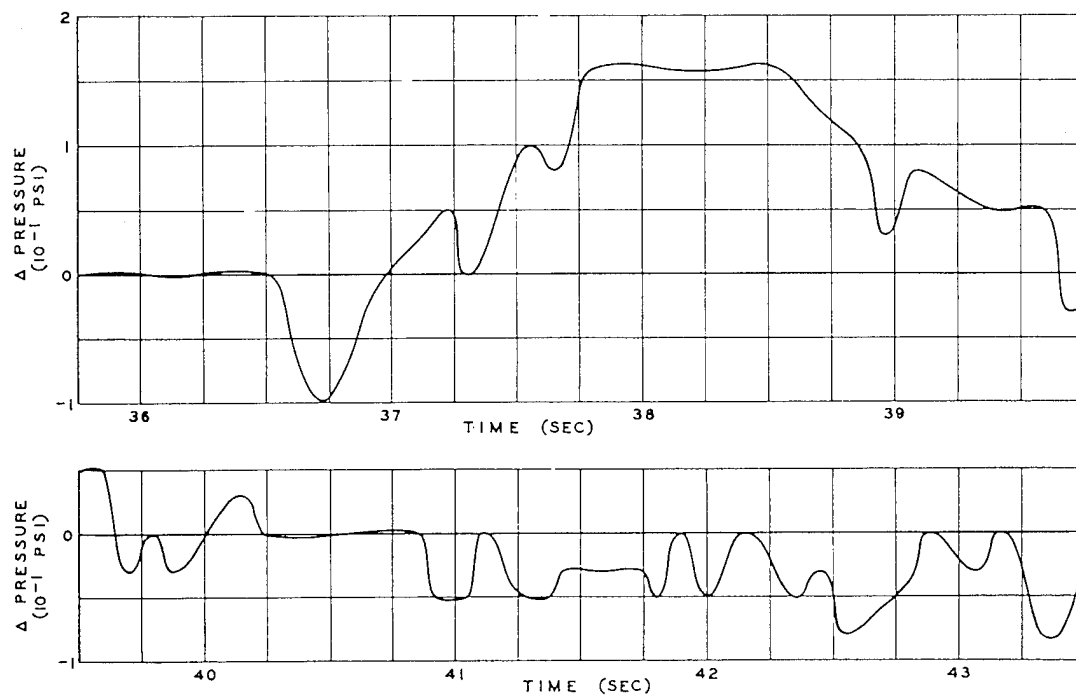


Fig. 7.42 Gauge Aerodynamic Pressure, 15% Chord, Top Left Wing Station 524, Channel B12, B-50D (340), George Shot

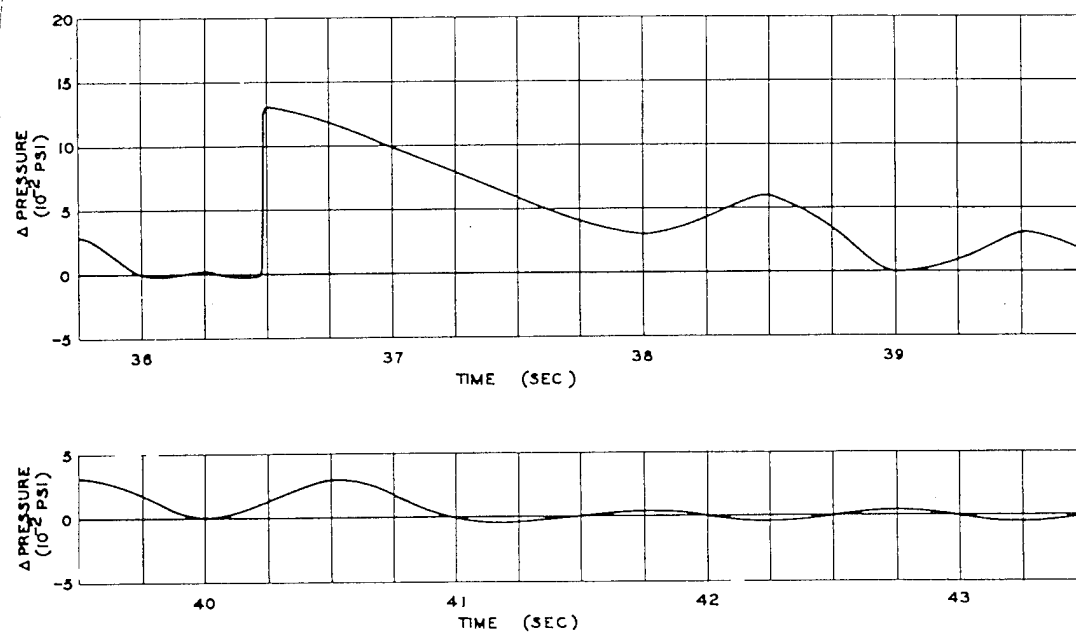


Fig. 7.43 Gauge Aerodynamic Pressure, 60% Chord, Top Left Wing Station 524, Channel B15, B-50D (340), George Shot

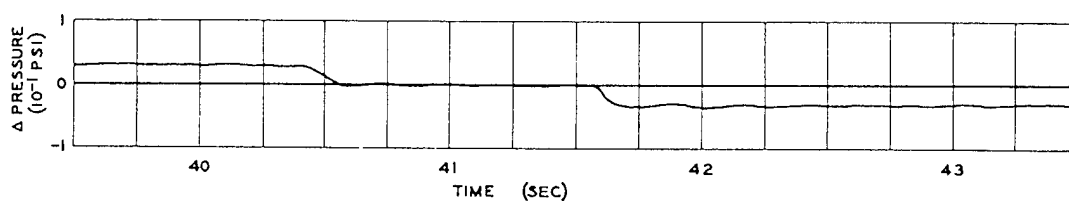
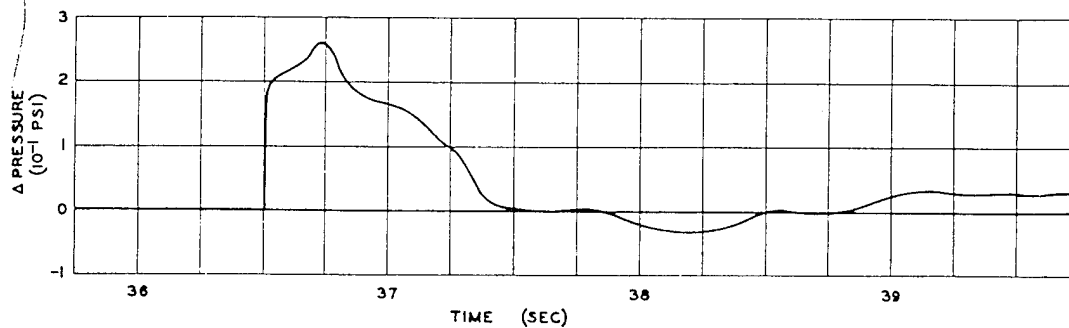


Fig. 7.44 Gauge Aerodynamic Pressure, 5% Chord, Bottom Left Wing Station 524, Channel B17, B-50D (340), George Shot

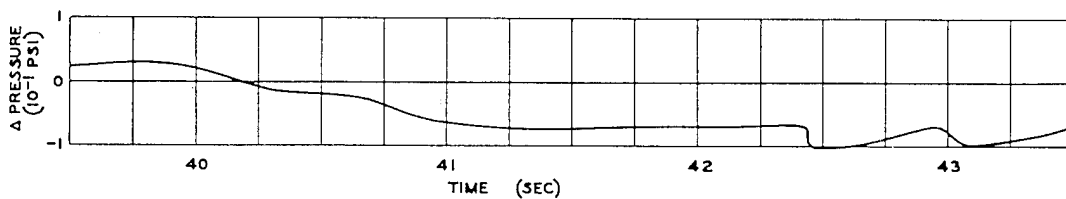
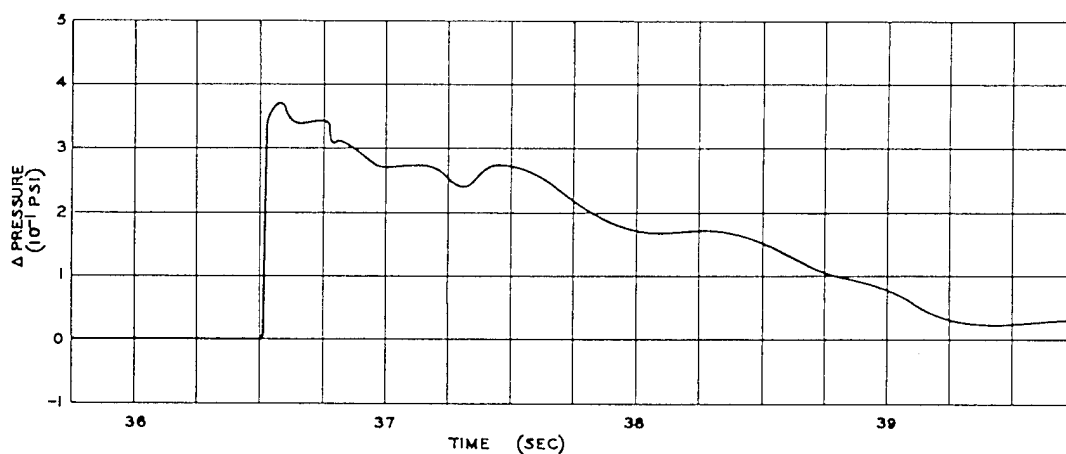


Fig. 7.45 Gauge Aerodynamic Pressure, 23% Chord, Bottom Left Wing Station 524, Channel B19, B-50D (340), George Shot

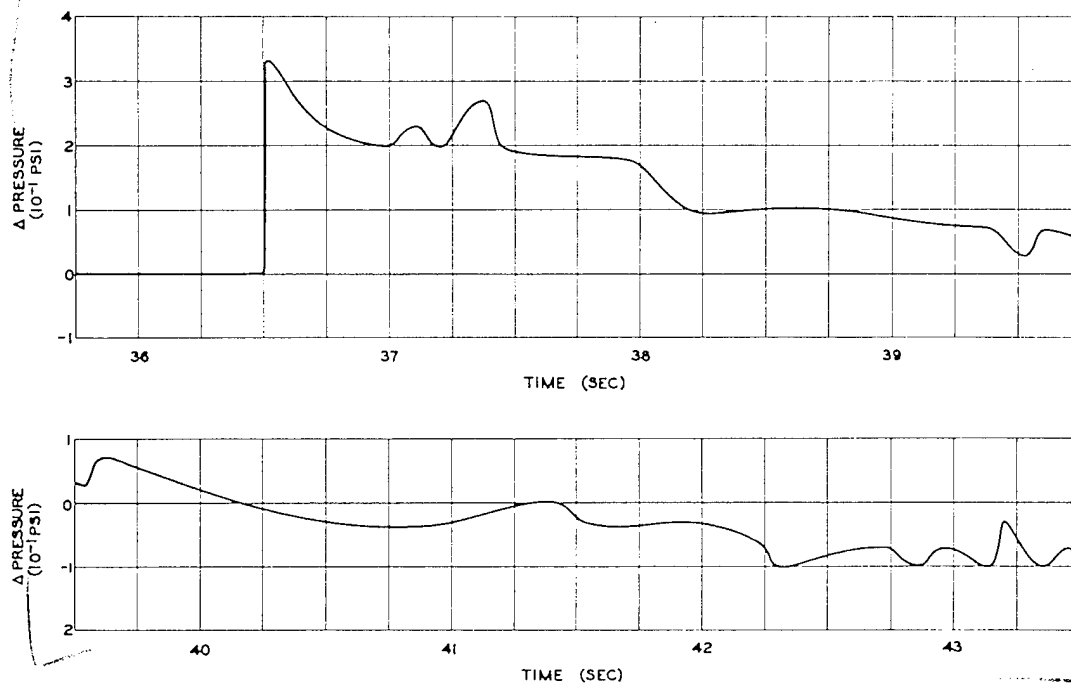


Fig. 7.46 Gauge Aerodynamic Pressure, 85% Chord, Bottom Left Wing Station 524, Channel B22, B-50D (340), George Shot

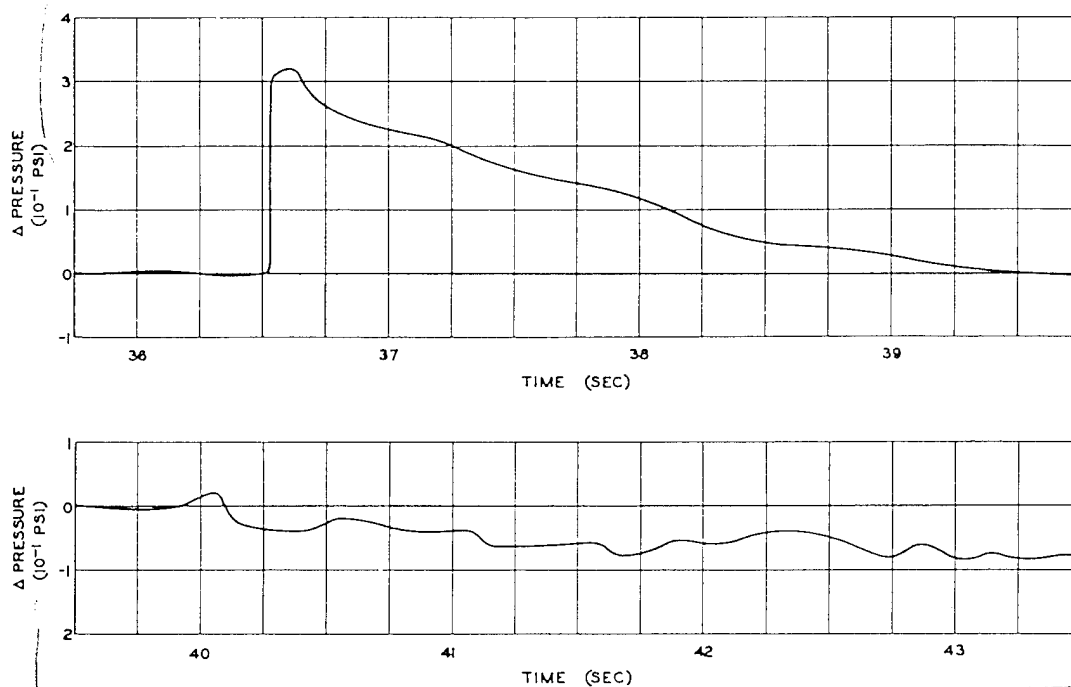


Fig. 7.47 Gauge Aerodynamic Pressure, Bottom Right-horizontal-stabilizer Station 170, Channel B23, B-50D (340), George Shot

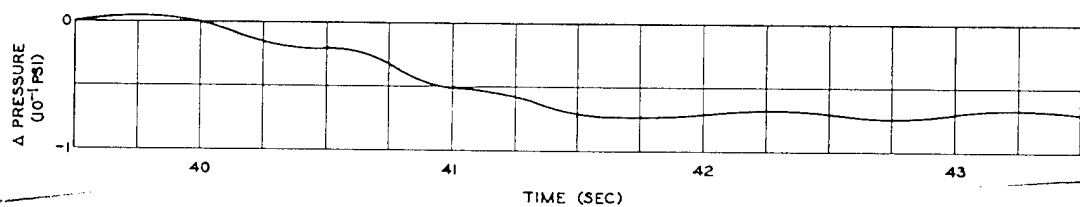
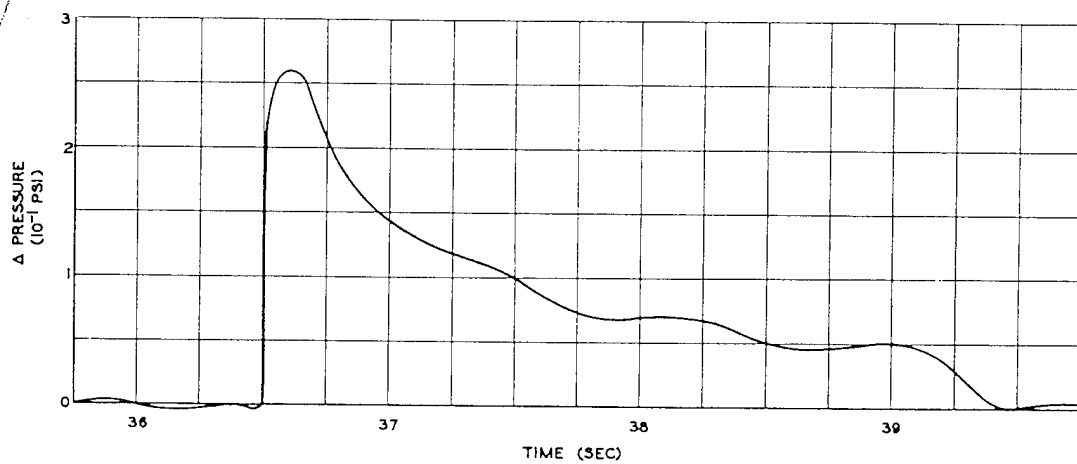


Fig. 7.48 Gauge Aerodynamic Pressure, Bottom Left-horizontal-stabilizer Station 170, Channel B24, B-50D (340), George Shot

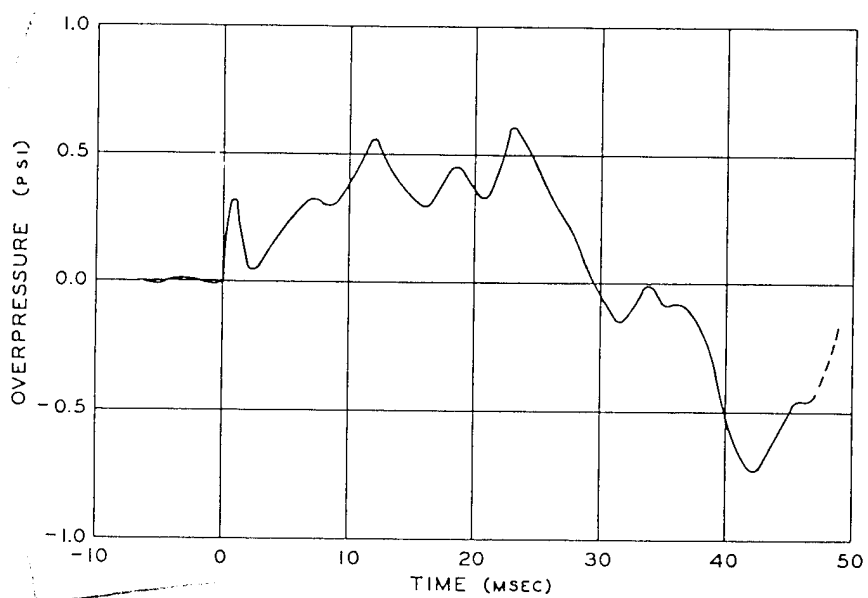


Fig. 7.49 High-frequency Pressure Record, Grace Position, George Shot

7.9.1 Flight Log

QB-17 airplane P was the last test airplane to take off since it was to be positioned at the lowest altitude. The mission was completed satisfactorily, and the flight data as reported¹ are as follows:

Time

Take-off, 0824

At assigned altitude, 0848

Shock arrival, 0931:04

Landing, 0946

Meteorological conditions at altitude

True altitude, 14,000 ft

Pressure altitude, 13,350 ft

Outside air temperature, +2°C

Wind direction (from), 260° (azimuth)

Wind velocity, 29 knots

Airplane parameters at shock arrival

Indicated airspeed, 130 knots

Ground speed, 278 ft/sec

Ground track azimuth, 352°

Horizontal angle from blast, 172° (azimuth)

Vertical angle from blast,* 13.4° (elevation)

Horizontal distance from blast, 58,850 ft

Slant distance from blast, 60,490 ft

Shock struck the airplane from ahead and slightly below

7.9.2 Airplane Condition

The instruments were checked prior to take-off, and several gauges were found to be bad. The plugs were removed from the pressure orifices just before a rain squall, and consequently the lines to the pressure transmitters filled with water. Of the other channels, only four did not check:

Channel 2—airspeed

Channel 7—wing bending, right wing root

Channel 13—wing torsion, right wing root

Channel 14—wing bending, mid-span right wing

The weight of the airplane at take-off was computed to have been 50,800 lb, with the c.g. at 30.5 per cent m.a.c. This condition included 1,700 gal (10,200 lb) of fuel in the main tanks and 500 gal (3,000 lb) in the Tokyo tanks. At the time of shock the gross weight was computed at 48,460 lb with 1,310 gal (7,860 lb) in the main tanks and still 500 gal (3,000 lb) in

the Tokyo tanks. The c.g. for this condition was at 30.1 per cent m.a.c.

7.9.3 Load Data

Seven channels of data were satisfactory from this mission. The data from channels 3, 4, 8, 9, 10, and 15 are presented in Figs. 7.50 through 7.55. Moisture prevented the collection of data from the other channels. The calibration data for channels 3, 4, and 8 are insufficient to establish a definite calibration curve. However, the records from these channels on the mission appear to be satisfactory, and, because of the small amount of data from this mission, these channels are presented. The missing calibration data have been approximated, and as a result the graphs of the mission data are open to question.

The sinusoidal frequency of approximately 180 cpm (see Sec. 7.4.4) again appears on channel 3 but was faired out when the graph in Fig. 7.50 was plotted. The frequency is shown on the graph of channel 8, Fig. 7.52. The high-frequency-recorder record is given in Fig. 7.56.

7.10 GENERAL CONCLUSIONS FROM GEORGE SHOT

The data from all test airplanes except B-50D (340) are very meager and are comparatively low in value. One particularly interesting aspect of these data was the comparison with the opinions of the crews. Almost unanimously the crew members agreed that the responses of the airplanes were practically undiscernible. However, the measured loads, even on QB-17 P, were definitely identifiable. The point to be made is that interrogation of crew members is a very poor method of establishing the magnitude of the applied loads. Apparently the loads are applied and released too quickly to allow the crew to be aware of the extent of the loading.

No evaluation of the discrepancy in time for shock-wave travel is possible from this shot since the majority of the times are based on crew reports. This situation arose from the need for the test crews to use the radio for voice transmission and reception.

REFERENCE

1. Navigator's Report, George Shot, prepared by ATU 3.4.2.

*Computed from data in Navigator's Report, reference 1.

~~SECRET~~

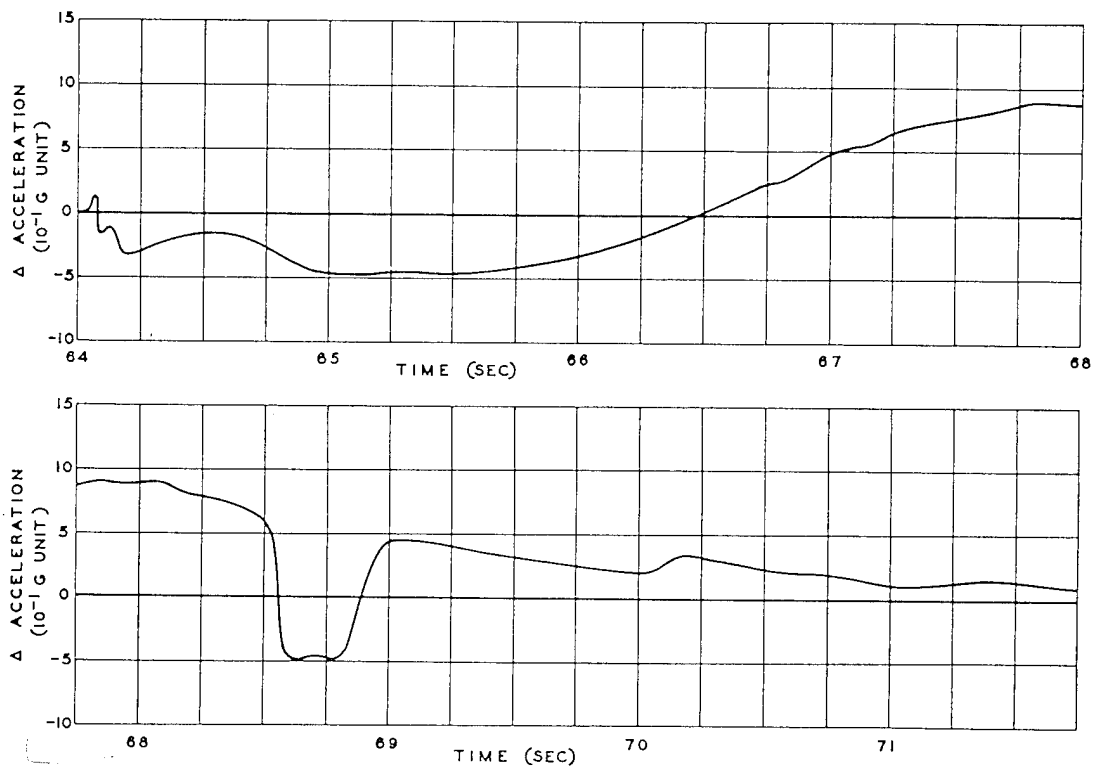


Fig. 7.50 Normal Acceleration, c.g., Channel 3, QB-17 P, George Shot

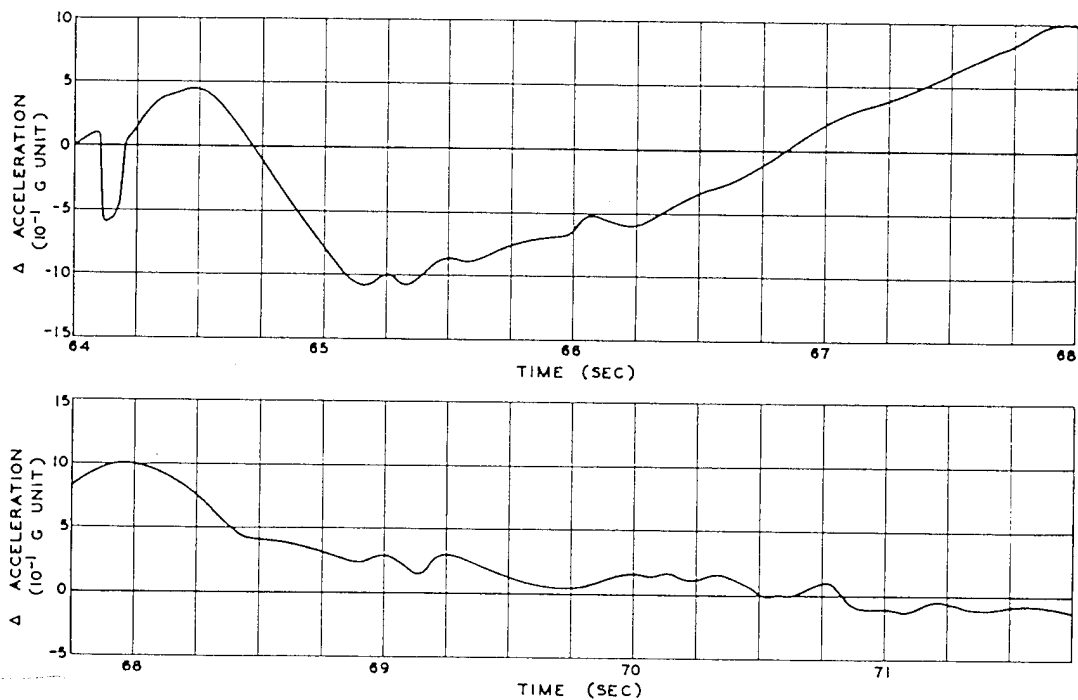


Fig. 7.51 Normal Acceleration, Aft Fuselage, Channel 4, QB-17 P, George Shot

~~SECRET~~

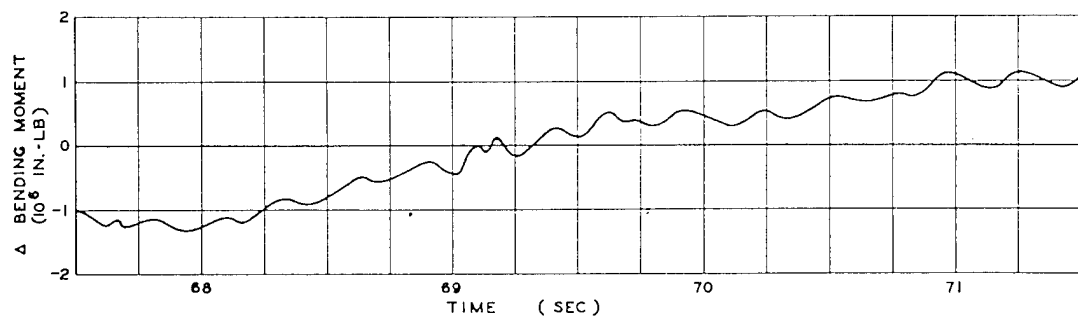
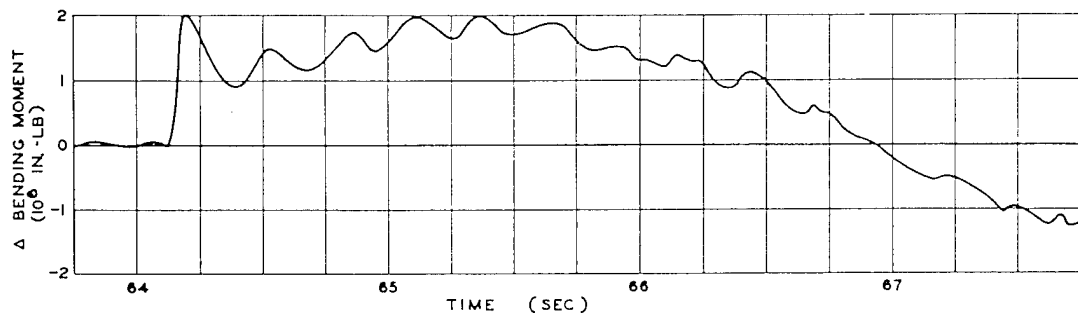


Fig. 7.52 Wing Bending, Left Wing Root, Channel 8, QB-17 P, George Shot

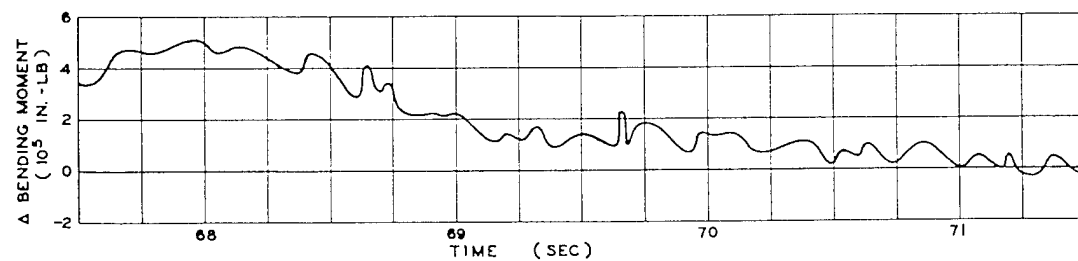
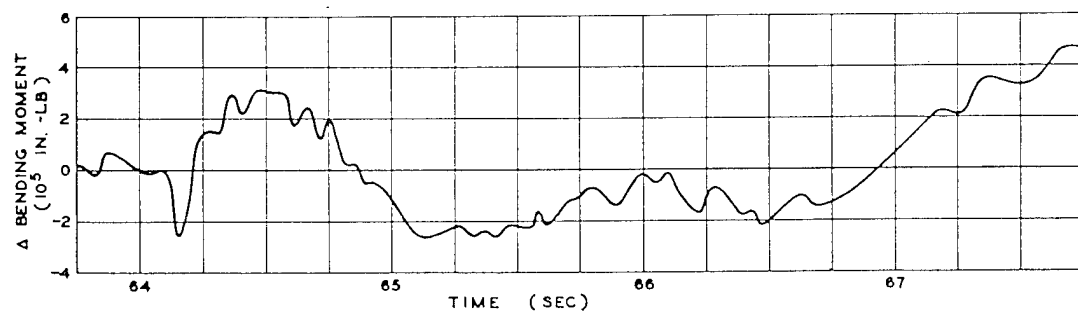


Fig. 7.53 Stabilizer Bending, Right Horizontal Stabilizer, Channel 9, QB-17 P, George Shot

~~SECRET~~

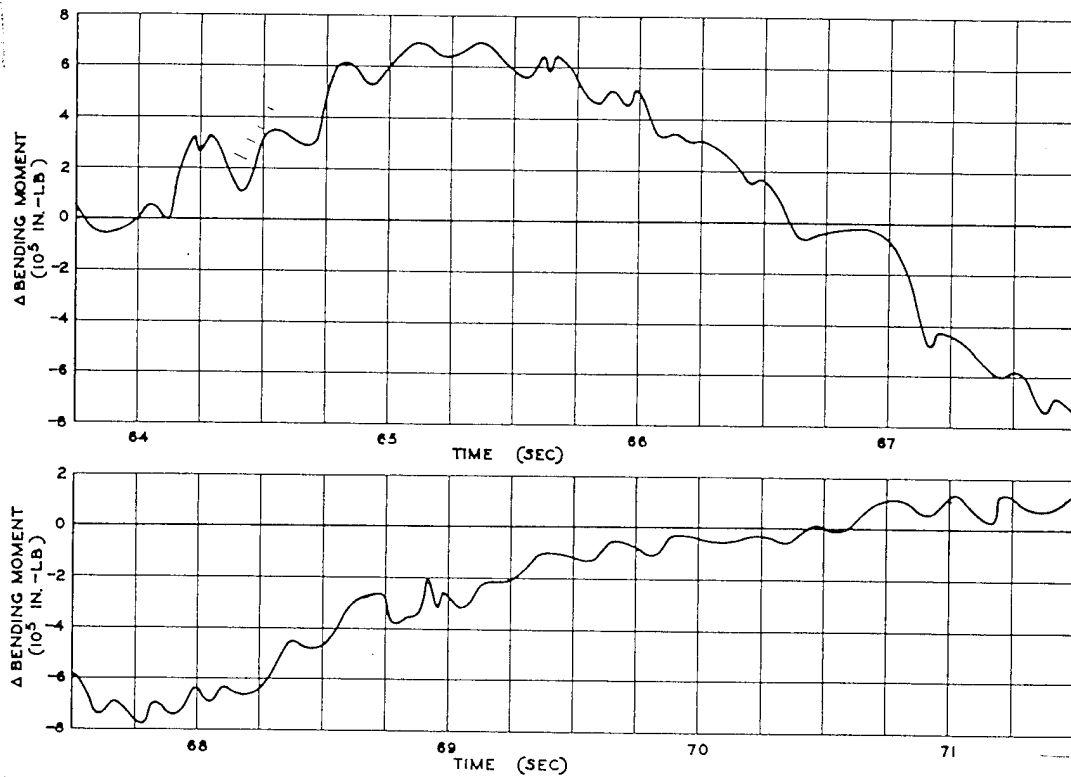


Fig. 7.54 Wing Bending, Outer Panel, Right Wing Station 19, Channel 10, QB-17 P, George Shot

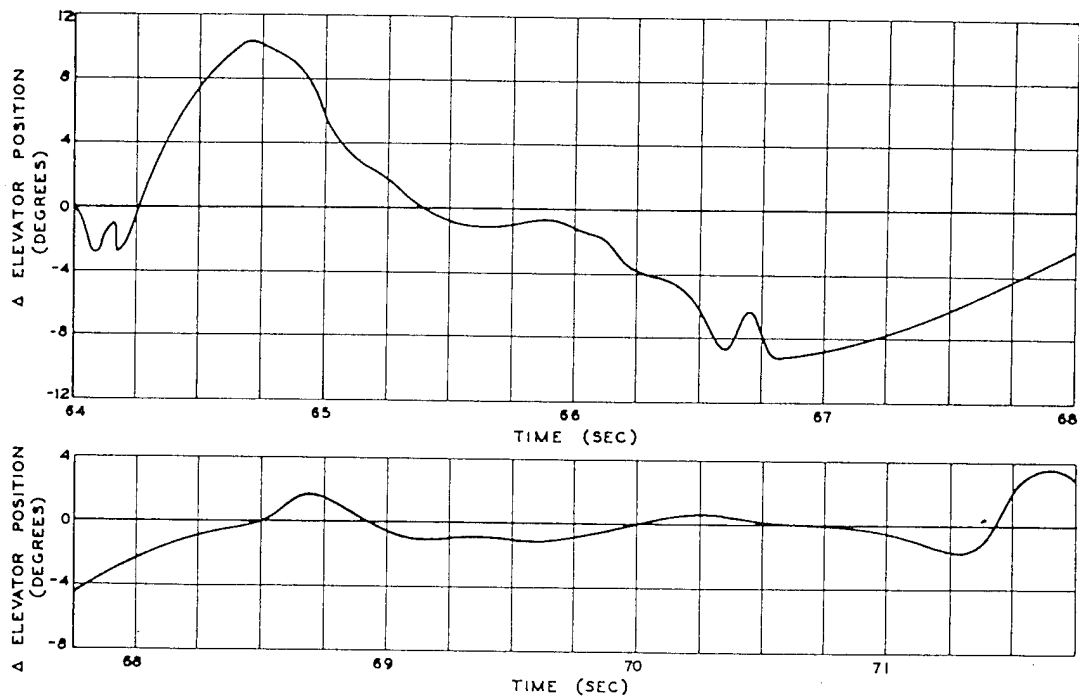


Fig. 7.55 Elevator Position, Channel 15, QB-17 P, George Shot

~~SECRET~~

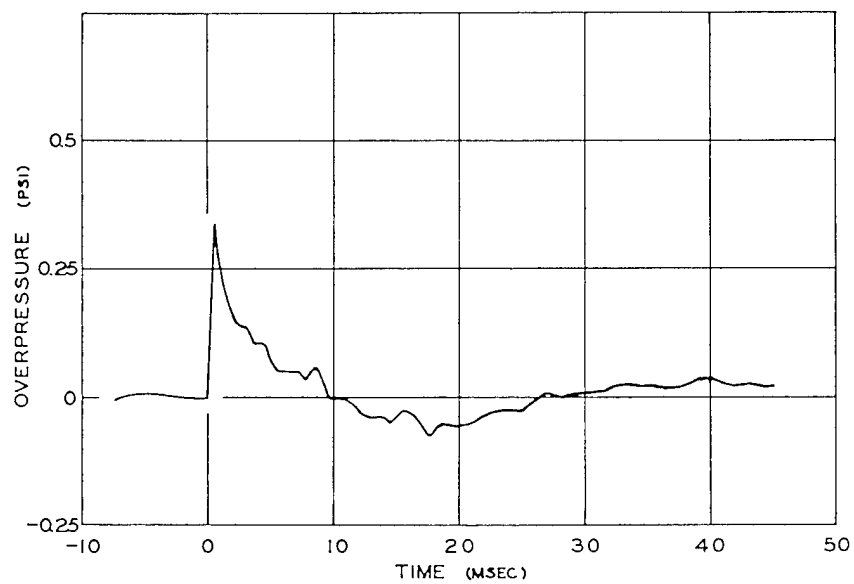


Fig. 7.56 High-frequency Pressure Record, Sally Position, George Shot

Chapter 8

Summary

Project 8.1 was generally successful in that the data which were collected appear to be sufficient to satisfy at least the initial requirements of the theory. There were two principal reasons for the failure to collect all the data that had been originally intended, although in normal flight-test experience complete success is the exception rather than the rule. First, the new and untried nature of the instruments combined with the one-shot nature of each test greatly complicated the operation. Second, more was attempted than could have reasonably been accomplished under the circumstances.

Using the size of this report as a measure, it is interesting to contemplate the potential size had all the data-gathering efforts been successful. The time which would have been required for the preparation of such a report is even more impressive.

8.1 INSTRUMENTATION

The problems involved in the instrumentation of aircraft to measure and record the effects of an atomic explosion are unique. The uniqueness is due to the "impulse" nature of the loading, the ambient conditions (corrosion as well as temperature and pressure variations from sea level to altitude), the requirement for automatic unattended operation in drone aircraft, and the emphasis on reliability to ensure the obtaining of data from tests which cannot be repeated. Although each of these conditions alone is not unusual in flight-test work, the combination of conditions demands special equipment. Other governmental agencies are concerned with the development of equipment to operate under various combinations of these

conditions. The development of instruments should logically be coordinated among these agencies.

It is apparent from the experience of this project that the combination of service-testing of instruments with the actual mission of collecting important data is poor practice. Such a combination not only increases the complexity of the operation and increases the personnel requirement in a restricted area, but also compromises the primary mission by preventing collection of some of the data, by reducing the reliability of data collected, and by occupying the time and effort of personnel who should be concerned with other matters. It is therefore necessary that equipment be employed on projects of this type only after it has been tested, accepted, and proved under field conditions.

Recommendation. A continuing Air Force project should be established at WADC with the necessary continuing responsibility, priority, personnel, and funds solely for the improvement and/or development of appropriate sensing, recording, telemetering, and associated equipment which will be suitable for collecting aircraft structural data from future atomic tests. The plans and progress of this project should be closely coordinated with similar efforts within other governmental agencies, and the end items should be standardized and catalogued in appropriate stock lists so that procurement and storage can be accomplished through normal channels.

8.2 OPERATION

In general, the organization and functioning of the operation as seen from the vantage point

~~SECRET~~

of Project 8.1 was very good. However, one suggestion is offered: One representative of the technical group should have been assigned to a staff position in each of the concerned Task Groups and in the particularly pertinent Task Units of at least the Air Task Group. This representative would have been able to assist the commanders in their responsibilities with regard to data collection and would have provided the technical groups with a channel of approach to the operating organizations.

8.2.1 Organization

The assignment of the instrument-maintenance and -operation section to the drone-operating organization solved the problem of coordination with the operating and training functions, but it greatly complicated the collection of data. For example, decisions by the technical group to add or delete items of equipment on the basis of current experience or data analysis were voided because the mission of the Air Task Group, as assigned by directives, specifically included the operation of certain equipment. That equipment was, therefore, to have been operated regardless of circumstances. Such resistance reduced the flexibility of operation and thus the effectiveness of the technical group.

In line with the division of responsibilities between the technical and the operating organizations, the Communications Section of the Air Task Group was to have been responsible for the installation of landlines between the radar and telemetering sites. The logistics of this responsibility were apparently lost among the great quantity of logistical support required for the communication networks, the Air Operation Center, and the other electronic equipment. To the technical organization this detail would have assumed its proper importance, and the necessity for ensuring a satisfactory installation would have been realized.

Recommendation. In future operations the technical organization should have the responsibility, along with the authority over and control of the personnel and facilities, for complete conduct of the data-gathering effort exclusive of the actual maintenance and operation of the aircraft. In order to make this organization effective, however, the specific areas of responsibility, the relative impor-

tance of the various technical efforts, and the necessity for close coordination must be clearly defined and mutually understood.

8.2.2 Facilities

The importance of certain facilities at the test site, such as steady electrical power, transportation, and air conditioning, was underestimated. Electrical power from the diesel generators was variable and uncertain because of the total loads being supported. In the alignment of the instruments a constant stable power source was very important. It was necessary, therefore, that the use of power be closely scheduled with other operations. Because this scheduling was impromptu, it was the cause of a great number of delays.

Vehicles for transportation of instruments and equipment and for use of project personnel on the job were in very short supply. The lack of this transportation was serious, although some relief in this regard was occasionally provided by the Air Task Group.

The presence of coral dust and moisture in the equipment was one important source of trouble. The equipment, in its assembled state, was reasonably well protected; however, when disassembled for maintenance, the equipment was quickly and seriously affected by dust and moisture. The hangar provided some protection, but leaks in the roof were invariably in vulnerable locations.

Photographic-processing facilities were in very short supply. Even by supplementing the equipment, as provided, with the available facilities of other organizations, it was impossible to avoid delays in the processing of data.

Recommendation. Careful plans, with coordination in the forward area, to include adequate power, transportation, work space, and photographic-processing facilities should be an important part of the arrangements for future projects.

8.2.3 Personnel

The shortage of technical personnel in the forward area was a definite handicap. The personnel in the Instrumentation Section were overworked beyond the point of marginal returns. Many of the technicians worked more than 12 hr per day, every day, including week

~~SECRET~~

ends, especially during the latter part of the operation. Such intensive effort reduced the efficiency of the men to such a point that much time was necessary to recheck and repair previous work.

In any such future program there should be one engineer assigned to each test airplane instead of one engineer to each type of airplane. This engineer with two or four technicians (depending on the size of the airplane and the extent of the instrumentation) should be able to maintain the instruments and the calibration of one test airplane. The instrument-repair and -overhaul section was also undermanned. Based on the experience of this project and assuming that equipment to be used on future tests will have been better tested before its use, the following ratios of men to instruments for maintenance have been evolved: one technician for every four recorders, one technician for every three air-borne telemeters, one technician for every two telemeter receivers, one technician for every six synchronizing systems, one technician for every tape-playback set, one technician for every two high-frequency pressure recorders, and one engineer for each principal type of instrument. In addition, the necessary "overhead" personnel, such as photographic technicians, supply clerks, typists, noncommissioned officers-in-charge, liaison men, and supervisors, depending on the size and type of the organization and the equipment involved, should be included. Such an organization for this project would have involved 68 technicians and 21 engineers in the forward area. The technicians may be either civilian or enlisted. However, if enlisted men are included, they should be relieved of the usual military duties. The number of personnel in the training and preparation phase of the project will need to be somewhat greater in order to have sufficient personnel to install the instruments and in order to select the better qualified and more amiable ones for the forward area.

Admittedly, this not only would have involved a large number of persons during the initial phases, but the size of the organization in the forward area would also have been considered unduly large in view of the restricted number of accommodations. However, in order to ensure a more profitable return on the investment of time and funds, the scope of the project

should have been curtailed until a reasonable balance between the effort and the permissible size of the organization had been achieved.

The organization, in the form to be used in the forward area, should be assembled and operated for a reasonable length of time in the Z.I. before departure in order to develop the related duties. This time could well be used to instrument the test airplanes. Also, the organization should remain intact after return to the Z.I. until the storage of the equipment and the preparation of the report have been completed.

Recommendations. The limits on the number of persons in the forward area and the allocations of living quarters should be established early in future operations while the scope of the technical effort is still capable of expansion or contraction without undue loss of time and money. The technical effort should be scrutinized closely to determine that no more is attempted than can be reasonably accomplished with the personnel.

8.3 DATA

The data collected and reported here appear to conform reasonably well to the theory of aircraft loading by blast. Generally, it is believed that the data are accurate to at least ± 5 per cent, except for a few instances as noted. In the instances of the radar location data, the recorded times for shock travel, the high-frequency pressure records, and certain of the tape channels the accuracy is better than ± 5 per cent.

Using the measurements from manned airplanes as a foundation and extending the information by means of the measurements from the drones, the techniques of extrapolation to other structures, unusual locations, and alternate or variable conditions should be established or at least indicated. It should be possible in the future, therefore, to add to the existing knowledge through the use of manned airplanes, principally. However, the extrapolation will unquestionably become nebulous in the higher ranges, and further verification will be necessary. For safety reasons such verification will require drone aircraft.

The relations of the blast loads to the loads due to maneuvers and to the loads experienced within the cloud are apparent from the records.

Although the normal tactics, either present or planned, do not include traverse of the cloud, the structural hazard in such a traverse is indicated by the loads on drone N on Easy shot (Sec. 6.5.5).

The relative importance of the heat in defining tactical limitations was very positively indicated by this operation. The loss of parts of control surfaces, the damage to the protected (foil-covered) control surfaces, and the burning of the tire all indicate the hazard to the large airplanes presently designed with such vulnerable areas. These data also indicate the need for further study of the many aspects of the heat problem, including the structural loads imposed by the thermal expansion.

The calibration curves are included as appendixes to this report (reproduced elsewhere, see page iv) for the benefit of those who will apply these data to theoretical calculations. These curves indicate the linearity of the calibrations, the sensitivity of the various channels, and the range of the calibration for comparison with the ranges of the measured data. In general, therefore, the calibrations are presented as substantiating evidence for the measured data.

Recommendation. The data as presented in this report should be generally accepted as accurate within 10 per cent (± 5 per cent) and should be applied to the theory to verify the techniques of computing the structural loads on aircraft in the vicinity of an atomic explosion.

8.4 FUTURE PLANS

Specific and detailed plans for further measurements of blast effects on aircraft in flight must necessarily await the assimilation of the data collected from this operation. Also, the nature, time, and extent of future measurements will depend upon supporting activities. Among these are the progress in the development of suitable instrumentation and, for drone tests, the rate at which radio-control equipment and techniques can be perfected for new types of aircraft. Both of these requirements must be satisfied before specific tests and plans can be prepared for coordination with the responsible agency.

An apparent and immediate need is for the study of radiant-energy emission and reception and the thermal effects on the airplane and crew. It is planned that this study will be con-

tinued at the earliest opportunity.

It will also be necessary to check the application and extrapolation of the theory to other configurations. It has been, therefore, proposed to Headquarters, USAF, that projects be established for the development of radio-control equipment for F-84F, B-29, and B-47 types of airplanes to be used in future tests of this type.

A proposal is presently being considered which will solve a part of the personnel and planning problems if it is acceptable. The plan involves a continuing contract with an engineering organization of suitable qualifications. The functions of the contractor will be as follows:

1. To maintain current and continuous liaison concerning the state and progress of the theoretical studies in order to determine the data which are needed to supplement the theory.
2. To maintain current detailed plans for the installation of instrumentation in the various types of airplanes which might be used for the tests. Plans are to be prepared for instrumentation as either manned airplanes or drones, if the alternatives are possible, and the plans are to be sufficiently detailed and complete to permit implementation on short notice.
3. To maintain organization arrangements and plans for the rapid expansion of an organization and the associated facilities which would be required to support the plans as prepared. The amount and extent of the expansion to be required will be dependent on the scope of the project and the funds available.

With such plans available on a current basis, it should be possible to plan and execute a considered program with a minimum of time in preparation. The flexibility of a contractor's organization should provide the solution to at least a part of the personnel problems. Developing instrumentation, arranging for modification of the airplanes, supervising the operation, and monitoring the contract would be retained as the direct functions of WADC. However, the severe drain on the supply of technical personnel from WADC would be greatly reduced if the proposed plan were accepted and adopted.

Recommendation. Future air-borne projects by the Air Force should, in any event, be tail-

[REDACTED] [REDACTED]

ored to the personnel limitations and should be much more modest in scope than Project 8.1 unless the USAF now, and the operating Task Force at the time of the tests, are willing to

support the program with personnel, funds, and facilities to the extent that justifies the existence of the effort both now and during the operation.